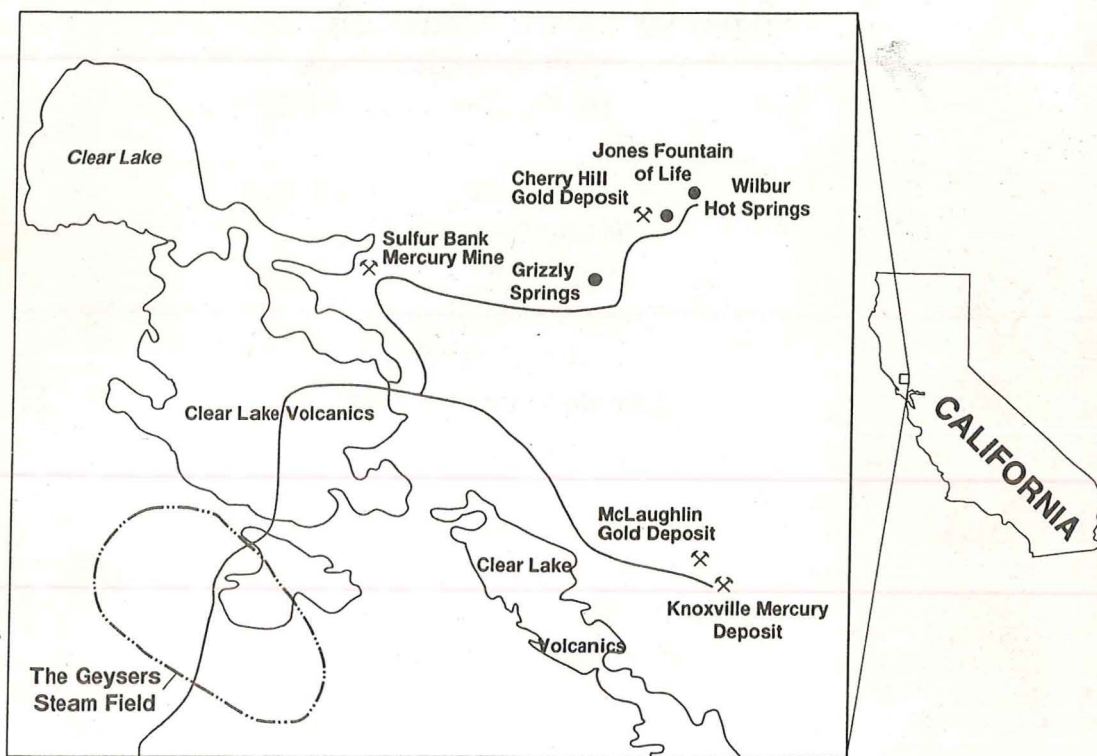


GL04381

GUIDEBOOK SERIES Volume 16

ACTIVE GEOTHERMAL SYSTEMS AND GOLD-MERCURY DEPOSITS IN THE SONOMA-CLEAR LAKE VOLCANIC FIELDS, CALIFORNIA

Edited by James J. Rytuba



Guidebook Prepared for Society of Economic Geologists Field Conference
27 September-1 October 1993

Series Editor: Tommy B. Thompson
SOCIETY OF ECONOMIC GEOLOGISTS

**GUIDEBOOK SERIES
of the
SOCIETY OF ECONOMIC GEOLOGISTS**

SERIES EDITOR: Tommy B. Thompson

**Printed by: Citizen Printing Co., Inc.
1309 Webster Avenue
Fort Collins, CO 80521**

*Additional copies of the guidebook may
be obtained from:*

Tommy B. Thompson
Department of Earth Resources
Colorado State University
Fort Collins, CO 80523 USA

OR

Society of Economic Geologists
5808 South Rapp St., Suite 209
Littleton, CO 80120 USA

Price (including postage in North America):

Society Members - \$US35.00

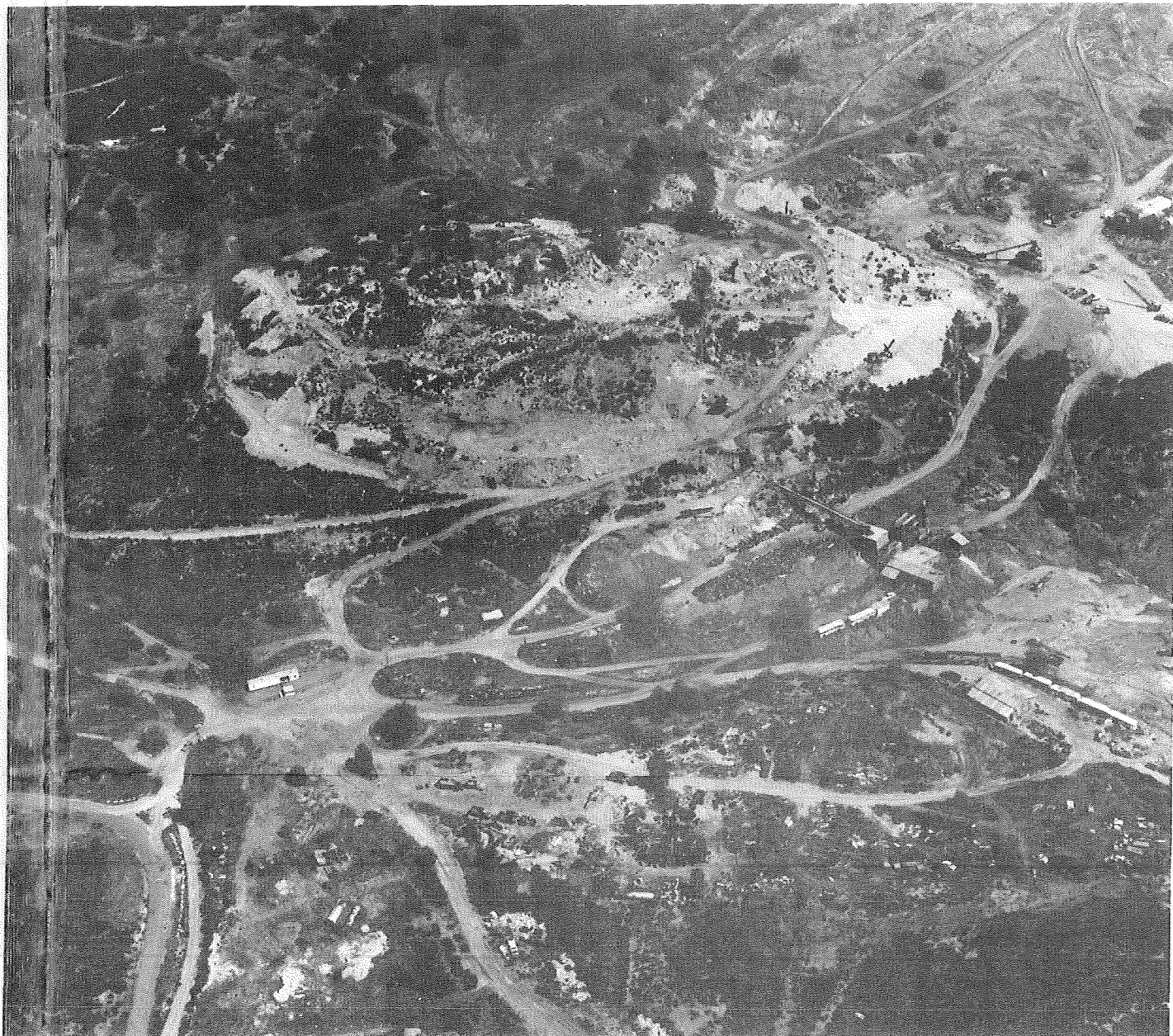
Non-members - \$US40.00

*For shipping outside of North America, please
include \$US5.00 with cost of guidebook.*

TABLE OF CONTENTS

Itinerary	ix
OVERVIEW OF ORE DEPOSITS AND ACTIVE GEOTHERMAL SYSTEMS IN THE SONOMA AND CLEAR LAKE VOLCANIC FIELDS	
The Geysers-Clear Lake area, California: thermal waters, mineralization, volcanism, and geothermal potential J. M. Donnelly-Nolan, M. G. Burns, F. E. Goff, E. K. Peters, and J. M. Thompson	1
Thermal-volcanic evolution in the California Coast Ranges Mian Liu	26
Epithermal precious-metal and mercury deposits in the Sonoma and Clear Lake volcanic fields, California J. J. Rytuba	38
DAY ONE-Papers	
Epithermal precious metals deposits of the Calistoga mining district Napa County, California, D. A. Enderlin	52
Relation of hot-spring gold mineralization to silica-carbonate mercury mineralization in the Coast Ranges, California W. J. Pickthorn	77
Silica carbonate alteration of serpentinite, implications for the association of precious metal and mercury mineralization in the Coast Ranges R. L. Sherlock, M. Amelia V. Logan, and E. Craig Jowett	90
DAY ONE-Road Logs	
The Sonoma volcanic field and associated gold and mercury deposits: road log J. J. Rytuba, D. A. Enderlin and R. J. McLaughlin	117
DAY TWO-Papers	
Geothermal setting of The Geysers steam field, northern California R. O. Fournier	124
Preliminary report on $^{40}\text{Ar}/^{39}\text{Ar}$ incremental heating experiments on feldspar samples from the felsite unit, Geysers Geothermal Field, California G. B. Dalrymple	131
The geysers felsite and associated geothermal systems, alteration, mineralization, and hydrocarbon occurrences J. B. Hulen and M. A. Walters	141
DAY TWO-Road Logs	
The Geysers geothermal area and mercury deposits in the Clear Lake volcanic field: Road log J. J. Rytuba, J. M. Donnelly-Nolan, and R. J. McLaughlin	153

DAY THREE-Papers	
The origin and significance of high-grade metamorphic xenoliths, Clear Lake Volcanics, California Jim Stimac	171
Chemical and isotopic constituents in the hot springs along Sulphur Creek, Colusa County, California J. M. Thompson	190
Gas geochemistry and guide for geothermal features in the Clear Lake Region, California F. Goff and Cathy Janik	207
Gold and mercury deposits in the Sulphur Creek District, California G. C. Nelson, J. J. Rytuba, R. J. McLaughlin, and R. M. Tosdal	262
DAY THREE-Road Logs	
Hot springs and deposits of mercury and gold in the Clear Lake volcanic field: Road log J. J. Rytuba, J. M. Donnelly-Nolan, and R. J. McLaughlin	270
DAY FOUR-Papers	
Regional geophysical setting of gold deposits in the Clear Lake region, California A. Griscom, R. C. Jachens, P. F. Halvorson, and R. J. Blakely	289
Overview of the McLaughlin precious metal mine, Napa and Yolo Counties, Northern California R. M. Tosdal, D. A. Enderlin, G. C. Nelson, and N. J. Lehrman	312
The genesis of the McLaughlin Mine sheeted vein complex, fluid inclusion and stable isotope evidence R. L. Sherlock	330
DAY FOUR-Road Logs	
McLaughlin gold and Knoxville mercury deposits: Road log J. J. Rytuba, D. A. Enderlin, R. J. McLaughlin, and J. M. Donnelly-Nolan	350



FRONTISPIECE

Aerial view of the Manhattan Mercury Mine prior to development of the McLaughlin gold deposit by Homestake Mining Company. The oval hill with numerous cuts and mine workings is the San Quentin hot-spring sinter that hosted the cinnabar ore body (note steam shovel on the right side of the sinter). The sinter was about 35 m thick and 130 m in maximum width and displayed many features typically found in active hot springs. The area of the sinter is now an open pit developed to mine the south orebody but large samples of the sinter have been preserved by Homestake Mining Company in a museum just outside the mine area. The sheeted vein complex was located directly beneath the sinter and contained 721,000 ounces of gold, about 25% of the gold within the McLaughlin deposit, in an area of about 60 meters by 60 meters in width over a vertical interval of 130 meters (Lehrman, 1986). Several mercury deposits have been mined in the Clear Lake volcanic field but only the Manhattan Mercury Mine has been developed into an economic epithermal gold deposit. In contrast to the development of the McLaughlin Mine, the Sulphur Bank Mercury Mine, the largest mercury deposit in the Clear Lake volcanic field, is presently inactive and has been declared an Environmental Protection Agency Superfund Site.

[photo courtesy of Homestake Mining Company]

INTRODUCTION

James J. Rytuba

U. S. Geological Survey, 345 Middlefield Road, Menlo Park, CA 94025

Since the discovery of gold and silver in the northern part of the Napa Valley in 1858, ore deposits and geothermal systems have drawn a variety of geologists to study one of the few areas in the United States where hot springs are actively depositing gold and mercury. The geothermal systems and very young precious-metal and mercury deposits occur in two adjacent volcanic fields, the older Sonoma volcanic field and the younger Clear Lake volcanic field. In the eastern foothills of the Napa Valley, precious metal deposits hosted by the Sonoma volcanic field produced only a small amount of gold and silver. The fertile soil and good drainage of the volcanic rocks in this area gave way to vineyards and wineries and the mines were closed and abandoned. The younger Clear Lake volcanic field has gone through several cycles of mineral and geothermal development. The hot springs in the volcanic field were developed initially for their supposed medicinal benefits although many of the springs contained toxic levels of mercury. Mercury and sulfur were mined from several of the deposits present throughout the volcanic field and spectacular samples containing plumes of native gold within cobbles of cinnabar were discovered in the Sulphur Creek District. In spite of the known association of gold and mercury, mercury mining dominated the mineral development within the volcanic field until the mid-1940's. Development of The Geysers for geothermal power in 1960 began a new phase of economic development, and geothermal power production has continued to be important in the western part of the volcanic field. The most recent mineral development was the discovery of the McLaughlin gold deposit in 1978 at the site of the old Manhattan Mercury Mine. Since that time exploration has continued for additional epithermal precious-metal deposits but without success.

This guidebook provides an overview of the geothermal systems and ore deposits in the Sonoma and Clear Lake volcanic fields. Several research papers in this guidebook provide important new concepts and data on the ore deposits, geothermal systems, and volcanic rocks within the two volcanic fields from the perspective of geologists, geochemists, geophysicists, and petrologists. In addition, a paper by Fraser Goff and Cathy Janik provides the first comprehensive field guide to the geothermal features within the Clear Lake volcanic field. This field conference and guidebook should provide the basis for new research and a better understanding of the processes that have contributed to the formation of the ore deposits and geothermal systems in the Clear Lake and Sonoma volcanic fields.

ACKNOWLEDGMENTS

Over the past two decades a large number of geologist, geochemists, and geophysicists have studied the geology and geothermal systems within the Sonoma and Clear Lake volcanic fields. A large number of research papers have been published in the past and many of these have been landmark papers in the development of our concepts in geothermal systems, epithermal ore deposits, and volcanism in the Coast Ranges. The present volume contains twenty new publications which summarize past work and present important new concepts in the geophysics, geochemistry, and geology of the volcanic and hydrothermal systems in the Clear Lake and Sonoma volcanic fields. The editor wishes to acknowledge the large amount of work that has gone into each of these papers and the consistently high quality of the presentations. In particular, the paper by Fraser Goff and Cathy Janik provides important information on the gas geochemistry of springs in the Clear Lake region as well as the first comprehensive field guide to geothermal features in the Clear Lake volcanic field. Although this field trip does not have time to visit all the springs described in their field guide, the guide is exceptionally well organized and a valuable resource for geologists who wish to visit these features in the future. Special recognition also goes to Ross Sherlock for providing two papers to this volume and which advance our understanding of the McLaughlin gold deposit and silica-carbonate mercury deposits.

Many reviewers provided high quality reviews in the face of very short deadlines and these significantly improved the manuscripts in this volume. Richard Tosdal and William Pickthorn significantly helped the production of this volume by providing two excellent papers that required no additional reformatting or editing.

The staff of Homestake Mining Company has been particularly helpful in preparation of the field trip and providing comprehensive papers on the McLaughlin gold deposit and new data on the Cherry Hill deposit. Special thanks go to Dean Enderlin of the McLaughlin Mine Staff for his help in planning for the field trip and providing the first comprehensive paper on epithermal precious metal deposits in the Sonoma volcanic field. Gordon Nelson of the McLaughlin Mine Staff was instrumental in preparing the field trip to the gold and mercury deposits in the Sulphur Creek district.

The editor wishes to thank his co-authors of the field trip guides for their contributions, suggestions, and help in providing new ideas on the geology and structure of this area.

Finally, thanks go to Ana Barrales, Susan Garcia, and Diana Mangin for providing help on short notice and helpful suggestions at the various stages of development of this guidebook.

NOTES

[reprinted with permission from Donnelly-Nolan, J.M., Burns, M.G., Goff, F.E., Peters, E.K., and Thompson, J.M., 1993, *Economic Geology*, v. 88, p. 301-316.]

**THE GEYSERS-CLEAR LAKE AREA, CA: THERMAL WATERS, MINERALIZATION,
VOLCANISM, AND GEOTHERMAL POTENTIAL**

**J. M. Donnelly-Nolan¹, M. G. Burns^{1,2}, F. E. Goff³,
E. K. Peters⁴, and J. M. Thompson¹**

¹U.S. Geological Survey, 345 Middlefield Road, Menlo Park CA 94025

²Harding Lawson Associates, 303 Second Street, San Francisco CA 94107

³Los Alamos National Laboratory, Los Alamos, NM 87545

⁴Geology Dept., Washington State University, Pullman WA 99164

ABSTRACT

Manifestations of a major thermal anomaly in the Geysers-Clear Lake area of northern California include the late Pliocene to Holocene Clear Lake Volcanics, The Geysers geothermal field, abundant thermal springs, and epithermal mercury and gold mineralization. The epithermal mineralization and thermal springs typically occur along high-angle faults within the broad San Andreas transform fault system that forms the western boundary of the North American plate in this area. The young volcanic rocks overlie Mesozoic marine rocks of the Great Valley sequence which have been thrust above the coeval Franciscan Complex and penecontemporaneously dropped back down along low-angle detachment faults.

Many of the waters of the region are non-meteoric as defined by their isotopic signature. One type of isotopically shifted water emerges from or near Great Valley sequence rocks and is the most chloride rich. It is interpreted to be evolved connate in origin. A second type, evolved meteoric water has moderate chloride contents, high boron contents, and high B/Cl ratios and is found locally in Franciscan rocks, notably at the Sulphur Bank mercury mine where it probably results from near-closed-system, repeated boiling of meteoric water in host rocks that also contribute organic components to the water. At the Sulphur Bank mine fracturing of otherwise impermeable Franciscan rocks by faulting has created a localized zone of permeability in which thermal water boils repeatedly with limited venting to the surface. Boron-rich fluids were apparently present at depth in The Geysers when intrusion of silicic magma occurred because the concealed intrusion of felsite is surrounded by a halo of tourmaline-bearing hornfels. The volume of this poorly dated early to middle Quaternary intrusive body probably exceeds the 100 km³ of erupted Clear Lake Volcanics. Similar intrusions may have occurred in the eastern part of the area at Wilbur Springs and the McLaughlin mine, where gold deposition and evidence of hydrothermal phenomena suggest more magmatic activity than is indicated by small exposed bodies of early Quaternary basaltic lava. The Clear Lake Volcanics are the present locus of volcanism in the northern Coast Ranges and other volcanic

centers are progressively older to the south. Geophysical data suggest that a large silicic magma body may be centered north of The Geysers steam field providing the heat for the geothermal field.

Geothermal power production has peaked at The Geysers and pressure declines indicate significant depletion of the fluid resource. The vapor-dominated field evolved from a pre-existing hydrothermal system within fractured, otherwise impermeable Franciscan metamorphic rocks. A deep water table of saline fluid has been postulated to be present under the steam field, but no chloride-rich water has been found at drillable depth. We propose that recently discovered, isotopically shifted steam in the northwest Geysers area indicates the presence not of deep connate water but rather of boiled-down, boron-rich Franciscan evolved meteoric water. This water is likely to be present in limited quantities and will not provide a significant hot water resource for geothermal power production at The Geysers or from the main Clear Lake volcanic field.

INTRODUCTION

The Geysers-Clear Lake area is located in the northern California Coast Ranges about 150 km north of San Francisco and about 50 km from the trace of the San Andreas fault (Fig. 1). In this area, rocks of the Coast Range ophiolite and the Mesozoic Great Valley sequence are thrust above the coeval Franciscan Complex and, in turn, this Mesozoic section is attenuated by numerous penecontemporaneous low-angle extensional faults (Jayko et al., 1987). These Mesozoic rocks are depositionally overlain by marine and nonmarine rocks of early Tertiary age and younger, and by the late Pliocene to Holocene Clear Lake Volcanics. The region is cut by many northwest- to north-trending faults with normal, strike-slip, and reverse components of movement. These faults are part of the broad San Andreas transform fault system separating the North American and Pacific plates. Subduction appears to have ended at the latitude of Clear Lake at about 3 Ma (McLaughlin, 1981), a million years prior to the inception of volcanism which was initially widespread, but in the past million years has focused near Clear Lake. There are numerous manifestations of a major thermal anomaly in the area, and geophysical data suggest the presence of a large silicic magma body under the main Clear Lake volcanic field. Numerous mercury deposits have been exploited and disseminated gold is currently being mined at the McLaughlin deposit. The area is famous for its thermal and mineral springs which display unusual chemical compositions. Geothermal power production is entirely from steam in The Geysers vapor-dominated field, which is located on the southwest margin of the volcanic field where drilling has identified a large concealed silicic intrusive body. The steam field is the largest power-producing geothermal field in the world, but in recent years production has declined. The boiling water table which earlier workers hypothesized to underlie the vapor-dominated zone (White et al., 1971) has remained elusive. This paper presents an overview of the Geysers-Clear Lake thermal anomaly, offers hypotheses to explain the chemical and isotopic variations in thermal waters of the region, and argues that significant volumes of water as a separate water-dominated reservoir are unlikely to be found in Franciscan rocks under the Clear Lake volcanic field or in The Geysers steam field.

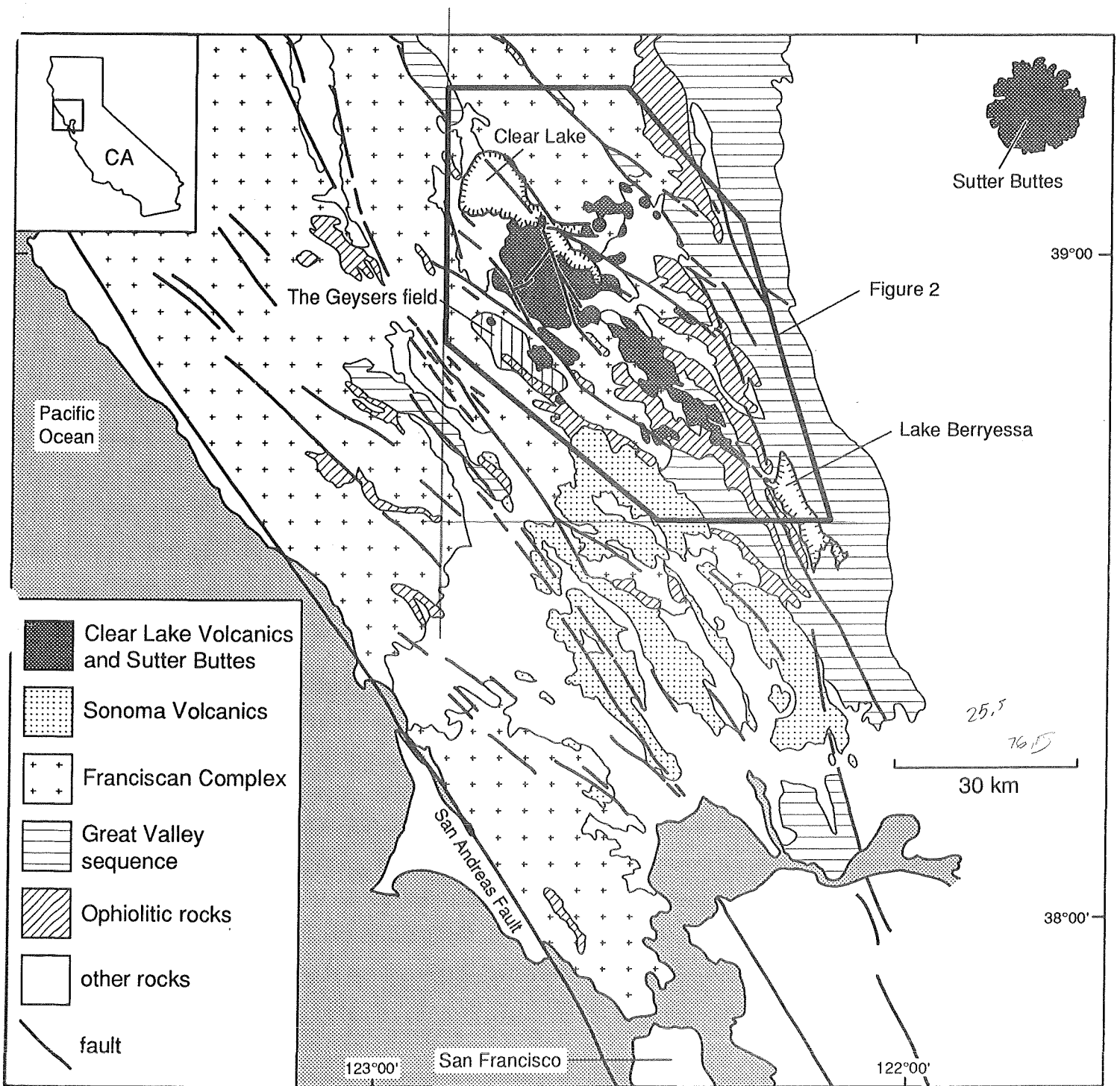


FIGURE 1. Location map of the Geysers-Clear Lake area, northern California, with generalized geology. Geology is adapted from Jennings and Strand (1960) and Wagner and Bortugno (1982). Only major high-angle faults are shown; contact between Franciscan Complex and Great Valley sequence is a low-angle fault.

GEOLOGIC AND TECTONIC SETTING

Bedrock geology

The Geysers-Clear Lake area is geologically complex with the Clear Lake volcanic field overlying the contact between Mesozoic rocks of the Franciscan subduction complex and the overthrust Coast Range ophiolite and time-equivalent fore-arc rocks of the Great Valley sequence (Figs. 1 and 2). These great formations consist largely of turbidite sequences deposited on oceanic basements in marine settings and later deformed at an obliquely convergent subduction margin (McLaughlin, 1981; McLaughlin and Ohlin, 1984). The terrigenous sedimentary rocks of the Franciscan Complex are grossly similar in lithology to Great Valley sequence rocks but differ in their petrography (Jayko and Blake, 1984). Franciscan rocks are also different in being highly deformed into numerous melanges and tectonostratigraphic terrane, and in containing high-pressure, low-temperature metamorphic rocks (McLaughlin and Ohlin, 1984). Most Franciscan rocks have been metamorphosed to laumontite, prehnite-pumpellyite, and/or lawsonite grade, whereas Great Valley sequence rocks are weakly metamorphosed to laumontite grade (Blake et al., 1988). The Great Valley sequence generally thickens rapidly to the east. Cutting across the area are large elongate bodies of serpentinite and associated ophiolitic rocks, particularly along northwest-trending faults related to the San Andreas transform fault system. Geologic mapping studies of Franciscan rocks in this area include those by Brice (1953), McNitt (1968a,b), Brice (1953), Swe and Dickinson (1970), Rich (1971), McLaughlin (1978), and McLaughlin et al. (1989).

Clear Lake Volcanics

The Clear Lake Volcanics are the northernmost and youngest of several Cenozoic volcanic fields that are progressively older to the south in the California Coast Ranges. Early geologic studies of the Clear Lake Volcanics include those of Anderson (1936), and Brice (1953). Subsequent work by Hearn et al. (1976, 1981) and Donnelly-Nolan et al. (1981) has shown that the Clear Lake Volcanics date from 2.1 Ma to about 10 ka and have an estimated erupted volume of 100 km³. Silicic lavas dominate and basalts are rare. The most voluminous rock type in the volcanic field is rhyodacite. No ash flow tuffs have been recognized. Volcanism has moved progressively northward within the volcanic field following an early phase when predominantly basaltic andesite lava erupted over a wide area (Fig. 3 and Hearn et al., 1981). Since about 1 Ma, volcanism has been localized south and east of Clear Lake, a long-lived lake that occupies a volcano-tectonic basin (Hearn et al., 1988; Sims et al., 1988).

Tectonic setting

Tectonic activity has controlled not only basin development, but also alignments of vents within the Clear Lake volcanic field (Hearn et al., 1988). Seismic evidence (Bufe et al., 1981; Oppenheimer, 1986) indicates that the Geysers-Clear Lake area is currently under extension. The extension is generated within the North American plate, between faults of the broad San Andreas transform fault system. The Geysers-Clear Lake area is apparently a pull-apart basin similar to those described by Crowell (1974; and see McLaughlin and Nilsen, 1982; Hearn et al., 1988).

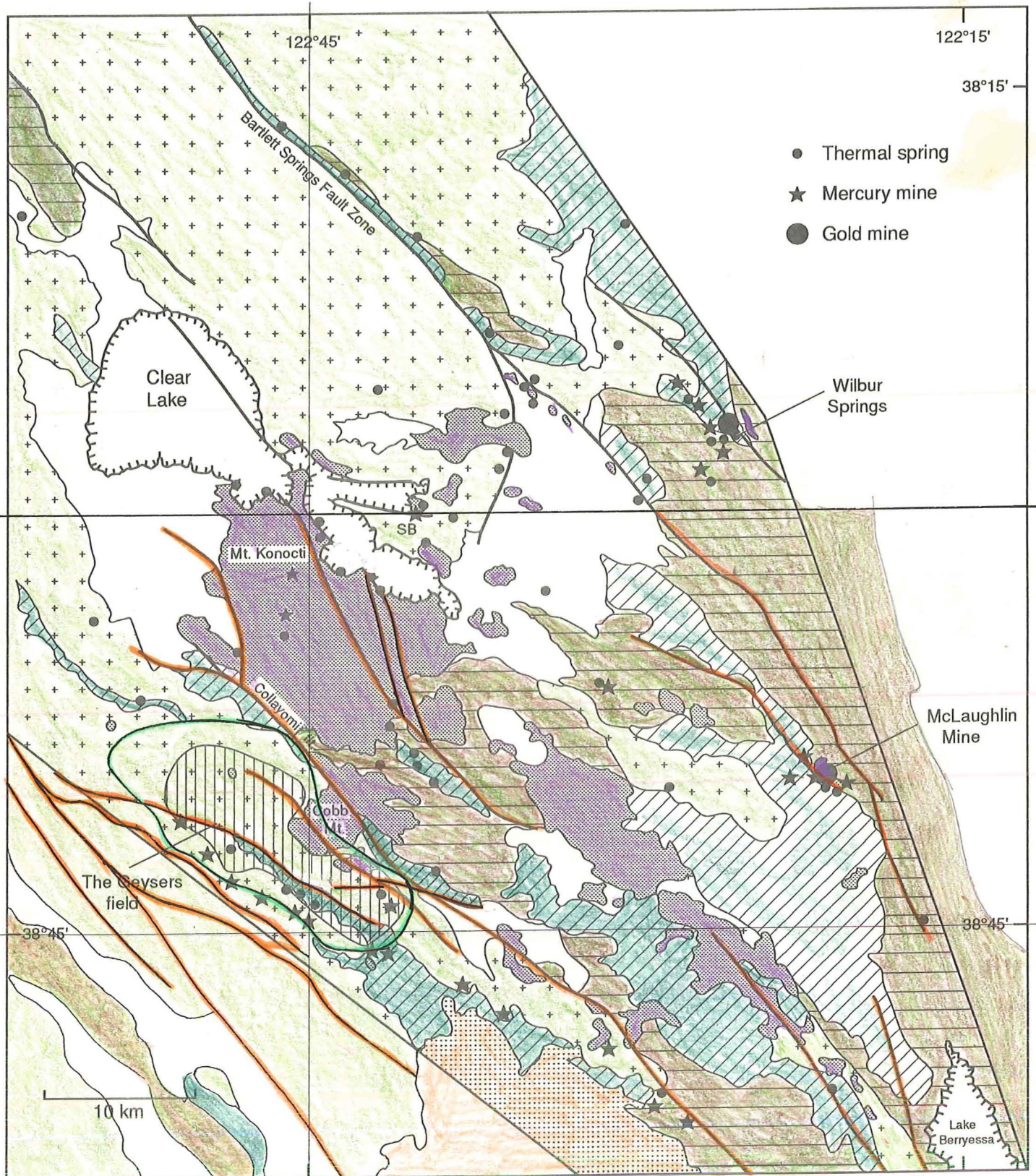


FIGURE 2. Enlarged geologic map of the Geysers-Clear Lake area. Patterns same as Figure 1, except that Clear Lake Volcanics are shown with a slightly lighter shade of gray. SB = Sulphur Bank mine.

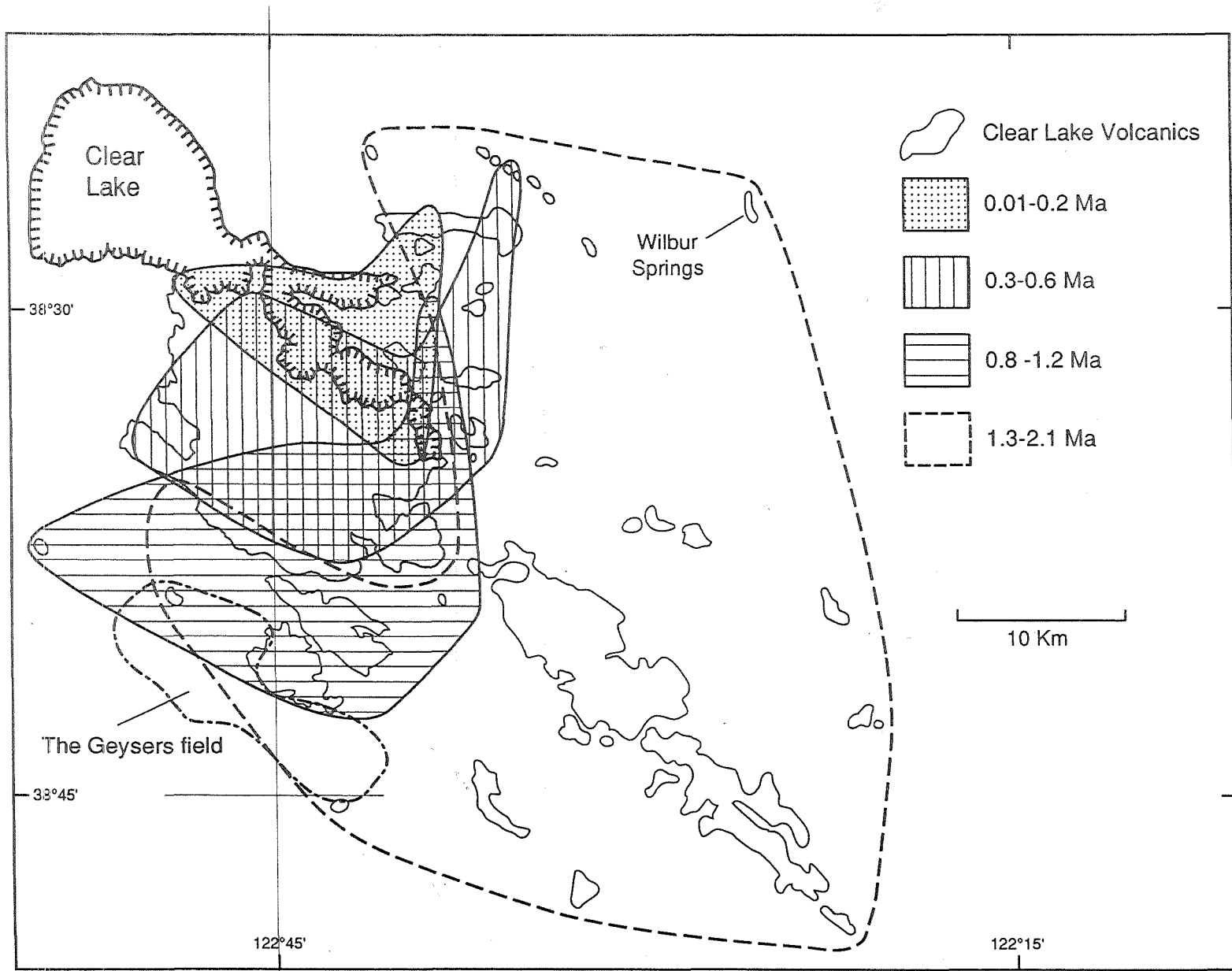


FIGURE 3. Distribution of Clear Lake volcanism. Areal limits of four periods of extrusive volcanic activity shown by patterns.

Subduction ceased off the coast of North America at the latitude of Clear Lake at about 3 Ma as the San Andreas transform fault propagated northward behind the Mendocino triple junction, leaving a "slab window" (Dickinson and Snyder, 1979) of asthenosphere under the Geysers-Clear Lake area. Primitive basaltic melts from the mantle, however, have rarely reached the surface and instead apparently have lodged in the crust to melt and assimilate crustal materials and form the more silicic magmas that dominate the eruptive products of the Clear Lake Volcanics.

The numerous faults that cut the Geysers-Clear Lake area provide important control on surface manifestations of the thermal anomaly. Thermal springs and epithermal Hg and Au mineralization are typically located along faults.

GEOPHYSICAL DATA

A major negative Bouguer gravity anomaly (Chapman, 1966) was the first geophysical evidence for magma under the Clear Lake area. Subsequent collection and interpretation of gravity data (Chapman, 1975; Isherwood, 1976, 1981) together with recognition of large teleseismic P wave delays (Iyer et al., 1979, 1981) indicate the presence of a large silicic magma body beneath the main Clear Lake volcanic field north of The Geysers steam field. Corroborative evidence is provided by a major heat flow anomaly in which values over much of the volcanic field exceed 4 heat flow units (HFU) and exceed 12 HFU in parts of the Geysers geothermal field (Walters and Combs, 1992). A lack of deep earthquake foci under the volcanic field provides supporting evidence for the existence of a magma body at depth (Bufe et al., 1981). Because no magnetic high is associated with the gravity low, Isherwood (1976) proposed that the magma body is above its Curie point of approximately 550°C.

THERMAL AND MINERAL WATERS

The Geysers-Clear Lake area is a focus for abundant thermal springs (Fig. 2) as well as mineralized cold springs. Numerous studies of the thermal and mineral waters of the area include those by Anderson (1892), Waring (1915), Allen and Day (1927), Berkstresser (1968), White et al. (1973), Barnes et al. (1973a, b), Goff et al. (1977), Thompson et al. (1981), and Donnelly-Nolan (1983). Thermal waters are here defined as those with temperatures >19°C. The hottest spring reported within the Geysers-Clear Lake area (80.5°C) outside of The Geysers steam field was found at Sulphur Bank mine (Dickson and Tunnell, 1968). However, a deposit of siliceous sinter that existed at the Manhattan (now McLaughlin) mine prior to gold mining indicates that boiling water may have been present there in the past (White et al., 1971).

Some mineralization is directly associated with thermal springs, most notably at Sulphur Bank mine (White and Roberson, 1962; Fig. 2), but also in the Wilbur Springs district where the chloride-rich waters contain gold, silver, mercury, and antimony and are depositing as much as 12 ppm of gold in spring precipitates (Peters, 1991). Fluid inclusion data (Lehrman, 1986; Thordsen, 1988; Peters, 1991) suggest that ore-depositing fluids at the McLaughlin gold mine (Fig. 2) were similar to those found today in the Wilbur Springs district.

Previously unpublished δD and $\delta^{18}O$ values for spring and well waters collected in and near the Geysers-Clear Lake area are listed in Table 1. Based on these values, waters of the Geysers-Clear Lake area fall into two major water types: meteoric and isotopically shifted. Within each of these two groups, there is more than one subtype.

Meteoric waters

Isotopic values for meteoric waters from the Geysers-Clear Lake area fall on or near the meteoric water line (Craig, 1961; Fig. 4). Meteoric waters include cold surface meteoric waters as well as thermal waters that are warm but dilute. Thermal meteoric springs are found at contacts between units and along fault zones. These waters are spatially related to the main Clear Lake volcanic field and appear to be geothermally heated meteoric waters that have resided at depth for relatively short time periods. On the other hand, carbonated meteoric waters are typically cold and contain high concentrations of bicarbonate, and low concentrations of other dissolved species. These CO_2 -rich waters are common just east and northeast of Clear Lake, particularly along the Bartlett Springs fault zone (Fig. 2). Although the water is meteoric, the carbon dioxide is probably produced by metamorphic reactions at depth (Barnes et al., 1973b).

Isotopically shifted waters

Evaporated water: One subtype of isotopically shifted water consists of evaporated water such as Clear Lake itself or other standing bodies of water. This is surface water which has undergone isotopic fractionation of both deuterium and oxygen such that the δ values are shifted to the right of the meteoric water line and fall on a steeper slope than the values of other nonmeteoric waters of the region. Data from such waters come from localities 15, 22, 34 and 35 and are given in Table 1.

Thermal surface waters in The Geysers: Data from thermal surface waters in The Geysers geothermal field are strongly shifted to the right from the meteoric water line (Craig, 1963). Compositions of these relatively dilute waters are strongly influenced by oxidation of H_2S gas resulting in sulfate, commonly their most abundant species. These waters are a mixture of heated ground water and condensed steam and are not samples of the water that boils to produce the steam in the vapor-dominated Geysers geothermal field (White et al., 1971). The isotopic compositions of springs in The Geysers are a result of high temperature evaporation (Craig, 1963). No samples of the deep water are reported to have been recovered.

Evolved connate waters: Isotopically shifted chloride-rich waters emerge from Great Valley sequence rocks in the eastern part of the Geysers-Clear Lake area, e.g. at Wilbur Springs (Figs. 2 and 4). The chloride content in these waters generally increases from west to east as Great Valley sequence marine sandstone and shale thickens eastward. White et al. (1973) termed these "evolved connate" waters -- waters that were originally deposited as oceanic pore waters (connate water) in the marine sediments. Subsequent rock-water interaction and dilution by meteoric waters has altered their chemical and isotopic compositions, thus the term evolved connate.

Table 1. Waters in and near the Geysers-Clear Lake area

Number	Name	T°C	δ 18O	δ D	Cl	B	B/Cl	Latitude	Longitude	Ref. no.
1	Open well nr. Seigler Spgs	31	-8.67	-60.3	24	1.6	0.067	38°52.9	122°41.1	6
2	Spring nr. Perini Hill	20	-8.24	-57.6	4	<.1		38°52.7	122°41.1	14
3	Horseshoe Spring	41.5	-7.30	-54.7	78	19	0.244	38°59.6	122°44.5	15
4	Konocti Harbor Inn	35	-7.06	-53.8	48	9	0.188	38°59.2	122°44.0	17
5	Kip Neasham's well	11	-8.16	-62.5	4	<.1		38°56.6	122°43.8	20
6	Clear Lake State Park	8	-7.93	-53.8	9.8	0.6	0.061	39°01.0	122°48.4	22
7	Perini Spring	17	-8.04	-55.0	6.2	<.1		38°53.0	122°38.6	24
8	Bardole Spring	17	-7.65	-55.6	4	1	0.250	38°52.3	122°38.1	25
9	Well, Konocti Cons. Camp	25	-8.59	-59.3	10		0.000	38°54.5	122°43.4	29
10	Spring, Diener Ranch	13	-8.24	-57.8	4.8	0.2	0.042	38°54.0	122°42.8	31
11	Well at Riviera	29.5	-7.97	-59.3	42	9	0.214	38°57.7	122°43.0	35
12	Gordon Warm Spring	36	-8.52	-57.9	41	1.3	0.032	38°50.1	122°43.6	42
13	Upper Bartlett Spring	16	-8.95	-63.0	8.4	<.1		38°11.0	122°42.0	48
14	Main Bartlett Spring	18.5	-8.90	-63.5	8.4	<.1		38°11.1	122°42.1	49
15	Upper Crabtree Spring	36	-1.90	-30.8	9.8	0.1	0.010	39°17.4	122°49.3	50
16	Main Crabtree Spring	41	1.75	-33.9	1240	277	0.223	39°17.5	122°49.4	51
17	Rice Fork, Eel River	25	-8.30	-61.9	9.1	0.33	0.036	39°17.3	122°49.1	52
18	Newman Spring	34.5	2.50	-29.6	3310	386	0.117	39°11.9	122°43.0	54
19	Pseudo Complexion Spring	27	-7.20	-55.0	115	<.1		39°11.9	122°30.3	55
20	Complexion Spring	19	6.25	-24.0	24100	31	0.001	39°10.2	122°31.2	56
21	Wilbur Spring	50	4.95	-22.7	9810	280	0.029	39°02.8	122°25.3	57
22	Clear Lake at C.L.Highlands	24	-2.15	-25.0	30	1.55	0.052	38°56.9	122°32.3	58
23	Grizzly Spring	20	0.55	-32.5	4210	140	0.033	39°00.1	122°29.9	59*
24	Sulphur Spring	20	-8.70	-63.2	331	18	0.054	39°05.8	122°31.4	60
25	Turkey Run Mine	22	-6.80	-53.6	1150	34.5	0.030	39°01.0	122°26.4	61
26	Jones Fountain of Life	61	6.65	-17.4	11900	271	0.023	39°02.0	122°26.7	62
27	Toby's well	24.5	-5.15	-45.9	140	4.6	0.033	39°02.1	122°25.6	63
28	Hayfield well	14.5	-7.55	-55.4	28.6	0.84	0.029	39°01.1	122°24.2	64
29	Blank Spring	44.5	2.55	-30.8	8050	158	0.020	39°01.4	122°26.0	65
30	Chalk Mountain Spring	24	-4.10	-44.4	2410	190	0.079	39°04.8	122°35.0	67
31	Cross Spring	18	-8.65	-60.3	13	0.1	0.008	39°02.5	122°35.4	68
32	Unnamed cold spring	19	-8.45	-59.9	22	<.1		39°03.2	122°35.3	69
33	Quigley Soda Spring	28	-5.30	-53.6	918	122	0.133	39°03.2	122°35.8	70
34	Herman Pit, Sulphur Bank	21	0.40	-18.6	205	395	1.927	39°00.1	122°39.8	71
35	Green Pool, Sulphur Bank	26	5.60	7.5	7	0.3	0.043	39°00.2	122°39.4	72
36	Pine Cone Spring	25.5	-7.60	-56.5	146	21.5	0.147	38°51.0	122°41.6	73
37	Spier's Spring	25.5	-6.85	-52.2	343	51.2	0.149	38°50.2	122°39.2	74

Table 1. Waters in and near the Geysers-Clear Lake area

38	Aetna Springs well#1	34	-7.65	-50.9	63	2.88	0.046	38°39.0	122°09.0	76
39	Aetna Springs well#2	33	-6.50	-48.6	287	80.6	0.281	38°39.0	122°09.0	77
40	Moki Beach Spring	27	-6.50	-48.6	58.6	13.5	0.230	39°01.0	122°48.1	79
41	Hog Hollow Spring	30	-8.40	-59.6	174	14.5	0.083	39°01.4	122°35.3	80
42	Unnamed Spg, Cache Fm.	22	-8.40	-59.1	27	34.5	1.278	38°57.0	122°34.3	81
43	Reid's well	25	-8.25	-58.8	136	115	0.846	38°58.2	122°38.5	82
44	Kono Tayee well	21.5	-8.15	-59.4	7.3	5.3	0.726	39°02.4	122°45.7	83
45	Howard Soda Spring	28.5	-8.40	-57.0	187	125	0.668	38°51.4	122°40.8	84
46	Holm's warm well	40	-7.05	-53.2	74	152	2.054	38°58.6	122°40.5	85
47	Zem-Zem Spring	21	-6.75	-48.9	157	8.9	0.057	38°45.3	122°17.1	86
48	Davis' Soda Spring	23	-8.50	-60.0	4	<.1		38°59.7	122°38.5	87
49	Spring in Sweet Hollow Ck.	22	-6.75	-55.1	561	49	0.087	39°01.1	122°35.0	88
50	Salt Lick Spring	24	-8.15	-56.2	419	48	0.115	39°06.0	122°36.4	89
51	Hildebrande Spring	25	-8.05	-56.1	8	<.1		38°55.5	122°46.2	90
52	Anderson Spring	42	-7.70	-48.3	4	<.1		38°46.5	122°42.4	91
53	Benmore Canyon well	21	-3.75	-45.6	4050	72.3	0.018	39°01.5	122°34.2	92
54	Magnesite Spring	20	-5.20	-49.4	1920	130	0.068	39°04.4	122°34.0	93
55	Gamer Sulfur Spring	22	-8.60	-59.6	9	0.42	0.047	39°04.7	122°41.9	94
56	Gamer's Salt Lick Spring	23	-2.85	-42.0	242	225	0.930	39°04.6	122°42.2	95
57	Gamer Cold Spring	16	-8.50	-58.5	5	0.1	0.020	39°05.0	122°41.8	96
58	Calistoga Geyser	100	-7.95	-52.4	206	12	0.058	38°36.0	122°36.0	97
59	Highway 20 Sulfur Spring	23	-6.55	-55.9	2080	41.5	0.020	39°01.0	122°29.4	98
60	Elgin Mine	54	6.55	-16.3	12100	220	0.018	39°03.5	122°28.5	99
61	Hough Spring	16	-9.20	-63.6	5	0.27	0.054	39°09.7	122°36.8	100
62	Allen Chalybeate Spring	20	-7.30	-59.1	481	41	0.085	39°09.6	122°39.9	101
63	Royal Spring	18	-8.30	-59.8	300	28	0.093	39°13.8	122°44.7	102
64	Riviera Beach Spring	34	-7.60	-53.9	31	13	0.419	38°57.5	122°42.2	103
65	Little Geysers	99	3.00	-22.8	3	0.1	0.033	38°46.0	122°44.9	104
66	Honeycutt well #2	49	-8.20	-57.5	101	16.3	0.161	38°56.4	122°43.8	105
67	Bennett's well	46	-8.35	-57.4	96	18	0.188	38°56.5	122°46.1	106

Notes:

Ref. no. is from Thompson et al. (1981)

Cl and B values in mg/l; isotopic values relative to SMOW.

* Cl and B data from a subsequent analyzed sample CLW-82-1 (J.M. Thompson, analyst); isotope data determined on a split of original sample

Isotope analyses performed at USGS, Menlo Park (oxygen by N. Nehring; deuterium by L. D. White), except #17, 19, 22, 27, 28, 31, 44, 51, 55, 57, 61 analyzed by L. Merlivat at Centre D'Etudes Nucleaires de Saclay, France

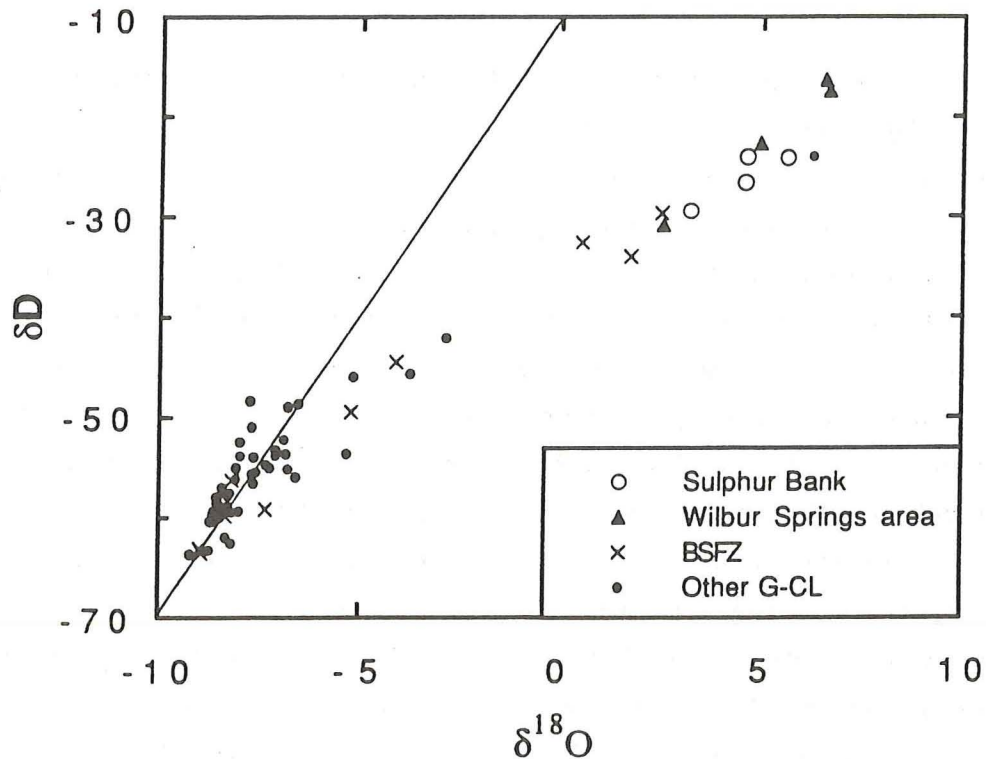


FIGURE 4. δD vs. $\delta^{18}O$ for waters of the Geysers-Clear Lake area. Data from Table 1 plus Sulphur Bank analyses from White et al. (1973). Strongly evaporated waters are not plotted (#15, 22, 34, 35, 65 in Table 1). Line is the meteoric water line of Craig (1961). BSFZ = Bartlett Springs fault zone; G-CL = the Geysers-Clear Lake area.

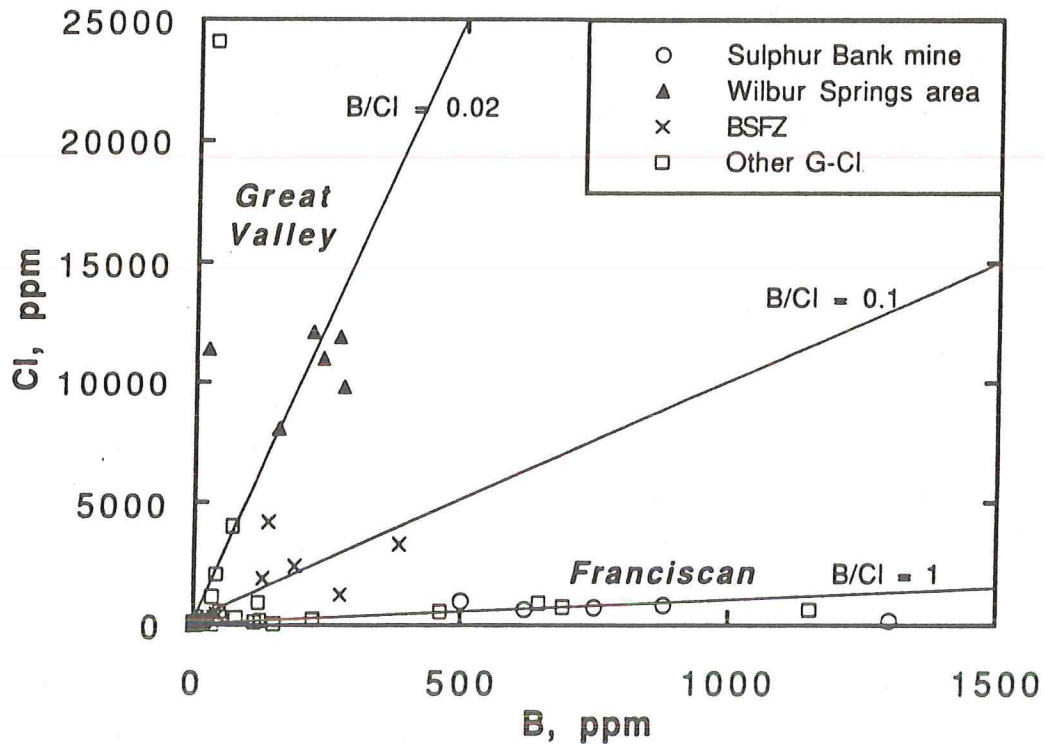


FIGURE 5. Boron vs. chloride for waters of the Geysers-Clear Lake area. Most of the data are from Table 1. Other data sources are White and Roberson (1962), Berkstresser, 1968, White et al. (1973), and Beall (1985). Lines of $B/Cl = 1, 0.1,$ and 0.02 are shown for comparison. Abbreviations same as Figure 4.

Evolved meteoric waters: Westward from Wilbur Springs, the salinity of emerging springs decreases. White et al. (1973) attributed this to the increasing role of "metamorphic water". White (1957, p. 1662) defined metamorphic water as "water that is or that has been associated with rocks during their metamorphism Metamorphic water is probably derived largely from hydrous minerals during recrystallization to anhydrous minerals." White et al. (1973) suggested that thermal waters at and near Sulphur Bank mine are metamorphic based on their high B/Cl and HCO₃/Cl ratios and their non-meteoric isotopic signature. These waters do not fit a simple model of dilution of evolved connate water nor do they emerge from Great Valley sequence rocks. Instead, they are associated with more highly metamorphosed Franciscan rocks. An example of this evolved meteoric water or "Franciscan water" is listed in Table 2, along with representative analyses of other water types.

Thermal and mineral waters of the Bartlett Springs fault zone

The Bartlett Springs fault zone (BSFZ) northeast of Clear Lake (Fig. 2) displays right-lateral strike-slip offset and is part of the San Andreas transform fault system. The Bartlett Springs fault zone is up to 1.5 km wide and shows a northwestward translation of fragments of Great Valley sequence and ophiolitic rocks (DePolo and Ohlin, 1984; McLaughlin et al., 1989), although it mostly crosses Franciscan terrane. Thermal and mineral springs are common along the fault zone (Figs. 2 and 4). They range in temperature from cold to 41°C, in chloride content from <10 to 3,310 mg/l, and in $\delta^{18}\text{O}$ values from -9.2 to +2.5 per mil. Bartlett Spring (Table 2), is an example of carbonated meteoric water, with low chloride and low $\delta^{18}\text{O}$ values but a large amount (2,750 mg/l) of bicarbonate. The hottest spring, Crabtree Hot Spring, has a chloride content of 1,240 mg/l, which is significantly lower than some other cooler springs along the fault zone. The lack of a strong correlation between chloride content and temperature is also typical of spring waters in other parts of the Geysers-Clear Lake area. Springs with higher chloride contents along the fault zone emerge from or near Great Valley sequence rocks.

THE GEYSERS

Despite the name of the steam field, no natural geysers exist anywhere in the Geysers-Clear Lake area. The name was suggested to early explorers by the fumarolic activity and steam rising from hot springs in what later became the earliest developed part of the steam field. Numerous geothermal wells are located in an area about 30 km NW-SE by approximately 5 km northeast-southwest in rugged Coast Range terrain. Power production began in the 1960's and increased (Barker et al., 1992) to nearly 2,000 megawatts before declining in the late 1980's to about 1,500 megawatts (Kerr, 1991). Porosity within rocks of the reservoir is very low. Most permeability occurs within fractures which contain the steam (McLaughlin, 1981).

High-resolution gravity data indicated as early as 1977 that reservoir depletion was occurring because steam being withdrawn was not being replaced (Isherwood, 1977). Isherwood also noted that the gravity data precluded the existence of a deep water table and instead argued for flashing of water to steam within pores in the reservoir rock. He predicted drastic pressure decay once the boiling front had exhausted the pore water available to the highly permeable fractures. Because only 25% of the produced steam is reinjected as liquid and there are no large sources of

TABLE 2. Examples of some water types in the Geysers-Clear Lake area

Water type	Meteoric	Thermal (meteoric)	Carbonated (meteoric)	Franciscan (nonmeteoric)	Great Valley sequence (nonmeteoric)	Mixed (F+GV)
Name	Perini spring	Gordon spring	Bartlett spring	Sulphur Bank	Wilbur Spring	Newman spring
Data source	1	1	1	2	1	1
T°C	17	36	18.5	69.5	50	34.5
pH	6.5	7	7	6.8	7.9	7
SiO ₂	61	126		42	131	134
Ca	5.5	5.5	89	20	2.5	162
Mg	5.3	21	470	55	44	520
Na	7.8	54	14	1190	9200	2500
K	2.9	5.0	1.4	23	445	56.5
Li	<.01	.15	.02	4.4	8.00	20
HCO ₃	69	275	2750	3290	7040	4290
SO ₄	1	.5	9	598	390	2
Cl	6.2	41	8.4	644	9810	3310
B	<.1	1.3	<.1	620	280	386
δD	-55.0	-57.9	-63.45	-24.1	-22.65	-29.60
δ ¹⁸ O	-8.04	-8.52	-8.90	+5.62	+4.95	+2.50
Latitude	38°53.0'	38°50.1'	39°11.1'	39°00.1'	39°02.8'	39°11.9'
Longitude	122°38.6'	122°43.6'	122°42.1'	122°39.8'	122°25.3'	122°43.0'
No. in Table 1	7	12	14		21	18

Chemical components in mg/l; isotopic values determined relative to SMOW.

Data sources: 1=Thompson et al. (1981)

2=White and Roberson (1962). Chemical analysis is of Geysers Spring,
isotopic analysis of Ink Spring

F+GV indicates Franciscan plus Great Valley

water immediately available, the future of power production in The Geysers steam field is in question (Barker et al., 1992; Kerr, 1991).

The steam field is adjacent to the southwest edge of the Quaternary Clear Lake volcanic field (Fig. 2). The geothermal field includes the 1.66 Ma basalt of Caldwell Pines and wraps around the northwest, west and south sides of the 1.0-1.1 Ma rhyolite and dacite dome of Cobb Mountain (Donnelly-Nolan et al., 1981). Otherwise, the geothermal field is entirely within an area of Franciscan Complex and rocks of the Coast Range ophiolite that are juxtaposed along fault zones. The reservoir rock is primarily a relatively brittle graywacke unit that is broken by fractures that can transmit the steam. To the northeast and southwest, respectively, are the major northwest-trending Collayomi and Mercuryville faults that appear to act as boundaries to the vapor-dominated system (McLaughlin,

1981). The steam field lies in an extensional environment with the least principal stress oriented at 105° (Oppenheimer, 1986), the same direction as the regional stress field that encompasses the Clear Lake Volcanics.

Geothermal drilling has revealed a large silicic intrusive body known as "the felsite" which reaches to within about 1 km of the surface south of Cobb Mountain (Thompson, 1992). The felsite has been K-Ar dated at 2.7-0.9 Ma (Schriener and Suemnicht, 1981; Thompson, 1991). Intrusive bodies identified in the subsurface near Cobb Mountain may be related to the main body and are Ar/Ar dated at 0.57 Ma (Pulka, 1991). However, recent $^{40}\text{Ar}/^{39}\text{Ar}$ age spectrum dating of four samples of the felsite indicates a minimum crystallization age of 1.3 - 1.4 Ma (Dalrymple, 1992), in accord with the age distribution of Clear Lake Volcanics shown in Figure 3. Volume estimates based on the contour map of the felsite indicate that the intrusive body is probably larger than the erupted volume of the volcanic field, which is estimated at 100 km³ (Donnelly-Nolan et al., 1981). Steam production seems to be related to the distribution of the felsite, such that the shallowest steam is near the shallowest reports of felsite (Hebein, 1986). Heat flow contours in The Geysers field also mimic the shape and location of the felsite body (Walters and Combs, 1992). Intrusion of the felsite was responsible for fracturing the adjacent brittle graywacke (McLaughlin et al, 1983; Sternfeld, 1989) and McLaughlin et al. (1983) reported evidence for multiple episodes of intrusion. The felsite is surrounded by an alteration halo of tourmaline-bearing hornfels (McLaughlin et al., 1983).

Studies of hydrothermal mineralogy in drill cores and cuttings indicate that a hot water system existed in The Geysers field prior to the current vapor-dominated system (Lambert, 1976; Sternfeld, 1981; Sternfeld and Elders, 1982; McLaughlin et al., 1983; Moore et al., 1989). K-Ar dating of adularia deposited in veins by the preexisting hot water system yielded an age of 0.69 Ma (McLaughlin et al., 1983). Estimated temperatures of the hot water system reach about 350°C based on fluid inclusion studies (Moore, in press) and vein mineralogy (McLaughlin et al., 1983), although most of the steam in The Geysers field possesses a uniform temperature of 240°C. Deuterium and oxygen isotopic studies of vein mineral assemblages indicate that the hot water system began with abundant meteoric water (Lambert, 1976; Sternfeld, 1981), although fluid inclusion studies by Moore (in press) indicate an early phase of high-temperature, high-salinity water related to the felsite intrusion.

No high chloride content springs are present in or near the steam field, although unusually high contents of chloride (to 120 ppm) (Haizlip and Truesdell, 1988) have been found in superheated steam with temperatures approaching 350°C (Walters et al., 1992). These findings for steam discovered in the northwestern part of The Geysers field in the 1980's, together with $\delta^{18}\text{O}$ values as high as 3 per mil, aroused speculation that this steam was boiling off a deep water table of connate water similar to water at Wilbur Springs (Haizlip, 1985; Haizlip and Truesdell, 1992; Walters et al., 1992; Truesdell et al., 1992).

MINERALIZATION

The Geysers-Clear Lake area has been one of the most productive in the United States for mercury, primarily from the Wilbur Springs, Knoxville, and Mayacmas districts and Sulphur Bank mine, although no mercury is currently being produced. More than a century ago Becker (1888) noted the strong correspondence

between the mercury ore deposits, thermal springs, and volcanism. He also doubted that mercury deposits would be found north of Clear Lake because of the lack of volcanic phenomena between Clear Lake and Mt. Shasta. A century later, no mercury deposits are known in the Coast Ranges north of Clear Lake.

Gold was mined in the late 1800's at the Clyde and Manzanita mines in the Wilbur Springs district (Watts, 1893), although the district is best known for its mercury mines. The mineralization occurs in rocks of the Great Valley sequence and the Coast Range ophiolite at the eastern edge of the Geysers-Clear Lake area, adjacent to a basaltic dike of Clear Lake Volcanics that is K-Ar dated at 1.66 Ma (McLaughlin et al., 1989). Gold and mercury mineralization occurs in rocks of the Great Valley sequence and the Coast Range ophiolite. Farther south, also at the eastern edge of the Geysers-Clear Lake area and at the fault contact between Great Valley sequence rocks and the Coast Range ophiolite, is the McLaughlin gold mine, a disseminated gold deposit discovered at the site of the former Manhattan mercury mine in the Knoxville district. Mineralization at the Manhattan-McLaughlin deposit is located in and adjacent to basaltic lava (Averitt, 1945; Lehrman, 1986) now dated at 2.2 Ma in age (Lehrman, 1986). Siliceous sinter deposits at the heart of the gold mineralization indicate that mineralization is related to former hot springs; only relatively cool mineralized springs now emerge in the district (e.g. Berkstresser, 1968).

No free gold has been found in the Mayacmas district which extends southeast from The Geysers for about 40 km and is located in rocks of the Franciscan Complex and the Coast Range ophiolite. Bailey (1946) and Yates and Hilpert (1946) recognized the strong association between quicksilver ore bodies and faults, particularly the northwest-trending faults that dominate the structural grain. The district follows the regional structural grain and is defined by a linear array of mercury deposits. Bailey (1946) pointed out the association between ore deposits, hydrothermal activity in The Geysers, and magma at depth. In The Geysers area, most of the mercury deposits lie outside and to the south and west of the producing steam field. Walters et al. (1992) suggested that this "halo" may have formed around the hydrothermal system that pre-dated the present vapor-dominated reservoir. Many of the deposits, particularly in the eastern Mayacmas district, are directly associated with outcrops of early Clear Lake volcanic rocks (Yates and Hilpert, 1946).

The Sulphur Bank mine was described by White and Roberson (1962, p. 397) as "the most productive mineral deposit in the world that is clearly related to hot springs." The mine is located at the east end of Clear Lake in an andesite flow of the Clear Lake Volcanics and in underlying rocks of the Franciscan Complex. No volcanic vents were found during the extensive mining operations, supporting the suggestion of LeConte and Rising (1882) that the andesite flow was derived from a cinder cone to the east and that mineralization is not related to vents but rather to faulting. Sims and White (1981) reported a radiocarbon age of $44,500 \pm 800$ years from a carbonized log in possible landslide deposits under the andesite flow. They also reported the results of mercury analyses of cored lake sediments from adjacent Clear Lake, which indicate that mineralization occurred in pulses beginning about 34,000 years ago.

Gold mineralization in the Geysers-Clear Lake area appears to be confined to areas with Great Valley sequence bedrock. No free gold is reported in Franciscan rocks. It is unknown whether the Great Valley sequence itself is the source of the gold, but the limited volume of such rocks in the western part of the area and their

complete absence in The Geysers geothermal field may account for the lack of gold mineralization in the main Clear Lake volcanic field, in The Geysers steam field, and in the Mayacmas mercury district.

INTERPRETATION OF THERMAL WATER CHEMISTRY

The correlation of water chemistry and isotopic composition with geology is strong in the Geysers-Clear Lake area and provides a framework for understanding the origins of the waters. We conclude that two types of thermal waters with nearly identical strongly shifted isotopic signatures exist in the Geysers-Clear Lake area, along with numerous mixtures of these two types, as well as in mixtures with meteoric water. One type is genetically related to Great Valley sequence rocks and the other to Franciscan rocks, and we believe that the two fluids were generated by very different processes.

Evolved connate waters of the Great Valley sequence

High chloride content, isotopically shifted nonmeteoric thermal waters are relatively common in the eastern part of the area where they emerge from Great Valley sequence rocks (Fig. 2; Barnes et al., 1975). Hot saline waters emerge in the Wilbur Springs mercury district, where they have chloride contents of about 12,000 mg/l, B/Cl weight ratios about 0.02, $\delta^{18}\text{O}$ values of 5 per mil, and δD values of -22 per mil (Table 1, 21, 26, 60). They are characterized as connate waters "derived from reaction of ancient ocean waters and marine sediments" (White et al., 1973, p. 547), now being forced out of the rocks by pressures higher than hydrostatic (Unruh et al., 1992). Even more saline but cooler waters emerge from and near Great Valley sequence rocks to the north and south of Wilbur Springs (e.g. 20, Table 1; Barnes et al., 1973b). The waters are no longer identical in composition to seawater and the process by which original ocean water is converted to an evolved connate water is not a simple process of dilution by meteoric water (White et al, 1973).

To the west, attenuated Great Valley sequence is thin where it overlies the Franciscan Complex and is covered by the main Clear Lake volcanic field. Variably dilute thermal waters that have a meteoric or near-meteoritic isotopic signature emerge throughout the main volcanic field, particularly along fault zones. Goff et al. (1977) noted that chloride contents in some of these waters are noticeably higher than in others, which they interpreted as indicating the presence of a component of evolved connate water. The authors used these chloride contents to predict the distribution of Great Valley sequence bedrock under the volcanic cover.

The evolved connate waters have a chloride-rich chemical composition, shifted isotopic signature, and a clear association with Great Valley sequence rocks. Their actual present-day chemical and isotopic composition may be strongly shifted by water-rock interactions, but we do not believe that these waters had a meteoric origin. Instead, we concur with White et al. (1973) that they represent evolved ancient seawater that was deposited with the host Mesozoic marine sedimentary rocks of the Great Valley sequence.

Evolved meteoric waters of the Franciscan Complex

Waters emerging from the Franciscan Complex are less easily characterized than Great Valley sequence waters. Thermal or mineralized springs are rare in Franciscan terranes where rocks of the Great Valley sequence rocks

are lacking nearby. Notable exceptions are the waters emerging at the Sulphur Bank mine. Analyses of well waters and thermal springs (now flooded) (White and Roberson, 1962; White et al., 1973) indicate high bicarbonate (about 3,000 ppm), moderate chloride (644-830 ppm), and high boron contents (620-880 ppm), such that B/Cl is nearly 1. Concentrations of iodine, bromine, and ammonia are also significant. Beall (1985) reports chemical analyses of waters from 4 wells in and near Sulphur Bank and from the Jorgensen-1 well located about 8 km south-southwest. The 5 analyses are very similar to the analyses of Sulphur Bank hot spring water, particularly in showing high boron contents (as high as 1,300 ppm) and B/Cl weight ratios approximately equal to 1.

A plot of boron vs. chloride (Fig. 5) shows that high chloride waters typically are relatively low in boron, whereas high boron waters are low in chloride. Franciscan thermal waters plot around the line B/Cl=1; evolved connate waters plot near the line B/Cl=0.2. Newman Springs (see Table 2), which emerges along the Bartlett Springs fault zone, is probably a mixture of the two water types plus some meteoric water. Waters from other thermal springs along the fault zone are probably also mixtures.

A map of areas determined by values of the B/Cl ratio for the Geysers-Clear Lake area (Fig. 6A) displays a very different pattern than the map of Cl content (Fig. 6B). The western part of the area has B/Cl ratios significantly higher than the eastern part where Great Valley sequence rocks and evolved connate fluids dominate. The B/Cl weight ratio of the main Wilbur Spring is 0.032, in contrast to a B/Cl weight ratio at Sulphur Bank mine of 0.96 (White et al., 1973). White et al. (1971) reported B/Cl weight ratios of 6.2 and 10 from two steam condensate springs in The Geysers. Haizlip and Truesdell (1988) report analyses of steam condensates and two dilute water entries in steam wells in The Geysers field. B/Cl weight ratios in these waters are greater than 1 in most cases, although a few lower values are reported. The extensive boron metasomatism indicated by the tourmaline-bearing hornfels at the margin of the felsite intrusion within The Geysers field and the boron minerals within it suggest that high boron fluids were present at the time of intrusion.

No saline fluid emerges at the surface anywhere near The Geysers steam field, and none of the springs emerging in the geothermal field give any indication of the chemistry of deep waters in the system. Furthermore, no deep waters have been sampled by drilling. White et al. (1971) proposed that a deep boiling brine underlies the steam field. Haizlip (1985) suggested that a connate fluid similar to the water emerging at Wilbur Springs is present under the northwest part of the geothermal field based on the isotopically enriched composition of the steam. However, the source of such a water is uncertain. The only other chloride-rich connate waters in the region are derived from Great Valley sequence rocks. No Great Valley sequence rocks are known to be present in or near The Geysers geothermal field. We conclude that no chloride-rich connate water is present in the steam field and that the shifted isotopic values are a result of local rock-water interaction with originally meteoric water, as suggested by Gunderson (1992).

At the Sulphur Bank mine, the moderately saline thermal water also has a shifted isotopic signature where the $\delta^{18}\text{O}$ value is 5 per mil and the δD value is about -25 per mil, values nearly identical to those of the chloride-rich evolved connate waters at Wilbur Springs. White et al. (1973) interpreted the Sulphur Bank water as metamorphic water. Donnelly-Nolan (1983) suggested an alternative explanation of multiple Rayleigh distillation

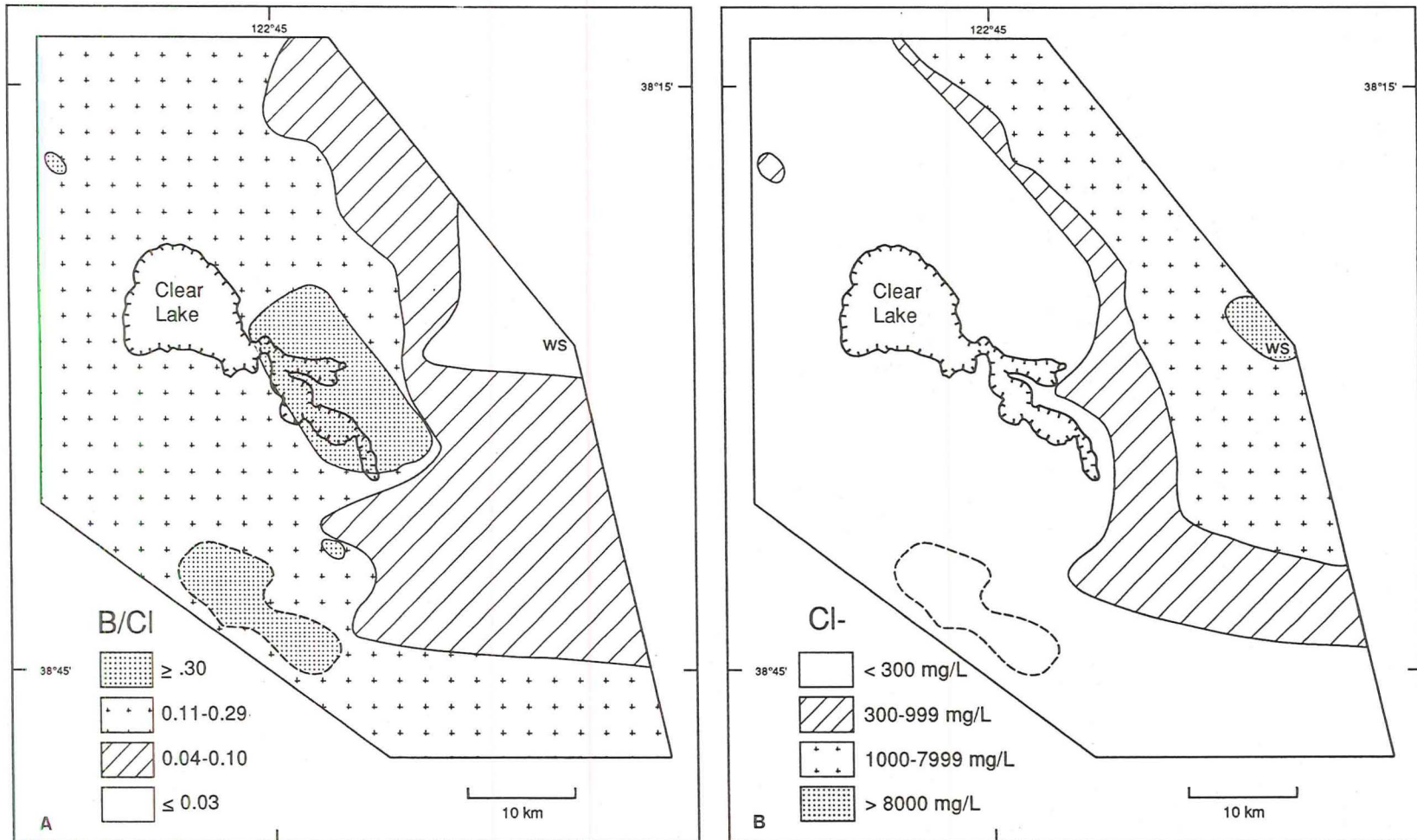


FIGURE 6. Maps showing distribution of chemical components in thermal waters of the Geysers-Clear Lake region: A. ratio of boron to chloride, B. chloride. Outline of The Geysers steam field shown by dashed line. B/Cl values for The Geysers field from Hazlip and Truesdell (1988). WS = Wilbur Springs.

by repeated boiling of a local isolated geothermal system. She further suggested that faulting might have created an isolated pocket of permeability within the otherwise relatively impermeable Franciscan rocks. Beall (1985) reported that of four geothermal exploration wells drilled in and near Sulphur Bank mine all encountered temperatures over 200°C but only one of the wells (one of two at the Sulphur Bank mine) produced a large amount of fluid. Beall (1985, p. 395) states that the productivity of the well “resulted from penetration of a steeply north plunging, pipelike zone of permeability at the intersection of three steeply dipping faults”. Waters from the four wells and an additional well drilled through Clear Lake Volcanics into underlying Franciscan rocks about 8 km south-southwest yield chloride contents of 195-990 ppm, boron contents of 500-1,300 ppm, and B/Cl weight ratios of 0.38 to 6.67. The fluids are similar in other ways to Sulphur Bank spring waters in having relatively high bicarbonate contents and, in some, high ammonia contents. In addition, the water from the Borax Lake well about 2 km south of Sulphur Bank mine has a $\delta^{18}\text{O}$ value of 5 per mil (J. J. Beall, unpublished data, 1985), the same as that for Sulphur Bank water.

Taken together, the evidence indicates that this moderate chloride, high boron, high B/Cl water is found only in Franciscan rocks, and only in localized areas. We infer that the limited occurrence of the water and its association with areas of high heat flow are evidence that it was produced by multiple boiling of an originally dilute, probably meteoric water. Limited recharge through the surrounding relatively impermeable rocks has combined with some venting at the surface to yield a more and more concentrated water. The thermal input in the Geysers-Clear Lake area from intruded magma at depth, and possibly the fracturing caused by the intrusions, has created local environments favorable to producing boiled-down, isotopically-shifted evolved meteoric water. Rock-water interaction with marine host rocks containing organic material and clays is the probable cause of the unusually high boron values, as well as elevated values of ammonia, iodine, and bromine.

Multiple near-closed-system boiling of meteoric water would produce a relatively small resultant volume of water and this may account for the scarcity of this distinctive Franciscan water as thermal springs in the region. We also propose that this same type of water is the source of the isotopically enriched fluid found in The Geysers steam field. Isotopic evidence obtained from minerals in drillcore and cuttings from The Geysers (Lambert, 1976; Sternfeld, 1981; McLaughlin et al., 1983) indicates that the system began as a hot water system dominated by meteoric water. Gunderson (1992) points out that $d^{18}\text{O}$ of steam increases with depth in the main Geysers field and that this shift is to be expected from the interaction of hot meteoric water with oxygen-rich, isotopically heavier Franciscan graywackes. Craig (1963) first pointed out this explanation for the oxygen shift. We conclude that rock-water interaction with isotopically similar host rocks is the simplest explanation for the similar isotopic values of the two chemically different waters — the Franciscan evolved meteoric water and the Great Valley sequence evolved connate water.

THERMAL INPUTS: DISTRIBUTION OF THE CLEAR LAKE VOLCANICS

The Clear Lake Volcanics erupted during four periods of time beginning at about 2 Ma (Donnelly-Nolan et al., 1981). The earliest eruptive period lasted from about 2.1 to 1.3 Ma and was by far the most widespread, with dominantly mafic lavas scattered over an area about 50 by 60 km (Fig. 3). These early lavas included basaltic eruptions in the Wilbur Springs district and at the site of the McLaughlin mine, both areas of mercury and gold mineralization. At the McLaughlin mine, there was abundant evidence of previous hot spring activity although only a small volume of basaltic lava is present. At Wilbur Springs, the volume of basaltic lava is also small and no younger lavas are present, but hot springs are actively depositing gold and mercury. A 2.9-km-deep geothermal drill hole (McLaughlin et al., 1989) did not encounter young volcanic rock, but the youthfulness and extent of mineralization, both at Wilbur Springs and at the McLaughlin mine, suggest that heat may be supplied by relatively young intrusive bodies that are similar to the one in The Geysers field but are below drillable depth.

$^{40}\text{Ar}/^{39}\text{Ar}$ dating of adularia from the Wilbur Springs district yields an age of 0.56 ± 0.14 Ma (Pearcy and Peterson, 1990). K-Ar dating of alunite at the McLaughlin mine gives 0.75 Ma (Lehrman, 1986). Adularia in a vein assemblage in drillcore from The Geysers steam field is K-Ar dated at 0.69 ± 0.03 Ma (McLaughlin et al., 1983). The similarity of these ages despite the 2-million-year time span of Clear Lake volcanism may reflect a widespread period of intrusion not reflected in the relatively limited areal extent of the second period of Clear Lake volcanism from 1.2 to 0.8 million years ago (Fig. 3). The hydrothermal systems in these three areas were apparently active during the 0.8- to 0.6-Ma time gap in eruptive volcanism. More detailed dating of The Geysers felsite intrusion may indicate whether the pause in eruptive volcanism is reflected in intrusive magmatic activity as well. The dating should also indicate whether late Pleistocene intrusions are present. If no intrusive rock younger than 0.57 Ma (Pulka, 1991) is present, then the current heat source for The Geysers geothermal field cannot be the intrusive felsite. Rejuvenation by later, deeper intrusions, as suggested by McLaughlin et al. (1983), or by structurally-controlled tapping of heat from the present magmatic heat source that is inferred to lie just to the north are likely explanations for the high heat flow at The Geysers steam field. Similarly, rejuvenation of the Wilbur Springs heat source by multiple episodes of intrusion may explain the current thermal activity.

The nearest volcanic activity contemporary with the Clear Lake Volcanics occurred at the Sutter Buttes, approximately 50 km northeast of the northeastern margin of the Clear Lake volcanic field (Fig. 1). Rhyolite and andesite domes erupted there from about 1.56 to 0.9 Ma (Hausback, 1991). It is possible that early Clear Lake basaltic magma intruded as far northeast as the Sutter Buttes. Hausback (1991) points out that inception of volcanism at the Sutter Buttes was nearly synchronous with the opening of the asthenospheric window that Dickinson and Snyder (1979) postulated to form after subduction ceased and the downgoing slab continued to sink. The Sutter Buttes may represent an outlier of the Clear Lake volcanic field. If so, other intrusive bodies may lie between Sutter Buttes and the Wilbur Springs-McLaughlin mine area, thus expanding possible sites of gold mineralization to the east.

CONCLUSIONS

Geologic and geophysical evidence indicates that a major thermal anomaly exists in the Geysers-Clear Lake area. The 2-m.y. history of volcanism and The Geysers geothermal field are the most obvious manifestations. Thermal springs and epithermal ore deposits result from the same heat source and their locations are controlled by faults of the San Andreas transform fault system in this plate margin setting.

Two types of isotopically shifted thermal waters are present in the Geysers-Clear Lake area and are strongly correlated with geology. One water is chloride rich and interpreted to be an evolved connate fluid derived from ancient seawater. It emerges at numerous locations in the eastern part of the area from weakly metamorphosed marine sandstones and shales of the Mesozoic Great Valley sequence. The other water is found in the more highly metamorphosed rocks of the coeval Franciscan Complex. It has a significantly lower chloride content but a higher boron content and B/Cl ratio. This water emerges at the surface in only a few places, most notably at the Sulphur Bank mine where the impermeable Franciscan bedrock is fractured by faulting. We conclude that the unusual water composition is produced by repeated near-closed-system boiling of meteoric water with contributions of organic material from the marine sedimentary host rocks. We propose that this evolved meteoric water is present within and boils to form the steam in The Geysers geothermal field. Because of the concentration processes that generate this water, large volumes of it are unlikely to be found as a separate exploitable phase. The long-term future of The Geysers geothermal field may depend on developing sources of surface water for recharge to the system.

The heat source for the Geysers-Clear Lake thermal anomaly is a long-lived magmatic system that powers The Geysers steam field and has controlled (together with faulting) the deposition of mercury and gold. At Wilbur Springs, both gold and mercury are depositing from evolved connate fluid. Near The Geysers, mercury deposits without gold were probably deposited from evolved meteoric fluids. Gold mineralization is focused in the eastern part of the area in Great Valley sequence rocks. The hot evolved connate fluids are known to transport gold, but whether the Great Valley sequence itself provides a source for the gold is unknown. The lack of Great Valley sequence rocks and their associated waters in the western part of the area may explain the lack of gold deposits there.

The Clear Lake Volcanics result from extension within a pull-apart basin in the San Andreas transform fault system. Extension over a slab window has allowed mantle melts to intrude the relatively thin crust and generate derivative silicic melts. Much of this silicic material never reached the surface, as documented in The Geysers. The volume of silicic intrusive rocks discovered at depth in The Geysers steam field probably exceeds the entire erupted volume of the Clear Lake volcanic field. Very likely, similar intrusive bodies exist elsewhere in the Geysers-Clear Lake area. Two possible locations are below drilled depths at Wilbur Springs and the McLaughlin gold mine where anomalously large amounts of heat are now or have in the recent past been concentrated. The widespread early basaltic phase of Clear Lake volcanism may have included basaltic intrusions parental to the Sutter Buttes, 50 km northeast of the margin of the Clear Lake Volcanics. If intrusive activity took place between the Sutter Buttes and the Wilbur Springs-McLaughlin mine area, then the possibility exists that gold mineralization could be found east of the presently recognized gold deposits.

ACKNOWLEDGEMENTS

We thank B. C. Hearn, Jr., R. J. McLaughlin, R. Gunderson, and *Economic Geology* reviewers for their comments. E.K.P. acknowledges a National Science Foundation grant EAR 8607003 to Ulrich Petersen and funding from the Homestake Mining Company. N. Nehring and L.D. White of the U.S. Geological Survey and L. Merlivat of the Centre D'Etudes Nucleaires de Saclay, France, provided isotopic analyses.

REFERENCES

- Allen, E. T., and Day, A. L., 1927, Steam wells and other thermal activity at "The Geysers", California: Carnegie Institution of Washington, Publication 378, 106 p.
- Anderson, C. A., 1936, Volcanic history of the Clear Lake area, California: *Geol. Soc. America Bull.*, v. 47, p. 629-663.
- Anderson, W., 1892, Mineral springs and health resorts of California: Bancroft and Co., San Francisco, 327 p.
- Averitt, Paul, 1945, Quicksilver deposits of the Knoxville district, Napa, Yolo, and Lake Counties, California: *Calif. Jour. Mines and Geol.*, v. 41, p. 65-89.
- Bailey, E. H., 1946, Quicksilver deposits of the western Mayacmas district, Sonoma County, California: *Calif. Jour. Mines and Geology*, v. 42, p. 199-230.
- Barker, B. J., Gulati, M. S., Bryan, M. A., and Riedel, K. L., 1992, Geysers reservoir performance: in Stone, Claudia, ed., *Monograph on The Geysers Geothermal Field: Davis, California, Geothermal Resources Council, Special Rept. No. 17*, p. 167-177.
- Barnes, I., Irwin, W. P., and Gibson, H. A., 1975, Geologic map showing springs rich in carbon dioxide or chloride in California: U. S. Geol. Survey, Water Resources Invest. Open-File Map.
- Barnes, I., Hinkle, M. E., Rapp, J. B., Heropoulos, C., and Vaughn, W. W., 1973a, Chemical composition of naturally occurring fluids in relation to mercury deposits in part of north-central California: U. S. Geol. Survey, Bulletin 1382-A, 19 p.
- Barnes, I., O'Neil, J. R., Rapp, J. B., and White, D. E., 1973b, Silica-carbonate alteration of serpentinite: Wall rock alteration in mercury deposits of the California Coast Ranges: *Econ. Geol.*, v. 68, p. 388-398.
- Beall, J. J., 1985, Exploration of a high temperature, fault localized, nonmeteoric geothermal system at the Sulphur Bank Mine, California: *Geothermal Resources Council, Transactions*, v. 9, p. 395-401.
- Becker, G. F., 1888, Geology of the quicksilver deposits of the Pacific slope: U. S. Geol. Survey Monograph 13, 486 p.
- Berkstresser, C. F., Jr., 1968, Data for springs in the northern Coast Ranges and Klamath Mountains of California: U. S. Geol. Survey Open-File Rept., 49 p.
- Blake, M. C., Jr., Jayko, A. S., McLaughlin, R.J., and Underwood, M. B., 1988, Metamorphic and tectonic evolution of the Franciscan Complex, northern California: in Ernst, W. G., ed., *Metamorphism and Crustal Evolution of the Western United States, Ruby Vol.*, v. 11, Prentice-Hall, Englewood Cliffs, New Jersey, p. 1035-1060.
- Brice, J. C., 1953, Geology of Lower Lake quadrangle, California: *Calif. Div. Mines and Geology, Bull.* 166, 72 p.
- Bufe, C. G., Marks, S. M., Lester, F. W., Ludwin, R. S., and Stickney, M. C., 1981, Seismicity of the Geysers-Clear Lake region: U. S. Geol. Survey Prof. Paper 1141, p. 129-137.
- Chapman, R. H., 1966, Gravity map of Geysers area: *Calif. Div. Mines and Geology, Mineral Information Service*, v. 19, no. 9, p. 148-149.
- Chapman, R. H., 1975, Geophysical study of the Clear Lake region, California: *Calif. Div. Mines and Geology, Spec. Rept.* 116, 23 p.
- Craig, Harmon, 1961, Isotopic variations in meteoric waters: *Science*, v. 133, p. 1305.
- Craig, Harmon, 1963, The isotopic geochemistry of water and carbon in geothermal areas: in Tongiorgi, E., ed., *Proc. Spoleto Conference on Nuclear Geology on Geothermal Areas*, p. 17-53.
- Crowell, J. C., 1974, Origin of late Cenozoic basins in southern California: *Soc. Econ. Paleontologists Mineralogists, Spec. Publ.* 22, p. 190-204.
- Dalrymple, G. B., 1992, Preliminary report on $^{40}\text{Ar}/^{39}\text{Ar}$ incremental heating experiments on feldspar samples from the felsite unit, Geysers geothermal field, California: U. S. Geol. Survey Open-File Rept. 92-407, 15 p.

- DePolo, C. M., and Ohlin, H. N., 1984, The Bartlett Springs Fault Zone: An eastern member of the California plate boundary system: *Geol. Soc. America, Abs. with Prog.*, v. 16, no. 6, p. 486.
- Dickinson, W. R., and Snyder, W. S., 1979, Geometry of subducted slabs related to San Andreas transform: *Jour. Geol.*, v. 87, p. 609-627.
- Dickson, F. W., and Tunnell, G., 1968, Mercury and antimony deposits associated with active hot springs in the western United States: *in* J. E. Ridge, ed., *Ore Deposits of the United States, 1933-1967, The Graton-Sales Volume*: New York, Am. Inst. Mining Metall. Petroleum Engineers, p. 1673-1701.
- Donnelly-Nolan, J., 1983, Diverse origins of thermal waters in the Geysers-Clear Lake geothermal area, northern California: Extended Abstracts for Fourth International Symposium on Water-Rock Interaction, Misasa, Japan, p. 123-126.
- Donnelly-Nolan, J. M., Hearn, B. C., Jr., Curtis, G. H., and Drake, R. E., 1981, Geochronology and evolution of the Clear Lake Volcanics: *U. S. Geol. Survey Prof. Paper 1141*, p. 47-60.
- Goff, F.E., Donnelly, J.M., Thompson, J.M., and Hearn, B.C., Jr., 1977, Geothermal prospecting in The Geysers-Clear Lake area, northern California: *Geology*, v. 5, p. 509-515.
- Gunderson, R. P., 1992, Distribution of oxygen isotopes and non-condensable gas in steam at The Geysers: *in* Stone, Claudia, ed., *Monograph on The Geysers Geothermal Field*: Davis, California, Geothermal Resources Council, Special Rept. No. 17, p. 133-138.
- Haizlip, J. R., 1985, Stable isotopic composition of steam from wells in the northwest Geysers, The Geysers, Sonoma County, California: *Geothermal Resources Council Transactions*, v. 9, pt. 1, p. 311-316.
- Haizlip, J. R., and Truesdell, A. H., 1988, Hydrogen chloride in superheated steam and chloride in deep brine at The Geysers geothermal field, California: *Proceedings, Thirteenth Workshop on Geothermal Reservoir Engineering*, Stanford University, Stanford, CA, January 19-21, 1988, p. 93-98.
- Haizlip, J. R., and Truesdell, A. H., 1992, Noncondensable gas and chloride are correlated in steam at The Geysers: *in* Stone, Claudia, ed., *Monograph on The Geysers Geothermal Field*: Davis, California, Geothermal Resources Council, Special Rept. No. 17, p. 139-143.
- Hausback, B. P., 1991, Eruptive history of the Sutter Buttes volcano - review, update, and tectonic considerations: *Geol. Soc. Am. Abs. with Prog.*, v. 23, no. 2, p. 34.
- Hearn, B. C., Jr., Donnelly, J. M., and Goff, F. E., 1976, Preliminary geologic map and cross-section of the Clear Lake volcanic field, Lake County, California: *U.S. Geol. Survey, Open-File Map 76-751* (scale 1:24,000).
- Hearn, B. C., Jr., Donnelly-Nolan, J. M., and Goff, F. E., 1981, The Clear Lake Volcanics: Tectonic setting and magma sources: *U. S. Geol. Survey Prof. Paper 1141*, p. 25-45.
- Hearn, B. C., Jr., McLaughlin, R. J., and Donnelly-Nolan, J. M., 1988, Tectonic framework of the Clear Lake basin, California: *Geol. Soc. America, Special Paper 214*, p. 9-20.
- Hebein, J. J., 1986, Conceptual schematic geologic cross-sections of The Geysers steam field: *Proceedings, Eleventh Workshop on Geothermal Reservoir Engineering*, Stanford University, Stanford CA, p. 251-257.
- Isherwood, W. F., 1976, Gravity and magnetic studies of The Geysers-Clear Lake geothermal region, California, U.S.A.: *Proceedings of the Second United Nations Symposium on the Development and Use of Geothermal Resources*, San Francisco, California, 20-29 May 1975, v. 2, p. 1065-1073.
- Isherwood, W. F., 1977, Reservoir depletion at The Geysers, California: *Geothermal Resources Council Transactions*, v. 1, p. 149.
- Isherwood, W. F., 1981, Geophysical overview of The Geysers: *U. S. Geol. Survey Prof. Paper 1141*, p. 83-95.
- Iyer, H. M., Oppenheimer, D. H., and Hitchcock, T., 1979, Abnormal P-wave delays in The Geysers-Clear Lake geothermal area, California: *Science*, v. 204, p. 495-497.
- Iyer, H. M., Oppenheimer, D. H., Hitchcock, T., Roloff, J. N., and Coakley, J. M., 1981, Large teleseismic P-wave delays in the Geysers-Clear Lake geothermal area: *U. S. Geol. Survey Prof. Paper 1141*, p. 97-116.
- Jayko, A. S., and Blake, M. C., Jr., 1984, Sedimentary petrology of graywacke of the Franciscan Complex in the northern San Francisco Bay area, California: *in* Blake, M. C., Jr., ed., *Franciscan geology of northern California*: *Pacific Section Soc. Econ. Paleontologists and Mineralogists*, v. 43, p. 121-134.
- Jayko, A. S., Blake, M. C., Jr., and Harms, T., 1987, Attenuation of the Coast Range ophiolite by extensional faulting, and nature of the Coast Range "thrust," California: *Tectonics*, v. 6, p. 475-488.
- Jennings, C. W., and Strand, R. G., 1960, *Geologic Map of California, Ukiah sheet*: *Calif. Div. of Mines and Geology*, 2 sheets, scale 1:250,000.
- Kerr, R. A., 1991, Geothermal tragedy of the commons: *Science*, v. 253, p. 134-135.
- Lambert, S. J., 1976, Stable isotope studies of some active hydrothermal systems: *Calif. Inst. of Technology, Ph. D. thesis*, 362 p.
- LeConte, J., and Rising, W. B., 1882, The phenomena of metalliferous vein formation now in progress at Sulphur Bank, California: *American J. Sci.*, 3rd. ser., v. 24, p. 23-33.

- Lehrman, N. J., 1986, The McLaughlin mine, Napa and Yolo counties, California: Nevada Bureau of Mines and Geology, Report 41, p. 85-89.
- McLaughlin, R. J., 1978, Preliminary geologic map and structural sections of the central Mayacmas Mountains and The Geysers steam field, Sonoma, Lake, and Mendocino Counties, California: U. S. Geological Survey Open-File Map 78-389, scale 1:24,000.
- McLaughlin, R. J., 1981, Tectonic setting of pre-Tertiary rocks and its relation to geothermal resources in the Geysers-Clear Lake area: U. S. Geol. Survey Prof. Paper 1141, p. 3-23.
- McLaughlin, R. J., and Nilsen, T. H., 1982, Neogene non-marine sedimentation and tectonics in small pull-apart basins of the San Andreas fault system, Sonoma County, California: *Sedimentology*, v. 29, p. 865-876.
- McLaughlin, R. J., Moore, D. E., Sorg, D. H., and McKee, E. H., 1983, Multiple episodes of hydrothermal circulation, thermal metamorphism, and magma injection beneath the Geysers steam field, California: *Geol. Soc. America Abs. with Programs*, v. 15, no. 5, p. 417.
- McLaughlin, R. J., and Ohlin, H. N., 1984, Tectonostratigraphic framework of the Geysers-Clear Lake region, California: *in* Blake, M. C., Jr., ed., *Franciscan geology of northern California*: Pacific Section Soc. Econ. Paleontologists and Mineralogists, v. 43, p. 221-254.
- McLaughlin, R. J., Ohlin, H. N., Thormahlen, D. J., Jones, D. L., Miller, J. W., and Blome, C. D., 1989, Geologic map and structure sections of the Little Indian Valley-Wilbur Springs geothermal area, northern Coast Ranges, California: U. S. Geol. Survey Map I-1706, scale 1:24,000.
- McNitt, J. R., 1968a, Geology of the Kelseyville Quadrangle, Sonoma, Lake, and Mendocino Counties, California: *Calif. Div. Mines and Geology, Map Sheet 9*, scale 1:62,500.
- McNitt, J. R., 1968b, Geology of the Lakeport Quadrangle, Lake County, California: *Calif. Div. Mines and Geology, Map Sheet 10*, scale 1:62,500.
- Moore, J. N., in press, Thermal and chemical evolution of The Geysers geothermal system, California: *Proceedings of 17th Workshop on Geothermal Reservoir Engineering, Stanford University, Jan. 29-31, 1992*, 6 p.
- Moore, J. N., Hulen, J. B., Lemieux, M. M., Sternfeld, J. N., and Walters, M. A., 1989, Petrographic and fluid inclusion evidence for past boiling, brecciation, and associated hydrothermal alteration above the Northwest Geysers steam field, California: *Geothermal Resources Council Transactions*, v. 13, p. 467-472.
- Oppenheimer, D. H., 1986, Extensional tectonics at The Geysers geothermal area, California: *Jour. Geophys. Research*, v. 91, p. 11,463-11,476.
- Pearcy, E. C., and Petersen, U., 1990, Mineralogy, geochemistry and alteration of the Cherry Hill, California hot-spring gold deposit: *Jour. Geochem. Exploration*, v. 36, p. 143-169.
- Peters, E.K., 1991, Gold-bearing hot spring systems of the northern Coast Ranges, California: *Econ. Geol.*, v. 86, p. 1519-1528.
- Pulka, F. S., 1991, Recent intrusives at Ford Flat and relationships to faulting and the geothermal heat source, Geysers geothermal field, California: *Geol. Soc. America Abs. with Prog.*, v. 23, no. 2, p. 90.
- Rich, E. I., 1971, Geologic map of the Wilbur Springs Quadrangle, Colusa and Lake Counties, California: U. S. Geol. Survey, Misc. Invest. Map I-538, scale 1:48,000.
- Schriener, A. Jr., and Suemnicht, G. A., 1981, Subsurface intrusive rocks at The Geysers geothermal area, California: U. S. Geol. Survey Open-File Rept. 81-355, p. 294-303.
- Sims, J. D., Rymer, M. J., and Perkins, J. A., 1988, Late Quaternary deposits beneath Clear Lake, California; Physical stratigraphy, age, and paleogeographic implications: *Geol. Soc. America, Special Paper 214*, p. 21-44.
- Sims, J. D., and White, D. E., 1981, Mercury in the sediments of Clear Lake: U. S. Geol. Survey Prof. Paper 1141, p. 237-241.
- Sternfeld, J. N., 1981, The hydrothermal petrology and stable isotope geochemistry of two wells in The Geysers Geothermal Field, Sonoma County, California: Univ. of Calif. Riverside, M. S. thesis, 202 p.
- Sternfeld, J. N., 1989, Lithologic influences on fracture permeability and the distribution of steam in the Northwest Geysers steam field, Sonoma County, California: *Geothermal Resources Council Transactions*, v. 13, p. 473-479.
- Sternfeld, J. N., and Elders, W. A., 1982, Mineral zonation and stable isotope geochemistry of a production well in The Geysers geothermal field, California: *Geothermal Resources Council Transactions*, v. 6, p. 51-54.
- Swe, W., and Dickinson, W. R., 1970, Sedimentation and thrusting of late Mesozoic rocks in the Coast Ranges near Clear Lake, California: *Geol. Soc. America Bull.* v. 81, p. 165-187.
- Thompson, J. M., Goff, F. E., and Donnelly-Nolan, J. M., 1981, Chemical analyses of waters from springs and wells in the Clear Lake volcanic area: U.S. Geol. Survey Prof. Paper 1141, p. 161-166.
- Thompson, R. C., 1992, Structural stratigraphy and intrusive rocks at The Geysers geothermal field, *in* Stone, Claudia, ed., *Monograph on The Geysers Geothermal Field*: Davis, California, Geothermal Resources Council Special Rept. No. 17, p. 59-63.

- Thordsen, J. J., 1988, Fluid inclusion and geochemical study of epithermal gold mineralization in the Wilbur Springs district, Colusa and Lake counties, California: Master's Thesis, Ohio State University, 229 p.
- Truesdell, A. H., Box, W. T., Jr., Haizlip, J. R., and D'Amore, 1992, A geochemical overview of The Geysers geothermal reservoir, *in* Stone, Claudia, ed., Monograph on The Geysers Geothermal Field: Davis, California, Geothermal Resources Council, Special Rept. No. 17, p. 121-132.
- Unruh, J. R., Davison, M. L., Criss, R. E., and Moores, E. M., 1992, Implications of perennial saline springs for abnormally high fluid pressures and active thrusting in western California: *Geology*, v. 20, p. 431-434.
- Wagner, D. L., and Bortugno, E. J., 1982, Geologic map of the Santa Rosa Quadrangle: California Div. of Mines and Geology, Regional Geologic Map Series, Map No. 2A, 5 sheets, scale 1:250,000.
- Walters, M., and Combs, J., 1992, Heat flow in the Geysers-Clear Lake geothermal area of northern California, U.S.A., *in* Stone, Claudia, ed., Monograph on The Geysers Geothermal Field: Davis, California, Geothermal Resources Council, Special Rept. No. 17, p. 43-53.
- Walters, M. A., Sternfeld, J. N., Haizlip, J. R., Drenick, A. F., and Combs, J., 1992, A vapor-dominated high-temperature reservoir at The Geysers, California, *in* Stone, Claudia, ed., Monograph on The Geysers Geothermal Field, Geothermal Resources Council, Special Rept. No. 17, p. 77-87.
- Waring, G. A., 1915, Springs of California: U. S. Geol. Survey, Water Supply Paper 338, 410 p.
- Watts, W. L., 1893, Colusa County: California Jour. of Mines and Geology, v. 11, p. 179-188.
- White, D. E., 1957, Magmatic, connate, and metamorphic waters: *Geol. Soc. America Bull.* v. 68, p. 1659-1682.
- White, D., Barnes, I., and O'Neil, J. R., 1973, Thermal and mineral waters of nonmeteoric origin, California Coast Ranges: *Geol. Soc. America Bulletin*, v. 84, p. 547-560.
- White, D. E., Muffler, L. J. P., and Truesdell, A. H., 1971, Vapor-dominated hydrothermal systems compared with hot-water systems: *Econ. Geol.*, v. 66, p. 75-97.
- White, D. E., and Roberson, C. E., 1962, Sulphur Bank, California, a major hot-spring quicksilver deposit: *Geol. Soc. America, Buddington Volume*, p. 397-428.
- Yates, R. G., and Hilpert, L. S., 1946, Quicksilver deposits of eastern Mayacmas district, Lake and Napa Counties, California: *California Jour. Mines and Geology*, v. 42, no. 3, p. 231-286.

THERMAL-VOLCANIC EVOLUTION IN THE NORTHERN CALIFORNIA COAST RANGES

Mian Liu

Department of Geological Sciences, University of Missouri, Columbia, MO 65211

INTRODUCTION

Numerous late Tertiary and Quaternary volcanic centers are scattered in the vicinity of the San Andreas Fault system across the northern California Coast Ranges (Fig. 1). These volcanic rocks are characterized by a clear age progression. The youngest volcanic rocks are found in the Clear Lake volcanic center (2.1-0.01 Ma) (Donnelly-Nolan et al., 1981). To the south, volcanic rocks become progressively older. In an area about 60-70 km north of Clear Lake, seismic tomography suggests an "unruptured magma chamber" marked by relatively low crustal velocity similar to that under Clear Lake (Benz et al., 1992).

A number of causes have been suggested for the Coast Ranges volcanism. Hearn et al. (1981) proposed that the volcanism resulted from northward motion of the North American plate over a hotspot relatively fixed in the mantle. However, the trend of the Coast Ranges volcanism is difficult to reconcile with the relative motion of the North American plate derived from global inversion of plate kinematics (Minster et al., 1974). An origin of arc-volcanism is also unlikely, since volcanic rocks in the northern Coast Ranges were erupted within 50-60 km of the plate boundary, whereas the Cascades arc-volcanism typically occurs about 300 km inboard of the plate boundary (Fox et al., 1985).

Most workers relate the Coast Ranges volcanism to thermal perturbations associated with the northward migration of the Mendocino triple junction (MTJ) (Dickinson and Snyder, 1979; McLaughlin et al., 1981; Furlong, 1984; Johnson and O'Neil, 1984; Fox et al., 1985; Liu and Furlong, 1992). Both geophysical and geological data generally agree with such a hypothesis. This paper summarizes current understanding of thermal perturbations associated with the MTJ migration and their links to the Coast Ranges volcanism.

THERMOTECTONIC EVOLUTION ASSOCIATED WITH THE MTJ MIGRATION

Plate tectonic reconstruction based on paleomagnetic patterns in the Pacific ocean basins indicates that the Pacific plate encountered the North American plate around 30 Ma (Fig. 2) (Atwater, 1970; 1989). Since then convergence between these two plates has been replaced by strike-slip motion along the San Andreas transform fault, which connects the transform-transform-trench Mendocino triple junction (MTJ) and the transform-ridge-trench Rivera triple junction (RTJ), and has been evolving as these two triple junctions move away from each other (Fig. 2). Atwater (1970) suggested that many major tectonic events in the western United States were related to this evolving geometry of plate boundaries. Dickinson and Snyder (1979) proposed that, because of the migration of the

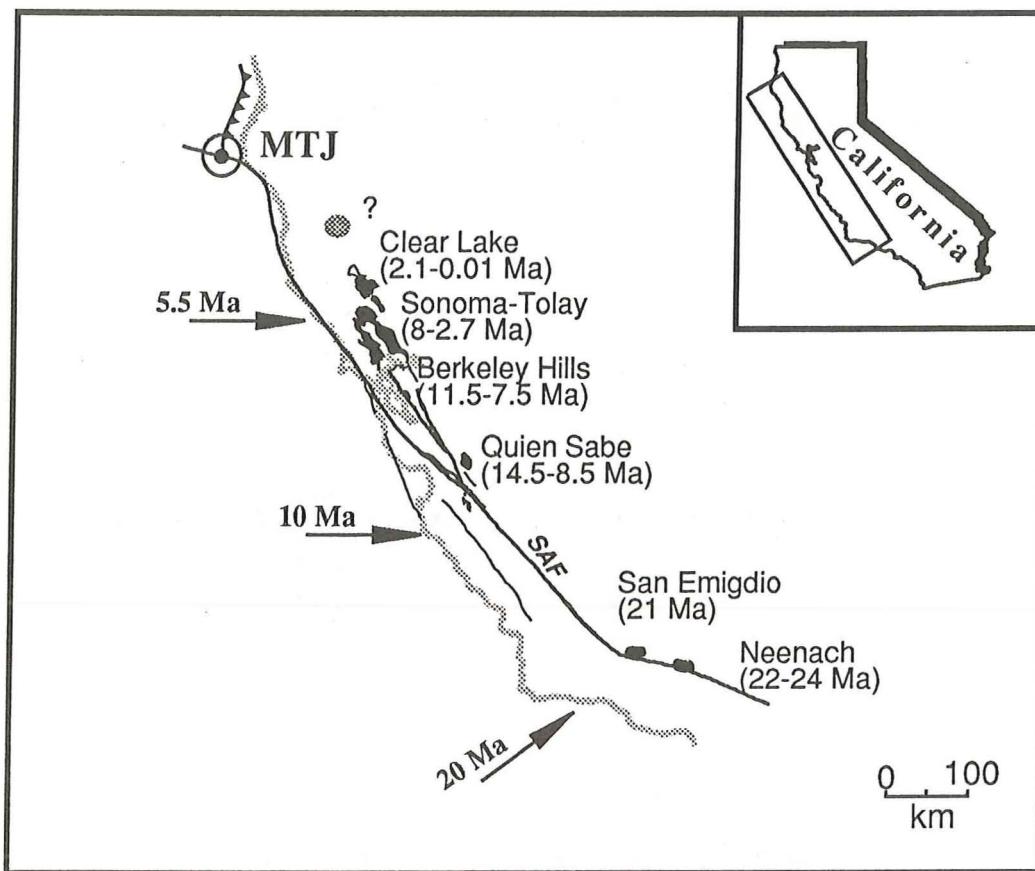


FIGURE 1. Distribution of Cenozoic volcanic rocks in the California Coast Ranges (dark areas). The insert indicates the map area. The gray curve is the coastline. Ages of the volcanic rocks are from Johnson and O'Neil (1984). The question mark indicates the region where a possibly unerupted magma chamber is suggested by seismic data (Benz et al., 1992). The long arrows indicate the approximate locations of the Mendocino Triple Junction (MTJ) at various times (from Atwater, 1989).

MTJ to the north and the RTJ to the south, a slabless window was created beneath the western United States which may have resulted in broad upwelling of the asthenosphere. The strongest thermal perturbations, however, are limited to a relatively narrow zone (50-100 km) west of the San Andreas fault, where northward migration of the subducting Gorda plate has allowed upwelling of the hot asthenosphere to a depth as shallow as the base of the crust (Furlong, 1984; Furlong et al., 1989).

Figure 2b illustrates the three dimensional geometry of plate boundaries around the MTJ, which has been migrating to the north with respect to the North America at the rate of relative motion between the North American and Pacific plates (McKenzie and Morgan, 1969). South of the MTJ, plate convergence (subduction under the North American plate) is replaced by strike-slip motion along the San Andreas fault. Northward migration of the subducting slab has created a slabless window beneath the western margin of the North American plate that has been filled by hot asthenosphere. Thermal perturbations associated with asthenospheric upwelling in the slabless window are tied with the MTJ and thus have been migrating to the north in the reference frame of the North American plate. The Coast Ranges volcanism was mainly caused by such thermal perturbations (Furlong, 1984; Johnson and O'Neil, 1984; Fox et al., 1985; Liu and Furlong, 1992).

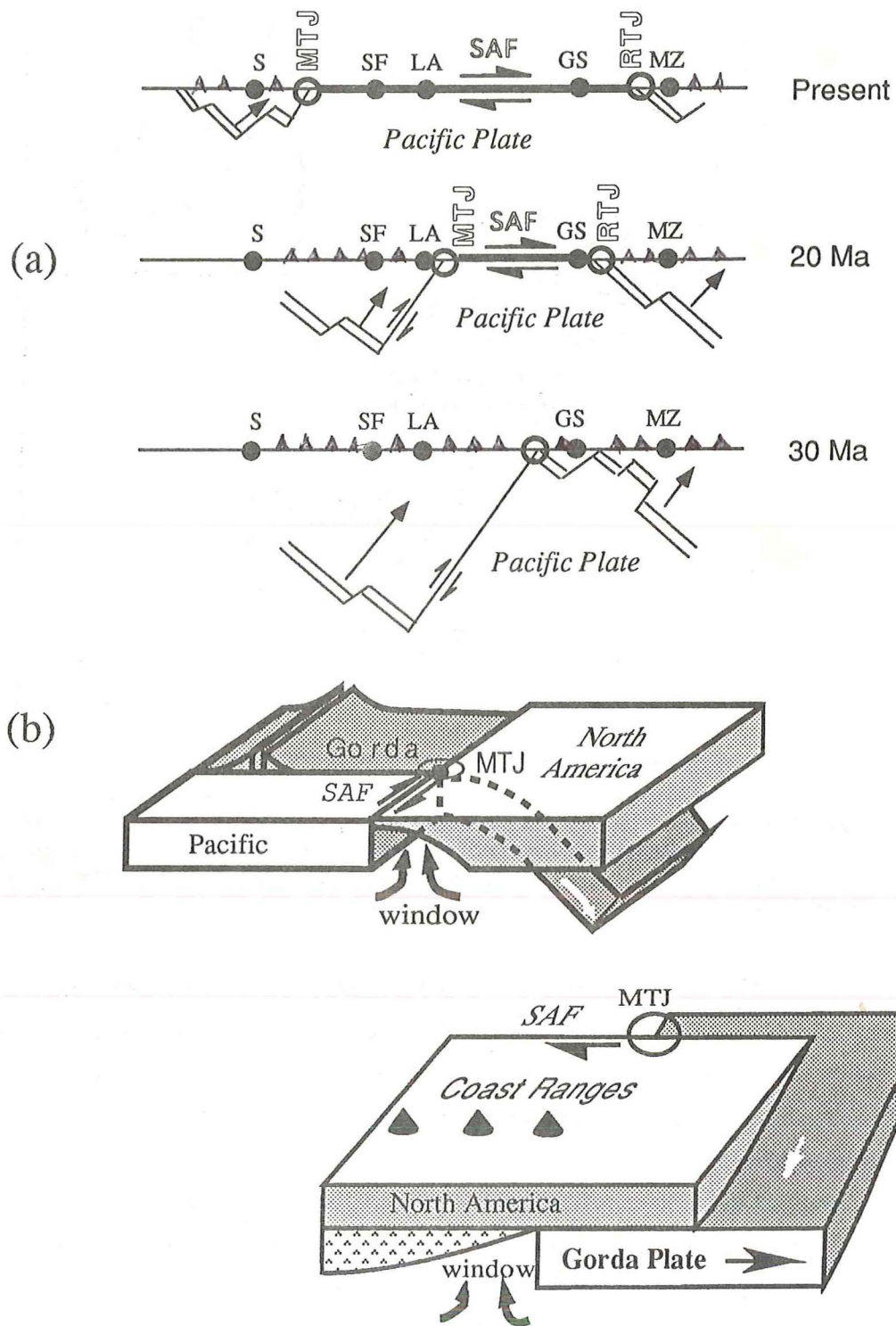


FIGURE 2.(a). Schematic model of relative motion between the North American and Pacific plates in the last 30 million years. The MTJ was formed about 30 Ma and has been migrating northward with respect to the North America. The thick solid line represents the San Andreas transform fault (SAF) which connects the MTJ and the Rivera triple junction (RTJ). S, Seattle; SF, San Francisco; LA, Los Angeles; GS, Guaymas; MZ, Mazatlan (modified from Atwater, 1970). **FIGURE 2.(b).** Sketches illustrating the three dimensional plate geometry around the MTJ. The northward migration of the subducting Gorda plate created a slabless window near its southern edge which was filled by upwelled asthenospheric material. In the wake of the MTJ, the upwelled asthenospheric material gradually cooled to attach to the surrounding plates as shown by the patterned area.

MAGMA GENERATION IN THE SLABLESS WINDOW

Although upwelling of the asthenosphere in the slabless window is commonly believed to be the major cause of the Coast Ranges volcanism, the time-dependent three-dimensional thermal perturbations in the wake of the MTJ are not fully understood. One important question concerning the thermal perturbations is what happened to the asthenospheric material filled in the slabless window. Did it cool conductively and attach to the surrounding lithosphere? Or could small-scale convection be induced below the slabless window, enhancing and prolonging thermal perturbations to the overlying crust? Using a two-dimensional (perpendicular to the strike of the San Andreas fault) numerical model simulating a coupled asthenosphere-lithosphere system, Liu and Furlong (1992) investigated the time-dependent thermal-dynamic evolution in the slabless window. They concluded that, within a reasonable range of model parameters, developing small-scale convection cells beneath the slabless window was unlikely. The asthenospheric material was dominated by conductive cooling after its initial upwelling in the slabless window. The resulting thermal perturbations are largely limited to the lower crust within a couple of million years after the passage of the MTJ (Fig. 3). It takes about 5 million years for most of the thermal signals to propagate to the surface. On the other hand, generation of mantle-derived magma is closely tied with the MTJ migration, since pressure-release partial melting occurs as soon as the upwelling asthenosphere crosses the mantle solidus.

Production of mafic magma in the slabless window depends chiefly on the initial temperature of the upwelling asthenosphere, the solidus of the mantle material, and the geometry of the slabless window. All these factors are associated with some uncertainties. Temperature of the asthenosphere beneath the lithosphere is in the range of 1200-1400°C as suggested by various studies (Jeanloz and Morris, 1986). The mantle material is generally represented by peridotite; and the commonly used solidus of peridotite is described by an empirical formula derived from melting experiments of garnet peridotites (McKenzie and Bickle, 1988). The major problem here is the geometry of the slabless window. The degree of pressure-release partial melting of the asthenosphere depends on the depth level it reaches, thus is controlled by the thickness of the conductive lid (mainly the crust) above the slabless window. Heat flow studies by Lachenbruch and Sass (1980) suggest that asthenosphere may have reached a level as shallow as 20 km in the wake of the MTJ. Seismic data indicate that crustal thickness in the northern California Coast Ranges is in the range of 30-45 km (Zandt, 1981). The width of the slabless window mainly affects the volume of magma production. Although direct constraints are not available, both seismic studies (Zandt, 1981) and heat flow modeling (Furlong, 1984) suggest a narrow (50-100 km) thin-lithosphere zone on top of the slabless window, bounded on the west by the San Andreas fault and thickening to the east at a dip of around 45° (Fig. 3). Using these constraints, up to 30% partial melting is predicted near the top of the slabless window; and the vertically integrated mafic magma may be up to 4-5 km thick (Liu and Furlong, 1992). It should be pointed out that Liu and Furlong's model did not consider variations of the window geometry during the MTJ migration and thermal processes in the south-north direction (see Fig. 2b). Variations of the geometry of the active slabless window may be important to the distribution of Coast Range volcanism and are discussed later.

Because a matrix of partially molten rocks cannot retain more than 1% basaltic melt fraction for a long period (Hunter and McKenzie, 1989), most mafic magma produced in the slabless window was likely extracted from

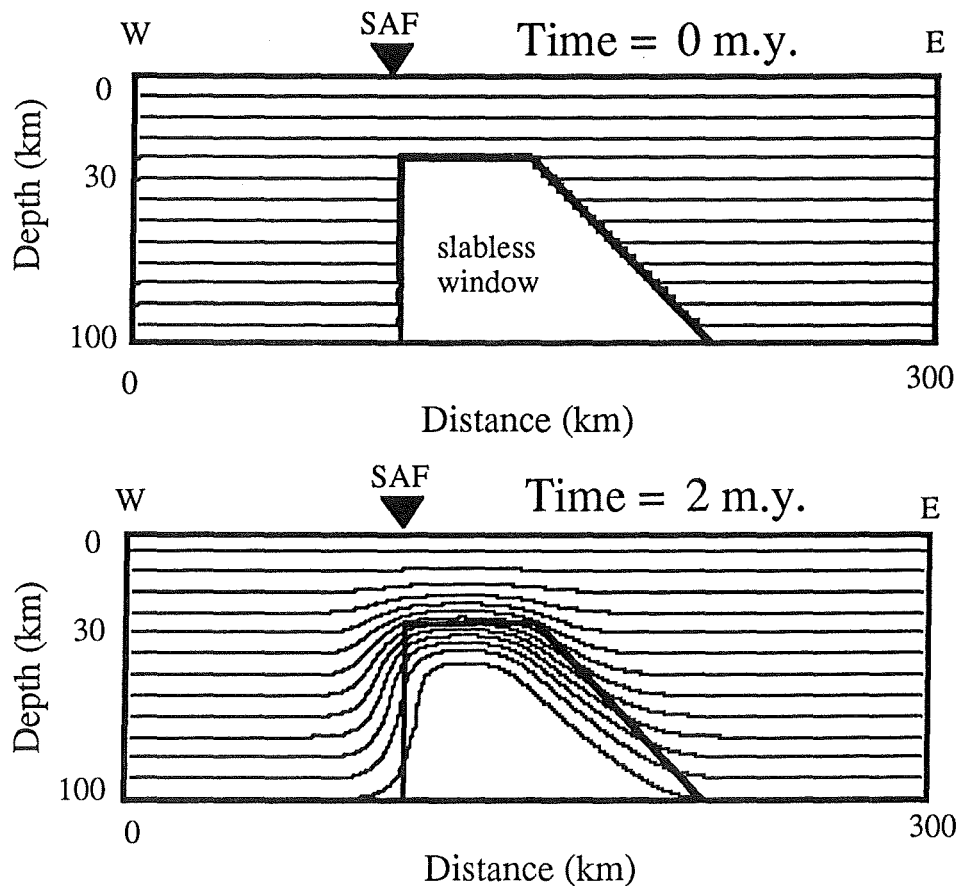


FIGURE 3. Modeled thermal evolution in lithospheric sections perpendicular to the direction of the MTJ migration. The solid triangle points to the surface position of the San Andreas fault (SAF). A linear geotherm is assumed for the lithosphere before the passage of the MTJ. Boundary conditions include fixed temperatures at the surface (0°C) and at the bottom (1300°C) of the lithosphere. The isothermal contours are at 100°C intervals. The slabless window created in the wake of the MTJ was filled by the asthenosphere at a uniform initial temperature of 1300°C which then cooled conductively. Within the first a few million years following the MTJ passage, most thermal perturbations are seen in the lower crust where temperatures may be raised over 800°C .

the partial melting zone by compaction. The characteristic extraction time was relatively small (10^4 years; see Liu and Furlong, 1992), thus production of basaltic magma was temporally linked to passage of the MTJ, as suggested by previous studies (Johnson and O'Neil, 1984, Fox et al., 1985).

Since only a small volume of basaltic magma has erupted (Hearn et al., 1976; Johnson and O'Neil, 1984), most of the asthenosphere-derived magma must be stored within and beneath the crust. The approximate storage depth of the major portion of basaltic magma may be constrained by surface heat flow data. Figure 4 shows the calculated surface heat flow anomalies in the wake of the MTJ with a 4-km basaltic sill emplaced at various depths. In comparison with measurements of surface heat flow in the northern Coast Ranges, it is clear that most of the basaltic magma must be stored in the deep crust (near 30 km, see curve C in Fig. 4). Otherwise, extremely high surface heat flow would be observed over large areas of northern California, which is not true. Seismic reflection data from the Coast Ranges area indicate a layer a few kilometers thick at the base of the crust with velocities appropriate

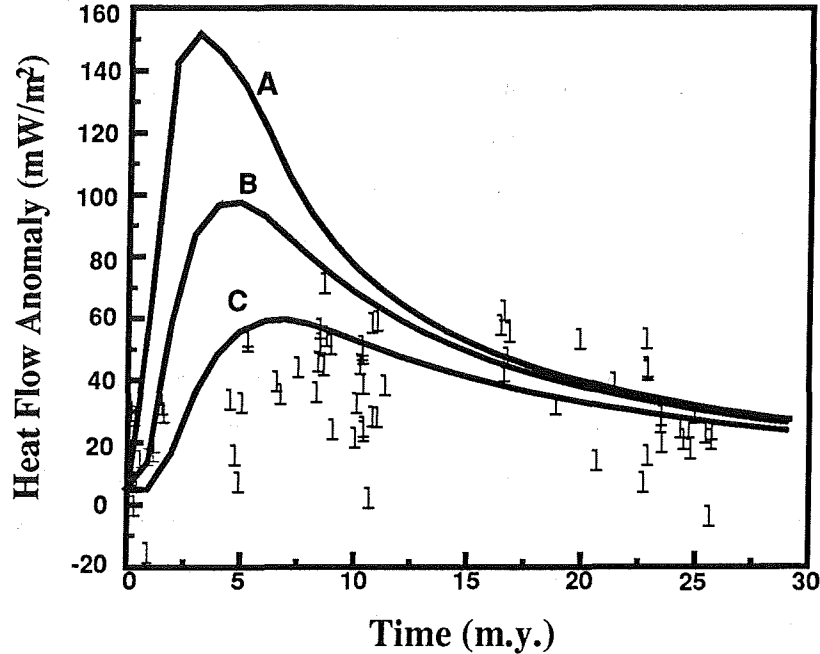


FIGURE 4. Comparison of measured surface heat flow anomalies in the Coast Ranges (solid bars; data are adapted from Lachenbruch and Sass (1980)) to model predictions (curves, from Liu and Furlong (1992)). The anomalies are relative to the background value (taken to be 42 mW/m^2 , the value of steady-state heat flow before the MTJ passage). Time is after the passage of the MTJ. Curves A and B are calculated with a 4-km basaltic sill intruded at 10 km and 20 km depth, respectively. Curve C shows the results when all mafic magma underplated at the base of the crust (at 30 km depth). The heat flow data are taken to represent regional thermal effects of the MTJ-related asthenospheric upwelling. Heat fluxes in the Clear Lake volcanic field are much higher ($>167 \text{ mW/m}^2$, see Walters and Combs, 1989) and are not plotted here, since they mainly reflect magmatism in the upper crust. See text for more discussion.

for gabbro, thus may be related to underplated basalts (Walter and Mooney, 1982; Blumling and Prodehl, 1983; Fuis and Mooney, 1990). However, the available seismic data are insufficient to be conclusive.

On the other hand, magmatism in upper crustal levels may be expected at volcanic centers. Walters and Combs (1989) reported high heat flux ($>167 \text{ mW/m}^2$) over a large area of the Clear Lake volcanic field. This may be caused by mafic intrusion at a depth shallower than 15 km (see Fig. 4) or silicic magma bodies at an even shallower depth. This is generally consistent with geophysical inversions which suggest a magma chamber lying about 7 km beneath the Geysers-Clear Lake area with a diameter of $\sim 20 \text{ km}$ (Chapman, 1975; Iyer et al., 1981; Oppenheimer and Herkenhoff, 1981). Additional evidence of high-level mafic intrusion is provided by xenoliths from Clear Lake, which indicate mixing between basaltic and silicic magmas in the middle crust (Stimac, this volume).

CRUSTAL ANATEXIS

To relate the northern Coast Ranges volcanism to the MTJ migration, we need to explain the generation of intermediate and rhyolitic magmas, which dominate the Clear Lake and Sonoma-Tolay volcanic fields (Donnelly-Nolan et al., 1981; Rytuba, this volume). Most of these silicic volcanic rocks bear clear geochemical and isotopic signatures indicating an origin of crustal anatexis (Johnson and O'Neil, 1984). Whereas some of the rhyolitic magmas at Clear Lake may have been resulted from mantle-derived basaltic precursors by multiple stages of crystal fractionation and crustal assimilation (Stimac, 1991). In general, volcanic sequences in the Coast Ranges indicate a complicated history of mafic intrusion, crustal partial melting, and mafic-silicic magma mixing (Hearn et al., 1981; Johnson and O'Neil, 1984; Stimac, 1991; Stimac, this volume).

Crustal anatexis may be caused by both thermal perturbations in the slabless window and intrusion/underplating of mafic magmas. Accurate calculations of crustal anatexis are difficult because of many uncertain factors. One major problem is the activity of water, which has large effects on partial melting of crustal material but is difficult to constrain. Normally, a fluid-absent condition can be assumed for deep crust (e.g., Vielzeuf and Holloway, 1988). However, the situation at the wake of the MTJ may be more complicated because of the previous period of subduction. Nonetheless, Liu and Furlong (1992) suggested that water-saturated crustal anatexis did not prevail in the wake of the MTJ, otherwise unreasonably high magma production would be predicted.

Some lower bounds on crustal partial melting may be derived by assuming dry crustal anatexis. Liu and Furlong (1992) simulated the time-dependent crustal anatexis in a two-dimensional numerical model. Major assumptions of the model include a 30 km crust of metasediments on top of a slabless window initially filled with hot asthenospheric material at a uniform temperature of 1300°C, and a 2-km thick basaltic sill with an initial temperature of 1200°C emplaced at various depth of the crust. Crustal anatexis is caused by heat diffused from the intrusive basalts and asthenospheric material filled in the slabless window. The results suggest that crustal anatexis mainly occurred in the lower crust (below ~15 km depth). No major crustal anatexis is predicted in the upper crust, even when mafic magmas intrude the upper crust, because heat carried by mafic magmas is insufficient to increase the upper crustal temperature over the relevant local solidus on a significant scale. Production of crustal melts depends on the mode of storage of mafic magmas (Fig. 5). When massive mafic magmas intrude the lower crust, more crustal anatexis is predicted because of heating by both intrusive magmas and asthenospheric material in the slabless window. The predicted crustal anatexis and temperature-pressure conditions are consistent with petrological studies of xenoliths from Clear Lake (Stimac et al., 1992; Stimac, this volume), which suggest occurrence of crustal anatexis and silicic-mafic magma mixing in the middle to lower crust. Temperature and pressure estimates for crustal xenoliths derived from mineral geothermometry and geobarometry range from 750°C to 910°C and 4.4 to 7.6 kb (Stimac et al., 1992; Stimac, this volume). Numerical results (Liu and Furlong, 1992) show that temperatures in a large portion of the lower crust above the slabless window may be raised to over 800°C, especially when a large volume of mafic magma intrudes the lower crust. Thus thermal perturbations associated with the MTJ migration may have caused regional recrystallization of the Franciscan complex to high-temperature and lower-pressure

granulite facies, transforming accretional assemblages into lithofacies typical of continental crust (Hearn et al., 1981; Stimac et al., 1992).

The predicted crustal anatexis in the wake of the MTJ is likely sufficient for the Coast Ranges volcanism. The peak rate of magma production by crustal anatexis in the northern Coast Ranges is predicted to be 2000 km³/m.y. when most of the mantle-derived magmas are pooled near the base of the crust, and up to 8000 km³/m.y.

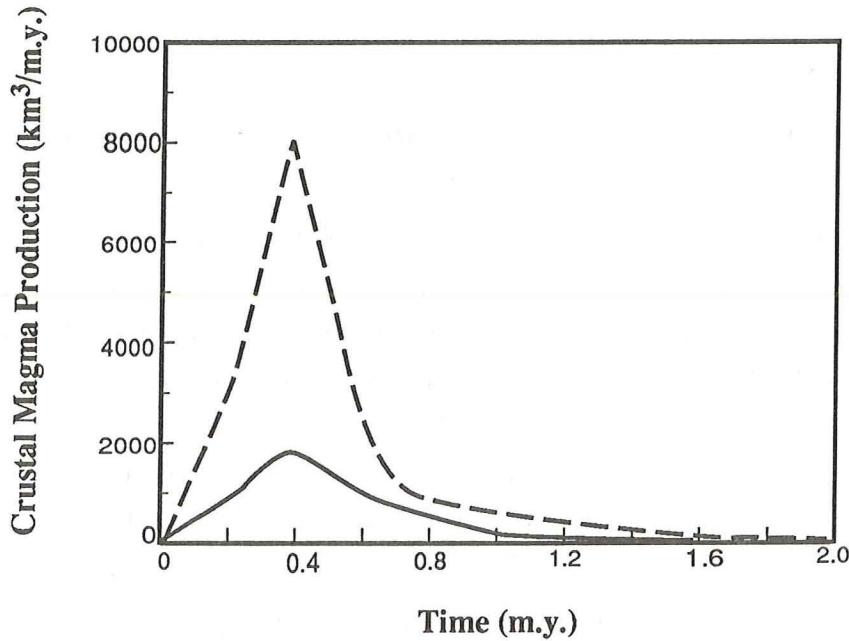


FIGURE 5. Incremental silicic magma production by crustal anatexis in the wake of the MTJ. The silicic magma production is calculated for the northern Coast Ranges assuming a MTJ migration rate of 5 cm/yr. The solid curve is for basaltic underplating only (at 30 km depth). The dashed curve shows higher rates of magma production when additional heating is provided by a 2-km mafic sill intruded in the lower crust (at 20 km depth).

when a large portion of the mafic magmas intrudes the lower crust (Fig. 5). The total magma production over a given area in the northern Coast Ranges may be roughly estimated by multiplying the peak magma production rate in Figure 5 with the time taken by the MTJ to migrate over the area. The time for the MTJ to migrate over the Clear Lake volcanic field was about one million years, thus the total volume of magma produced at Clear Lake is predicted to be about 2000-8000 km³. Although the actual ratio between intrusive and eruptive magmas is unknown, such a magma production is probably more than adequate for erupting 100 km³ volcanic rocks in this area. Because of many uncertainties involved in the calculations, these results need to be interpreted with caution. For instance, the predicted magma production would be lower if the lower crust consists of some mafic material instead of all metasediments as assumed in the model.

Figure 5 also suggests that most crustal melts were generated within one million years following the passage of the MTJ. However, silicic melts may take much longer to separate from the partial melting zones than mafic melts because of their high viscosity. Compaction becomes ineffective in extracting silicic melts. Most silicic magma may have been transported from partial melting zones when melt fraction exceeded the so-called critical melt

fraction, which is around 30-50% for granitic magma (Wickham, 1987). When this happens, the whole system of the partial melting zone behaves like a fluid with crystal suspensions. Crustal anatexis with melt fractions over 50% is predicted when significant amount of mafic magma intrudes the lower crust (Liu and Furlong, 1992). When most basaltic magmas is pooled at the base of the crust, the predicted degree of crustal partial melting is lower, and the melts may not be effectively transported to the surface. Variations of melt fraction in the crust may be a major factor influencing distribution of volcanism in the Coast Ranges.

DISTRIBUTION OF COAST RANGES VOLCANISM AND THE RATE OF THE MTJ MIGRATION

Thermal-magmatic modeling (Liu and Furlong, 1992) showed that significant magmatism was associated with the MTJ migration, thus supporting the link between the passage of the MTJ and the Coast Ranges volcanism. However, such a model predicts continuous thermal perturbations beneath the California Coast Ranges. How can this prediction be reconciled with the scattered and uneven distribution of volcanism (Fig. 1)?

Seismic tomography of the northern Coast Ranges shows that there is indeed a continuous low velocity zone stretching from Clear Lake all the way to Cape Mendocino (Benz et al., 1992). This low velocity zone reaches a depth below 100 km, supporting the asthenosphere-rooted thermal perturbations in the slabless window. Most significant velocity variations are seen in the upper crust, suggesting that crustal structure may be a major factor in forming the scattered volcanic centers in the northern Coast Ranges. Volcanic eruption at Clear Lake may be facilitated by tensional stresses induced by strike-slip motion along the broad San Andreas fault system that has led to the formation of the Clear Lake basin (Hearn et al., 1988). On the other hand, crust north of Clear Lake was likely under more compression in the last 5 m.y. (Page and Engeberston, 1984). Rotation of the Gorda plate and overriding by the Pacific plate in the last a few millions of years (Riddihough, 1984) may have contributed to the lack of volcanism in that region.

However, crustal structure is not the only controlling factor. Liu and Furlong (1992) showed that the general spatial-temporal distribution of Coast Ranges volcanism was closely correlated with the variation of the MTJ migration rates (Fig. 6). The relatively voluminous volcanism in northern California corresponds to relatively fast (> 5 cm/yr) migration of the MTJ in the last 10 m.y. Volcanic rocks older than 20 m.y. are sparse and smaller in volume, and the MTJ migration was slower over that period. The limited evidence of volcanism between 10 and 20 Ma corresponds to a period of very slow migration of the MTJ (~ 1.8 cm/yr). This correlation is unlikely a coincidence, because every stage of volcanic evolution in the Coast Ranges was closely related to the rate of the MTJ migration. Magma production over any area in the Coast Ranges was largely determined by the intensity of thermal perturbations which is directly related to the size of the active slabless window; and the rate of the MTJ migration determines the rate at which new slabless window was created. When the MTJ moved slowly, conductive cooling became important in the slabless window. More asthenospheric material may have attached to the surrounding plates, resulting in a smaller active slabless window. On the other hand, faster MTJ migration created new slabless window

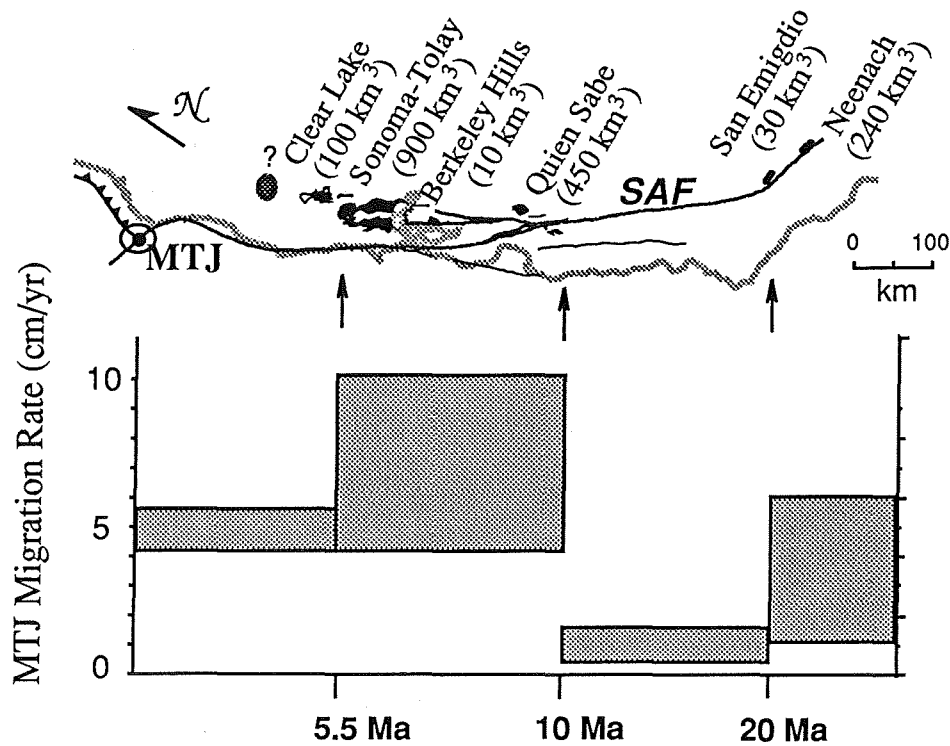


FIGURE 6. Correlation between the distribution of volcanic rocks in the Coast Ranges (top) and variations of the MTJ migration rate (bottom). The size of the boxes in the bottom figure indicates the uncertainties of the MTJ migration rates (from Atwater, 1989). The approximate location of the MTJ at various times (from Atwater, 1989) is indicated by the arrows.

at a higher rate. The size of the active slabless window was also bigger in this case since less asthenospheric material was attached. A smaller slabless window means less crustal anatexis; and crustal melts may not be effectively transported to the surface if melt fraction is lower than 30-50%. Although other factors, such as stress state in the crust and erosion, may have also played a large role, the strong correlation between the volume of volcanic rocks and the MTJ migration rates shown in Figure 6 suggests that variations in the MTJ migration rate may be the dominate cause for the uneven distribution of volcanic rocks in the northern Coast Ranges.

CONCLUSIONS

1. Cenozoic volcanism in the northern California Coast Ranges was caused by thermal perturbations associated with the northward migration of the Mendocino Triple Junction. Filling of hot asthenospheric material in the slabless window in the wake of the MTJ may have produced up to 4-5 km of mafic magma and drastically changed the thermal structure of the overlying crust.

2. Most of the mafic magmas were stored near the base of the crust; and crustal anatexis occurred mainly in the lower to middle crust (>15 km depth). Production of silicic magma in the northern California Coast Ranges was

likely over 2000 km³/m.y., but only a small portion of the magma was erupted. Thermal perturbations in the wake of the MTJ may have been sufficient to cause regional metamorphism of the lower and middle crust to granulite facies, converting the accretional assemblage of the Franciscan complex to lithofacies typical of continental crust.

3. The uneven distribution of the Coast Ranges volcanism was mainly related to variations of the MTJ migration rate. Changes of stress states in the crust may also have played a large role in volcanic eruptions in the northern Coast Ranges.

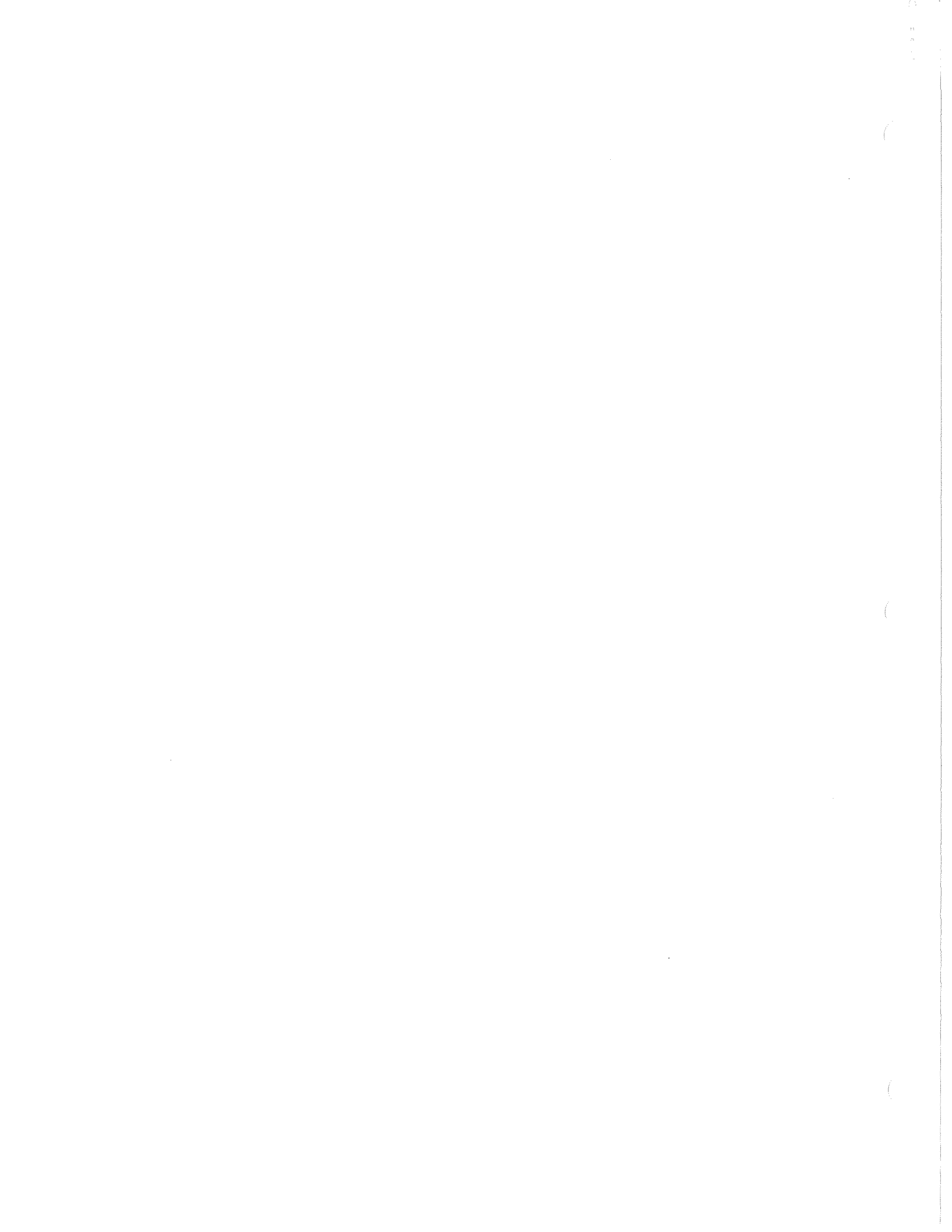
ACKNOWLEDGMENTS

Jim Stimac is thanked for his careful and helpful review. This work is partially supported by the Research Board of the University of Missouri .

REFERENCES

- Atwater, T., 1970, Implications of plate tectonics for the Cenozoic tectonic evolution of western North America: *Geol. Soc. Am. Bull.*, v. 81, p. 3513-3536.
- Atwater, T., 1989, Plate tectonic history of the northeast Pacific and western North America, in *The Geology of North America, Vol. N, The Eastern Pacific Ocean and Hawaii*, edited by Winterer, E.L., Hussong, D.M., and Decker, R.W., p.21-72, Geological Society of America, Boulder, Colo.
- Benz, H.M., Zandt, G., and Oppenheimer, D.H., 1992, Lithospheric structure of northern California determined from teleseismic images of the upper mantle: *J. Geophys. Res.*, v. 97, p. 4791-1807.
- Blumling, P., and Prodehl, C., 1983, Crustal structure beneath the eastern part of the Coast Ranges (Diablo Range) of central California from explosion seismic and near surface earthquake data: *Phys. Earth Planet. Inter.*, v. 13, p. 13-326.
- Chapman, R.H., 1975, Geophysical study of the Clear Lake region, California: *Calif. Div. Mines and Geology, Special Report v. 116*, 23p.
- Dickinson, W.R., and Snyder, W.S., 1979, Geometry of subducted slabs related to the San Andreas transform: *J. Geol.*, v. 87, p. 609-627.
- Donnelly-Nolan, J.M., Hearn, B.C., Jr., Curtis, G.H., and Drake, R.E., 1981, Geochronology and evolution of the Clear Lake volcanics, in *Research in the Geysers-Clear Lake Geothermal Area, North California*: *U.S. Geol. Surv. Prof. Pap.*, v. 1141, p. 47-60.
- Fox, K.F., Jr., Fleck, R.J., Curtis, G.H., and Meyer, C.E., Implications of the northwestwardly younger age of volcanic rocks in west-central California: *Geol. Soc. Am. Bull.*, v. 96, p. 647-654.
- Fuis, G.S., and Mooney, W., 1990, Lithospheric structure and tectonics from seismic-refraction and other data: *U.S. Geol. Surv. Prof. Pap.*, v. 1515, p. 207-238.
- Furlong, K.P., 1984, Lithospheric behavior with triple junction migration: An example based on the Mendocino triple junction: *Phys. Earth Planet. Inter.*, v. 36, p. 213-223.
- Furlong, K.P., Hugo, W.D., and Zandt, G., 1989, Geometry and evolution of the San Andreas Fault zone in northern California: *J. Geophys. Res.*, v. 94, p. 3100-3110.
- Jachens, R.C., and A. Griscorn, 1983, Three-dimensional geometry of the Gorda plate beneath northern California: *J. Geophys. Res.*, v. 88, p. 9375-9392.
- Jeanloz, R., and Morris, S., 1986, Temperature distribution in the crust and mantle: *Annu. Rev. Earth Planet. Sci.*, v. 14, p. 377-415.
- Johnson, C.M., and O'Neil, J.R., 1984, Triple junction magmatism: A geochemical study of Neogene volcanic rocks in western California: *Earth Planet. Sci. Lett.*, v. 71, p. 241-262.
- Hearn, B.C., Jr., Donnelly-Nolan, J.M., and Goff, F.E., 1976, Preliminary geologic map and cross-section of the Clear Lake volcanic field, Lake County, California: *U.S. Geological Survey Open-file Report*, 76-751.
- Hearn, B.C., Jr., Donnelly-Nolan, J.M., and Goff, F.E., 1981, The Clear Lake Volcanics: Tectonic setting and magma sources, in *Research in the Geysers-Clear Lake Geothermal Area, North California*: *U.S. Geol. Surv. Prof. Pap.*, v. 1141, p. 24-45.
- Hearn, B.C., Jr., McLaughlin, R. J., and Donnelly-Nolan, J.M., 1988, Tectonic framework of the Clear Lake basin, California: *GSA Special Paper v. 214*, p. 9-20.

- Hunter, R.H., and McKenzie, D., 1989, The equilibrium geometry of carbonate melts in rocks of mantle composition: *Earth Planet. Sci. Lett.*, v. 92, p. 347-356.
- Iyer, H.M., Oppenheimer, D.H., Hitchcock, T., Roloff, J.N., and Coakley, J.M., 1981, Large teleseismic P-wave delays in the Geysers-Clear Lake geothermal area, in *Research in the Geysers-Clear Lake Geothermal Area, North California: U.S. Geol. Surv. Prof. Pap.*, v. 1141, p. 97-116.
- Lachenbruch, A.H., and Sass, J.H., 1980, Heat flow and energetics of the San Andreas fault zone: *J. Geophys. Res.*, v. 85, p. 6185-6222.
- Liu, M., and Furlong, K. P., 1992, Cenozoic Volcanism in the California Coast Ranges: Numerical Solutions: *J. Geophys. Res.*, v. 97, p. 4941-4951.
- McKenzie, D., and Morgan, W.J., 1969, Evolution of triple junctions: *Nature*, v. 224, p. 25-133.
- McKenzie, D., and M.J. Bickle, 1988, The volume and composition of melt generated by extension of the lithosphere: *J. Petrol.*, v. 29, p. 625-679.
- McLaughlin, J.R., 1981, Tectonic setting of pre-Tertiary rocks and its relation to geochemical resources in the Geysers-Clear Lake area, in *Research in the Geysers-Clear Lake Geothermal Area, North California: U.S. Geol. Surv. Prof. Pap.*, v. 1141, p. 3-24.
- Minster, J.B., Jordan, T.H., Molnar, P., and Haines, E., 1974, Numerical modeling of instantaneous plate tectonics: *Roy. Astron. Soc. Geophys. J.*, v. 36, p. 541-576.
- Oppenheimer, D.H., and Herkenhoff, K.E., 1981, Velocity-density properties of the lithosphere from three-dimensional modeling at the Geysers-Clear Lake region, California: *J. Geophys. Res.*, v. 86, p. 6057-6065.
- Page, B.M., and Engebreston, D.C., 1984, Correlation between geological record and computed plate motions for central California: *Tectonics*, v. 3, p. 133-155.
- Riddihough, R.P., 1984, Recent movement of the Juan de Fuca plate system: *J. Geophys. Res.*, v. 89, p. 6980-6994.
- Stimac, J.A., 1991, Evolution of the silicic magmatic system at Clear Lake, California from 0.65 to 0.3 Ma, Ph.D. dissertation, Queen's University, Kingston, Ont., Canada.
- Stimac, J. A, Goff, F.E., and Glassley, W.E., 1992, Crustal xenoliths in the Clear Lake volcanics, California: Transformation of Franciscan assemblage rocks to continental crust?[abs]: *Eos, Trans. AGU*, 73, 505.
- Vielzeuf, D., and Holloway, J.R., 1988, Experimental determination of the fluid-absent melting relations in the pelitic system: Consequences for crustal differentiation: *Contrib. Mineral. Petrol.*, v. 98, p. 257-276.
- Walter, A.W., and Mooney, W.D., 1982, Crustal structure of the Diablo and Gabilan Ranges, central California: A reinterpretation of existing data: *Bull. Seismol. Soc. Am.*, v. 72, p. 1567-1590.
- Walters, M., and Combs, J., 1989, Heat flow regime in the Geysers-Clear Lake area of northern California, U.S.A: *Geothermal Resources Council, Transactions*, v. 13, p. 491-502.
- Wickham, S.M., 1987, The segregation and emplacement of granitic magmas: *J. Geol. Soc. London*, v. 144, p. 281-273.
- Zandt, G., 1981, Seismic images of the deep structure of San Andreas fault system, central coast ranges, California: *J. Geophys. Res.*, v. 86, p. 5039-5052.
- Zandt, G., and Furlong, K.P., 1982, Evolution and thickness of the lithosphere beneath coastal California: *Geology*, v. 10, p. 376-381.



EPITHERMAL PRECIOUS-METAL AND MERCURY DEPOSITS IN THE SONOMA AND
CLEAR LAKE VOLCANIC FIELDS, CALIFORNIA

(1993)

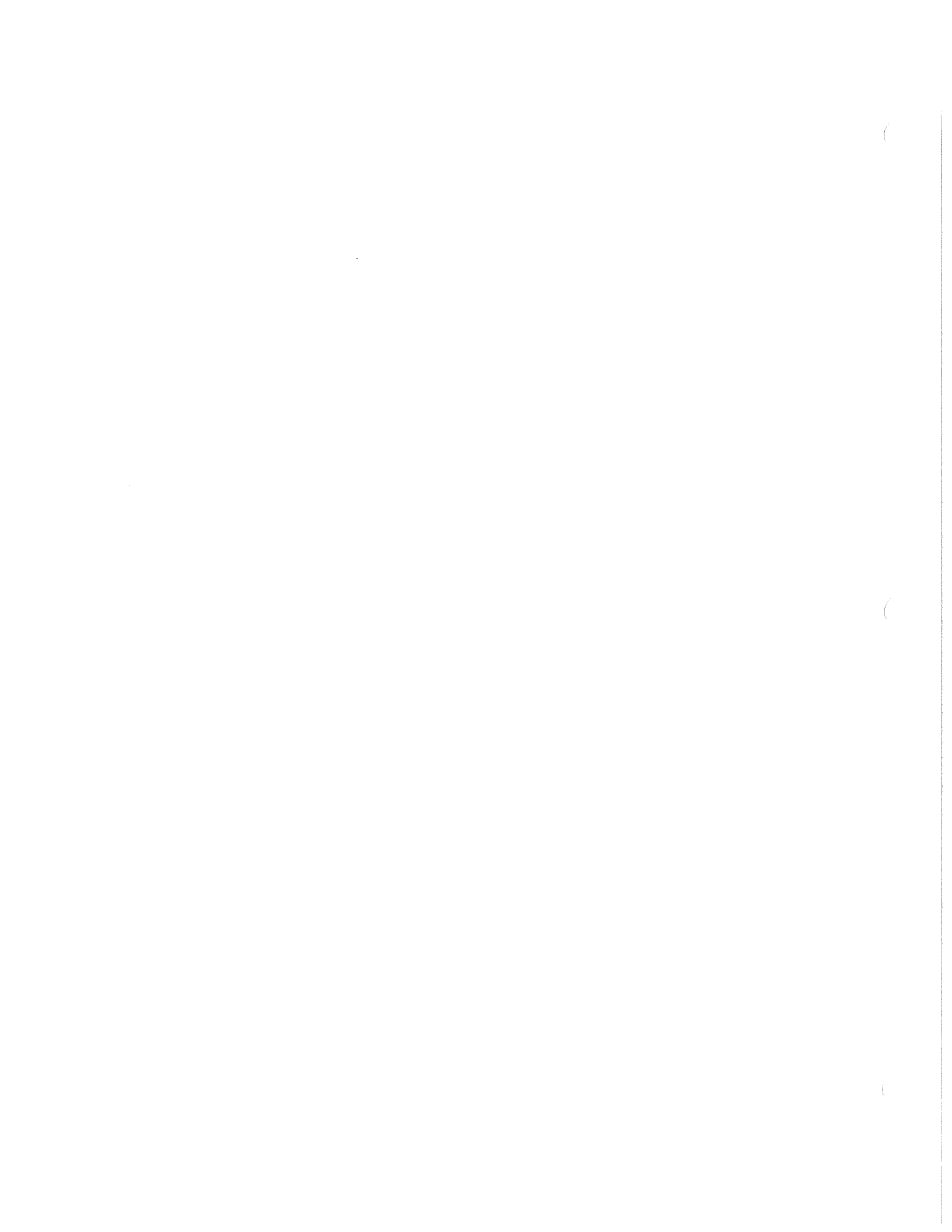
James J. Rytuba

U. S. Geological Survey, 345 Middlefield Road, Menlo Park, CA 94025

ABSTRACT

Epithermal precious-metal and mercury deposits are present in the Sonoma and Clear Lake volcanic fields of central California and several hot springs in the Clear Lake volcanic field are presently depositing mercury and gold. The deposits and hot springs are associated with late Miocene to Holocene volcanic centers developed above a zone of thin crust and hot asthenosphere termed a slab window (Dickinson and Snyder, 1979, Benz and others, 1992) as the end of Pacific plate subduction was marked by the passage of the Mendocino triple junction along the California coast. Mercury deposition is actively occurring at the Sulphur Bank mercury mine, but no precious metals are present there because the geothermal system is vapor-dominated. In the water dominated geothermal systems at Wilbur Springs (Peters, 1990, Donnelly and others, 1993) and springs near the Cherry Hill gold deposit, both cinnabar and gold are being deposited (Percy and Petersen, 1990). Transport of mercury and gold is in a fluid which also contains high concentrations of petroleum and associated methane and CO₂ derived from thermal degradation of organic matter in sedimentary rocks (Peabody, 1989). Chemical and isotopic analysis of oxygen and deuterium of the hot springs indicate that three types of fluid are present: moderate chloride, isotopically heavy, evolved formation fluid equilibrated with oceanic sedimentary rocks; evolved meteoric water; and isotopically light meteoric water (Peters, 1990, 1991, Sherlock and Jowett, 1992, and Donnelly-Nolan and others, 1993). High concentrations of Hg, As, Sb, Au, and Ag occur in precipitates from hot springs composed dominantly of the isotopically heavy fluid, but not in the moderate-temperature, oxidized springs that are mixtures of these two fluid types (Peters, 1990, Donnelly-Nolan and others, 1993).

The McLaughlin gold deposit (initial reserves of 2.9 million oz of gold) is economically the most important deposit in the Clear Lake and Sonoma volcanic fields. This precious metal-mercury hydrothermal system developed within and adjacent to andesitic vents and dikes emplaced along the Stony Creek fault zone (Lehrman, 1986). Gold occurs in opal, chalcedony, and quartz veins, and the highest gold values typically occur in amber to brown opal containing petroleum. Gold occurs in several sites within the petroleum-bearing opal: as a filling of 20-50 micron- diameter oval voids representing large fluid inclusions; as 2-4 micron size crystals that coalesce to form dendrites of gold along primary vein banding; and in syneresis cracks which cut the vein banding. Oxide phases of Ga, In, Sn, and Ni are present within the petroleum-bearing opal. The isotopically heavy McLaughlin ore fluid



plots in the field of andesitic magma volatiles (Hedenquist and Aoki, 1990, Giggenbach, 1987) and evolved formation waters (Sherlock and Jowett, 1992) suggesting that these two components are present. Andesitic vents and dikes at the McLaughlin gold deposit suggest that a larger intrusion underlies the area and provided the heat source for the hydrothermal system. Andesitic vents along the Stony Creek fault provided a conduit for volatiles degassing from the intrusion to become entrained within the hydrothermal fluid composed of gas-oil-field water derived from the Great Valley sequence. The McLaughlin gold deposit reflects the complex interaction of three types of fluid each transporting a different elemental suite: evolved gas-oil field formation water transporting petroleum, Ga, In, Sn, Ni, and Hg; andesitic magmatic fluid transporting Au, Ag, Hg, Sb, and As; and near-surface meteoric water.

Prospective areas for precious metal hot-spring deposits occur in the volcanic-structural environment above the thin crust and hot asthenosphere within the slab window in the Coast Ranges and parts of the Great Valley sequence where blind thrusts and associated faults are intruded by Pliocene to Holocene intrusive rocks. Mercury deposits with little or no gold content form along major structures from gas-oil field fluids with little or no magmatic component in the fluid and contain petroleum, Ni, Ga, In, Sn, and other transition elements. Epithermal gold deposits contain a significant magmatic component characterized by Au, Ag, As, Sb, and Hg as well as a gas-oil- field fluid component characterized by petroleum and transition metals. Both deposit types may occur along the same structures.

INTRODUCTION

Epithermal precious-metal and mercury deposits occur throughout the Sonoma and Clear Lake volcanic fields of central California and several hot springs in the Clear Lake volcanic field are actively depositing mercury and gold. Middle Tertiary to Holocene volcanic activity in the Sonoma and adjacent Clear Lake volcanic fields is characterized by basaltic-andesite to rhyolitic flows, domes, tuffs, and cinder cones (Donnelly-Nolan and others, 1981, Fox and others, 1985). Volcanic activity has progressed systematically northward along the San Andreas transform fault as the end of Pacific plate subduction was marked by the passage of the Mendocino triple junction northward along the coast of California (McLaughlin, 1981, Hearn and others, 1981, and Fox and others, 1985). Most of the ore deposits and hot springs are localized adjacent to small volcanic centers developed within a broad zone of right-lateral faulting associated with the San Andreas transform fault.

Recent studies (Peters, 1990, 1991, Sherlock and Jowett, 1992, and Donnelly-Nolan and others, 1993) of hot springs in the Clear Lake volcanic field have provided important information on the composition of the hydrothermal fluid and insight into processes related to the formation of epithermal precious-metal and mercury deposits. Mercury deposition was noted in the early part of the century during mining at the Sulphur Bank mercury mine, and White and Roberson (1962) described the vapor-dominated geothermal system and the acid-sulfate alteration associated with the mercury mineralization. More recently, deposition of cinnabar and gold have been recognized in the water-dominated geothermal systems such as Wilbur Springs and other springs adjacent to the

Cherry Hill gold deposit in the Sulphur Creek district (Peters, 1990, Percy and Petersen, 1990). Geochemical and isotopic data from these gold-depositing hot springs has provided a basis for understanding the genesis of the precious-metal deposits in the Clear Lake volcanic field (Peters, 1990,1991, Sherlock and Jowett, 1992, and Donnelly-Nolan and others, 1993), although there is no consensus on the source of the gold-mercury-bearing hydrothermal fluids. This paper reviews previous research on the hot springs and ore deposits and provides new data on the mineralogy of the McLaughlin deposit. Prospective terranes for further exploration for epithermal precious-metal deposits are delineated, based on a genetic model.

GEOLOGY

The Sonoma and Clear Lake volcanic fields are composed of numerous small to moderate volume volcanic centers that occur over a broad area of thin crust developed after subduction-related tectonism and volcanism ceased. The volcanism in these volcanic fields resulted from the influx of hot asthenosphere into the area previously occupied by the subducting slab termed the slab window (Fig. 1) (Dickinson and Snyder, 1979, Benz and others, 1992). The area above the slab window defines the broad area in which volcanic activity occurred and, in the case of the Clear Lake volcanic field it, it encompasses not only the Pliocene volcanic rocks of the Clear Lake area but also the cryptodomes and intrusions within the northern part of the Great Valley as well as the Pliocene volcanic rocks of Sutter Buttes. The age of the Sonoma volcanic field is late Miocene to Pliocene, and it occurs just to the south of the Pliocene to Holocene Clear Lake volcanic field. Although both fields are characterized by basaltic-andesite to rhyolitic flows, domes, tuffs and cones (Donnelly-Nolan and others, 1981), the Sonoma volcanic field is more silicic and contains a regionally extensive ash-flow sheet, the Miocene Sonoma tuff (Fox and others, 1985). Volcanic vents and edifices have not been documented in the Sonoma Volcanics because of widespread alteration, and because faulting associated with the San Andreas transform fault has disrupted the volcanic sequence. No plutonic equivalents of the Sonoma Volcanics are present at the surface but a large gravity and magnetic low in the central part of the volcanic field likely reflects a small batholith related to source of the Sonoma Tuff. In contrast, volcanic vents and edifices are well preserved within the younger and less tectonically disrupted Clear Lake volcanic field. A Pleistocene batholith emplaced at a shallow level occurs in the southwestern part of the Clear Lake volcanic field and The Geysers geothermal field is developed in the upper part of the batholith and overlying graywacke of the Franciscan assemblage (Thompson, 1989). This vapor-dominated geothermal system is the largest producing geothermal field in the United States. A magma body associated with the youngest volcanism in the Clear Lake volcanic field occurs on the north flank of the batholith and is the heat source for the Geysers field (Iyer and others, 1981).

Epithermal precious-metal and mercury deposits within the Sonoma and Clear Lake volcanic fields are hosted in Cenozoic volcanic rocks and the pre-Tertiary accretionary complex which forms the basement rocks of the volcanic fields. Mercury and precious-metal vein deposits in the Sonoma Volcanics have had only a small production in the past. The largest and most productive mercury and precious metal deposits occur in the eastern part

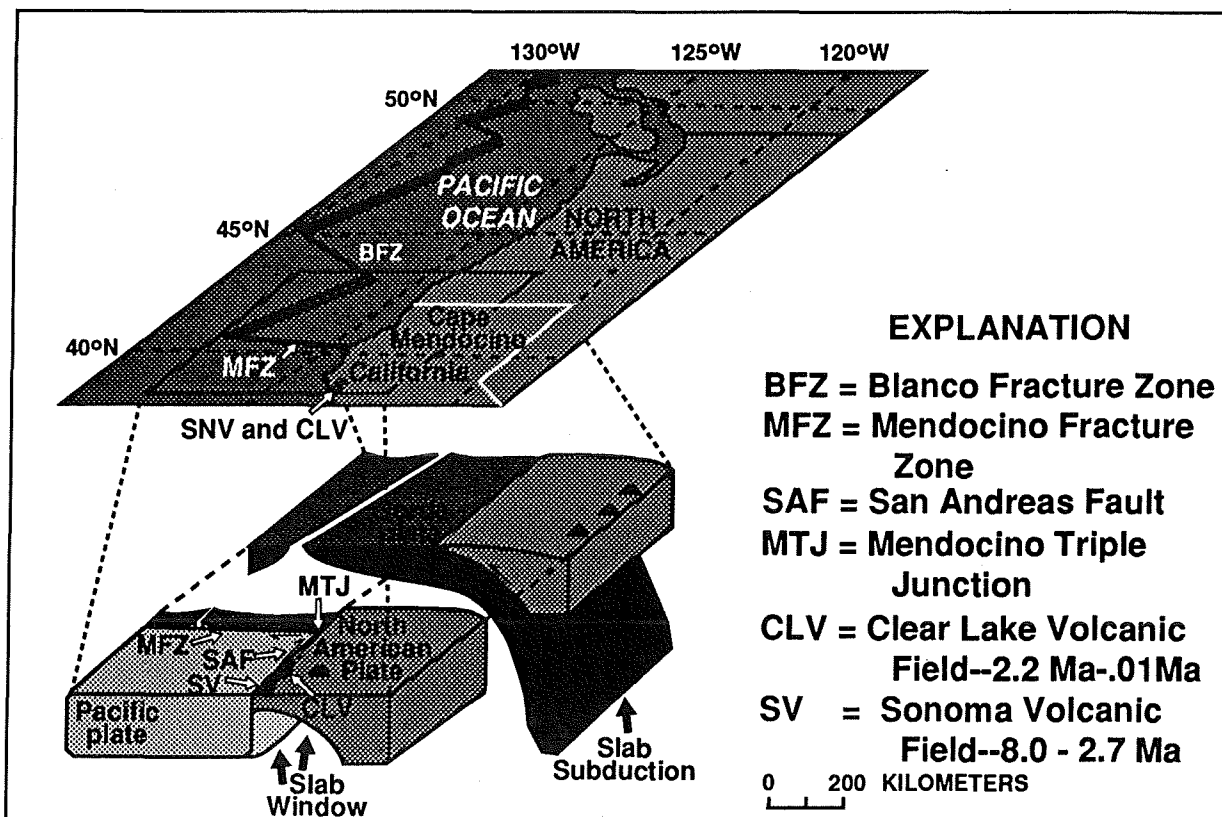


FIGURE 1. Tectonic and volcanic setting of the Sonoma and Clear Lake volcanic fields showing location of thin crust and hot asthenosphere above the slab window. Modified from Benz and others (1992)

of the Clear Lake volcanic field. Several hot springs in the Clear Lake volcanic field presently deposit mercury and gold and are located in the area of the largest gold and mercury deposits (Fig. 2). Mercury deposition is occurring at the Sulphur Bank mercury mine, the fifth largest mercury producer in the U. S. having produced 130,000 flasks of mercury. Fumarolic vents occur both above and below the level of the lake which fills the open pit developed for mining mercury and sulfur. Native sulfur, cinnabar, and pyrite are being deposited from a vapor-dominated geothermal system at this site (White and Roberson, 1962). These deposits contain no precious metals because only native mercury and H_2S can be transported in the vapor. In the water-dominated geothermal systems such as Wilbur Springs and other springs adjacent to the Cherry Hill gold deposit, mercury and gold are being deposited together (Peters, 1990, Percy and Petersen, 1990, Donnelly-Nolan and others, 1993). Mercury and gold are transported in a fluid containing high concentrations of H_2S and varying amounts of petroleum, CO_2 , and methane (Thompson, 1979, personal communication). The mercury deposits also commonly contain petroleum and pyrobitumen. The petroleum is derived from thermal degradation of organic matter in sedimentary rocks, and the CO_2 and methane are dissociation products of the polycyclic aromatic hydrocarbons (Peabody, 1989). The Cherry Hill, West End, and Manzanita gold deposit, located within the central part of the Sulphur Creek district, were previously mined for mercury and gold. The deposit consists of high-grade gold-quartz-adularia-carbonate veins

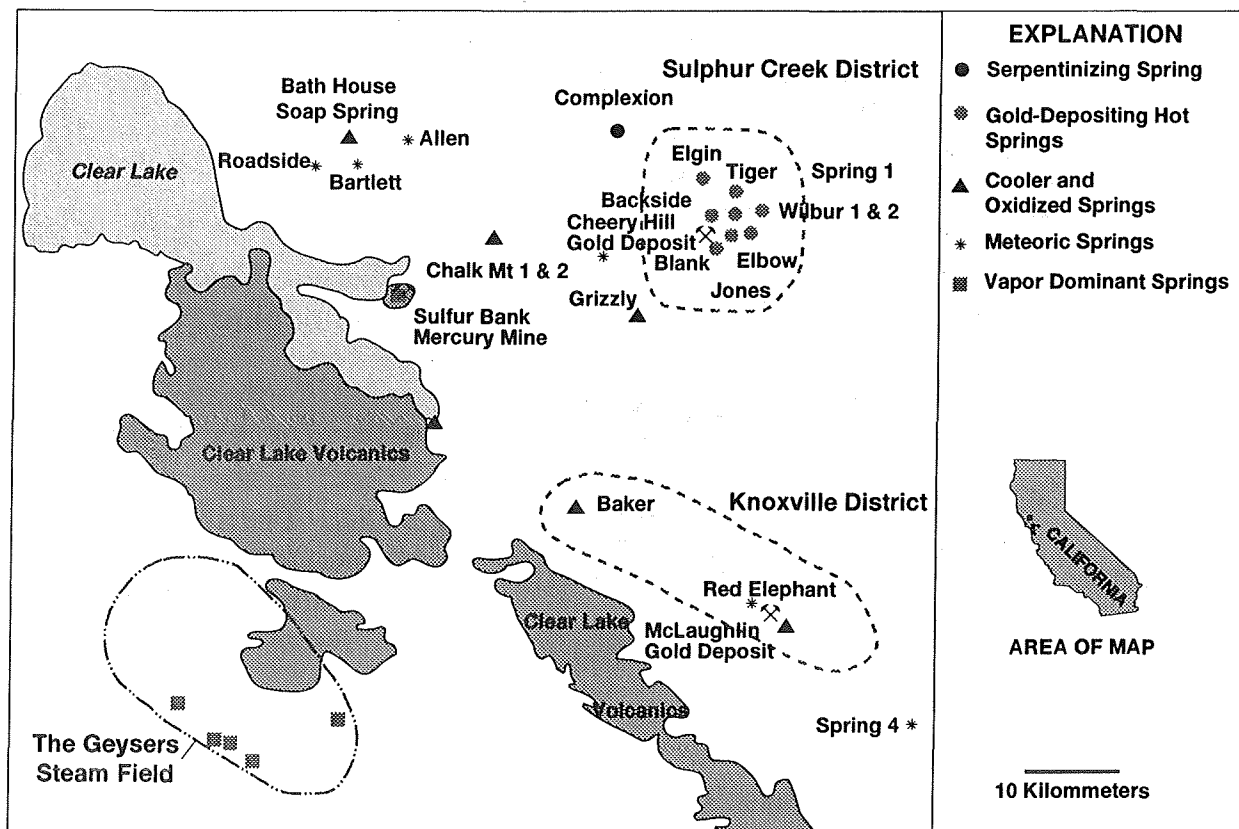


FIGURE 2. Location of mercury and gold deposits, hot springs, and the Geysers geothermal area in the Clear Lake volcanic field. Modified from Peters (1991).

containing abundant petroleum compounds. Hot springs adjacent to the deposit are actively depositing gold and reflect the waning stage of mineralization at this very young gold deposit (Pearcy and Petersen, 1990, Donnelly-Nolan and others, 1993).

The McLaughlin gold deposit, discovered in 1978 with initial reserves of 2.9 million oz of gold at a grade of 0.152 oz /ton, is economically the most important deposit in the Clear Lake volcanic field. Several andesitic vents, plugs, and dikes were emplaced at about 2.2 Ma along the Stony Creek fault zone and the gold-mercury hydrothermal system developed during this volcanic event and continued to at least 0.75 Ma (Lehrman, 1986). Warm springs depositing a travertine terrace on the east flank of the McLaughlin deposit may reflect the waning stage of the hydrothermal system. Prior to discovery of the gold deposit, the area was known as the Manhattan mercury mine and produced about 17,000 flasks of mercury. Large sinter terraces interbedded with hydrothermal explosion breccias hosted the mercury mineralization which consisted of cinnabar and native mercury. Mercury was also produced from the basal lithic tuffs of an andesitic vent termed the Johntown neck.

McLAUGHLIN GOLD DEPOSIT

Two distinct ore bodies occur within the McLaughlin gold deposit. The north ore body consists of several high grade chalcedony and quartz veins as well as a stockwork of veins hosted by siltstones of the Great Valley sequence and altered serpentinite. The south ore body also is composed of high grade veins but also contains a sheeted vein developed in the pressure shadow of a large basalt fragment within the serpentine melange (Lehrman, 1986). The sheeted vein is about 60 meters by 60 meters in width and is developed over a vertical interval of 130 meters and contains 721,000 ounces of gold, about 25% of the gold within the deposit (Lehrman, 1986). Crosscutting veins in the deposit are common and reflect multiple periods of fracturing and deposition of gold and silica.

Vein banding is defined by several silica phases which include white to clear opal, amber to brown opal, and clear to milky quartz and chalcedony. The amber to brown color of the opal results from petroleum deposited along with the opal. Deposition of petroleum-bearing opal was episodic and it is commonly interlayered with clear opal or quartz. The highest grades of gold typically occur within the petroleum-bearing opal. In some of the veins, petroleum occurs in sufficient concentration to fill large voids and vugs. These froth veins are common throughout many of the mercury deposits in the Coast Ranges of California (Bailey, 1959). Other phases particularly common in the petroleum-bearing veins are acicular stibnite crystals which occupy vugs that are partly filled with petroleum. The high content of petroleum indicates that the hydrothermal fluid was highly reducing and that the oxygen fugacity was buffered by $\text{CO}_2\text{-CH}_4$. Under these chemical conditions, gold is transported as a bisulfide complex. *

The texture of the petroleum-bearing opal is characterized by numerous oval voids ranging from 20 to 50 microns in diameter (Fig. 3). This texture does not occur in the clear quartz or chalcedony. The voids represent large fluid inclusions that contained fluid having a high content of petroleum and vapor composed of CO_2 and CH_4 . Gold commonly lines the circular voids within the opal, and larger gold grains are formed from the coalescence of gold-filled cavities (Fig. 4a). This is more clearly seen in the SEM back scatter image (Fig. 4b), where the gold is the highly reflective and outlines the oval void. Other phases which occur within the voids include pyrite, chalcopyrite, silver-antimony-zinc sulfosalts, barite, and various sodium-calcium-chloride silicate phases.

Gold also occurs in other sites within the petroleum bearing opal. A typical occurrence is for the gold to occur along primary vein banding as 2-4 micron-size grains which coalesce to form layers of dendritic gold (Fig. 5a, 5b). Gold also occurs in syneresis cracks which cut the primary banding in the opal (Fig. 6). Other phases which occur in the syneresis cracks include silver-antimony sulfide and pyrite. Dehydration of the opal to form syneresis cracks occurred very late in the vein paragenesis and indicates that some of the gold and sulfides were introduced after silica deposition.

Anhedral grains of gallium-indium-tin oxide (Fig. 7) occur as small, 1-4 micron size grains disseminated throughout the petroleum-bearing opal in veins from the north ore body. Nickel-oxide grains commonly occur as disseminated grains localized along fractures within the petroleum-bearing opal in both the north and main ore bodies. The occurrence of these phases is unusual in epithermal gold deposits. The close spatial association of these

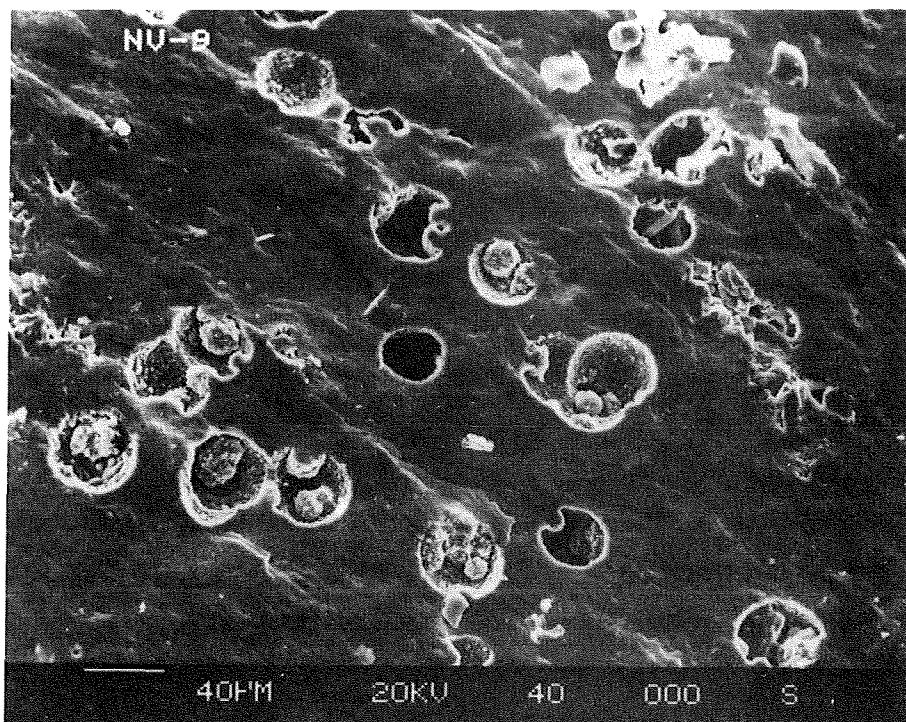


FIGURE 3. SEM photo of oval void texture in petroleum bearing opal from a gold vein in the north ore body at the McLaughlin gold deposit. Voids are large fluid inclusions up to 50 microns in diameter which were filled with fluid, petroleum, and vapor.

phases with the petroleum-bearing opal indicate that they were introduced along with the petroleum compounds. Nickel, cobalt, and other transition elements are important catalysts in the formation of petroleum, and these elements along with gallium, indium, and tin are commonly present in high concentrations in some petroleum fields as porphyrin complexes (Valkovic, 1978). Other elements such as mercury have been recognized to occur in very high concentrations in some of the gas and petroleum fields in California (Hinkle, 1971).

CHEMISTRY OF FLUIDS IN THE CLEAR LAKE VOLCANIC FIELD

Three distinct types of fluids have been recognized within the Clear Lake volcanic field based on chemical and isotopic analysis of oxygen and deuterium of hot-spring fluids (Peters, 1990, 1991, Sherlock, 1991, Sherlock and Jowett, 1992, and Donnelly-Nolan and others, 1993). One type of fluid is characterized by heavy oxygen and deuterium isotopes (Fig. 8) and moderately high concentrations of chloride and H_2S . Hot springs composed of this fluid are depositing Hg, As, Sb, Au and Ag at Wilbur Springs and other springs adjacent to the Cherry Hill gold deposit the Sulphur Creek district (Peters, 1990, 1991, Donnelly-Nolan and others, 1993). This fluid is derived from Late Jurassic to Early Cretaceous pore and connate fluid equilibrated with either oceanic sedimentary rocks of the

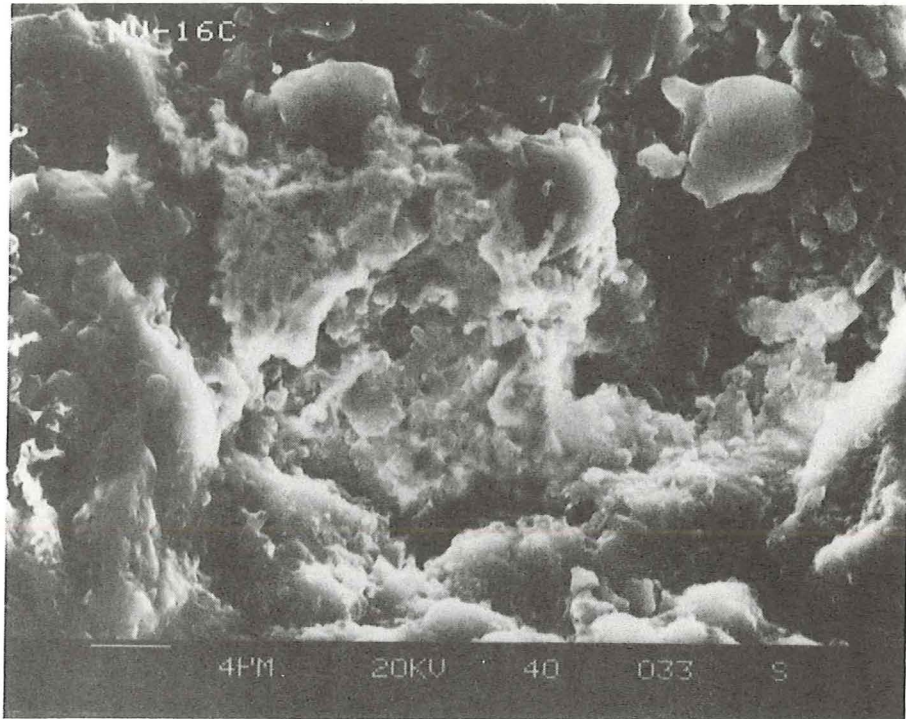


FIGURE 4 a. SEM image of gold within an oval void in petroleum bearing opal from a gold vein in the north ore body at the McLaughlin gold deposit.

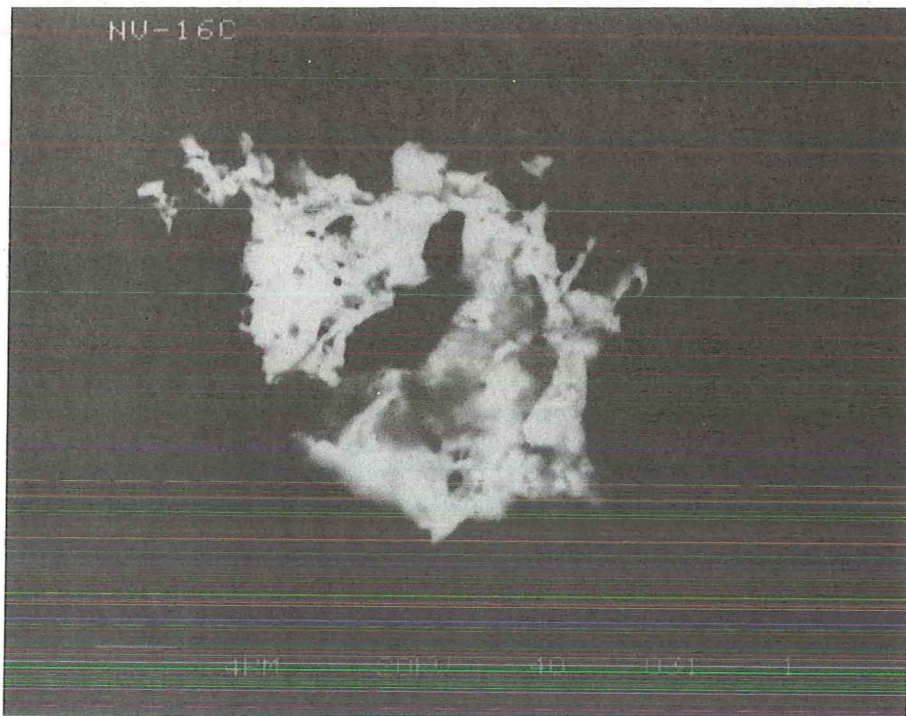


FIGURE 4b. Backscatter SEM image of gold grain, the white area, outlining oval void shown in figure 4a.

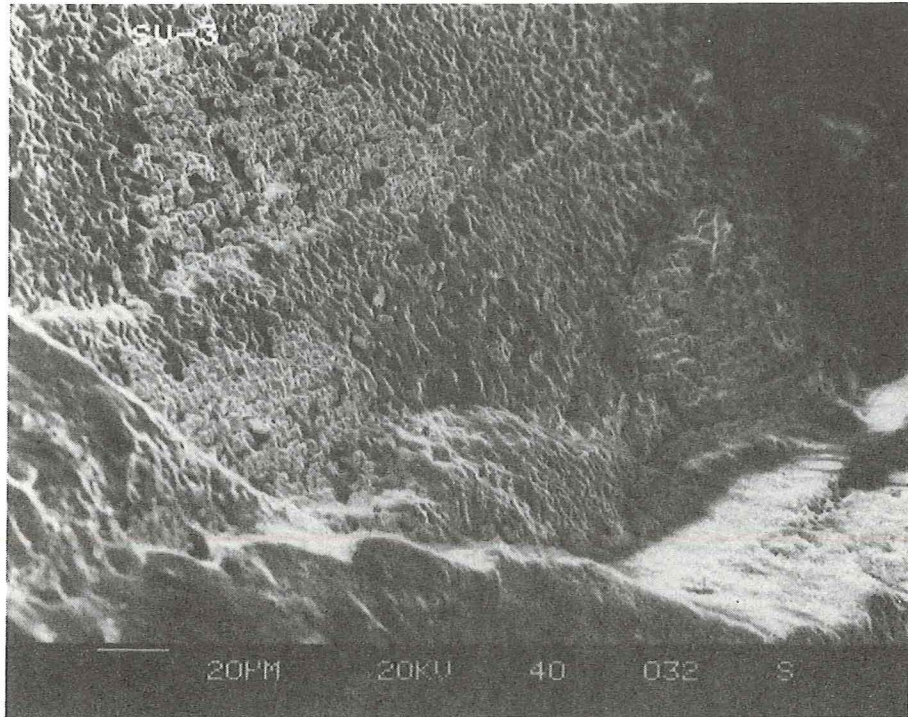


FIGURE 5a. SEM image of coalescing gold grains forming dendritic gold in the sheeted vein of the main ore body at the McLaughlin gold deposit. Three separate fracture surfaces are shown each displaying the surface of primary layering in the vein.

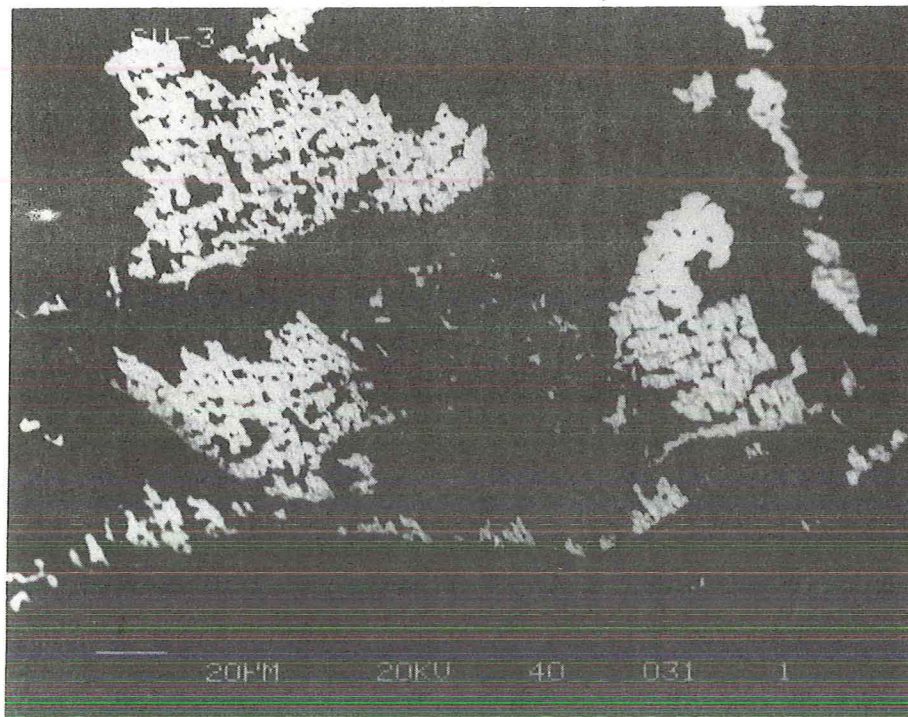


FIGURE 5b. Backscatter SEM image of figure 5a with gold delineated by the white areas and silica in dark gray.

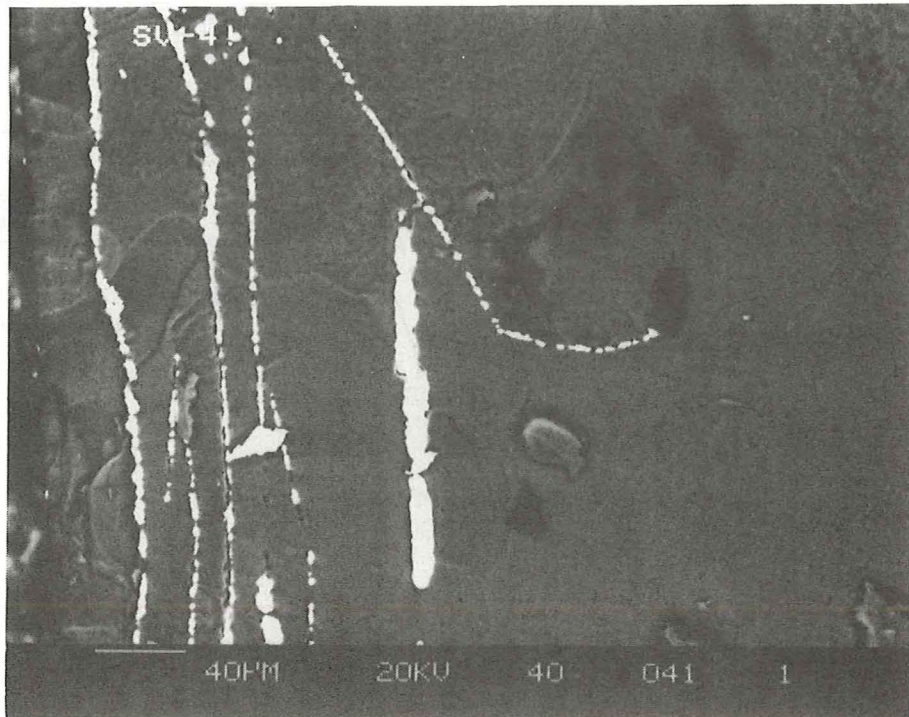


FIGURE 6. SEM image of gold and silver sulfosalts occurring along primary banding in the vein and in an arcuate syneresis crack which cuts the primary depositional banding in the sheeted vein of the main ore body at the McLaughlin gold deposit.

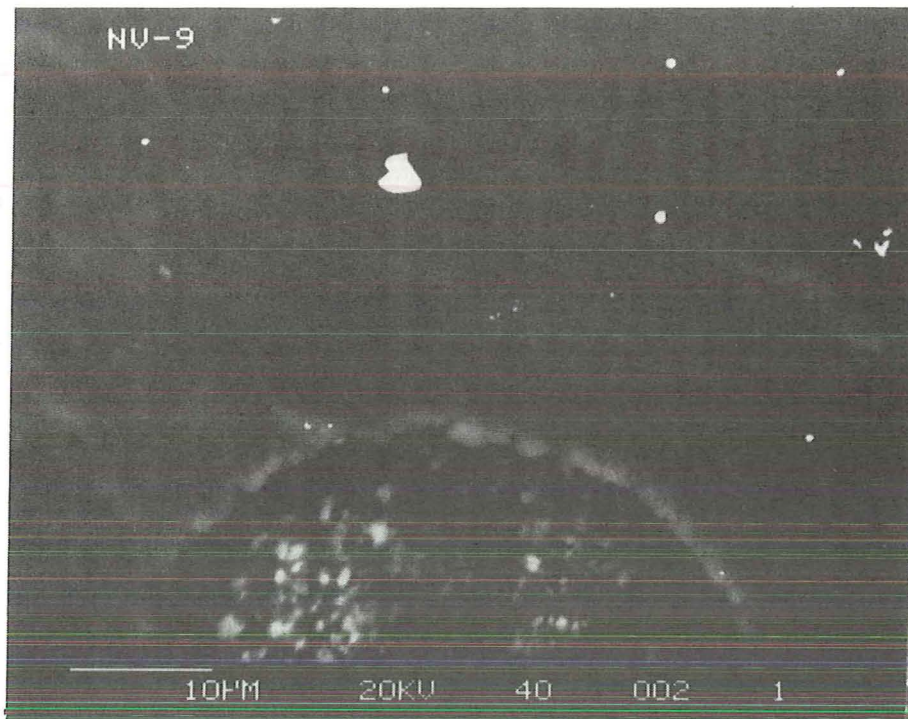


FIGURE 7. Backscatter SEM image of high-reflectivity gallium-indium-tin-oxide phase, bright-white grains, in petroleum-bearing opal, dark-gray area, from a gold vein in the north ore body at the McLaughlin gold deposit.

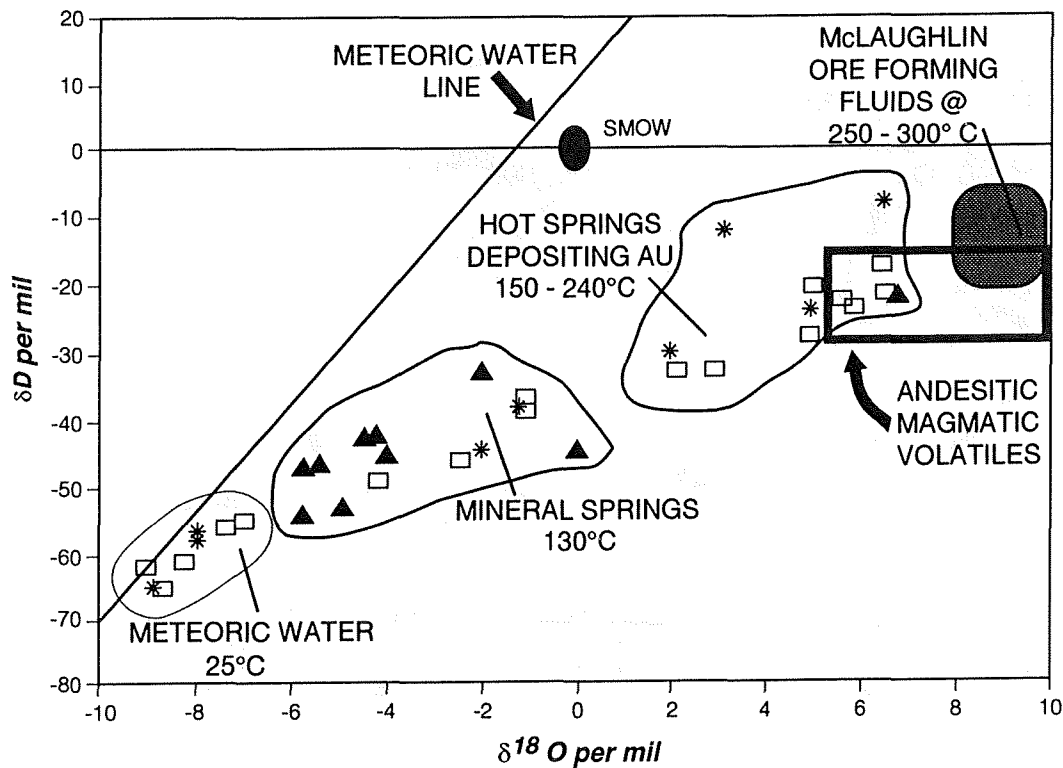


FIGURE 8. Plot of oxygen and deuterium isotopes in hot-spring fluids from the Clear Lake volcanic field modified from Peters, 1990, 1991, Sherlock, 1991, Sherlock and Jowett, 1992, and Donnelly-Nolan and others, 1993. Data for McLaughlin hydrothermal fluid from Sherlock and Jowett, 1992. Field of andesitic magmatic water from Hedenquist and Aoki (1990) and Giggenbach (1992).

Franciscan Complex (Sherlock and Jowett, 1992) or sedimentary rocks of Great Valley sequence (Donnelly-Nolan and others, 1993, Peters, 1990). Considering the complex geologic history of the Franciscan Complex, it is unlikely that original pore waters would be retained in these rocks. It is more likely that the source region for the fluid is the Great Valley sequence, a relatively undisturbed sequence of marine sedimentary rocks. Dating of iodine using ^{129}I isotope in hot spring water of this type of fluid indicates that the iodine source has a minimum age of 60-80 Ma which is consistent with the source being from the Great Valley Sequence (Fehn and others, 1992). The second type of fluid is meteoric water that has not equilibrated with country rocks and is characterized by light oxygen and deuterium isotopes and low concentration of chloride and H_2S (Donnelly-Nolan and others, 1993, Sherlock and Jowett, 1992, Peters, 1992). Moderately warm hot springs that are not depositing gold and mercury are a mixture of meteoric water and the isotopically heavy formation water (Fig. 8) (Donnelly-Nolan and others, 1993, Sherlock and Jowett, 1992, Peters, 1992). The third type of fluid is evolved meteoric water that has exchanged with rocks of the Franciscan complex during closed system boiling and characterizes the hydrothermal fluid at the Sulphur Bank Mine (Donnelly-Nolan and others, 1993).

Isotopic data on the sheeted vein from the main ore body at the McLaughlin gold deposit indicate that the hydrothermal fluid was isotopically heavy with respect to oxygen and deuterium and similar to the isotopically heavy

fluids depositing gold and mercury in the hot springs at Wilbur Springs (Sherlock and Jowett, 1992) (Fig. 8). Although the gold-depositing hot springs and the McLaughlin hydrothermal fluid have similar isotopic signatures, these isotopically heavy fluids can be generated by other mechanisms and do not necessarily reflect a unique single source for the fluid. Magmatic fluids derived from degassing andesitic magma are isotopically heavy (Hedenquist and Aoki, 1990, Giggenbach, 1987, 1992) and plot in the same field as the McLaughlin ore fluid (Fig. 8). It is thus possible that there is a component of magmatic fluid in the gold-depositing springs and at the McLaughlin gold deposit. The presence of several small volume andesitic intrusions and vents at McLaughlin indicate that a larger intrusion underlies the area and provided the heat source for the hydrothermal system. The large magnetic low between McLaughlin and the Sulphur Creek district (Griscom and others, this volume), may in part reflect the presence of a larger plutonic body. Andesitic vents emplaced along the Stony Creek fault at McLaughlin, such as the Johntown neck, provided a conduit for volatiles degassing from the shallow intrusion. This magmatic component would become entrained within the hydrothermal fluid composed of isotopically heavy gas-oil field formation water derived from the Great Valley sequence. The typical epithermal geochemical suite of Au, Ag, As, Sb, and Hg reflects the magmatic component in the hydrothermal fluid, and the petroleum, Ga, In, Ni, and Hg geochemical suite reflects the gas-oil-field formation-water component of the hydrothermal fluid. In the near surface, meteoric water would mix with these two isotopically heavy waters.

CONCLUSION

Evidence from hot springs and ore deposits in the Clear Lake volcanic field and ideas proposed by Donnelly-Nolan and others (1993) provide the basis for the following genetic model for the formation of mercury and hot-spring precious metal deposits. At convergent plate boundaries, such as in the Coast Ranges of California, pore and connate fluid trapped within oceanic sediments chemically exchanges with the host rocks during diagenesis and low-grade metamorphism to form moderately high-chloride, isotopically heavy oxygen and deuterium fluid. Thermal degradation of organic matter contributes petroleum compounds and high concentrations of CO₂, H₂S, and methane to the fluid. During faulting and folding of the Late Jurassic to Early Cretaceous Great Valley Sequence, this evolved formation fluid migrated into structural traps to form fluid-gas reservoirs with varying amounts of petroleum. These fluid-gas reservoirs were well developed throughout parts of the Central Valley of California and along the Coast Range Fault where it bounds the folded Great Valley sequence. During the late Miocene to Holocene, andesitic magmas were emplaced within a broad zone developed above the slab window as the end of Pacific plate subduction was marked by the passage of the Mendocino triple junction (Fig. 1). The Sonoma and Clear Lake volcanic fields developed within the strike slip and extensional fault zone associated with the San Andreas transform fault, while in the Central Valley of California andesitic intrusions as well as the Sutter Buttes dome field were emplaced. Tectonic activity temporally associated with the volcanism permitted movement of the gas-oil field fluid into major structures such as the Stony Creek fault. Hydrothermal systems developed in the vicinity of the andesitic intrusions emplaced along major structures and andesitic vents and associated faults provided a conduit for

volatiles degassing from shallow intrusions. This magmatic component was entrained within the hydrothermal fluid and was the source of the Au, Ag, As, Sb, and Hg. The elemental suite of Ga, In, Ni, Sn, Hg, and petroleum was introduced with the gas-oil field water derived from the Great Valley sequence. Mercury deposits with high contents of transition metals and petroleum formed from a hydrothermal fluid composed essentially of gas-oil field formation water. These mercury deposits would contain only low levels of precious metals. Precious-metal deposits formed where the magmatic component of the hydrothermal fluid was large, such as at McLaughlin where an intrusion and associated vents introduced a large magmatic component to the hydrothermal system. The McLaughlin gold deposit reflects the complex interaction of three types of fluid each transporting a different elemental suite: evolved gas-oil field formation water; magmatic from degassing andesitic magma; and near surface meteoric water.

Exploration for hot spring precious metal deposits in the Coast Ranges of California has focused on evaluating previously known mercury districts for their gold content and has met with limited success. Gold was recognized long ago in some of the mercury deposits and mined at the Manzanita mercury mine from 1865 to 1891, where about 3,000 oz of gold was recovered (Whitney, 1865, and Bradley, 1916). Although there is a close association of gold and mercury in some of the mercury deposits, only some of the mercury deposits have potential for epithermal precious-metal deposits. The genetic model presented above indicates that mercury deposits form along major structures where gas-oil field fluids are localized. These structures may also localize emplacement of andesitic magma and where this occurs, the hydrothermal system will have a precious-metal component and hot spring gold deposits may form in this volcanic-structural environment. Magmatic activity associated with the slab window not only occurs in the Coast Ranges but also occurs in the broad area of the Great Valley of California. This large area of the Central Valley is permissive for hot-spring precious metal deposits (Donnelly-Nolan and others, 1993). The most highly prospective areas include parts of the Great Valley sequence where blind thrusts and associated faults have been intruded by Pliocene to Holocene crypto-domes and intrusions.

REFERENCES

- Bailey, E. H., 1959, Froth veins, formed by immiscible hydrothermal fluids in mercury deposits, California: Geological Society of America Bulletin, vol. 70, no. 5, p. 661-663.
- Benz, H. M., Zandt, G., and Oppenheimer, D. H., 1992, Lithospheric structure of Northern California from teleseismic images of the upper mantle: Journal of Geophysical Research, v. 97, no. B4, p. 4791-4807.
- Bradley, W. W., 1916, The counties of Colusa, Glenn, Lake, Marin, Napa, Solano, Sonoma, Yolo: California Mining Bureau Fourteenth Report State Mineralogist, p. 173-370.
- Dickinson, W. R., and Snyder, W. S., 1979, Geometry of subducted slabs related to the San Andreas transform: J. Geol., v. 87, p. 609-627.
- Donnelly-Nolan, J. M., Hearn, B. C. Jr., Curtis, G. H., and Drake, R. E., 1981, Geochronology and evolution of the Clear Lake Volcanics: U. S. Geological Survey Professional Paper 1141, p. 47-60.
- Donnelly-Nolan, J. M., Burns, M. G., Goff, F. E., Peters, E. K., and Thompson, J. M., 1993, The Geysers-Clear Lake area, California: thermal waters, mineralization, volcanism, and geothermal potential: Econ. Geol., v. 88, p. 301-316.
- Fehn, U., Peters, E. K., Tullai-Fitzpatrick, S., Kubik, P. W., Sharma, P. Teng, R. T. D., Gove, H. E., and Elmore, D., 1992, ^{129}I and ^{36}Cl concentrations in waters of the eastern Clear Lake area, California: Residence times and source ages of hydrothermal fluids: Geochimica and Cosmochimica Acta, v. 5 p 1-19.
- Fox, K. F. Jr., Fleck, R. J., Curtis, G. H., and Meyer, C. E., 1985, Potassium-argon and fission-track ages of the Sonoma volcanics in an area north of San Pablo Bay, California: U. S. Geological Survey Map MF-1753.

- Fox., K. F. Jr., Fleck, R. J., Curtis, G. H., and Meyer, C. E., 1985, Implications of the northwestwardly younger age of the volcanic rocks of west-central California: *Geological Society of America Bulletin*, v. 96, p. 647-654.
- Giggenbach, W. F., 1987, Redox processes governing the chemistry of fumarolic gas discharges from White Island, New Zealand: *Applied Geochemistry*, v. 2, p. 143-161.
- Giggenbach, W. F., 1992, Isotopic shifts in waters from geothermal and volcanic systems along convergent plate boundaries and their origin: *Earth and Planetary Science Letters*, v. 113, p. 495-510.
- Griscom, Andrew, Jachens, R. C., Halvorson, P. F., and Blakely, R. J. 1993, Regional geophysical setting of gold deposits in the Clear Lake region, California, *in* J. J. Rytuba ed., *Active geothermal systems and gold-mercury deposits in the Sonoma-Clear Lake volcanic fields: California, Soc. Econ. Geol. Guidebook Series*, (this volume)
- Hearn, B. C. Jr., Donnelly-Nolan, J. M., and Goff, F. E., 1981, The Clear Lake volcanics: tectonic setting and magma sources: U. S. Geological Survey Professional Paper 1141, p. 25-45.
- Hedenquist, J. W., and Aoki, M., 1990, Meteoric interaction with magmatic discharges in Japan, and its significance regarding the potential for mineralization: *Symposium on high-temperature acid fluids and associated alteration and mineralization (Geological Survey of Japan)*, p. 63-73.
- Hinkle, M. E., 1971, Determination of mercury in crude oils: U. S. Geological Survey Professional Paper 750B, p. B171-174.
- Iyer, H. M., Oppenheimer, D. H., Hitchcock, T., Roloff, J. N., and Coakely, J. M., 1981 Large teleseismic P-wave delays in the Geysers-Clear Lake geothermal area: U. S. Geological Survey Professional Paper 1141, p. 97-116.
- Lehrman, N. J., 1986, The McLaughlin Mine, Napa and Yolo Counties, California *in* Precious metal mineralization in hot springs systems, Nevada-California. *ed.* J. V. Tingley and H. F. Bonham, Jr.: Nevada Bureau of Mines and Geology Report 41, pp. 85-89.
- McLaughlin, R. J., 1981, Tectonic setting of the Pre-Tertiary rocks and its relation to geothermal resources in the Geysers-Clear Lake area: U. S. Geological Survey Professional Paper 1141, p. 3-23.
- Peabody, C. E., 1989, Association of petroleum and cinnabar in mercury deposits of the California Coast Ranges: Ph. D. dissertation, Stanford University, Stanford, California, 256 p.
- Pearcy, E. C., and Petersen, U., 1990, Mineralogy, geochemistry and alteration of the Cheery Hill, California hot-spring gold deposit *in* Epithermal gold mineralization of the circum-pacific, geology, geochemistry, origin and exploration, II *editor* J. W. Hedenquist, N. C. White and G. Siddeley, *Journal of Geochemical Exploration*, v. 36, no 1/3, pp. 143-170.
- Peters, E. K., 1990, The aqueous geochemistry of the Clear Lake area, northern California, and its implications for hot-spring gold deposit. Unpublished Ph. D. dissertation, Harvard University, Cambridge, Massachusetts, 237 p.
- Peters, E. K., 1991, Gold-bearing hot spring systems of the northern Coast Ranges, California: *Economic Geology*, v. 86, p. 1519-1528.
- Sherlock, R. L., and Jowett, E. C., 1992, The McLaughlin hot-spring gold-mercury deposit and its relationship to hydrothermal systems in the Coast Ranges of northern California, USA: *in* Kharaka, Y. K., and Maest, A. S., *Water-rock interaction, Proceedings of the 7th international symposium on water -rock interaction*, v. 2, p. 979-982.
- Thompson, J. M., 1979, A reevaluation of geothermal potential of the Wilbur Hot Springs area, California: *Geothermal Resources Council, Transactions*, v. 3, p. 729-731.
- Thompson, R. C., 1989, Structural and intrusive rocks at the Geysers geothermal field: *Geothermal Resources Council, Transactions*, v. 13, p. 481-485.
- Valkovic, 1978, Trace elements in petroleum, Tulsa, Oklahoma: The Petroleum Publishing Company, 133 p.
- White, D. E., and Roberson, C. E., 1962, Sulphur Bank, California, a major hot spring quicksilver deposit: *in* Buddington Volume, *Geological Society of America*, pp. 339-357.
- Whitney, J. D., 1865, *Geological Survey of California: Geology*, vol. I, Report of progress and synopsis of the field work from 1860 to 1864, 498 p.

**EPITHERMAL PRECIOUS METALS DEPOSITS OF THE CALISTOGA MINING DISTRICT
NAPA COUNTY, CALIFORNIA**

Dean A. Enderlin

**Homestake Mining Company, McLaughlin Mine
26775 Morgan Valley Rd., Lower Lake, CA 95457**

ABSTRACT

The Calistoga Mining District, is one of three districts in the northern California Coast Ranges, where epithermal precious metals deposits have been economically mined. The district produced over 1.5 million ounces of silver (with lesser amounts of gold, copper and lead) intermittently over a 76 year period. The Palisade and Silverado mines were the two producers of the district.

Precious metals enrichment is associated with northeast-striking, en échelon quartz + chalcedony + adularia vein systems, hosted by flows and pyroclastic rocks of the Tertiary Sonoma Volcanics. Basement rocks are part of the Mesozoic and early Cenozoic Franciscan Complex, composed largely of tectonized marine sediments and dismembered ophiolite. Silver dominates gold by 74:1, and occurs in various sulfides, sulfosalts and selenides. Gold occurs in its native state, but is rarely macroscopic. In addition, this system is highly enriched in Cu, Sb, Zn, Pb, As and Ba, and contains anomalous concentrations of Se, Cd, Hg, Te, Ga, Tl, Mo and Bi.

Veins formed at +200 m depths, along dilational segments of northeast-striking (sinistral) conjugate Reidel shears, associated with a zone of San Andreas-style dextral wrench faulting. The zone of alteration and vein propagation is restricted to a corridor 1.5 km wide by 14.5 km long. This corridor appears to be structurally related to a local dilational jog in a 305°-striking dextral shear zone. The orientation of the optimal plane of extension was approximately 196° (right hand rule), dipping 74°. Because the volcanic pile has deformed as a homogeneous medium, a comparison of 595 vein and shear joint attitudes, taken in the Silverado and Palisade vein systems, provides a means of determining finite strain ellipsoid axes for vein formation. Based on these data, the orientation of Z is calculated to be 202°, plunging 18° and X at 106°, plunging 16°. Because of scatter in the data, the above axes are assigned error limits of ±15°. These values do not take into account the possibility of post-mineral rotation.

Fluid inclusion geothermometry indicates that this was a boiling system, with temperatures averaging 212° and 249° for the Palisade and Silverado veins, respectively. The mineralizing fluids were low salinity (~1.0 wt. % NaCl equivalent), NaCl-dominated, and possibly enriched in CO₂. They are believed to be evolved meteoric waters, chemically and isotopically similar to those of the Geysers and McLaughlin systems. Metals were presumably transported as bisulfide and (to a lesser extent) chloride complexes. Precipitation was triggered by CO₂ and H₂S partitioning in response to fault-induced increases in vertical permeability.

INTRODUCTION

The Northern California Coast Ranges have been the site of over one hundred and thirty years of sporadic mining activity. Mercury deposits were the primary focus of interest, although the region did not entirely escape the eyes of nineteenth century gold prospectors. Anomalous precious metals values, though not ubiquitous, have been recognized in association with some of the epithermal systems. Three mining districts in the region stand out as having significant precious metals production; the Knoxville (McLaughlin), Sulphur Creek (Wilbur Springs) and Calistoga districts. Ranking second of the three, in terms of production dollar value, Calistoga district represents a significant, yet poorly studied epithermal precious metals system. This paper presents the production and exploration history of the district, summarizes the results of past and present research on the deposits, and proposes a structural and geochemical model for the system.

The Calistoga Mining District is located in the vicinity of the town of Calistoga, at the head of the Napa Valley wine grape growing region in northwestern Napa County, California (Fig. 1). Precious metals mines and prospects are concentrated along the western flank of the Howell Mountains, a range of hills bounding the northeastern edge of the upper Napa Valley. The mines and prospects of the district extend along a 1.5 km wide, southeast-trending corridor, extending from the south peak of Mount St. Helena (elev. 1,220 m MSL) to Dutch Henry Canyon (elev. 150 m MSL), a distance of approximately 15 km. Mercury mining in the district was limited to two small mines, known as the Kellett and Yellowjacket mines.

EXPLORATION HISTORY

Exploration for precious metals in the region probably began in the early 1850's, inspired by the discovery of gold in the Sierra Nevada foothills. The lack of coarse placer gold in the northern California Coast Ranges undoubtedly quelled the interest of these early prospectors. The first discovery of Ag-Au deposits in Calistoga district reportedly occurred in the winter of 1858-59 (Menefee, 1873), coinciding with the discovery of the Comstock Lode in western Nevada. Increased public awareness of the occurrence of silver, stirred by the Comstock discovery, led to a silver "excitement" in this district, beginning in late 1859. Dozens of claims were staked in the vicinity of Mount St. Helena, and prospectors soon radiated outward from that point. The district was then known as the Buckeye Mining District (Calistoga having not yet been established). The excitement persisted through 1860, but quickly ebbed as reports of illegitimate assays spread. The influx of prospectors to the region did, however, result in important discoveries of mercury ore, including the X.L.C.R. deposit in the Knoxville Mining District (Menefee, 1873).

Prospecting and intermittent mining continued from the 1870's through the 1950's, with the intensity of activities directly associated with fluctuations in the silver price. The most active periods were the mid-1870's, late 1880's, late 1920's and the 1930's. Production records are incomplete, so the precious metals output of the district is unclear. The two mines of the district, the Palisade and Silverado, probably produced a total of 1.5 to 2.0 million ounces of silver and 12,000 to 15,000 ounces of gold (Davis, 1948; Swearingen, 1957).

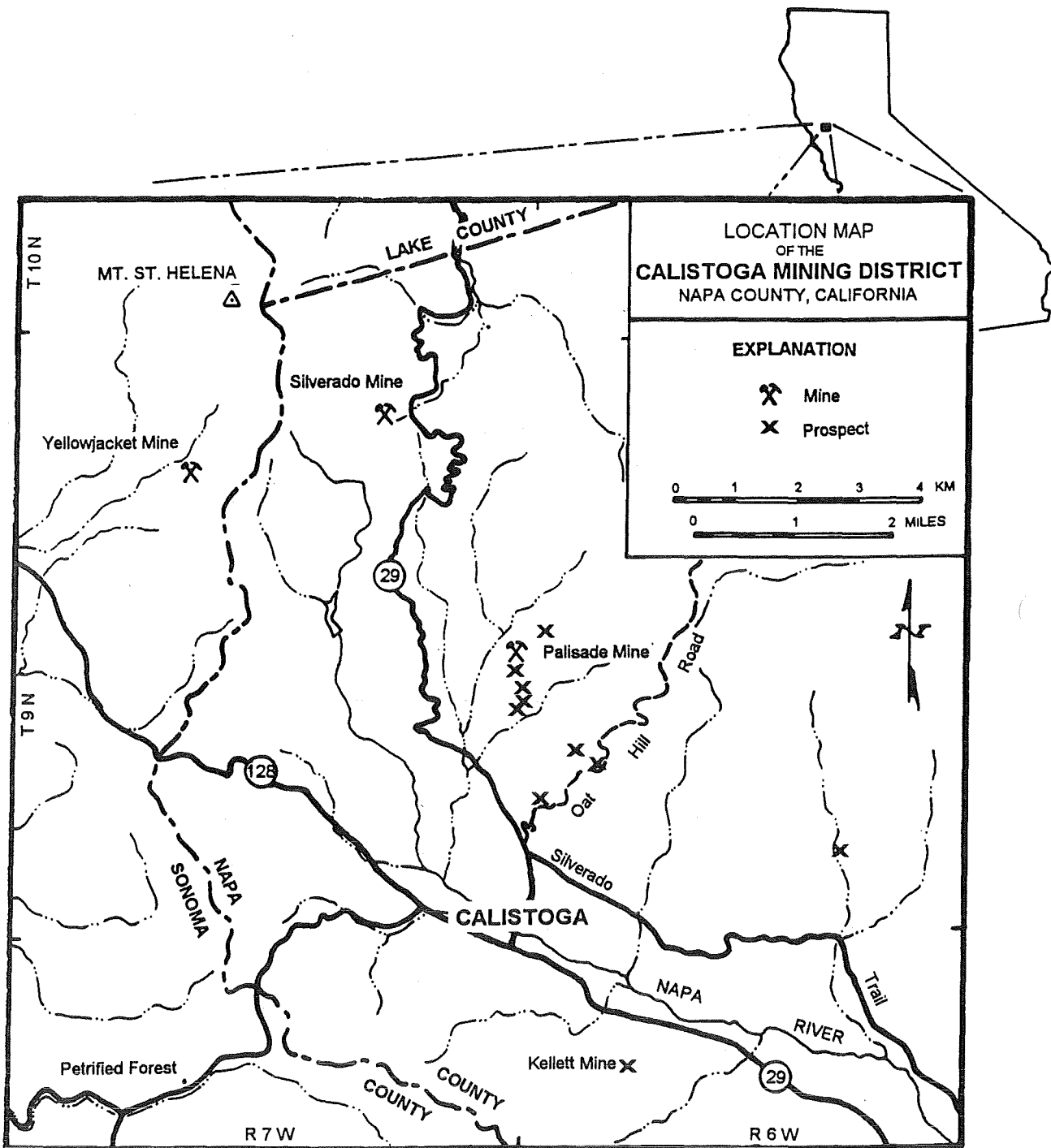


FIGURE 1. Location map of the Calistoga Mining District.

PRINCIPAL MINES AND PRODUCTION

The Calistoga Gold & Silver mine (Silverado) was the first producing mine of the district. Its popular name, Silverado, was taken from the boomtown that sprung up nearby in 1874. The mine was located on the southeast flank of Mount St. Helena, near the center of the south half of section 2, township 9 north, range 7 west, at elevation 820 m (Fig. 1). The heart of the mining activity was a northeast-striking vein system, known as the Monitor Ledge (Fig. 3). At its northern terminus, the ledge projected in bold relief, exposing approximately 60 vertical meters of the steeply dipping vein system. Production came from stopes off of two levels, driven southwestward into this face (Fig. 2). The strike length of the "pay-zone" was estimated at 137 m (Raymond, 1875), and based on the limits of the workings, its vertical extent was less than 120 m.

The original claim was staked in 1872 by Alexander Badlam Jr., a nephew of Calistoga's founder, Sam Brannan (Issler, 1948). The mine was brought into production in 1874, and operated intermittently until early 1876. Ore was processed by a ten-stamp mill, located 1.8 km southeast of the mine. The Washoe process (pan amalgamation) was used to extract the precious metals. Production was reportedly valued at \$93,000 in gold and silver from 2,300 tons of ore milled during this period (Irelan, 1890).

The mine was reopened by the Silverado Mining Company in 1890. The renewed activities concentrated in the extension of an old cross-cut, driven about 60 m below the 1870's workings, but no ore was produced. The Mount St. Helena Mining Company took control of the property in 1901, and received patent to two claims in 1905. In 1902, they reportedly shipped 1000 tons of old dump material (assaying \$1.10 per ton gold, and \$2.65 silver) to the Copper King Smelting Company, Contra Costa County, California (Bradley, 1915). That same year, 34 tons of sorted ore were also shipped to the Selby smelter in Contra Costa County (Bradley, 1915). Two railroad car loads of ore, reportedly netting \$42 per ton, were shipped to the Mountain Copper Company smelter in Contra Costa County in 1918 (Hamilton, 1921), and at least one other car load was shipped from Calistoga in 1919. No other production is recorded, although an attempt was made to reopen the mine in conjunction with operations at the Palisade mine in 1930. The mine is now a part of the Robert Louis Stevenson State Park.

The other producing silver-gold mine of the district was the Palisade mine. It was located 4.3 km southeast of the Silverado mine (Fig. 1), in the northeast quarter of section 24, township 9 north, range 7 west, at elevation 213 m. Mining activity at the Palisade mine focused on two northeast striking veins, known as the Easley and the Palisade (Fig. 3). The Easley vein was considered the "main vein" of the mine (Grigsby, 1923).

The original Palisade mine claim group consisted of ten claims plus other landholdings. The two most important claims were the Old Discovery (Palisade) and Ida Easley. The Palisade claim was originally staked in November 1876, by James C. Bivens and Robert F. Grigsby. It was relocated and named the Old Discovery in 1882, by John J. Johnson, and patented in 1887. The Ida Easley claim was staked in October 1876, by W. Hugh Easley and James C. Bivens, and was patented in 1889.

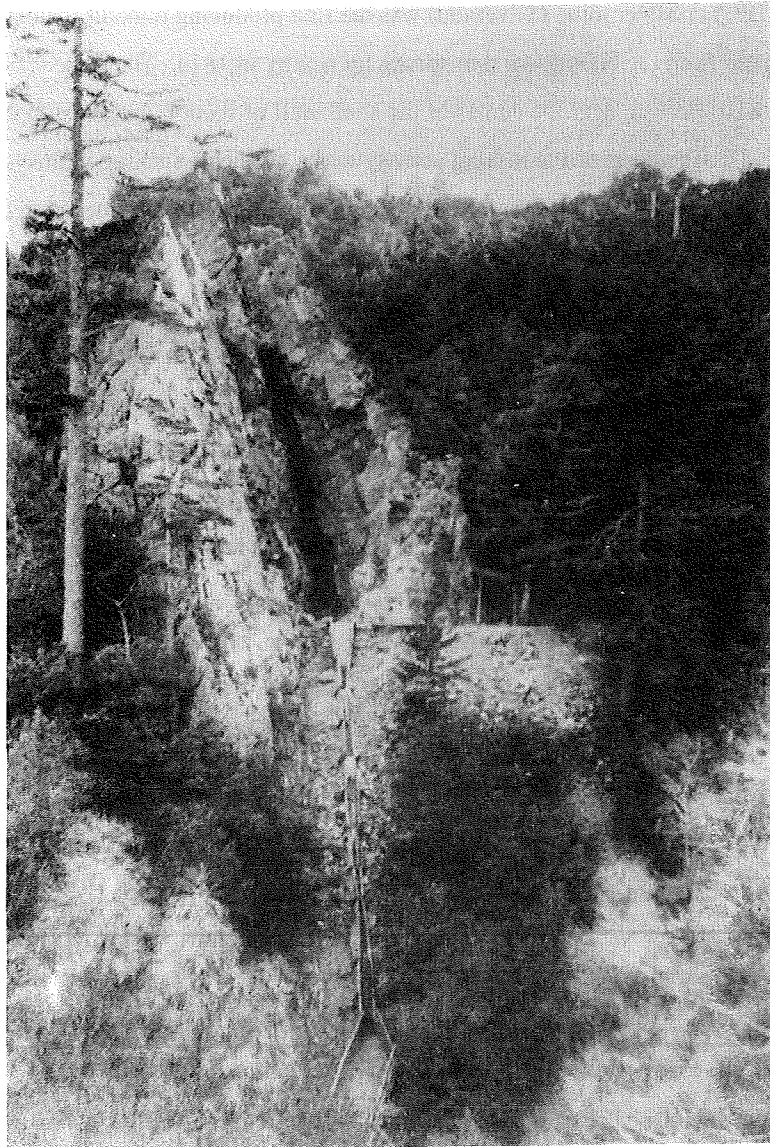


FIGURE 2. Open cut and ore chute on the Monitor Ledge, Silverado mine, circa 1900. View is looking southwest. From Osbourne, 1911.

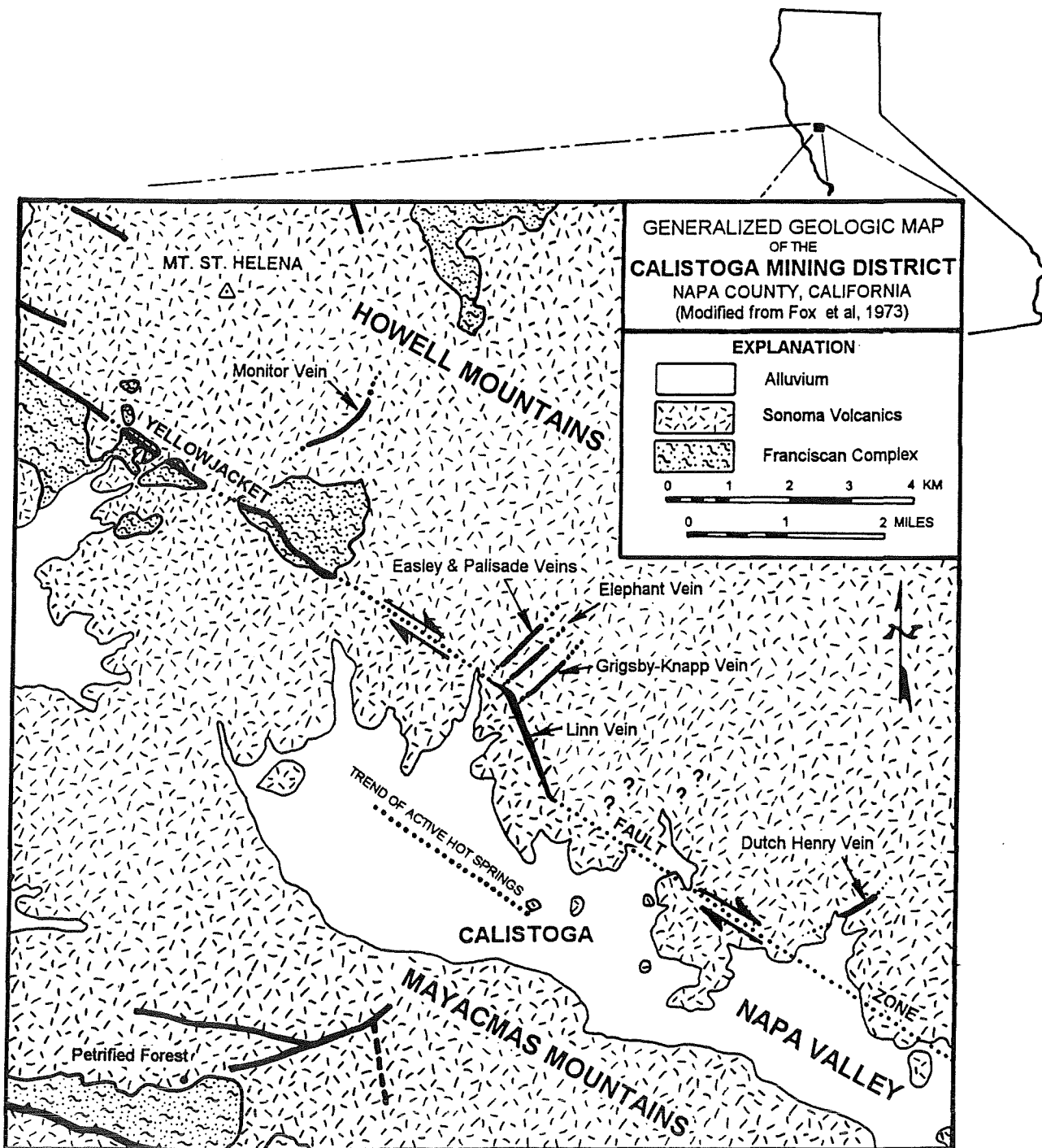


FIGURE 3. Generalized geologic map of the Calistoga Mining District, Napa County, California.

Test ore shipments from the Ida Easley and the neighboring Twin claim were made to the Selby smelter as early as 1880 and 1881. Although the results of the tests were reportedly favorable, title disputes over the claims impeded these early attempts to open the mine. In 1882, control of the most important claims of the district was secured by Robert F. Grigsby. Grigsby organized the Palisade Mining Company, with partners John J. Johnson and James Bain. In 1888, after several test ore shipments to Nevada and Bay Area smelters, the Palisade Mining Company constructed a mill, using machinery from the old Calistoga (Silverado) mill on Mt. St. Helena. To enhance silver recovery, a White's rotary chloridizing furnace was added to the circuit. Grigsby and his partners operated the mine through 1892, when depressed silver prices and the death of Grigsby's son in a mill accident forced the mine to close. The property remained idle for three decades.

In 1924, the property was leased to the newly organized Palisades Mining Company. Initial activities focused on reworking of the old dumps. Four railroad car-loads of dump material, shipped to the Kennett smelter (Shasta County) in early 1925, reportedly netted \$300 per car. During the process of rehabilitating the old mill in October 1925, a fire broke out and consumed the structure. It was rebuilt the following year, and was operated through 1928. The new mill used the Vandercook mercuric-cyanide process.

Operations at the Palisade mine changed hands repeatedly in the following years, reflecting the marginal economics of the period and difficulties in maintaining mill throughput. The Banner Development Company operated the mine from 1929 through 1930, using a six-cell Kraut flotation circuit (Averill, 1929). Concentrates were shipped to the Selby smelter. A receiver operated the property for a short period in 1931 (Davis, 1948). The list of operators that followed included the Calistoga Mining and Development Company (1933-1934), Coast Range Mining Company (1935-1937), Graham Loftus Oil Corporation (1937-1941), and Helena Consolidated Mines (January, 1941-August, 1941). The Palisade mine closed in August 1941, due to materials shortages and wartime labor demands. The mill building and all equipment were dismantled and removed in the following months.

A last attempt was made to reopen the mine in the late 1950's. A 50 ton flotation plant was installed, and the stopes above the mill level were evaluated for mining. The effort was performed on a small scale with limited capital, and no production resulted. The mill burned in 1964.

The bulk of the production at the Palisade mine came from the Easley vein. During the life of the mine, seven major levels were developed on it. The first, or mill level, was a 427 m long, Z-shaped tunnel, connecting the original surface hoisting works in King Canyon with the mill in the canyon to the north. The original (1885-1892) mine stopes were developed from this and from the 160 ft. (49 m) level, the latter accessed via a vertical shaft. The main stope was off the 160 ft. level, measuring 213 m long, 1.2 m wide, and extending 52 m on dip (Kellett, undated). These stopes yielded nearly \$300,000 in gold and silver (Davis, 1948). The ore averaged \$24.50 per ton, with the gold portion valued at \$3 to \$4 (Grigsby, 1923).

The 270 ft. (82 m), 400 ft. (122 m), 600 ft. (183 m) and 700 ft. (213 m) levels were added in the period from 1925 to 1941. Ore was hoisted to the mill level via a central winze, inclined westward along the Easley vein. Stopes were developed from all levels. Ore from the 700 ft. level was reportedly low grade (Crutchfield, 1953). The poor ore grades, combined with disappointing exploratory drilling results, persuaded the operators not to develop

deeper levels.

Incomplete state production figures for 1925 through 1941 (1936 and 1940 unavailable) report \$684,669 in silver and \$292,795 in gold produced from the Palisade mine in that period (Davis, 1948). U.S. Bureau of Mines records indicate that the mine also produced 65,001 pounds of copper and 768 pounds of lead (Swearingen, 1957). From 1937 to 1941, the average ore assay was approximately \$12.00 in silver and \$2.00 in gold per ton (Crutchfield, 1953).

GEOLOGIC SETTING

Calistoga lies within the Santa Rosa structural block (Fox, 1983) of the Coast Ranges geomorphic province. The local geology is dominated by Tertiary volcanics, covering a highly deformed Mesozoic or early Cenozoic basement (Fig. 3). Both rock packages have been deformed in the San Andreas transform fault system. The most obvious local physiographic feature related to this deformation is the Napa Valley, a structural basin (graben) formed by syn- and post-volcanic transtensional downwarping along Quaternary faults and folds.

The basement rock is part of the Franciscan Complex, a collection of complexly tectonically and positionally juxtaposed masses of moderately metamorphosed marine sediments with subordinate amounts of greenstone and chert (Berkland et al., 1972; McLaughlin, 1977). Minor amounts of limestone, blueschist, serpentinite, amphibolite and eclogite are also present, with the high grade metamorphics generally confined to zones of mélangé (McLaughlin, 1977). The Franciscan Complex is the product of tectonic and sedimentary processes in the trench environment of an obliquely convergent Mesozoic and early Cenozoic subduction zone. It may be the product of several episodes of structural aggregation, so its age varies from place to place (Fox, 1983). Locally, it is assigned an age no younger than Eocene, and is possibly pre-Tertiary (Fox, 1983). Where exposed in local erosional windows through the overlying volcanics, the Franciscan basement consists of disrupted graywacke-rich turbidite sequences and ophiolitic material dominated by serpentinitized peridotite. Compiled regional geology (Fox et al., 1973; Wagner et al, 1982) reveals a well defined northwest linearity of the serpentinite belts in the Franciscan. Locally, the most notable of these is a belt exposed on the southwest flank of Mount St. Helena (Fig. 3), in the vicinity of the Yellowjacket mercury mine (3.2 km northwest of the Palisade mine). A similar serpentinite body in Conn Valley (20 km to the southeast), lies on the same trend, and presumably connects with the former beneath the Tertiary volcanic cover. This belt parallels the axial trend of the upper Napa Valley graben (Fig. 3), as well as nearby minor fold belts in the Howell Mountains.

Miocene-Pliocene volcanics in the Calistoga area are part of the Sonoma Volcanics, as named by Weaver (1949). The erosional remnants of the field span a northwest-aligned belt 90 km long and 30 km wide (Fox, 1983). Calistoga lies at the northwest fringe of the field. Several attempts have been made to divide the volcanic field into various members (Weaver, 1949; Osmont, 1905), but the complex lithologic and temporal variations make simple subdivisions inappropriate. Overall, it can be said that the Sonoma Volcanics underwent a gross evolution from mafic flows to silicic volcanoclastics, with the youngest units lying in the Calistoga area. Reported K-Ar age

determinations range from 8.9 ± 4.5 m.y. to 2.9 ± 0.2 m.y., with the youngest examined unit being a welded tuff capping Mount St. Helena (Mankinen, 1972).

In the area of Calistoga Mining District, three distinct episodes of volcanism are evident. The earliest generation is characterized by pumiceous and lithic-rich pyroclastics, some appearing water-lain. Being the basal unit in the local volcanic pile, it hosts widespread fossil flora, including the Petrified Forest of California (3.5 m.y. K-Ar age by Everndon and James, 1964), and rare fossil fauna. The lithic component includes a variety of mafic Sonoma Volcanic fragments and rock of the Franciscan assemblage. While widespread in the Mayacmas Mountains, west of Calistoga, there are only scattered exposures of these deposits on the flanks of the northern Howell Mountains, based on mapping by Fox et al. (1973).

Local andesitic eruptions appear to have been synchronous with, or closely preceded, the emplacement of the pumiceous, lithic-rich pyroclastics. A thick sequence of andesitic flows and coarse pyroclastic rocks of this generation is exposed in an erosional window along the flank of the Howell Mountains immediately north of Calistoga. Where the andesite sequence is covered by younger volcanics, east of Calistoga, its persistence is clearly expressed by a southeast-trending positive gravity anomaly identified by Chapman et al. (1982). These andesites are typically highly propylitized, and form poor outcrops. No age determinations are currently available.

The second episode of volcanism is represented by widespread silicic tuffaceous deposits. This sequence is the product of numerous explosive eruptions and minor flows, apparently emanating from a variety of eruptive centers. It includes both proximal and distal vent facies pyroclastics, complexly commingled due to redistribution by successive eruptions. Rhyolitic tuffs, tuff breccias and flows dominate the lower part of this sequence. Higher in the pile, agglomerates, lahar deposits and welded tuffs dominate. The lahar deposits and agglomerates contain as much as 80% vitrophyre, the increased proportion of glass probably representing the degassed culmination of an eruptive cycle. Rhythmically bedded tuffaceous sandstone is also associated with this sequence in at least one locality north of Calistoga (Crutchfield, 1953). Deposits emplaced in the second episode of volcanism are extensive in the northern Howell Mountains. They also constitute the bulk of the volcanic pile forming Mount St. Helena. Only one K-Ar age, from welded tuff on Mount St. Helena (previously noted), is reported for rocks of this generation near Calistoga.

The third episode is characterized by renewed andesitic volcanism. Eroded andesitic intrusives and flows are scattered through the Howell Mountains north of Calistoga, with several displaying well-developed columnar joint patterns. Their cross-cutting and/or superpositional relationship with the second episode volcanics confirms their placement as the youngest units in the local volcanic succession. No age determinations are available.

Mild syn- and post-volcanic deformation is apparent throughout the district, but clear interpretations are elusive due to the difficulties in correlating volcanic units. Gravity data and drill logs from geothermal wells in the Calistoga area offer a glimpse at the degree of deformation. These data support the interpretation of the Napa Valley as a structural basin or series of linked structural basins. The upper Napa Valley, which follows a more westerly trend than its lower (southern) extremity, is a broad asymmetric syncline plunging to the southeast (Taylor, 1981). The deepest portion of the basin lies along the western flank of the valley, based on interpreted gravity data compiled

by Chapman et al. (1982). The volcanic-alluvial pile thickens to at least 600 m beneath the valley floor at Calistoga (based on well logs) and then abruptly thins and is elevated in the Mayacmas Mountains that form the western flank of the valley. It is likely that this 760+ m step in the paleosurface is the result of displacement along a northwest-striking marginal growth fault system underlying the western valley floor. This form of deformation is consistent with San Andreas-style transtensional forces and crustal thinning above a post-subduction asthenospheric "slab window" (Dickinson and Snyder, 1979). The normal fault displacement may well have been syn-volcanic, as is the case with the structurally similar Clear Lake basin (Hearn et al., 1988), 40 km to the north.

Geothermal activity appears to have closely followed the cessation of local volcanism. An early period of geothermal activity is indicated by the precious metals vein systems of the district, and a moderate-temperature geothermal system persists to the west of the older deposits. The early systems were active around 2.6 to 1.4 Ma, based on K-Ar age determinations of vein matter (McLaughlin and others, this volume). The present-day system extends along a northwest-striking linear trend, controlled by inferred deep-seated fault conduits disrupting the bedded basin sediments and pyroclastics (Taylor, 1981).

STRUCTURE AND VEIN GEOMETRY

Vein geometries associated with the silver-gold deposits are related to a zone of San Andreas-style dextral shear. The controlling shear system is poorly expressed in the volcanic pile, but the most likely candidate appears in the Franciscan basement as a near vertical serpentinite belt bearing 305° (right hand rule). This belt, herein referred to as the Yellowjacket fault zone (Fig. 3), projects beneath the Howell Mountains on the east flank of the Napa Valley, and is exposed in erosional windows near the Yellowjacket mine and Conn Valley.

En échelon argillic alteration zones and siliceous vein systems occupy the volcanics adjacent to the projection of the controlling shear system, forming a mineralized corridor approximately 1.5 km wide and at least 14.5 km long. The veins typically strike northeasterly, and occur at irregular intervals along the northwest trend. An exception to the typical orientation is the northwest-striking Linn vein system, which extends southeastward from the vicinity of the Palisade mine, for a distance of about 2,000 m (Fig. 3).

Important northeast-striking vein systems in the corridor include (from north to south) the Silverado (Monitor), Easley, Palisade, Elephant (Old Discovery), Grigsby-Knapp, Manuel, Sunnyside and Dutch Henry veins. Two of these, the Manuel and Sunnyside, are reported in historical accounts, but have not been investigated by the author. The Silverado and Palisade veins have been studied in detail, and lower hemisphere (Schmidt) stereograms for each are included in Figures 4 and 5.

Because of its excellent exposure, the Silverado vein system offers the best opportunity for structural analysis. The trend of this sinuous vein swarm is traceable for about 760 m on the south flank of Mount St. Helena. The veins pinch, dilate and splay according to changes in strike. Maximum dilation occurs along more north-northeast striking segments (typically 190° to 205° strike, dipping 65° to 75°). The open cut at Silverado was developed in one of these dilational segments, where the mined width of the vein swarm was 1.8 to 7.6 m

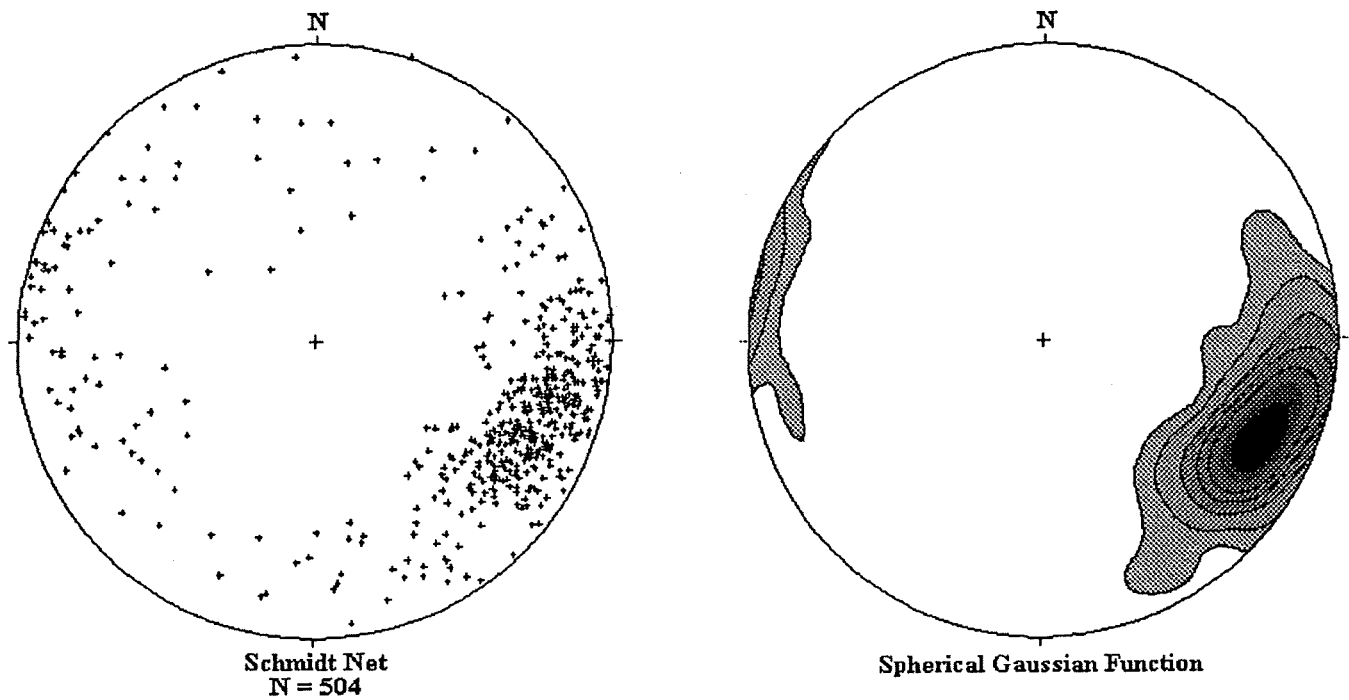


FIGURE 4. Stereogram set showing Silverado vein and shear-joint poles (contoured and uncounted). Contours represent increments of 2% of 1% area, using Spherical Gaussian Function.

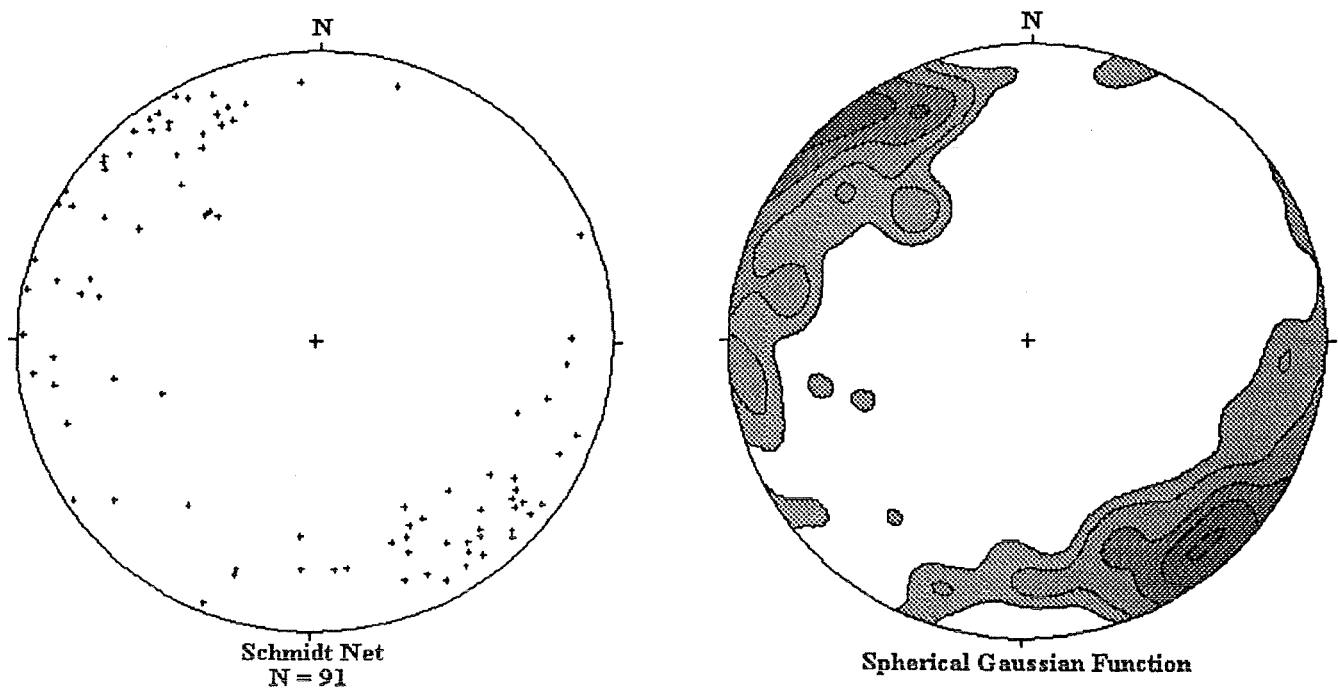


FIGURE 5. Stereogram set showing Palisade mine vein and shear joint poles (contoured and uncounted). Contours represent increments of 2% of 1% area, using Spherical Gaussian Function.

(Raymond, 1875; Hamilton, 1916). The average vein and shear-joint orientation in the walls of this stope is 205° , dipping 68° ($n=182$). Strikes of veins and shear-joints along the entire trend ($n=504$) undulate about a common axis, striking $\sim 335^\circ$ and plunging $66^\circ (\pm 15^\circ)$.

Palisade mine structural data is sparse. Underground, the average strike of the developed portions of the Easley and Palisade veins was 186° (Averill, 1929). Where mined, the Easley vein ranged from 1.2 to 7.3 m wide and dipped 63° to 75° west (Hamilton, 1916; Averill, 1929). The Palisade vein reportedly averaged 1.2 m in width, dipping 57° west (Averill, 1929). A diffuse set of quartz stringers of the Palisade set, is exposed in outcrops near the Palisade mine shaft. The attitudes of these stringers ($n=91$) are nearly parallel with the east-northeast striking (pinch) segments of the Silverado vein set, implying that the two deposits are structurally similar (Figs. 4 and 5). The more northerly attitudes of Palisade mine veins associated with the mined ore shoots (presumably dilational) are also consistent with observations made at Silverado.

Dilation on north-northeast striking segments and pinching on east-northeast striking segments of the Palisade and Silverado vein systems is indicative of sinistral shear along the vein trends. The average strike of the plane of maximum dilation in these systems is approximately 196° , dipping 74° , based on combined data from the mine stopes. This strike corresponds closely to dike trends (extensional planes) measured by Fox (1983). It can be considered the approximate orientation of the Y - Z plane of the finite strain ellipsoid ($X>Y>Z$) extant during vein emplacement, assuming that post-mineral rotation has not taken place. The Y strain axis, derived by measuring the axis of vein girdling, lies at $\sim 335^\circ$, plunging $66^\circ (\pm 15^\circ)$. The derivation of the Y strain axis, combined with the average plane of extension, fixes the Z (contractional) strain axis at $\sim 202^\circ$, plunging $18^\circ (\pm 15^\circ)$ and the X (extensional) strain axis at $\sim 106^\circ$, plunging $16^\circ (\pm 15^\circ)$. Because these veins are the product of simple shear, the principal stress and finite strain ellipsoids are only coaxial along their respective intermediate axes, s_2 and Y . It is likely that the Z and X finite strain axes have been rotated clockwise, with respect to their original principal stress counterparts, s_1 and s_3 , due to torsional forces associated with wrench faulting. The amount of rotation is probably not great, given the relatively short duration of the vein-forming episode and apparently limited post-volcanic offset along the Yellowjacket fault zone. Therefore, it can be concluded that the orientation of the maximum principal stress (s_1) at the time of vein formation, was directed northward or north-northeastward. These data and interpretations support and augment structural observations made by Fox (1983), and confirm that these veins formed in response to stresses related to the San Andreas wrench fault system. Under Fox's adaptation of the simple shear model, the northeast-striking faults hosting vein systems would be en échelon conjugate Reidel (R') shears.

The Linn vein system follows a strike that is unique among vein sets of the district. It is the most massive body of siliceous veining and brecciation exposed in the district, and is also mineralogically unusual. At its widest point (about 600 m south of the Palisade mine shaft), the Linn vein system is 15 to 30 m wide. The Linn vein system, as a package, strikes 330° , and is vertical or steeply dipping to the northeast, however, vein orientations within this zone are not clear. It lies immediately west of the Easley, Palisade, Elephant and Grigsby-Knapp vein systems, forming an apparent barrier, across which the other veins do not pass (Fig. 3). Unlike the other vein systems of the district, the Linn vein system is dominated by hydrothermal breccia, and rarely displays planar veins.

Being of a more northerly strike than the overall strike of the Yellowjacket fault trend, it is conceivable that the Linn vein system formed along a strike inflection of the latter. Dextral motion on the Yellowjacket trend, would have a dilational effect on such a segment.

The northeast-striking conjugate Reidel shears (dominant vein systems) and the northwest-striking Yellowjacket fault trend display a nearly orthogonal relationship. Such a relationship does not reconcile well with conventional Mohr-Coulomb faulting theory. However, recent observations of conjugate strike-slip faults in California and Japan (Thatcher and Hill, 1991), indicate that mutually perpendicular conjugate shear sets are *typical*, rather than exceptional features. The orthogonal geometry was noted by Thatcher and Hill (1991) as being particularly well developed in regions of extensional strike-slip, characterized by elevated heat flow and recent volcanism. Such observations are consistent with, and applicable to, the northern California Coast Ranges.

Fox (1983) applied the terminology of Tchalenko and Ambraseys (1970) to deformational features of the Santa Rosa structural block. Using this model, the Yellowjacket (305°) shear system would be classified as a P fault. Faults of this type develop as older faults are rotated in advanced stages of deformation (Freund, 1974). Fox (1983) hypothesized that shear activity shifted throughout the wrench zone, as older faults rotated and became inactive. The cessation of volcanism in the Sonoma Volcanics may well have coincided with the rotation of older strike-slip faults away from preferred orientations as volcanic conduits. In this case, the P fault(s) near Calistoga would have been most likely to propagate in the waning stages of Sonoma volcanism. This cycle may have repeated itself to the northeast in the Clear Lake Volcanics, where emplacement of the McLaughlin deposit was controlled by similar post-volcanic shears. Complicating the issue of the origin of the P faults of the region, is the likelihood that their fabric in the basement rocks is partly inherited from the earlier period of subduction. In this case, certain zones, such as the Yellowjacket serpentinite-dominated fault zone, may have accommodated right-lateral slip simply because they were inherent planes of weakness approximately paralleling the ideal shear direction. The cessation of movement along such faults is still best explained by their ultimate rotation away from favorable slip directions.

VEIN MINERALOGY

Because of the long closure of the Calistoga mines, access to the workings and underground vein exposures is nearly impossible. As a result, collection of vein matter typifying that which was actually mined is difficult. The Silverado mine affords the best opportunity to study the veins. The vein sets there are well exposed, both in outcrop and in shallow mine workings. Although the heart of the orebody has been stoped, the vein remnants in the walls of the old workings are undoubtedly similar (albeit lower in grade) than the stoped material.

Silverado Mine

Vein filling at Silverado was incremental, with stages of crudely banded growth punctuated by hydrothermal brecciation and cockade quartz healing. Vein matter consists of quartz, chalcedony and adularia. Few carbonates are present, although quartz pseudomorphs preserve patterns of early carbonates (presumably calcite) on the walls of the

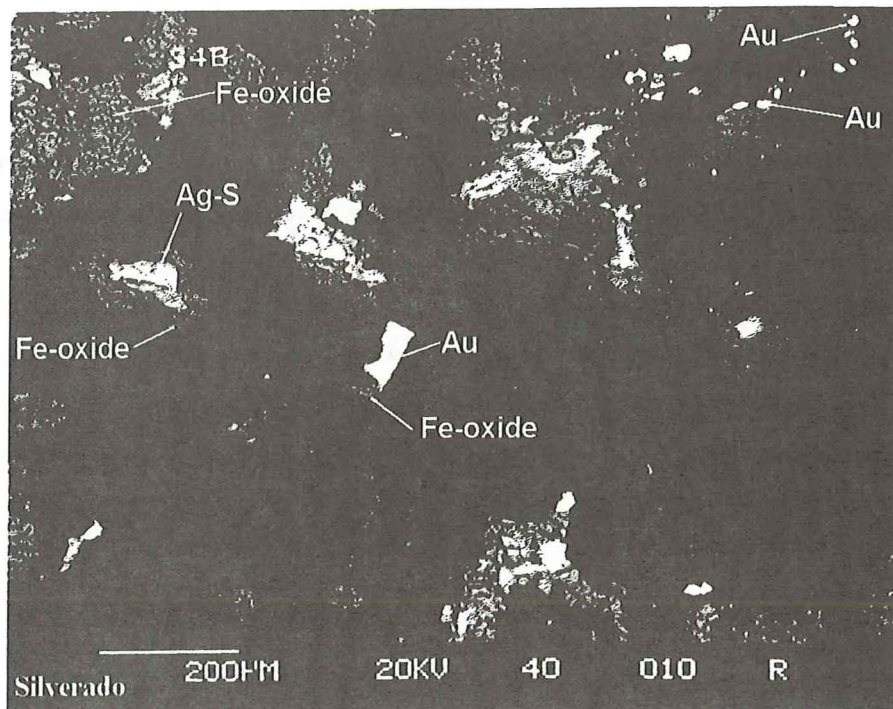


FIGURE 6. S.E.M. backscatter image of Silverado mine vein matter in polished section, showing distribution of silver sulfides and gold in quartz. Photo courtesy J. Rytuba, U.S. Geological Survey.

main stope. First recognized at Silverado by Crutchfield (1953), this material is characterized by a lattice-blade network of thin, rhombic plates forming tetrahedral and polyhedral cavities. Identical textures have been photodocumented by Morrison, et al, (undated). They are interpreted to be the product of quartz growth along blades and lamellar partings of primary calcite during replacement.

The main stage of silver mineralization at Silverado is characterized by crustiform-colloform banded quartz, chalcedony and adularia. The adularia crystals are typically macroscopic. They appear as colorless euhedral needles in quartz, radiating in clusters from common loci. Fine sulfides occur in varying concentrations in the crudely banded, sucrosic quartz matrix surrounding the adularia. Chalcopyrite dominates, and is the only macroscopic sulfide in this zone. It occurs as equant, subhedral to anhedral crystals up to 0.3 mm, and is typically rimmed by extremely fine-grained, dark sulfides. Under high magnification, these sulfides can be seen to also rim fine sphalerite grains, with the encapsulating mineral appearing as greenish, roughened blebs in both cases (Crutchfield, 1953). They are tentatively identified as argentite (Crutchfield, 1953).

Dark sulfides also occur individually, as disseminated minute grains and aggregates in bands of clear, sucrosic quartz, and appear to be concentrated along irregular quartz grain boundaries, forming a moss-like texture. Microprobe analysis of this material revealed the presence of silver sulfides and selenides associated with a secondary iron-antimony oxide (Rytuba, 1992, personal communication). Native gold (Fig. 6) and a silver-antimony sulfide (pyrargyrite?) were also noted, the former associated with silver selenides. The silver selenide (Ag-Se-S phase) is presumably aguilarite (Ag_4SeS).

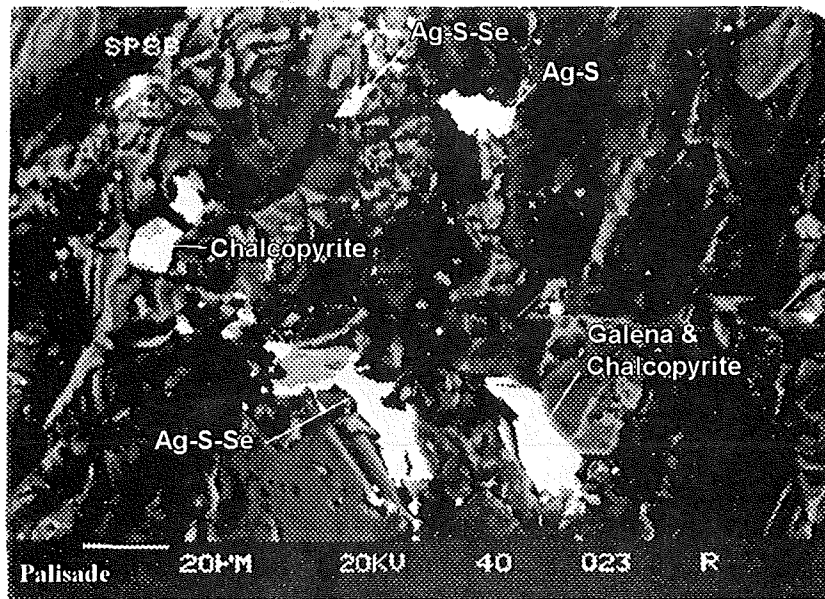


FIGURE 8. S.E.M. backscatter image of Palisade mine vein matter in polished section, showing distribution of silver and base metal sulfides in quartz. Photo courtesy J. Rytuba, U.S. Geological Survey.

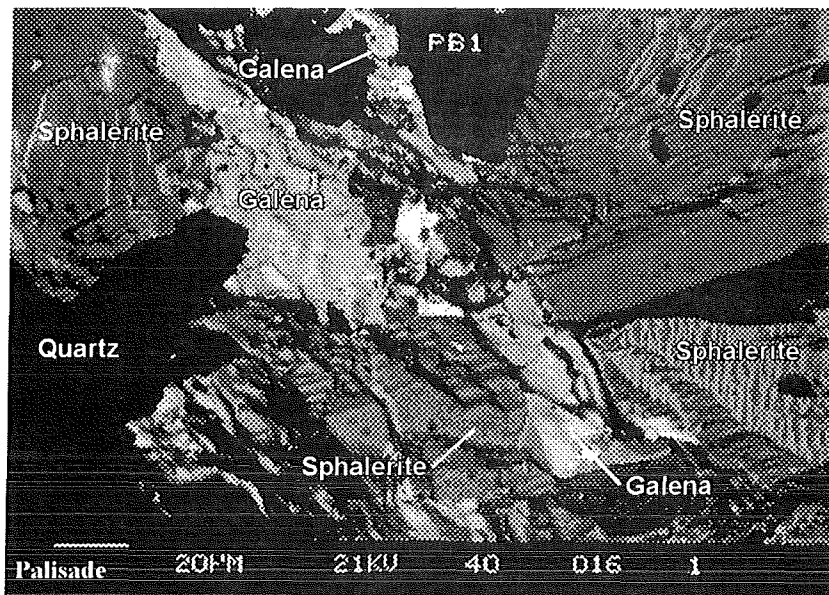


FIGURE 9. S.E.M. backscatter image of Palisade mine vein matter in polished section, showing distribution of base metal sulfides in quartz. Photo courtesy J. Rytuba, U.S. Geological Survey.

Although samples of Palisade vein matter collected by the author have yielded gold values as high as 142 ppm (4.1 oz/ton), the gold is rarely seen (Fig. 7). Only one macroscopic gold grain in quartz (associated with chalcopyrite and argentite) has ever been observed by the author. Two minute gold particles, each measuring approximately 0.1 mm, were also obtained by panning in a stream cutting the Palisade outcrops. These grains were rough and reddish in color. The accompanying heavy minerals included epidote (~50%), ilmenite, zircon, magnetite, hematite, chalcopyrite and pyrite.

Supergene marcasite and selenite samples have also been collected from the Palisade mine (Crutchfield, 1953). The marcasite is stalactitic, with larger columns measuring over 15 cm in length. This material is the product of descending acid sulfate waters, and was probably collected from upper levels of the mine. The zeolite, heulandite, is also present in highly argillized, amygdaloidal andesite(?) found near the mine, but its relationship to the vein systems is unclear.

Microprobe analyses of vein matter from the Palisade dumps, indicate the presence of an Ag-Se-S phase in association with argentite, chalcopyrite and galena (Rytuba, 1992, personal communication)(Fig. 8). Results of geochemical analyses indicate that selenium and (to a lesser degree) tellurium are intimately associated with silver enrichment in the veins of this district. Concentrations as high as 787 ppm Se and 14 ppm Te have been detected in Palisade mine ore. A lead-bismuth sulfide associated with pyrite, and a titanium oxide (anatase?) associated with quartz-adularia, have also been recognized from microprobe analyses of Palisade vein matter (Rytuba, 1992, personal communication).

Other Prospects

Numerous shallow prospects are scattered along the alignment of en échelon veins of the district, and their mineralogy closely resembles that of the Palisade and Silverado deposits. The Dutch Henry vein is the southernmost documented vein of the trend (Fig. 3). It resembles Silverado, texturally, with abundant quartz lattice-blades after carbonates. Fine sulfides and native gold are dispersed through crudely crustiform-colloform bands of sucrosic quartz with microscopic adularia. Microprobe analyses of this material by Rytuba (1992, personal communication) indicate the presence of silver and copper sulfide phases, presumably argentite and chalcopyrite. A titanium oxide, similar to that observed in Palisade mine vein matter, was noted, as well as a Fe-Ni-Cr phase and a cerium phosphate. Elevated selenium and silver concentrations, up to 72 ppm and 1,430 ppm, respectively, suggest that silver selenides are present in the Dutch Henry vein system, as they are in the Palisade and Silverado systems.

The Linn vein system forms the only structurally dissimilar vein trend of the district (Fig. 3), and its textural features are also, in part, unique. Overall, its most common texture is cockade quartz growth around fragments of wallrock. In fact, the Linn vein exhibits more hydrothermal breccia than any other vein of the district. Quartz lattice-blades after carbonate are also present, but to a lesser degree than in the Silverado and Dutch Henry systems. At a point about 920 m south of the Palisade mine shaft, a chalcedonic portion of the Linn vein exhibits its most noteworthy textural features: mottled color bands and syneresis cracks. These textures are indicative of

silica precipitation as a gelatinous material, and their presence suggests a high degree of silica supersaturation, relative to quartz, in the vein-forming fluid (Fournier, 1985). Fine sulfides are present throughout the various portions of the Linn vein system, but detailed mineralogical studies have not been conducted.

WALLROCK ALTERATION

Propylitic alteration is widespread in the first generation andesites near Calistoga, and is characterized by an assemblage of chlorite, calcite and albite, with lesser epidote and possible titanite (Crutchfield, 1953).

Ferromagnesium minerals in the volcanics are typically altered to chlorite and calcite, as a result of this process. It appears that propylitization occurred in an early event, preceding silicification and sulfidation (Crutchfield, 1953).

Argillic alteration is widespread in the district, typically extending as a halo a few meters laterally from each of the major vein systems. It is characterized by bleaching and sulfidation of the surrounding rock, and is often accompanied by streaks of pervasive silicification. Narrow, en échelon argillic alteration patterns also occur away from the siliceous veins. The best examples of these lie on Mount St. Helena, above the Silverado mine, where structurally controlled argillic alteration patterns parallel the Silverado vein system, and persist to the crest of the south peak. No advanced argillic alteration has been recognized in the district.

Pervasive silicification is restricted to close proximity with the vein systems, and is more common in wallrocks of the Palisade mine than at Silverado (Crutchfield, 1953). Wallrock at the Palisade mine is andesite of the first generation of volcanism. Wallrock at Silverado is silicic lapilli tuff and tuff breccia of the second generation of volcanism. Tuffaceous units should be more susceptible to pervasive silicification than flows, due to their relatively greater porosity and permeability, but in these cases the opposite holds true. In either case, pervasive silicification is minor in Calistoga district.

GEOCHEMISTRY

Maximum values (in parts per million) for selected elements, obtained from a set of 84 Calistoga district vein samples are depicted graphically in Fig. 10. These results are based on recent fire assay, I.C.P. and atomic absorption analyses. It should be noted that the full element suite was not run for *all* the samples. Although average values are typically much lower than the maximum values, the chart serves to illustrate the orders of magnitude of concentration of the various metals in the heart of the system. Tungsten is the one exception, with values invariably below detection limits (less than 1 ppm), and is not depicted in the chart.

Silver, copper, zinc and antimony values range into the 10,000's of ppm, with lead, arsenic and barium in the 1,000's. Gold and selenium range into the 100's of ppm, while mercury, thallium, cadmium, gallium and tellurium values peak in the 10's. Molybdenum and bismuth values fall below 10 ppm, but are anomalous. Mercury, thallium and barium are the only elements that show a negative correlation with precious metals enrichment in this district. The average Ag: Au ratio is 74:1 (n=84).

MAXIMUM VALUES FOR SELECTED ELEMENTS: CALISTOGA DISTRICT

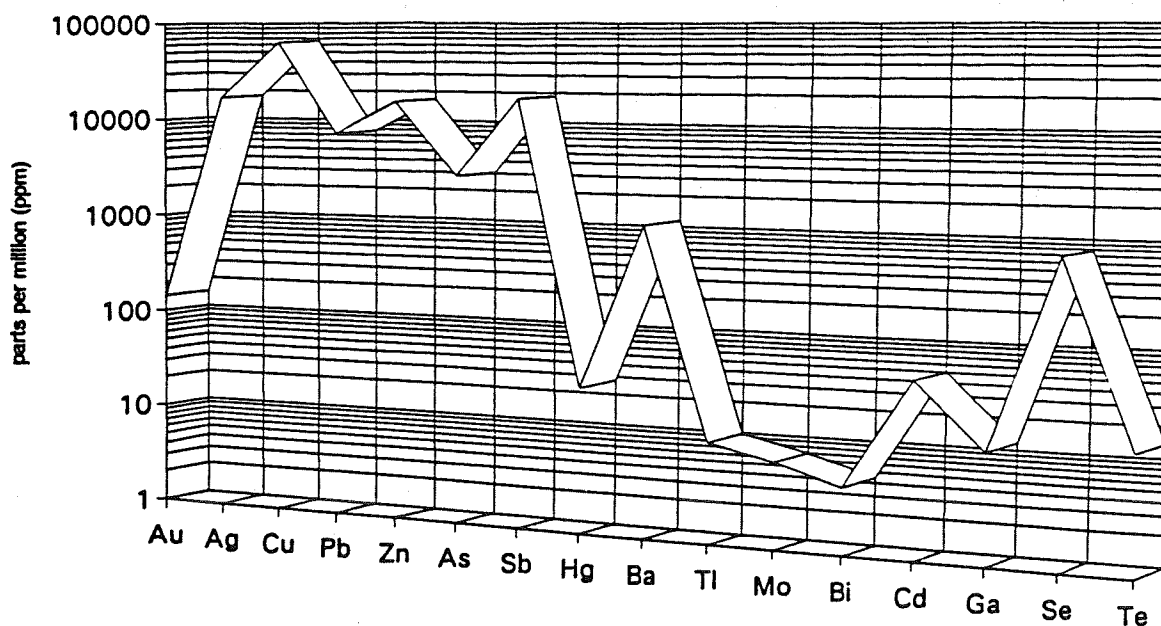


FIGURE 10. Maximum values for selected elements: Calistoga district.

Fluid inclusion and stable isotope studies of Silverado and Palisade vein matter have recently been published by Sherlock (1993), and the following summarized information is drawn entirely from his work.

Silverado Mine

Four samples of Silverado vein matter from outcrops were found to contain both liquid- and vapor-dominated primary fluid inclusions. The vapor content ranges from ~10% to ~90% in a coeval population, with high-vapor inclusions being less common. Of 28 inclusions analyzed, the homogenization temperatures were found to range from 224°C to 272°C, with the average being 249°C. In two cases, approximately simultaneous homogenization of vapor-to-liquid and liquid-to-vapor was noted in coeval inclusions. This phenomenon is suggestive of fluid boiling during formation of the inclusions. The average calculated salinity (from 16 inclusions) was found to be 0.87 wt. % NaCl equivalent.

In all cases, a third phase was observed in Silverado inclusions. This phase was tentatively identified as liquid CO₂, based on melting temperatures and crushing tests. This assumption needs further testing, because it leads to calculated boiling depths that are irreconcilable with local geology.

Oxygen and deuterium isotope data were derived for two samples, using vein quartz and fluid inclusions, respectively. Calculated $\delta^{18}\text{O}_{\text{H}_2\text{O}}$ and corresponding δD values were found to be -4.9 per mil and -89 per mil for one sample, and -2.0 per mil and -92 per mil for the second.

Palisade Mine

One sample of vein matter from a stope between the 600 and 400 foot levels (author's collection) was analyzed by Sherlock. Fluid inclusions were found to be nearly identical to those of Silverado. Homogenization temperatures were somewhat lower, ranging from 198° to 226°, and averaging 212°. Average calculated fluid salinity was found to be 1.0 wt. % NaCl equivalent, based on final melting point depressions measured in four inclusions. A third phase, similar to that observed at Silverado, was noted.

Due to lack of sufficient material, no deuterium values were derived. The $\delta^{18}\text{O}_{\text{H}_2\text{O}}$ value for one sample of vein quartz was found to be -1.6 per mil.

DISCUSSION

Precious metals deposits of the Calistoga Mining District compare well with established geochemical and structural models of epithermal vein systems. Their mineralogy, metal credits and textural features are indicative of the deep levels of boiling and open space filling in a hot-springs precious metals system.

Structural control of precious metals veins in Calistoga District is tied directly to San Andreas-style wrench faulting. The Yellowjacket fault zone is the most likely master shear system. This zone strikes 305°, parallels the overall trend of the vein systems, and forms the western boundary of the "mineral corridor." It is interpreted to be a rotated dextral shear (P fault), associated with large scale, 330° dextral wrench (Fox, 1983). The vein systems are orthogonal to the Yellowjacket fault zone, and formed along sinistral (conjugate Reidel) shears that propagated northeastward from the master structure.

No master shear control along the east fringe of the vein systems is apparent, although one may exist. The master (P) shear fabric is widespread in the region, and it is conceivable that the conjugate Reidels link between parallel master structures. Some suggestion of this is indicated by the presence of the Linn vein system, which forms an anomalous, 330°-striking zone of veins and hydrothermally cemented wallrock breccia along the projected Yellowjacket fault trend. This segment was dilational, and appears to occupy a large (2,000 m) jog of the master shear trend. Sibson (1987) observed that such jogs form particularly favorable sites for epithermal mineralization. The abundance of silicified wallrock breccia associated with silica gel textures in the Linn vein system is indicative of hydraulic implosion and rapid adiabatic chilling of inflowing hydrothermal fluids in a zone of high fluid pressure differentials. Rapid slip transfer in a fault jog interior can generate the necessary pressure differentials to account for these features (Sibson, 1987). The Linn vein system is centrally located in the 14.5 km long mineralized corridor. The symmetrical distribution of the conjugate Reidel vein systems surrounding this segment suggests that it may be an "energy sink," translating strain across a northward step in the Yellowjacket fault trend. This model calls for syn-tectonic formation of the veins, with vein and wallrock brecciation corresponding to major seismic events. Incipient (coseismic) strain would have been focused along the Linn segment, with residual adjustments occurring in the adjacent "linking fracture network" of conjugate Reidel shears.

Ore shoots (zones of maximum dilation) developed along north-northeast striking segments of the

undulating conjugate Reidel shears, as would be expected in San Andreas-style shear. Movement along the conjugate Reidels was incremental, resulting in polyepisodic rupturing accompanied by hydrothermal brecciation. Considering the small number of individual veins within each of the conjugate Reidel shear systems, and in spite of the approximate 1 million year life of the system, it is clear that there were only a few hydrothermal rupturing events. This, perhaps, marks the greatest genetic difference between this system and the McLaughlin system, where deformation was apparently less prolonged (~500,000 yrs), but sealing-rupturing cycles were repetitive.

The ore and gangue mineral assemblages, and their associated textural features, correspond to the lower Crustiform-Colloform Superzone of Morrison et al. (undated), and the zone of overlap between the base and precious metal horizons of Buchanan (1981). The quartz + chalcedony + calcite + adularia gangue mineral assemblage, together with observed homogenization and melting phenomena in fluid inclusions (Sherlock, 1993), indicates that the ore forming fluid was a boiling, low salinity, NaCl type fluid. Simultaneous calcite and adularia crystallization occurs where vertical pressure-temperature gradients in the system allow partitioning of CO₂ and H₂S from the fluid. The corresponding rise in pH initiates rapid rates of crystallization of calcite and the disordered K-feldspar -- adularia (Morrison et al., undated). Quartz and chalcedony deposition, following or contemporaneous with calcite-adularia growth, is primarily the result of adiabatic cooling and concentration of silica in the boiling liquid fraction (Fournier, 1985).

Native gold and silver sulfides, sulfosalts and selenides are associated with siliceous portions of the veins. Their deposition was presumably linked to the destabilization of metallic bisulfide complexes associated with H₂S partitioning (Romberger, 1990). Early base metal sulfides are also present, and are typically encrusted, or replaced, by the silver sulfides and sulfosalts. The spatial and temporal association of these base metal sulfides with boiling-related features, suggests that they may be the products of both chloride and bisulfide transport. Work by Brown (1986) indicates that bisulfide complexes in the deep aquifer environment of a hot spring can account for nearly all dissolved copper. The low salinity of the fluids (~1.0 wt. % NaCl equivalent) favors this transport mechanism. However, the early placement of base metals in the paragenetic sequence is consistent with destabilization of chloride complexes, which can occur during CO₂ partitioning and prior to H₂S partitioning (Sherlock, 1993). It is likely that a combination of the two mechanisms was involved.

Fluid inclusion geothermometric studies by Sherlock (1993) indicate that the temperature of the ore forming fluids in the Silverado and Palisade systems, ranged from 198°C to 272°C, averaging 212°C and 249°C, respectively. Minimum calculated depths of formation, based on the above temperatures and inferred 2.2 molal CO₂ content, are ~780 m to ~1,000 m (Sherlock, 1993). Given the relative youth of this hot springs system, and moderate topographic relief, the unroofing of 1,000 m of the volcanic pile is unlikely. Vertically jointed, columnar andesite capping the north peak of Mount St. Helena is one of the uppermost units of the local volcanic sequence. This unit presumably lies within a few tens of meters of the paleosurface at the time of vein formation. The Silverado vein outcrop is 370 m lower in elevation than the summit of Mount St. Helena, implying that its depth of formation was approximately 400 m below the paleosurface. If the third phase in Silverado fluid inclusions is not CO₂, then the hydrostatic boiling curve is intersected at ~400 m, rather than ~1,000 m (Sherlock, 1992, personal communication).

Similarly, the depth of formation of the Palisade system is reduced to ~200 m, if the CO₂ content is reconsidered. This shallower depth value, like its counterpart at Silverado, reconciles well with the apparent degree of erosion of the volcanic pile.

Stable isotope data from Calistoga veins are consistent with evolved meteoric fluids, with deuterium values similar to modern meteoric water (Sherlock, 1993). Oxygen shows a positive shift to isotopically heavier values due to water/rock interaction (Sherlock, 1993). The early geothermal system near Calistoga was the product of convective circulation and concentration of these meteoric fluids. The source of the metals remains to be determined.

A remnant of the older geothermal system still exists at Calistoga, in the form of modern, moderate-temperature hot springs. Prior to drilling and development of the geothermal resource, surface springs and hot pools were extensive. Small mounds of siliceous sinter were also present near the original Springs Ground at Calistoga (Allen and Day, 1927). Surface hot springs are now limited to the northwest fringe of the field, where the "hot water" table is generally unaffected by development of the geothermal resource (Youngs and Higgins, 1981). The modern system is characterized by low salinity, NaCl-type waters, presumably derived from convection of meteoric fluids (Taylor, 1981). Present day structural control of the geothermal system appears to be a northwest-trending fault zone (Taylor, 1981), based on the alignment of the hotter springs and bore holes. The ascending fluids are complexly mixed with surface waters migrating laterally through the gently dipping valley floor sediments and volcanoclastics. This relationship, and the lack of deep information, makes a clear interpretation of the permeability constraints of the deep fluids difficult. A recent comparison of Calistoga geyser eruption intervals with regional seismicity, indicates that variations in geyser eruptive behavior are precursory to, and coincident with, large earthquakes in a 250 km radius (Silver and Valette-Silver, 1992). Such variations are attributed to permeability changes due to pre- and coseismic strain, and demonstrate the close tie of the hydrothermal system to modern large-scale regional deformation. The modern system is fluid-dominated, but somewhat cooler than that which emplaced the veins. Reservoir temperatures in deep bore holes (~570 m) at the heart of the system, peak between 137°C and 167°C (Kelley, 1981), with a general increase in temperature with depth (Taylor, 1981).

ACKNOWLEDGMENTS

The author would like to acknowledge the contributions of several individuals, who generously supplied key information for use with this report. To Norm Lehrman, of Homestake Mining Company, goes the author's greatest appreciation, for his support and encouragement of academic studies in the work environment at the McLaughlin mine.

The author wishes to thank Dr. Ross Sherlock, of the University of British Columbia, for his generous exchange of unpublished geochemical data during the course of his thesis work. The author's appreciation is also extended to Richard Tosdal and James Rytuba, of the U.S.G.S. at Menlo Park, for their generous exchange of data and knowledge in their respective fields.

REFERENCES

- Allen, E. T., and Day, A. L., 1927, Steam wells and other thermal activity at "The Geysers", California: Carnegie Institution of Washington Publication No. 378, pp. 98-100.
- Averill, C. V., 1929, 25th Report of the State Mineralogist: California Division of Mines, pp. 237-238.
- Becker, G. F., 1888, Geology of the quicksilver deposits of the Pacific Slope: United States Geological Survey Monograph 13, pp. 370, 388, 471, 472.
- Berkland, J. O., Raymond, L. A., Kramer, J. C., Moores, E. M., and O'Day, Michael, 1972, What is Franciscan?: American Association of Petroleum Geologists Bulletin, v. 56, no. 12, pp. 2295-2302.
- Bradley, W. W., 1915, Mines and mineral resources of the counties of Colusa, Glenn, Lake, Marin, Napa, Solano, Sonoma, Yolo: California State Mining Bureau, Chapters of the state mineralogist's report biennial period 1913-1914, pp.97-99, 104-105, 127.
- Brown, K. L., 1986, Gold deposition from geothermal discharges in New Zealand: Economic Geology. v. 81, pp. 979-983.
- Buchanan, L. J., 1981, Precious metals deposits associated with volcanic environments in the southwest *in* Relations of tectonics to ore deposits in the southern cordillera *edited by* W. R. Dickinson and W. D. Payne: Arizona Geological Society Digest v. XIV, pp. 237-262.
- Chapman, R. H., Youngs, L. G., and Chase, G. W., 1982, Gravity, structure, and geothermal resources of the Calistoga area, Napa and Sonoma Counties: California Geology, v. 35, no. 8, pp. 175-183.
- Crutchfield, W. H. Jr., 1953, The geology and silver mineralization of the Calistoga District, Napa County, California: University of California (Berkeley) M.A. thesis, (71 p., map, scale 1:35,000).
- Davis, F. F., 1948, Mines and mineral resources of Napa County: California Journal of Mines and Geology, vol. 44, pp. 159-188.
- Dickinson, W. R., and Snyder, W. S., 1979, Geometry of subducted slabs related to San Andreas transform: Jour. Geology, v. 87, p. 609-627.
- Evernden, J. F., and James, G. T., 1964, Potassium-argon dates and the Tertiary florae of North America: American Journal of Science, v. 262, no. 8, pp. 25-56.
- Fournier, R. O., 1985, Silica minerals as indicators of conditions during gold deposition in Geologic characteristics of sediment- and volcanic-hosted disseminated gold deposits -- search for an occurrence model *edited by* E. W. Tooker: U.S. Geological Survey Bulletin 1646, pp. 15-26.
- Fox, K. F., Jr., 1983, Tectonic setting of late Miocene, Pliocene, and Pleistocene rocks in part of the Coast Ranges north of San Francisco, California: U.S. Geological Survey Professional Paper 1239, 33 p.
- Fox, K. F., Jr., Sims, J. D., Bartow, J. A., and Helley, E. J., (compilers), 1973, Preliminary geologic map of eastern Sonoma County and western Napa County, California: U.S. Geological Survey Miscellaneous Field Studies Map MF-483, scale 1:62,600, 4 sheets.
- Freund, Raphael, 1974, Kinematics of transform and transcurrent faults: Tectonophysics, v. 21, no. 1-2, pp 93-134.
- Grigsby, R. A., 1923, Outline report on the Palisade mining property: Unpublished hand-written report. (5 p., with map and cross-section).
- Hamilton, Fletcher, 1916, Report XIV of the state mineralogist: California State Mining Bureau, pp. 269-271.
- Hamilton, Fletcher, 1921, Report XVII of the state mineralogist: California State Mining Bureau, pp. 158-159.
- Hearn, B. C. Jr., McLaughlin, R. J., and Donnelly-Nolan, J. M., 1988, Tectonic framework of the Clear Lake basin, California: Geological Society of America Special Paper 214, p. 9-20.
- Irelan, W. Jr., 1890, Tenth annual report of the state mineralogist: California State Mining Bureau, p. 363.
- Issler, A. R., 1948, Silverado 1874: Unpublished manuscript compiled for Napa County Historical Society, Napa, California, 13 p.
- Kellett, Fred, (undated), The Palisade mine: Unpublished hand-written report. (5 p. with cross-section).
- Kelley, F. R., 1981, Thermal springs and wells and radiometric ages of rocks in the Santa Rosa Quadrangle: California Division of Mines and Geology, accompanying Regional Geologic Map Series, Map No. 2A (Geology), Sheet 4, pp. 8-9.
- Mankinen, E. A., 1972, Paleomagnetism and potassium-argon ages of the Sonoma Volcanics, California: Geological Society of America Bulletin, v. 83, no. 7, p. 2063-2072.
- McLaughlin, R. J., 1977, The Franciscan assemblage and Great Valley sequence in The Geysers-Clear Lake region of northern California, *in* Field Trip Guide to The Geysers-Clear Lake area, (California): Geological Society of America, Cordilleran Section, April 1977, p. 2-24.
- McLaughlin, R. J., 1993, (*Title pending), in this volume.
- Menefee, C. A., 1873, Historical and Descriptive Sketchbook of Napa, Sonoma, Lake and Mendocino: Napa City, California: Reporter Publishing, pp. 88-92.
- Morrison, G., Guoyi, D., and Subhash, J., (undated), Textural zoning in epithermal quartz veins: AMIRA Project P 247 field manual, James Cook University (Queensland), 33 p.

- Osbourne, Katharine D., 1911, Robert Louis Stevenson in California. Chicago: A. C. McClurg & Co., p. 92.
- Osmont, V. C., 1905, A geological section of the Coast Ranges north of the Bay of San Francisco: University of California Publications, Department of Geology Bulletin, v. 4, no. 3, p. 39-87.
- Raymond, R. W., 1875, The seventh annual report of the United States Commissioner of Mining Statistics: House of Representatives. 43d Congress, 2d Session. Ex. Document No. 177, pp. 178-179.
- Romberger, S. B., 1990, Geochemistry of epithermal precious metals deposits in Gold '90, *edited by* D. M. Hausen, D. N. Halbe, E. U. Petersen and W. J. Tafuri: S.M.E. proceedings of the Gold '90 symposium, pp. 181-188.
- Rytuba, J. J., 1992-1993, U.S. Geological Survey, Menlo Park, California.
- Sherlock, R. L., 1992, University of Waterloo, Ontario, Canada.
- Sherlock, R. L., 1993, The geology and geochemistry of the McLaughlin mine sheeted vein complex, northern Coast Ranges, California: University of Waterloo, Ontario, Ph.D. thesis, 309 p.
- Sibson, R. H., 1987, Earthquake rupturing as a mineralizing agent in hydrothermal systems: *Geology* v. 15, pp. 701-704.
- Silver, P. G., and Valette-Silver, N. J., 1992, Detection of hydrothermal precursors to large Northern California earthquakes: *Science* v. 257, pp. 1363-1368.
- Swearingen, J. D., 1957, Untitled: Unpublished manuscript on Palisade mine, 16 p.
- Taylor, G. C., 1981, Calistoga geothermal resource area: *California Geology*, v. 34, no. 10, pp. 208-217.
- Tchalenko, J. S., and Ambraseys, N. N., 1970, Structural analysis of the Dasht-e Bayaz (Iran) earthquake fractures: *Geological Society of America Bulletin*, v. 81, no. 1, pp. 41-59.
- Thatcher, W., and Hill, D. P., 1991, Fault orientations in extensional and conjugate strike-slip environments and their implications: *Geology* v. 19, pp. 1116-1120.
- Wagner, D. L., and Bortugno, E. J. (compilers), 1982, Geologic map of the Santa Rosa Quadrangle, California, 1:250,000: California Division of Mines and Geology, Regional Map Series, Map No. 2A (Geology), Sheet 4.
- Weaver, C. E., 1949, Geology of the Coast Ranges immediately north of San Francisco Bay region, California: *Geological Society of America Memoir* 35 (242 p., pls. 6 and 7, scale 1:62,500).
- Youngs, L. G., and Higgins, C. T., 1981, Moderate-temperature geothermal resource, Calistoga, Napa County, California: *California Geology*, v. 34, no. 4, pp. 67-72.

**RELATION OF HOT-SPRING GOLD MINERALIZATION TO
SILICA-CARBONATE MERCURY MINERALIZATION
IN THE COAST RANGES, CALIFORNIA**

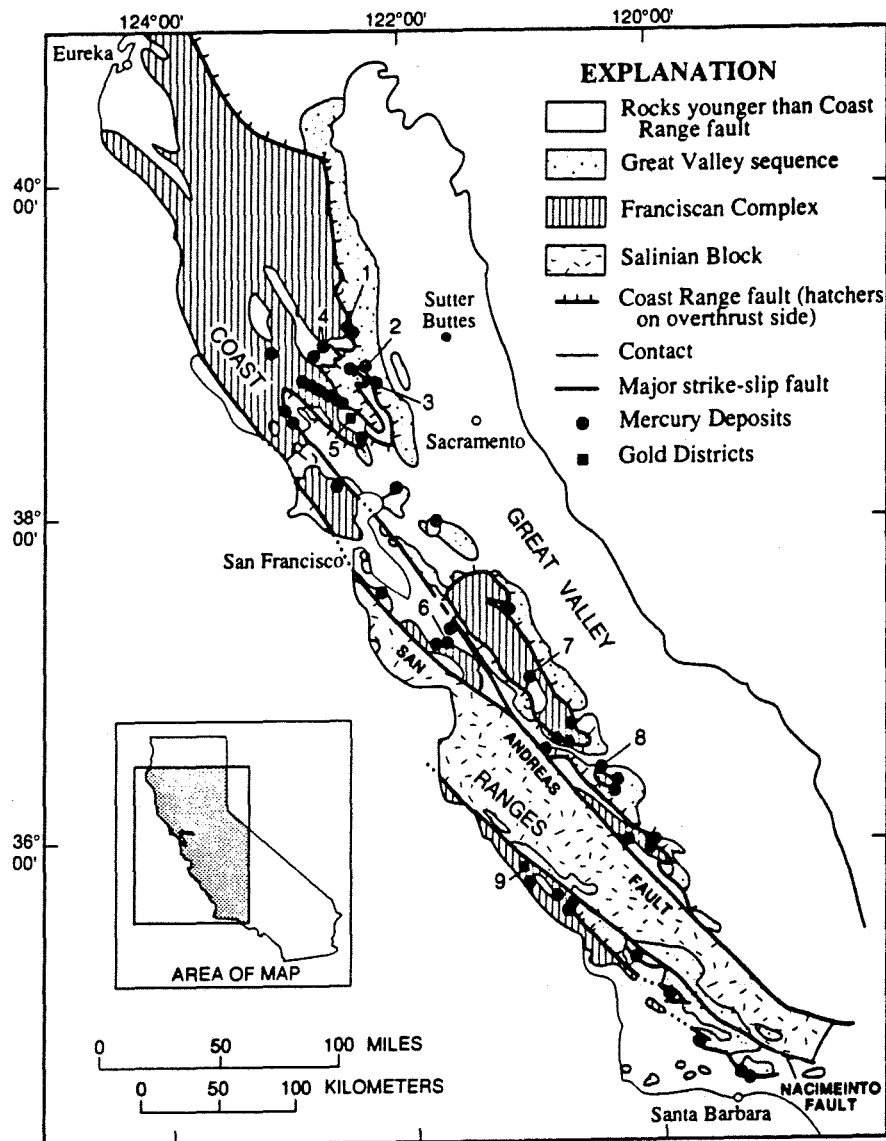
William J. Pickthorn

U. S. Geological Survey, 345 Middlefield Rd, Menlo Park, CA 94025

INTRODUCTION

The discovery of the McLaughlin hot-spring type gold deposit in the old Knoxville mercury district sparked considerable interest and research into the origin and relation of mercury and epithermal gold mineralization in the California Coast Ranges Province. Silica-carbonate mercury mineralization occurs throughout the Coast Ranges, from Santa Barbara County in the south to Lake and Colusa counties in the north (Fig. 1). Since their discovery in the mid 1800's California's Coast Ranges mercury deposits have produced over 50% of the total production for the United States, and two of the mines, the New Almaden mine in Santa Clara County and the New Idria mine in San Benito County, rank as the fifth and sixth largest producing deposits in the world respectively (Bailey and others 1973). Prior to the discovery of the McLaughlin gold deposit in 1978, lode gold production from the Coast Ranges was very minor with an estimated total of about \$750,000, with two thirds of this production from the Palisade and Silverado mines in the Calistoga silver-gold district (Clark, 1976). Notable quantities of lode gold have been produced from only two other areas; the Los Burros district in south western Monterey County where mesothermal gold-bearing quartz veins occur in Franciscan Complex rocks; and, from the Knoxville and Sulfur Creek mercury mining districts where gold was produced as a byproduct. The McLaughlin and Cherry Hill epithermal gold deposits (Fig. 1) were subsequently discovered in the Knoxville and Sulfur Creek mining districts respectively. Current reserves at the McLaughlin mine are estimated at 3 million oz gold (Lehrman, 1986).

Much of the research into the origin and relation of the silica-carbonate mercury and epithermal gold mineralization in the Coast Ranges has focused on thermal springs in and around the Knoxville and Sulfur Creek mining districts and in the Geysers Geothermal Area to the west. Gold-bearing precipitates are currently forming at several hot springs in the Sulfur Creek district and cinnabar is being deposited in active springs in the Sulfur Bank mine about 20 km to the west (White, 1981; Peters, 1991). Chemical and isotopic analyses of the spring waters, precipitates, and gangue and ore minerals suggests that the ore-forming fluids for the mercury and gold mineralization were non-meteoric or evolved-meteoric waters, and that the Au and Hg mineralizing fluids had different sources (Peters, 1991, 1993; Sherlock and Jowett, 1992; Donnelly-Nolan and others, 1993). There is clearly a spatial relation between the epithermal gold mineralization and silica-carbonate mercury mineralization, and this paper examines a possible genetic relation between the two deposit types.



- | | |
|---|--|
| <ol style="list-style-type: none"> 1. Wilbur Springs Hg District (Cherry Hill Au) 2. Knoxville Hg District (McLaughlin Au) 3. Oat Hill Hg Mine 4. Sulfur Bank Hg Mine | <ol style="list-style-type: none"> 5. Calistoga Ag-Au District 6. New Almaden Hg Mine 7. Stayton Hg District 8. New Idria Hg Mine 9. Los Burros Au District |
|---|--|

FIGURE 1. Generalized geologic map of the California Coast Range and location of mercury and gold occurrences. Numbers refer to locations mentioned in the text (modified from Bailey et al., 1973)

REGIONAL GEOLOGY

The Coast Ranges Province, extending for approximately 1,000 km along the California coast, is comprised of three major rock units: the Salinian Block, the Franciscan Complex, and the Great Valley sequence (Fig 1). The Great Valley sequence consists predominantly of weakly metamorphosed Upper Jurassic and Cretaceous marine sedimentary rocks, including conglomerate, mudstone, and sandstone, depositionally overlying oceanic crust known as the Coast Range ophiolite (Bailey and others, 1964; McLaughlin and Pessagno, 1978). The Great Valley sequence represents fore-arc basin or arc-trench gap deposits derived from the Sierran and Klamath island arc terranes to the east and north (Dickinson, 1970; Ingersoll and others, 1977).

The Franciscan Complex is separated from the Great Valley sequence and Coast Range ophiolite by the Coast Range fault. The Franciscan Complex is composed of weakly to moderately metamorphosed, highly deformed turbidite deposits and mafic volcanic and intrusive rocks. The sedimentary rocks consist of sandstone, shale, chert, and the mafic rocks are commonly serpentinized. The Franciscan Complex is a highly faulted tectonic melange with juxtaposed large blocks of contrasting composition and metamorphic grade. Largely coeval in age to the Great Valley sequence, the Franciscan Complex is considered to represent trench fill deposits formed westward of the Great Valley fore-arc basin. The Complex was underthrust and accreted to the North American plate margin along an oblique northeast trending subduction zone (Dickinson, 1970; Blake and Jones, 1974). Metamorphic mineral assemblages in the Franciscan Complex ranges from the zeolite to blue-schist facies, typical of the low-temperature high-pressure subduction zone environment.

The Salinian Block is a granitic-metamorphic complex consisting of Paleozoic to Mesozoic age plutonic and high-grade metamorphic rocks. This fault-bounded block separates a main Coast Ranges metamorphic belt from a slice of Franciscan Complex and Great Valley sequence rocks to the west (Fig. 1). The Salinian Block is related to crystalline rocks which are found approximately 500 km to the south, and has been displaced northward by movement along the San Andreas and Nacimiento transform fault systems.

Depositionally overlying the Franciscan Complex and Great Valley sequence are dominantly marine sedimentary rocks ranging from Paleocene to Pliocene in age, and late Tertiary to Recent age volcanic rocks. The sedimentary rocks are predominantly sandstone, shale, mudstone, and conglomerate, and, while commonly forming thick accumulations are generally of restricted aerial extent (Page, 1966). The volcanic rocks in the Coast Ranges Province are divided into two groups. A set of volcanics rocks approximately 22-24 Ma in age is found throughout the Coast Ranges and in the Central Valley, and a sequence of volcanics which decrease in age from approximately 15 Ma in the south to .02 Ma in the north (fig. 2) (Fox and others., 1985; Stanley, 1987). These volcanic rocks are interpreted to have formed from primitive basaltic material which has assimilated considerable crustal material before erupting (Hearn and others., 1981; Donnelly-Nolan and others, 1993). The volcanic rocks range in composition from basalt to rhyolite, and are present as flows, domes, tuffs, and breccia. The Sonoma Volcanics in northern California (Fig. 2) include significant volumes of ash-flow tuff and welded tuff which are considered to be result of a caldera forming event (J. Rytuba, pers. comm.).

STRUCTURE

Accretion and underthrusting of the Franciscan Complex against the Coast Range ophiolite and Great Valley sequence began in Late Jurassic and Cretaceous time along an oblique subduction margin. The San Andreas fault system formed approximately 40 m.y. ago as the spreading centers and transform fault systems associated with the Pacific and Farallon plates came in contact with the North American plate margin (Atwater, 1970; Blake and Jones, 1978; McLaughlin, 1981). Northward migration of the triple junction formed by the intersection of the Pacific, Farallon, and North American plates, caused a change from subduction to broad right-lateral transform shear along the North American plate margin. Changes in relative motion between the North American and Pacific plate also caused the formation of extensional basins within the San Andreas fault system and in the Coast Ranges (Blake and Jones, 1978). A northward migration of volcanism within the California Coast Ranges began about 15 m.y. closely following the passing of the triple junction (Fig. 2). Hearn and others. (1981) attribute this to movement of the North American plate over a stationary mantle plume or hot spot, however, McLaughlin (1981) favors a model for magma emplacement that is tied to the northward migration of the triple junction and the crustal extension within the Coast Ranges and San Andreas fault system. Dickinson and Snyder (1979) attribute the source of the volcanism to the formation of a "slab window", a triangular zone of extension present near the propagating end of the San Andreas transform fault, which caused an upwelling of mantle material beneath the Coast Ranges complex.

Major thrust and strike-slip faults are found throughout the Coast Ranges Province. This is related in part to the oblique convergence in the subduction zone, which caused the formation of strike-slip as well as thrust features during accretion, and the broad zone of right lateral strike-slip faulting in the San Andreas transform fault system associated with the relative northward movement of the Pacific Plate to the North American plate. Many of these faults are evidently very deep seated and have acted as conduits for mineralizing fluids and volcanism, as well as present day spring activity.

THERMAL AND MINERAL SPRINGS

Thermal and mineral springs of varying chemical and isotopic composition are found throughout the Coast Ranges Province. Studies of the springs, particularly in the vicinity of Clear Lake and Geysers Geothermal Area, have focused on the origin of the spring waters and their relation to mercury and gold mineralization. High-HCO₃⁻ springs produced by metamorphic devolatilization of Franciscan Complex rocks, springs of moderately saline fluid derived from the Great Valley sequence marine sediments, and meteoric water dominated springs, have been identified.

Mineral springs from throughout the Coast Ranges have been analyzed to test the hypothesis that they might represent present-day analogs of the silica-carbonate mercury hydrothermal systems. White and others. (1973) determined that there were two isotopically similar, but chemically distinct, waters present in mercury-bearing springs from the Sulfur Creek mercury district and the Sulfur Bank mercury mine 20 km to the west. Waters from both areas are enriched in deuterium (approximately 40 per mil) and O¹⁸ (approx. 13 per mil) compared to local

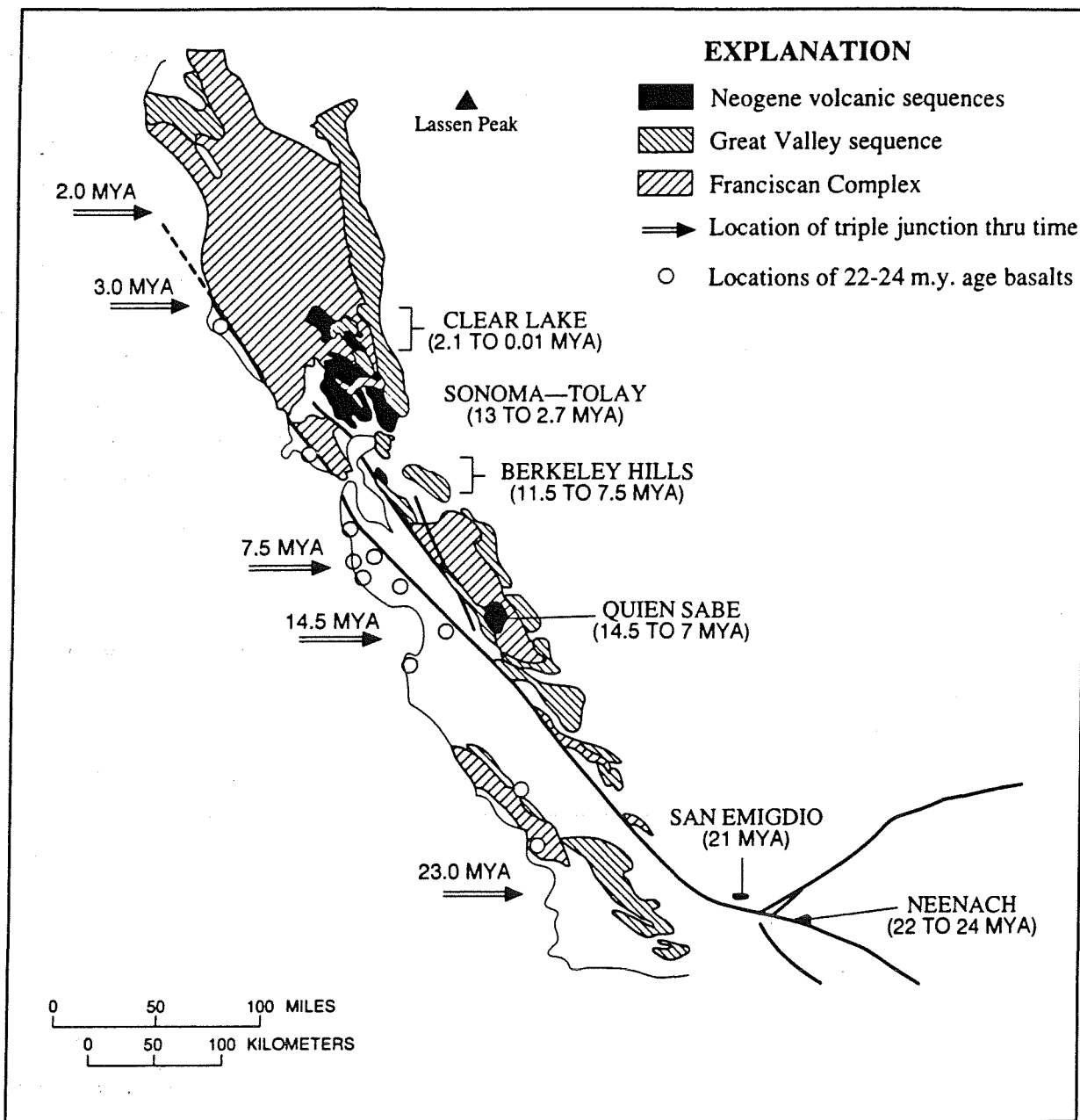


FIGURE 2. Generalized geologic map showing location and age of volcanic rocks in the Coast Range and location of the triple junction thru time. (modified from Johnson and O'Neil, 1984; Fox et al., 1985; and Stanley, 1987).

meteoric waters. However, in the Sulfur Creek district spring waters have high Cl^- content and lower HCO_3^- and B, whereas those in the Sulfur Bank mine are low in Cl^- and higher in B and HCO_3^- (Table 1).

The Sulfur Creek district is located in Great Valley sequence rocks near the Coast Range fault. The isotopic composition of the high Cl^- spring fluids ($\delta^{18}\text{O}$ +1 to +11‰ and δD -10 to -40‰; White and others., 1973; Peters, 1991) is distinct from local meteoric water (approximately $\delta^{18}\text{O}$ -8‰ and δD -60‰). They are essentially chemically and isotopically identical to oil-field waters from the Central Valley just to the east. Based on their isotopic signature and high- Cl^- content White and others. (1973) and Barnes (1970) considered these springs to represent connate or modified connate fluids derived from dewatering and low-grade metamorphism of the Great Valley sequence marine sediments. Strontium and Iodine isotopic analyses of the spring fluids also suggest a Great Valley source (Fehn and others., 1992). $^3\text{He}/^4\text{He}$ ratios indicate that the heat source for the thermal springs is most likely related to the Clear Lake volcanic rocks (Peters, 1993).

In contrast, the high- HCO_3^- low- Cl^- fluids found in springs to the west at the Sulfur Bank mine, and similar springs elsewhere in the Franciscan assemblage, were considered to represent a metamorphic fluid released during progressive regional metamorphism and devolatilization of the Franciscan Complex marine sediments (White, 1974; White and others. 1973; Barnes, 1970). Evolution of this fluid occurred after compaction had removed the high- Cl^- marine pore waters (White and others., 1973). In support of this idea, analyses of whole rock and vein materials in the Franciscan Complex from throughout the Coast Ranges by Magaritz and Taylor (1976) indicate that a fluid produced by devolatilization reactions during blueschist metamorphism would be chemically and isotopically very similar to the high carbonate springs. Conversely, Donnelly-Nolan (1983) suggested that the Sulfur Bank spring water was not a metamorphic fluid, but rather the result of multiple Rayleigh distillation of a meteoric fluid by repeated boiling. An argument against this "evolved meteoric" water model is that it requires boiling and separation of the vapor phase at a fairly low temperature and it is unlikely that the fluid could maintain a high HCO_3^- concentration (up to 13,000 ppm, Barnes and others., 1973) under these conditions.

SPRING TYPE	Cl^-	HCO_3^-	B	δD	$\delta^{18}\text{O}$	ref.
FRANCISCAN WATERS (incl. Sulfur Bank spring)	530 to 830	2,500 to 13,000	620 to 750	-27 to -24	+0.2 to +5.6	1,2,3,4
GREAT VALLEY WATERS (incl. Sulfur Creek District springs)	9,700 to 11,000	2,700 to 7,800	310 to 240	-10 to -40	+1.0 to +11.0	1,2,3
METEORIC WATER	---	---	---	-70 to -60	-10.3 to -8.1	1,2

TABLE 1. Range of values for chemical and stable isotope analyses of springs in the California Coast Ranges. Cl^- , HCO_3^- , and B reported in ppm; δD and $\delta^{18}\text{O}$ reported in per mil relative to SMOW. References: 1. White and others., 1973; 2. Barnes and others., 1973; 3. Peters, 1991; 4. Peters, 1993.

MERCURY DEPOSITS

Mercury mineralization throughout the California Coast Ranges is found predominantly associated with serpentinites along major faults in the Franciscan Complex, and in the base of the Great Valley sequence along or near the Coast Range fault. Many of the serpentinites are considered to have been structurally emplaced or plastically "intruded" along the faults from depth. The majority of the mercury deposits are defined as the silica-carbonate type. The silica-carbonate alteration is the result of interaction of the serpentinite with CO₂-rich fluids at low temperatures and replacement of the host by the silica phases quartz, chalcedony, and opal, and the carbonate phases magnesite and dolomite. Petrographic and chemical studies of several of the mercury deposits indicate that they formed in a shallow near surface environment at <200°C (Henderson, 1969; Peabody and Einaudi, 1992). Stable isotope analyses of the silica and carbonate alteration minerals indicate that $\delta^{18}\text{O}$ of the mineralizing fluid was relatively heavy, in the range of -3 to +8‰ (Table 2), and the carbon was from an organic source (Boctor and others., 1987; Peabody and Einaudi, 1992;).

Barnes and others (1973) were first to suggest that the Coast Ranges mercury deposits were of metamorphic origin. They related the high-bicarbonate, low-chloride spring waters directly to the silica-carbonate alteration of serpentinites associated with mercury mineralization and considered the ore fluid to be near surface mixture of Franciscan metamorphic and meteoric waters. At the Sulfur Bank mine a high-HCO₃⁻ spring is currently depositing cinnabar. A possible model for the metamorphic origin of the mercury deposits would closely parallel one developed for mesothermal gold-quartz vein systems in low- to moderate-grade metamorphic rocks in which fluids and ore constituents are derived from the host rocks by regional metamorphic processes (see Goldfarb and others., 1986). During prograde metamorphism, water and other volatiles such as CO₂, CH₄, H₂S, and N₂ are released during various devolatilization reactions. If the pressure of this metamorphic fluid exceeds the confining pressure of the enclosing rocks, either by hydrofracturing due to increasing temperature and/or pressure or by a decrease in the confining pressure due to cessation of compressional tectonics or uplift, the fluid and ore constituents will then migrate to lower pressure areas higher up in the rock package along deep-seated structures such as faults. This model for mesothermal gold-quartz deposits is very applicable to the tectonic development of the Coast Ranges and the formation of the silica-carbonate mercury deposits. A metamorphic fluid release can be related to the change from compression tectonics to transform and dilation following the passing of the triple junction. The mercury deposits, like the volcanic rocks, apparently decrease in age northward, Pliocene to Pleistocene at the New Almaden mine and Quaternary at Sulfur Bank (Peabody and Einaudi, 1992). These mercury deposits may represent a higher level analog or extension of mesothermal gold systems.

Conversely, several authors have suggested that devolatilization of the Franciscan Complex and mercury mineralization are directly related to heating from upwelling mantle material or volcanic intrusions rather than the product of regional metamorphic processes (Moiseyev, 1971; Studemeister, 1984; Peabody and Einaudi, 1992). Although this may be a viable process for localized areas, the widespread distribution of mercury occurrences throughout the Coast Ranges (including the rocks outboard of the Salinian Block where volcanism is generally absent) argue against this model. The lack of correlation between mercury mineralization and areas of volcanic

DEPOSIT TYPE	$\delta^{18}\text{O}$ quartz	δD fluid inclusions	Calculated $\delta^{18}\text{O}$ fluid	ref.
Silica-carbonate mercury deposits	+18.5 to +24.6	---	-3 to +8	1,2,5
Hot-spring gold deposits	+18 to +31	-30 to -15	+8 to +10	3,4
Calistoga Ag-Au district	+4.2 to +12.6	---	-9 to -6	5

TABLE 2. Stable isotope analyses of quartz and fluid inclusion waters from silica-carbonate mercury and hot-spring gold deposits and veins in the Calistoga Ag-Au district, Coast Ranges, California, and calculated oxygen isotope composition of the ore-fluid. δD and $\delta^{18}\text{O}$ reported in per mil relative to SMOW. References: 1. Boctor and others, 1987; 2. Peabody and Einaudi, 1992; 3. Peters, 1991; 4. Sherlock and Jowett, 1992; 5. this study.

activity, and the absence of metamorphic-fluid dominated hydrothermal systems and associated alteration of the volcanics, suggest that magmatism not an important process in the formation of the mercury deposits. For example, in the Sonoma Volcanics, alteration and veining is related to a meteoric fluid (Table 2).

A second type of mercury deposit in which the alteration is predominantly silicification is found in several areas along or near the Coast Range fault. In the Knoxville and Sulfur Creek mercury districts opalite mercury mineralization is found in hot-spring deposits spatially associated with older silica-carbonate mineralization. Similar active thermal springs in the Sulfur Creek district, identified by White and others (1973) as Great Valley high Cl^- type fluid, are currently depositing mercury-bearing sulfide minerals (see also Peters, 1991, 1993). Springs with similar chemical compositions outside of the silica-carbonate districts do not carry significant mercury suggesting that the mercury in the opalite deposits is remobilized from the older silica-carbonate mineralization. Two of the opalite mercury systems have also been identified as carrying economic concentrations of gold (the McLaughlin and Cherry Hill deposits). Other opalite mercury occurrences associated with silica-carbonate mineralization are found at the Oat Hill mercury mine south of the Knoxville district and in the Stayton mercury district in northern San Benito County (Vradenburgh, 1982).

GOLD DEPOSITS

The McLaughlin and Cherry Hill systems lie at the contact between rocks of the Great Valley sequence and serpentinized Coast Range ophiolite along the Stony Creek fault zone, just to the east of the Coast Range fault (Percy and Peterson, 1990; McLaughlin and others., 1989). These gold-bearing systems represent a hot-spring environment with subaerial sinter, pervasive silicification, and near-surface argillic alteration associated with the mineralization (Lehrman, 1986; Percy and Peterson, 1990; Sherlock and Jowett, 1992). Ore at the McLaughlin and Cherry Hill deposits occurs principally as sheeted and stockwork veins and microveinlets, most less than 1 cm wide, in highly fractured adularized and silicified sedimentary rocks and serpentinite. At the McLaughlin deposit, some of the near surface brecciation is considered typical of that produced by hydrothermal over-pressuring and hydrofracturing (Sherlock and Jowett, 1992). However, most of the fracturing and brecciation is related to tectonic processes (Tosdal, pers. comm.). Fluid inclusion studies and a vertical zonation from base-metal enrichment at depth

zoning up through gold and silver to mercury at the sinter, are consistent with ore deposition in a boiling system (Peters, 1991; Sherlock and Jowett, 1993). Boiling and ore deposition at the McLaughlin deposit occurred in the range of 160° to 200°C (Sherlock, 1993). In contrast, at the Cherry Hill deposit the zones of intense fracturing and brecciation are only related to tectonic processes and there is little or no direct evidence of boiling. This suggests that the boiling and hydrofracturing are not necessary for the production of ore-grade mineralization (Percy and Peterson, 1990).

Both the McLaughlin and Cherry Hill hot-spring deposits are located in major silica-carbonate mercury districts and were the sites of byproduct gold production from the mercury mining. These hot-spring deposits also had opalite mercury mineralization associated with the sinter and in the near-surface. However, the chemistry of the gold-bearing hot spring fluid was significantly different from that which produced the older silica-carbonate mineralization. Stable isotope and fluid inclusion analyses of ore samples from the McLaughlin deposit indicate that the hydrothermal fluid associated with the gold and opalite mercury mineralization was isotopically heavy, $\delta^{18}\text{O}$ +8 to +10‰ and δD -30 to -15‰ (Table 2), low- to moderate-salinity, with minor CO_2 , CH_4 , and H_2S (Peters, 1991; Sherlock and Jowett, 1992). Although the hot-spring and silica-carbonate ore fluids are isotopically similar, the low CO_2 content hot-spring fluid could not have produced the silica-carbonate alteration assemblage (Barnes, and others, 1973; Peabody and Einaudi, 1992). Several thermal springs in the Sulfur Creek district are isotopically and chemically similar to the fluid determined to be responsible for the hot-spring gold mineralization, and are currently depositing an auriferous sulfide precipitate (Percy and Peterson, 1990; Peters, 1991, 1993). These springs are among the high-Cl⁻ group identified by White and others (1973) and Barnes (1970) as fluids derived from dewatering of the Great Valley marine sediments. Many similar saline springs are found throughout the Coast Ranges along or near the Coast Range fault, but only those in the Sulfur Creek district have been identified as carrying significant gold (Thompson and others, 1981; Peters, 1991).

Two other areas of precious metal mineralization occur in the Coast Ranges Province. The largest historical production of gold was from the Calistoga silver-gold district in north-western Napa County approximately 15 mi to the southwest of the McLaughlin mine. Principal production came from the Silverado and Palisade mines where quartz veins up to 5 meters thick occur in andesite and silicified rhyolite of the Sonoma Volcanics. Oxygen isotope values range from +4.2 to +5.9‰ for quartz from the Silverado main vein to +7.4 to +12.6‰ for samples of opaline silica and vein material from several prospects to the south. Assuming deposition over a temperature range of 100° to 200°C, the oxygen isotope composition of the hydrothermal fluid was approximately -6 to -9‰. This value is essentially identical to present day meteoric water and significantly different from the silica-carbonate and hot-springs gold hydrothermal fluids.

A second area with historic gold production is the Los Burros district in southern Monterey county (Fig. 1) where gold-bearing quartz veins occur in highly sheared and faulted high-metamorphic grade Franciscan Complex rocks. The veins are localized along shears and in fracture zones, often accompanied by fault gouge. Vein mineralogy consists of calcite and minor chalcopyrite, pyrite, arsenopyrite, and free gold (Hart, 1966). These veins are mineralogically and structurally similar to mesothermal veins found in metamorphosed turbidite rocks

worldwide which are considered to have formed by metamorphic processes. Similar small-scale vein systems may be present elsewhere in the Coast Ranges. Many streams draining Franciscan Complex rocks were mined by small-scale placer operations during the Depression and several occurrences of narrow gold-bearing quartz veins in the metamorphosed Franciscan Complex rocks, including in the hills just south of San Francisco, have also been reported (Clark, 1976).

DISCUSSION

Three components appear to relate directly to the origin of the hot-spring gold mineralization at the McLaughlin and Cherry Hill deposits: the apparent spatial relation to silica-carbonate mercury mineralization, the presence of volcanic rocks or other heat source, and the proximity to the Great Valley sequence or Coast Range fault and associated saline fluid. Presently, the only known hot-spring gold deposits in the Coast Ranges Province are found associated with recent volcanism and high Cl^- thermal spring activity in or near older silica-carbonate mercury mineralization. To evaluate the potential for similar deposits elsewhere in California Coast Ranges we need to understand which, if any, of these components are essential for the formation of the hot-spring gold mineralization.

There appears to be no simple direct correlation of hot-spring gold mineralization with either silica-carbonate mercury mineralization or volcanism in the Coast Ranges Province. Silica-carbonate mercury deposits are found throughout the Coast Ranges, and with the exception of those deposits which have evidence of later hot spring activity, significant gold is not reported with the mercury mineralization. Although sulfides from several of the silica-carbonate deposits have been determined to contain trace quantities of gold (Vradenburgh, 1982), the two largest mercury mines in the Coast Ranges, the New Almaden and New Idria mines, have reported no detectable gold. Volcanic rocks are also found along the entire length of the Coast Ranges, and outside of the veins in the Calistoga district there is no other gold mineralization which can be tied specifically only to volcanic activity.

There also appears to be no direct correlation of hot-spring gold mineralization to silica-carbonate mercury mineralization or volcanism in close proximity to the Great Valley sequence, source of the saline hydrothermal ore fluids present in the McLaughlin and Cherry Hill deposits. At the New Idria mercury mine which is located along the Coast Range fault and much of the ore is localized in Great Valley sedimentary rocks, and the Sutter Buttes volcanic rocks which intrude the Great Valley sediments, there is no evidence of hot-spring type alteration or mineralization.

At the Sulfur Bank mine there is a spatial association of mercury mineralization and volcanic rocks. Mercury mineralization occurs in Franciscan Complex metasediments and overlying Clear Lake volcanic rocks. Alteration associated with the mineralization is dominantly amorphous silica and kaolinite (Wells and Ghiorso, 1988). Although similar to the opalite mineralization associated with the hot-spring gold mineralization, springs in the mine pit which are reported to be currently depositing mercury-bearing minerals are the high HCO_3^- low Cl^- fluids considered to be derived from the metamorphosed Franciscan Complex rocks (White and others, 1973). Samples of marcasite contain traces of gold but no precious metal mineralization has been identified. This deposit

most likely is of the silica-carbonate type but the absence of reactive serpentinite and boiling in the hydrothermal system give it the appearance of an opalite occurrence.

Although the silica-carbonate deposits and the hot-springs deposits were formed by significantly different hydrothermal fluids, there appears to be a direct relation between the two systems. The silica-carbonate mercury deposits are localized along major structural features throughout the Coast Ranges and are considered to have formed from fluids derived from low- to moderate-grade metamorphic devolatilization of the Franciscan accretionary complex. Mesothermal gold-bearing quartz veins, also considered to be related to regional metamorphic processes, occur in higher-grade Franciscan assemblage metamorphic rocks and may represent deeper levels in the silica-carbonate system. In contrast, the McLaughlin and Cherry Hill hot-springs gold deposits were formed by moderately saline connate fluids most likely derived from the Great Valley sequence rocks. Similar saline spring systems in the Sulfur Creek silica-carbonate mercury district are currently depositing a gold-bearing sulfide precipitate. However, saline springs that are spatially unrelated to silica-carbonate mineralization have not been identified as carrying significant quantities of gold or mercury. This, and the spatial association of the McLaughlin and Cherry Hill deposits with the older silica-carbonate mineralization, suggests that the source of the gold and mercury for the hot-spring deposits is remobilization from the preexisting silica-carbonate mercury and deeper gold systems. Saline waters from the Great Valley sequence that percolated into Coast Range fault and adjacent Franciscan assemblage rocks along faults and fractures were heated by the intrusion of recent volcanics and scavenged or remobilized the gold and other ore constituents. The hydrothermal fluids were then channeled along the same structures which focused the silica-carbonate mercury systems. The idea of deposits forming by remobilization of preexisting mineralization is not new and is common in the Chinese literature.

CONCLUSIONS

The epithermal gold and mercury mineralization at the McLaughlin and Cherry Hill deposits, although formed from a different hydrothermal fluid, is genetically related to the local silica-carbonate mercury mineralization. Saline thermal springs driven by a volcanic heat source remobilized the gold from depth and the mercury from the upper levels of the silica-carbonate system and redeposited them in a near-surface hot-spring environment. Similar systems may be present at the Oat Hill mine and in the Stayton district where opalite mercury mineralization has been reported associated with silica-carbonate and volcanic rocks. These two areas are also reported to contain anomalous gold values (Wiebelt, 1956; Yates and Hilpert, 1946) and may be the sites of hot-spring gold mineralization.

REFERENCES

- Atwater, Tanya, 1970, Implications of plate tectonics for the Cenozoic tectonic evolution of western North America: Geological Society of America Bulletin, vol. 81, pp. 3513-3536.
- Bailey, E. H., Clark, A. L., and Smith, R. M., 1973, United States Mineral Resources: Mercury: U. S. Geological Survey Professional Paper 820, pp. 401-414.
- Bailey, E. H., Irwin, W. P., and Jones, D. L., 1964, Franciscan and related rocks, and their significance in the geology of western California; California Division of Mines and Geology Bulletin 183.
- Barnes, Ivan, 1970, Metamorphic waters from the Pacific tectonic belt of the west coast of the United States: Science, vol. 168, pp. 973-975.
- Barnes, Ivan, O'Neil, J. R., Rapp, J. B., and White, D. E., 1973, Silica-carbonate alteration of serpentine: Wall rock alteration in mercury deposits of the California Coast Ranges: Economic Geology, vol. 68, pp. 388-398.
- Blake, M. C., Jr., and Jones, D. L., 1974, Origin of Franciscan melanges in northern California: Society of Economic Paleontologists and Mineralogists Special Publication 19, pp. 345-357.
- Blake, M. C., Jr., and Jones, D. L., 1978, Allochthonous terranes in northern California?- A reinterpretation, *in* Mesozoic paleogeography of the western United States: Society of symposium, 2d, April 1978, Proceedings, pp. 397-400.
- Boctor, N. Z., Shieh, Y. N., and Kullerud, G., 1987, Mercury ores from the New Idria mining district, California: Geochemical and stable isotope studies: Geochimica et Cosmochimica Acta, vol. 51, pp. 1705-1715.
- Clark, W. B., 1976, Gold districts of California; California Division of Mines and Geology Bulletin 193, 186p.
- Dickinson, W. R., 1970, Clastic sedimentary sequences deposited in shelf, slope, and trough settings between magmatic arcs and associated trenches: Pacific Geology, vol. 3, pp. 15-30.
- Dickinson, W. R., and Snyder, W. S., 1979, Geometry of triple junctions related to the San Andreas transform: Journal of Geophysical Research, vol. 84, pp. 561-572.
- Donnelly-Nolan, J. M., 1983, Diverse origins of thermal waters in the Geysers-Clear Lake area, northern California: International Symposium on Water-Rock Interaction, 4th, Misasa, Japan, August 29-September 3, 1983, Extended Abstracts, pp. 123-126.
- Donnelly-Nolan, J. M., Burnes, M. G., Goff, F. E., Peters, E. K., and Thompson, J. M., 1993, The Geysers-Clear Lake area, California: Thermal waters, mineralization, volcanism, and geothermal potential: Economic Geology, vol. 88, pp. 301-316.
- Fox, K. F., Jr., Fleck, R. J., Curtis, G. H., and Meyer, C. E., 1985, Implications of the northwardly younger age of the volcanic rocks of west-central California: Geological Society of America Bulletin, vol. 96, pp. 647-654.
- Goldfarb, R. J., Leach, D. L., Miller, M. L., and Pickthorn, W. J., 1986, Geology, metamorphic setting and genetic constraints of epigenetic lode-gold mineralization within the Cretaceous Valdez Group, south-central Alaska; in Keppie, J. D., Boyle, R. W., and Haynes, S. J., eds., Turbidite-Hosted Gold Deposits, Geological Association of Canada Special Paper 32, pp. 87-106.
- Hart, E. W., 1966, Mines and mineral resources of Monterey County, California: California Division of Mines and Geology County Report 5, 142p.
- Hearn, B. C., Donnelly-Nolan, J. M., and Goff, F. E., 1981, The Clear Lake Volcanics: Tectonic setting and magma sources: U. S. Geological Survey Professional Paper 1141, pp. 25-45.
- Henderson, III, F. B., 1969, Hydrothermal alteration and ore deposition in serpentinite-type mercury deposits: Economic Geology, vol. 64, pp. 489-499.
- Ingersoll, R. V., Rich, E. I., and Dickinson, W. R., 1977, Field trip guide to the Great Valley sequence: Geological Society of America, Cordilleran Section, Annual Meeting, 73d, April 1977, 72p.
- Johnson, C. M., and O'Neil, J. R., 1984, Triple junction magmatism: a geochemical study of Neogene volcanic rocks in western California: Earth and Planetary Science Letters, vol. 71, pp. 241-262.
- Lehrman, N., 1986, The McLaughlin mine, Napa and Yoly Counties, California: Nevada Bureau of Mines and Geology Report 41, pp. 85-89.
- Magaritz, M. and Taylor, H. P., 1976, Oxygen, hydrogen, and carbon isotope studies of the Franciscan formation, Coast Ranges, California: Geochimica et Cosmochimica Acta, vol. 40, pp. 215-234.
- McLaughlin, R. J., 1981, Tectonic setting of pre-Tertiary rocks and its relation to geothermal resources in the Geysers-Clear Lake area: U. S. Geological Survey Professional Paper 1141, pp. 3-23.
- McLaughlin, R. J., Ohlin, H. N., Thormahlen, D. J., Jones, D. L., Miller, J. W., and Blome, C. D., 1989, Geologic map and structure sections of the Little Indian Valley-Wilbur Springs geothermal area, northern Coast Ranges, California: U. S. Geological Survey Miscellaneous Investigations Series Map I-1706, 1:24,000.
- McLaughlin, R. J., and Pessagno, E. A., Jr., 1978, Significance of age relations above and below Upper Jurassic ophiolite in The Geysers-Clear Lake region, California: U. S. Geological Survey Journal of Research, vol. 6, pp. 715-726.
- Moiseyev, A. N., 1971, A non-magmatic source of mercury deposits: Economic Geology, vol. 66, pp. 591-601.

- Page, B. M., 1966, Geology of the Coast Ranges of California: California Division of Mines and Geology Bulletin 190, pp. 253-276.
- Peabody, C. E., and Einaudi, M. T., 1992, Origin of petroleum and mercury in the Culver-Baer cinnabar deposit, Mayacmas district, California: *Economic Geology*, vol. 87, pp. 1078-1103.
- Pearcy, E. C., and Peterson, Ulrich, 1990, Mineralogy, geochemistry and alteration of the Cherry Hill, California hot-spring gold deposit: *Journal of Geochemical Exploration*, vol. 36, pp. 143-169.
- Peters, E. K., 1991, Gold-bearing hot spring systems of the Northern Coast Ranges, California; *Economic Geology*, vol. 86, pp. 1519-1528.
- Peters, E. K., 1993, D - ^{18}O enriched waters of the Coast Range Mountains, northern California: Connate and ore-forming fluids: *Geochimica et Cosmochimica Acta*, vol. 57, pp. 1093-1104.
- Sherlock, R. L., and Jowett, E. C., 1992, The McLaughlin hot-spring gold-mercury deposit and its relationship to hydrothermal systems in the Coast Ranges of northern California; in Kharaka and Maest, eds, Water-Rock Interaction, Balkema, Rotterdam, pp. 979-982.
- Stanley, R. G., Implications of the northwestwardly younger age of the volcanic rocks of west-central California: Alternative Interpretation: *Geological Society of America Bulletin*, vol. 98, no. 5, pp. 612-614.
- Studemeister, P. A., 1984, Mercury deposits of western California: An Overview: *Mineralium Deposits*, vol. 19, pp. 202-207.
- Thompson, J. M., Goff, F. E., and Donnelly-Nolan, J. M., 1981, Chemical analyses of waters from springs and wells in the Clear Lake volcanic area: U. S. Geological Survey Professional Paper 1141, pp. 161-166.
- Vredenburg, L. M., 1982, Tertiary gold bearing mercury deposits of the Coast Ranges of California: *California Geology*, vol. 35, pp. 23-27.
- Wells, J. T., and Ghiorso, 1988, Rock alteration, mercury transport, and metal deposition at Sulfur Bank, California: *Economic Geology*, vol. 83, pp. 606-618.
- White, D. E., 1974, Diverse origins of hydrothermal ore fluids: *Economic Geology*, vol. 69, pp. 954-973.
- White, D. E., 1981, Active geothermal systems and hydrothermal deposits: *Economic Geology 75th Anniversary Volume*, pp. 392-423.
- White, Donald, Barnes, Ivan, and O'Neil, J. R., 1973, Thermal and mineral waters of nonmeteoric origin, California Coast Ranges: *Geological Society of America Bulletin*, vol. 84, pp. 547-560.
- Wiebelt, F. J., 1956, Quien Sabe Antimony Mine, San Benito County, California; U. S. Bureau of Mines, Report of Investigation 5192.
- Yates, R. G., and Hilpert, L. S., 1946, Quicksilver deposits of the eastern Mayacamas District, Lake and Napa Counties, California: *California Journal of Mines and Geology*, vol. 42, no. 3, pp. 231-286.

SILICA CARBONATE ALTERATION OF SERPENTINITE, IMPLICATIONS FOR THE ASSOCIATION OF PRECIOUS METAL AND MERCURY MINERALIZATION IN THE COAST RANGES

Ross L. Sherlock¹, M. Amelia V. Logan² and E. Craig Jowett²

¹Mineral Deposit Research Unit, Department of Geological Sciences, University of British Columbia, Vancouver, B.C. V6T 1Z4

²Department of Earth Sciences, University of Waterloo, Waterloo, Ont. N2L 3G1

ABSTRACT

Silica carbonate alteration of serpentinite is ubiquitous in the Coast Ranges of northern California, occurring in barren, Hg-rich and auriferous hydrothermal systems. The alteration is formed by the low temperature reaction of CO₂-rich fluids with serpentinite minerals. The alteration is considered to be an exchange of cations with little net gain or loss of oxygen. The major element flux is characterized by the addition of silica and CO₂ and a depletion in all other cations. The trace element flux is different for each suite examined. Barren silica carbonate assemblages are not elevated in any of the trace elements analyzed. Mercury-rich suites are elevated in Hg and the auriferous suites are elevated in Au, As, Sb and Hg. The mineralogical changes resulting from the alteration is a halo of magnesite around a core of silicified serpentinite. The variation in alteration minerals may reflect variations in fluid temperature. Oxygen isotopes suggest that the alteration is low temperature around 20°C, and that the mineral-springs were likely active at the site of the McLaughlin deposit prior to and after the hot-spring activity, that formed the McLaughlin ore body. The sulfur isotopic composition from a variety of mercury deposits and active hydrothermal systems show fairly consistent values of about 0‰, indicating a magmatic source.

INTRODUCTION

This study was initiated, to determine the mass flux and stable isotope systematics of silica carbonate alteration of serpentines and associated mercury mineralization. Silica carbonate alteration of serpentinite is ubiquitous, in the Coast Ranges of northern California, occurring in barren, Hg-rich, and Au-Hg systems. The alteration is structurally controlled and is formed by low temperature CO₂-rich fluids (Barnes et al., 1973a). Previous studies (Barnes et al., 1973a,b; White et al., 1973; Peters, 1991, 1993; Sherlock, 1993) have demonstrated that mineral-springs issuing from silica carbonate assemblages are isotopically and geochemically related to higher temperature auriferous hot-springs. The problem addressed in this study is whether the silica carbonate alteration is related to a higher temperature auriferous hydrothermal system, and if geochemical analysis of silica carbonate assemblages can be used to evaluate their auriferous potential.

This study consists of three parts: (1) a study of the mass flux that results in the silica carbonate alteration; (2) the oxygen isotope systematics of the alteration and the implications for evolution of the hydrothermal fluids; (3) a reconnaissance study of the sulfur isotopes from various mercury deposits, gold-mercury deposits and active hydrothermal systems throughout the northern Coast Ranges. Each of the three topics will be discussed separately.

Twenty-one samples were selected for a detailed study from three locations that are representative of barren, potentially auriferous (Hg-rich), and auriferous hydrothermal systems (Fig. 1). The sites chosen were a silica carbonate assemblage at Soda Springs near Lake Pillsbury (barren, n = 7); the Knoxville deposit (potentially auriferous Hg-rich, n = 8); and the McLaughlin deposit (auriferous, n = 6). Care was taken to sample only silica carbonate assemblages with no macroscopic veining. Samples from each suite ranged from intensely altered to unaltered serpentinite.

A total of thirteen samples of silica carbonate were analyzed for oxygen isotopes from the three silica carbonate assemblages. Samples ranged from pristine serpentinite to intensely altered silica carbonate. Five isotopic analysis of mineral-spring fluids that are active around the silica carbonate assemblages are also included.

Sulfur isotopes were conducted on twenty five samples from fourteen mercury deposits and five active hydrothermal systems throughout the northern Coast Ranges (Fig. 1).

LOCAL GEOLOGY

Soda Springs, Lake Pillsbury

The Soda Springs (Fig. 2) silica carbonate assemblage was selected for the barren suite because it has an active mineral-spring issuing from the center of the alteration and no mercury production has been reported from the area. The area is underlain by serpentinite. The location of the spring is likely controlled by a northwest trending fault that originates at the Coast Range Thrust and is defined by a belt of serpentinite (Fig. 1). This is the same structure that controls Bartlett Springs, Chalk Mountain and the Abbot and Turkey Run mercury deposits. The mineral-spring is low temperature, CO₂-rich with associated calcareous travertine and amorphous iron oxide precipitates. The silica carbonate alteration extends in a halo around the spring.

Knoxville-McLaughlin

There is a continuous zone of serpentinite extending from the McLaughlin to the Knoxville deposits (Fig. 3). In both the Knoxville and McLaughlin deposits the serpentinite is on the footwall side of the Stony Creek fault and forms the Coast Range Ophiolite (Shervais and Kimbrough, 1985). Silica carbonate alteration within this zone is restricted to the McLaughlin and Knoxville deposits with the alteration being most intense at the Stony Creek fault.

The Knoxville silica carbonate assemblage (Fig. 3) was chosen as the Hg-rich, potentially auriferous suite because it was a large mercury producer and it is spatially related to the McLaughlin gold deposit. The structural features controlling the alteration are northwest striking fault splays originating at the Stony Creek fault. Alteration increases in intensity surrounding these faults.

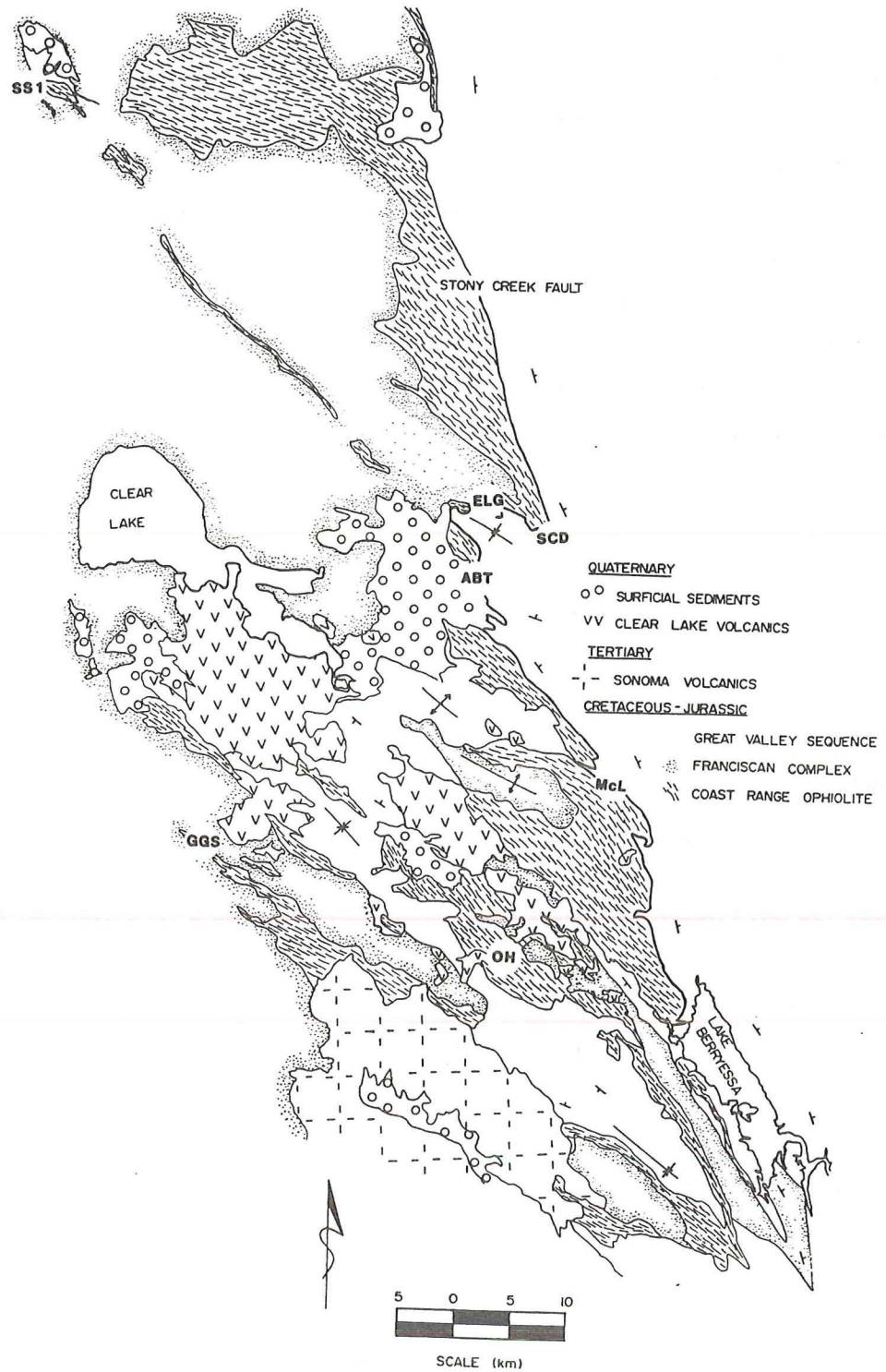


FIGURE 1. Sample location map. McL, McLaughlin and Knoxville silica carbonate suites; SS1, Soda Springs at Lake Pillsbury silica carbonate suite. The samples for sulfur isotopes were taken from the: GGS, Geysers Geothermal System; OH, Oat Hill District; McL, McLaughlin District; ABT, Abbot District; SCD, Sulphur Creek District; and ELG, Elgin District. The abbreviations correspond to the districts used in table three. Geology is compiled from McLaughlin et al. (1978), McLaughlin et al. (1990), Wagner and Bortugno (1982) and Chapman et al. (1974).

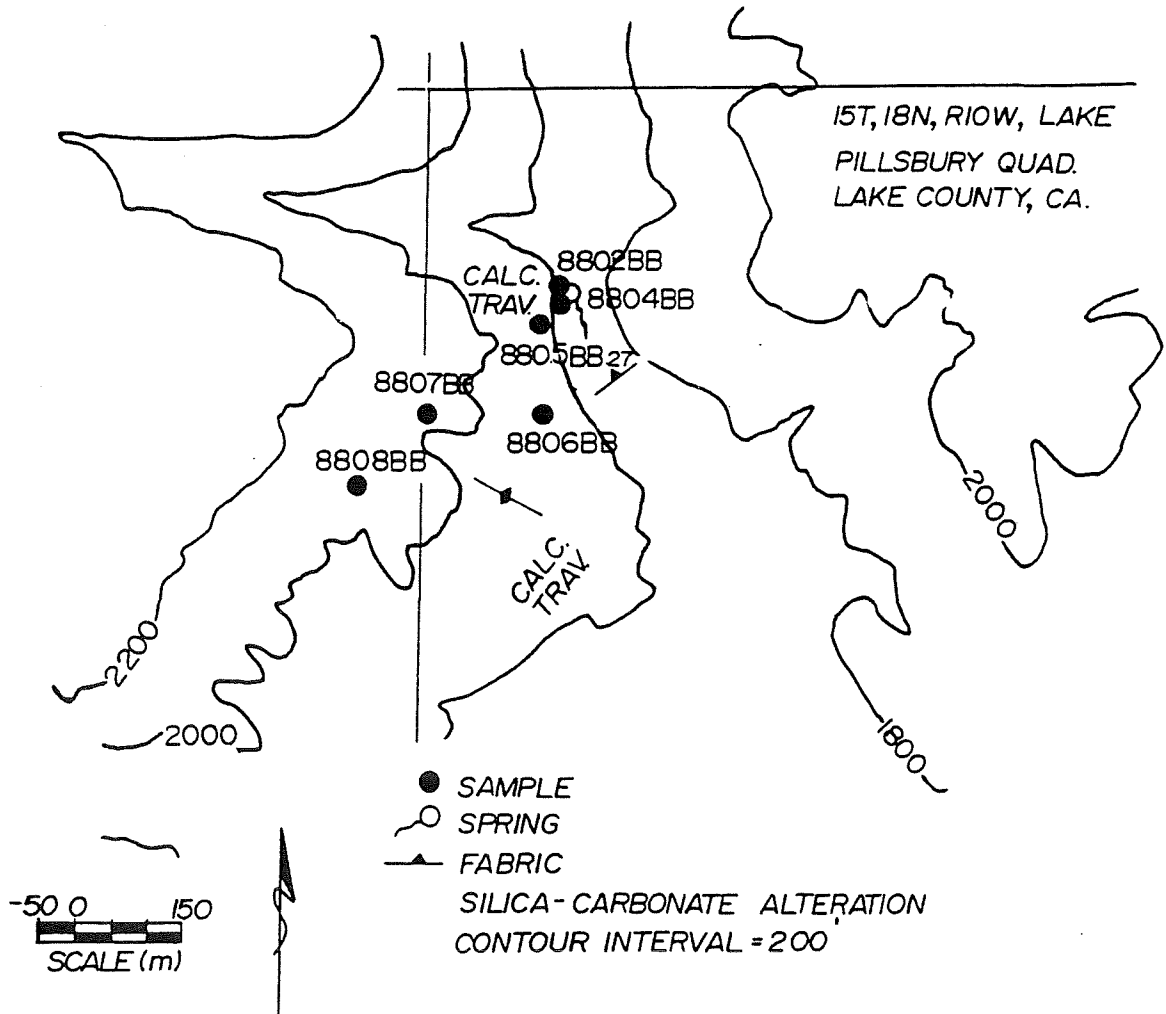


FIGURE 2. Sample location map for the Soda Springs silica carbonate assemblage at Lake Pillsbury.

Samples of silica carbonate from the McLaughlin south pit (Fig. 3) were chosen as representative of an auriferous system. The silica carbonate itself is not auriferous but is cut by auriferous veining, suggesting that it is an early alteration assemblage, possibly pre-mineralization. Structures controlling the alteration at McLaughlin are similar to those at the Knoxville deposit, northwest striking fault splays from the Stony Creek fault localize and control the intensity of alteration.

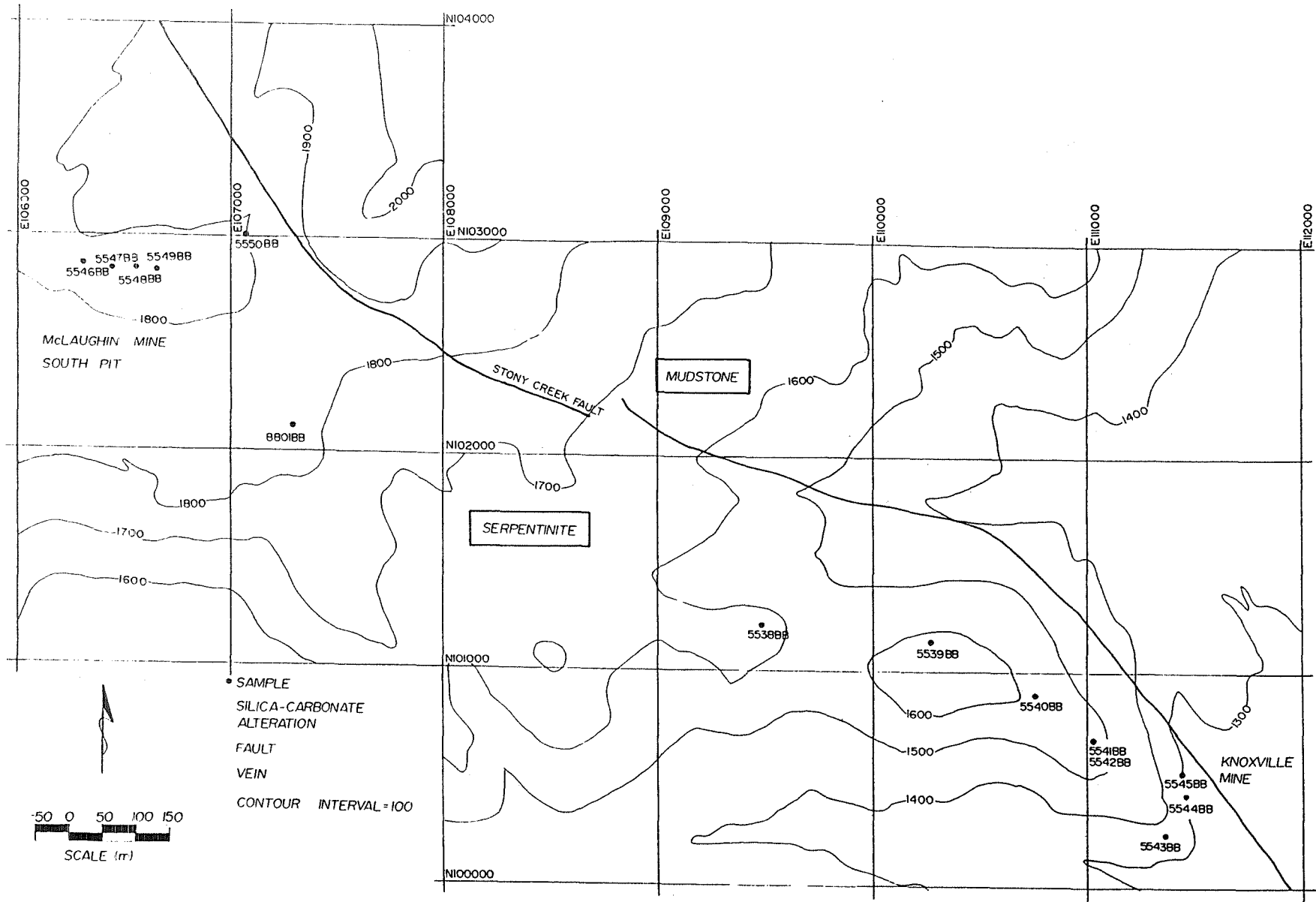


FIGURE 3. Sample location map for the Knoxville and McLaughlin deposits silica carbonate assemblages.

ANALYTICAL TECHNIQUES

Major and trace elements were analyzed by x-ray fluorescence at X-Ray Assay Lab in Toronto. Total iron is reported as Fe^{3+} . Trace elements were analyzed by inductively coupled plasma spectrometry at Geochemical Services Inc. in Sparks, Nevada. Gold assays were performed by graphite furnace fire assay with an atomic absorption finish at Geochemical Services Inc. Rare earth elements were analyzed by instrumental neutron activation at the University of Waterloo. Specific gravity measurements were performed on an air comparison pycnometer. Whole rock $\delta^{18}\text{O}$ analysis were performed on selected samples by first heating the samples to 300°C for 2 hours to remove any absorbed water, than oxygen extraction and $\delta^{18}\text{O}$ analysis performed using standard techniques with a gas source mass spectrometer at the University of Western Ontario. Silicate $\delta^{18}\text{O}$ data are reported with respect to SMOW. Sulfur isotopes were conducted on sulfide separates and on native sulfur. The sulfide separates were prepared using a modified technique of Tuttle et al. (1986). The separates were reacted with copper sulfide to sulfur dioxide using the technique of Fritz et al. (1974) and analyzed at the University of Waterloo. Sulfur isotopes are reported with respect to CDT. Oxygen analysis of spring fluids were conducted by CO_2 equilibration using the techniques of Fritz et al. (1986). Deuterium analysis of spring fluids were conducted by zinc reduction using the techniques of Coleman et al. (1982). All water analysis were performed at the Environmental Isotope Laboratory at the University of Waterloo and are reported with respect to SMOW.

PETROGRAPHY

The petrographic relations are similar for each of the three suites, and will be treated in the same section. Fresh serpentinite is dominantly lizardite with minor amounts of chrysotile. Up to 5% chromite and magnetite are typically present. The presence of mesh-textured lizardite suggests that the protolith was a dunite (Wicks and Whittaker, 1977; Wicks et al., 1977). Fresh samples (5538BB, 5539BB, 5540BB) were collected on a traverse between the Knoxville and McLaughlin silica carbonate assemblages (Fig. 3), and fresh samples (8808BB and 8806BB) from the Soda Springs silica carbonate body were collected distal to the alteration (Fig. 2).

Two phases of alteration have been identified on the basis of petrographic relations. The first phase is characterized by an assemblage of lizardite and magnesite. The magnesite is present as shapeless masses replacing the lizardite and as veinlets cross-cutting the lizardite. Also present are various forms of the serpentinite minerals within cross-cutting veinlets. These veinlets have high second order birefringence and are optically distinct from the mesh textured lizardite. However, examination of the minerals with a XRF microprobe at the University of Toronto was unable to distinguish between the two phases. These veinlets, of highly birefringent serpentinite, are only present in samples that contain magnesite, and appear to be overprinted by the magnesite. Samples demonstrating this style of alteration are: 5541BB, 5542BB, from the Knoxville deposit; 5550BB, 8801BB, from the McLaughlin deposit; and 8804BB, 8807BB from Soda Springs.

A second phase of alteration is intense silicification with minor magnesite. This style of alteration is characterized by complete silicification of serpentinite minerals, with preservation of the original serpentinite textures. Samples displaying this alteration have very high SiO_2 contents ($> 85\%$), and are what is typically

identified as intense silica carbonate alteration. The silica is opalin in nature and replaces the serpentinite on a very fine scale preserving the serpentinite mesh textures. Samples displaying this alteration are: 5543BB, 5544BB, 5545BB, Knoxville deposit; 5546BB, 5547BB, 5548BB, 5549BB, McLaughlin deposit; and 8802BB, 8803BB, 8805BB, Soda Springs.

The alteration of serpentinite appears to be a halo of carbonate flooding around a core of intensely silicified serpentinite. The serpentinite textures are preserved on a very fine scale. There is no evidence for overprinting of the phases of alteration, they appear to be coeval. Similar alterations have been described at the New Almaden mercury deposit in California (Bailey and Everhart, 1964), and at the Culver Baer deposit (Peabody and Einaudi, 1992). The main difference is that the strongly altered silica carbonate assemblages examined in this study do not contain the carbonate and silica veinlets that are present at the Culver Baer deposit.

GEOCHEMISTRY

Primary Geochemistry

Fresh serpentine is characterized by very low Al_2O_3 , TiO_2 , Zr and REE contents (Table 1). The samples are very depleted in light REE with an upward sloping REE trend (Sherlock, 1993). Chondrite normalized abundances of REE are between 0.1 and 1. The chemistry supports the petrographic observations that the protolith of these samples was a dunite (Schandl and Naldrett, 1992).

Gresens Analysis

Using the general metasomatic equation of Gresens (1967), and the technique of Appleyard (1990), the mass flux of elements during alteration can be calculated using equation 1.

$$DX_n = a (FV * [r^b / r^a] * X^{b,a} - X^a) \quad (1)$$

Where DX_n is the gain or loss of element n in producing rock b (altered) from rock a (parent); FV (volume factor) is the ratio of the volume of rock a to the volume of rock b if element n is considered immobile; a is the initial mass of rock a ; $X^{b,a}$ is the weight fraction of component n ; and $r^{a,b}$ is the density of the parent and altered rock respectively.

Equation one is a linear equation with two unknowns DX_n and FV . If more than one element is immobile, or the same element with multiple parent rocks, then the FV values for those elements will be similar when $DX_n = 0$. A cluster of FV values indicates possible immobility of the respective elements, and the FV value is termed the zero change volume factor (FV°). By calculating the FV° values for each element in a parent-daughter relationship and plotting the values on a histogram the immobile elements can be readily determined by a clustering of FV° values. Once the immobile elements and the appropriate volume change is determined then DX_n can be calculated for each element in each altered sample by applying the determined FV° value.

TABLE 1

Soda Springs

	8802BB	8803BB	8804BB	8804BB repeat	8805BB	8806BB	8806BB repeat	8807BB	8808BB
SiO ₂ % (1)	84.5	77.6	45.7	44.6	78.2	40.7	40.3	48.2	38.4
Al ₂ O ₃ % (1)	0.42	0.58	1.54	1.52	1.71	2.55	2.58	1.82	2.10
Fe ₂ O ₃ % (1)	9.15	9.15	8.71	8.83	7.55	8.69	8.75	8.01	8.74
MgO % (1)	1.3	2.5	24.6	24.1	1.5	32.5	31.9	26.0	35.3
CaO % (1)	0.16	0.16	0.53	0.61	0.18	0.60	0.67	0.34	0.08
Na ₂ O % (1)	0.09	0.37	<0.01	0.02	<0.01	<0.01	<0.01	<0.01	<0.01
K ₂ O % (1)	0.15	0.14	0.08	0.11	0.26	<0.01	0.06	0.07	0.04
P ₂ O ₅ % (1)	0.02	0.02	0.02	0.02	0.02	0.01	0.02	0.02	0.02
MnO % (1)	0.08	0.15	0.13	0.13	0.07	0.14	0.14	0.13	0.15
S % (1)	0.11	<0.01	<0.01	0.02	0.03	<0.01	<0.01	0.01	<0.01
LOI % (1)	6.70	7.93	17.80	17.80	8.39	13.70	13.80	13.50	13.50
Total	102.71	98.56	99.11	97.76	97.88	98.89	98.22	98.10	98.33
Specific Gravity g/cc	2.21	2.47	2.74		2.39	2.74		2.64	2.78
Cr ppm (1)	3510	4250	3240	3210	3300	3340	3310	3250	3440
Ti ppm (1)	64	69	239		217	425		200	321
Co ppm (1)	109	81	102		70	91		99	105
Ni ppm (1)	1580	2370	2510		930	2170		2380	2530
Ba ppm (1)	1040	667	1290	1330	675	71	80	161	95
Rb ppm (1)	22	21	27	16	38	25	28	24	13
Sr ppm (1)	108	23	70	78	28	47	48	<10	<10
Zr ppm (1)	22	15	<10	<10	29	<10	<10	<10	<10
Nb ppm (1)	34	31	24	25	12	23	14	16	17
Ce ppm (2)									
Sm ppm (2)									
Eu ppm (2)									
Yb ppm (2)									
Lu ppm (2)									
Ag ppb (3)	10	5	10	6	14	10		10	10
Au ppb (3)	<2	<2	2	<2	<2	<2		5	2
As ppm (3)	1.14	1.14	0.36	<0.25	1.23	0.40		<0.25	0.69
Hg ppm (3)	0.10	<0.02	0.07	0.05	0.66	0.38		0.43	0.37
Sb ppm (3)	0.07	<0.05	<0.05	<0.05	0.33	0.06		0.06	0.14
Cu ppm (3)	8.81	7.58	9.93	11.10	11.70	20.60		16.30	30.40
Pb ppm (3)	0.29	0.13	0.25	0.54	0.54	0.17		0.31	0.61
Zn ppm (3)	14.60	23.20	22.80	24.40	27.20	16.90		19.60	21.70
Tl ppm (3)	0.69	1.49	0.64	0.62	0.95	0.53		<0.50	<0.50

- (1) X-ray Assay Laboratory
(2) University of Waterloo
(3) Geochemical Services Inc.

This Study

Criteria used for selecting the parent composition are distance from megascopic alteration, petrographic absence of alteration and chemical analysis that is consistent with fresh serpentinite. Since the McLaughlin and Knoxville silica carbonate bodies are connected by a continuous zone of serpentinite, parent samples were taken between the alteration zones (samples 5538BB, 5539BB & 5540BB). Parent samples for the Soda Springs at the Lake Pillsbury silica carbonate were spatially removed from the active springs (samples 8806BB & 8808BB).

Volume Change

Previous studies have suggested that silica carbonate alteration is a constant volume process (Bailey and Everhart, 1964; Barnes et al., 1973a). This assumption is based on the preservation of original serpentinite textures. To preserve the serpentinite mesh textures the alteration must have a small volume change, but a zero volume change is unwarranted. Volume change is a three dimensional process and is proportional to the radius cubed. To observe a 10% volume change in one dimension, a 2.2% length change must be observed. This is a very small change observed petrographically, however, it is significant when determining mass flux.

As a result of the Gresens analysis oxygen is used to constrain the volume change. The FV^o for oxygen is very well clustered for each parent composition, and is also clustered with various transition elements. The FV^o for the transition elements did not always cluster with oxygen which is attributed to variations in the primary chemistry of the samples. Using oxygen, with one exception, volume changes were calculated to be less than 10%. One sample (5549BB) had a larger volume change of 21%. These overall small volume changes are consistent with the preservation of serpentinite textures.

The use of oxygen to constrain volume change in a hydrothermal environment is unusual. This does not mean that oxygen has not been exchanged with the fluid, isotopic data indicates that exchange has occurred. A constant oxygen suggests that the alteration is dominated by cation exchange with little net gain or loss in oxygen. The use of oxygen as an immobile element is analogous to a Barth Cell (Barth 1948, 1952; McKie, 1966).

Results of Gresens Analysis

Histograms were plotted for two representative samples from each of the suites. Samples that displayed the initial magnesite alteration are labeled weakly altered serpentinite and samples that were intensely silicified are labeled intensely altered serpentinite. The mass flux data was normalized to the primary rock composition and are presented as percent mass flux (Fig. 4a,b; 5a,b; 6a,b). This displays the relative mobility of the elements without biasing the data to more abundant elements. A negative percent mass flux indicates a depletion in that element, to a maximum of 100%, and a positive percent mass flux indicates an enrichment in that element with no maximum. Elements labeled ND were below the detection limit and could not be treated in this manner. Elements without a visible histogram bar have an elemental flux of less than 1 percent. Only elements that are consistently above the detection limit are considered.

Major Elements

Similar trends in major element chemistry were found in all three of the silica carbonate assemblages, as a result all three assemblages will be treated in the same section. The alteration is characterized by the addition of Si and CO₂ and the loss Al, Fe³⁺, Mn, and Mg (Fig. 4a,b; 5a,b; 6a,b). The samples that have a lizardite-magnesite assemblage have a small enrichment in silica and a corresponding small depletion in other major cations. Samples that are intensely silicified show an extreme silica enrichment and a depletion in other major cations. There is no intermediate composition, the samples are either composed of the lizardite-magnesite assemblage or the opalin silica assemblage.

Mass flux of Si vs Mg displays a linear relationship (Fig. 7), suggesting coherent mobility of these elements. These plots are affected by the actual magnitude of the elemental flux. The alteration trend is typically from an initial 40 to a final 90 wt.% SiO₂. Therefore, all elements will show a systematic depletion with Si enrichment simply as a result of the magnitude of silica enrichment. However, these plots show linear relationships within the regions where silica has been only slightly enriched, suggesting that the relationship is due to coherent mobility. The plot of Si vs Mg flux also illustrates the two groups of alteration assemblages. The low Si and Mg flux is characterized by the lizardite-magnesite assemblage and the high Si and Mg flux is characterized by the opalin silica assemblage.

Trace Elements

The trace element mass flux calculations are strongly affected by their low primary abundance in the parent rock composition. Unless the altered rock is strongly enriched in a trace element, the variations in the percent mass flux likely represent natural variation in the rock composition. Only trace elements of epithermal affinity were considered.

Soda Springs: The trace elements were generally below the detection limit in all the samples examined from this suite (Fig. 4a,b).

Knoxville deposit: High silica samples show a strong increase in Hg (Fig. 5a,b). The samples also show a variable flux of other trace elements, however, they are not significantly elevated in any of the samples. The histogram does show a ~40% mass flux in Sb, however, this is largely a result of the very low primary abundance of these elements in the host rock. The 40% mass flux of Sb is the result of an increase from 86 ppb in the parent sample to 160 ppb in the altered rock. This is a very small addition of Sb and is not likely a meaningful variation.

McLaughlin deposit: High silica samples show an extreme enrichment in As and Sb and moderate enrichment in Au, and Hg (Fig. 6b). Samples with low silica show little variation in trace element contents (Fig. 6a).

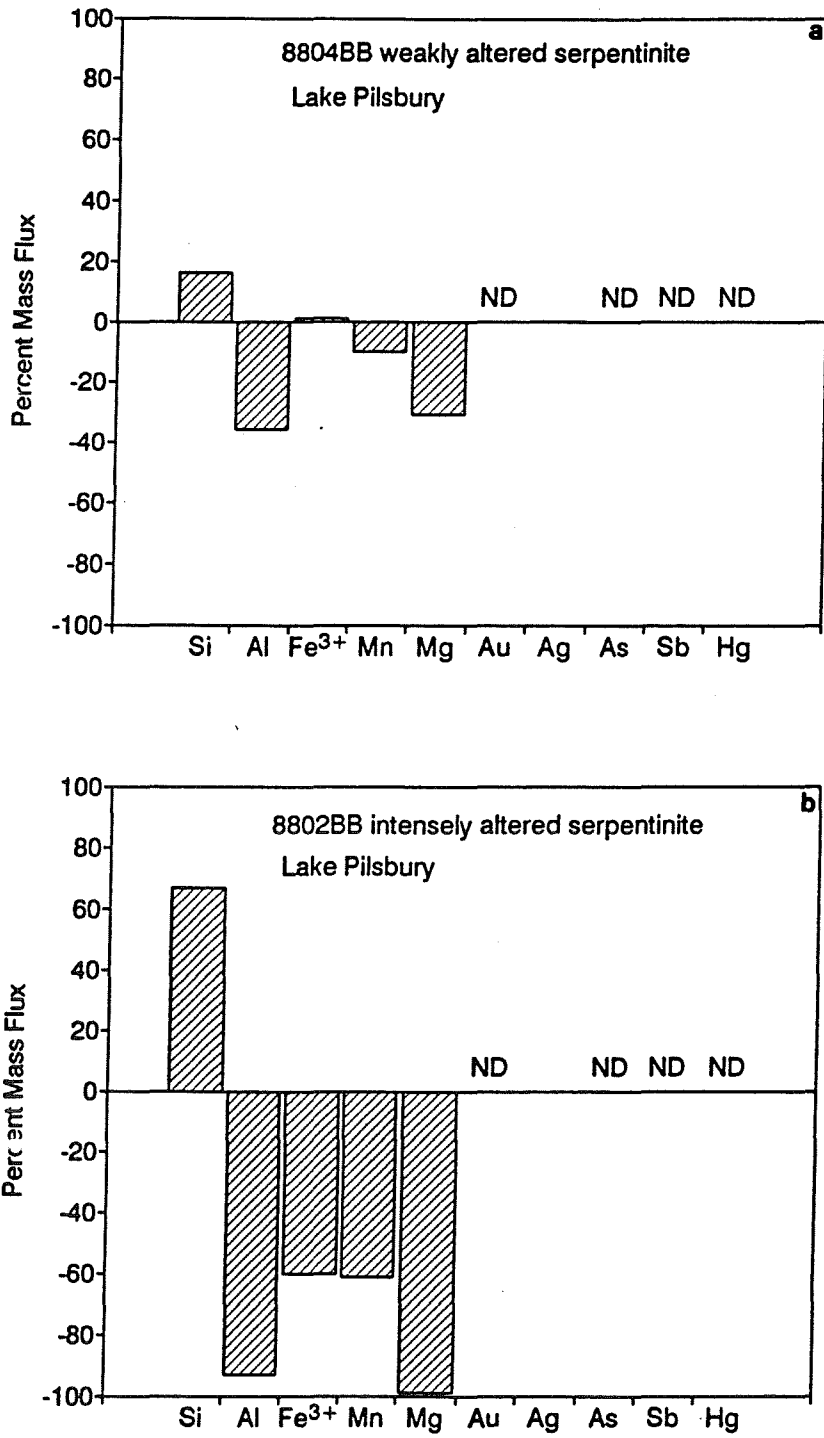


FIGURE 4. Histogram showing percent mass flux for (a) weakly altered and (b) intensely altered silica carbonate from the Soda Springs suite.

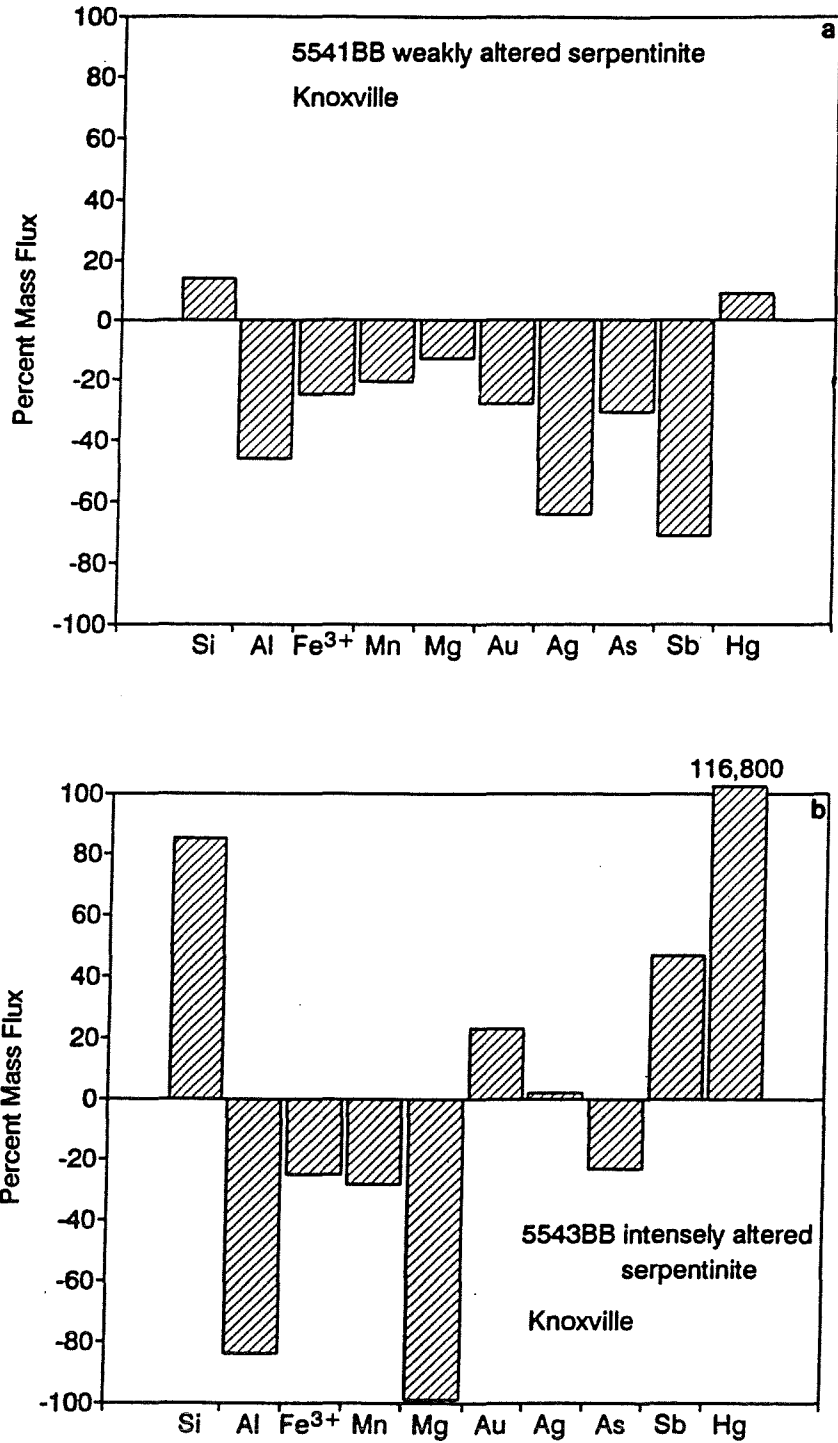


FIGURE 5. Histogram showing percent mass flux for (a) weakly altered and (b) intensely altered silica carbonate from the Knoxville suite.

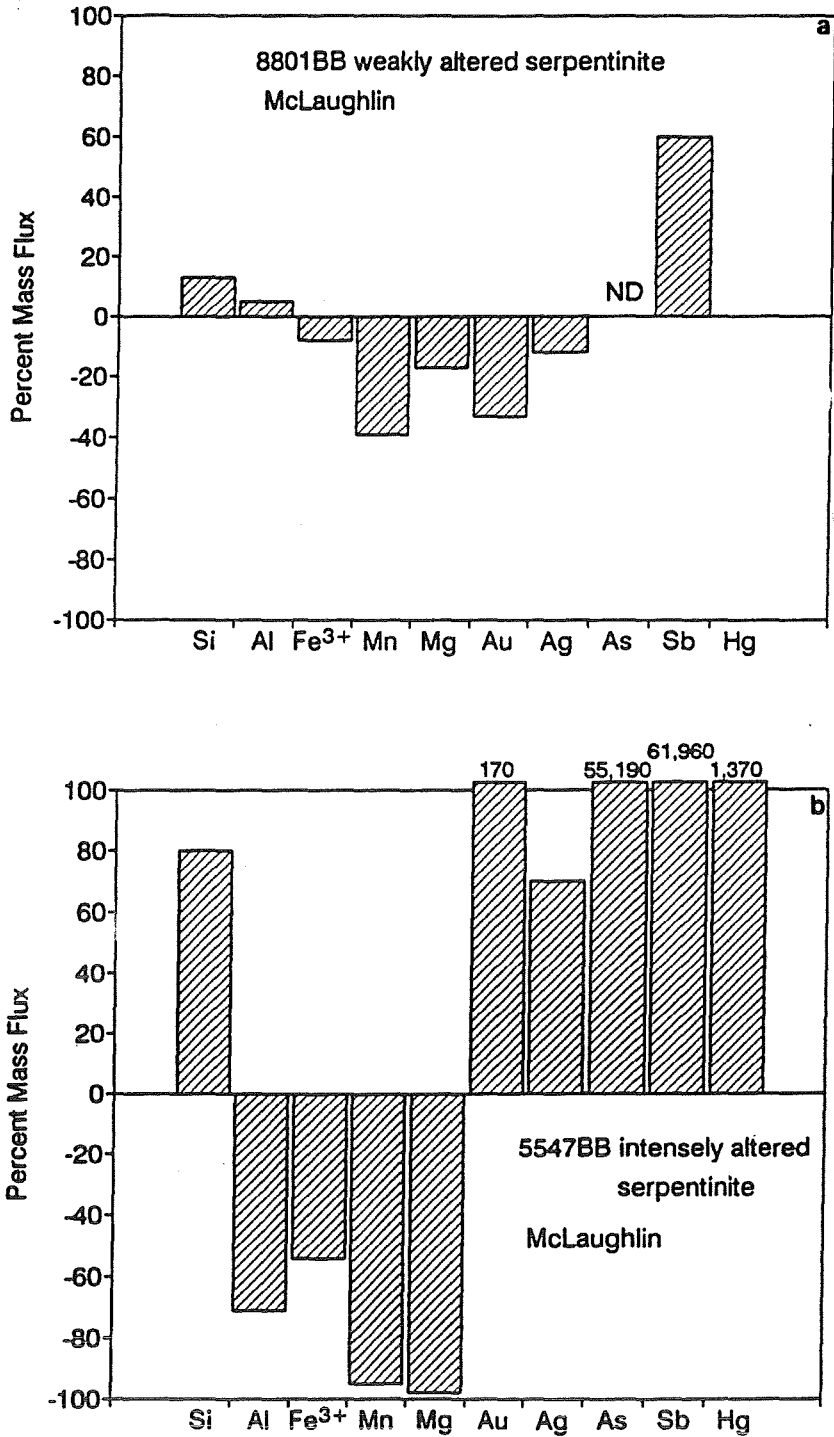


FIGURE 6. Histogram showing percent mass flux for (a) weakly altered and (b) intensely altered silica carbonate from the McLaughlin suite.

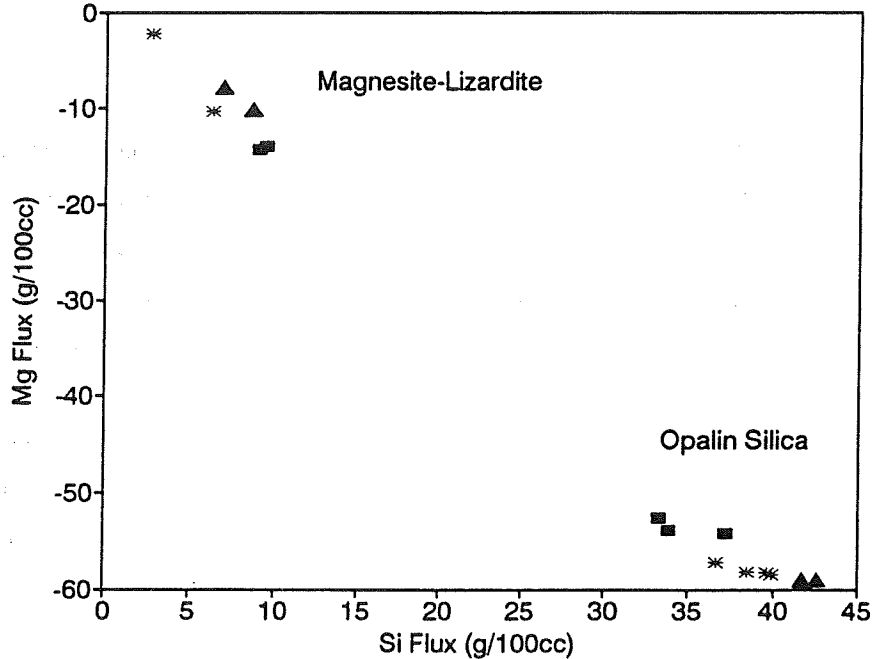
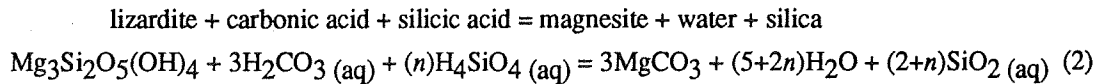


FIGURE 7. Plot of calculated Mg flux vs Si flux silica for carbonate alteration. The data are clustered in two groups representing the magnesite-lizardite and the opalin silica assemblages. Triangle, Knoxville suite; asterisk, McLaughlin Suite; and square, Soda Springs suite.

DISCUSSION

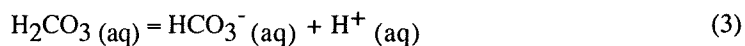
Petrography and major element mass flux calculations indicate that the process of silica carbonate alteration is the same for the three silica carbonate assemblages examined. The initial phase of alteration is magnesite replacing lizardite, represented by reaction 2.



The mass balance calculations indicate that silica is added during the first stage. The addition of silica is represented by the prefix n in reaction 2. This suggests that in addition to silica liberated by the alteration of lizardite to magnesite additional silica was added to the system. The silica is likely submicroscopic opalin silica. Talc was not observed in any of the samples examined, which is consistent with the petrology of Peabody and Einaudi (1992). Barnes et al (1973a) suggest that talc is not stable at the low temperatures of these springs.

Excess acid produced or consumed by reaction 2 is likely buffered by the carbonic acid - bicarbonate equilibrium reaction (3).

carbonic acid - bicarbonate equilibrium reaction



Reaction 3 is in equilibrium at a specific pH which can be calculated, at mineral-spring temperatures, using a van't Hoff extrapolation and data from Garrels and Christ (1965). The carbonic acid - bicarbonate equilibrium occurs at a pH of 6.4 at 17°C. The measured pH of Soda Springs at Lake Pillsbury is 6.46 at 17°C (Barnes et al., 1973a). The similarity between measured and calculated pH suggests that the fluid pH is buffered by the carbonic acid - bicarbonate equilibrium. This is not restricted to Soda Springs, all the mineral-springs show a near neutral pH, and are likely buffered by this reaction.

The second and final stage of the alteration is the replacement of pre-existing serpentinite minerals with opal and minor magnesite, also represented by reaction 2. The difference in the two stages is that initially magnesite was the main alteration mineral and in the second stage silica was the main alteration mineral. The difference in alteration assemblages can be explained by the effect of temperature. The solubility of carbonate increases with decreasing temperature and the solubility of silica decreases with decreasing temperature. The zones dominated by carbonate could be areas of higher fluid temperature than the silica dominated assemblages. Since the carbonate dominated zones occur as a halo around the silica dominated zones, this variation may represent the path of fluid flow, with the fluids migrating from the hotter surrounding area into a fault zone where the fluids cooled by vertical migration and /or mixing with local groundwater.

The main difference in the results of this study and the results of previous studies on silica carbonate alteration (Bailey and Everhart, 1964; Barnes et al. (1973a); Peabody and Einaudi, 1992) is that here the alteration is not considered a constant volume process. And that the metasomatic process involved in the alteration is characterized by the addition of silica in large amounts and the loss of magnesium.

Discrimination Criteria

The three suites of samples show different patterns of trace element enrichment within the high silica samples. The Soda Springs suite is not significantly elevated in any of the trace elements analyzed. The Knoxville suite shows a strong increase in Hg, however, Ag, Au and Sb show little change. The McLaughlin suite shows a strong increase in As and Sb and a moderate enrichment in Au and Hg. The enrichment in As and Sb in silica carbonate assemblages is a potential discrimination tool for identifying auriferous hydrothermal systems.

The enrichment in As and Sb in the McLaughlin silica carbonate may have been superimposed on the alteration assemblage by the latter precious metal hydrothermal system. If this is the case, then the metals were added without modifying the oxygen isotopic composition of the silica carbonate assemblage. In either case, if the As and Sb anomalies are introduced by the silica carbonate altering fluids or if they were introduced by a latter hot-spring event their presence is still useful as a discrimination tool to identify possible precious metal mineralization.

SILICATE OXYGEN ISOTOPES

Introduction

Previous work (Barnes et al., 1973a,b; White, 1973; Peters, 1991, 1993; Sherlock, 1993) have defined a distinct difference between hot-springs and mineral-springs, based largely upon their isotopic signatures. The Coast Range hydrothermal systems show a well defined linear relationships on a $\delta^{18}\text{O}$ - δD plot (Barnes et al., 1973b; White et al., 1973; Peters, 1991, 1993). Hot-springs commonly have oxygen isotopic compositions of 5 to 9‰, and meteoric water has a oxygen isotopic composition of -9.0‰, mineral-springs plot intermediate between hot-springs and meteoric water. Isotopic analysis of the silica carbonate alteration can be used to infer the temperature of alteration and the isotopic composition of the altering fluids.

Soda Springs

Some spectacularly heavy $\delta^{18}\text{O}$ values ranging from 9.8 to 39.2‰ were obtained from the Soda Springs suite. These values are 5 to 6‰ heavier than values seen for the Knoxville or McLaughlin samples.

Knoxville and McLaughlin Deposits

Results for samples from the McLaughlin and Knoxville deposits have similar oxygen isotopic compositions ranging from 8.3 to 33.9‰.

DISCUSSION

Temperature of Alteration

Soda Springs

The Soda Springs silica carbonate assemblage has a mineral-spring issuing from the center of it (Fig. 2). The oxygen isotopic composition of the spring has been determined by Barnes et al. (1973a) to be -2.03‰, and by Sherlock (1993) to be -2.06‰ (Table 2). The isotopic composition of the amorphous silica at the discharge site is 39.2‰. If the fluid and the rock are in isotopic equilibrium, then the temperature of alteration is 17.5°C based on the fractionation between H_2O and amorphous silica (Kita et al., 1985). This temperature is very close to the measured temperature of 17°C (Barnes et al., 1973a) and strongly suggests that the mineral-springs and the opalin silica are in isotopic equilibrium.

Knoxville

A mineral-spring discharges onto the slope between McLaughlin and Knoxville (Fig. 2). The oxygen isotopic composition of the spring has been determined to be -4.37‰ (Table 2). The amorphous silica in the silica carbonate assemblage at Knoxville has an average oxygen isotopic composition of 33.5‰. If the fluid and the rock are in isotopic equilibrium, then the temperature of the alteration is 15.6°C. The actual temperature of the spring was

not determined due to the low volume of the spring, but it was cool to touch consistent with the calculated temperature.

McLaughlin deposit

The oxygen isotopic composition of the silica carbonate from the McLaughlin deposit averages 32.3‰, which is isotopically the most enriched suite of samples observed at McLaughlin. The oxygen isotope composition of hydrothermal silica that is related to the precious metal mineralizing event ranges from 18.2 to 31.5‰ with a maximum at the sinter. The oxygen isotopic composition of the hot-spring fluids that formed McLaughlin deposit have been determined to be ~ 9.3‰ (Sherlock, 1993). If these fluids formed the silica carbonate assemblage at ~20°C than the amorphous silica would have a oxygen isotopic composition of 45.9‰, which is not observed. Another possibility is that the McLaughlin silica carbonate assemblage formed from a hot-spring fluid (9.3‰) at slightly elevated temperatures. If this is the case the equilibrium temperature is ~86°C. This temperature is well above what is observed in mineral-springs. The isotopic composition of the McLaughlin silica carbonate indicates that it did not form from hot-spring type fluids.

The hot-spring fluids at McLaughlin have a low CO₂ content (Sherlock, 1993). A fluid with a low CO₂ content would not produce a silica carbonate assemblage (Barnes et al., 1973a; Peabody and Einaudi, 1992), which supports the isotopic data. The isotopic similarities between the McLaughlin and the Knoxville silica carbonate assemblages, and the low CO₂ content of the McLaughlin hot-spring fluids suggests that the fluids that formed the McLaughlin silica carbonate assemblage were low temperature, CO₂-rich mineral-springs.

Evolution of Spring Fluids

The silica carbonate alteration at McLaughlin is the earliest alteration event recognized, possibly pre-mineralization. The isotopic composition of the silica carbonate, and the low CO₂ content of the main ore forming hot-spring fluids, suggest that there was mineral-spring activity at the site of the McLaughlin deposit prior to the onset of the hot-spring activity. There is also active mineral springs presently discharging into the San Quentin pit and onto the hill surrounding the deposit (Table 2).

This suggests an evolution of spring fluids with time. Initially a low temperature CO₂-rich fluid was dominate, forming the silica carbonate assemblages. As a results of volcanism (increased thermal input) and/or possibly due to a more suitable structural setting (better plumbing), the temperature and volume of the hydrothermal activity increased and the McLaughlin deposit formed. At this stage fluids are isotopically heavier, much hotter and CO₂-poor. The hot-spring system eventually waned, likely as a result of the cooling of the volcanic center, and hydrothermal activity was dominated by mineral-springs that are presently discharging into the San Quentin pit, and marginal to the McLaughlin deposit.

TABLE 2

SILICATE ISOTOPIC DATA

Sample #	Location	$\delta^{18}\text{O}$
8802BB	Soda Springs	39.2
8805BB		37.4
8806BB		104.
8808BB		9.8
5538BB	Knoxville	11.7
5541BB		16.1
5542BB		21.6
5543BB		32.4
5544BB		33.9
5544BB repeat		33.3
5546BB	McLaughlin	32.2
5547BB		32.4
5550BB		8.3
8801BB		10.4

MINERAL-SPRING ISOTOPIC DATA

Sample #	Location	$\delta^{18}\text{O}$	δD
90-M-VF	Fluids from vugs in veining. 1590 elev. N104240, E106110	-5.8	-54
McL #6	San Quentin dewatering well, ~1430 elev.	-1.9	-32
90-M-60	Calcareous travertine with small spring. N101090 E107090	-4.4	-42
DDH819	Gaseous spring discharging from diamond drill hole 819, at the McLaughlin Mine N110920 E103192	-5.8	-47
Soda Springs at Lake Pillsbury	Gaseous spring discharging from the center of a silica carbonate alteration zone	-2.1	-38

The variation in CO₂ content is possibly due to the volume of hydrothermal fluid involved. Peabody and Einaudi (1992), Des Marais et al. (1981) and Peters (1993) have suggested that CO₂, in the Geysers area and in the mineral springs, is derived from oxidation of organic material. If this is the case then an increase in the volume of hydrothermal fluid circulating would decrease the proportion of hydrocarbons and result in a CO₂-poor fluid. If the amount of water circulating was quite small, as is typical of the mineral springs, then the proportion of hydrocarbons increase and result in a CO₂-rich fluid.

SULFUR ISOTOPES

Sulfur isotopic analysis were conducted on cinnabar separates from various mercury deposits throughout the northern Coast Ranges as well as on native sulfur collected from argillic alteration zones associated with active hydrothermal systems (Table 3; Fig. 1). The mercury mineralization, in all the districts except the Geysers Geothermal System, is present along late fractures within silica carbonate altered rocks. Only rarely is mineralization in siliceous hydrocarbon-rich froth veins (Bailey, 1959). The mercury mineralization observed from these deposits is exclusively cinnabar, metacinnabar was not observed in this study. For these deposits mineralization appears to be the result of vapor phase transport of mercury, since the cinnabar is present along late fractures with no associated gangue minerals. In the deposits from the Geysers Geothermal System the mercury mineralization is present within siliceous veinlets that cross cut the silica carbonate assemblage. The cinnabar is restricted to the veinlets, and in one case, at the Rattlesnake deposit, native mercury was observed associated with the cinnabar. For the deposits in the Geysers Geothermal System the mercury mineralization is likely the result of fluid phase transport of the mercury. The mercury mineralization in all the deposits examined is late in the paragenetic sequence, occurring after the silica carbonate alteration.

The data are relatively consistent for each type of sample. The $\delta^{34}\text{S}$ for the cinnabar separates range from 7.40 to 1.53‰ with an average of 3.88‰. The $\delta^{34}\text{S}$ values for the native sulfur ranges from -2.35 to 2.59‰ with an average of 0.12‰ (Table 3, Fig. 8).

The range of $\delta^{34}\text{S}$ values observed in this study is very similar to the range in data seen from cinnabar at the New Idria Mining District in the Coast Ranges of California. Cinnabar, from the New Idria district have $\delta^{34}\text{S}$ values that range from 1.3 to 4.4‰ (Boctor et al., 1987). The data are also similar to the isotopic composition of sulfur observed at the McLaughlin deposit. The sulfur isotopic composition of the deep ore fluids at McLaughlin is -2.0 to -1.0‰. The sulfur composition in the near surface environment is variable ranging up to 7.36‰, which is attributed to fractionation as a result of phase separation above the boiling horizon (Sherlock, 1993).

Peters (1993) observed a range of sulfur composition from reduced sulfur in the active hot-springs of the Sulphur Creek District from 4.7 to 5.9‰. Peters (1993) also reported the sulfur isotopic compositions of sulfate from 3 mineral springs at 6.6, 7.0, and one sample at 20.2‰. With the exception of the very heavy sample the range in data is very similar to the data observed in the near surface environment at the McLaughlin deposit (Sherlock, 1993).

TABLE 3

Sample #	Location	District	Location	Mineral	$\delta^{34}\text{S}$
HM-2	Harrison	McL	T12N, R5W, 35	HgS	3.65
RM-16-1	Reed	McL	T12N, R5W, 25	HgS	1.56
	repeat				1.98
RE-14	Red Elephant	McL	T11N, R5W, 3	HgS	7.40
KM-15-1	Knoxville	McL	T11N, R4W, 7	HgS	4.43
	repeat				4.53
TP-3	Twin Peaks	OH	T9N, R6W, 4	HgS	3.69
CO-11	Corona	OH	T10N, R6W, 32	HgS	3.58
RS-4	Rattlesnake	GGs	T11N, R8W, 31	HgS	2.10
EM-5	Eureka	GGs	T11N, R8W, 32	HgS	2.14
BM-6	Buckman	GGs	T11N, R9W, 29	HgS	1.82
CM-7	Contact	GGs	T11N, R8W, 32	HgS	7.31
CB-8	Culver Baer	GGs	T11N, R9W, 24	HgS	1.53
ER-9	Eagle Rock	GGs	T11N, R9W, 15	HgS	6.34
CRM-10	Crystal	GGs	T11N, R8W, 5	HgS	2.07
Geysers-1	Sulphur Bank Area	GGs	T11N, R9W, 13	native S	-2.35
Geysers-2	Sulphur Bank Area	GGs	T11N, R9W, 13	native S	0.16
Geysers-4	Sulphur Bank Area	GGs	T11N, R9W, 14	native S	-1.55
Geysers-5	Sulphur Bank Area	GGs	T11N, R9W, 14	native S	-1.78
Geysers-6	Sulphur Bank Area	GGs	T11N, R9W, 14	native S	-1.84
Geysers-7	Sulphur Bank Area	GGs	T11N, R9W, 14	native S	-1.15
TR-13	Turkey Run	SCD	T14N, R5W, 32	HgS	6.39
Elgin-1	Elgin	SCD	T14N, R6W, 13	native S	2.59
	repeat				2.59
MAN-1	Manzanita	SCD	T14N, R5W, 29	native S	2.31
MAN-2	Manzanita	SCD	T14N, R5W, 29	native S	3.35
Wilbur-1	Wilbur Spring	SCD	T14N, R5W, 29	native S	0.39
Elbow-1	Elbow Spring	SCD	T14N, R5W, 29	native S	0.24

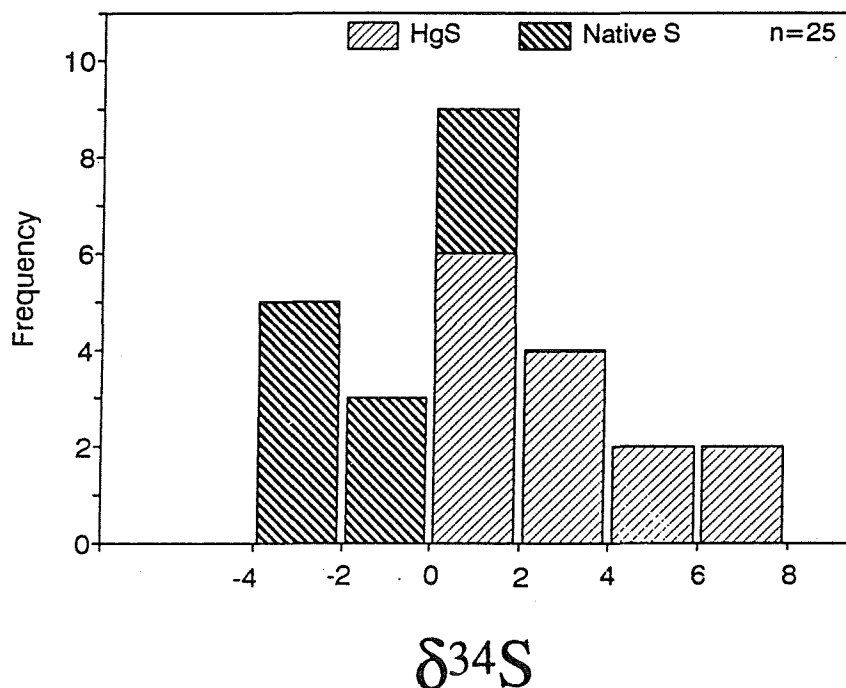


FIGURE 8. Histogram of sulfur isotopic composition for cinnabar and native sulfur samples.

DISCUSSION

Sulfur Source

The isotopic composition of the sulfur from the mercury deposits and the active hot-springs reported in this study can be used to infer a sulfur source. Sulfate minerals were not observed in any of the samples, which suggests that the isotopic composition determined for the sulfides is representative of the composition of the hydrothermal system. The similar isotopic composition of the sulfur from the various localities over such a large area suggests that the sulfur source for all the hydrothermal systems examined is similar.

At the low temperatures seen in this study sulfur isotopic equilibrium is unlikely (i.e. Boctor et al., 1987). If the hydrothermal system is open to the surface and undergoing phase separation then sulfur is partitioned into a vapor phase and the isotopic composition would vary due to fractionation between the liquid and vapor phase. Although equilibrium cannot be demonstrated the sulfur isotopic data cluster around 0‰ and show no systematic variation between localities.

Sulfur of this composition is not likely to have been derived from sedimentary sulfate at temperatures observed in the mineral-springs. Sedimentary sulfate has an isotopic composition of ~15 to 20‰ (Ohmoto and Rye, 1979). To produce the range in isotopic compositions observed in this study a fractionation of 15 to 20‰ is required. The fractionation between sulfate and H₂S is quite large; a 20‰ shift would require a temperature of 303°C, and a fractionation of 15‰ would require a temperature of 396°C. These temperatures are very high, well above any temperatures observed in these hydrothermal systems.

The sulfur isotopic composition of near 0‰ is consistent with a magmatic source (Ohmoto and Rye, 1979). Most of the mercury deposits and hydrothermal systems are spatially and probably temporally related to Clear Lake Volcanic rocks making a magmatic sulfur source geologically reasonable. Another possibility is that the sulfur was derived from the leaching of reduced sulfur from volcanic derived sediments in the Franciscan Complex.

ASSOCIATION OF PRECIOUS METAL AND MERCURY MINERALIZATION

The ubiquitous presence of silica carbonate alteration in barren, potentially auriferous (Hg-rich) and auriferous systems suggests that the alteration process is common to many hydrothermal systems in the Coast Ranges. This is supported by the similar mass flux calculations for the major elements from all the suites examined, and the similar sulfur isotope compositions. The oxygen isotope characteristics suggest that it is a low temperature process occurring in a CO₂-rich environment. Based on the timing of the alteration at McLaughlin and the presence of active mineral-springs in and around the mine it is likely that the mineral-spring phase may be part of the evolution of a hot-spring system.

The association of silica carbonate alteration and mercury mineralization may be a result of the brittle nature of the silica carbonate assemblage, since the mineralization occurs along late fractures in the silica carbonate. The few cases in the Mayacmas district where mercury mineralization is hosted by greywacke, such as the Oat Hill and Eagle Rock Mines, the mineralization occurs as disseminated cinnabar within the greywacke. The greywacke does not contain any serpentinite minerals that are susceptible to being replaced by a brittle silica carbonate assemblage. If the host rock was not initially altered to a brittle assemblage then the mercury mineralization may not be concentrated in fracture networks, and economic concentrations of cinnabar may not be produced. The mineralization is likely facilitated by the gaseous nature of the mineral springs which may transport mercury in a vapor phase.

Mercury mineralization at the McLaughlin deposit was hosted mainly as coatings on late cross-cutting fractures and as pervasive pigmentation in the siliceous sinter (Lehrman, 1986). This may be analogous to the silica carbonate hosted mineralization. The sinter was a brittle assemblage and mercury mineralization occurred along the late fractures possibly as a result of vapor phase transport of mercury.

The silica carbonate alteration is a low temperature process, likely occurring at temperatures around 20°C. By analogy, the associated mercury mineralization is also low temperature. Precious metal mineralization is not likely to occur in mercury deposits unless the system shows evidence for higher fluid temperatures and fluid volumes. This would manifest itself as the preservation of a sinter and large multistage vein swarms. It is possible

that evidence for the higher temperature hydrothermal system could be obscured by landslides or other ground cover and the only evidence of hydrothermal activity is the silica carbonate alteration. If this is the case then elevated concentrations of As and Sb in the silica carbonate may indicate the presence of a hidden auriferous system and exploration activities should be focused in this area.

CONCLUSIONS

Silica carbonate is an ubiquitous alteration in the northern Coast Ranges. The alteration is formed by the low temperature reaction of CO₂-rich fluids with serpentinite. The alteration is best considered to be an exchange of cations with little net gain or loss of oxygen. The major element mass flux is characterized by the addition of Si and CO₂, and a depletion in all other cations. The trace element flux is different for each of the suites examined. Barren silica carbonate assemblages are not elevated in any of the trace elements analyzed. Mercury rich suites are elevated in Hg and auriferous suites are elevated in Au, As, Sb and Hg. This variation in trace element enrichment may be used as an exploration criteria for discriminating between barren and potentially auriferous hydrothermal systems.

The alteration took place in two phases, the initial phase is a carbonate flooding of serpentinite which forms a halo around the silica-rich phase. This variation in alterations minerals may be the effect of temperature gradients. The carbonate-rich areas may be zones of higher temperature and the silica rich zones may be lower temperature. The silica rich cores may represent areas where the fluids are migrating in structurally controlled dilatant zones cooling as they ascend.

Oxygen isotopes suggest that the alteration is low temperature, around 20°C. The silica carbonate alteration at McLaughlin likely did not form from the main ore forming hot-spring fluids, but formed from early mineral-spring activity at the site. The main ore forming hot-spring event was superimposed on the silica carbonate alteration which formed the McLaughlin deposit. Presently there are mineral-springs discharging into the mine workings and onto the hill sides surrounding the deposit. This suggests that the mineral-springs were part of the evolution of a late hydrothermal system that formed the McLaughlin deposit. The precious metal hydrothermal system may have evolved as a result of increased thermal input and/or increased fluid flow. This suggests that Hg-rich silica carbonate assemblages are not likely to contain precious metal mineralization unless it has been superimposed by a higher temperature hydrothermal system.

The sulfur isotopic composition from a variety of mercury deposits and active hydrothermal systems show a fairly consistent values at about 0‰. This composition indicates that the sulfur source for the hydrothermal systems is likely magmatic in origin.

ACKNOWLEDGMENTS

This study was initiated to develop exploration criteria for discriminating between potentially auriferous and non-auriferous silica carbonate assemblages. This work would not have been possible without the support of Homestake Mining Company, U.S. Exploration, Stan Caddey, Peter Schwarzer and Norman Lehrman. Funding for this research was provided by a grant from Homestake Mining Company, as well a employment during field work,

and a NSERC (grant URF0037724 to E.C. Jowett). Financial support was also provided by an Ontario Post Graduate Scholarship to R.L. Sherlock. We would like to thank Dr. J. Rytuba and the USGS for the opportunity to present our research in this forum.

REFERENCES

- Appleyard, E.C., 1990, Mass balance corrections applied to lithochemical data in mineral exploration: *in* Modern Exploration Techniques, *edited by* L.S. Beck and C.T. Harper, Sask. Geol. Soc. Special Pub. 10, p. 27-40
- Bailey, E.H., 1959, Froth veins, formed by immiscible hydrothermal fluids in mercury deposits, California: *Bull. Geol. Soc. of America*, v. 70, p. 661-664
- Bailey, E.H., and Everhart, D.L., 1964, Geology and quicksilver deposits of the New Almaden District, Santa Clara County, California: U.S. Geol. Survey Prof. Paper, 360, 206 pp.
- Barth, T.W.F., 1948, Oxygen in rocks, a basis for petrographic calculations: *Jour. of Geology*, v. 56, p. 50-60
- Barth, T.W.F., 1952, *Theoretical Petrology*: Wiley, New York
- Barnes, I., O'Neil, J.R., Rapp, J.B., and White, D.E., 1973a, Silica carbonate alteration of serpentinite: wall rock alteration in mercury deposits of the California Coast Ranges: *Econ. Geol.*, v. 68, p. 388-398
- Barnes, I., Hinkle, M.E., Rapp, J.B., Heropoulos, C., and Vaughn, W.W., 1973b, Chemical composition of naturally occurring fluids in relation to mercury deposits in part of north central California: *U.S. Geol. Survey Bull.*, 1382-A, 19 pp.
- Boctor, N.Z., Shieh, Y.N., and Kullerud, G., 1987, Mercury ores from the New Idria Mining District, California: geochemical and stable isotope studies: *Geochim et Cosmochim. Acta*, v. 51, p. 1705-1715
- Chapman, R.H., Bishop, C.C., Chase, G.W., and Gasch, J.W., 1974, Bouguer gravity map of California, Ukiah sheet. California Division of Mines and Geology
- Coleman, M.I., Shepherd, T.J., Durham, J.J., Rouse, J.E., and Moore, G.R., 1982, Reduction of water with zinc for hydrogen isotope analysis: *Analytical Chemistry*, v. 54, p. 993-995
- Des Marais, D.J., Donchin, J.H., Nehring, N.L., and Truesdell, A.H., 1981, Molecular carbon isotopic evidence for the origin of geothermal hydrocarbons: *Nature*, v. 292, p. 826-828
- Fritz, P., Drimmie, R.J., and Nowiki, V.K., 1974, Preparation of sulfur dioxide for mass spectrometer analyses by combustion of sulfides with copper oxide: *Analytical Chemistry*, v. 46, p. 164-166
- Garrels, R.M., and Christ, C.L., 1965, *Solutions, minerals and equilibria*: Jones and Bartlett, 450 pp.
- Gresens, R.L., 1967, Composition volume relationships of metasomatism: *Chem. Geol.*, v. 2, p. 47-65
- Kita, I., Taguchi, S., and Matsubaya, O., 1985, Oxygen isotope fractionation between amorphous silica and water at 34-93°C: *Nature*, v. 314, p.63-64
- Lehrman, N.J., 1986, The McLaughlin Mine, Napa and Yolo Counties, California: *in* Precious-Metal Mineralization in Hot-Springs Systems, Nevada-California, *edited by* J.V. Tingley and H.F. Bonham, Jr., Nevada Bureau of Mines and Geology Report 41, p. 85-89
- McKie, D., 1966, Fentization: *in* Carbonatites, *edited by* O.F. Tuttle and J. Gittins, Wiley, New York, p. 261-294
- McLaughlin, R.J., 1978, Preliminary geologic map and structural sections of the central Mayacmas mountains and the Geysers steam field, Sonoma, Lake, and Mendocino Counties, California: U.S. Geol. Survey, Open File Report 78-389.
- McLaughlin, R.J., Ohlin, H.N., Thormahlen, D.J., Jones, D.L., Miller, J.W., and Blome, C.D., 1990, Geologic map and structural sections of the Little Indian Valley-Wilbur Springs geothermal area, northern Coast Ranges, California: U.S. Geol. Survey Misc. Invest. Series Map 1-1706
- Ohmoto, H., and Rye, R.O., 1979, Isotopes of sulfur and carbon: *in* Geochemistry of Hydrothermal Ore Deposits, *edited by* H.L. Barnes, Wiley, p. 509-567
- Ohmoto, H., and Lasaga, A.C., 1982, Kinetics of reactions between aqueous sulfates and sulfides in hydrothermal systems: *Geochim. et Cosmochim. Acta*, v. 46, p. 1727-1745
- Peabody, C.E., and Einaudi, M.T., 1992, Origin of petroleum and mercury in the Culver-Baer cinnabar deposit, Mayacmas district, California: *Econ. Geol.*, v. 87, p. 1078-1103
- Peters, E.K., 1991, Gold-bearing hot spring systems of the northern Coast Ranges, California: *Econ. Geol.*, v. 86, p. 1519-1528
- Peters, E.K., 1993, $\delta^{18}\text{O}$ enriched waters of the Coast Range Mountains, northern California: connate and ore-forming fluids: *Geochim. et Cosmochim. Acta*, v. 57, p. 1093-1104
- Schandl, E.S., and Naldrett, A.J., 1992, CO_2 metasomatism of serpentinites, south of Timmins, Ontario: *Can. Min.*, v. 30, p. 93-109
- Sherlock, R.L., 1993, The geology and geochemistry of the McLaughlin Mine sheeted vein complex, northern Coast Ranges, California. Unpub. Ph.D. Thesis, University of Waterloo, 309 pp.

- Shervais, J.W., and Kimbrough, D.L., 1985, Geochemical evidence for the tectonic setting of the Coast Range Ophiolite: a composite island arc-oceanic crust terrane in western California: *Geology*, v. 13, p. 35-38
- Tuttle, M.L., Goldhaber, M.B., and Williamson, D.L., 1986, An analytical technique for determining forms of sulfur in oil shales and associated rocks: *Talanta*, v. 33, p. 953-961
- Wagner, D.L., and Bortugno, E.J., 1982, Santa Rosa quadrangle: U.S. Geol. Survey, Regional Map Series, Map No. 2A.
- White, D., Barnes, I., and O'Neil, J.R., 1973, Thermal and mineral waters of nonmeteoric origin, California Coast Ranges. *Geol. Soc. of America Bull.*, v. 84, p. 547-560
- Wicks, F.J., and Whittaker, E.J.W., 1977, Serpentine textures and serpentinization: *Can. Min.*, v. 15, p. 459-488
- Wicks, F.J., Whittaker, E.J.W., and Zussman, J., 1977, An idealized model for serpentine textures after olivine: *Can. Min.*, v. 15, p. 448-458

DAY ONE

THE SONOMA VOLCANIC FIELD AND ASSOCIATED GOLD AND MERCURY DEPOSITS: ROAD LOG

James J. Rytuba¹, Dean A. Enderlin², and Robert McLaughlin¹

¹U.S. Geological Survey, 345 Middlefield Road, Menlo Park CA 94025

²Homestake Mining Company, McLaughlin Mine 26775 Morgan Valley Rd., Lower Lake, CA 95457

This tour begins at the Red Lion Hotel in Santa Rosa and ends in Healdsburg. Load into vans at the Red Lion Hotel parking lot. The road log begins at the Mark West-River Road exit from Highway 101, about 10.5 to the north of the Red Lion Hotel. The route for the trip is shown in Figure 1.

Mileage

0.0	0.0	Exit Highway 101 at Mark West-River Road exit and proceed east onto Mark West Road.
6.2	6.2	Turn into parking area on left side of road to examine road cut of sandstone containing volcanoclastic deposits from the Sonoma volcanic field. STOP 1.

STOP 1 . CONTINENTAL SANDSTONE AND CONGLOMERATE AND TUFFACEOUS SEDIMENTS FROM THE SONOMA VOLCANIC FIELD

Exposures in roadcut consist of massively bedded continental clastic beds of the Pliocene Huichica Formation. Interstratified with sandstone and pebble conglomerate are tuffaceous sediments and reworked tuff consisting of ash and large pumice fragments are . The pumiceous beds were derived from the tuff of Petrified Forest which interfinger with the upper part of the Huichicha Formation, dated at 3.7 Ma (Fox and others, 1985). These beds unconformably overlie rocks of the Franciscan Complex and Great Valley sequence and are time equivalent to the tuff of Petrified Forest, the upper member of the Sonoma Volcanics exposed about 8 km to the east. The tuffaceous beds are the western most exposures of pyroclastic rocks vented from the Sonoma volcanic field and represent reworked pyroclastic rocks typically present at the distal parts of large volcanic ash-flow fields.

4.1	10.3	Intersection with Petrified Forest Road, turn left.
0.8	11.1	Turn left into commercial development for the Petrified Forest and park in lot. STOP 2.

volume). The veins consist of quartz-barite-pyrite and cut argillically altered ash flow tuff. An altered felsic intrusive in which pyrite is concentrated along fractures and flow foliation is exposed in the fault zone.

Retrace route back to Silverado Trail and turn left.

-
- | | | |
|------|-------|--|
| 0.8 | 23.6 | Turn right onto Silverado Trail. |
| 3.2 | 26.8 | Intersection of Highway 29 and Silverado Trail, proceed straight ahead. |
| 8.0 | 34.8 | Turn left onto Mount St. Helena summit road. This road is gated and a key from the California State Park Service office at north of St. Helena can be obtained. |
| 1.55 | 36.35 | Park on left side of road where road widens just before sharp turn. Walk down trail on left side of road and follow path for about 20 feet to exposure of Silverado vein. STOP 4. |
-

STOP 4. SILVERADO VEIN AND OVERVIEW OF THE SONOMA VOLCANIC FIELD.

The Silverado vein (Fig. 2) is well exposed in the outcrop above and to the west of the main stope, which delineates the width and attitude of the vein. The safest place to view and sample the vein is in the first exposure to the left of the path. The Silverado mine was placed into production in 1874 and is one of only two mines in the Calistoga mining district to have had significant precious-metal production. Similar epithermal vein systems extend discontinuously southward from the Silverado mine for a distance of about 15 km and define a northwest trending zone about 1.5 km in width (Enderlin, this volume). The vein systems formed along conjugate Reidel shears that propagated northeastward from a northwest trending wrench fault associated with the San Andreas transform system (Fox, 1983; and Enderlin, this volume). Host rocks for the Silverado veins are the 3.5 Ma tuff of Petrified Forest, and the 3.0 Ma rhyolite of Calistoga, a flow-dome and pyroclastic unit (Fox and others, 1985). The less altered lithic tuffs are exposed in the road cut about 200 feet up the road from this stop. The Silverado veins extend for distance of 760 m and typically strike 190° to 205°(Enderlin, this volume).

The Silverado veins display typical epithermal textures of crustiform and colloform banded quartz, adularia, and chalcedony. The assemblage calcite-pyrite-arsenopyrite characterized the earliest stage of deposition and bladed calcite is typically replaced by quartz. This texture (Fig. 3) is well exposed on the base of the large outcrop to the right, downslope from the main vein and path. Pyrite and chalcopryrite are the most common sulfides. Minor fine grained sphalerite, pyrrargyrite, silver-sulfides and silver-selenides are associated with the pyrite and chalcopryrite. Native gold grains up to 100 microns in diameter are commonly present in quartz bands and hydrocarbons have been noted within quartz vugs. Fluid inclusions consist of coeval vapor- and fluid-rich inclusions which have an average homogenization temperature of 249 °C and a salinity of 0.87 per cent equivalent NaCl (Sherlock, 1993). The fluid inclusions indicate that the hydrothermal system was boiling and stable isotopic analysis indicate that the fluids were dominantly meteoric (Sherlock, 1993; Pickthorn, this volume). Adularia in the veins has been K-Ar dated at 2.6±0.07 Ma (D. H. Sorg, written communication, 1993; in McLaughlin and others, this volume).

Retrace route back to Highway 29

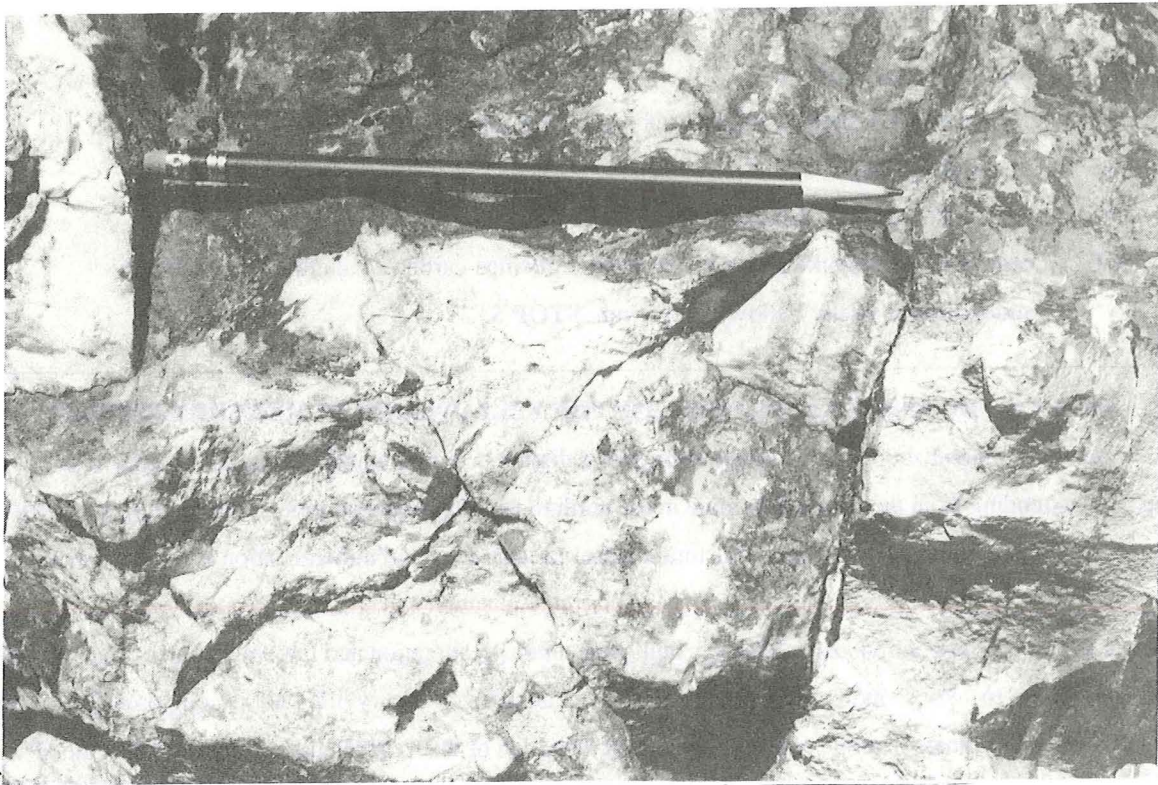


FIGURE 2. Silverado vein consisting of banded quartz and adularia. Dark sulfide zone contains base metals and visible gold.



FIGURE 3. Vein just below main exposed Silverado vein consisting of quartz after bladed calcite.

- 1.55 37.9 Turn right onto Highway 29.
- 6.35 44.25 Intersection of Highway 29 and Tubbs lane, turn right.
- 1.35 45.6 Turn right on Highway 128.
- 7.5 54.3 Turn right onto Ida Clayton road.
- 2.3 56.6 Park vehicles and hike up road to exposures of silica-carbonate alteration and mercury mineralization of the Yellowjacket trend. **STOP 5.**

STOP 5. SILICA-CARBONATE ALTERATION OF THE YELLOWJACKET MERCURY DEPOSIT

Mercury mineralization in the western Mayacmas district occurred along a 25 km long, northwest-trending zone extending from the Cloverdale mine in the north to the Yellowjacket mine in the south (Bailey, 1946, and Yates and Hilpert, 1946). The primary structural control for alteration and mineralization is the northwest-trending, steeply dipping Mercuryville fault zone. Mercury mineralization and silica-carbonate alteration of serpentinite are present discontinuously along this fault zone although alteration and mineralization extend outside the fault zone for up to a km or more. The serpentinite present along the Mercuryville fault is composed dominantly of chrysotile and subordinate lizardite and is derived from alteration of the Coast Range ophiolite. The zone of silica-carbonate alteration and mercury mineralization continues to the southeast from the Yellowjacket mine where it is then covered by the Sonoma Volcanics to the southwest of Mount St. Helena (McLaughlin, 1978; 1981). The age relationship of the silica-carbonate alteration and related mercury mineralization have not been clearly documented although Bailey (1946) indicates an age contemporaneous with volcanism in the Sonoma volcanic field. On a regional scale, the southeast extension of the zone of silica-carbonate alteration extends into the volcanic rocks but is characterized by epithermal precious metal vein systems such as the Silverado and Palisades veins (Enderlin, this volume). At the Palisades precious metal deposit Sorg (in McLaughlin and others, this volume) obtained a 1.4 ± 0.04 Ma age on adularia in mineralized veins. This age is anomalously young, possibly indicating late injection of Clear Lake Volcanics related intrusives beneath the older Sonoma volcanics.

In this road cut, typical features of silica-carbonate alteration are easily examined. Marcasite and pyrite are common in the silica-carbonate alteration and oxidation of these sulfides causes the iron oxide coating on the surface of these rocks. Late quartz veins in the silica-carbonate alteration locally contain abundant petroleum and froth vein textures occur in some of these veins.

Turn around and retrace route.

- 2.3 58.9 Turn right onto Highway 28.
- 9.8 68.7 Follow Highway 28 as it makes a left turn here.
- 3.9 72.6 Turn left onto Healdsburg Ave.
- 1.8 74.4 At stoplight turn right on Dry Creek Road.
- 0.2 74.6 At stoplight turn left onto Grove and then first right into parking lot of Dry Creek Inn.

REFERENCES

- Axelrod, D. I., 1944, The Sonoma flora, *in* Chaney, R. W., ed., Pliocene floras of California and Oregon: Carnegie Institution of Washington, Publication 553, p. 167-206.
- Bailey, E. H., 1946, Quicksilver deposits of the western Mayacmas district, Sonoma County, California: *Calif. Jour. Mines and Geology*, v. 42, p. 199-230.
- Chaney, R. W., 1944, Introduction, *in* Chaney, R. W., ed., Pliocene floras of California and Oregon: Carnegie Institution of Washington, Publication 553, p. 1-20.
- Enderlin, D. A., 1993, Epithermal precious metal deposits of the Calistoga mining district Napa County, California, *in* Rytuba, J. J., ed., Active geothermal systems and gold-mercury deposits in the Sonoma-Clear Lake volcanic fields, California: Soc. Econ. Geol. Guidebook Series, (this volume).
- Evernden, J. F., and James, G. T., 1964, Potassium-argon dates and the Tertiary floras of North America: *American Journal of Science*, v. 262, no. 8, pp. 25-56.
- Fox, K. F., Jr., 1983, Tectonic setting of late Miocene, Pliocene, and Pleistocene rocks in part of the Coast Ranges north of San Francisco, California: U. S. Geological Survey Prof. Paper 1239, 33 p.
- Fox, K. F., Jr., Fleck, R. J., Curtis, G. H., and Meyer, C. E., 1985, Potassium-argon and fission-track ages of the Sonoma Volcanics in an area north of San Pablo Bay, California: U. S. Geol. Survey Miscellaneous Field Studies Map MF-1753.
- McLaughlin, R. J., 1978, Preliminary geologic map and structural sections of the central Mayacmas Mountains and The Geysers steam field, Sonoma, Lake, and Mendocino Counties, California: U. S. Geol. Survey Open-File Map 78-389, scale 1:24,000.
- McLaughlin, R. J., 1981, Tectonic setting of pre-Tertiary rocks and its relation to geothermal resources in the Geysers-Clear Lake area: U. S. Geological Survey Prof. Paper 1141, p. 3-23.
- Pickthorn, W. J., 1993, Relation of hot-spring gold mineralization to silica-carbonate mercury mineralization in the Coast Range, California, *in* Rytuba, J. J., ed., Active geothermal systems and gold-mercury deposits in the Sonoma-Clear Lake volcanic fields, California: Soc. Econ. Geol. Guidebook Series, (this volume).
- Sherlock, R. L., 1993, The geology and geochemistry of the McLaughlin mine sheeted vein complex, northern Coast Ranges, California: University of Waterloo, Ontario, Ph. D. thesis, 309 p.
- Yates, R. G., and Hilpert, L. S., 1946, Quicksilver deposits of eastern Mayacmas district, Lake and Napa Counties, California: *California Jour. Mines and Geology*, v. 42, no. 3, p. 231-286.

GEOTHERMAL SETTING OF THE GEYSERS STEAM FIELD, NORTHERN CALIFORNIA

Robert O. Fournier

U.S. Geological Survey MS-910, 345 Middlefield Road, Menlo Park, CA 94025, USA

INTRODUCTION

The Geysers–Clear Lake area, located about 150 km north of San Francisco, is mainly underlain by Jurassic and Cretaceous rocks of the Franciscan assemblage (composed dominantly of a melange of graywacke and argillite with lesser amounts of altered mafic igneous rocks, radiolarian chert, serpentine, limestone, and very minor blocks of blueschist, eclogite, and amphibolite), the Great Valley sequence (mainly siltstone and argillite in the Clear Lake region), and associated ophiolitic rocks that accumulated in marine settings, and that later were deformed at an obliquely convergent subduction margin (McLaughlin, 1977, 1981; McLaughlin and Ohlin, 1984; Thompson, 1989). Later strike-slip movement on northward-propagating faults of the San Andreas transform system, some of which pass through The Geysers–Clear Lake area, cut and offset the thrust sheets, and shut down subduction at the latitude of Clear Lake about 3 Ma (Atwater, 1970; Blake and others, 1978; Dickinson and Snyder, 1979). Simultaneously, behind a northward-migrating triple junction, there also has been a northward migration of volcanic centers in the Coast Ranges of California above a window of anomalously shallow asthenosphere, with the most recent volcanic activity focused in the Clear Lake region (Dickinson and Snyder, 1979; Hearn et al., 1981; McLaughlin, 1981; Fox et al., 1985).

GEOLOGY

The Geysers geothermal system is clearly related to the Clear Lake volcanic activity and associated intrusions (Figs. 1 and 2) that have K/Ar dates ranging from about 2.5 Ma to 0.03 Ma or less (Hearn et al., 1976; Donnelly-Nolan et al., 1981; Thompson, 1989). The main part of this volcanic field is younger than 1.0 Ma, and much of the central part is younger than 0.6 Ma (Hearn et al., 1976; Donnelly-Nolan et al., 1981). The Geysers geothermal reservoir lies to the southwest of the volcanic field (Fig. 1). However, extensive deep drilling has shown that the productive reservoir (mainly in graywacke) is centered above and partly within an intrusive body of silicic rocks, informally called felsite, that is elongate in a NW-SE direction (Fig. 2), and that has age dates ranging from 0.9 Ma to 2.7 Ma (Schriener and Suemnicht, 1981; Thompson, 1989). The discordant ages may be the result of contamination of felsite cuttings by older graywacke (Schriener and Suemnicht, 1981). The direction of elongation of the felsite corresponds with the general NW-SE structural grain of the region that is dominated by faults of the San Andreas system and by the earlier low-dipping, predominantly NW-trending shear fabric of the Franciscan assemblage. Rhyolitic and dacitic extrusive rocks that form Cobb Mountain adjacent to the steam reservoir (Fig. 1) have K/Ar ages of about 1.0 to 1.1 Ma (Hearn et al., 1976; Donnelly-Nolan et al., 1981). Cobb Mountain is

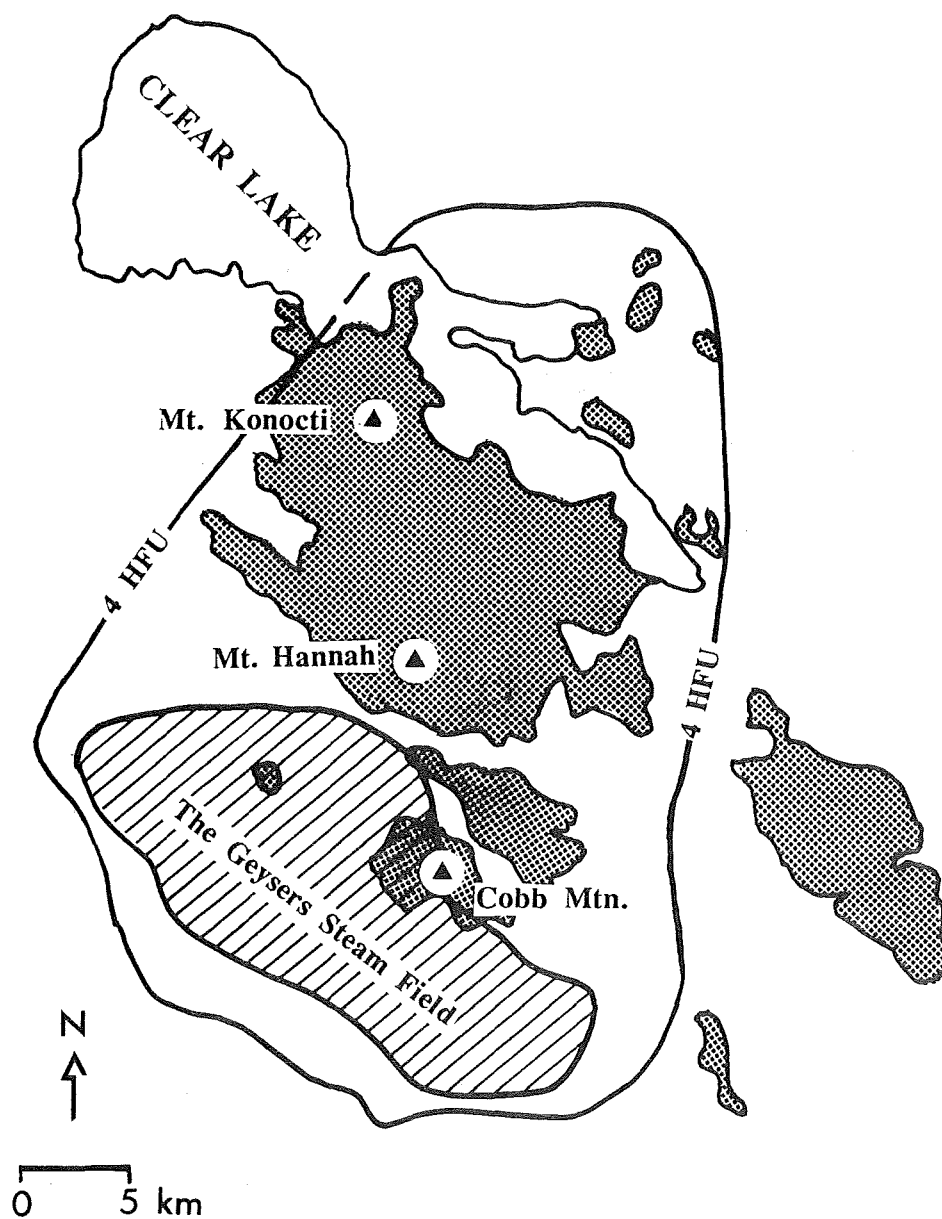


FIGURE 1. The Geysers–Clear Lake volcanic field, thermal anomaly, and steam reservoir. The heavy line shows the thermal anomaly outlined by the 4 HFU (168 mWm^{-2}) contour (from Walthers and Combs, 1989). The distribution of extrusive volcanic rocks (simplified after Hearn et al., 1976) is shown by stipples and the area underlain by the steam reservoir (from Williamson, 1990) is hachured.

probably the extrusive equivalent of the buried felsite intrusion. In addition, extensive geophysical studies, including gravity and magnetic (Isherwood, 1976), P-wave delay (Iyer, 1984), and heat flow (Walthers and Combs, 1989), all are consistent with the presence of a large body of molten or partly molten rock centered beneath Mt. Hannah (Fig. 1), a 0.9-Ma volcano (Donnelly-Nolan et al., 1981) in the central part of the Clear Lake volcanic field. A deep drill hole on the upper flank of Mt. Hannah encountered a nearly linear geothermal gradient and a bottom-hole temperature near 400°C at a depth of about 3.6 km (Fournier, 1991). The evidence is strong that shallow silicic intrusives

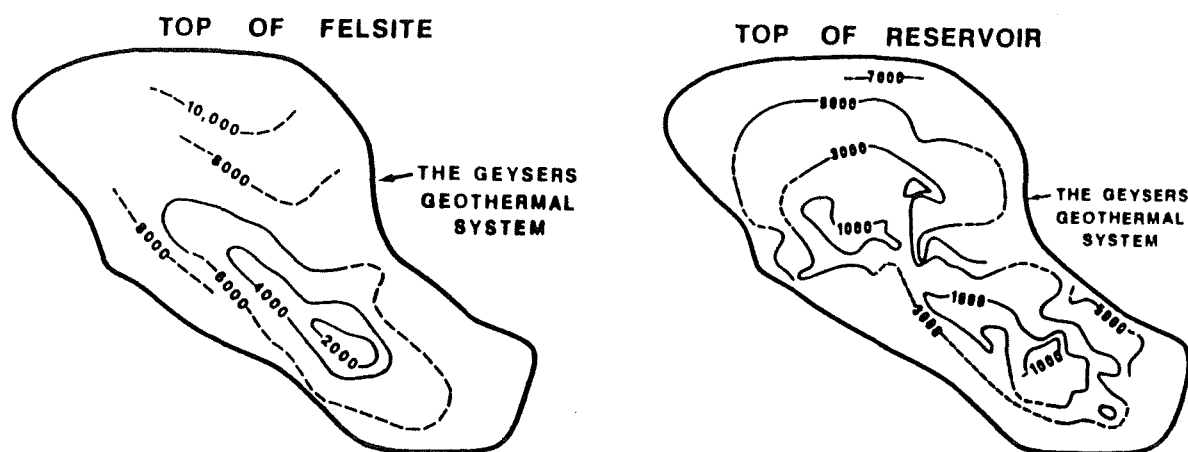


FIGURE 2. (a) Top of felsite and (b) Top of steam reservoirs, both shown within the bounding area of The Geysers steam field. Contours are in feet below sea level. From Williamson (1990).

beneath the steam field provided the heat that initiated the hydrothermal system, and that heat from still partly molten material intruded to a relatively shallow depth at the northern side of the steam field, beneath Mt. Hannah, may be sustaining the hydrothermal activity.

In addition to high temperatures at relatively shallow depths, presently exploitable geothermal reservoirs must have sufficient porosity and permeability to sustain the production of hot fluids for long periods of time at high rates of discharge. Goff et al. (1977) stress that both the northeast and southwest sides of the steam field appear to be bounded by major faults that trend NW-SE. Cores from within the steam reservoir between these major fault zones show that much of the porosity is fracture-related (Gunderson, 1989). Furthermore, although there are some steeply dipping fractures related to movement on the still active San Andreas fault system, there is a dominance of near-horizontal fractures in graywacke that appear to be related to older low-angle faulting (Thompson and Gunderson, 1989). In contrast, there is a strong predominance of vertical fractures in felsite that Thompson and Gunderson (1989) attribute to regional stresses and to local stresses generated during intrusion and cooling of magma. Sternfeld (1989) concludes that the dominant mechanisms for fracturing in the steam reservoir are shear fracturing and hydraulic fracturing induced by the emplacement of intrusions. McLaughlin (1981) called attention to the importance of open-fracture networks in graywacke within the steam reservoir, and noted the major change in lithology to Great Valley sequence rocks and ophiolites to the northwest of The Geysers field, across a major fault. Sternfeld (1989) and Walther and Combs (1989) also stress the influence of lithology on fracture permeability and conclude that of the sedimentary rocks in the region, only graywacke appears to be brittle enough to propagate and

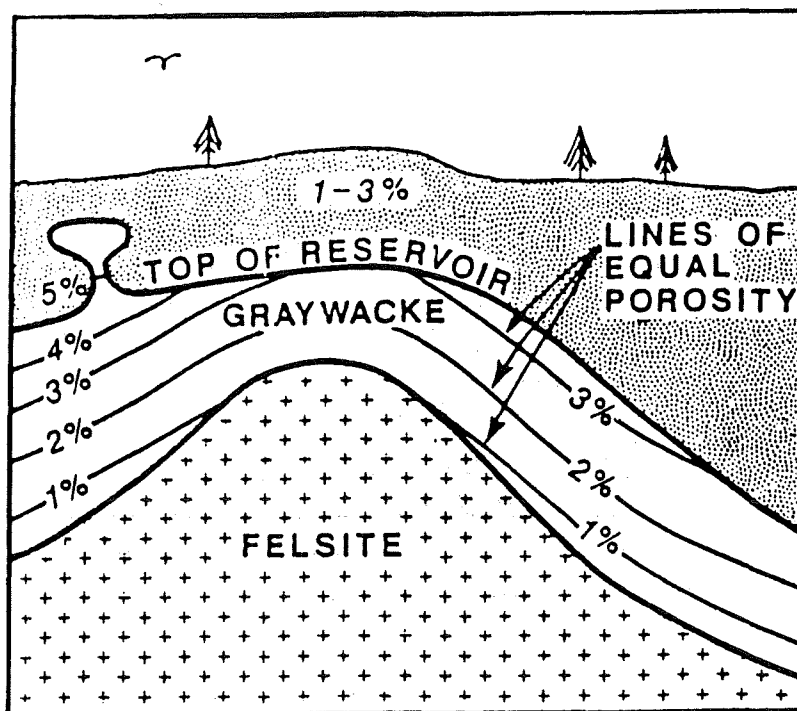


FIGURE 3. Schematic cross-section illustrating how matrix porosity of Geysers reservoir graywacke is related to the felsite intrusion. From Gunderson (1990).

maintain open fractures. However, this generalized view of a primary lithologic control on where brittle fractures may occur and persist is probably an oversimplification of a complex situation in which the degree of metamorphism also plays a major role (written communication, R. J. McLaughlin, 1991). Nevertheless, drilling to the northwest of The Geysers field has shown that rock sequences composed mainly of siltstone, argillite, and serpentine are unproductive.

An additional factor that influences permeability is the degree to which hydrothermal alteration increases or decreases porosity. There is ubiquitous calcite filling fractures in graywacke outside the reservoir, while little calcite remains in fractures within the reservoir. Therefore, it appears that dissolution of calcite and reaction of calcite with clays to form denser silicates with a net decrease in volume have been important processes in increasing porosity and permeability within the reservoir (Gunderson, 1990). On the other hand, graywacke within the reservoir becomes less permeable as the felsite is approached (Fig. 3), probably as a result of increased silicate mineral deposition in veins, and recrystallization of graywacke at high temperatures (Thompson and Gunderson, 1989; Gunderson, 1990).

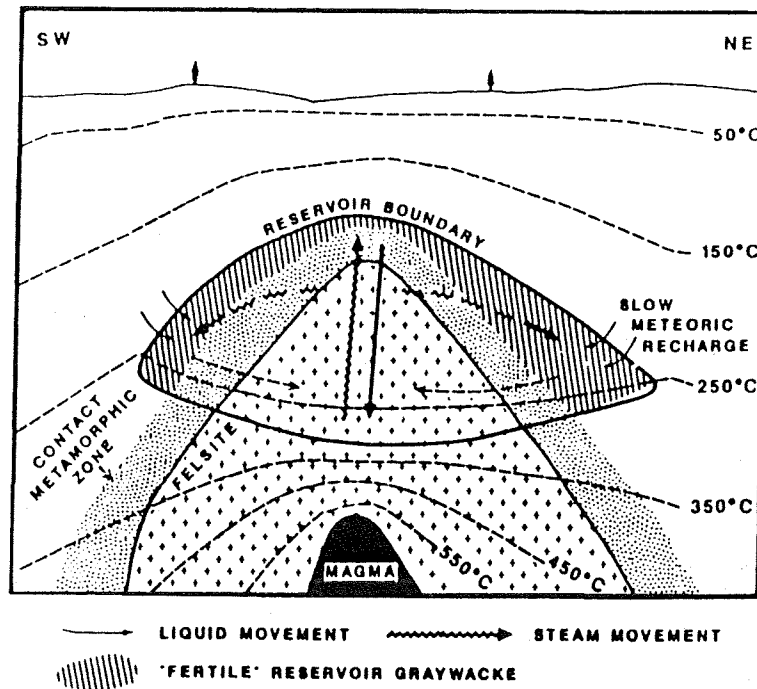


FIGURE 4. Schematic model of pre-exploitation Geysers reservoir showing contact metamorphic zone of hornfels and flow of steam and water. Hachured area represents reservoir rocks containing calcite and organic material. Diagram is not to scale. From Gunderson (1989).

The evolution of the magmatic/hydrothermal system has been complex, and it is possible that there were multiple episodes of felsite intrusion. During and shortly after magmatic injection, contact metamorphic processes formed boron-rich hornfels in graywacke immediately adjacent to the felsite (Fig. 4). This fine-grained hornfels is generally rich in biotite, quartz, tourmaline, adularia, and ilmenite (Sternfeld, 1989). A few high-temperature (325–400°C), very saline (NaCl > 25 equivalent weight percent) fluid inclusions that may be samples of evolved magmatic fluids have been found in vein minerals near the top of the felsite (J. N. Moore, written communication, 1989). At an early stage in the hydrothermal activity a convecting hot water-dominated system with temperatures as high as 300–350°C extended throughout the region that is now vapor-dominated with present temperatures close to 240°C (McLaughlin et al., 1983; Moore et al., 1989; Sternfeld, 1989). Early high-temperature veins contain hydrothermally deposited quartz, epidote, albite, pyrite, actinolite, adularia, pyrrhotite, tourmaline, hornblende amphibole, pyroxene, and ilmenite (McLaughlin et al., 1983; Sternfeld, 1989). Superimposed on this earlier mineral zonation is a second generation of minerals characterized by prehnite and axinite (Sternfeld, 1989). There are also later veins of quartz ± adularia ± chlorite ± white mica ± pyrite. Adularia from these late veins has been dated at 0.69 ± 0.03 Ma (McLaughlin et al., 1983). The fluids in the hot water-dominated stage of the reservoir generally had salinities in the range 0.36 to 1.7 equivalent weight percent NaCl, and CO₂ contents as high as 3.8 weight percent (Moore et al., 1989). The system changed from hot water- to vapor-dominated when fluid discharge began to

exceed recharge while abundant heat continued to be supplied from below (White et al., 1971). This change probably came about because of decreasing permeability at those boundaries of the system where recharge had been active, possibly caused by deposition of calcite as recharge water was heated.

ACKNOWLEDGMENTS

This summary is based entirely on the work of others. I have relied heavily upon the results of extensive regional and local geologic mapping, age dating, and geophysical characterizations of The Geysers–Clear Lake area that were carried out by many members of the U.S. Geological Survey as part of the Geothermal Research Program. The manuscript was greatly improved by the very detailed and helpful reviews of J. M. Donnelly-Nolan and R. J. McLaughlin. I especially wish to acknowledge the major contributions to our understanding of The Geysers reservoir made by the many company geologists and geophysicists who have worked there, and to acknowledge and thank their companies who have allowed them to publish their results and interpretations. In particular, recent publications by staff members of the UNOCAL Geothermal Division and the GEO Operator Corporation were of great value to me in the preparation of this report. Figures 2, 3, and 4 were prepared originally by UNOCAL geologists, and are reproduced here with UNOCAL's permission.

REFERENCES

- Atwater, Tanya, 1970, Implications of plate tectonics for the Cenozoic tectonic evolution of western North America: *Geol. Soc. Amer. Bull.*, v. 81, p. 3513–3536.
- Blake, M. C., Jr., Campbell, R. H., Dibblee, T. W., Jr., Howell, D. G., Nilsen, T. H., Normark, W. R., Vedder, J. C., and Silver, E. A., 1978, Neogene basin formation in relation to plate-tectonic evolution of San Andreas fault system, California: *Amer. Assoc. Petroleum Geologists Bull.*, v. 62, p. 344–372.
- Dickinson, W. R., and Snyder, W. S., 1979, Geometry of subduction slabs related to San Andreas transform: *Jour. Geol.*, v. 87, p. 609–627.
- Donnelly-Nolan, J. M., Hearn, B. C., Jr., Curtis, G. H., and Drake, R. E., 1981, Geochronology and evolution of the Clear Lake Volcanics: *U.S. Geol. Survey Prof. Paper 1141*, p. 47–60.
- Fournier, R. O., 1991, The transition from hydrostatic to greater than hydrostatic fluid pressure in presently active continental hydrothermal systems: *Geophys. Res. Ltrs.*, v. 18, p. 955–958.
- Fox, K. F. Jr., Fleck, R. F., Curtis, G. H., and Meyer, C. E., 1985, Potassium-argon and fission-track ages of the Sonoma Volcanics in an area north of San Pablo Bay, California: *U.S. Geol. Survey Misc. Field Studies Map MF-1753*, 9 p.
- Goff, F. E., Donnelly, J. M., Thompson, J. M., and Hearn, B. C., 1977, Geothermal prospecting in The Geysers–Clear Lake area, northern California: *Geology*, v. 5, p. 509–515.
- Gunderson, R. P., 1989, Distribution of oxygen isotopes and non-condensable gas in steam at The Geysers: *Geothermal Resources Council Transactions*, v. 13, p. 449–454.
- Gunderson, R. P., 1990, Reservoir porosity at The Geysers from core measurements: *Geothermal Resources Council Transactions*, v. 14, part II, p. 1661–1665.
- Hearn, B. C., Jr., Donnelly, J. M., and Goff, F. E., 1976, Geology and geochronology of the Clear Lake Volcanics, California: *Proc. Second United Nations Symposium on the Development and Use of Geothermal Resources*, May 20–29, 1975, San Francisco, Calif., v. 1, p. 423–428.
- Hearn, B. C., Jr., Donnelly, J. M., and Goff, F. E., 1981, The Clear Lake Volcanics: Tectonic setting and magma sources: *U.S. Geol. Survey Prof. Paper 1141*, p. 25–45.
- Isherwood, W. F., 1976, Gravity and magnetic studies of The Geysers–Clear Lake geothermal region, California, USA: *Proc. Second United Nations Symposium on the Development and Use of Geothermal Resources*, May 20–29, 1975, San Francisco, Calif., v. 2, p. 1065–1073.

- Iyer, H. M., 1984, Geophysical evidence for the locations, shapes and sizes, and internal structures of magma chambers beneath regions of Quaternary volcanism: *Phil. Trans. R. Soc. Lond.* v. A 310, p. 473–510.
- McLaughlin, R. J., 1977, The Franciscan Assemblage and Great Valley Sequence in The Geysers–Clear Lake Region of Northern California, *in* Field Trip Guide to The Geysers–Clear Lake area for the Cordilleran Section of the Geological Society of America, April 1977, p. 3–12.
- McLaughlin, R. J., 1981, Tectonic setting of pre-Tertiary rocks and its relation to geothermal resources in The Geysers–Clear Lake area: U.S. Geol. Survey Prof. Paper 1141, p. 3–23.
- McLaughlin, R. J., Moore, D. E., Sorg, D.H., and McKee, E. H., 1983, Multiple episodes of hydrothermal circulation, thermal metamorphism, and magma injection beneath The Geysers steam field, California (abstract): *Geol. Soc. Amer. Abstracts With Programs*, v. 14, p. 417.
- McLaughlin, R. J., and Ohlin, N. O., 1984, Tectonostratigraphic framework of The Geysers-Clear Lake region, California, *in* Blake, M. C., Jr., ed., *Franciscan Geology of Northern California: Pacific Section S.E.P.M.*, v. 43, p. 221–254.
- Moore, J. N., Hulen, J. B., Lemieux, M. M., Sternfeld, J. N., and Walters, M. A., 1989, Petrographic and fluid inclusion evidence for past boiling, brecciation, and associated hydrothermal alteration above the northwest Geysers steam field: *Geothermal Resources Council Transactions*, v. 13, p. 467–472.
- Schriener, A., Jr., and Suemnicht, G. A., 1981, Subsurface intrusive rocks at The Geysers geothermal area California, *in* Silberman, M. L., Field, C. W., and Berry, A. L., eds., *Proceedings of the Symposium on Mineral Deposits of the Pacific Northwest: U.S. Geol. Survey Open-File Report 81–355*, p. 295–302.
- Sternfeld, J. N., 1989, Lithologic influences on fracture permeability and distribution of steam in the northwest Geysers steam field, Sonoma County, California: *Geothermal Resources Council Transactions*, v. 13, p. 473–479.
- Thompson, R. C., 1989, Structural stratigraphy and intrusive rocks at The Geysers geothermal field: *Geothermal Resources Council Transactions*, v. 13, p. 481–485.
- Thompson, R. C., and Gunderson, R. P., 1989, The orientation of steam-bearing fractures at The Geysers geothermal steam field: *Geothermal Resources Council Transactions*, v. 13, p. 487–490.
- Walthers, M., and Combs, J., 1989, Heat flow in The Geysers–Clear Lake area of Northern California, U.S.A.: *Geothermal Resources Council Transactions*, v. 13, p. 491–502.
- White, D. E., Muffler, L. J. P., and Truesdell, A. H., 1971, Vapor-dominated hydrothermal systems compared with hot-water systems: *Econ. Geol.*, v. 66, p. 75–97.
- Williamson, K. H., 1990, Development of a reservoir model for The Geysers geothermal field, *in* Claudia Stone, ed., *Monograph on The Geysers Geothermal Field: Geothermal Resources Council, Special Rept. No. 17*, p. 77–87.

PRELIMINARY REPORT ON $^{40}\text{Ar}/^{39}\text{Ar}$ INCREMENTAL HEATING EXPERIMENTS ON
FELDSPAR SAMPLES FROM THE FELSITE UNIT, GEYSERS GEOTHERMAL FIELD,
CALIFORNIA

G. Brent Dalrymple

U.S. Geological Survey, Menlo Park, CA 94025

INTRODUCTION

This is a progress report on some preliminary $^{40}\text{Ar}/^{39}\text{Ar}$ incremental heating experiments on feldspar separates from four samples of the felsite unit, a complex silicic batholith that intrudes the overlying Franciscan Complex (Late Jurassic to Late Cretaceous) and underlies the Geysers Geothermal Field, northern California (Schriener and Suemnicht, 1981; Thompson, 1989, 1991). The felsite unit is only found in the subsurface but it appears to be an elongate body whose axis trends northwest-southeast and whose surface is shallowest in the southeast part of the field (Figure 1). It ranges in composition from granite to granodiorite (Schriener & Suemnicht, 1981; Thompson, 1991).

The apparent coincidence of the heat flow anomaly within the Geysers field (Walters and Combs, 1989) with the distribution of felsite within and below the zone of steam production suggests that the felsite unit may be the primary source of heat. Presently available K-Ar ages (0.9 Ma to 2.7 Ma) suggest, however, that the felsite unit may be too old to be the primary source of heat for the present thermal activity. Resolution of this apparent paradox should be of interest for the purposes of both exploration and field management. If the felsite unit is young (<1 Ma), for example, then it should be hot wherever it is found. If the felsite unit is old (>1 Ma), on the other hand, then it may be relatively cold outside of the region of present production. The felsite unit also may be a complex body emplaced over a significant interval of time with both older and younger parts. Regardless of its age, the felsite unit appears to play an important role in the geothermal field and its intrusion and thermal history is of interest.

The age of the felsite unit is not known. Schriener and Suemnicht (1981) reported K-Ar ages of 1.6 ± 0.4 Ma on sanidine, 2.7 ± 0.3 Ma on biotite, and 2.5 ± 0.4 Ma on whole rock felsite. The samples for their study came from cutting recovered from wells that penetrate the felsite unit in the subsurface. Thompson (1991) mentions unpublished age measurements, presumably K-Ar, of as young as 0.9 Ma. McLaughlin and others (1983) reported a K-Ar age of 0.69 ± 0.03 Ma on adularia separated from veins that intrude Franciscan rocks above, and presumably associated with, the felsite unit. The details of these limited age studies have not been published and it is, therefore, difficult to evaluate their significance.

The K-Ar method is remarkably reliable in simple systems, e.g., volcanic rocks. In more complex systems, however, it is subject to errors from Ar loss due to thermal events and alteration, and (rarely) from excess ^{40}Ar due to contamination, incomplete degassing, and elevated ^{40}Ar partial pressures (Dalrymple

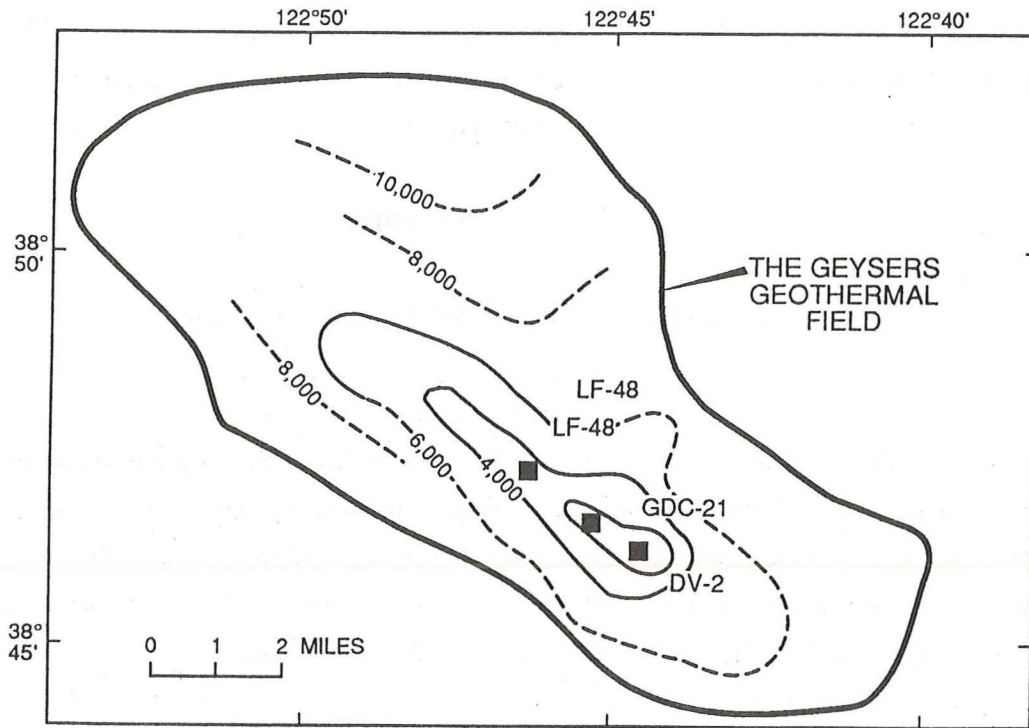


FIGURE 1. Location of core samples showing approximate boundary of geothermal reservoir and generalized top of the felsite unit. Contours in feet below sea level. From Thompson (1991) and Gunderson (1991).

and Lanphere, 1969). The felsite unit has been subjected to elevated temperatures, fluid and gas flow, and alteration over an extended period of time. It is, therefore, a complex system and K-Ar ages are probably of limited, if any, value. The discordance in its reported ages suggests that the felsite unit is not an undisturbed system and, therefore, cannot be reliably dated by conventional K-Ar methods. Also unknown is the degree to which the dated cuttings samples might be contaminated with material from the older Franciscan rocks.

In the $^{40}\text{Ar}/^{39}\text{Ar}$ method the sample is irradiated with fast neutrons, along with a *monitor mineral* of known age, to induce the reaction $^{39}\text{K}(n,p)^{39}\text{Ar}$. The age of the sample is then calculated from the $^{40}\text{Ar}/^{39}\text{Ar}$ ratio after determining the fraction of ^{39}K converted to ^{39}Ar (expressed by the neutron conversion efficiency factor, J) by analyzing the monitor mineral. Appropriate corrections for interfering Ar isotopes produced from K and Ca, and for contaminating atmospheric Ar must also be applied in the age calculations. The $^{40}\text{Ar}/^{39}\text{Ar}$ method can be used in two different ways. If all of the Ar is released by fusing the sample in a single heating, the result is a *total fusion age*, which is analogous to, and interpreted the same as, a conventional K-Ar age. If the argon is released from the sample in steps by incrementally heating the sample to progressively higher temperatures, the result is a series of ages known as an *age spectrum*.

The $^{40}\text{Ar}/^{39}\text{Ar}$ age spectrum method has the advantage of providing information about the degree to which the system has been disturbed or contaminated. In many instances it is possible to determine a crystallization age for

a sample that has lost a significant fraction of its radiogenic ^{40}Ar due to thermal or chemical (alteration) disturbance. In others it is possible to determine a minimum crystallization age for a disturbed sample. Regardless of the degree of disturbance or contamination, the method nearly always gives information about the reliability of the sample as a geochronometer and so the apparent ages measured in this way are easily evaluated. In some instances, information about the thermal history of the sample can be extracted from age spectra. For a recent and thorough description of $^{40}\text{Ar}/^{39}\text{Ar}$ methods, see McDougall and Harrison (1988).

The purposes of this preliminary study were three. The first and most important goal was to determine if $^{40}\text{Ar}/^{39}\text{Ar}$ age spectrum analyses of sufficient precision could be made on feldspars from the felsite unit. The ability to measure precise $^{40}\text{Ar}/^{39}\text{Ar}$ age spectra on small samples of very young rocks is a relatively recent development, and it was felt from the outset that there was no point in undertaking a detailed geochronological study of the Geysers subsurface rocks if precise and detailed age spectra could not be obtained on these samples. The second goal was to determine a reliable, if only preliminary, minimum age for the felsite unit. The third goal, assuming success for the first goal, was to use the information obtained from the preliminary results to design a sensible $^{40}\text{Ar}/^{39}\text{Ar}$ research program with the goal of determining the age and (perhaps) some information about the thermal history of the felsite unit.

The preliminary experiments reported here have resulted in precise $^{40}\text{Ar}/^{39}\text{Ar}$ age spectra on feldspar separated from four samples of the felsite unit, thereby fulfilling the first goal, and a reliable minimum age of 1.3-1.4 Ma for the parts of the felsite unit sampled, thereby fulfilling the second. An analysis of the age spectrum data to determine what, if any, thermal history information might be extracted from these four samples or from future analyses of other samples has not commenced. These preliminary data indicate that a more comprehensive $^{40}\text{Ar}/^{39}\text{Ar}$ study of the felsite unit, and perhaps of selected samples from the overlying Franciscan Complex, will be productive.

SAMPLE DESCRIPTIONS AND LOCATIONS

The samples studied were from cores taken from the felsite unit below the first steam entry and, for two of the cores, within the geothermal reservoir (Figure 1, Table 1; Gunderson, 1990,1991). The wells have not been logged and so the temperatures at the sample depths are not known with certainty, but data from surrounding wells indicates that the temperatures should be in the range 243-249 °C (R. P. Gunderson, personal communication, 1992).

The samples studied came from two core segments from DV-2 (DV-2B, DV-2E) and one each from GDC-21 and LF-48. The parts of the cores used for mineral separation and dating were selected to avoid the most highly altered parts of the core segments, which surround fractures. The samples have not yet been studied petrographically and the descriptions that follow are based on only a cursory thin section examination. All four of the samples appear to be approximately rhyolite to quartz monzonite in composition.

Table 1. Location of cores from the felsite unit (Gunderson, 1990, 1991).

Well	Sample From	Core interval (drilled depth, ft.)	Core elev. (ft., MSL)	Felsite elev. (ft., MSL)
DV-2	steam entry	3,708-3,718	-665	-300
GDC-21	reservoir	5,864-5,868	-3,310	-1,500
LF-48	reservoir	8,089-8,096	-4,805	-3,000

Sample LF-48 is porphyritic with phenocrysts (2-3 mm) of quartz, K-feldspar, plagioclase, and rare biotite in an equigranular groundmass (avg. \sim 0.1 mm) of quartz, feldspar, and rare mafic minerals. Most of the groundmass feldspar is altered to clays(?) but many of the K-feldspar phenocrysts show relatively minor alteration.

Sample DV-2B and DV-2E are similar to LF-48 but more highly altered, except that the groundmass of DV-2B has a somewhat coarser grain size (0.2-0.3 mm). The groundmass in both of these samples is highly altered and recrystallized and contains abundant white mica and amphibole. Some of the K-feldspar phenocrysts are only slightly to moderately altered.

Sample GDC-21 contains rare phenocrysts of K-feldspar (2-3 mm). The rock has a poikilitic texture with crystals (1 mm) of quartz, K-feldspar, and rare plagioclase enclosing small crystals of plagioclase, biotite, and minor accessory minerals. Both the ground mass and phenocrystic K-feldspar is slightly altered but optically continuous.

Sample GDC-21 is by far the least altered of the samples, with DV-2B and DV-2E the most altered.

ANALYTICAL METHODS

Selected sections of the four core pieces were crushed and sieved to 150-250 μ m. Potassium-feldspar crystals (which, because of the sizing, were presumably phenocrysts) were separated from the sized fractions using heavy liquids. The feldspar was etched in 10% HF for 5-10 minutes to remove adhering alteration products and the feldspar was then cleaned ultrasonically and washed in distilled H₂O.

The feldspar samples were packaged in Al-foil envelopes, sealed in a quartz vial along with aliquots of 85G003 (sanidine from the Taylor Creek Rhyolite of Elston (1968), the neutron flux monitor mineral, 27.92 Ma), shielded with Cd foil, and irradiated in the core of the U.S. Geological Survey TRIGA reactor for 2 hours, where they received an integrated fast neutron flux of 1.2×10^{17} nvt. The reactor characteristics, corrections for interfering Ar isotopes produced from K and Ca, and irradiation procedures are described in detail by Dalrymple and others (1981). The monitor minerals were measured on a $^{40}\text{Ar}/^{39}\text{Ar}$ continuous laser system that incorporates a high-sensitivity MAP-216 rare-gas mass spectrometer optimized for Ar analyses (Dalrymple, 1989). The Geysers feldspar samples were measured on a similar system equipped with a double-vacuum resistance furnace.

The *J*-value curve determined from measurements of the four packets of the monitor mineral (85G003) is shown in Figure 2. The figure shows the weighted mean values calculated from multiple analyses of crystals from

each packet, where weighting is by the inverse of the estimated variance of each individual run (Taylor, 1982). A total of 26 analyses were made on the monitor mineral packets and the errors (best of Taylor) of the weighted means range from 0.09% to 0.15%. The J values applied to each sample is found by interpolation of the curve in Figure 2. The errors in the J values applied to the age spectrum calculations for these samples is less than 0.5%.

PRELIMINARY RESULTS

The $^{40}\text{Ar}/^{39}\text{Ar}$ analytical data for the four samples are listed in Table 2 and the age spectra shown in Figure 3. The number of increments in the age spectra range from 16 for GDC-21 to 19 for DV-2B and DV-2E.

The age spectra indicate that the four samples have been disturbed by thermal events, alteration, or both. The first few gas increments of each of the spectra have high apparent ages. This is often caused by ^{39}Ar loss due to ^{39}Ar recoil from ^{40}K sites near the surfaces of mineral grains and the apparent ages calculated from such increments do not have any geologic age significance. Although the feldspar grains are too large for significant ^{39}Ar recoil effects, the alteration products visible in thin section are very fine-grained and recoil of ^{39}Ar from these phases is not unexpected.

The overall patterns of the age spectra are more-or-less typical of samples that have undergone thermal loss of Ar, with low apparent ages in the low-temperature steps increasing to higher apparent ages in the intermediate- and high-temperature steps. The decrease in apparent age for the high-temperature steps in samples DV-2B and DV-2E are consistent with ^{39}Ar recoil effects but such "humped" age spectra also occur in altered samples. The cause of the "saddle" in the age spectrum of GDC-21 is, at present, unknown. How much of the disturbance of the four age spectra is due to thermal causes and how much to alteration is not known but further analyses on a broader suite of samples plus a more detailed analysis of the present data may clarify this question. The feldspar from these samples is altered, however, and it is very likely that alteration effects are important. It also may be significant that the feldspar from GDC-21, which is the least altered of the four samples, has the highest intermediate- and high-temperature increment ages (see below).

It is virtually impossible for either thermal events or alteration to disturb an age spectrum in such a way that the apparent ages for the bulk of the intermediate- and high-temperature increments exceed the crystallization age of the sample, the increments at the extremes, i.e., near 100% ^{39}Ar released, excepted. A conservative interpretation, therefore, is that the intermediate- and high-temperature maxima in the age spectra are minimum ages. Accordingly, the results from sample GDC-21 suggest that the crystallization age of the part of the felsite unit sampled by the three cores is at least 1.3-1.4 Ma. The results also indicate that the interpretation of conventional K-Ar and total fusion $^{40}\text{Ar}/^{39}\text{Ar}$ ages from the felsite unit is equivocal and that if the crystallization age of the felsite unit can be determined, it will be by $^{40}\text{Ar}/^{39}\text{Ar}$ age spectrum methods.

TABLE 2. Analytical data for $^{40}\text{Ar}/^{39}\text{Ar}$ age spectrum data on K-feldspar from the felsite unit, Geysers Geothermal Field, California.

Temp. (°C)	$^{40}\text{Ar}/^{39}\text{Ar}$	$^{37}\text{Ar}/^{39}\text{Ar}^{\text{a}}$	$^{36}\text{Ar}/^{39}\text{Ar}$	$^{40}\text{Ar}_{\text{rad}}^{\text{b}}$ (%)	$^{40}\text{Ar}_{\text{K}}^{\text{b}}$ (%)	$^{36}\text{Ar}_{\text{Ca}}^{\text{b}}$ (%)	K/Ca	^{39}Ar (%)	Age ^c (Ma)
<u>DV-2B (J = 0.0003154) Total gas age = 0.684 ± 0.006 Ma</u>									
450	15.714	0.000981	0.04416	16.9	0.0	0.0	499.6	5.9	1.513 ± 0.035
500	4.752	0.001782	0.012298	23.4	0.1	0.0	274.9	3.5	0.633 ± 0.031
550	3.442	0.001269	0.008949	23.0	0.1	0.0	386.0	4.9	0.451 ± 0.022
625	3.062	0.001583	0.007373	28.7	0.2	0.0	309.5	6.6	0.499 ± 0.017
700	2.568	0.003106	0.005650	34.8	0.2	0.0	157.8	5.3	0.508 ± 0.020
775	3.726	0.003351	0.008655	31.2	0.1	0.0	146.2	4.2	0.662 ± 0.026
850	3.035	0.002769	0.007121	30.5	0.2	0.0	176.9	1.2	0.527 ± 0.089
925	2.430	0.002424	0.005050	38.4	0.2	0.0	202.1	1.5	0.531 ± 0.068
1000	2.952	0.001881	0.006238	37.4	0.2	0.0	260.5	3.2	0.628 ± 0.034
1050	3.077	0.001650	0.006363	38.7	0.2	0.0	297.0	5.3	0.678 ± 0.021
1080	2.738	0.001335	0.005479	40.7	0.2	0.0	367.1	5.6	0.633 ± 0.019
1110	2.548	0.001005	0.004598	46.5	0.2	0.0	487.4	7.3	0.673 ± 0.015
1130	2.132	0.000732	0.003118	56.6	0.2	0.0	669.2	6.6	0.686 ± 0.016
1150	1.9957	0.000642	0.002486	62.9	0.3	0.0	763.8	7.8	0.714 ± 0.0
1175	1.9006	0.000473	0.002302	63.9	0.3	0.0	1035	9.6	0.691 ± 0.0
1200	2.503	0.000485	0.004454	47.2	0.2	0.0	1010	9.0	0.672 ± 0.012
1250	1.8699	0.000242	0.002579	59.0	0.3	0.0	2026	9.7	0.627 ± 0.011
1300	3.043	0.000609	0.006400	37.7	0.2	0.0	804.0	1.0	0.653 ± 0.103
1500	7.220	0.000852	0.02011	17.6	0.1	0.0	575.1	1.8	0.724 ± 0.059
<u>DV-2E (J = 0.0003170) Total gas age = 0.894 ± 0.008 Ma</u>									
500	97.26	0.003949	0.2907	11.7	0.0	0.0	124.1	0.7	6.487 ± 0.259
525	27.33	0.004393	0.08679	6.1	0.0	0.0	111.6	1.2	0.958 ± 0.116
575	19.542	0.002932	0.06018	9.0	0.0	0.0	167.1	2.8	1.003 ± 0.059
625	9.995	0.002603	0.03085	8.7	0.1	0.0	188.2	2.9	0.499 ± 0.048
675	11.208	0.002298	0.03409	10.1	0.0	0.0	213.2	2.9	0.646 ± 0.048
725	8.982	0.002066	0.02704	11.0	0.1	0.0	237.2	3.0	0.564 ± 0.046
800	7.563	0.001799	0.02263	11.5	0.1	0.0	272.4	3.9	0.498 ± 0.035
875	3.609	0.001562	0.010215	16.2	0.1	0.0	313.6	1.5	0.334 ± 0.082
950	5.744	0.002041	0.017347	10.7	0.1	0.0	240.1	2.6	0.351 ± 0.051
1000	7.842	0.002122	0.02339	11.8	0.1	0.0	230.9	3.8	0.529 ± 0.037
1050	8.042	0.001924	0.02324	14.5	0.1	0.0	254.6	6.3	0.669 ± 0.025
1100	6.917	0.002108	0.018667	20.2	0.1	0.0	232.5	11.1	0.798 ± 0.017
1150	5.767	0.002106	0.013683	29.8	0.1	0.0	232.7	18.6	0.982 ± 0.013
1180	4.390	0.001756	0.008696	41.4	0.1	0.0	279.0	19.7	1.038 ± 0.010
1210	4.548	0.001772	0.009851	35.9	0.1	0.0	276.5	12.4	0.933 ± 0.013
1250	4.505	0.002164	0.010485	31.1	0.1	0.0	226.4	3.9	0.802 ± 0.034
1325	6.716	0.005555	0.016981	25.2	0.1	0.0	88.21	1.2	0.968 ± 0.108
1450	15.413	0.003489	0.04482	14.0	0.0	0.0	140.4	0.7	1.237 ± 0.184
1550	11.195	0.02534	0.02377	37.2	0.0	0.0	19.34	0.8	2.382 ± 0.1

GDC-21 (J = 0.0003117) Total gas age = 1.169 ± 0.008 Ma

500	11.195	0.02534	0.02377	37.2	0.0	0.0	19.34	0.8	2.342 ± 0.150
550	7.297	0.017874	0.014572	40.9	0.1	0.0	27.41	0.9	1.679 ± 0.130
625	2.911	0.013899	0.004982	49.3	0.2	0.1	35.25	3.6	0.807 ± 0.033
700	1.5566	0.015966	0.003108	40.8	0.3	0.1	30.69	4.6	0.357 ± 0.026
775	1.6368	0.014544	0.002625	52.4	0.3	0.1	33.69	4.2	0.482 ± 0.029
850	1.9272	0.010351	0.003228	50.3	0.3	0.1	47.34	1.6	0.545 ± 0.074
925	2.324	0.008024	0.003941	49.7	0.2	0.1	61.07	1.3	0.649 ± 0.094
1000	2.705	0.006575	0.003586	60.7	0.2	0.0	74.53	3.3	0.922 ± 0.036
1050	3.255	0.005188	0.002843	74.0	0.2	0.0	94.45	6.1	1.354 ± 0.020
1100	2.789	0.003624	0.001536	83.6	0.2	0.1	135.2	17.5	1.310 ± 0.008
1130	2.378	0.002625	0.000920	88.4	0.2	0.1	186.6	18.7	1.181 ± 0.007
1160	2.352	0.002340	0.000722	90.7	0.2	0.1	209.4	22.6	1.199 ± 0.006
1200	2.765	0.004204	0.001058	88.5	0.2	0.1	116.6	13.2	1.376 ± 0.010
1250	4.659	0.03627	0.006625	57.9	0.1	0.1	13.51	1.1	1.517 ± 0.110
1400	21.49	0.05775	0.05489	24.5	0.0	0.0	8.48	0.3	2.962 ± 0.382
1550	199.28	0.03264	0.6291	6.7	0.0	0.0	15.01	0.1	7.509 ± 1.357

LF-48 (J = 0.0003136) Total gas age = 0.931 ± 0.006 Ma

450	57.81	0.007400	0.15878	18.8	0.0	0.0	66.21	0.8	6.149 ± 0.152
500	19.898	0.006168	0.05232	22.3	0.0	0.0	79.45	1.3	2.506 ± 0.080
550	9.518	0.004224	0.02588	19.6	0.1	0.0	116.0	2.0	1.055 ± 0.048
625	3.521	0.003380	0.007755	34.8	0.1	0.0	145.0	2.0	0.692 ± 0.045
850	2.251	0.003195	0.004926	35.1	0.2	0.0	153.4	2.0	0.447 ± 0.045
700	2.004	0.003967	0.004361	35.4	0.3	0.0	123.5	5.1	0.402 ± 0.018
775	2.073	0.003969	0.005035	28.0	0.2	0.0	123.5	2.3	0.328 ± 0.040
925	2.011	0.003028	0.003771	44.4	0.3	0.0	161.8	2.4	0.504 ± 0.038
1000	2.091	0.003297	0.003871	45.1	0.2	0.0	148.6	2.8	0.533 ± 0.032
1050	3.059	0.002794	0.005680	45.0	0.2	0.0	175.4	4.4	0.778 ± 0.021
1080	3.007	0.002754	0.005269	48.1	0.2	0.0	177.9	4.5	0.818 ± 0.021
1110	2.682	0.002471	0.003537	60.8	0.2	0.0	198.3	10.7	0.923 ± 0.010
1130	2.269	0.001970	0.002027	73.4	0.2	0.0	248.7	16.5	0.942 ± 0.007
1150	2.077	0.001565	0.001298	81.3	0.2	0.0	313.1	17.6	0.955 ± 0.006
1175	2.086	0.001422	0.001113	84.0	0.2	0.0	344.6	18.7	0.991 ± 0.006
1200	2.287	0.002196	0.001725	77.5	0.2	0.0	223.1	6.0	1.003 ± 0.015
1250	3.652	0.008950	0.006526	47.1	0.1	0.0	54.75	0.7	0.972 ± 0.125
1400	19.460	0.009326	0.05667	13.9	0.0	0.0	52.54	0.2	1.532 ± 0.482

a Corrected for ^{37}Ar decay, half-life=35.1 days.

b Subscripts: rad, radiogenic; K, potassium-derived; Ca, calcium derived.

c Decay constants: $\lambda_{\epsilon}=0.581 \times 10^{-10} \text{yr}^{-1}$, $\lambda_{\beta}=4.692 \times 10^{-10} \text{yr}^{-1}$. Errors assigned to individual ages are estimates of the

standard deviation of analytical precision and do not include the error in J, which is 0.5%.

$(^{36}\text{Ar}/^{37}\text{Ar})_{\text{Ca}}=0.000269 \pm 2$, $(^{39}\text{Ar}/^{37}\text{Ar})_{\text{Ca}}=0.000670 \pm 5$, $(^{40}\text{Ar}/^{39}\text{Ar})_{\text{K}}=0.0051 \pm 4$.

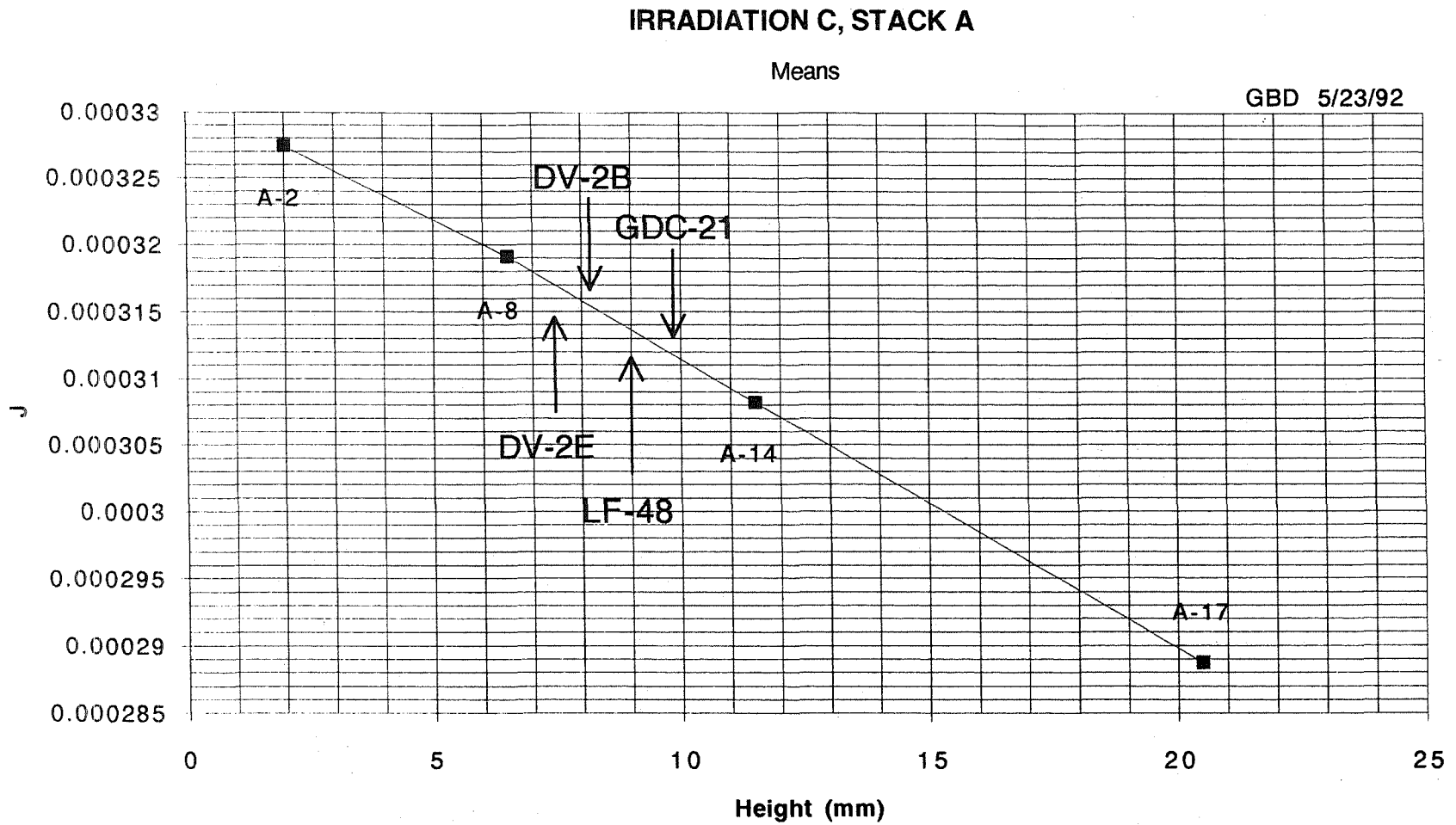


FIGURE 2. *J*-curves showing mean values (squares) for packets of the monitor mineral (85G003, 27.92 Ma) and the locations within the sample stack of the four Geysers K-feldspar samples.

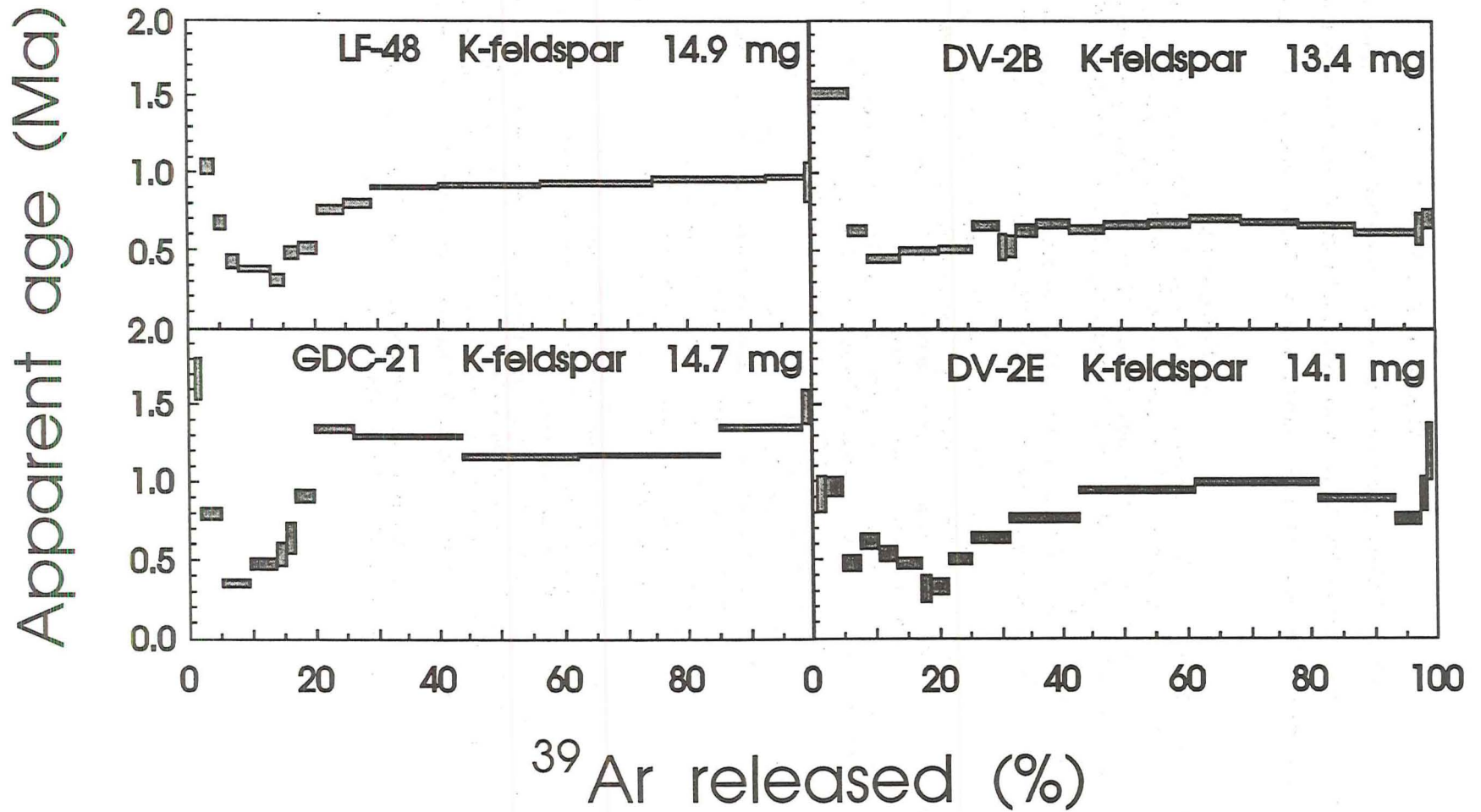


FIGURE 3. $^{40}\text{Ar}/^{39}\text{Ar}$ age spectra for four samples of potassium feldspar from core samples of the felsite unit, Geysers geothermal field. The thickness of the shaded bars is two standard deviations of precision of the calculated age.

ACKNOWLEDGMENTS

I thank UNOCAL Corporation for making the samples available, the Geothermal Division of the Department of Energy for funding this preliminary study, Mike McWilliams of Stanford University for making his laboratory available for some of the measurements, and Robert Fournier for reviewing the manuscript.

REFERENCES

- Dalrymple, G. B., 1989, The GLM continuous laser system for $^{40}\text{Ar}/^{39}\text{Ar}$ dating: Description and performance characteristics, in Shanks, W. C. III, and Criss, R. E., eds., *New frontiers in stable isotopic research: Laser Probes, Ion Probes, and small-sample analysis*: U.S. Geological Survey Bulletin 1890, p. 89-96.
- Dalrymple, G. B., and Lanphere, M. A., 1969, *Potassium-Argon Dating*: San Francisco, W. H. Freeman and Company, 258 p.
- Dalrymple, G. B., Alexander, E. C., Jr., Lanphere, M. A., and Kraker, G. P., 1981, Irradiation of samples for $^{40}\text{Ar}/^{39}\text{Ar}$ dating using the Geological Survey TRIGA reactor: U.S. Geological Survey Professional Paper 1176, 55 p.
- Elston, W. E., 1968, Terminology and distribution of ash flows of the Mogollon-Silver City-Lordsburg region, New Mexico: Arizona Geological Society, S. Arizona, Guidebook 3 (S. R. Titley, ed.), p. 231-240.
- Gunderson, R. P., 1990, Reservoir matrix porosity at the Geysers from core measurements: Geothermal Resources Council Transactions, vol. 14, part II, p. 1661-1665.
- Gunderson, R. P., 1991, Porosity of reservoir graywacke at the Geysers: Geothermal Resources Council, Monograph on the Geysers Geothermal Field, Special Report No. 17, p. 89-93.
- McDougall, I., and Harrison, T. M., 1988, *Geochronology and Thermochronology by the $^{40}\text{Ar}/^{39}\text{Ar}$ method*: New York, Oxford University Press, 212 p.
- McLaughlin, R. J., Moore, D. E., Sorg, D. H., and McKee, E. H., 1983, Multiple episodes of hydrothermal circulation thermal metamorphism, and magma injection beneath the Geysers steam field, California: Geological Society of America Abstracts with Programs, vol. 15, no. 5, p. 417.
- Schriener, A., and Suemnicht, G. A., 1981, Subsurface intrusive rocks at the Geysers geothermal area, California, in Silberman, M. L., Field, C. F., and Berry, A. L., eds., *Proceedings of the symposium on mineral deposits of the Pacific northwest, Corvallis, OR, March 20-21, 1980*: U.S. Geological Survey Open-File Report 81-355, p. 295-302.
- Taylor, J. R., 1982, *An introduction to Error Analysis*: Mill Valley, CA, University Science Books, 270 p.
- Thompson, R. C., 1989, Structural stratigraphy and intrusive rocks at the Geysers geothermal field: Geothermal Resources Council Transactions, vol. 13, p. 481-485.
- Thompson, R. C., 1991, Structural stratigraphy and intrusive rocks at the Geysers geothermal field: Geothermal Resources Council, Monograph on the Geysers Geothermal Field, Special Report No. 17, p. 59-63.
- Thompson, R. C., and Gunderson, R. P., 1991, The orientation of steam-bearing fractures at the Geysers geothermal field: Geothermal Resources Council, Monograph on the Geysers Geothermal Field, Special Report No. 17, p. 65-68.
- Walters, M., and Coombs, J., 1989, Heat flow regime in the Geysers-Clear Lake area of northern California: Geothermal Resources Council Transactions, vol. 13, p. 491-502.

1993
in Active geothermal systems and gold-mercury deposits
in the Sonoma-Clear Lake volcanic fields, California:
Society of Economic Geologists, Guidebook Series,
v. 16, pl. 141-152.

THE GEYSERS FELSITE AND ASSOCIATED GEOTHERMAL SYSTEMS, ALTERATION, MINERALIZATION, AND HYDROCARBON OCCURRENCES

Jeffrey B. Hulen¹ and Mark A. Walters²

¹University of Utah Research Institute, Salt Lake City, UT 84108

²Russian River Energy Company, Santa Rosa, CA 95401

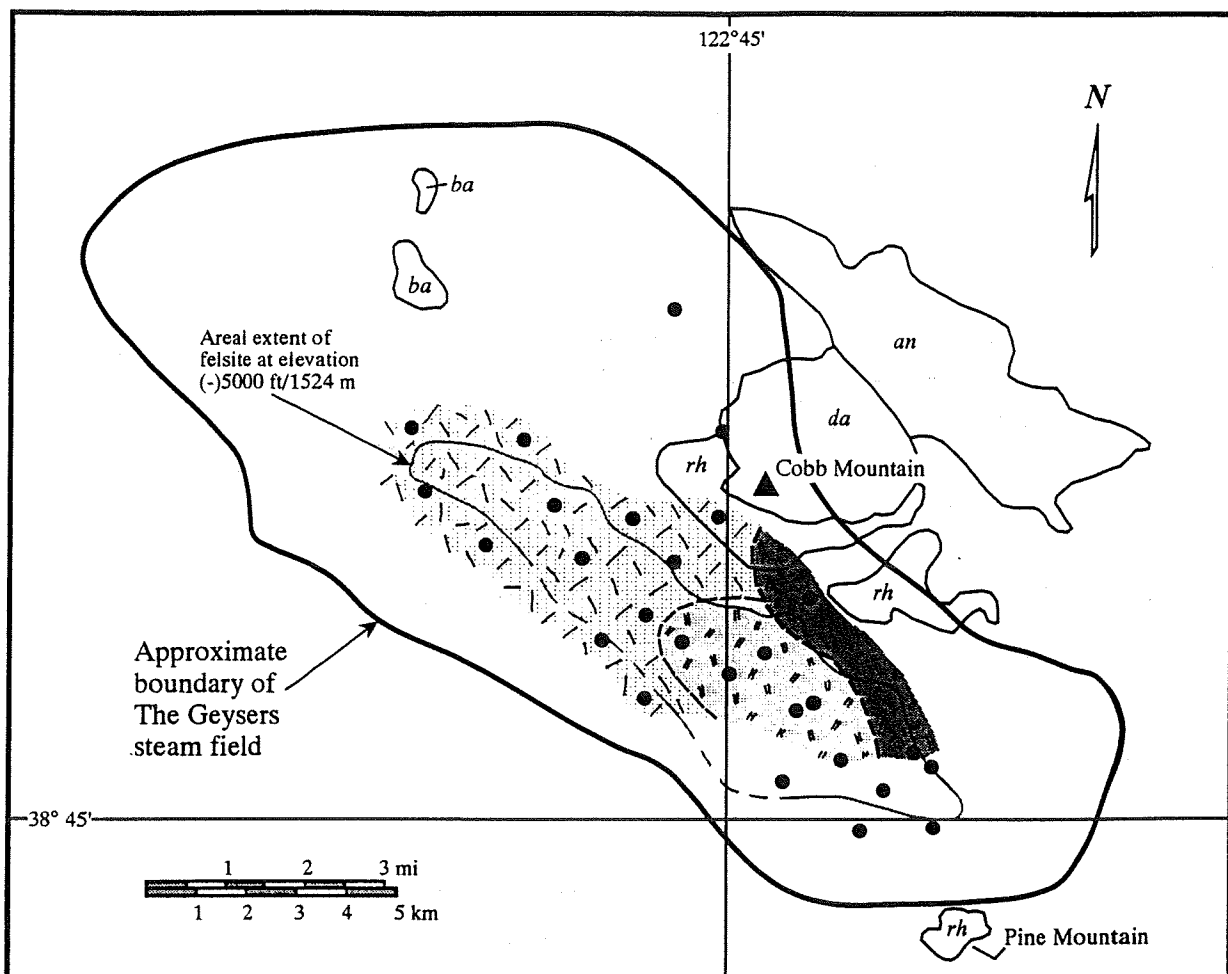
INTRODUCTION

The Geysers "felsite" (a designation of common usage in the geothermal community and thus retained for this article) is a young, wholly concealed, hypabyssal intrusive complex of batholithic dimensions within and beneath The Geysers steam field in the Mayacmas Mountains of northwest-central California (Fig. 1). The felsite was first penetrated by geothermal wells in the 1970's, but because these air-drilled boreholes yielded extremely minute (typically <0.1 mm in diameter) cuttings, the igneous nature of the body long eluded recognition. Bailey (1946) speculated that fumaroles at The Geysers signaled such a hidden intrusive, but the first detailed descriptions and chemical analyses of the felsite were published by Schriener and Suemnicht of Unocal Corporation (1981).


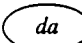

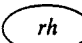


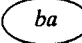
The Geysers felsite shows a clear correlation with the extent and configuration of the currently exploited vapor-dominated geothermal system (Figs. 1 and 2). A portion of this system is actually hosted by the felsite (e.g. Beall and Box, 1992), and above the pluton the remainder of the steam reservoir occurs in rocks which are hydrothermally altered and mineralized in concentric zones centered on the deep intrusive (Hulen and Nielson, 1993; Hulen and others, 1992; Moore, 1992; Walters and others, 1992; Hebein, 1986; McLaughlin and others, 1983). This alteration records the prior presence of a high-temperature, liquid-dominated hydrothermal system which appears to have "dried out" to yield the modern vapor-dominant regime (e.g. Moore, 1992; McLaughlin and others, 1983). The surface projection of the steam field includes and is encircled by numerous but scattered, commonly hydrocarbon-rich mercury deposits (e.g. Peabody and Einaudi, 1992), though these deposits also range well beyond the field to the southeast (Donnelly-Nolan and others, 1993). In view of these relationships, it seems highly likely that the modern steam reservoir, the prior liquid-dominant system, and at least some of the mercury deposits and associated hydrocarbons are genetically affiliated. The nature of that affiliation is explored briefly in this article.

GEOLOGIC SETTING

The Geysers felsite and steam field occur in complexly deformed, texturally and compositionally variable Franciscan metamorphic rocks locally overlain by rhyolitic to basaltic volcanic rocks of the southernmost reaches of the Plio-Pleistocene Clear Lake volcanic field (Donnelly-Nolan and others, 1993; McLaughlin, 1981; Hearn and others, 1981). The Franciscan rocks were deposited initially in a deep-ocean-floor environment, then modified by



Explanation

The Geysers Felsite (subsurface; at top of pluton)	Nearby Clear Lake Volcanics* (surface)
 Hornblende-pyroxene-biotite granodiorite	 Dacite
 Leucocratic biotite rhyolite porphyry	 Rhyolite
 Pyroxene-biotite granite	 Andesite
	 Basalt

● Felsite-study well locations (at top of felsite; under investigation where unpatterned)

* from Hearn et al., 1981

FIGURE 3. Interim geologic map of the surface of the Geysers felsite (from Hulen and Nielson, 1993). Three major intrusive phases have been recognized to date at the top of the pluton. The east Geysers granodiorite is temporally and geochemically similar to the overlying Cobb Mountain dacite, and may be this volcanic rock's magmatic equivalent.

CONFIGURATION, COMPOSITION, TEXTURE, AND GEOCHRONOLOGY OF THE GEYSERS FELSITE

Based on penetrations by more than 100 deep geothermal wells (R. P. Gunderson, pers. comm., 1990), the subsurface areal extent of The Geysers felsite may exceed 20 X 5 km (Fig. 1) -- batholithic dimensions. The volume of this composite intrusive body could easily be more than 100 km³, larger than the entire erupted volume of the Clear Lake volcanic field (Donnelly-Nolan and others, 1993).

The felsite is a distinctly elongate, northwest-trending (parallel to major faults of the San Andreas system) igneous body which plunges along strike both to the northwest and southeast (Fig. 1). Measured elevations at the top of the pluton range from about 152 m/500 ft below sea level to more than 2286 m/7500 ft subsea. The felsite has not been penetrated in northwest Geysers geothermal wells, but its deep presence there is inferred from the subsurface distribution of biotite- and tourmaline-rich hornfels (which mantles the felsite elsewhere in the steam field; Walters and others, 1992; Sternfeld, 1981).

Figure 3 is an in-progress geologic map of the top of the Geysers felsite (from Hulen and Nielson, 1993). Rather than being a simple single-intrusive igneous body, the felsite is a composite pluton with at least three major phases -- there are probably more but these are the ones readily recognized from the field's typical small-diameter air-drilled cuttings and the four short conventional cores available from the central and southeast Geysers.

The shallowest major felsite phase, occurring in the southeast Geysers, is rhyolite porphyry (Fig. 3) -- a leucocratic rock with phenocrysts of quartz, sparse plagioclase, and potassium feldspar embedded in a granophyric to micrographic groundmass. The quartz phenocrysts are prominently rounded and embayed. Phenocrysts and matrix alike incorporate sparse, nest-like aggregates of accessory, acicular, early-crystallized rutile. This porphyry is invariably hydrothermally altered (silicification, potassium metasomatism, local sericitization, quartz-tourmaline veining), so its whole-rock geochemistry (e.g. 76-77% SiO₂) necessarily departs from a purely primary composition. Dalrymple (1992) has determined, utilizing high-precision ⁴⁰Ar/³⁹Ar techniques, that this altered and thermally disturbed unit is older than 1.3 Ma --too old to have been a magmatic source for the overlying Cobb Mountain rhyolites (Fig. 3), K-Ar (sanidine)-dated at 1.11-1.15 Ma (Donnelly-Nolan and others, 1981), but permissively related genetically to the 2.04 m.y.-old Pine Mountain rhyolite to the south (Fig. 3; Donnelly-Nolan and others, 1981).

Orthopyroxene-biotite granite dominates the top of the felsite in the central and northwest-central Geysers (Fig. 3). Most samples from this rock type are exceedingly small-diameter drill cuttings, so we cannot say to what extent the unit is porphyritic. A single core of this rock does contain rounded and embayed quartz phenocrysts in a fine-crystalline hypidiomorphic-granular groundmass. Like the rhyolite porphyry, this granite is apparently a high-silica (77% SiO₂) variety, though its composition has clearly been modified in part by hydrothermal alteration and vein mineralization. The rock also contains scattered accessory acicular rutile "nests" in addition to trace amounts of allanite. Cuttings of the granite were dated (K/Ar -- biotite) at 1.6 and 2.4 Ma for Schriener and Suemnicht (1981); Dalrymple (1992) obtained, for a more recently collected core sample, a ⁴⁰Ar/³⁹Ar (K-feldspar) minimum age of 1.3 Ma. As with the rhyolite porphyry, the magma which yielded this granite could not have supplied the Cobb

Mountain rhyolites, but could have been contemporaneous with the older rhyolite of Pine Mountain.

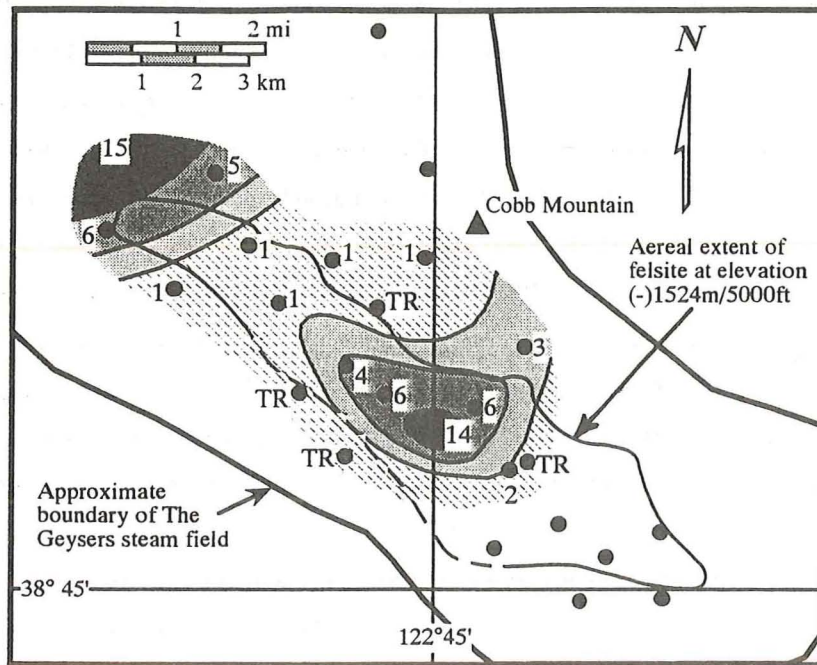
Apparently the youngest and certainly the most mafic of the three major felsite phases is a distinctive, dark-colored granodiorite occurring at depth in the eastern portion of the steam field (Fig. 3). This rock is microcrystalline to fine-crystalline and euhedral-granular, containing intricately zoned plagioclase crystals. Apatite is a conspicuous and relatively abundant accessory mineral; the acicular rutile "nests" of the granite and rhyolite are absent. Both orthopyroxene and clinopyroxene are abundant, the latter apparently replacing the former. Hornblende replaces both pyroxenes, and biotite partially replaces all other mafic minerals. A core collected from this intrusive is only weakly altered and contains 67% SiO₂; thus, it appears chemically to be a true granodiorite. Pulka (1991) has dated this core (⁴⁰Ar/³⁹Ar -- potassium feldspar) at 0.952-1.192 Ma. Thus, the granodiorite is both temporally and geochemically similar to an overlying dacite (66% SiO₂; 1.06-1.08 Ma -- K/Ar) of the Clear Lake volcanic field at Cobb Mountain (Fig. 3; Hearn and others, 1981; Schriener and Suemnicht, 1981; Donnelly, 1977).

Below the top of the felsite, the east Geysers granodiorite appears locally to have partially assimilated older granites in the pluton to form hybrid intrusives of limited vertical and lateral extent. These hybrid phases overall are mineralogically and texturally similar to the granodiorite but host vaguely-defined domains more reminiscent of the granites and containing acicular rutile. The hybrid rocks are also intermediate in chemical composition between the granodiorite and granite or rhyolite porphyry; whole-rock geochemical analysis of a core sample of this hybrid rock from a depth of 1788 m/5866 ft in the central Geysers, for example, yielded an SiO₂ value of 72% SiO₂. The hybrid phases could represent either true magma mixing or partial assimilation of granite by granodioritic magma.

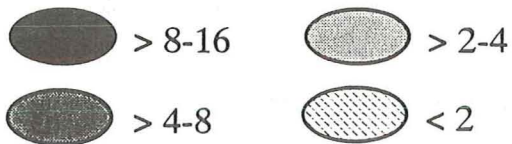
In addition to the major intrusive phases in the main body of the felsite, numerous dikes have been documented in the overlying Franciscan sequence. For example, Pulka (1991) discovered dikes ranging in composition from basalt to rhyolite in geothermal wells of the southeast Geysers. One of the rhyolitic dikes yielded a ⁴⁰Ar/³⁹Ar date (potassium feldspar) of 0.57 Ma (Pulka, 1991), about half that of the granodiorite described above; these younger Geysers intrusives have no known extrusive counterparts. An even younger and still-cooling pluton has been postulated to underlie the northwest Geysers sector of the steam field, where, although no felsic intrusive rocks have been encountered, deep reservoir temperatures are as high as 342°C -- more than 100°C higher than in the "typical" Geysers vapor-dominated regime (Truesdell and others, 1993; Williams and others, 1993; Walters and others, 1992; Moore, 1992; White and others, 1971).

HYDROTHERMAL ALTERATION AND MINERALIZATION

The entire explored Geysers felsite as well as overlying Franciscan rocks are hydrothermally altered. Portions of the pluton as well as enveloping hornfels and metagraywacke locally host very high concentrations (up to at least 33 vol. %) of secondary minerals such as tourmaline, ferroaxinite, and various calc-silicates as well as iron and copper sulfide phases including pyrrhotite and chalcopyrite (e.g. Hulen and Nielson, 1993; Moore, 1992; Walters and others, 1992; Sternfeld, 1989; McLaughlin and others, 1983). At and near the present ground surface above the felsite, rich cinnabar deposits are commonly accompanied by silica-carbonate alteration, and many contain oil and other hydrocarbons such as curtisite and ozocerite (Fig. 4; Peabody and Einaudi, 1992; Bailey, 1946; Ransome and



Wt% tourmaline plus ferroaxinite



- Felsite-study well locations (at top of felsite; under investigation where no data shown)

FIGURE 5. Distribution and concentration of secondary borosilicate minerals in the upper 61 m/200 ft of the Geysers felsite (from Hulen and Nielson, 1993).

DISCUSSION AND CONCLUSIONS

The spatial correlation of The Geysers steam field with the felsite and its associated hydrothermal alteration/mineralization and contact-metamorphic halos as well as shallow mercury and hydrocarbon occurrences argues in favor of common or related processes in the evolution of these features. The texture, composition, and zoning characteristics of the felsite and related alteration assemblages as well as the widespread occurrence in and above the pluton of altered and mineralized hydrothermal breccias suggest that the steam field could represent the waning effects of one or more huge porphyry-copper-style magmatic-meteoric hydrothermal systems (an idea first explored by White and others, 1971). We do not suggest that an actual porphyry copper deposit has formed within or above the deep Geysers felsite, but rather that a weakly mineralizing porphyry-type system in the following ways "prepared the ground" and led to ultimate occupation by the steam reservoir: (1) mechanical rock rupture by forceful intrusion and/or natural, high-temperature hydrothermal fracturing and brecciation to create vital secondary porosity and permeability (Walters and others, 1992; Sternfeld, 1989); (2) further porosity enhancement by hydrothermal carbonate-dissolution (e.g. Hulen and others, 1992; Thompson and Gunderson, 1992); and (3) creation of still more pore space through replacement of hydrous minerals by denser anhydrous phases (Gunderson, 1992). These changes were effected in a hot-water system which gradually "dried out" to form the modern steam field (Moore, 1992; McLaughlin and others, 1983; Sternfeld, 1981; White and others, 1971). The porphyry connection at The Geysers is even more compelling when the tourmaline-rich and commonly hydrothermal-breccia hosted porphyry coppers of the South American Andes are considered (Hollister, 1978).

We suggest that The Geysers is, in essence, a "porphyry steam" deposit -- one which, with 2000 MW installed electrical generating capacity and an estimated replacement value of between 2 and 6 billion dollars (S. Sanyal, pers. comm. with Walters, 1993) -- qualifies as a world-class if ephemeral "orebody". The heat engines driving the Geysers geothermal systems -- both liquid-and vapor-dominated -- have undoubtedly been individual plutons in the deeply concealed felsite. The felsite is petrographically, geochemically, geochronologically and almost certainly geneally related to the Pliocene-Holocene Clear Lake volcanic field. The critical difference is that most of the felsite magmas (with the possible exception of the east Geysers granodiorite -- and Pine Mountain rhyolite?) failed to reach the surface to form flows, domes, or pyroclastic deposits. Magmatic volatiles therefore accumulated to the point where they induced widespread hydraulic rock rupture, helping to create a plumbing network within which felsite-heated, high-temperature hydrothermal fluids could effectively circulate. The network was enhanced by hydrothermal carbonate-dissolution at modern-day reservoir levels, but sealed by deposition of various hydrothermal minerals at higher elevations to form or reinforce what would become the steam field's essentially impermeable caprock.

ACKNOWLEDGMENTS

Hulen's felsite research, initially suggested by Rich Gunderson of Unocal Corporation, is being sponsored by the U.S. Department of Energy's Geothermal Division, contract DE/AC07/90ID12929; said support does not necessarily constitute an endorsement of the views expressed in this article. We thank Unocal and Calpine

Corporations as well as NCPA for access to samples, insight into the steam field, and permission to publish. We appreciate the thoughtful reviews of G. B. Dalrymple and R. J. McLaughlin. Bob Turner produced the figures. Merrienne Tolbert processed the manuscript.

REFERENCES

- Bailey, E.H., 1946, Quicksilver deposits of the western Mayacmas district, Sonoma County, California: Calif. Bur. Mines, Rept. 42 of the State Mineralogist, p. 200-230.
- Beall, J.J., and Box, W.T., Jr., 1992, The nature of steam-bearing fractures in the south Geysers reservoir *in* C. Stone, ed., Monograph on The Geysers geothermal field: Geoth. Resour. Council., Spec. Rept. 17, p. 69-78.
- Dalrymple, G.B., 1992, Preliminary report on $^{40}\text{Ar}/^{39}\text{Ar}$ incremental heating experiments on feldspar samples from the felsite unit, Geysers geothermal field, California: U.S. Geol. Survey, Open-File Rept. 92-407, 15 p.
- Donnelly, J.M., 1977, Geochronology and evolution of the Clear Lake volcanic field: Berkeley, Univ. Calif., Ph.D. Diss., 48 p.
- Donnelly-Nolan, J.M., Hearn, B.C., Jr., Curtis, H., and Drake, R.E., 1981, Geochronology and evolution of the Clear Lake Volcanics *in* R.J. McLaughlin and J.M. Donnelly-Nolan, eds., Research in the Geysers-Clear Lake geothermal area, northern California: U.S. Geol. Surv., Prof. Paper 1141, p. 47-60.
- Donnelly-Nolan, J.M., Burns, M.G., Goff, F.E., Peters, E.K., and Thompson, J.M., 1993, The Geysers-Clear Lake area, California -- Thermal waters, mineralization, volcanism, and geothermal potential: Econ. Geol., v. 88, p. 301-316.
- Gunderson, R.P., 1992, Porosity of reservoir graywacke at The Geysers *in* C. Stone, ed., Monograph on The Geysers geothermal field: Geoth. Resour. Council., Spec. Rept. 17, p. 89-93.
- Hearn, B.C., Jr., Donnelly-Nolan, J., and Goff, F., 1981, The Clear Lake Volcanics -- Tectonic setting and magma sources *in* R.J. McLaughlin and J.M. Donnelly-Nolan, eds., Research in the Geysers-Clear Lake geothermal area, northern California: U.S. Geol. Survey, Prof. Paper 1141, p. 25-45.
- Hebein, J.J., 1986, Conceptual schematic geologic cross sections of The Geysers steam field: Stanford Univ., 11th Workshop on Geoth. Res. Eng. (Jan. 21-23, 1986), Proc., p. 251-257.
- Hollister, V.F., 1978, Geology of the porphyry copper deposits of the western hemisphere: New York, American Inst. Mng., Met., and Petrol. Eng., 219 p.
- Hulen, J.B., Nielson, D.L., and Martin, W., 1992, Early calcite dissolution as a major control on porosity development in The Geysers steam field, California -- Additional evidence from Unocal well NEGU-17: Geoth. Resour. Council., Trans., v. 16, p. 167-174.
- Hulen, J.B., and Nielson, D.L., 1993, Interim report on geology of the Geysers felsite: Geoth. Resour. Council., Trans., v. 17, 10 p., in press.
- Lambert, S.J., 1976, Stable-isotope studies of some active geothermal systems: Pasadena, Calif. Inst. Tech., Ph.D. Diss., 174 p.
- McLaughlin, R.J., 1981, Tectonic setting of pre-Tertiary rocks and its relation to geothermal resources in the Geysers-Clear Lake area *in* R.J. McLaughlin and J.M. Donnelly-Nolan, eds., Research in the Geysers-Clear Lake geothermal area, northern California: U.S. Geol. Survey, Prof. Paper 1141, p. 25-45.
- McLaughlin, R.J., and Ohlin, H.N., 1984, Tectonostratigraphic framework of the Geysers-Clear Lake region, California: Soc. Econ. Paleontologists and Mineralogists, Pacific Sec., v. 43, p. 221-254.
- McLaughlin, R.J., Moore, D.E., Sorg, D.H., and McKee, E.H., 1983, Multiple episodes of hydrothermal circulation, thermal metamorphism, and magma injection beneath The Geysers steam field, California (abs.): Geol. Soc. America, Abs. with Progr., v. 15, p. 417.
- Moore, J.N., 1992, Thermal and chemical evolution of The Geysers geothermal system, California: Stanford Univ., 17th Workshop on Geoth. Res. Eng., Preprint, 6 p.
- Peabody, C.E., and Einaudi, M.T., 1992, Origin of petroleum and mercury in the Culver-Bear cinnabar deposit, Mayacmas district, California: Econ. Geol., v. 87, p. 1078-1102.
- Pulka, F., 1991, Subsurface geology at Ford Flat, Geysers geothermal field, northern California: Houghton, Mich. Tech. Univ., M.S. Thesis, 324 p.
- Ransome, A.L., and Kellogg, J.L., 1939, Quicksilver resources of California: Calif. Div. of Mines and Geol., State Mineralogists Rept., v. 35, p. 383-401.
- Schriener, A., Jr., and Suemnicht, G.A., 1981, Subsurface intrusive rocks at The Geysers geothermal area, California *in* M.L. Silberman C.W. Field, and A.L. Berry, eds., Proceedings of the symposium on mineral deposits of the Pacific Northwest: U.S. Geol. Survey, Open-File Rept. 81-355, p. 295-302.

- Sternfeld, J.N., 1981, The hydrothermal petrology and stable-isotope geochemistry of two wells in The Geysers geothermal field, Sonoma County, California: Riverside, Univ. Calif., M.S. Thesis (Rept. UCR/IGPP 81/7), 202 p.
- Sternfeld, J.N., 1989, Lithologic influences on fracture permeability and the distribution of steam in the northwest Geysers steam field, Sonoma County, California: Geoth. Resour. Council, Trans., v. 13, p. 487-490.
- Stone, C. (ed.), 1991, Monograph on The Geysers geothermal field: Geoth. Resour. Council, Spec. Rept. 17, 327 p.
- Thompson, R.C., 1992, Structural stratigraphy and intrusive rocks at The Geysers geothermal field in C. Stone, ed., Monograph on The Geysers geothermal field: Geoth. Resour. Council, Spec. Rept. 17, p. 59-63.
- Thompson, R.C., and Gunderson, R.P., 1992, The orientation of steam-bearing fractures at The Geysers geothermal field in C. Stone, ed., Monograph on The Geysers geothermal field: Geoth. Resour. Council, Spec. Rept. 17, p. 65-68.
- Truesdell, A., Walters, M., Kennedy, M., and Lippmann, M., 1993, An integrated model for the origin of The Geysers' geothermal field: Geoth. Resour. Council, Trans., v. 17, in press.
- Unocal Corporation, Geysers Geothermal Corporation, NCPA, GEO Operator Corporation, Santa Fe Geothermal Corporation, and California Department of Water Resources, 1992, Top-of-felsite map in C. Stone, ed., Monograph on The Geysers geothermal field: Geoth. Resour. Council, Spec. Rept. 17, in pocket.
- Walters, M.A., Haizlip, J.R., Sternfeld, J.N., Drenick, A.F., and Combs, J., 1992, A vapor-dominated, high-temperature reservoir at The Geysers, California in C. Stone, ed., Monograph on The Geysers geothermal field: Geoth. Resour. Council, Spec. Rept. 17, p. 77-87.
- White, D.E., Muffler, L.J.P., and Truesdell, A.H., 1971, Vapor-dominated systems compared with hot-water systems: Econ. Geol., v. 66, 75-97.
- Williams, C., Glanis, S.P., Moses, T.H., and Grubb, F.V., 1993, Heat flow studies in the northwest Geysers geothermal field, California: Geoth. Resour. Council, Trans., v. 17, in press.
- Yates, R.G., and Hilpert, L.S., 1946, Quicksilver deposits of the eastern Mayacmas district, Lake and Napa Counties, California: Calif. Jour. Mines and Geol., v. 42, p. 231-286.

DAY TWO

THE GEYSERS GEOTHERMAL AREA AND MERCURY DEPOSITS IN THE CLEAR LAKE VOLCANIC FIELD: ROAD LOG

James J. Rytuba, Julie M. Donnelly-Nolan and Robert J. McLaughlin

U.S. Geological Survey, 345 Middlefield Road, Menlo Park CA 94025

This tour begins at the Lytton Springs exit from Highway 101 north of Healdsburg and proceeds through The Geysers and ends at Clearlake Highlands. The route for the trip is shown in Figures 1 and 2.

Mileage

0.0		Exit Highway 101 at Lytton Spring exit and proceed east over railroad tracks; turn left.
1.3	1.3	At intersection of two-lane Alexander Valley Road, turn left.
1.95	3.25	At intersection with Highway 128 turn left.
1.85	5.1	Highway 128 turns right; proceed straight and follow signs to The Geysers.
0.6	5.7	Turn left onto Geysers Road.
8.7	14.4	Park on left side of Geysers Road. Overview of the Culver Baer mercury deposit and the controlling fault structure. STOP 1

STOP 1 . CULVER BAER MERCURY DEPOSIT

The Culver Baer mercury deposit lies at the northwest end of the Mayacmas quicksilver district as delineated by Bailey (1946) and Yates and Hilpert (1946). The mercury mineralization is within the northeast trending, steeply dipping Mercuryville fault zone, an important structural boundary of The Geysers hydrothermal system northeast of the Culver Baer deposit. The Mercuryville fault zone is aligned with, and partly excavated along upper Devils Den Canyon by the north branch of Little Sulphur Creek. Epithermal mineralization and hydrothermal alteration are distributed discontinuously along this fault zone for at least 6 km northwest and 15 km southeast of the Culver Baer Mine workings. Production from the mine totaled 12,644 flasks and occurred primarily from 1872 to 1882 with intermittent production until 1944. Recent work in the subsurface of The Geysers (Hulen and Walters, this volume; Schriener and Suemnicht, 1981; Thompson, 1991; Hulen and Nielson, 1993; McLaughlin and others, 1983) indicates that a large silicic hypabyssal composite intrusive complex, predominantly of granitic to quartz dioritic, composition extends locally to within 1 km of the surface and underlies the area beneath The Geysers just northwest of the Culver Baer Mine. The intrusive body, known as "the felsite", has ages ranging from 2.6 to 0.5 Ma in age (Hulen and Walters, this volume). These young intrusive rocks along with buried roots of the Sonoma Volcanics to the southeast have provided the heat sources for The Geysers hydrothermal system, and the Mayacmas

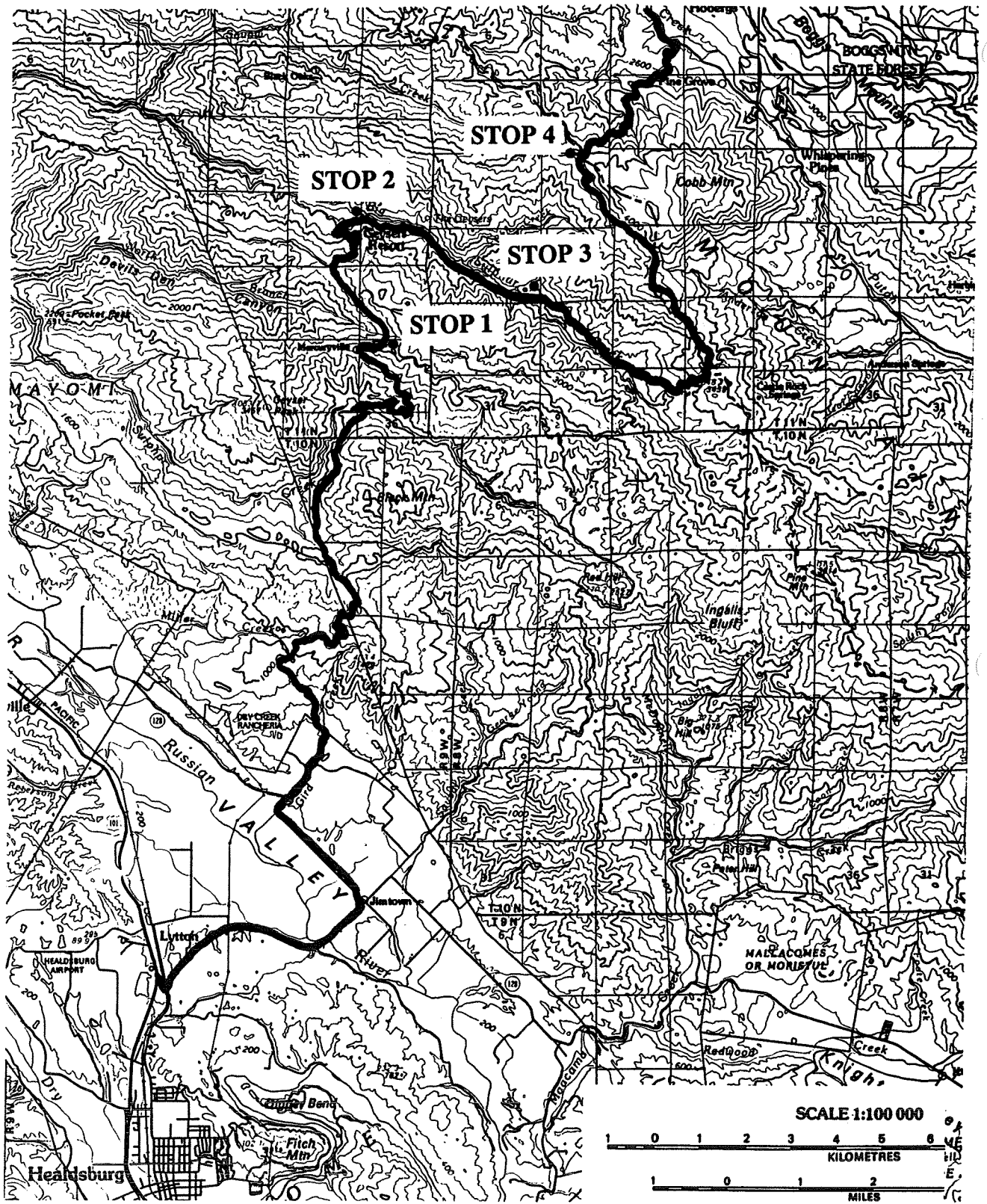


FIGURE 1. Route map for morning of Day 2: from Lytton Springs exit from Highway 101 through The Geysers.

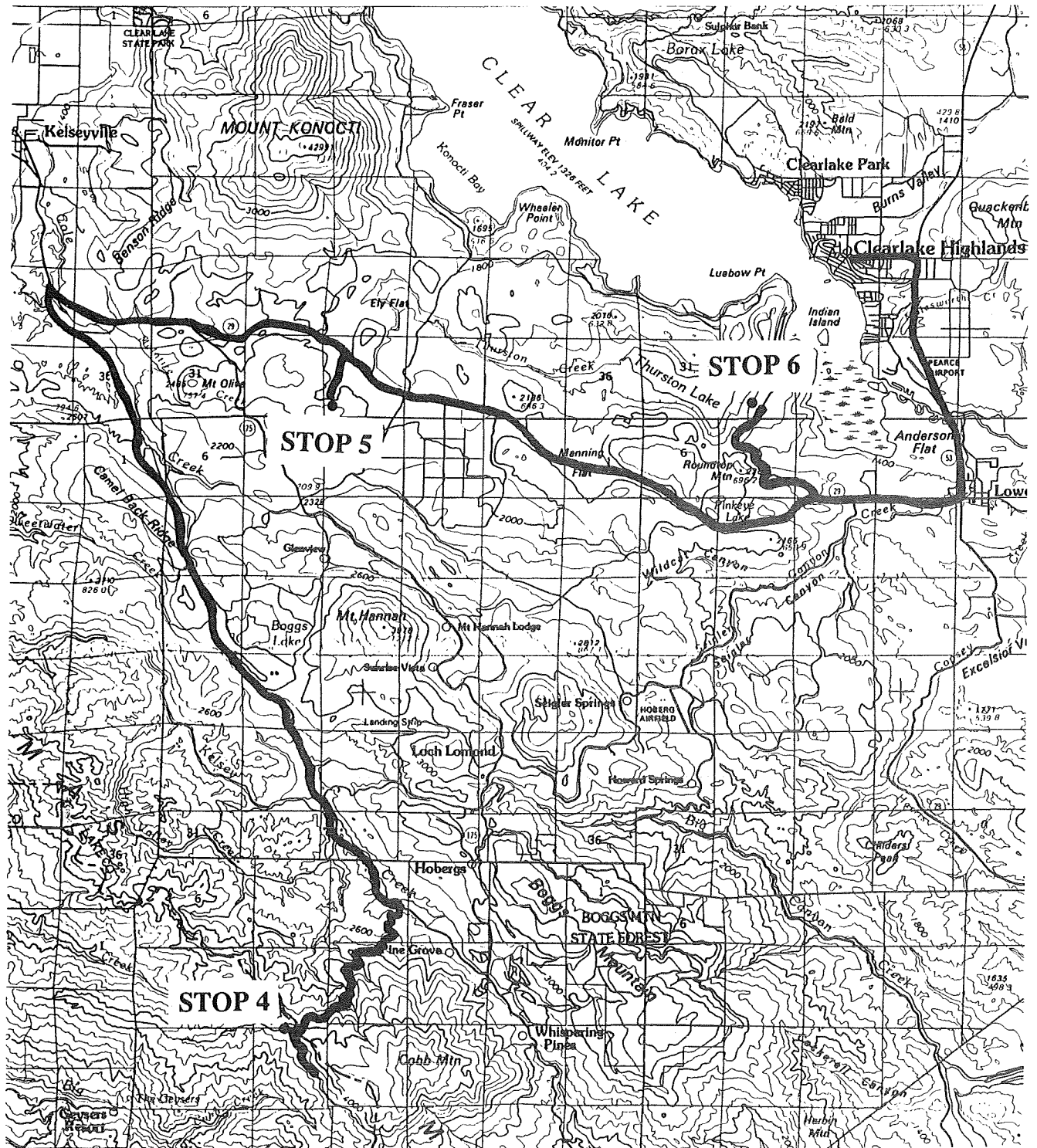


FIGURE 2. Route map for afternoon of Day 2: from The Geysers through the Clear Lake volcanic field to Clearlake Highlands.

mercury district. In the westernmost part of the district the mercury mineralization forms a partial elliptical halo around the western and southern parts of the intrusive complex (see Figure 4 in Hulen and Walters, this volume; and Walters and others, 1991).

Mercury mineralization is associated with silica-carbonate rock, a product of the hydrothermal alteration of serpentinite. Penetratively sheared argillite (melange) occupies the hanging wall block of the Mercuryville fault and massive to thin-bedded, lithic, arkosic metasandstone (graywacke) occupies the footwall block. The serpentinite interleaved along the Mercuryville fault is composed dominantly of chrysotile and subordinate lizardite (Peabody, 1990) and can be traced southeastward into rocks of the Coast Range ophiolite and overlying Great Valley sequence covered by the Sonoma Volcanics of Mount St. Helena (McLaughlin, 1978; 1981). The sheared argillite and melange and metasandstone are assigned to the Central belt of the Franciscan Complex of Early Jurassic to Late Cretaceous age.

The Culver Baer mercury deposit, the Mercuryville fault zone, and The Geysers steam field all occupy the northeast limb of the Mayacmas antiform, with an axis at this latitude that is approximately aligned with the northwest trend of the upper reaches of Little Sulphur Creek Canyon. The interbedded metasandstone and argillite in the footwall of the Mercuryville fault zone at the Culver Baer Mine are the structurally lowest rocks exposed in The Geysers region, because they occupy the core of the Mayacmas antiform. These rocks extend beneath The Geysers steam field to the northeast.

The following description of the deposit is summarized from Peabody (1990). Mercury ore is found within the serpentinite bodies where they are altered to a silica-carbonate, primarily in the alteration core where silicification was most intense (Fig. 3). A mesh texture of veinlets consisting of quartz-chalcedony-magnesite-pyrite is present. Cinnabar is the primary ore mineral, present in silicified breccias, veinlets, as disseminations, and as acicular crystals filling vugs. Petroleum commonly is found in quartz veins and vugs up to 14 cm in diameter, and solid petroleum residue and rarely froth veins are present. Peripheral to the deposit, serpentinite is altered along fractures to an assemblage of magnesite+magnetite to form a mesh texture of veinlets that typically contain only small amounts of cinnabar. At least five generations of veins have been identified and include, from early to late: (1) N. 15° E. to N. 30° W. magnesite+quartz+minor mercury veins, (2) N. 10° E. to N. 30° W., 40-40° SE dip, quartz+chalcedony+mercury veins, (3) ladder veins, (4) low-angle breccias with high-grade mercury in quartz+petroleum matrix, and (5) clear quartz+mercury veins (Fig. 3). Quartz in the high-grade cinnabar breccias of type 4 contains two phase inclusions that homogenize at 90° to 185°C with a maximum occurring in the 130° to 145°C range. The mineral assemblages indicate that CO₂, H₂S, Hg and petroleum were added to the serpentinite as a vapor phase and deposited from a condensate in the nearsurface environment where meteoric water mixed with the condensate. Carbon isotopes indicate that isotopically light magnesite was derived from an organic source that reflects both a terrigenous and marine component likely derived from the Franciscan Complex.

Although the timing of mercury mineralization is not well constrained it is likely that the hydrothermal systems closely followed volcanism in this area. Paragenetically late adularia in veins from a drill core of metasandstone in the steam field, north of Big Sulphur Creek at The Geysers just to the northeast of the Culver Bear

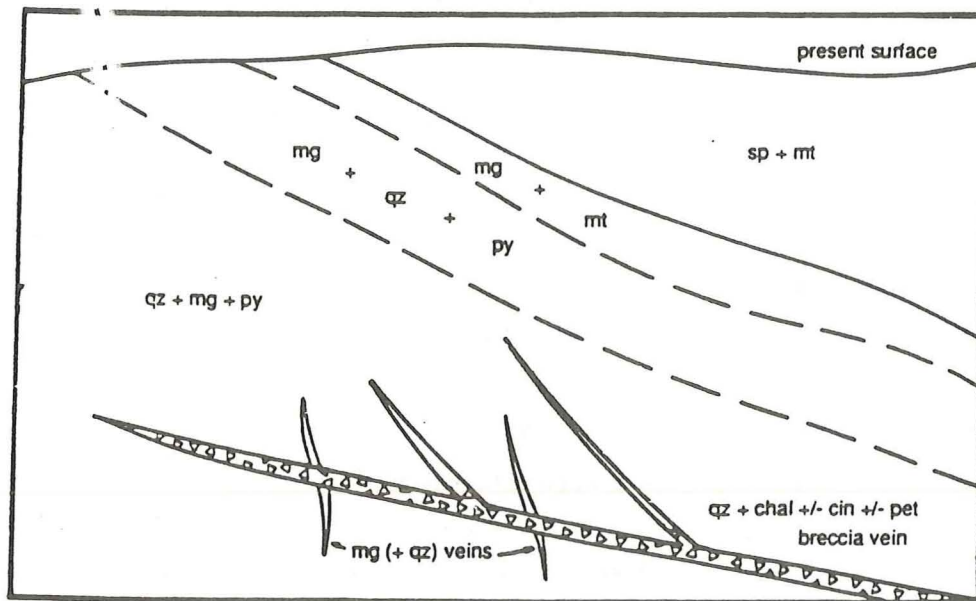


FIGURE 3. Schematic cross section through the Culver Baer mercury deposit showing alteration zoning from core of quartz+magnesite+pyrite to unaltered serpentinite. High-grade ore was deposited in late-stage quartz-cemented breccias. Chal= chalcedony, cin=cinnabar, mg=magnesite, mt=magnetite, pet=petroleum, py=pyrite, qz= quartz, and sp=serpentine. From Peabody (1990).

Mine, is K-Ar dated at 0.69 Ma (McLaughlin and others, 1983). Very late trace amounts of cinnabar were also found in a quartz-adularia vug in the same core indicating that mercury mineralization occurred shortly after deposition of the quartz and adularia at The Geysers. Another line of evidence that constrains the timing of mercury mineralization at the Culver Baer Mine is the timing of first appearance of cinnabar-bearing silica-carbonate rock in the sedimentary record. In Devils Den Canyon, which drains the Culver Baer Mine and Mercuryville area, cobbles and pebbles of silica-carbonate rock containing cinnabar are locally concentrated in the very recent alluvium. At the confluence of Devils Den Canyon and Little Sulphur Creek, a few cobbles of silica-carbonate rock, one with cinnabar, were observed in a high terrace estimated, on the basis of elevation and surface weathering, to be about 0.5 Ma (E. J. Helley, oral commun., 1978). Nearby, unnamed older, steeply tilted and folded fluvial gravel along the Maacama fault contains sporadic volcanic clasts derived from the older Sonoma Volcanics. These deformed gravels also are interbedded with rhyolitic to dacitic welded tuff of the Sonoma Volcanics, suggesting an age younger than about 4 Ma for the gravels (McLaughlin, 1978). A single clast of silica-carbonate rock with no mercury mineralization found in these gravels suggest that, although hydrothermal circulation had been established, large-scale unroofing of the Mayacmas mercury district had not yet occurred, nor had there as yet been extensive mercury mineralization. These relations conservatively constrain mercury deposition to sometime between 4.0 and 0.7 Ma. The appearance of cinnabar in 0.5 Ma terrace deposits could indicate that mineralization occurred around 0.6 to 0.7 Ma, followed by rapid unroofing by 0.5 Ma.

If mineralization depths at the Culver Baer Mine were in the range 200 to 1,000 m, as suggested by Peabody and Einaudi (1992), then uplift rates in this area between 0.7 and 0.5 Ma were about 1 to 5 mm/yr, which is high compared to average regional geodetically determined uplift rates observed in the Coast Ranges. At this rate of uplift Franciscan metasandstone with traces of cinnabar, presently at a depth of about 91 m, at 0.6 Ma was probably between 700 and 3,100 m deep.

-
- | | | |
|------|-------|---|
| 0.75 | 15.15 | Optional stop. Park on side of road and hike down hill to open pit workings of the Culver Bear mercury deposit. |
| 2.15 | 17.3 | Park on side of road at Geysers overlook. STOP 2. |
-

STOP 2. OVERVIEW OF THE GEYSERS GEOTHERMAL AREA

From this overlook you can observe the principal zone of present day hydrothermal leakage from The Geysers hydrothermal system (Fig. 4). Hydrothermal venting occurs along a series of steep dipping faults and fractures aligned with, and along the lower south-facing slopes of, Big Sulphur Creek Canyon. The rocks from which the geothermal reservoir vents consist here predominantly of Late Cretaceous (Cenomanian or younger) lithic metasandstone of the Franciscan Complex, which overlies Early Jurassic to early Late Cretaceous ribbon chert and Early Jurassic or older basalt flows. These rocks, referred to as The Geysers terrane by McLaughlin and Ohlin (1984) are part of a melange that, at depth, structurally overlies the same metasandstone (Devils Den terrane of McLaughlin and Ohlin (1984)) as that in the footwall of the Mercuryville fault zone. The zone of hydrothermal leakage along Big Sulphur Creek Canyon is capped in this area by a thick (as much as 460 m) 35° to 45° northeast dipping unit of serpentinite that has been thermally metamorphosed to actinolite±tremolite±antigorite±chlorite. This ultramafic cap tapers down dip to the northeast, where it is cut out by northeast-dipping thrust and reverse faults that bound the serpentinite in the subsurface. To the northwest, the serpentinite is abruptly cut out by faulting but the outcrop length of the unit to the southeast is about 10 km. At its southeast end, northeast of the Socrates Mine, the serpentinite is structurally overlain by partially serpentinized peridotite of the Coast Range ophiolite.

Surface venting of the present Geysers hydrothermal system occurs sporadically along the southwest contact of the serpentinite as hot springs, fumaroles, and boiling mud springs. Surface alteration is characterized by acid-leached, argillic zones with associated native sulphur and sulfate-bearing alteration-mineral assemblages. In addition, steep faults, which locally cut the serpentinite, are also the focus of hot springs and fumaroles, particularly at the Little Geysers and vicinity to the southeast along Big Sulphur Creek. Several of these steep faults are delineated by linear zones of silica-carbonate alteration in the serpentinite and by leached argillic gouge in the metaclastic rocks. The prominent northwest-trending bleached zone of argillic alteration visible from this vantage point along the southwest-facing slopes of Big Sulphur Creek (Fig. 4) is predominantly in metasandstone, radiolarian chert, and metabasalt, which crop out beneath the impermeable serpentinite cap rock. At depth, open fractures and faults in these reservoir rocks are sealed by quartz-carbonate assemblages below the serpentinite in the upper part of the reservoir. The serpentinite cap is structurally overlain on the north side of Big



FIGURE 4. Overview of hydrothermal alteration along Big Sulphur Creek; the white areas are bleached and acid leached metasandstone. In the distance metaserpentine, which forms the cap rock of the geothermal system, is exposed below metabasalt and chert capping the ridge. Note production pipes from steam field along hillside and power plant on upper right horizon.

Sulphur Creek Canyon by the same, structurally repeated, pillow basalt flows, flow breccias, cherts, metasandstones, and melange that lie beneath the serpentinite.

The Mercuryville fault zone represents a zone of conduits along which The Geysers hydrothermal system was formerly vented (McLaughlin, 1981). It is now well established that, with time, the present vapor-dominated system at The Geysers evolved from one or more fluid-dominated systems as indicated by paragenetic relations of the alteration mineral assemblages present in veins and vugs in the subsurface of the steam field (McLaughlin and others, 1983; Sternfeld and Elders, 1982; Lambert, 1976; Hulen and Walters, this volume). This vapor-dominated system presently vents along northwest-trending faults and fractures aligned with Big Sulphur Creek, beneath a major northeast-dipping thrust fault just northeast of the Culver Baer Mine. Steam wells drilled between Big Sulphur Creek and the Mercuryville fault zone have been, at best, marginal producers. Mercury mines and prospects, silica-carbonate alteration of serpentinite, and intense hydrothermal alteration are notably concentrated along the Mercuryville fault trend and scattered to the north of the fault. Given the northeastward dip of the structural grain of the rocks and major faults cutting the Franciscan Complex along the north flank of the Mayacmas antiform, the above data suggest that when The Geysers system was dominated by hot water, it extended up dip and southwest of the present vent area. During that time, faults of the Mercuryville zone served as primary conduits for fluid venting. As the system boiled off and (or) cooled, the boiling interface shrank down-dip and northeastward, sealing fractures in the hanging wall of the fault zone with quartz-carbonate assemblages, and forming a cap rock. Carbonaceous woody plant debris present in minor, but locally abundant concentrations in the footwall metasandstones along the Mercuryville fault zone, may have been a major source for liquid hydrocarbons found associated with mercury mineralization. Mercury mineralization is paragenetically late and assumed to be associated with the vapor phase or with condensation above the steam zone at The Geysers.

-
- | | | |
|-----|-------|--|
| 1.1 | 18.4 | Continue along Geysers Road and through gate. |
| 1.8 | 20.4 | Cross creek and then turn left and proceed up hill. |
| .25 | 20.45 | Turn left and park on either side of road adjacent to production pipelines. STOP 3. |
-

STOP 3. SURFICIAL EXPRESSION OF THE GEYSERS AND PRODUCTION OF STEAM

The water you see here is steam condensate which gives no indication of the composition of the water that is boiling to form the steam in the Geysers (Fig. 5). None of this deep water has been sampled. White and others (1971) hypothesized that a boiling water table is present at some great depth, but in holes extending to depths greater than 3 km, this deep water table has not been encountered. The steam apparently forms by boiling of water in fractures in the reservoir rocks that are composed primarily of graywacke and to a lesser extent, of felsite. In recent years, isotopically shifted steam has been found in deep wells in the northwest Geysers. $\delta^{18}\text{O}$ values as high as 3 per mil aroused speculation that this steam was boiling off a deep water table of connate water similar to that at Wilbur Springs (Haizlip, 1985; Haizlip and Truesdell, 1991; Walters and others, 1991; Truesdell and others, 1992). However, Donnelly-Nolan and others (1993) have argued, instead, that no such deep water table exists and that

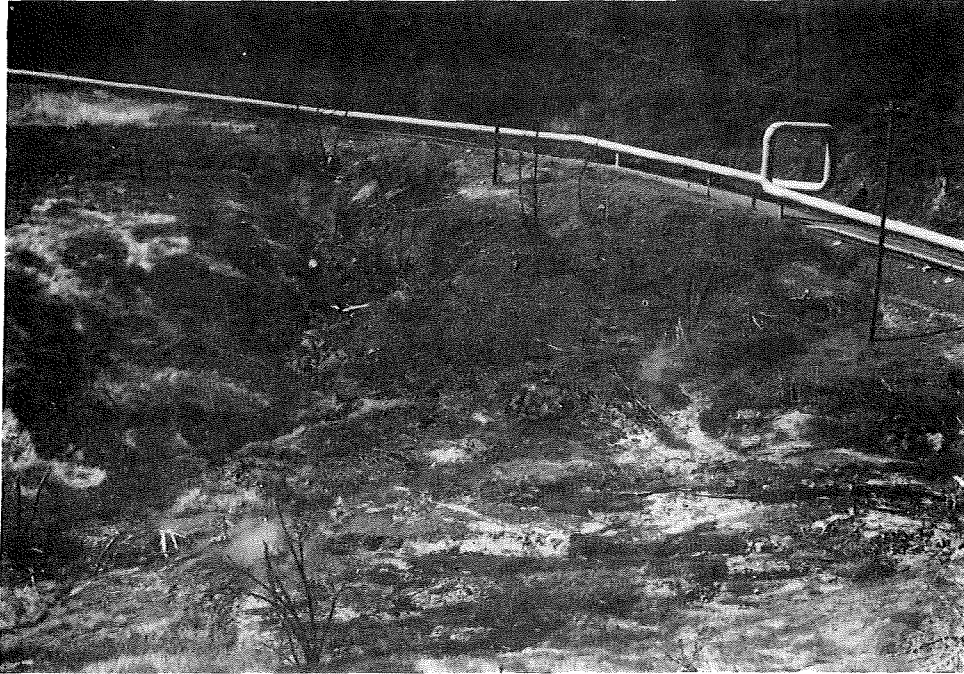


FIGURE 5. Steam condensate and gas vents at The Geysers. Leakage from the steam field occurs along high-angle faults that penetrate the serpentine cap rock of the geothermal system. Pipes in background along road transfer steam to power plants.

water that is present in the fractures is produced by near-closed-system boiling of originally meteoric water circulating in the Franciscan Complex. Connate waters found in the Geysers-Clear Lake area are closely associated with Great Valley sequence sedimentary rocks, which are not present in The Geysers.

Large-scale development and production from The Geysers (note that there are no geysers present: just fumaroles and hot springs) began in 1960 with a 12 MW plant. Development accelerated between 1982 and 1988 (Barker and others, 1992) with an average of 150 MW/ yr of new capacity added. Maximum capacity of 2,042 MW was reached in 1989. However, since 1987, total steam deliverability has decreased. Fluid injection from Big Sulphur Creek began in 1980 but quantities of water available for injection are limited and the benefits from this program have not been quantified easily. It is expected that production will continue for at least 50 years but at a significantly reduced level (Barker et al., 1992). The most recent proposal for increasing injection has been with the use of reclaimed water from the sewage disposal system in the Clear Lake area.

0.35	20.8	Retrace route to intersection of paved road near creek and turn left.
2.2	23.0	Turn out for Little Geysers overview.
0.3	23.3	Turn right onto graveled Socrates Mine road.
0.4	23.7	Turn right onto Pine Flat Road
0.4	24.1	Sharp left turn.
0.45	24.55	Turn left on to Socrates Mine Road.

- | | | |
|------|-------|---|
| 0.35 | 24.9 | Bear right onto paved road. |
| 0.25 | 25.15 | Turn left onto John Kincade Road. |
| 5.85 | 31.0 | Turn right |
| 0.45 | 31.45 | Pull over into large flat area on left side of road at Geysler Rock. STOP 4. |

STOP 4. GEYSER ROCK OVERVIEW OF CLEAR LAKE VOLCANIC FIELD

Looking north from Geysler Rock you can see Mt. Konocti and Clear Lake (Fig. 6). Farther to the southeast is Mt. Hannah, which lies at the center of a 25-milligal negative gravity anomaly (Chapman, 1975, Isherwood, 1981), at the focus of an electrical resistivity anomaly (Stanley and others, 1973; Isherwood, 1981) that approximately mimics the gravity anomaly, and at the center of a low-velocity anomaly (Iyer, 1988). Between Geysler Rock and Mt. Hannah is the northwest-trending Collayomi fault zone, beyond which no dry steam has been found. The Collayomi is one of several segments of the San Andreas transform fault system that cut through the Geyslers-Clear Lake region. A branch fault of the Collayomi was activated during the 1906 San Francisco earthquake (Hearn and others, 1988) (although the San Andreas itself is aseismic in this area). Seismicity in the region is mostly focused along northwest-trending faults except for a concentration of seismicity in The Geyslers production field, which is induced by development (Eberhart-Phillips and Oppenheimer, 1984).

Immediately southeast of us is Cobb Mountain, a 1.1 Ma composite rhyolite and dacite dome of the Clear Lake Volcanics. Flows of the Clear Lake volcanic field are distributed over an area from the upper arm of Clear Lake southeast nearly to Lake Berryessa (about 60 km) and from The Geyslers northeast to Wilbur Springs (more than 40 km). However, the largest volume of these late Pliocene to Holocene (?) volcanic rocks lies within view between here and Clear Lake. Total erupted volume is about 100 km³. Nearly 100 volcanic units have been mapped, mostly separate flows and domes and a few tephra deposits (Hearn and others, in press). The earliest phase of Clear Lake volcanism was dominated by widespread eruption of mafic lavas, although the oldest dated unit in the field is the rhyolite of Pine Mountain at 2.06 ± 0.02 Ma. Pine Mountain is about 10 km southeast of Geysler Rock, near the southern end of the felsite body, as depicted by Hulen and Walters (this volume). Volume calculations suggest that the volume of the felsite body probably exceeds the total erupted volume of the volcanic field. If Griscom and others (this volume) are correct, then the felsite is a pluton-size body, most of which is at least 5 km thick. No intrusive body has been penetrated by drilling northeast of the Collayomi fault zone, but a tourmalinized zone at the base of the Neasham #1 well at Sulphur Mound Mine (day 2, stop 5) suggests that an intrusive contact may lie just below the 3,673 m-deep hole. Buried plutons may also be present in the Wilbur Springs and McLaughlin mine areas which could help to explain the focus of heat and mineralization at those localities.

See Griscom and others (this volume) for a review of geophysical data and models. They concluded that a shallow, hot, siliceous pluton is the cause of the greater than 20-milligal gravity anomaly focused under Mt. Hannah. The top of the inferred body is somewhat deeper than 3-4 km. This conclusion largely supports the earlier work of Chapman (1975) and Isherwood (1981) but other recent work disputes the shallow depth of the magma body.



FIGURE 6. Overview of the Clear Lake volcanic field and basement rocks in the Mayacmas Mountains from Geyser Rock overlook.

About 5 km northwest of Geysler Rock, along the ridge crest of the Mayacmas Mountains, is an area of large pine trees, the Caldwell Pines, where the 1.66 Ma basalt of Caldwell Pines caps the ridge. Flow rock overlies a diatreme of fragmental material containing basalt of Caldwell Pines mixed with Franciscan rocks. This olivine- and clinopyroxene-phyric basalt is isotopically and chemically the most primitive lava in the Clear Lake volcanic field. It has an $^{87}/^{86}\text{Sr}$ ratio of 0.70316 (Futa and others, 1981) and an Mg number of 74. The basalt locally overlies a thin unit of fluvial gravel containing rounded and water-polished cobbles of Franciscan-derived lithologies, implying that the gravel is the residuum of a 1.6 Ma or older uplifted fluvial surface. Remnants of the basalt persist at somewhat lower elevations to the northeast, suggesting northeastward tilting, consistent with uplift of the Mayacmas Mountains and crustal shortening across the northeast dipping imbricate thrust system that underlies The Geysers. To the northeast of Collayomi Valley, fluvial terrace gravels along the Collayomi fault contain clasts derived from Cobb Mountain and Caldwell Pines volcanic units. The Collayomi fault appears to be an important bounding structure to production on the northeast side of the steam field. Geysler Rock is a large block of mafic breccia that is a knocker within the melange of the Franciscan Complex.

The steam field is underlain at depths largely below 2 km (Hulen and Walters, this volume), by a hypabyssal granitic to quartz dioritic intrusive complex dated at about 2.6 Ma to 0.5 Ma. The present heat source beneath the steam field may be associated with a very young phase of this felsite intrusive complex (Schriener and Suemnicht, 1981, Pulka, 1991, Dalrymple, this volume). This young heat source may have created its own spreading center in the shallow crust (McLaughlin and others, this volume) resulting in the ongoing uniaxial extension in this area (Oppenheimer, 1986). Around the periphery of the intrusive complex, the Franciscan wall rocks are extensively tourmalinized by contact thermal metamorphism. The Franciscan metaclastic and metaigneous wall rocks have undergone Cretaceous metamorphism to low-temperature, high-pressure pumpellyite-lawsonite- and glaucophane-lawsonite-bearing assemblages. Around the felsite intrusive, these rocks have been overprinted by vein fillings and replacement assemblages including quartz-adularia±tourmaline and actinolite±tremolite±chlorite ±epidote which indicate temperatures in the range of 290°C-350°C around the margin of the felsite. The vein-mineral assemblages were deposited from a hot-water system initiated during and (or) following episodes of intrusion. A drill core fragment of micro-granitic felsite from beneath the southwestern part of The Geysers from a depth of about 1.1 km is shattered by abundant microfractures that are rehealed and mineralized by quartz and tourmaline, suggesting that intrusion of the felsite was followed by lithification, brecciation, and then by introduction of a new magma source, which healed and tourmalinized fractures created in the earlier episode of brecciation. The tourmaline veinlets are further cut by quartz+adularia veins, indicating a later, lower temperature, hot water system that was overprinted on the higher temperature tourmalinization. Later stage adularia is present in quartz veins at depths as shallow as about 400 m near The Geysers Resort, where it is cogenetic with chlorite, illite, pyrite, and quartz, all probably deposited from greater than 210°C water. The adularia from this phase was K-Ar dated at 0.69 ± 0.03 Ma. Later stages of mineral phases deposited as encrustations and replacement minerals in open spaces and vugs in adularia veins include datolite, pyrite, galena, sphalerite, calcite, and minor cinnabar. This latest

mineralization may have been associated with increased temperature, decreased pressure, and change over to a vapor-dominated hydrothermal system (McLaughlin and others, 1983).

-
- | | | |
|------|-------|--|
| 0.55 | 31.0 | Exposures of rhyolite on Cobb Mountain along roadside. |
| 2.25 | 34.25 | Gate at Bottle Rock road. |
| 0.05 | 34.3 | Turn left on Bottle Rock Road |
| 2.5 | 35.8 | In this roadcut silica-carbonate alteration is localized along a strand of the northwest-trending Collayomi fault zone that cuts the lower part of a major slab of Coast Range ophiolite. This segment of the Collayomi fault zone has acted as an area of hydrothermal leakage. The fault clearly displaced the altered ultramafic rocks southwestward above and over terrace gravels. The presence of rhyolite clasts derived from Cobb Mountain and of basalt derived from Caldwell Pines in these gravels shows that the terrace deposits are younger than about 1.0 Ma and that faulting is very young. |
| 2.85 | 38.65 | Large outcrops of rhyolite of Thurston Creek consisting of obsidian and flow banded rhyolite. |
| 0.75 | 39.4 | View of Mount Konocti, Clear Lake, and Bell Mine. Optional stop. Pull over into gravel driveway on right. Walk down gravel road about 400 ft to examine obsidian outcrops. These flow banded obsidians are part of the rhyolite of Thurston Creek (approximately 0.6 Ma). BE CAREFUL WITH SHARP OBSIDIAN FRAGMENTS |
| 0.1 | 39.5 | Return back to Bottle Rock Road and continue north (right) |
| 2.7 | 42.2 | Turn right at intersection onto Highways 29-- 175. |
| 1.3 | 43.5 | Bear left on Highway 29 at split with Highway 175. |
| 2.3 | 45.8 | Turn right off Highway 29 at entrance to Sulphur Mound Mine (left gate).
Proceed up road past crusher for aggregate mining to upper most pit |
| 0.55 | 46.35 | Park in open pit and examine exposures of bedded tuffs in workings at
Sulfur mound. Mining has cut back into the hill and the pit occurs in a natural valley. STOP 5. |
-

STOP 5. SULPHUR MOUND MINE

Walk south to the white, excavated scarp in bedded rhyolitic airfall tuff. This hydrothermally altered area is the site of active sulfur deposition by fumaroles and has been mined in recent years for agricultural sulfur. Cinnabar was prospected for and mined in this valley, probably near the turn of the century (see also Stop 1 Day 1 in Goff and Janik, 1993, this volume; Stop 11 in Donnelly-Nolan and others, 1977). Note the strong smell of H₂S and patches of sulfur-rich ground. Look for pieces of acid-etched, flow-banded obsidian and sulfur-cemented obsidian tuff breccia. The rocks are altered to an advanced-argillic assemblage of kaolinite+quartz+opal as a result of near-surface oxidation of H₂S vapor derived from the underlying geothermal system. Native sulfur and the resulting H₂SO₄ cause acid leaching of the volcanic rocks.

Stimac and Wark, 1992) used textural, mineralogical, and chemical data to demonstrate that the dacitic lavas are mixtures of a rhyolitic end member and a basaltic andesite end-member. Stimac (1991) and Stimac and others (1992) hypothesized that, at about 0.6 Ma, a large silicic magma chamber approximately 20 km across existed in the Mt. Konocti area and that the rhyolite of Thurston Creek erupted from this body. Mafic magma and cumulates are hypothesized to underlie the chamber. Following eruption of rhyolite, cooling, and some crystallization, the single body segmented into several smaller sub-systems; mafic magma continued to intrude and cumulates grew. At a later stage, dacites were produced by an increased flux of mafic magma into the system and mixing of the silicic and mafic magma.

Turn around and retrace route back to Highway 29.

- 1.8 57.3 Turn left at intersection of Highway 29.
- 1.9 59.2 Intersection of Highway 29 and Highway 53 in Lower Lake, turn left and proceed on Highway 53.
- 2.95 62.15 Turn left (west) at stoplight and proceed into town of Clearlake.
- 0.35 62.5 Turn left into parking lot of El Grande Hotel. End of second day.

References

- Bailey, E. H., 1946, Quicksilver deposits of the western Mayacmas district, Sonoma County, California: California Journal of Mines and Geology, Report 42 of the State Mineralogist, p. 200-230.
- Barker, B. J., Gulati, M. S., Bryan, M. A., and Riedel, K. L., 1992, Geysers reservoir performance: *in* Claudia Stone, ed., Monograph on The Geysers Geothermal Field: Davis, California, Geothermal Resources Council, Special Rept. No. 17, p. 167-177.
- Beall, J. J., 1985, Exploration of a high temperature, fault localized, nonmeteoric geothermal system at the Sulphur Bank mine, California: Geothermal Resources Council Trans., v. 9, p. 395-401.
- Chapman, R. H., 1975, Geophysical study of the Clear Lake region, California: California Division of Mines and Geology Special Report 116, 23 p.
- Dalrymple, G. B., 1993, Preliminary report on $^{40}\text{Ar}/^{39}\text{Ar}$ incremental heating experiments on feldspar samples from the felsite unit, Geysers geothermal field, California: *in* J. J. Rytuba ed., Active geothermal systems and gold-mercury deposits in the Sonoma-Clear Lake volcanic fields, California: Soc. Econ. Geol. Guidebook Series, (this volume)
- Dellinger, M., and Cooper, G., 1990, Greenhouse heating with low-temperature geothermal resources in Lake County, California: Geothermal Resources Council Transactions, v. 14, no. 1, p. 321-328.
- Donnelly-Nolan, J. M., Hearn, B. C., Jr., and Goff, F. E., 1977, The Clear Lake Volcanics, California: Geology and field trip guide, *in* Field Trip Guide to the Geysers-Clear Lake Area, for the Cordilleran Section of The Geological Society of America, April, 1977.
- Donnelly-Nolan, J. M., Hearn, B. C. Jr., Curtis, G. H., and Drake, R. E., 1981, Geochronology and evolution of the Clear Lake Volcanics: U. S. Geological Survey Professional Paper 1141, p. 47-60.
- Donnelly-Nolan, J. M., Burns, M. G., Goff, F. E., Peters, E. K., and Thompson, J. M., 1993, The Geysers-Clear Lake area, CA: thermal waters, mineralization, volcanism, and geothermal potential: Econ. Geol., v. 88 p. 301-316.
- Eberhart-Phillips, Donna, and Oppenheimer, D. H., 1984, Induced seismicity in The Geysers Geothermal area, California: Journal of Geophysical Research, v. 89, p. 1191-1207.
- Futa, Kiyoto, Hedge, C. E., Hearn, B. C., Jr., and Donnelly-Nolan, J. M., 1981, Strontium isotopes in the Clear Lake Volcanics: U.S. Geological Survey Professional Paper 1141, p. 61-66.
- Goff, F. E., and Janik, C. J., 1993, Gas geochemistry and guide for geothermal features in the Clear Lake region, California, *in* J. J. Rytuba ed., Active geothermal systems and gold-mercury deposits in the Sonoma-Clear Lake volcanic fields, California: Soc. Econ. Geol. Guidebook Series, (this volume)
- Goff, F. E., Shevenell, M. L., Gardner, J. N., Vuataz, F. D., and Grisby, C. O., 1988, The hydrothermal outflow plume of Valles caldera, New Mexico and a comparison with other outflow plumes: Jour. Geophysical Research, v. 93 (B6), p. 6041-6058.

- Griscom, Andrew, Jachens, R. C., Halvorson, P. F., and Blakely, R. J., 1993, Magnetic and gravity interpretation of gold deposits in the Clear Lake region, California, *in* J. J. Rytuba ed., Active geothermal systems and gold-mercury deposits in the Sonoma-Clear Lake volcanic fields, California: Soc. Econ. Geol. Guidebook Series, (this volume)
- Haizlip, J. R., 1985, Stable isotopic composition of steam from wells in the northwest Geysers, The Geysers, Sonoma County, California: Geothermal Resources Council Transactions, v. 9, pt. 1, p. 311-316.
- Haizlip, J. R., and Truesdell, A. H., 1992, Noncondensable gas and chloride are correlated in steam at The Geysers: *in* Claudia Stone, ed., Monograph on The Geysers Geothermal Field: Davis, California, Geothermal Resources Council, Special Rept. No. 17, p. 139-143.
- Hausback, B. P., 1991, Eruptive history of the Sutter Buttes volcano - review, update, and tectonic considerations: Geol. Soc. Am. Abs. with Prog., v. 23, no. 2, p. 34.
- Hearn, B. C., Jr., Donnelly-Nolan, J. M., and Goff, F. E., in press, Geologic map and structure sections of the Clear Lake Volcanics, northern California: U.S. Geological Survey Miscellaneous Investigations Map.
- Hearn, B. C., Jr., McLaughlin, R. J., and Donnelly-Nolan, J. M., 1988, Tectonic framework of the Clear Lake basin, California: Geol. Soc. America, Special Paper 214, p. 9-20.
- Hulen, J. B., and Walters, M. A., 1993, The Geysers felsite and associated geothermal systems, alteration, mineralization, and hydrocarbon occurrences, *in* J. J. Rytuba ed., Active geothermal systems and gold-mercury deposits in the Sonoma-Clear Lake volcanic fields: California, Soc. Econ. Geol. Guidebook Series, (this volume)
- Hulen, J. B., and Nielson, D. L., 1993, Interim report on geology of the Geysers felsite: Geothermal Resource Council Trans., v. 17, in press
- Isherwood, W.F., 1981, Geophysical overview of The Geysers: U.S. Geological Survey Professional Paper 1141, p. 83-95.
- Iyer, H. M., 1988, Seismological detection and delineation of magma chambers beneath intraplate volcanic centers in western U.S.A.: *in* C.-Y. King, and Roberto Scarpa, eds., Modeling of Volcanic Processes, Friedr. Vieweg & Sohn, Braunschweig/Wiesbaden p. 1-56
- Lambert, S. J., 1976, Stable isotope studies of some active hydrothermal systems: Calif. Inst. of Technology, Ph. D. thesis, 362 p.
- McLaughlin, R. J., 1978, Preliminary geologic map and structural sections of the central Mayacmas Mountains and The Geysers steam field, Sonoma, Lake, and Mendocino Counties, California: U. S. Geological Survey Open-File Map 78-389, scale 1:24,000.
- McLaughlin, R. J., 1981, Tectonic setting of pre-Tertiary rocks and its relation to geothermal resources in the Geysers-Clear Lake area: U. S. Geol. Survey Prof. Paper 1141, p. 3-23.
- McLaughlin, R. J., and Ohlin, H. N., 1984, Tectonostratigraphic framework of the Geysers-Clear Lake region, California: *in* Blake, M. C., Jr., ed., Franciscan geology of northern California: Pacific Section Soc. Econ. Paleontologists and Mineralogists, v. 43, p. 221-254.
- McLaughlin, R. J., Moore, D. E., Sorg, D. H., and McKee, E. H., 1983, Multiple episodes of hydrothermal circulation, thermal metamorphism, and magma injection beneath the Geysers steam field, California: Geol. Soc. America Abs. with Programs, v. 15, no. 5, p. 417.
- McLaughlin, R. J., Sorg, D. H., Moore, D. E., and Donnelly-Nolan, J. M., 1993, Tectonic setting and evolution of hydrothermal systems, volcanism, and epithermal mineralization in the Geysers-Clear Lake region and northern Coast Ranges, California, *in* J. J. Rytuba ed., Active geothermal systems and gold-mercury deposits in the Sonoma-Clear Lake volcanic fields: California, Soc. Econ. Geol. Guidebook Series, (this volume)
- Oppenheimer, D. H., 1986, Extensional tectonics at The Geysers geothermal area, California: Jour. Geophys. Research, v. 91, p. 11,463-11,476.
- Peabody, C. E., 1990, Association of petroleum and cinnabar in mercury deposits of the California Coast Ranges, USA: Stanford University Ph. D. thesis, 256 p.
- Peabody, C. E., and Einaudi, M. T., 1992, Origin of petroleum and mercury in the Culver-Bear cinnabar deposit, Mayacmas district, California: Econ. Geol. v. 87, p. 1078-1102.
- Pulka, F. S., 1991, Recent intrusives at Ford Flat and relationships to faulting and the geothermal heat source, Geysers geothermal field, California: Geol. Soc. America Abs. with Prog., v. 23, no. 2, p. 90.
- Schriener, A., Jr., and Suemnicht, G. A., 1981, Subsurface intrusive rocks at The Geysers geothermal area, California: U. S. Geol. Survey Open-File Rept. 81-355, p. 294-303.
- Stanley, W. D., Jackson, D. B., and Hearn, B. C., Jr., 1973, Preliminary results of geoelectrical investigations near Clear Lake, California: U.S. Geological Survey Open-File Report, 20 p.
- Sternfeld, J. N., and Elders, W. A., 1982, Mineral zonation and stable isotope geochemistry of a production well in The Geysers geothermal field, California: Geothermal Resources Council Transactions, v. 6, p. 51-54.

- Stimac, J. A., 1991, Evolution of the silicic magmatic system at Clear Lake, California from 0.6 to 0.3 Ma: Queen's University Ph. D. thesis, 399 p.
- Stimac, J. A., and Pearce, T. H., 1992, Textural evidence of mafic-felsic magma interaction in dacite lavas, Clear Lake, California: *American Mineralogist*, v. 77, p. 795-809.
- Stimac, J. A., Pearce, T. H., Donnelly-Nolan, J. M., and Hearn, B. C., Jr., 1990, The origin and implications of undercooled andesitic inclusions in rhyolites, Clear Lake Volcanics, California: *Journal of Geophysical Research*, v. 95, p. 17,729-17,746.
- Stimac, J. A., and Wark, D. A., 1992, Plagioclase mantles on sanidine in silicic lavas, Clear Lake, California: implications for the origin of rapakivi texture: *Geological Society of America Bulletin*, v. 104, p. 728-744.
- Stimac, J. A., and Goff, F., and Hearn, B. C., Jr., 1992, Petrologic considerations for hot dry rock geothermal site selection in the Clear Lake region, California: *Geothermal Resource Council Trans.*, v. 16, p. 191-198.
- Truesdell, A. H., Box, W. T., Jr., Haizlip, J. R., and D'Amore, 1992, A geochemical overview of The Geysers geothermal reservoir, *in* Claudia Stone, ed., *Monograph on The Geysers Geothermal Field*: Davis, California, Geothermal Resources Council, Special Rept. No. 17, p. 121-132.
- Thompson, R. C., 1992, Structural stratigraphy and intrusive rocks at The Geysers geothermal field, *in* Claudia Stone, ed., *Monograph on The Geysers Geothermal Field*: Davis, California, Geothermal Resources Council, Special Rept. No. 17, p. 59-63.
- Walters, M. A., Sternfeld, J. N., Haizlip, J. R., Drenick, A. F., and Combs, J., 1992, A vapor-dominated high-temperature reservoir at The Geysers, California, *in* Claudia Stone, ed., *Monograph on The Geysers Geothermal Field*: Davis, California, Geothermal Resources Council, Special Rept. No. 17, p. 77-87.
- White, D. E., Muffler, L. J. P., and Truesdell, A. H., 1971, Vapor-dominated hydrothermal systems compared with hot-water systems: *Econ. Geol.*, v. 66, p. 75-97.
- Yates, R. G., and Hilpert, L. S., 1946, Quicksilver deposits of the eastern Mayacmas District, Lake and Napa Counties, California: *Calif. Journal of Mines and Geology*, v. 42, no. 3, p. 231-286.

THE ORIGIN AND SIGNIFICANCE OF HIGH-GRADE METAMORPHIC XENOLITHS, CLEAR LAKE VOLCANICS, CALIFORNIA

Jim Stimac

Earth and Environmental Sciences, MS-D462
Los Alamos National Laboratory, Los Alamos, NM 87545

INTRODUCTION

The Clear Lake Volcanics (~2.1 to 0.01 Ma) are the youngest of a series of volcanic fields in the northern Coast Ranges of California whose ages roughly parallel the timing of northerly migration of the Mendocino triple junction (Dickinson and Snyder, 1979; Johnson and O'Neil, 1984; Fox et al., 1985). There is compelling chemical, isotopic, and textural evidence that partial melting of crustal rocks played a major role in magmatism at Clear Lake (Futa et al., 1981; Hearn et al., 1981; Johnson and O'Neil, 1984). Physical evidence includes the presence of high-grade metamorphic xenoliths in many basaltic to andesitic lavas of the area (Brice, 1953; Hearn et al., 1981). The xenolith suite is dominated by high-T, low-P granulite facies schist and gneiss, but also includes mafic igneous inclusions interpreted as cognate with the Clear Lake Volcanics (Stimac, 1991). Together, this suite is thought to represent fragments of mid- to lower-crustal mafic intrusions and their contact aureoles (Stimac et al., 1992a).

Exposed basement rocks in the Clear Lake area include the Late Jurassic to Late Cretaceous Franciscan Complex (FC), the Middle Jurassic Coast Range ophiolite (CRO), and the Late Jurassic to Early Cretaceous Great Valley sequence (GVS) (McLaughlin, 1981; McLaughlin and Ohlin, 1984). The metamorphic xenoliths do not resemble exposed graywackes of the FC and GVS, although they could represent the residuum of partial melting and recrystallization of graywacke and intermediate to mafic igneous rocks of the FC or GVS. This indicates that either the exposed country rocks are metamorphosed to higher grade at depth, or sialic basement underlies them. If the xenolith suite represents FC or GVS rocks, then it appears that mantle upwelling and crustal magmatism at the southern edge of the Gorda plate has converted accreted melange to lithofacies typical of continental crust over the past 3 m.y. (Stimac et al., 1992a).

This study briefly describes three important xenolith occurrences in host lavas nearly spanning the age range of volcanism at Clear Lake. These examples shed light on the nature of the middle crust of the region, and the assimilation process that formed the host lavas. The xenolith suite also provides evidence bearing on broader issues such as the relationship of granulite facies metamorphism to magmatism, and processes of crustal growth at continental margins.

CONTAMINATED LAVAS AND THE XENOLITH SUITE

Previous Studies

In his study of the volcanic rocks of the Lower Lake Quadrangle, Brice (1953) noted the presence of both

cognate and accidental xenoliths in the andesite of Perini Hill (APH) and older basalts. He was particularly impressed by the abundance of quartz aggregates and quartz xenocrysts (known locally as "Clear Lake diamonds") present in mafic rocks. Brice divided accidental xenoliths into siliceous and aluminous types. His siliceous types included sandstone, chert, quartz, and quartz-rich schist, whereas aluminous types included pelitic schist and partially reacted orthopyroxene xenocrysts containing inclusions of quartz, plagioclase, biotite, garnet, or cordierite.

Hearn et al. (1981) expanded the description of the inclusion suite. They noted that quartz aggregates and schistose to granular-textured xenoliths occurred in the APH unit, and less commonly in other andesitic to basaltic rocks of the region. Like Brice, they linked the presence of quartz in mafic to intermediate lavas to the disintegration of quartz-rich metamorphic rocks. Hearn et al. (1981) also pointed out that the fabric and mineralogy of the xenoliths probably resulted from regional metamorphism, and suggested that high-grade sialic basement rocks may underlie the Franciscan Complex in the Clear Lake area. A study by Wilson (1981) indicated that zircons in the APH unit, crustal xenoliths, and metagraywacke of the Franciscan Complex were similar in morphology and color, and could have a common parentage.

Inclusion-Bearing Volcanic Units

Inclusions of the type described above are present in Clear Lake volcanic rocks ranging in composition from basaltic andesite to andesite (54-63 wt% SiO₂). Extensive sampling of new and previously described localities indicate that the most important inclusion-bearing volcanic units are the: (1) andesites of Perini Hill (APH), Grouse Springs (AGS), Seigler Canyon (ASC), Split Top Ridge (AST), and Salmina Flat (ASF), (2) "early basalts" (BE), and (3) the younger basaltic andesites of Roundtop Mountain (BR), North Cone (BN), and High Valley (BHV) (Fig. 1). Thus xenoliths are found in mafic rocks spanning nearly the full age range of the volcanic field. Although I will concentrate on xenolith occurrences dominated by high-T, low-P granulite-facies rocks, rare chert, serpentinite, and graywacke xenoliths are also present in some units, especially young mafic rocks in the northeastern portion of the volcanic field (e.g. BN).

Petrographic and isotopic features of basaltic to andesitic units containing from 0 to 15% xenoliths are summarized in Table 1. Strontium and oxygen isotopic data for these samples clearly reflect the influence of crustal assimilation in units which contain xenoliths, even though identifiable xenoliths were excluded from the analyzed samples. Relatively primitive mafic magmas that lack xenoliths (units BC, BE/SN, and BB) have $^{87/86}\text{Sr}$ ratios <0.7032 and $\delta^{18}\text{O} \leq 8\text{‰}$, whereas mafic rocks exhibiting petrographic evidence of assimilation (the remaining samples in Table 1) have higher $^{87/86}\text{Sr}$ ratios and $\delta^{18}\text{O}$ values, ranging up to 0.70529 and +10.6‰ respectively. Quartz xenocrysts and metamorphic xenolith samples range from 0.706 to 0.708 in $^{87/86}\text{Sr}$ and +11 to +15‰ in $\delta^{18}\text{O}$, indicating that they are of metasedimentary origin (Stimac et al., in prep.). Xenolith-bearing mafic rocks are also strongly enriched in incompatible trace elements, such as Rb, Ba, Th, Ce, Hf, and Y, relative to uncontaminated mafic rocks such as BE/SN (Fig. 2A). Crustal xenoliths exhibit incompatible element enrichment patterns similar to the most contaminated lavas, indicating that assimilation of a crustal component is largely responsible for the incompatible trace element signature of xenolith-bearing lavas (Fig 2B).

THE ORIGIN AND SIGNIFICANCE OF HIGH-GRADE METAMORPHIC XENOLITHS, CLEAR LAKE VOLCANICS, CALIFORNIA

Jim Stimac

Earth and Environmental Sciences, MS-D462
Los Alamos National Laboratory, Los Alamos, NM 87545

INTRODUCTION

The Clear Lake Volcanics (~2.1 to 0.01 Ma) are the youngest of a series of volcanic fields in the northern Coast Ranges of California whose ages roughly parallel the timing of northerly migration of the Mendocino triple junction (Dickinson and Snyder, 1979; Johnson and O'Neil, 1984; Fox et al., 1985). There is compelling chemical, isotopic, and textural evidence that partial melting of crustal rocks played a major role in magmatism at Clear Lake (Futa et al., 1981; Hearn et al., 1981; Johnson and O'Neil, 1984). Physical evidence includes the presence of high-grade metamorphic xenoliths in many basaltic to andesitic lavas of the area (Brice, 1953; Hearn et al., 1981). The xenolith suite is dominated by high-T, low-P granulite facies schist and gneiss, but also includes mafic igneous inclusions interpreted as cognate with the Clear Lake Volcanics (Stimac, 1991). Together, this suite is thought to represent fragments of mid- to lower-crustal mafic intrusions and their contact aureoles (Stimac et al., 1992a).

Exposed basement rocks in the Clear Lake area include the Late Jurassic to Late Cretaceous Franciscan Complex (FC), the Middle Jurassic Coast Range ophiolite (CRO), and the Late Jurassic to Early Cretaceous Great Valley sequence (GVS) (McLaughlin, 1981; McLaughlin and Ohlin, 1984). The metamorphic xenoliths do not resemble exposed graywackes of the FC and GVS, although they could represent the residuum of partial melting and recrystallization of graywacke and intermediate to mafic igneous rocks of the FC or GVS. This indicates that either the exposed country rocks are metamorphosed to higher grade at depth, or sialic basement underlies them. If the xenolith suite represents FC or GVS rocks, then it appears that mantle upwelling and crustal magmatism at the southern edge of the Gorda plate has converted accreted melange to lithofacies typical of continental crust over the past 3 m.y. (Stimac et al., 1992a).

This study briefly describes three important xenolith occurrences in host lavas nearly spanning the age range of volcanism at Clear Lake. These examples shed light on the nature of the middle crust of the region, and the assimilation process that formed the host lavas. The xenolith suite also provides evidence bearing on broader issues such as the relationship of granulite facies metamorphism to magmatism, and processes of crustal growth at continental margins.

CONTAMINATED LAVAS AND THE XENOLITH SUITE

Previous Studies

In his study of the volcanic rocks of the Lower Lake Quadrangle, Brice (1953) noted the presence of both

cognate and accidental xenoliths in the andesite of Perini Hill (APH) and older basalts. He was particularly impressed by the abundance of quartz aggregates and quartz xenocrysts (known locally as "Clear Lake diamonds") present in mafic rocks. Brice divided accidental xenoliths into siliceous and aluminous types. His siliceous types included sandstone, chert, quartz, and quartz-rich schist, whereas aluminous types included pelitic schist and partially reacted orthopyroxene xenocrysts containing inclusions of quartz, plagioclase, biotite, garnet, or cordierite.

Hearn et al. (1981) expanded the description of the inclusion suite. They noted that quartz aggregates and schistose to granular-textured xenoliths occurred in the APH unit, and less commonly in other andesitic to basaltic rocks of the region. Like Brice, they linked the presence of quartz in mafic to intermediate lavas to the disintegration of quartz-rich metamorphic rocks. Hearn et al. (1981) also pointed out that the fabric and mineralogy of the xenoliths probably resulted from regional metamorphism, and suggested that high-grade sialic basement rocks may underlie the Franciscan Complex in the Clear Lake area. A study by Wilson (1981) indicated that zircons in the APH unit, crustal xenoliths, and metagraywacke of the Franciscan Complex were similar in morphology and color, and could have a common parentage.

Inclusion-Bearing Volcanic Units

Inclusions of the type described above are present in Clear Lake volcanic rocks ranging in composition from basaltic andesite to andesite (54-63 wt% SiO₂). Extensive sampling of new and previously described localities indicate that the most important inclusion-bearing volcanic units are the: (1) andesites of Perini Hill (APH), Grouse Springs (AGS), Seigler Canyon (ASC), Split Top Ridge (AST), and Salmina Flat (ASF), (2) "early basalts" (BE), and (3) the younger basaltic andesites of Roundtop Mountain (BR), North Cone (BN), and High Valley (BHV) (Fig. 1). Thus xenoliths are found in mafic rocks spanning nearly the full age range of the volcanic field. Although I will concentrate on xenolith occurrences dominated by high-T, low-P granulite-facies rocks, rare chert, serpentinite, and graywacke xenoliths are also present in some units, especially young mafic rocks in the northeastern portion of the volcanic field (e.g. BN).

Petrographic and isotopic features of basaltic to andesitic units containing from 0 to 15% xenoliths are summarized in Table 1. Strontium and oxygen isotopic data for these samples clearly reflect the influence of crustal assimilation in units which contain xenoliths, even though identifiable xenoliths were excluded from the analyzed samples. Relatively primitive mafic magmas that lack xenoliths (units BC, BE/SN, and BB) have ^{87/86}Sr ratios <0.7032 and $\delta^{18}\text{O} \leq 8\text{‰}$, whereas mafic rocks exhibiting petrographic evidence of assimilation (the remaining samples in Table 1) have higher ^{87/86}Sr ratios and $\delta^{18}\text{O}$ values, ranging up to 0.70529 and +10.6‰ respectively. Quartz xenocrysts and metamorphic xenolith samples range from 0.706 to 0.708 in ^{87/86}Sr and +11 to +15‰ in $\delta^{18}\text{O}$, indicating that they are of metasedimentary origin (Stimac et al., in prep.). Xenolith-bearing mafic rocks are also strongly enriched in incompatible trace elements, such as Rb, Ba, Th, Ce, Hf, and Y, relative to uncontaminated mafic rocks such as BE/SN (Fig. 2A). Crustal xenoliths exhibit incompatible element enrichment patterns similar to the most contaminated lavas, indicating that assimilation of a crustal component is largely responsible for the incompatible trace element signature of xenolith-bearing lavas (Fig 2B).

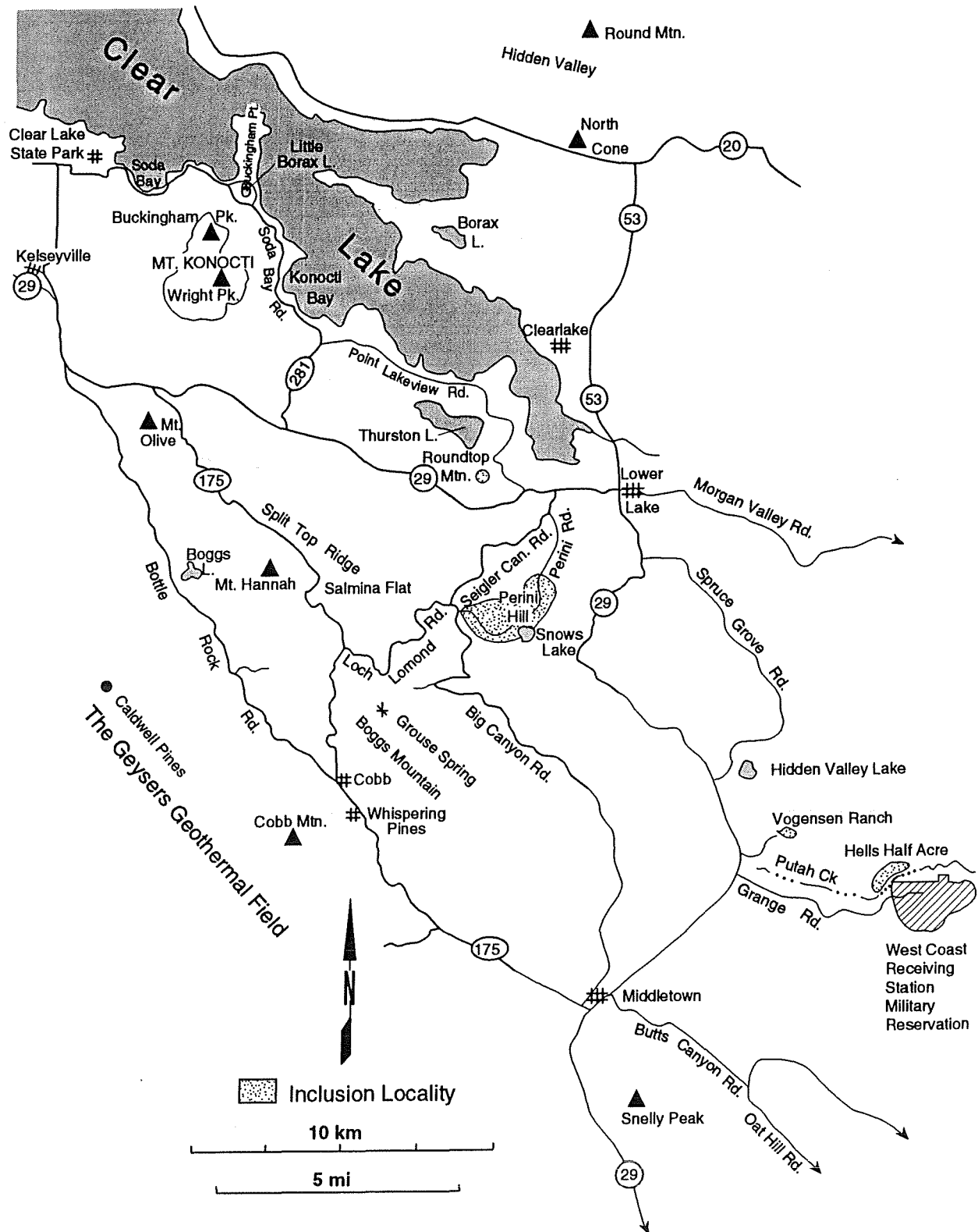


FIGURE 1. Selected inclusion localities in the central and southeastern portions of the Clear Lake volcanic field. Samples from the andesite of Perini Hill (APH) were collected from a number of localities along Perini Road. Samples of the basaltic andesite of Roundtop Mountain (BR) were collected primarily from the excavated portion of the cinder cone, owned by Konocti Rock Company. Samples of older basaltic andesite and andesite (unit BE of Hearn et al., 1976) were collected primarily from two localities: (1) a prominent mesa described by Brice (1953) as Hill 1812. This mesa is located on the Vogensen Ranch, SE of Hidden Valley Lake (BE/V); and (2) along Putah Creek in the Hells Half Acre area (BE/HHA).

Table 1. Modal and Isotopic Data for Selected Basaltic to Andesitic Rocks from the Clear Lake Volcanic Field.

UNIT	Mg#	OL	CPX	OPX	PL	HB	ILM	QTZ	X	^{87/86} Sr	δ ¹⁸ O
BC	74	7-15	1-2	-	<1	-	-	-	-	0.70308	+6.6-7.0(pl)
BE/SN	63	4	-	-	-	-	tr	-	-	0.70312	+7.9(pl)
BB	66	3	2	-	1	-	-	1	-	0.70319	+7.9(wr)
BHV	56	3-5	5-15	2-5	10	-	-	<1	<1	0.70402	+8.5-9.3(wr)
BN	55	1	<1	-	2	-	-	1	<1	NA	NA
BR	63	5	<1	-	<1	-	-	1	<1	0.70368	+8.0-8.8(wr)
BE/V	67	10	3	2	1	-	-	4	<1-2	0.70529	+10.6(wr)
APH	59	tr	<1	3-5	3-5	tr	-	2	2-5	0.70402	+10.0(wr)
AGS	67	<1	2	1	2-5	<1	-	1	1	NA	NA
ASC	65	<1	5	7	7	-	tr(i)	tr	tr	NA	+8.7(pl)
AST	66	1-3	4	2	12	tr	tr	tr	tr	0.70391	+10.6(wr)
ASF	47	tr	8	14	16	tr	2	1	1	0.70463	+10.3(pl)
BE/HHA	61	4	7	3	10	-	tr	1-2	2-15	NA	NA

UNIT ABBREVIATIONS: BC, basalt of Caldwell Pines; BE/SN, early basalt/Snelly Peak; BB, basaltic andesite of Buckingham Peak; BHV, basaltic andesite of High Valley; BN, basaltic andesite of North Cone; BR, basaltic andesite of Roundtop Mountain; BE/V, early basaltic andesite/Vogensen Ranch; APH, andesite of Perini Hill; AGS, andesite of Grouse Springs; ASC, andesite of Seiglar Canyon; AST, andesite of Split Top; ASF, andesite of Salmina Flat; BE/HHA, basaltic andesite and andesite of Hells Half Acre. See map by Hearn et al. (1976) for unit descriptions and locations. MINERAL ABBREVIATIONS: OL, olivine; CPX, clinopyroxene; OPX, orthopyroxene; PL, plagioclase; HB, hornblende; ILM, ilmenite; QTZ, quartz; X, xenoliths; tr, trace; (i) occurs as inclusions in phenocrysts; "-", not observed; NA, not analysed. NOTES: Mg# (molar Mg/[Mg+0.85FeT]) based on whole-rock chemical analyses (see Stimac, 1991). Modal estimates (vol%) based on visual estimates in outcrops, hand samples, and thin sections. ^{87/86}Sr data from Futa et al. (1981) and Bullen, unpub. data; Whole-rock (wr) and plagioclase (pl), δ¹⁸O values from J. Stimac et al. (in prep).

Inclusion Types

The term "inclusion" is used in this paper to encompass all rock and mineral aggregates (with or without interstitial glass) that appear to be foreign to the host rock, but I will exclude discussion of quenched mafic inclusions because they are common only in the silicic rocks of the Clear Lake Volcanics (see Stimac and Pearce, 1992). Both metamorphic xenoliths (accidental), and plutonic igneous inclusions (interpreted to be cognate) are present in mafic to intermediate volcanic rocks at Clear Lake. These inclusions can be further divided into four major types based on mineralogy and texture (Table 2). The main distinctions between M1 and M2 metamorphic xenoliths are: (1) the dominance of Al-rich minerals (garnet, cordierite, sillimanite) in M1 xenoliths, and (2) the dominance of orthopyroxene-clinopyroxene±quartz assemblages in M2 xenoliths. These types are roughly equivalent to the aluminous and silicic types of Brice (1953).

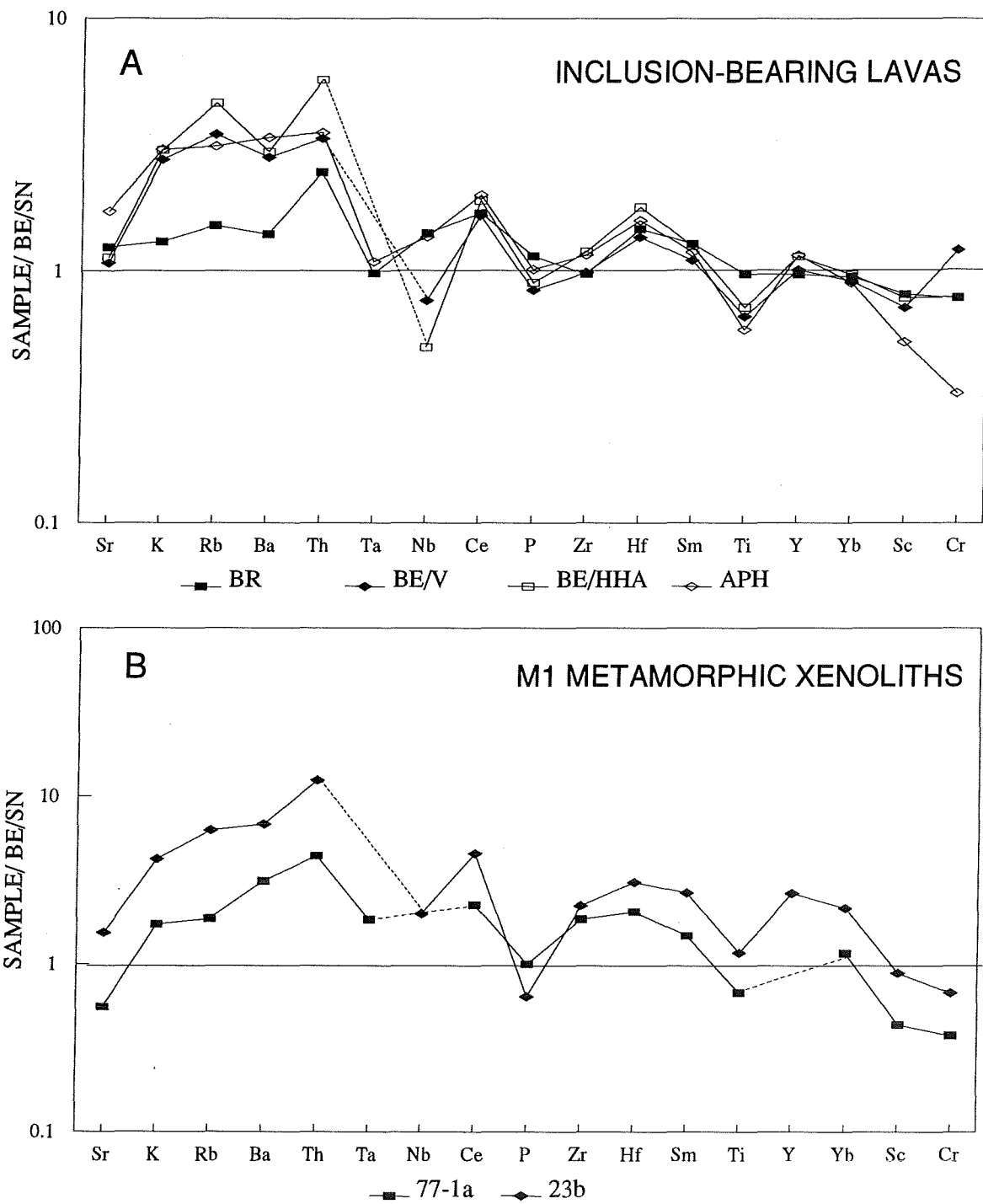


FIGURE 2. Spiderdiagrams of selected xenolith-bearing mafic to intermediate rocks (A) and M1 crustal xenoliths (B). All samples are normalized to the basalt of Snelly Peak, a relatively primitive basalt listed in Table 1. Note that relative enrichments in K, Rb, Ba, Th, Ce, Hf, and Y in the xenolith-bearing units are similar to enrichment patterns in the M1 xenoliths (see Stimac, 1991 for whole-rock data and methods).

Table 2. Summary of Inclusion Types from Clear Lake volcanic rocks.

INCLUSION TYPE	MINERALOGY	FEATURES
Metamorphic (M1)	PL-OPX-BT-CRD ± GAR ±SILL ±SP ±ILM	fn.gr. compositionally layered Al-rich gneiss and schist
Metamorphic (M2)	PL-OPX-CPX ± QTZ ± ILM	fn.gr. compositionally layered quartzofeldspathic gneiss and schist
Plutonic Igneous (PI1)	PL-OPX-CPX ± OL ± ILM ± HB	med.gr. pyroxene gabbro to gabbro-norite
Plutonic Igneous (PI2)	PL-OPX-BT ± QTZ ± ILM	med.gr. to cr.gr. bio-qtz gabbro to diorite

ABBREVIATIONS: OL, olivine; OPX, orthopyroxene; CPX, clinopyroxene; PL, plagioclase; BT, biotite; HB, hornblende; ILM, ilmenite; QTZ, quartz; GAR, garnet; CRD, cordierite; SP, hercynitic spinel; SILL, sillimanite. NOTES: Most xenoliths contain interstitial glass.

Medium- to coarse-grained plutonic igneous inclusions are present in association with metamorphic xenoliths in some rocks. These inclusions are mainly noritic gabbros, quartz-pyroxene gabbros, and biotite-quartz gabbros and diorites with SiO₂ from ~48 to 58 wt%. They consist of plagioclase-orthopyroxene-clinopyroxene±opaque oxides±olivine±amphibole assemblages (PI1), or plagioclase-orthopyroxene-biotite±quartz±ilmenite assemblages (PI2)(Table 2). Accessory apatite and zircon are present in some PI2 inclusions. Plutonic inclusions can be distinguished from metamorphic xenoliths by their granular, non-layered texture, and lack of aluminous minerals.

Individual plutonic inclusions exhibit textures that indicate incomplete to complete crystallization, and partial reaction with the host magma. In some PI1 inclusions, euhedral to subhedral plagioclase and pyroxene crystals lacking reaction or exsolution textures project into glass which contains quench crystals of feldspar. These relationships are more consistent with incomplete crystallization than partial melting. Other PI1 and PI2 inclusions lack interstitial glass, and show evidence of reaction with the host magma including fine-fritting of plagioclase, and complex pyroxene recrystallization. The complete lack of metamorphic fabrics and the evidence for incomplete solidification indicates that these inclusions are broadly related to their host rocks rather than representing pre-existing mafic crustal rocks.

M1 and M2 xenoliths are most abundant, accounting for a high proportion of all inclusions sampled. PI1 inclusions are present in low abundance in a number of units including ASF, ASC, APH, and BE/HHA, whereas PI2 inclusions are only known from localities along Putah Creek (BE/HHA). In the remainder of this paper I will focus on three inclusion occurrences at Perini Hill (APH), Roundtop Mountain (BR), and Hell's Half Acre (BE/HHA), which illustrate the range of inclusion and host rock types present at Clear Lake (Fig. 1).

The andesite of Perini Hill

The andesite of Perini Hill (APH) outcrops over an area of 10 km² in the central portion of the Clear Lake volcanic field (Hearn et al., 1976)(Fig. 1). The unit reaches a maximum thickness of about 200 m at Perini Hill, and has an estimated eruptive volume of 0.5 km³. The APH unit has not been dated, but must be younger than 1.02 Ma based on a K-Ar date on the underlying tuff of Bonanza Springs (Donnelly-Nolan et al., 1981). Combined stratigraphic, K-Ar, and paleomagnetic evidence indicated that the APH unit was erupted between about 0.97 and 0.90 Ma.

The APH unit contains abundant xenoliths and xenocrysts derived from metamorphic and plutonic igneous rocks in various stages of reaction with the host magma (Fig. 3). Typical hand samples contain from 2 to 5% identifiable xenoliths (Table 1). Most of these xenoliths are small (<5 cm), but rare examples range up to 15 cm in long dimension (Brice, 1953). Three of the four inclusion types are present (M1, M2, and P11), but M1 and M2 types comprise >90% of the inclusion population. Regional and contact metamorphic fabrics and mineralogies are preserved in the cores of larger (>2 cm) xenoliths (Fig. 3A). Most xenoliths display a concentric recrystallization at their margins related to reaction with the host magma (Fig. 3B). Progressive replacement of the original xenolith mineral assemblage by calcic plagioclase and magnesian orthopyroxene ± hercynitic spinel ± ilmenite is most common. Rhyolitic to dacitic glass is generally present along grain boundaries at xenolith margins, and filling cracks and small pockets elsewhere.

Detailed examination of the apparent phenocryst population (defined as crystals >0.3 mm) indicates that the cores of a high proportion of all crystals, including plagioclase and orthopyroxene, were inherited from crustal rocks. Single xenocrysts of aluminous minerals such as garnet and cordierite are variably mantled by magmatic reaction products (Fig. 3C), whereas xenocryst minerals that were stable in the host magma, such as plagioclase and orthopyroxene, exhibit compositionally distinct magmatic overgrowths (Figs. 3D and 3E). Because plagioclase in the majority of xenoliths was more sodic than that crystallizing in the host magma, plagioclase derived from crustal rocks is typically fritted, with clear overgrowths of more calcic composition (Fig. 3A). A high proportion (>50%) of all plagioclase in the APH unit larger than 0.3 mm consists of partially fritted, sodic cores, jacketed by clear, more calcic rims (cf. Figs. 3B and 3D), and is probably crustal in origin. Similarly, orthopyroxene phenocrysts commonly contain Al- and Fe-rich cores and Ca- and Mg-rich rims, separated by sharp interfaces (Fig. 3E). Comparison to orthopyroxene in xenoliths indicates that these Al- and Fe-rich cores were derived from a crustal source, and were subsequently overgrown by orthopyroxene of more Ca- and Mg-rich composition.

Very rare P11 inclusions consisting of plagioclase, orthopyroxene, and hornblende are present in the APH unit. Reaction textures such as fine-fritting of plagioclase and overgrowths of orthopyroxene on hornblende indicate that these inclusion were not in equilibrium with the host magma. Subhedral hornblende crystals up to 5 mm are also present as phenocrysts in some samples (Fig. 3D), but are not abundant.

The compositional differences between plagioclase and orthopyroxene in crustal xenoliths versus those crystallizing from the host magma indicate that the APH unit is not simply a partial melt of crust with residual crystals (restite), but rather, is a complex mixture of crustal melt and entrained crystalline debris with a mafic magma

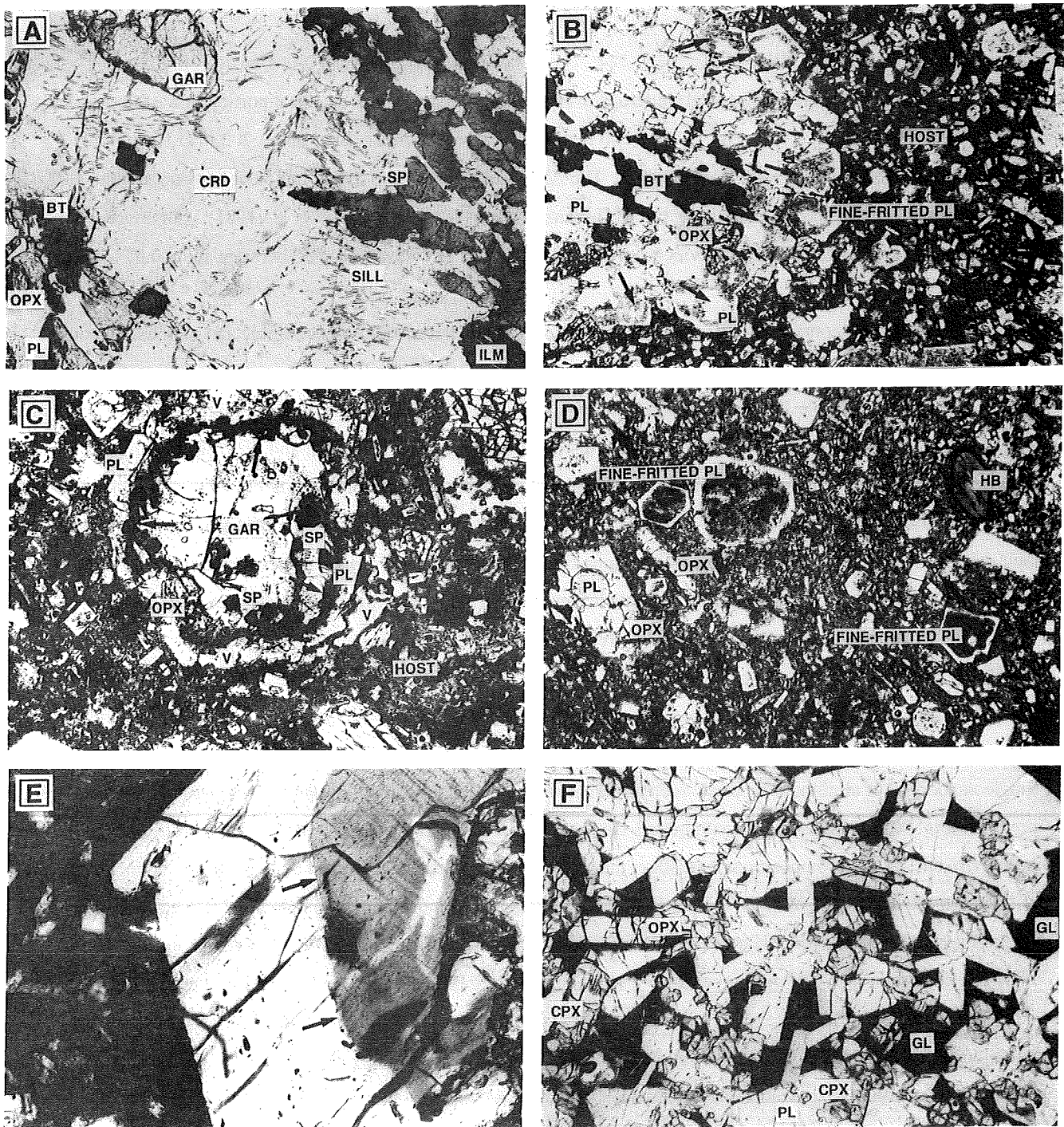


FIGURE 3. Textural relations in xenoliths and xenolith-bearing rocks (see Tables 1 and 2 for mineral abbreviations). (A) Core of M1 xenolith SCL23B consisting of a cordierite poikiloblast enclosing almandine, sillimanite needles, and hercynitic spinel. Biotite, orthopyroxene, ilmenite, and plagioclase can be seen at the bottom edge of the poikiloblast. Field of view ~2 mm. (B) Edge of small M1 xenolith exhibiting reaction with the host magma at its margin. Plagioclase at the margin is characterized by sodic cores with fine-fritted regions (arrows) and clear, more calcic overgrowths. The core of the xenolith consists primarily of clear sodic plagioclase, biotite, and orthopyroxene. Biotite is only found within the core of the xenolith. Field of view ~8 mm. (C) Inclusion-rich almandine garnet xenocryst with complex reaction mantle. Proceeding from the inner contact, the mantle consists of (1): relatively coarse-grained spinel and orthopyroxene, (2) very fine-grained intergrowth (symplectite) of spinel, opx, and glass (marked by arrows), and (3) coarse-grained plagioclase and lesser orthopyroxene. Field of view ~4 mm. (D) The APH unit, containing phenocrysts of plagioclase, orthopyroxene, and rare hornblende. A high proportion of plagioclase phenocrysts have fine-fritted cores and clear, calcic overgrowths. Orthopyroxene poikiloblasts (up to 1.5 cm in long dimension) containing rounded inclusions of plagioclase, biotite, quartz, and cordierite are also common (lower left). Field of view ~8 mm. (E) Orthopyroxene with xenocrystic Fe-Al-rich core and magmatic Mg-Ca-rich overgrowth, separated by a sharp interface (marked by arrows). Field of view ~2 mm. (F) Plutonic inclusion (PI1) consisting of plagioclase, orthopyroxene, clinopyroxene, and interstitial glass. Field of view ~8 mm.

much richer in Ca and Mg. The presence of rare Mg-olivine (Fo₈₁₋₉₀) and clinopyroxene phenocrysts in the APH unit is also consistent with the involvement of more mafic magma in the early stages of assimilation.

Early Olivine-basalts

Early olivine basalt, basaltic andesite, and andesite (mapped collectively as BE by Hearn et al., 1981) outcrop as an extensive plateau-like highland northeast of Middletown, and as scattered outcrops east of Clear Lake. This sequence of mafic lavas comprises some of the oldest volcanic rocks at Clear Lake, ranging in age from 1.33 to 1.64 Ma (Donnelly-Nolan et al., 1981). The older mafic rocks have not been studied in detail, but Brice (1953) estimated that this sequence consists of at least three lava flows with a composite thickness of ~170 m in the central portion of their outcrop area. He described quartz aggregates up to 15 cm in length, and siliceous and aluminous xenoliths as common in some lavas.

Further sampling has revealed that diatreme(?) breccias near the base of the sequence in the Hells Half Acre area contain up to 15% inclusions of widely ranging texture and mineralogy (Table 1). Basaltic andesite lavas overlying this basal breccia and capping mesas at the nearby Vogensen ranch contain <1 to 6% xenoliths and xenocrystic debris. The xenolith suite in the Hells Half Acre area includes all four types listed in Table 2, with metamorphic and cumulate types present in roughly equal proportions, but PI2 inclusions are only found along Putah Creek (Fig. 1).

The host rocks range from olivine-rich basaltic andesites (BE/V) to plagioclase and pyroxene andesites (BE/HHA). Olivine compositions in these rocks are surprisingly Mg-rich, ranging from Fo₈₂ to Fo₉₁. The combination of relatively high Mg# for the lava (Table 1), and Mg-rich olivine phenocrysts suggests that these rocks are mixtures of relatively unfractionated mantle-derived basalt with variable proportions of crustal melt and residual crystalline debris. As with the APH unit, most of the plagioclase and orthopyroxene in these rocks can be attributed to disaggregation of crustal rocks.

Crustal xenoliths are similar in size and composition to those found in APH, but they have generally suffered more extensive reaction with the host magma. Surface weathering is also more pronounced in some porous samples. Rare, large (up to 10 cm) schistose to gneissic xenoliths containing quartz layers up to several centimeters in width support previous workers' conclusions that quartz aggregates in mafic rocks of the region represent disaggregation products of these rocks (Brice, 1953; Hearn et al., 1981). Plutonic inclusions consist of plagioclase-orthopyroxene-clinopyroxene±olivine (PI1) and plagioclase-orthopyroxene-biotite±quartz±ilmenite (PI2). Some inclusions contain abundant interstitial glass (Fig. 3F), whereas others contain little or no glass.

Basaltic Andesite of Roundtop Mountain

The basaltic andesite of Roundtop Mountain consists of a young lava flow and cinder cone located near Thurston Lake (Fig. 1). The lava flow has a maximum thickness of 20 m, and the cinder cone is 200 m high, giving the unit an estimated total volume of ~0.1 km³ (B.C. Hearn et al., map in press). The unit is undated, but is presumed to be Pleistocene in age due to the well preserved morphology of the flow and cone deposits. It overlies

dacitic rocks dated at <0.5 Ma (Donnelly-Nolan et al., 1981). The cinder cone is currently being mined for ornamental stone by the Konocti Rock Company. This operation has greatly increased the amount of exposed rock, allowing better sampling of the xenolith suite.

The basaltic andesite is nearly aphyric, with sparse olivine (Fo₇₉₋₈₈), and Mg-rich clinopyroxene phenocrysts. Quartz is the most abundant xenocryst mineral, present at <1 to 1% abundance (Table 2). Xenoliths are even less abundant, comprising much less than 1% of the rock. The xenolith suite consists primarily of unusually quartz-rich M2 rocks. Some xenoliths are dominated by plagioclase, orthopyroxene, and biotite, whereas others consist almost entirely of quartz, with lesser plagioclase and pyroxene. Layering in a few larger samples suggests that the protolith was a banded gneiss, with quartz-rich and quartz-poor layers. Moreover, glass-rich pockets at the contact between these layers in some xenoliths suggests that disaggregation would most likely take place parallel to layering. Some xenoliths have suffered extensive partial melting and consist of loosely aggregated, rounded crystals in an interconnected matrix of vesicular dacitic glass. It is clear from these examples that in some cases, partial melting along grain boundaries leads to dispersion of xenolithic debris in the form of single crystals.

XENOLITH PARAGENESIS

Metamorphic Xenoliths

The mineralogies of M1 metamorphic xenoliths in the Clear Lake occurrences are similar to the mineralogy of the residuum in fluid-absent partial melting experiments of pelitic or semi-pelitic starting material held at temperatures and pressures typical of the middle to lower crust (Thompson, 1982; Vielzeuf and Holloway, 1988; Patiño Douce and Johnson, 1991). However, both M1 and M2 xenoliths are characterized by complexly overprinted fabrics indicating multiple episodes of recrystallization and partial melting (e.g. Fig. 3A). Compositional layering and foliation characteristic of regional metamorphism are well preserved in some xenoliths, but appear to be partially overprinted by static recrystallization in others.

The paragenesis of metamorphic xenoliths is summarized in Figure 4A. The protoliths of M1 metamorphic xenoliths are not well known, but appear to have been eugeosynclinal(?) sedimentary rocks. Protoliths for M2 xenoliths were certainly less aluminous than M1, and could have been either intermediate to mafic volcanic rocks, or lithic-rich volcanic sediments derived from them. Prograde regional metamorphic assemblages in M1 are dominated by sodic plagioclase (PLAG1), Fe-Al-rich orthopyroxene (OPX1), biotite, garnet, and sillimanite, whereas M2 is dominated by plagioclase (PLAG1), orthopyroxene (OPX1), clinopyroxene, biotite, and quartz. I suspect that K-feldspar and quartz were present in some protoliths, but have been completely consumed by partial melting reactions.

The textures and mineralogies of some M1 xenoliths indicate that contact metamorphism and partial melting increased the modal proportions of cordierite, plagioclase, orthopyroxene, and ilmenite at the expense of garnet, sillimanite, biotite, K-feldspar, clinopyroxene, and quartz (Fig. 4A). The remaining biotite is Ti-rich (5-7 wt% TiO₂), and is locally replaced by orthopyroxene and ilmenite. These types of mineralogic transformations are typical of high-temperature contact aureoles of dioritic, gabbroic, and anorthositic plutons (Berg, 1977; Harris, 1981; Speer, 1982; Droop and Charnley, 1985; Grant and Frost, 1990; Pattison and Tracy, 1991), and high-T, low-P

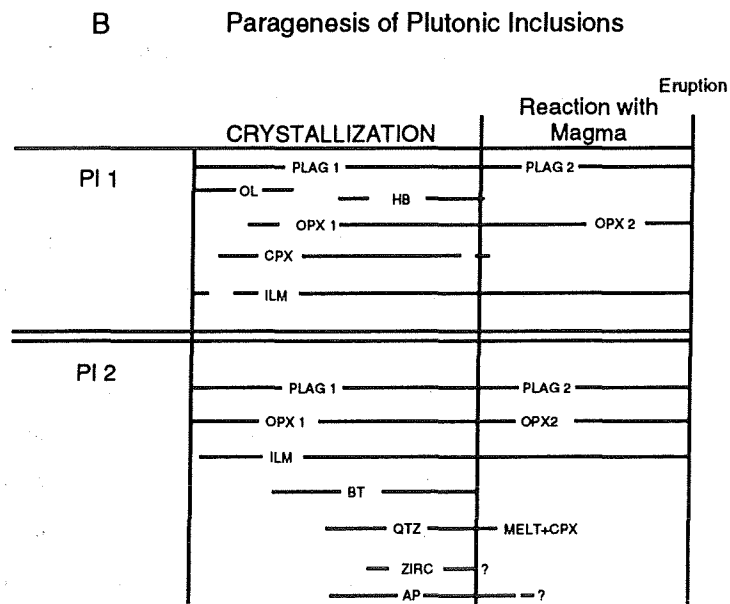
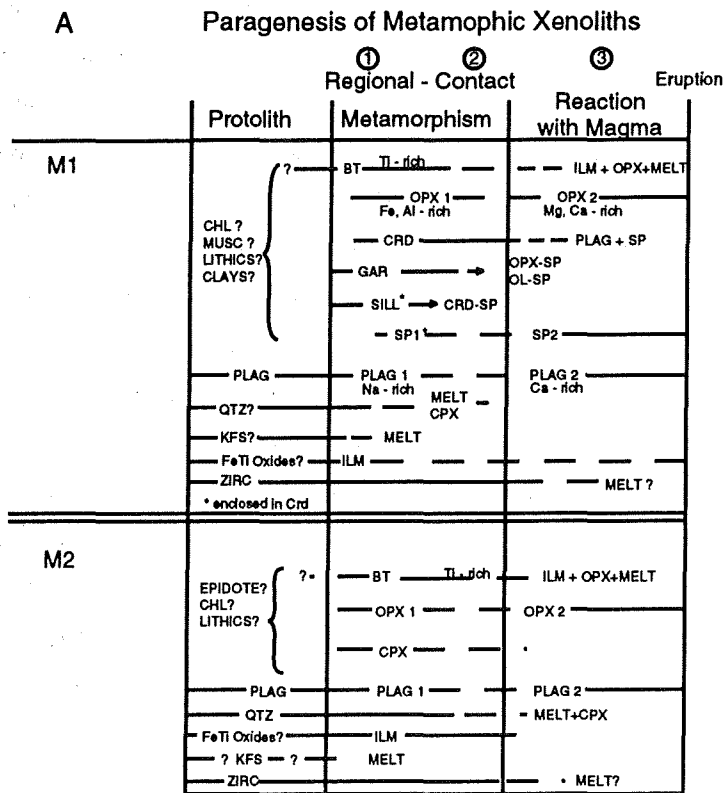


FIGURE 4. Paragenesis of metamorphic (A) and plutonic igneous (B) inclusions based on textural relations and mineral composition data. Diagrams portray the progressive mineralogical transformations resulting from (1) regional metamorphism, (2) contact metamorphism, and (3) direct reaction with magma (see text for details).

granulite terrains inferred to have formed by magmatic underplating (Young et al., 1989; Dempster et al., 1991).

Direct exposure of xenoliths and xenocrysts to the host magma led to further reaction and partial melting (Fig. 4A). Concentric recrystallization at xenolith margins indicates progressive replacement of the original mineral assemblage by calcic plagioclase and Mg-rich orthopyroxene \pm hercynitic spinel \pm ilmenite. Similarly, single xenocrysts of aluminous minerals underwent simple dissolution and were mantled by various combinations of plagioclase, orthopyroxene, hercynitic spinel, and ilmenite, whereas metamorphic plagioclase and orthopyroxene were overgrown by more calcic and magnesian compositions (Figs. 3 and 4A). Quartz was rounded and embayed, and mantled by augite coronas. The formation of reaction mantles on quartz and aluminous xenocrysts appears to have impeded complete dissolution by limiting further exposure to the host magma.

The paragenesis of plutonic inclusions is summarized in Figure 4B. Plutonic inclusions contain variable amounts of interstitial glass, suggesting a range of degrees of solidification. Based on size and shape, the first minerals to crystallize were olivine (typically rimmed by orthopyroxene), plagioclase, orthopyroxene, and clinopyroxene. Minerals mantling early-formed minerals or restricted to interstices between large crystals include hornblende, quartz, zircon, and apatite. Biotite and ilmenite are present both as inclusions in early-formed minerals, and as late crystallizing phases. Direct reaction with magma has led to overgrowths or recrystallization of plagioclase and orthopyroxene to compositions in equilibrium with the host magma in some inclusions.

Mineralogical Constraints on Temperature and Pressure

Host Rocks

Olivine-phyric basaltic andesites (BR and BE/V) yield liquidus temperatures from 1165 to 1175°C, whereas pyroxene-phyric andesites (ASF and BE/HHA) yield crystallization temperatures ranging from 873 to 1108°C (Table 3). No temperature estimates could be obtained for the APH unit, but it likely had a pre-eruption temperature similar to or below closely related two-pyroxene andesites.

Metamorphic Xenoliths

Mineral assemblages preserved in the cores of some metamorphic xenoliths allow estimation of the conditions of regional and contact metamorphism. Temperature estimates based on Fe-Mg ratios in coexisting cordierite, garnet, orthopyroxene from M1 xenoliths range from 750-890°C (Table 3). Temperature estimates based on two-pyroxene thermometry of M2 xenoliths yield a similar range (793-855°C). Pressure estimates based on the Al content in orthopyroxene coexisting with garnet (Harley, 1984) and cordierite-garnet equilibria (Martignole and Sisi, 1981) in M1 xenoliths range from 4.4 to 7.6 kb (Table 3; Stimac et al., 1992a). The range of P-T conditions inferred through thermobarometry is consistent with (1) the complete lack of muscovite or andalusite in M1 xenoliths, which suggests that conditions were above muscovite breakdown (645°C at 3 kb), and above the andalusite-sillimanite inversion, and (2) the lack of kyanite, sapphirine, sapphirine-quartz, and spinel-quartz assemblages, which suggests P less than ~9 kb and T less than ~1050°C (Harley and Hensen, 1990).

Plutonic Inclusions

Medium- to coarse-grained inclusions with plutonic textures (PI) are present in association with

Table 3. Summary of Thermobarometry for Inclusions and Host Rocks

SAMPLE	UNIT	TEMPERATURE (°C)	PRESSURE (kb)
SCL109A	BE/V	1175 (1)	-
SCL27	BR	1165 (1)	-
SCL71F	ASF	873-942 (2)	-
SCL96	BE/HHA	950-1108 (2)	-
SCL23A	APH/M2	814-836 (2)	-
SCL88C	APH/M2	775-810 (2)	-
SCL23B	APH/M1	780-850 (4)	4.4-5.2@nH ₂ O=0; 5.8-6.3@nH ₂ O=0.4 (6)
FP80-19	APH/M1	805-890 (4); 750-900 (3)	6.0-6.7 (5); 5.2-5.8@nH ₂ O=0; 6.3-7.6@nH ₂ O=0.4 (6)
H77-1A	APH/M1	-	5.8-6.2 (5)
SCL95D	BE/HHA/PI1	1113-1187 (2)	-
SCL140C	BE/HHA/PI1	1109-1147 (2)	-
SCL140A	BE/HHA/PI1	947-1070 (2)	-
SCL139A	BE/HHA/PI1	930 (2)	-
SCL71A	ASF/PI1	732-883 (2)	-

METHODS: (1) Olivine-liquid thermometry (Roeder and Emslie, 1970); (2) Two-pyroxene thermometry (Davidson and Lindsley, 1985); (3) OPX-GARNET thermometry (Harley, 1984); (4) CRD-GARNET thermometry (Bhattacharya et al., 1988); (5) OPX-GARNET barometry (Harley and Green, 1982); (6) CRD-GARNET barometry (Martigole and Sisi, 1981). NOTES: See Tables 1 and 2 for unit abbreviations. All two-pyroxene temperatures calculated at P=4 kb; T increases about 5°C/kb. Errors on two-pyroxene temperatures are typically ±60-85°C (see Davidson and Lindsley, 1985).

metamorphic xenoliths in some mafic rocks. Some PI1 inclusions have cumulate textures with abundant interstitial glass, whereas others lack interstitial glass and display a range of recrystallization and exsolution textures, indicating a range of solidification. Two-pyroxene thermometry yields a range of temperatures that correlates well with the degree of solidification as estimated by the proportion of interstitial glass. Inclusions with the highest proportion of interstitial glass (up to 20%), indicating incomplete crystallization, yield temperatures ranging up to 1187°C, whereas inclusions with little or no glass (<5%), indicating complete crystallization yield temperatures as low as 732°C. This suggests that plutonic inclusions are fragments of partially to completely solidified mafic intrusions cognate with the Clear Lake Volcanics (Stimac, 1991; Stimac et al., 1992a). Chemical data for these inclusions is also consistent with this idea (Stimac, 1991).

INFERENCES CONCERNING THE STRUCTURE OF THE CRUST AND THE CLEAR LAKE MAGMATIC SYSTEM

Geophysical evidenced suggests that the crust in the Clear Lake region is from 24 to 30 km thick, and is directly underlain by hot asthenosphere (Lachenbruch and Sass, 1980; Mooney and Weaver, 1989; Benz et al., 1992;

Castillo and Ellsworth, 1993). Inferred crustal cross sections of the region typically consist of 12 to 18 km of Franciscan-like material underlain by 12 to 14 km of gabbroic and mafic crystalline rocks (Fig. 5). However, recent wedge-tectonic models for the upper and middle crust beneath the Coast Ranges based on seismic reflection and refraction studies (Fuis and Mooney, 1990; Wentworth et al., 1984, 1990; Unruh and Moores, 1992) suggest that a metamorphic basement from the western Sierra Nevada and Klamath Mountains could underlie the FC in the Clear Lake region. These rocks include slates, phyllites, and associated andesitic metavolcanic rocks of the Jurassic Mariposa and Galice Formations. Therefore, the metamorphic xenolith suite present in volcanic rocks at Clear Lake could represent metasedimentary and metavolcanic rocks derived from either Sierran or Klamath basement that extends beneath the FC and GVS, or FC rocks metamorphosed to granulite facies since emplacement.

Considering the depths implied by thermobarometry, it seems most likely that the xenolith suite was derived from near the base of the FC, which is thought to extend to depths of 12-18 km in the northern Coast Ranges (Fig. 5). If the crust below 18 km depth is composed primarily of mafic crystalline rocks (Mesozoic oceanic crustal rocks and/or younger gabbroic intrusions), then the deepest portion of the FC which is dominated by metasedimentary rocks is precisely that portion of the crust most susceptible to anatexis. The boundary between metasedimentary and mafic crystalline rocks would also be characterized by large density and rheological contrasts, which would tend to inhibit upward migration of mafic magmas.

The Clear Lake magmatic system can be envisioned as a simplified two-level system, driven by triple junction migration and concomitant decompression melting within the underlying asthenosphere (see Dickinson and Snyder, 1979; Johnson and O'Neil, 1984; and Liu and Furlong, 1992; and Liu, this volume for discussion of regional tectonic controls on magmatism). The focus of the resulting volcanism has shifted north and east with time (Donnelly-Nolan et al., 1981; Hearn et al., 1981; Stimac et al., 1992b). The deep part of the system (lower to mid-crustal levels) is dominated by mafic intrusions, granulite-facies metamorphism, and partial melting of metasedimentary protoliths. This system gives rise to variably contaminated and hybridized intermediate to silicic magmas, some of which eventually migrate to higher crustal levels (Stimac et al., 1992b). The upper level system consists primarily of numerous localized clusters of small silicic magma bodies, rather than a single large silicic reservoir (Stimac, 1991; Stimac and Pearce, 1992). Although some large, upper to mid-crustal crustal intrusive complexes have resulted (Schriener and Suemnicht, 1981; Thompson, 1991; Griscom and Jachens, this volume), most of these upper crustal magma bodies were relatively small, and probably crystallized very quickly unless recharged at regular intervals.

The inclusion suite described in this paper is most likely from the midcrust, and perhaps the uppermost portion of the mafic lower crust (about 12 to 18 km depth). This suite represents fragments of mid-crustal rocks, mafic intrusions, and their partially molten wall rocks. It appears that multiple intrusions in this portion of the crust produced partially molten regions which were easily assimilated by later pulses of magmatism, giving rise to the observed range of mantle-crustal hybrids (BR, BE/V, BE/HHA, APH). The preponderance of xenoliths in lavas erupted in approximately the first million years of volcanism suggests that the most intense period of mafic intrusion and related metamorphism occurred shortly after passage of the Mendocino triple junction. This is also

implied by the wide distribution and relatively high proportion of mafic and highly contaminated intermediate rocks erupted from 2.1 to 0.8 Ma. However, it should be noted that sparse xenoliths are also present in some of the youngest mafic lavas.

This model of the magmatic system is based mainly on detailed textural, mineralogical, and chemical study of volcanic rocks and inclusions, but it is also consistent with heat flow and geophysical evidence that suggests the presence of localized partial melt at depths >6 km over a broad region (Isherwood, 1981; Iyer et al., 1981; Eberhart-Phillips, 1986; Benz et al., 1992; Liu and Furlong, 1992; Liu, this volume; Griscom and Jachens, this volume). The model also implies that formation of high-T, low-P granulites may be directly linked to high magmatic heat flux into relatively thin crust, and that this process is likely to be an important contributor to "cratonization" at some continental margins.

CONCLUSIONS

The xenolith suite at Clear Lake is composed of high-grade metamorphic rocks with complexly overprinted fabrics and partial melting textures, as well as noritic to gabbroic rocks with cumulate textures. Together, these rocks represent fragments of deep crust, partially solidified mafic intrusions, and their contact aureoles brought to the surface by later pulses of mafic magmatism (Stimac et al., 1992a). Metapelitic xenoliths record progressive recrystallization and partial melting reactions which have increased the modal proportions of cordierite, plagioclase, orthopyroxene, and ilmenite at the expense of garnet, sillimanite, and biotite. The lack of K-feldspar and quartz in many pelitic xenoliths is attributed to partial melting. Temperature and pressure estimates for metamorphic xenoliths range from ~750-900°C and 4.4-7.6 kb (Stimac et al., 1992a). Plutonic inclusions yield temperatures from ~730-1190°C, correlating with the degree of solidification observed. These inclusions represent either Sierran or Klamath basement that extends beneath the FC and GVS, or FC rocks metamorphosed to granulite facies since emplacement.

The Clear Lake magmatic system consists of a deep zone dominated by mantle-derived basalt intrusion, granulite metamorphism, and partial melting of crustal rocks, and a shallow zone consisting of more silicic magma reservoirs. Multiple intrusions of basalt triggered partial melting at mid-crustal levels and led to production of a variety of crust-mantle hybrids, some of which were erupted as xenolith-bearing basaltic andesite to andesite lavas. Other batches of andesitic to rhyolitic magma produced in this zone fractionated and migrated to higher levels, where they formed clusters of mid- to upper-crustal silicic magma bodies.

ACKNOWLEDGMENTS

The author thanks Julie Donnelly-Nolan, Bob McLaughlin, Fraser Goff, Carter Hearn, and Dave Jacobs for enlightening discussions and sharing of samples and unpublished data. This manuscript benefitted from reviews by Julie Donnelly-Nolan, Fraser Goff, and Andy Griscom. Tom Bullen is gratefully acknowledged for providing unpublished Sr isotopic data. Eric Montoya and James Archuleta drafted the figures. Dave Mann and Carlos Montoya prepared many thin sections of xenoliths and host rocks. This project was funded mainly by a Director's

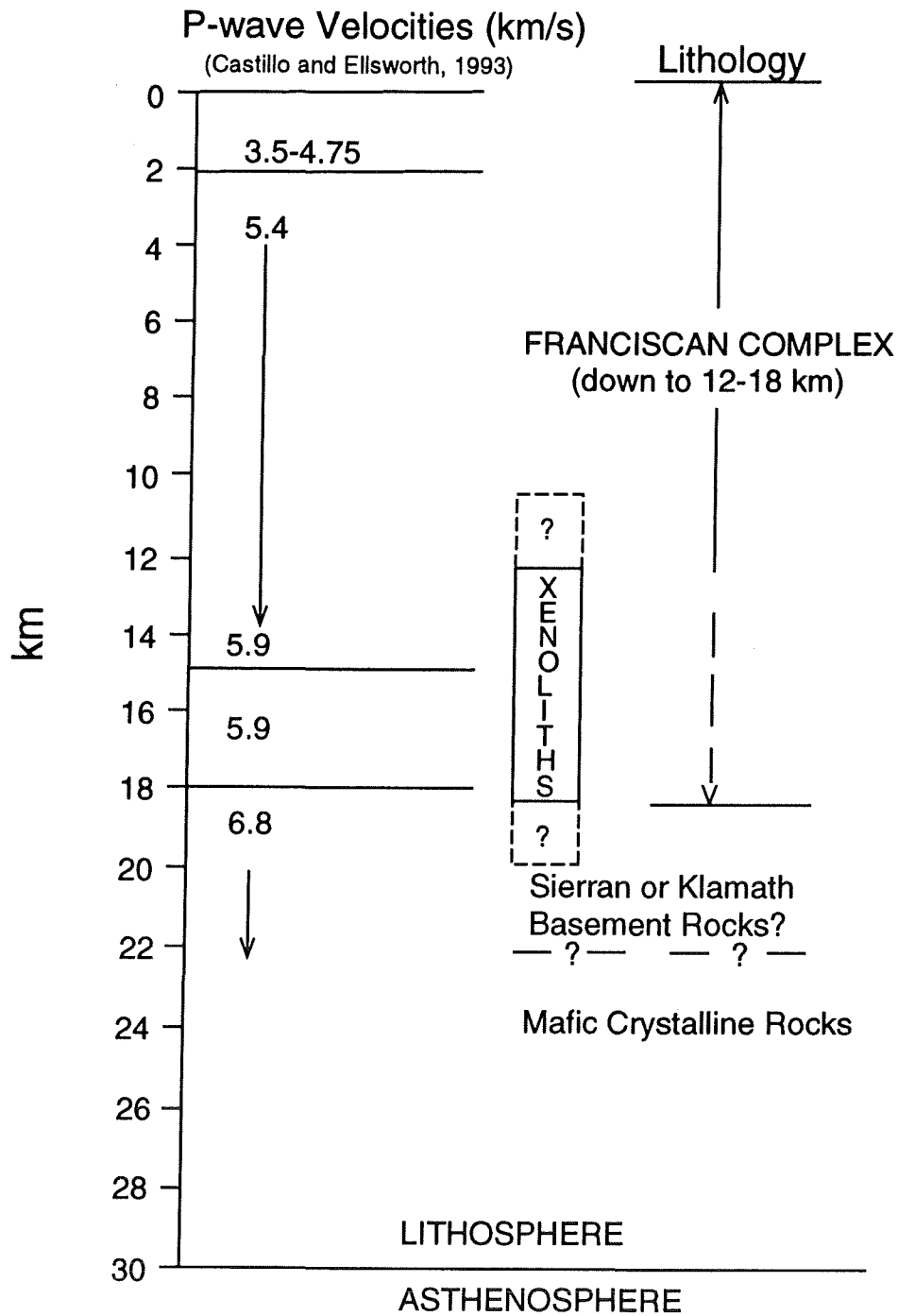


FIGURE 5. Inferred crustal structure in the Clear Lake region. The P-wave velocities shown are from the model of Castillo and Ellsworth (1993), which was derived from study of earthquakes in the vicinity of the Maacama and Bartlett Springs faults. The lithologies shown are generalized from those inferred or suggested by various authors (Wentworth et al., 1984, 1990; Eberhart-Phillips, 1986; Mooney and Weaver, 1989; Fuis and Mooney, 1990; Castillo and Ellsworth, 1993). The crustal depths represented by xenoliths are inferred from thermobarometry (see Table 3).

post-doctoral appointment at Los Alamos National Laboratory. Some samples were collected during Ph.D. field work which was funded by Queen's University, NSERC grant 8709 to T. Pearce, and Sigma Xi.

REFERENCES

- Benz, H.M., Zandt, G., and Oppenheimer, D.H., 1992, Lithospheric structure of northern California determined from teleseismic images of the upper mantle: *J. Geophys. Res.*, v. 97, p. 4791-4807.
- Berg, J.H., 1977, Regional geobarometry in the contact aureoles of the anorthosite Nain Complex, Labrador: *J. Petrol.*, v. 18, p. 399-430.
- Bhattacharya, A., Mazumdar, A.C., and Sen, S.K., 1988, Fe-Mg mixing in cordierite: constraints from natural data and implications for cordierite-garnet geothermometry in granulites: *Am. Mineral.*, v. 73, p. 338-344.
- Brice, J.C., 1953, Geology of the Lower Lake Quadrangle, California: California Division of Mines Bull. 166, p. 34-49.
- Castillo, D.A., and Ellsworth, W.L., 1993, Seismotectonics of the San Andreas fault system between Point Arena and Cape Mendocino in northern California: implications for the development and evolution of a young transform: *J. Geophys. Res.*, v. 98, p. 6543-6560.
- Davidson, P.M., and Lindsley, D.H., 1985, Thermodynamic analysis of quadrilateral pyroxenes: *Contrib. Mineral. Petrol.*, v. 91, p. 383-404.
- Dempster, T.J., Harrison, T.N., Brown, P.E., and Hutton, D.H.W., 1991, Low-pressure granulites from the Ketilidian mobile belt of Southern Greenland: *J. Petrol.*, v. 32, p. 979-1004.
- Dickinson, W.R., and Snyder, W.S., 1979, Geometry of triple junctions related to San Andreas transform: *J. Geophys. Res.*, v. 84, p. 561-572.
- Donnelly-Nolan, J.M., Hearn, B.C., Jr., Curtis, G.H., and Drake, R.E., 1981, Geochronology and evolution of the Clear Lake volcanics, in *McLaughlin, R.J., and Donnelly-Nolan, J.M., eds., Research in the Geysers-Clear Lake geothermal area, northern California: U.S. Geol. Surv. Prof. Paper 1141*, p. 47-60.
- Droop, G.T.R., and Charnely, N.R., 1985, Comparative geobarometry of pelitic hornfels associated with the Newer Gabbros: a preliminary study: *J. Geol. Soc. London*, v. 142, p. 53-62.
- Eberhart-Phillips, D., 1986, Three-dimensional velocity structure in northern California Coast Ranges from inversion of local earthquake arrival times: *Bull. Seism. Soc. Am.*, v. 76, p. 1025-1052.
- Ellis, D.J., 1986, Garnet-liquid Fe²⁺-Mg equilibria and implications for the beginning of melting in the crust and subduction zones: *Am. J. Sci.*, v. 286, p. 765-791.
- Fox, K.F., Jr., Fleck, R.J., Curtis, G.H., and Meyer, C.E., 1985, Implications of the northwestwardly younger age of the volcanic rocks of west-central California: *Geol. Soc. Am. Bull.*, v. 96, p. 647-654.
- Fuis, G.S., and Mooney, W.D., 1990, Lithospheric structure and tectonics from seismic-refraction and other data: in *Wallace, R.E., ed., The San Andreas fault system: U.S. Geol. Surv. Prof. Pap. 1515*, p. 207-236.
- Futa, K., Hedge, C.E., Hearn, B.C., and Donnelly-Nolan, J.M., 1981, Strontium isotopes in the Clear Lake volcanics: in *McLaughlin, R.J., and Donnelly-Nolan, J.M., eds., Research in the Geysers-Clear Lake geothermal area, northern California: U.S. Geol. Surv. Prof. Pap. 1141*, 259p.
- Grant, J.A., and Frost, B.R., 1990, Contact metamorphism and partial melting of pelitic rocks in the aureole of the Laramie Anorthosite Complex, Morton Pass, Wyoming: *Am. J. Sci.*, v. 290, p. 425-472.
- Griscom, A., and Jachens, B., 1993, Geophysical constraints on crustal structure in the Clear Lake area: this volume.
- Harley, S.L., 1984, An experimental study of the partitioning of Fe and Mg between garnet and orthopyroxene: *Contrib. Mineral. Petrol.*, v. 86, p. 359-373.
- Harley, S.L., and Green, D.H., 1982, Garnet-orthopyroxene barometry for granulites and peridotites: *Nature*, v. 300, p. 697-701.
- Harley, S.L., and Hensen, B.J., 1990, Archaean and Proterozoic high-grade terranes of East Antarctica (40-80°E): a case study of diversity in granulite facies metamorphism: in *Ashworth, J.R., and Brown, M., eds., High-temperature metamorphism and crustal anatexis, The Mineralogical Society Series, No. 2*, p. 320-370.
- Harris, N., 1981, The application of spinel-bearing metapelites to P/T determinations: an example from South India: *Contrib. Mineral. Petrol.*, v. 76, p. 229-233.
- Hearn, B.C., Jr., Donnelly-Nolan, J.M., and Goff, F.E., 1981, The Clear Lake Volcanics: tectonic setting and magma sources: in *McLaughlin, R.J., and Donnelly-Nolan, J.M., eds., Research in the Geysers-Clear Lake geothermal area, northern California: U.S. Geol. Surv. Prof. Pap. 1141*, 259p.
- Hearn, B.C., Jr., Donnelly, J.M., and Goff, F.E., 1976, Preliminary geologic map and cross-section of the Clear Lake volcanic field, Lake County, California: U.S. Geol. Surv. Open-File Report 76-751, scale 1:24,000.
- Isherwood, W.F., 1981, Geophysical overview of the Geysers: in *McLaughlin, R.J., and Donnelly-Nolan, J.M.,*

- eds., Research in the Geysers-Clear Lake geothermal area, northern California: U.S. Geol. Surv. Prof. Paper 1141, p. 83-95.
- Iyer, H.M., Oppenheimer, D.H., Hitchcock, T., Roloff, J.N., and Coakley, J.M., 1981, Large teleseismic P-wave delays in the The Geysers-Clear Lake geothermal area: *in* McLaughlin, R.J., and Donnelly-Nolan, J.M., eds., Research in the Geysers-Clear Lake geothermal area, northern California: U.S. Geol. Surv. Prof. Paper 1141, p. 97-116.
- Johnson, C.M., and O'Neil, J.R., 1984, Triple junction magmatism: a geochemical study of Neogene volcanic rocks in western California: *Earth Planet. Sci. Letters*, v. 71, p. 241-262.
- Lachenbruch, A.H., and Sass, J.H., 1980, Heat flow and energetics of the San Andreas fault zone: *J. Geophys. Res.*, v. 85, p. 6185-6222.
- Liu, M., 1993, Thermal-Volcanic evolution in the California Coast Ranges: this volume.
- Liu, M., and Furlong, K.P., 1992, Cenozoic volcanism in the California Coast Ranges: numerical solutions: *J. Geophys. Res.*, v. 97, p. 4941-4951.
- Martignole, J., and Sisi, J.-C., 1981, Cordierite-garnet-H₂O equilibrium: a geological thermometer, barometer and water fugacity indicator: *Contrib. Mineral. Petrol.*, v. 77, p. 38-46.
- McLaughlin, J.R., 1981, Tectonic setting of pre-Tertiary rocks and its relation to geothermal resources in the Geysers-Clear Lake area: *in* McLaughlin, R.J., and Donnelly-Nolan, J.M., eds., U.S. Geol. Surv. Prof. Pap. 1141, p. 3-23.
- McLaughlin, J.R., and Ohlin, H.N., 1984, Tectonostratigraphic framework of the Geysers-Clear Lake Region, California: *in* Blake, M.C., Jr., ed., *Franciscan Geology of Northern California: Pacific Section S.E.P.M.*, v. 43, p. 221-254.
- Mooney, W.D., and Weaver, C.S., 1989, Regional crustal structure and tectonics of the Pacific Coastal States: California, Oregon, and Washington: *Geol. Soc. Am. Memoir* 172, p. 129-161.
- Patiño Douce, A.E., and Johnson, A.D., 1991, Phase equilibria and melt productivity in the pelitic system: implications for the origin of peraluminous granitoids and aluminous granulites: *Contrib. Mineral. Petrol.*, v. 107, p. 202-218.
- Pattison D.R.M., and Tracy, R.J., 1991, Phase equilibria and thermobarometry of metapelites: *in* Kerrick, D.M., ed., *Contact Metamorphism, MSA Reviews in Mineralogy*, v. 26, p. 105-206.
- Roeder, P.L., and Emslie, R.F., 1970, Olivine-liquid equilibrium: *Contrib. Mineral. Petrol.*, v. 29, p. 99-124.
- Schriener, A., and Suemnicht, G.A., 1981, Subsurface intrusive rocks at the Geysers geothermal area, California: *in* Silberman, M.L., Field, C.F., and Berry, A., eds., *Proceedings of the symposium on mineral deposits of the Pacific northwest, Corvallis, OR, U.S. Geol. Surv. Open-File Report* 81-355, p. 295-302.
- Speer, J.A., 1982, Metamorphism of the pelitic rocks of the Snyder Group in the contact aureole of the Kiglapait layered intrusion, Labrador: effects of buffering partial pressures of water: *Can. J. Earth Sci.*, v. 19, p. 1888-1909.
- Stimac, J.A., 1991, Evolution of the silicic magmatic system at Clear Lake, California from 0.6 to 0.3 Ma: unpublished Ph.D. thesis, Queen's University, Kingston, Canada, 399p.
- Stimac, J.A., Goff, F., and Glassley, W.E., 1992a, Crustal xenoliths in the Clear Lake Volcanics, California: Transformation of Franciscan Assemblage Rocks to Continental Crust?: *EOS*, v. 73(43), p. 505.
- Stimac, J.A., and Goff, F., and Hearn, B.C., Jr., 1992b, Petrologic considerations for hot dry rock geothermal site selection in the Clear Lake region, California: *Geothermal Resource Council Trans.*, v. 16, p. 191-198.
- Stimac, J.A., and Pearce, T.H., 1992, Textural evidence of mafic-felsic magmas interaction in dacitic lavas, Clear Lake, California: *Am. Mineral.*, v. 77, p. 795-809.
- Thompson, A.B., 1982, Dehydration melting of pelitic rocks and the generation of H₂O-undersaturated granitic liquids: *Am. J. Sci.*, v. 282, p. 1567-1595.
- Thompson, R.C., 1991, Structural stratigraphy and intrusive rocks at the Geysers geothermal field: *Geotherm. Res. Council Monograph on the Geysers Geothermal Field, Special Report No. 17*, p. 59-63.
- Unruh, J.R., and Moores, E.M., 1992, Quaternary blind thrusting in the Southwestern Sacramento Valley, Ca.: *Tectonics*, v. 11(2), p. 192-203.
- Vielzeuf, D. and Holloway, J.R., 1988, Experimental determination of the fluid-absent melting relations in the pelitic system: *Contrib. Mineral. Petrol.*, v. 98, p. 257-276.
- Wentworth, C.M., Blake, M.C., Jr., Jones, D.C., Walter, A.W., and Zoback, M.D., 1984, Tectonic wedging associated with emplacement of the Franciscan assemblage, California Ranges: *in* *Franciscan Geology of Northern California*, M.C. Blake, Jr., ed., *S.E.P.M., Pacific Section*, v. 43, p. 163-173.
- Wentworth, C.M., Zoback, M.D., 1990, Structure of the Coalinga area and thrust origin of the earthquake, *in* Rymer, M.J., and Ellsworth, W.L., eds., *The Coalinga California earthquake of May 2, 1983: U.S. Geol. Surv. Prof. Pap.* 1487, p. 41-67.
- Wilson, F.A., 1981, Preliminary investigation of accessory zircons from volcanic and sedimentary rocks from Clear

- Lake: in McLaughlin, R.J., and Donnelly-Nolan, J.M., eds., U.S. Geol. Surv. Prof. Pap. 1141, p. 251-259.
- Young, E.D., Anderson, J.L., Clarke, H.S., and Thomas, W.M., 1989, Petrology of biotite-cordierite-garnet gneiss of the McCullough Range, Nevada I. Evidence for Proterozoic low-pressure fluid-absent granulite grade metamorphism in the southern Cordillera: *J. Petrol.*, v. 30, p. 39-60.

CHEMICAL AND ISOTOPIC CONSTITUENTS IN THE HOT SPRINGS ALONG SULPHUR CREEK, COLUSA COUNTY, CALIFORNIA

J. Michael Thompson

U.S. Geological Survey, Menlo Park, California

ABSTRACT

Hot springs along Sulphur Creek in Colusa County, California, have been recognized for about 130 years. Several researchers have proposed that the hot spring fluid there is derived from mixing of "connate" or "evolved connate" water which is derived from ancient seawater deposited in the Mesozoic sedimentary rocks. This water, which is similar in composition to Complexion Spring, mixes with meteoric water to form Wilbur Springs and other hot spring waters along Sulphur Creek. A $\delta D - \delta^{18}O$ plot shows that Complexion Spring really does not plot along this trend; it must be isotopically modified to plot along the trend. Tuscan Springs, which is located 140 km NNE of Wilbur Springs, just NE of Red Bluff, has chemical and isotopic characteristics which are similar to the Sulphur Creek hot springs. Tuscan Springs vent from the Chico Formation of the Great Valley sequence and indicate that Tuscan Springs and Wilbur Springs are both derived from waters originating in the Great Valley sequence. Also $\delta^{11}B$ correlates well with Cl, δD and $\delta^{18}O$, which originate in the Great Valley sequence, suggesting a similar source for the higher $d^{11}B$ values. Chemical geothermometry of the Sulphur Creek hot springs indicates a reservoir temperature of ~ 180 °C. This temperature agrees with measured homogenization temperatures from fluid inclusion which range from 150 to 180 °C. The calculated cation geothermometer temperatures are affected by the presence of dissolved Mg, even though the concentrations appear low.

HOT SPRINGS HISTORY

Hot springs along Sulphur Creek (Fig. 1), Colusa County, in the Wilbur Springs Mining District, have been known for about 130 years. Many of these hot springs reportedly had adjacent resorts (Anderson, 1892). Guests were often referred to these accommodations by their doctors to treat or cure various medical conditions. The resorts consisted of a primary structure for cooking and serving meals, registration, small rooms and an office. Small nearby cabins were also built for housing complete families. Dr. Winslow Anderson, an advocate of spring-water therapy, visited this area in 1889 as part of his investigations on the mineral springs and health resorts of California (Anderson, 1892). According to Anderson (1892) springs in this area were good for treating chronic skin diseases and persistent rheumatism. In 1910, G. A. Waring also visited these hot springs as part of his investigations concerning the various types of springs in California (Waring, 1915). Their reports of these early researchers established a chemical and descriptive baseline for the hot-spring waters.

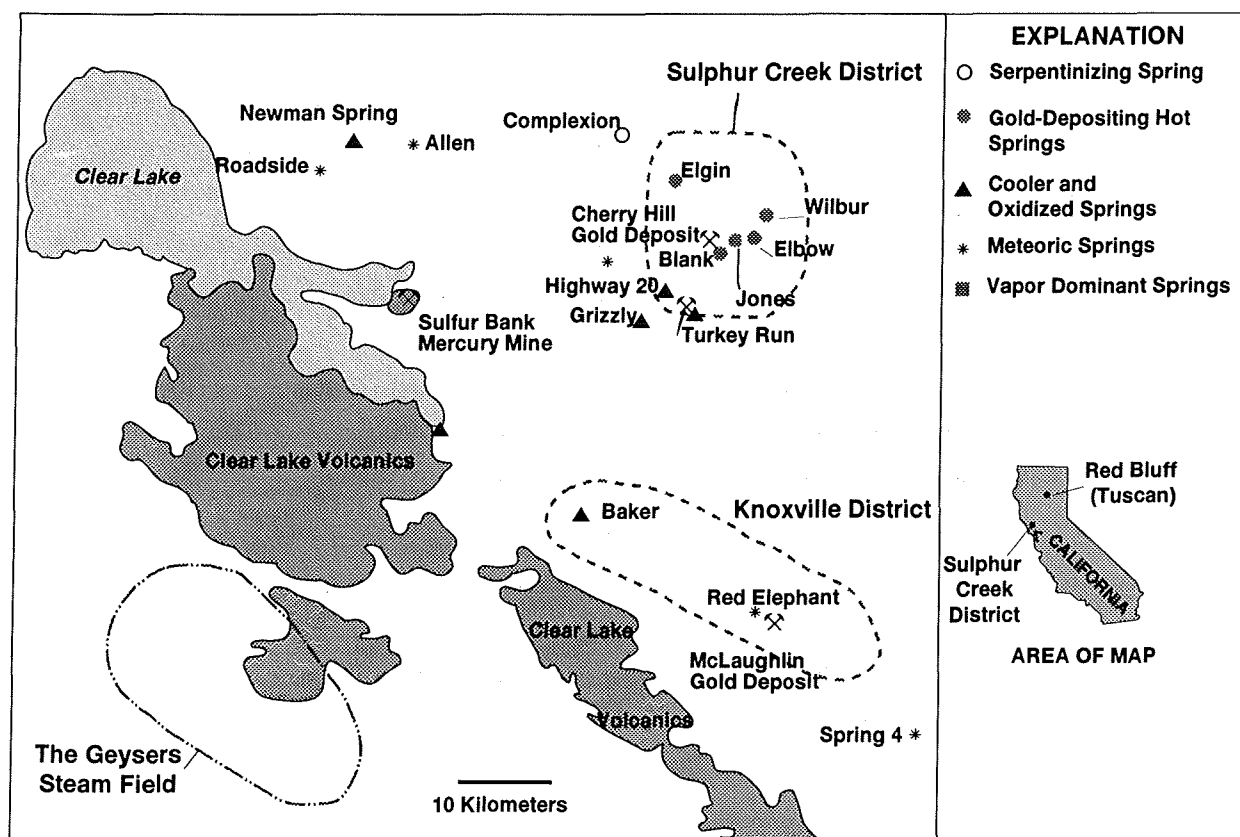


FIGURE 1. Location map of the Sulphur Creek District, The Geysers Steam Field, The Clear Lake Volcanics, the Sulfur Bank Mine and associated springs.

Waring (1915) reported that a small resort with two or three cabins had been constructed at Blank's Hot Spring. When the nearby Wide Awake (Wideawake according to Waring) mining shaft was sunk, the hot-spring discharge terminated and the resort closed. Later, after the mercury was mined out and the mining shaft abandoned and partially filled, the springs resumed flowing and are still flowing. This may be one of the oldest recorded effects of human development on the discharge of hot-spring water.

Waring (1915) also reported that there was a resort at Jones' Hot Spring. According to Waring (1915), the spring owners decided to drill a shallow well near where gas discharged. After completion, high volumes of saline water discharged from the well under artesian pressure. Directly above the well, the owners constructed a 4 m tall concrete tower. The associated gas and hot water caused the water to spurt up and flow down over the tower, giving the tower the name Jones' Fountain of Life. Today, some water still discharges from the ruins of the tower, but most of the water and gas discharge from a vent at the NE corner of the tower. This intermittent flow of water and gas from the Jones' Fountain of Life has been called "geysing" by some. However, because the water is flowing through a drilled well, this feature cannot be considered a true geyser. The so-called "geysing" is predictable: the interval ranges from 45 to 60 minutes and the duration is 15 to 20 minutes.

Where the water from Jones' Fountain of Life intersects Sulphur Creek, a small larvae about 5 cm long flourishes. Waring (1915) reported that these organisms were locally called "duck worms." Also, at the bottom of the discharge channel where the drainage intersects Sulphur Creek, cinnabar is depositing. According to Vincent Resh, University of California, Berkeley, the "Duck Worms" are the larval stage of the "Soldier Fly" (oral communication, 1993). These larvae are also found at Newman Springs, about 14 km NW of Jones' fountain of Life. The relatively high ratio of Mg:Ca and high Li concentrations are favorable for the growth of the "Duck Worm" (V. Resh, oral communication, 1993).

Anderson (1892) reported a chemical analysis of Wilbur Springs from the Wilbur Springs Resort. A fire occurred sometime between Anderson's visit in 1889 and Waring's visit in 1910 and destroyed the resort. Waring (1915) reported that the owners apparently decided not to rebuild on the original site but rather to move. They purchased Simmons Hot Springs, constructed a new resort, and changed the name to Wilbur Hot Springs. Thus the current Wilbur Springs location was described by Anderson (1892) as Simmons Hot Springs. The original Wilbur Springs is in the vicinity of the Elgin Mine hot springs, about 10 km up Sulphur Creek from the current Wilbur Springs. The Wilbur Springs resort is the only surviving hot spring resort and is now used for relaxation and recreation as well as for drug rehabilitation.

CHEMISTRY

Recently, numerous analyses of the Main Spring at Wilbur Springs and other hot springs along Sulphur Creek (for example, Blank's Spring, Elgin Mine springs and Jones' Fountain of Life) have been published (White, Hem and Waring, 1963; Berkstresser, 1968, White, Barnes and O'Neil, 1973; Thompson, 1979; Thompson and others, 1981; Peters, 1990, 1991; and Goff and others, 1993).

Analyses of the hot-spring water indicates that it has a salinity about half that of sea water (Table 1), but it is depleted in Mg (~40 mg/L), Ca (~1 mg/L), and SO_4 (~400 mg/L) compared to a sea water analysis reported in Hem (1989). The water is also enriched in HCO_3 (~4000 mg/L), Li (~12 mg/L), I (~20) and SiO_2 (~160 mg/L) compared to sea water. Additionally, the Sulphur Creek hot-spring waters are unusually high in dissolved H_2S (~150 mg/L), NH_3 (~100 mg/L) and B (~200 mg/L). White and others (1963) considered these "spring waters similar in composition to oil-field brines of the sodium-chloride type." The most likely source of the H_2S , NH_3 , B, and I is thermal decomposition of marine sediments. The H_2S , NH_3 and some CO_2 may originate from decomposition of organic matter in the sediments. The sedimentary constituents are probably derived from the Great Valley sequence to the east.

Peabody (1989) described the occurrence of petroleum throughout Wilbur Springs District and its chemical composition. The presence of steranes in the petroleum demonstrated that the source was from a "marine environment of deposition" (Peabody, 1989, p. 122) and that the distribution of alkylated naphthalenes and phenanthrenes indicated the petroleum to be fairly mature. The chemical data on the petroleum indicate that the petroleum was "generated from relatively immature organic matter in response to a heating event of short duration". This short heating event may have been the emplacement of basaltic andesite about 2 Ma (Hearn and others, 1981,

Table 1. Chemical Analyses of spring waters in the vicinity of Sulphur Creek; constituents in mg/L

name	date	latitude	longitude	temp	pH	Eh meas.	Eh. calc.	SiO ₂	Al	Fe(T)	Fe(II)	Fe(III)	Mn	As	Ca	Mg	Sr	B
Cold Saline Waters																		
Complexion Spring ¹	19-Mar-70	39°10.2'	122°31.2'	10	12.1	nr		24	na	na	na	na	na	na	0.7	0.8	na	na
Complexion Spring ²	15-Aug-78	39°10.2'	122°31.2'	19	11.3	nr		31	na	na	na	na	0.01	0.7	0.55	0.1	1.0	1.9
Complexion Spring ³	Aug-87	39°10.2'	122°31.2'	17	11.2	-0.241		1	na	na	na	na	na	na	0.5	0.1	na	na
Complexion Spring ⁴	9-Mar-91	39°10.2'	122°31.2'	9	10.8	nr		15	na	na	na	na	na	0.5	3.7	22.9	0.5	na
sea water ⁵	nr	nr	nr	nr	nr	nr	na	6	0.001	.003	na	na	.002	0	410	1350	8	0.0
Hot Springs waters																		
Bailey Mineral Well ²	28-Jun-82	39°01.8'	122°25.8'	88	8.24	nr	na	277	na	na	na	na	.05	3.3	449	0.16	18	8.5
Bailey Mineral Well ²	29-Jun-82	39°01.8'	122°25.8'	nr	8.1	nr	na	308	na	na	na	na	.13	2.8	493	5.39	20	9.2
Blank's Spring ³	Aug-87	39°01.4'	122°26.0'	44	7	-0.418	na	174	na	na	na	na	na	na	4	77	na	na
Blank's Spring ²	5 Jun 92	39°01.4'	122°26.0'	44	7.86	-0.401	-0.630	119	na	.08	.06	.02	.01	1.6	3.0	44.5	5.4	na
Elbow Spring ³	Aug-87	39°02.1'	122°25.5'	62	8	-0.467	na	198	na	na	na	na	na	na	1	11.9	na	na
Elbow Spring ²	17 Sep 90	39°02.1'	122°25.5'	59	8.08	-0.024	-0.252	67.4	<.01	.07	na	na	.11	.5	1.2	3	1.4	1.0
Elgin Mine Spring ²	15-Feb-85	39°03.5'	122°28.5'	67	8.15	na	na	150	na	na	na	na	.04	na	4.16	24	1.4	10.3
Elgin Mine Spring ³	Aug-87	39°03.5'	122°28.5'	67	7.4	-0.461	na	234	na	na	na	na	na	na	4	26.7	na	na
Jone's Fountain of Life ²	7-Sep-88	39°02.0'	122°26.7'	56	7.72	na	na	78	.089	na	na	na	.06	na	2.23	31.3	1.2	2.1
Jone's Fountain of Life ³	Aug-87	39°02.0'	122°26.7'	58	7.7	-0.452	na	126	na	na	na	na	na	na	2	34	na	na
Jone's Fountain of Life ²	17-Sep-90	39°02.0'	122°26.7'	59	8.47	-0.308	na	85	<.01	na	na	na	.08	1.1	4.4	32.2	1.1	1.2
Jones' Fountain of Life ⁴	9-Mar-91	39°02.0'	122°26.7'	62	7.88	na	na	89	na	na	na	na	na	1.2	5.6	41	1.1	
Jone's Fountain of Life ²	5-Jun-92	39°02.0'	122°26.7'	56	7.96	na	-0.345	85	na	0.04	0.04	0.005	.01	1.6	3.7	23.4	3.0	6.0
Wilbur Main Spring ²	7-Sep-88	39°02.8'	122°25.3'	53	7.08	na	na	168	.126	na	na	na	.06	na	2.26	41.3	2	1.9
Wilbur Main Spring ³	Aug-87	39°02.8'	122°25.3'	54	7.3	-0.384	na	282	na	na	na	na	na	na	2	41.3		
Wilbur Main Spring ²	6-Jun-90	39°02.8'	122°25.3'	52	8.35	na	na	140	na	na	na	na	.05	.5	1.61	37.7	3.5	2.4
Wilbur Main Spring ⁴	9-Mar-91	39°02.8'	122°25.3'	56	7.68	na	na	199	na	na	na	na	na	12.2	5.6	54.8	2	
Wilbur Main Spring ²	5-Jun-92	39°02.8'	122°25.3'	58	7.95	-0.633	-0.28	185	na	0.08	0.04	0.04	.01	2.2	3.3	30.6	5.4	4.6
Tuscan Springs ⁶	14-Dec-55	40°14.5'	122°06.7'	29	8.4	na	na	15	.9	na	na	na	.3	na	19	17	13	na
Tuscan Springs ²	30-Jul-79	40°14.5'	122°06.7'	31	8.45	na	na	16	.4	na	na	na	.01	na	20	18.4	na	na
Mixed waters																		
Baker Soda Spring ³	nr	38°00.2'	122°29.8'	25	6.8	-0.009	na	58	na	na	na	na	na	na	100	316	na	na
Baker Soda Spring ⁴	7-Mar-91	38°00.2'	122°29.8'	21	7.34	na	na	88	na	na	na	na	na	0.7	92.6	279	2	na
Grizzly Spring ⁴	9-Mar-91	39°00.1'	122°29.9'	19	7.05	na	na	90	na	na	na	na	na	0.9	52.3	686	13	na
Hiway 20 Sulfur Spg ¹	30-Sep-76	39°01.0'	122°29.4'	23	7.57	na	na	24	na	na	na	na	.05	na	3.5	5	na	na
Newman Springs ⁴	12-Mar-91	39°11.9'	122°43.0'	30	7.25	na	na	179	na	na	na	na	na	1.4	154	529	3.7	na
Turkey Run Mine ¹	26-Jun-76	39°01.0'	122°26.4'	22	7.62	na	na	70	na	na	na	na	.25	na	21	770	na	na
Spring Four ³	nr	38°46.75'	122°16.5'	26	7.6	0.07	na	60	na	na	na	na	na	na	24	136	na	na
Cold Waters																		
Red Elephant Mine ³	nr	38°51.5'	122°24.0'	18	7.8	0.008	na	54	na	na	na	na	na	na	10	10.7	na	na
Roadside ³	nr	39°12.2'	122°43.0'	26	7.1	0.095	na	12	na	na	na	na	na	na	88	17	na	na
Wilbur cold (meteoric) ²	7-Sep-88	39°02.3'	122°25.2'	27	7.67	na	na	41	na	na	na	na	.01	na	8.6	196	0.1	0.6
Wilbur cold (meteoric) ²	5-Jun-92	39°02.3'	122°25.4'	nr	7.3	na	na	41	na	.07	.06	.01	.07	na	13	109	0.3	0.2

table 1 con't

table 1 con't

name	Na	K	Li	Rb	Cs	NH ₄	HCO ₃	SO ₄	Cl	F	B	Br	I	H ₂ S	δD	δ ¹⁸ O	δ ¹³ C	δ ¹¹ B	δ ³⁴ S	Cat.	An.	Bal. %
Cold Saline Waters																						
Complexion Spring	12000	305	na	na	na	20	1990	60	18200	na	210	na	na	na	6.2	2.22	na	na	na	586	692.92	-4.18
Complexion Spring	15100	329	0.8	0.44	0.8	33	1389	42	22370	0.17	23	98	48	<.05	-24	6.25	na	na	na	667.21	654.63	0.48
Complexion Spring	13600	586	8.3	na	na	128	1650	59	20600	2.3	22	60.7	42	na	11	3.8	na	8.72	na	614.88	609.45	0.22
Complexion Spring	11845	335	0.1	na	na	112	0	49	17260	0.14	17	56.2	na	na	2.8	2.25	na	na	na	532.09	487.86	2.17
sea water	10500	390	0.17	0.12	0	na	142	2700	19000	1.3	5	67	0.06		0	0	na	na	na	na	na	na
Hot Springs waters																						
Bailey Mineral Well	5470	457	2.75	1.26	1.75	1.2	324	84	9820	0.38	85	na	na	<.01	-12.5	8.1	na	na	na	272.5	284.07	-1.04
Bailey Mineral Well	5920	412	2.94	1.29	2.14	na	247	104	10110	0.33	99	na	na		-5	11.4	na	na	na	293.51	291.4	0.18
Blank's Spring	6900	469	8.3	na	na	220	6100	10	8200	1.3	173	22	16	212	-33	2.1	-1.85	na	4.7	332.05	331.56	0.04
Blank's Spring	7590	438	7.6	3	0.96	na	7090	27	9360	1.92	257	na	na	110	-26	3.8	na	na	na	346.25	380.89	-2.38
Elbow Spring	11000	510	13.8	na	na	230	8600	10	12800	0.2	324	37	23.1	294	-16	8.5	-2.45	7.8	4.7	507.28	502.23	0.25
Elbow Spring	9200	459.8		5.21	0.59	0.86	370	7382	182	11880	6.58	294	na	na	54.7	54.7	-14.6	9.03	na	433.51	460.23	-1.49
Elgin Mine Spring	8900	478	11.9	4.6	6.2	360	8270	90	11000	2.6	220	na	na	0.8	-16.4	6.06	-4.58	na	na	423.21	447.84	-1.41
Elgin Mine Spring	8970	508	13.2	na	na	340	7200	10	11300	1.7	216	34	23	na	-18	6.4	na	7.1	na	426.31	437.05	-0.62
Jones' Fountain of Life	9770	475	8.92	0.99	1.61	420	7470	112	11430	4.4	340	na	na	198	-20	6.5	-4.23	na	na	464.37	447.47	0.13
Jones' Fountain of Life	9400	510	13.9	na	na	290	7200	10	11300	1.7	281	34	17.3	258	-22	6.5	-0.01	na	4.9	442.9	437.0	3
Jones' Fountain of Life	9339	461	7.12	0.89	1.23	351	7113	168	10720	5.6	288	11.7	na	60.9	-22	7.5	na	na	na	441.38	422.76	1.08
Jones' Fountain of Life	9740	513	14	na	na	218	8250	170	11210	5.15	300	32.1	na	na	-22.6	6.99	na	na	na	454.54	455.23	-0.04
Jones' Fountain of Life	9450	461	10.9	2.12	1.35	na	7680	336	11500	2.68	269	na	na	56.6	-18	6.9	na	na	na	426.52	457.39	-1.75
Wilbur Main Spring	8520	452	8.25	0.93	1.5	290	6690	39	10310	2.5	312	na	na	40	-34	5	-4.86	na	na	402.93	401.41	0.09
Wilbur Main Spring	8500	430	11.8	na	na	250	6710	10	9930	1.5	259	27	17.5	248	-21	5	-1.5	na	5.1	399.78	390.36	0.6
Wilbur Main Spring	8420	359	11	0.99	1.36	121	6959	40	10651	3.9	296	na	na	125	-21	6.08	-5.8	9.5	na	386.91	415.53	-1.78
Wilbur Main Spring	8580	460	12.1	na	na	214	7375	157	10710	3.32	285	30.1	na	na	-25.2	6.01	na	na	na	403.37	426.42	-1.39
Wilbur Main Spring	8560	451	9.73	2.35	1.32	na	7060	14	11150	1.65	269	na	na	na	-20	6.3	na	na	na	387.96	430.6	-2.6
Tuscan Springs	7900	59	2	na	na	167	1370	0	11800	5	201	25.3	1.3	172	na	na	na	na	na	357.03	355.55	0.1
Tuscan Springs	7270	35.8	1.7	0.24	1.2	195	488	47	11420	5.7	178	23.7	na	100	-12.3	-9.78	na	na	na	330.71	331.39	-0.05
Mixed waters																						
Baker Soda Spring	2530	242	6	na	na	135	4090	70	2520	0.6	173	11.2	8.6	na	-37	-1.1	-1.3	-1.8	na	155.57	139.61	2.7
Baker Soda Spring	2600	207	6.25	na	na	138	4650	0	2985	0.52	171	11.1	na	na	-38.9	-1.6	na	na	na	154.51	160.45	-0.94
Grizzly Spring	2686	45	3.8	na	na	16.5	4845	12	3750	0.4	167	16.1	na	na	-36.5	0.14	na	na	na	178.49	185.46	-0.96
Hiway 20 Sulfur Spg	1550	34	0.53	na	na	na	498	7	2080	6.7	42	na	na	na	-55.85	-6.55	na	na	na	68.95	67.33	-0.6
Newman Springs	2340	54	22.6	na	na	86.2	5319	35	3181	0.37	336	11.8	na	na	-35.2	2.49	na	na	na	162.41	161.26	0.18
Turkey Run Mine	1064	34.8	1.68	na	na	na	2300	2390	1150	5.2	35	3.1	na	na	-53.5	-6.8	na	na	na	111.8	120.17	-1.8
Spring Four	193	16.8	1	na	na	na	850	22	198	0.6	40	0.5	0.4	na	-55	-7	na	na	na	21.35	20.01	1.63
Cold Waters																						
Red Elephant Mine	15	1	1	na	na	na	120	1	10	0.2	<10	<.1	0	na	-56	-7.4	na	na	na	2.2	2.27	-0.81
Roadside	30	1	1	na	na	na	360	14	10	0.2	<10	<.1	0	na	-61	-8.2	na	na	na	7.26	6.48	2.83
Wilbur cold (meteoric)	13	0.37	0.01	na	na	na	1110	9	28	0.03	0	na	na	na	-59	-8.4	-14.4	na	na	17.12	19.17	-2.83
Wilbur cold (meteoric)	37	1.31	0.01	na	na	na	687	42	33	0.08	2	na	na	na	-60.1	-4.7	na	na	na	11.25	13.06	-3.73

¹ Thompson and others, 1981; ² unpublished data of Thompson; ³ Peters, 1990; ⁴ Goff and others, 1993; ⁵ Hem, 1989; White and others, 1963.

Donnelly-Nolan and others, 1981) or perhaps a more recent intrusion as hypothesized by Donnelly-Nolan and others (1993). Peabody's work supports the concept of a marine origin for the hot-spring components.

Because of the relatively high concentrations of H_2S and NH_3 , the waters are considered to be reducing. The measured oxidation-reduction potentials (measured Eh's), using a Pt billet electrode and a Ag/AgCl reference electrode (a combination redox electrode), range from -0.200 to -0.400 V. Eh values can also be calculated from the activity ratio of Fe^{+2}/Fe^{+3} using the Nernst Equation. For ground water studies this is the more commonly used half cell versus the Standard Hydrogen Electrode (SHE). The Eh as determined from the iron couple ranges from + 0.100 to + 0.300 V which is clearly more oxidizing than that measured. Another redox couple which may be applicable is the H_2S/SO_4 couple. Using the computer program WATEQ (Ball and others, 1987) to calculate the redox value, this redox couple yields values ranging from -0.250 to -0.350 V, much closer to the measured value. Because the concentrations of H_2S and SO_4 are substantially higher than those for Fe(II) and Fe(III) and the calculated Eh values calculated from the H_2S/SO_4 couple are closer to those measured with a combination Pt electrode, the H_2S/SO_4 couple is probably controlling the redox state of the water.

The presence of high gas pressures in this area was first noted by Waring's (1915) report that the owners of Jones' Hot Spring drilled out a gas vent and encountered an artesian pressure significant enough to propel water out of the ground and into the air. Very little was known about the composition of the spring gases until Thompson (1979) published three analyses of Wilbur Spring gases. Nehring (1981) reported 11 gas analyses from the Clear Lake volcanic field west of Wilbur Springs, but did not report anything from this area. Recently, Goff and others (1993) reported the analyses of 9 springs and a shallow well near Borax Lake from throughout the Clear Lake volcanic field, including one from the Sulphur Creek area. For comparison Goff reported that seven of these samples were collected by two different procedures, the so-called "caustic" (Giggenbach and Goguel, 1988) and "water displacement" procedures. For the "water displacement" procedure, a glass funnel is filled with water which is then displaced by gas; the gas is then transferred into an evacuated 100 ml gas tube (W. C. Evans, oral communication, 1993). From the gas compositions in Table 2, Jones' Fountain of Life samples are observed to have high concentrations methane (~50 - 60 percent) compared to Wilbur Springs (~3 percent) despite the relative proximity of the two springs (~1 km). Jones' Fountain of Life has an interval which ranges from 45 to 60 minutes and a duration of 15 to 20 minutes. Perhaps this is the only methane powered intermittent spring or "geyser." Jones' Fountain of Life is also high in H_2 (~0.1 percent) compared to Wilbur Springs (<0.003 percent)

ISOTOPIC STUDIES

The origin of the Wilbur Springs-type fluid has been elusive. Because the Cl concentrations for the Sulphur Creek hot springs are about half that of sea water, many investigators have proposed that the water is derived from a diluted and modified sea water source (the "connate" water of White, 1957 and the "evolved connate" water of White and others, 1973 and Donnelly-Nolan and others, 1993). One spring having Cl concentrations slightly greater than sea water is Complexion Spring which is located 17.5 km NW of Jones' Fountain of Life. Barnes and others (1972) described the water at Complexion Spring as a serpentinizing fluid because 1) the fluid pH

Table 2. Composition of spring gases in percent.

Name	date	temp	CO ₂	H ₂ S	NH ₃	He	H ₂	Ar	O ₂	N ₂	CH ₄	C ₂ H ₆	total percent	Calc ⁴ Temp
			←----- vol % -----→											
Wilbur (main spg) ¹	11 Dec 77	nr	54.2	2.66	.622	nd	.000936	.319	4.19	29	2.36	nd	93.35	188
Wilbur (main spg) ¹	11 Dec 77	nr	69.3	2.94	0	nd	.00266	.217	1.26	18.8	3.33	nd	95.85	211
Wilbur (main spg) ¹	16 Aug 78	53	76.7	2.92	.0324	nd	.000108	.188	.634	15.1	3.28	nd	98.85	143
Jones' Fount. of Life ²	16 Aug 78	60	32.5	.001	.182	nd	.145	.0135	.104	2.95	60.4	nd	96.35	189
Jones' Fount. of Life ³	9 Mar 91	61.9	40.6	.369	.0024	nd	.0353	.0353	.0943	6.76	51.9	nd	99.84	227
Jones' Fount. of Life ³	9 Mar 91	61.9	47.2	0.6	nd	.0013	.108	.0118	.144	2.28	51.1	nd	101.39	266
Baker Soda Spring ³	12 Mar 91	21.3	98.9	.001	.0002	.0022	.001	.0062	.11	.392	.714	nd	100.01	122
Gas Spring ³	12 Mar 91	10.0	96.1	.001	.0003	nd	.001	nd	nd	2.81	1.107	nd	100.04	119
Grizzly Spring ³	9 Mar 91	19.4	98.3	.001	.00001	nd	.001	.0073	.292	.289	1.11	nd	100.01	119

¹ Thompson, 1979; ² previously unreported; ³ Goff and others, 1993; ⁴ D'Amore and Panichi (1980) equation.
nd, not detected; nr, not recorded

is high (~ 11); 2) the Ca and Mg concentrations are exceptionally low; 3) the SiO₂ concentration is low compared to other waters in the vicinity and also for a water of such a high pH; and 4) the deuterium and oxygen-18 values are high compared to meteoric water. Barnes and others (1972), Peters (1990), Donnelly-Nolan and others (1993), Fehn and others (1992) and Peters (1993) have proposed that the Wilbur Springs water-type is derived from a Complexion Spring water-type. However, the deuterium and oxygen-18 values for Complexion Spring do not plot along the same trend as Wilbur Springs and other springs along Sulphur Creek (Fig. 2). Even if Wilbur Springs is considered to be derived from Complexion Springs by dilution with meteoric water, the ammonia, boron and hydrogen sulfide concentrations in Complexion Spring are substantially lower than those in Wilbur Springs, the opposite of what is expected.

A spring water that appears to be a better match, both chemically and isotopically, to Wilbur Springs is Tuscan Springs. Tuscan Springs, which are located just NE of Red Bluff, California, approximately 140 km NNE of Wilbur Springs, discharge through sediments of the Chico Formation and have deuterium and oxygen-18 values that plot on the trend for Sulphur Creek hot springs (Fig. 2). Additionally, Tuscan Springs have similar concentrations of H₂S, NH₃, B and Cl (Table 1). Perhaps the Sulphur Creek hot-spring water originates in the Great Valley sequence, rather than from anything immediately adjacent to Sulphur Creek. The difference in spring orifice temperature, which ranges from about 20 to 40 °C, or deep aquifer temperature, may account for some of the slight differences in water chemistry.

As can be observed from Table 1, the concentration of boron is unusually high in the Sulphur Creek hot spring waters. Peters (1990) and Donnelly-Nolan (1993) have shown that plots of chloride versus boron for these waters are linear. Additionally, Peters (1990) reports seven $\delta^{11}\text{B}$ values and here two more, determined by Tom Bullen, USGS, are reported (Table 1). The $\delta^{11}\text{B}$ values reported for the Sulphur Creek hot springs range from +7.1 to +9.5. The value reported by Peters for Allen springs (+17.8) seems unusually high for springs from this area (about twice as high as Complexion Spring, $\delta^{11}\text{B}=+8.7$) and will be neglected here because the values are unusually elevated compared to other springs in the area and because the B concentrations are low. Bassett (1990) suggested that low total boron concentrations may affect the determination of $\delta^{11}\text{B}$ values; samples with low boron concentrations apparently have falsely high $\delta^{11}\text{B}$ values. Plots of $\delta^{11}\text{B}$ values correlate well with chloride concentrations and $\delta^{18}\text{O}$ and dD values (Figs. 2, 3 and 4) and inversely with magnesium concentration (Fig. 6). Because the $\delta^{11}\text{B}$ correlates so well with Cl, $\delta^{18}\text{O}$ and dD, the B is presumed to originate in the Great Valley sequence. The elevated magnesium in the Sulphur Creek springs apparently arises from near-surface dissolution of serpentine in a high CO₂ environment. Thompson and others (1992) described similar reactions for the Konocti Bay fault zone on the west side of Clear Lake. From Figure 5, as the magnesium concentration increases by the dissolution of serpentine, any boron thus liberated apparently contributes low $\delta^{11}\text{B}$ values. However, for serpentine Peters (1990) report two $\delta^{11}\text{B}$ values: +8.8 and +31.5. Although the reported error for the two values is ± 0.5 , the boron concentrations are low; .005 to .01 mol/kg (Peters, 1990). Again, low B concentration values seem to affect the isotopic value (Bassett, 1990).

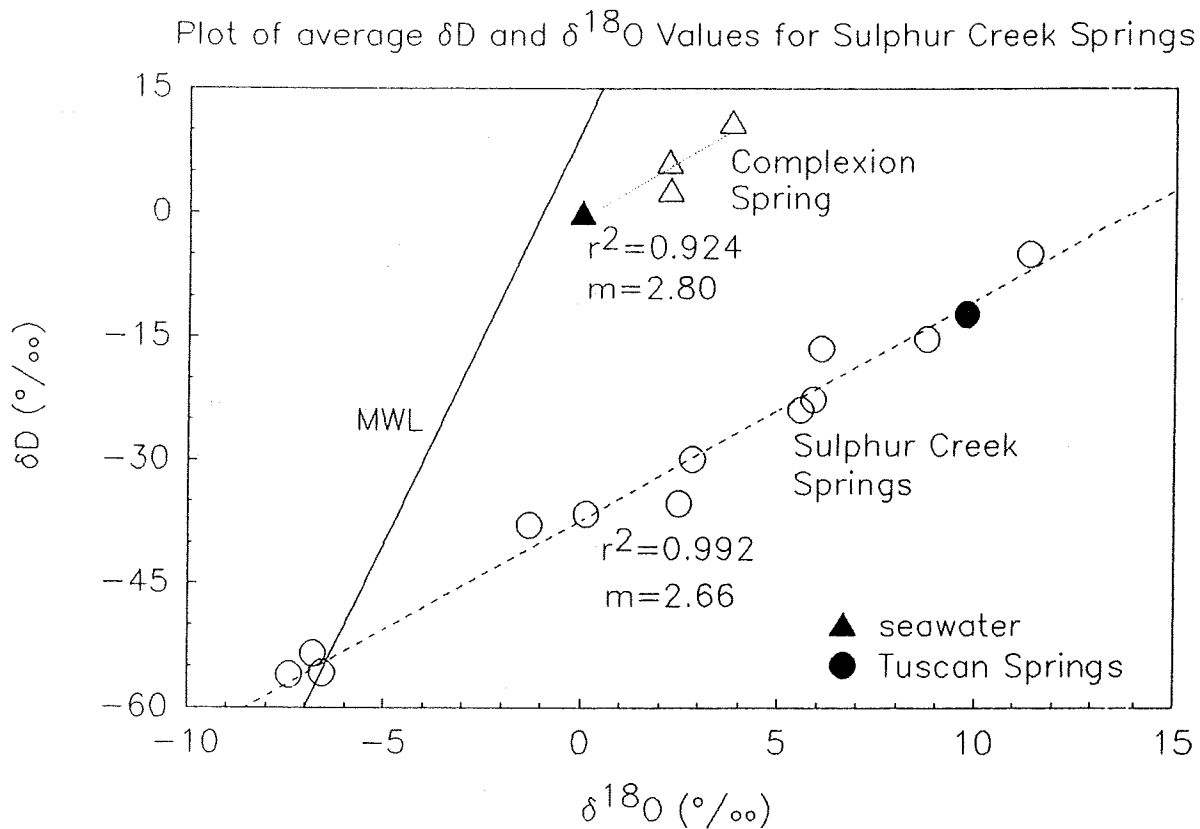


FIGURE 2. Plot of average δD and $\delta^{18}O$ values for Sulphur Creek Springs.

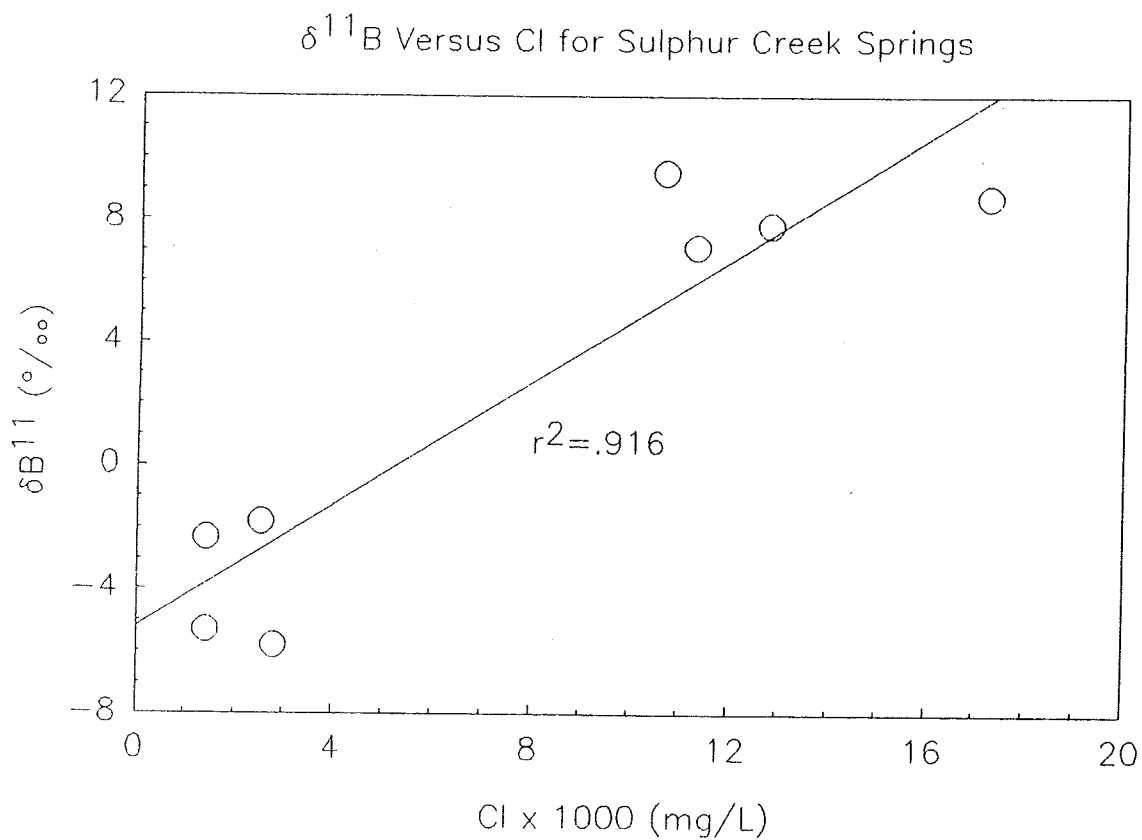


FIGURE 3. Plot of $\delta^{11}B$ values versus Cl concentration for Sulphur Creek Springs.

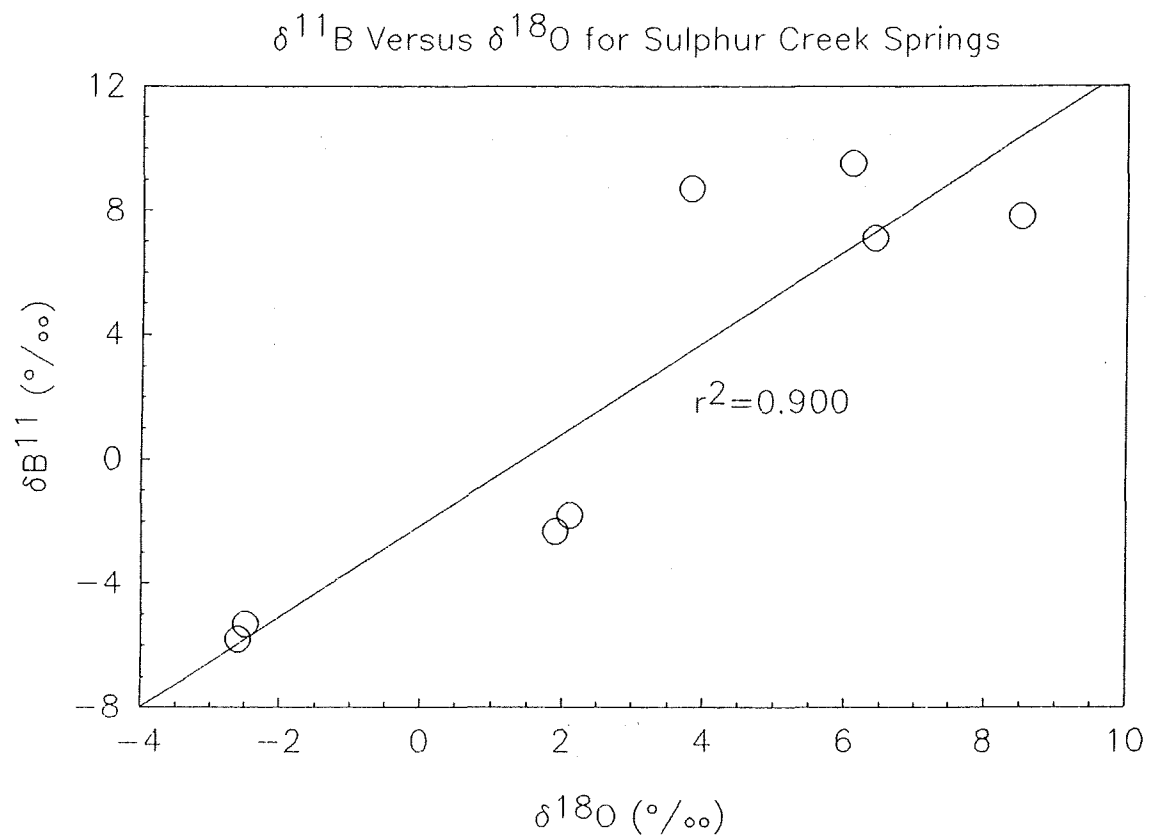


FIGURE 4. Plot of $\delta^{11}\text{B}$ values versus $\delta^{18}\text{O}$ values for Sulphur Creek Springs.

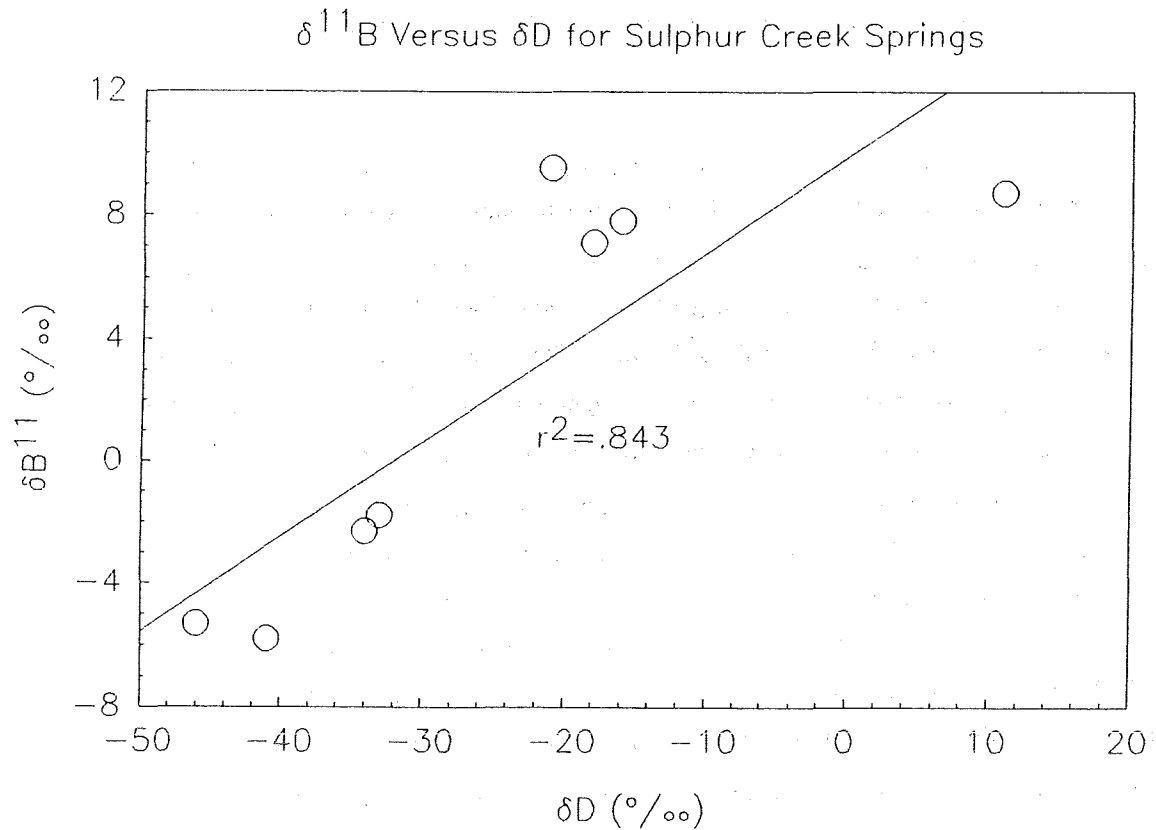


FIGURE 5. Plot of $\delta^{11}\text{B}$ values versus δD values for Sulphur Creek Springs.

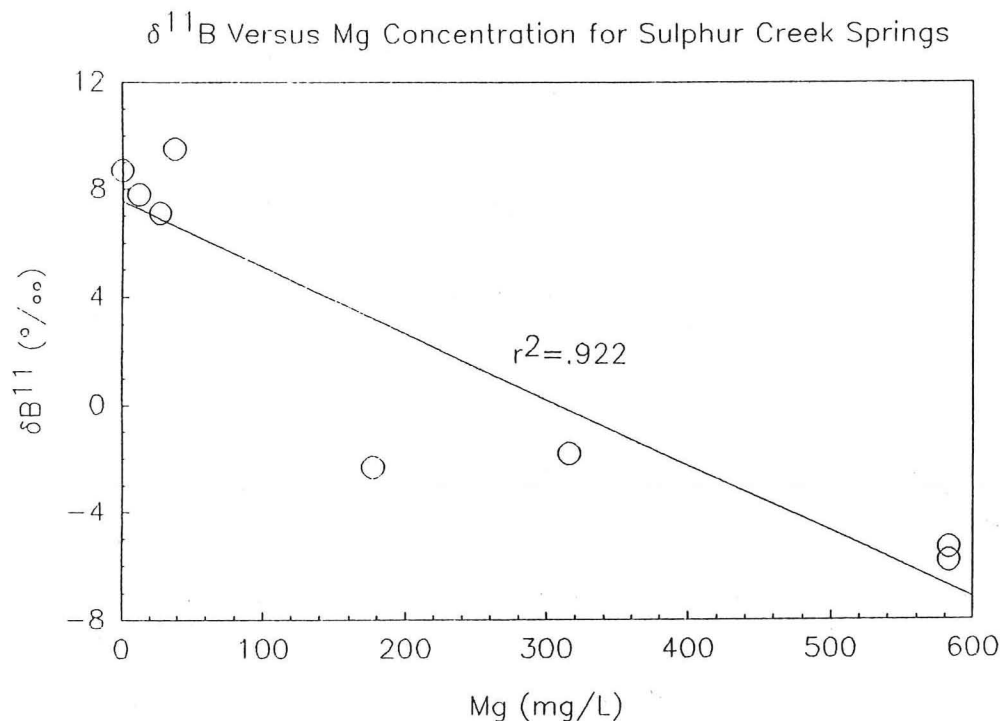


FIGURE 6. Plot of $\delta^{11}\text{B}$ values versus Mg concentration for Sulphur Creek Springs.

The carbon-13 values for the hot springs along Sulphur Creek appear heavy for volcanically heated hot springs. Peters (1993) suggested that the source of the HCO_3^- may be marine carbonate, but allow that some of it may be magmatic. The $\delta^{13}\text{C}$ values range from -5.8 to -1.85 (Table 1). Assuming no mixing effects, Barnes (1984) reported that $\delta^{13}\text{C}$ on mantle derived CO_2 ranges from -8.1 to -4.7 and Craig (1958) reported that $\delta^{13}\text{C}$ on marine limestones range from -4 to +3. Because the $\delta^{13}\text{C}$ from HCO_3^- over-laps the ranges of these two different sources of carbon, mixing of carbon sources is indicated. The light source of $\delta^{13}\text{C}$ may be mantle derived CO_2 having a $\delta^{13}\text{C}$ value of -7 or perhaps CO_2 arising from the oxidation of the locally abundant petroleum which may have a $\delta^{13}\text{C}$ value near -20. The heavy source is more equivocal. Two ranges seem possible: any value suggested by Craig for marine limestone or values determined by Oscarson and others (1992) for carbonates from the Warnick Canyon, just east of Sulphur Creek, may be used. Recently, Oscarson and others (1992) reported $\delta^{13}\text{C}$ values on HCO_3^- from those spring waters ranges from +5.6 to +8.4, with a mean of +7.1. The mean value for $\delta^{13}\text{C}$ on HCO_3^- from the Sulphur Creek hot springs is -4.0. If the end members $\delta^{13}\text{C}$ values are mantle CO_2 at -7.0 and carbonate carbon at +7.1, then the amount of mantle CO_2 is estimated to be ~80 percent. If the source of the lighter carbon is petroleum, then the amount of lighter carbon is estimated to be ~40 percent. Because the hot spring fluid

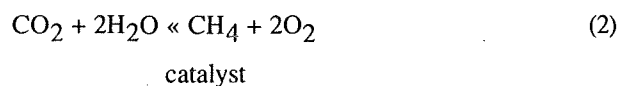
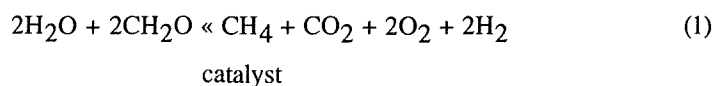
is so reducing, oxidation of petroleum to form CO₂ does not seem likely. Thus mantle derived CO₂ may account for 80 percent of the CO₂ in the Sulphur Creek hot springs.

ESTIMATED RESERVOIR TEMPERATURE

Just as the origin of the hot spring fluid for hot springs along Sulphur Creek has been controversial, the deep reservoir temperature is also uncertain. White and others (1973) reported the deep temperature to range from 200 to 350 °C based on a oxygen-18 equilibration between sediments and water. Muffler and others (1978) reported the reservoir for the Sulphur Creek area to be about 150 °C. Using the Na-K and the Na-K-Ca geothermometers, Thompson (1979) reported the reservoir temperature to be at least 220 °C. Sun Energy Development Company (Sunedco) drilled the Bailey Mineral No. 1 well near Blank's Spring in 1980. According to Ed Western (oral communication, 1982) of Sunedco, maximum measured temperatures in the well were near 180 °C. These correspond fairly well with the fluid inclusion temperature measurements reported by Thordsen (1988) for the nearby Manzanita mine.

As discussed by Thompson and others (1992), magnesium concentrations arising from serpentine dissolution readily influence the calculation of the reservoir temperature. Table 3 shows the indicated temperatures using various cation and silica geothermometers. Figure 7 shows a ternary plot of Na-K-Mg of Giggenbach (1988) as modified by Fournier (1990). Such a plot indicates that water collected from the Bailey Mineral No.1 well in 1982 was in approximate temperature equilibrium with common rock-forming minerals at 180 °C. The plot also indicates that the highest temperature spring water should be found in the vicinity of the Elgin mine. The cation geothermometers that indicate the "best" calculated temperature compared to fluid inclusion homogenization temperatures are the Na-Li (Kharaka and Mariner, 1990), the Mg-Li (Kharaka and Mariner, 1990) and the K-Mg (Giggenbach, 1988) geothermometers.

Estimated temperatures based on gas composition (Table 2) using the equation by D' Amore and Panichi (1980) range from 143-211 °C at Wilbur Springs to 189 -266 °C at Jones' Fountain of Life. The high concentrations of methane at Jones' Fountain of Life, which is usually an indication of a cooler environment, is more than compensated by the 50x increase in hydrogen. The increase in hydrogen and methane may be caused by the reactions:



and

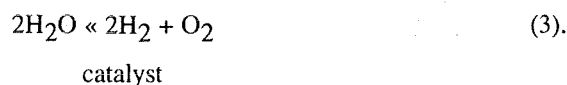


Table 3. Calculated geothermometer temperatures in °C for hot springs in the vicinity of Sulphur Creek; same source as table 1; geothermometer equations from Fournier (1992); Cond, Conductive Quartz, Ad Qtz, Adiabatic Quartz; Chal, Chalceony; α -crist, α cristobalite; β crist, β cristobalite; amor. SiO₂, amorphous silica; Qtz temp, silica geothermometer; T, Truesdell, F&T, Fournier and Truesdell, F, Fournier; G, Giggenbach; β 1/3 and β 4/3 Na-K-Ca geothermometer; F&M, Fouillac and Michard; K&M, Kharaka and Mariner.

name	temp meas	Cond Qtz	Ad Qtz	Chal	α crist	β crist	amor SiO ₂	Qtz temp	T	F&T	F	A	G	1/3	4/3	R	F&M Na-Li	K&M Na-Li	G K-Mg	K&M Mg-Li
Hot Saline Waters																				
Bailey Mineral Well	88	203	187	186	155	105	79	204	168	164	202	177	218	207	262	0.02	43	117	289	201
Bailey Mineral Well	nr	211	194	196	163	113	87	213	151	145	188	161	205	197	251	0.59	43	116	193	137
Blank's Spring	44	171	161	148	121	71	48	171	148	143	186	159	203	251	715	14	87	157	147	127
Blank's Spring	44	147	141	122	97	48	26	147	134	128	174	145	192	245	756	9.17	77	148	154	133
Elbow Spring	62	179	168	158	130	80	56	180	116	109	159	128	178	251	1144	2.28	89	159	185	179
Elbow Spring	58.9	116	115	88	66	18	-2	117	122	115	164	134	182	250	1008	0.65	49	122	211	168
Elgin Mine	67	161	153	137	111	61	39	161	128	121	169	139	187	239	735	4.74	93	162	169	160
Elgin Mine	67	191	177	172	142	92	67	192	133	126	173	143	191	244	760	4.96	98	167	169	161
Jones' Fountain of Life	56	124	121	96	73	25	5	124	120	113	162	131	181	242	869	6.15	72	143	163	145
Jones' Fountain of Life	58	151	144	125	100	51	29	151	129	122	170	140	188	250	916	6.23	99	167	165	159
Jones' Fountain of Life	58.6	128	125	100	77	29	9	128	121	114	163	133	182	234	720	6.47	63	135	162	136
Jones' Fountain of Life	61.9	131	127	103	80	32	11	131	127	120	168	138	186	237	710	7.33	97	166	161	156
Jones' Fountain of Life	55.6	128	125	100	77	29	9	128	120	113	162	132	181	236	752	4.79	84	155	168	157
Wilbur Main Spring	53	168	159	146	118	69	45	169	127	120	168	138	186	245	834	8.33	75	146	156	137
Wilbur Main Spring	54	205	188	188	156	106	80	206	123	116	165	134	183	243	844	8.73	95	164	155	149
Wilbur Main Spring	52	157	149	133	107	57	35	157	110	102	153	122	172	233	831	9.46	91	161	150	149
Wilbur Main Spring	55.6	180	168	158	130	80	56	180	128	121	169	139	187	235	673	10.53	96	165	152	145
Wilbur Main Spring	58.3	175	164	153	125	75	51	175	127	120	168	138	186	240	758	6.31	83	154	162	148
Mixed waters																				
Baker Soda Spring	25	109	109	80	59	11	-8	109	182	179	213	190	229	215	270	48.02	129	194	104	97
Baker Soda Spring	21.3	130	127	103	80	31	11	130	163	159	198	173	215	205	263	48.22	130	195	101	100
Grizzly Spring	19.4	131	128	104	81	32	12	132	51	41	100	64	121	131	189	87.58	96	165	54	76
Hiway 20 Sulfur Spg	23	70	75	39	21	-24	-40	71	66	56	114	79	135	155	279	11.76	28	101	107	88
Newman Springs	29.5	173	162	150	123	73	49	173	69	60	117	82	138	135	158	71.75	260	296	61	128
Turkey Run	22	118	117	90	68	20	0	118	91	82	137	103	156	154	191	93.24	103	171	47	56
Spring Four	26	111	110	81	60	13	-7	111	172	168	205	181	221	174	124	76.92	193	246	50	63

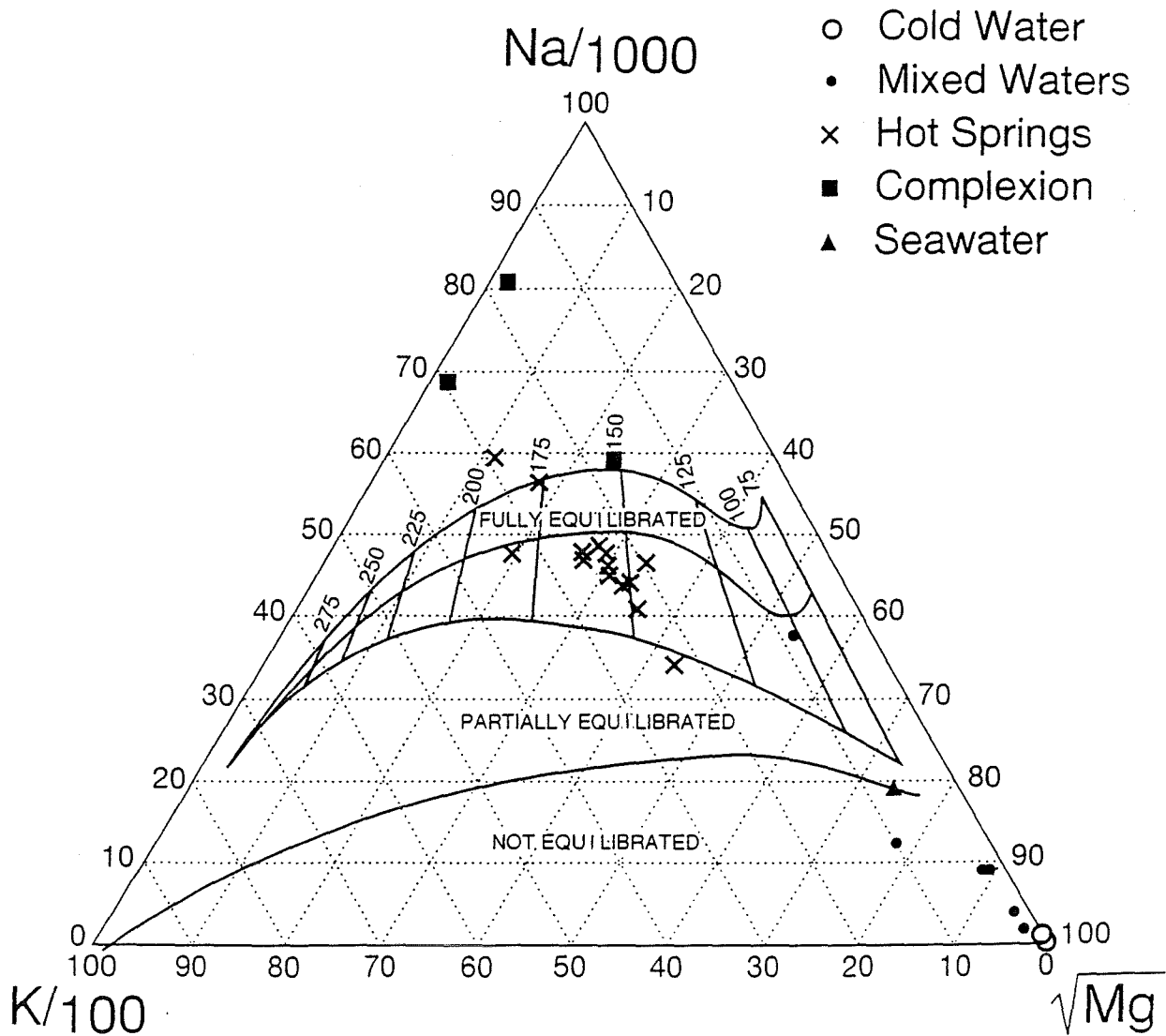


FIGURE 7. A ternary Giggenbach (1988) plot as modified by Fournier (1990) for Sulphur Creek Springs showing that the maximum temperature is near 180 °C.

Equation 1 is the decomposition of general organic matter (a simple sugar) in the presence of heat and some catalyst to form some of the gases found at Wilbur Springs and Jones' Fountain of Life. Equation 2 is a synthetic reaction to make methane from water and CO₂. Equation 3 is the breakdown of water at some elevated temperature in the presence of a catalyst. Without a catalyst, the breakdown will not occur at Eh's below about 1.23 V which are too negative for the conditions here. As mentioned previously NH₄ and H₂S probably arise from the decomposition of organic sediments. Specifically, these components arise from the decomposition of amino acids, liberating CO₂ and NH₄, and the hydrolysis of disulfide linkages and decomposition of various thiol compounds, leading to mercaptans and H₂S.

From the principle of Le Châtelier, the potential driving force of these reactions is the formation of metal oxides: the amount of oxygen in the spring gases at Wilbur Springs (~ 1 percent) is more than that at Jones' Fountain of Life (0.1 percent). Thus any molecular oxygen generated at Jones' by any of these reactions is immediately used to oxidize a yet-to-be-identified metal which precipitates as the oxide from solution. Because the Eh values appear to be more oxidizing at Jones' Fountain of Life (-0.2 to 0.0 V) than at Wilbur Springs (-0.4 to -0.1 V), such reactions may be occurring. However, for the only year in which data are available for Fe(II) and Fe(III), the data suggest that Jones' Fountain of Life is a more reducing environment than Wilbur Springs. More analyses for Fe(II), Fe(III), H₂S and SO₄ and more direct Eh measurements may help solve this ambiguity.

CONCLUSIONS

The hypothesis that Wilbur Spring type fluid is derived from a Complexion Springs type fluid may be in error. A sample of Tuscan Springs water, a chemically and isotopically similar spring located NE of Red Bluff, plots along the trend for the Sulphur Creek hot springs. This observation suggests that whatever the source of the H₂S, NH₃, B and Cl is to the Sulphur Creek hot-spring water, it must also contribute to Tuscan Springs. Tuscan Springs is discharging from the Chico Formation member of the Great Valley sequence. Thus the Wilbur Springs water type must also originate in the Great Valley sequence. High concentrations of NH₃, CO₂, H₂S and B suggest that these species originated from marine sediments. This is supported by analyses of the petroleum which also suggests that the petroleum matured rapidly from marine sediments. Plots of $\delta^{11}\text{B}$ correlate well with Cl, $\delta^{18}\text{O}$ and δD which suggests a marine origin for the B.

The amount of magnesium in these waters, although relatively low, is sufficient to cause an affect on the calculated reservoir temperatures using the Na-K and Na-K-Ca geothermometers. The Mg-Li and K-Mg geothermometers indicate temperatures similar to those found in drill-holes. Homogenization temperatures from fluid inclusions are substantially less than either the Na-K-Ca or Na-K geothermometers predicted. A ternary Mg-Na-K plot indicates that the highest temperatures present should be near 180 °C. This temperature agrees with homogenization temperature of fluid inclusions for this area. The highest predicted temperatures are in the vicinity of the Elgin Mine (the original Wilbur Springs). At Jones' Fountain of Life, gas geothermometry, although limited, indicates that maximum temperatures are near 220 °C. The abundance of reduced gases such as CH₄, NH₃

and H₂ in Jones' Fountain of Life, particularly H₂, suggests that elevated rates of organic decomposition are occurring there. Formation of significant H₂ affects the temperature calculation.

ACKNOWLEDGMENTS

Numerous colleagues at the USGS and elsewhere made this report possible. I especially thank Bill Carothers, Julie Donnelly-Nolan, Fraser Goff, Kirstin Peters, Jim Thordsen, and Al Waibel for numerous discussions. I thank Julie Donnelly-Nolan and Jim Rytuba for critical reviews.

REFERENCES

- Anderson, 1892, Mineral springs and Health Resorts of California: The Bancroft Company, San Francisco, 384 p.
- Ball, J. W., Nordstrom, D. K., and Zachman, D. W., 1987, WATEQ4F--A personal computer FORTRAN translation of the geochemical model WATEQ2 with revised data base: U.S. Geological Survey Open-File Report 87-50, 108 p.
- Barnes, I., 1984, Volatiles of Mount St. Helens and their origins: *Journal of Volcanology and Geothermal Research*, v. 22, p. 133-146.
- Barnes, I., Rapp, J. B., and O'Neil, J. R., 1972, Metamorphic assemblages and the direction of flow of metamorphic fluids in four instances of serpentinization: *Contributions to Mineralogy and Petrology*, vol. 35, p. 263-276.
- Bassett, R. L., 1990, A critical evaluation of the available measurements for the stable isotopes of boron: *Applied Geochemistry*, v. 5, p. 541-554.
- Berkstresser, C. F., Jr., 1968, Data for springs in the northern Coast Ranges and Klamath Mountains of California: U.S. Geological Survey Open-File Report, October 1968, 49 p.
- Brook, C. A., Mariner, R. H., Mabey, D. R., Swanson, J. R., Guffanti, M., and Muffler, L. J. P., 1979, Hydrothermal convection system with reservoir temperatures ≥ 90 °C in Muffler, L. J. P. (editor) *Assessment of Geothermal Resources of the United States--1978*: U.S. Geological Survey Circular 790, p. 64.
- Craig, H., 1958, The geochemistry of the stable carbon isotopes: *Geochimica et Cosmochimica Acta*, v. 3, p. 53-92.
- D' Amore, F. and Panichi, C., 1980, Evaluation of deep temperatures of hydrothermal systems by a new gas geothermometer: *Geochimica et Cosmochimica Acta*, v. 44, p. 549-556.
- Donnelly-Nolan, J. M., Hearn, B. C., Curtiss, G. H., and Drake, R. E., 1981, Geochronology and evolution of the Clear Lake Volcanics in R. J. McLaughlin and J. M. Donnelly-Nolan (editors), *Research in the Geysers-Clear Lake Geothermal Area, northern California*: U.S. Geological Survey Professional Paper 1141, p. 47-60.
- Donnelly-Nolan, J. M., Burns, M. G., Goff, F. E., Peters, E. K., and Thompson, J. M., 1993, The Geysers-Clear Lake area, California: Thermal waters, mineralization, volcanism, and geothermal potential: *Economic Geology*, v. 88, p. 301-316.
- Fehn, U., Peters, E. K., Tullai-Fitzpatrick, S., Kubik, P. W., Sharma, P., Teng, R. T. D., Gove, H. E., and Elmore, D., 1992, ¹²⁹I and ³⁶Cl concentrations in waters of the eastern Clear Lake area, California, residence times and source ages of hydrothermal fluids: *Geochimica et Cosmochimica Acta*, v. 56, p. 2069-2079.
- Fournier, R. O., 1990, The interpretation of Na-K-Mg relations in geothermal waters: *Geothermal Resources Council Transactions*, v 14, p. 1421-1425.
- Giggenbach, W. F., 1988, Geothermal solute equilibria. Derivation of Na-K-Mg-Ca geoindicators: *Geochimica et Cosmochimica Acta*, v. 52, p. 2749-2765.
- Giggenbach, W. F., and Goguel, R. L., 1988, Collection and analysis of geothermal and volcanic water and gas samples: Department of Scientific and Industrial Research, Petone, New Zealand, p. 37-51.
- Goff, F. E., Adams, A. I., Trujillo, P. E., Counce, D., and Mansfield, J., 1993, Geochemistry of thermal/mineral waters in the Clear Lake Region, California, and implications for Hot Dry Rock Geothermal Development: Las Alamos National Laboratory Report LA-12510-HDR, 23 p.
- Hearn, B. C., Jr., Donnelly-Nolan, J. M., and Goff, F. E., 1981, The Clear Lake Volcanics: Tectonic, setting and magma sources in R. J. McLaughlin and J. M. Donnelly-Nolan (editors), *Research in the Geysers-Clear Lake Geothermal Area, northern California*: U.S. Geological Survey Professional Paper 1141, p. 25-45.

- Hem, J. D., 1989, Study and interpretation of the chemical characteristics of natural water, Third Edition: U.S. Geological Survey Water-Supply Paper 2254, 264 p.
- Kharaka, Y. K., and Mariner, R. H., 1989, Chapter 6, Chemical geothermometers and their application to formation waters from sedimentary basins *in* Naeser, N. D., and McCulloh, T. H., (editors) Thermal History of Sedimentary Basins: Springer-Verlag, New York, p. 99-117.
- Nehring, N. L., 1981, Gases from springs and wells in the Geysers-Clear Lake area *in* R. J. McLaughlin and J. M. Donnelly-Nolan (editors), Research in the Geysers-Clear Lake Geothermal Area, northern California: U.S. Geological Survey Professional Paper 1141, p. 205-209.
- Oscarson, R. L., Presser, T. S., and Carothers, W. W., 1992, Ca-Mg carbonate deposits, Warnick Canyon, Colusa County, California: U. S. Geological Survey Open-File Report 92-707, 32 p.
- Peabody, Carey Evans, 1989, Association of petroleum and cinnabar in mercury deposits of the California Coast Ranges, USA: Ph.D. Dissertation for Stanford University, 256 p.
- Peters, Elsa Kirsten, 1990, The aqueous geochemistry of the Clear Lake Area, Northern California, and its implications for hot spring gold deposits: Harvard University Ph.D. Dissertation, 237 p.
- Peters, E. K., 1991, Gold-bearing hot springs systems of the northern coast ranges, California: Economic Geology, v 86, p. 1519-1528.
- Thompson, J. M., 1979, A reevaluation of the geothermal potential of the Wilbur Hot Springs area, California: Geothermal Resources Council Transactions, vol. 3, 729-731.
- Thompson, J. M., Goff, F. E., and Donnelly-Nolan, J. M., 1981, Chemical analyses of waters from springs and wells in the Clear Lake Volcanic area *in* R. J. McLaughlin and J. M. Donnelly-Nolan (editors), Research in the Geysers-Clear Lake Geothermal Area, northern California: U.S. Geological Survey Professional Paper 1141, p. 183-191.
- Thompson, J. M., Mariner, R. H., White, L. D., Presser, T. S., and Evans, W. C., 1992, Thermal waters along the Konocti Bay fault zone, Lake County, California: a reevaluation: Journal of Volcanology and Geothermal Research, v. 53, p167-183.
- Thorsden, James Joseph, 1988, Fluid inclusion and geochemical study of epithermal gold mineralization in the Wilbur Springs District, Colusa and Lake Counties, California: Ohio State University MS dissertation, 228 p.
- Waring, G. A., 1915, Springs of California: U.S. Geological Survey Water-Supply Paper 338, 410 p.
- White, D. E., 1957, Magmatic, connate, and metamorphic waters: Geological Society of America Bulletin, v. 68, p. 1659-1682.
- White, D. E., Hem, J. D., and Waring, G. A., 1963, Chapter F. Chemical composition of subsurface waters *in* Fleischer, Michael (Technical Editor) Data of Geochemistry: U.S. Geological Survey Professional Paper 440-F, 67 p.
- White, D. E., Barnes, I., and O'Neil, J. R., 1973, Thermal and mineral waters of non-meteoritic origin, California Coast Ranges: Geological Society of America Bulletin, v. 84, p. 547-560.

GAS GEOCHEMISTRY AND GUIDE FOR GEOTHERMAL FEATURES IN THE CLEAR LAKE REGION, CALIFORNIA

Fraser Goff¹ and Cathy J. Janik²

¹ Earth and Environmental Science Division, Los Alamos National Laboratory, Los Alamos, NM 87544

² Branch of Volcanic and Geothermal Processes, U. S. Geological Survey, Menlo Park, CA 94025

INTRODUCTION

Thermal/mineral waters of the Clear Lake region, California are among the most challenging geothermal fluids in the world to study because they display enormous chemical and isotopic diversity and do not geochemically resemble fluids in typical, high-temperature ($\geq 200^\circ\text{C}$) geothermal systems (Goff et al., 1993a, 1993b). The Clear Lake region contains no boiling hot springs, hot fumaroles, or springs actively depositing sinter, features commonly linked with high-temperature reservoirs. Regionally, the fluids display tremendous variations in chemical and isotopic composition, caused more by variations in bedrock composition than by subjacent magmatic heat sources (Goff et al., 1977; Thompson et al., 1981a; 1992; Donnelly-Nolan et al., 1993). The distribution of fluids is roughly coincident with the late Tertiary and Quaternary Clear Lake volcanic field (2.1 Ma to 10 ka; Donnelly-Nolan et al., 1981; Hearn et al., 1981). The region lies northeast of The Geysers steam field, the largest geothermal field in the world, yet drilling of approximately 25 exploration wells has not found a commercially exploitable geothermal system. Because conditions in most of these wells are very hot ($\geq 200^\circ\text{C}$ at 2000 m) but relatively impermeable, the Clear Lake region is rated as one of the best hot dry rock geothermal prospects in the United States (Goff and Decker, 1983).

Gas geochemistry is becoming more widely used for geothermal prospecting, especially in areas where spring chemistry is ambiguous or where spring waters are not directly derived from deep reservoirs (Goff et al., 1985; 1991; Janik et al., 1991; 1992). Geothermal gases commonly originate from sources much deeper than the spring waters in which they vent; thus the chemical and isotopic composition of gases can yield information on magmatic and mantle processes as well as subsurface equilibration temperatures (Giggenbach, 1980; D'Amore and Panichi, 1980; Welhan et al., 1988; Giggenbach and Matsuo, 1991). No systematic gas sampling has been conducted across the Clear Lake region, although data exist from a few topical studies (Barnes et al., 1973a; Nehring, 1981; Thompson et al., 1981b; Peters, 1993). We present herein preliminary results from an on-going gas investigation that evaluates geothermal potential and searches for possible magmatic and mantle contributions to the gases.

METHODS

Two principal types of gas samples have been collected for this project. "Caustic" samples are taken in ~300 ml evacuated glass bottles that contain ~150 ml of 4N NaOH solution (Fahlquist and Janik, 1992). These collection bottles are specifically designed for gas features that discharge large proportions of acid gases (CO_2 , H_2S , NH_3 , HCl , etc.) and/or steam. "Flow-through" samples are obtained in ~125 ml glass bottles with stopcocks at both ends. These

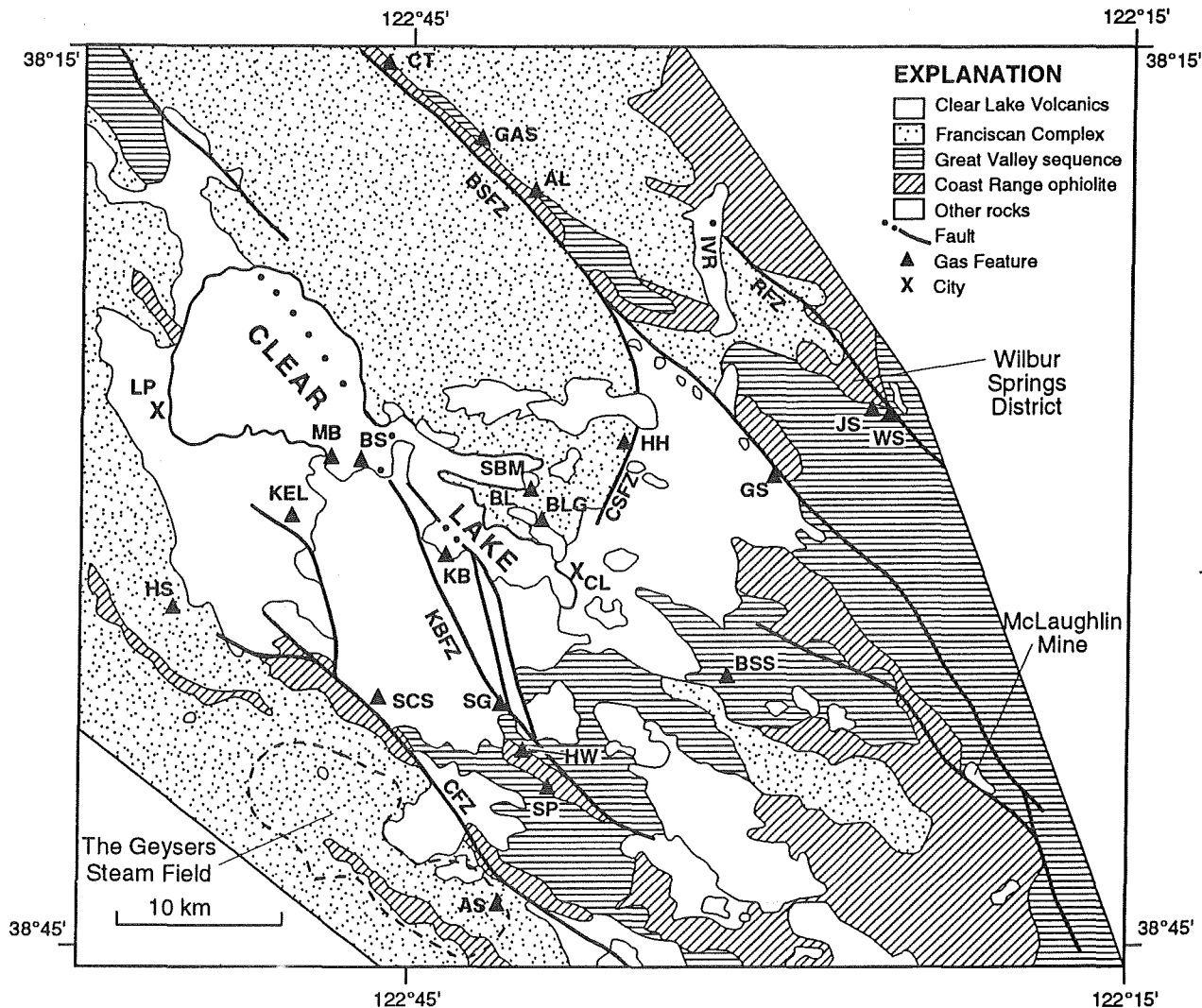


FIGURE 1. Generalized geologic map of the Clear Lake region, California, showing locations of gas sampling sites for the present study. BSFZ = Bartlett Springs fault zone; CFZ = Collayomi fault zone; CSFZ = Cross Spring fault zone; KBFZ = Konocti Bay fault zone; RFZ = Resort fault zone; BL = Borax Lake; IVR = Indian Valley Reservoir; LP = Lakeport; CL = Clearlake. Gas features: AL = Allen Springs; AS = Anderson Hot Springs; BLG = Borax Lake Gas Well; BS = Big Soda Spring; BSS = Baker Soda Spring; CT = Crabtree Hot Springs; GAS = Gas Spring; GS = Grizzly Springs; HH = Hog Hollow Spring; HS = Highland Springs; HW = Howard Hot Springs; JS = Jones Hot Spring; KB = Konocti Bay Gas Vent; KEL = Kelseyville Methane Well; MB = Moki Beach Gas Vent; SBM = Sulphur Bank Mine; SCS = Sulphur Creek Spring; SG = Siegler Hot Springs; SP = Spiers Springs; WS = Wilbur Hot Springs (figure modified from Donnelly-Nolan et al., 1993).

samples work best for gas features that contain substantial amounts of air components (N_2 , O_2 , Ar) and/or water insoluble organic compounds (Evans et al., 1988). Collection procedures and analytical methods for bulk gas chemistry and $\delta^{13}C$ - CO_2 composition are described in Trujillo et al. (1987), Evans et al. (1988), and Fahlquist and Janik (1992). Results of our investigations, selected results of previous studies, and results of helium isotope research are listed in Table 1. Descriptions of individual gas features can be found in the field trip guide that follows. The regional geology, regional tectonics, and magmatic history of the Clear Lake region (Fig. 1) has been most recently summarized by Donnelly-Nolan et al. (1993).

Table 1: Gas analyses of geothermal features in the Clear Lake region, California (values in mol-% except where noted).

Sample No.	Description	Date	Collection Temp. (°C)	CO ₂	H ₂ S	H ₂	CH ₄	C ₂ H ₆	N ₂	NH ₃	Ar	O ₂	He	Total	¹³ C-CO ₂ (‰)	R/R _A ¹	T-DP (°C) ²
Caustic Gas Samples³																	
CL91-1A	Herman Pit, Sul. Bank Mine	03/06/91	10.1	88.6	0.0325	0.0000	10.51	0.0000	2.66	0.0018	0.0107	0.0801	0.0200	99.93	-9.7 ⁴	7.5	(96)
CL91-1B	Herman Pit, Sul. Bank Mine	03/06/91	10.1	87.1	0.0169	0.0000	9.98	0.0000	2.56	0.0010	0.0153	0.1545	0.0077	98.95	—	—	(105)
N	Herman Pit, Sul. Bank Mine	?/??	"cold"	93.3	0.13	0	5.46	0.024	1.31	—	0.0072	0	0	100.26	-14.1(?)	—	(108)
CL91-2	Big Soda Spring	03/06/91	31.3	99.8	0.0000	0.0000	0.146	0.0008	0.014	0.0003	0.0005	0.0029	0.0000	100.00	-11.9	—	(56)
CL92-42	Big Soda Spring	06/04/92	31.0	99.7	0.0000	0.0000	0.252	0.0008	0.053	0.0002	0.0012	0.0181	0.0000	100.03	—	—	(86)
CL91-5	Baker Soda Spring	03/07/91	21.3	98.8	0.0000	0.0000	0.714	0.0006	0.392	0.0002	0.0062	0.110	0.0022	100.01	-10.5	5.2	(50)
P	Baker Soda Spring	?/??	257	98.3	0.0076?	0.0003	0.980	0.000	0.54	0.00	0.0093	0.18	0.0026	100.01	-11.3	4.0	78
CL91-12	Jones Hot Spring	03/09/91	61.9	40.7	0.369	0.0353	51.9	0.147	6.76	0.0024	0.0353	0.0943	0.0000	99.99	-10.7	1.7	135
CL92-34	Jones Hot Spring	06/02/92	57.0	53.3	0.976	0.184	44.0	0.0872	2.22	0.149	0.0000	0.0000	0.0000	100.87	-9.3	—	121
P	Jones Hot Spring	?/??	587	45.2	0.770	0.24	49.6	0.000	4.08	0.013	0.042	0.013	0.00095	99.93	-10.0	1.6	126
P	Wilbur Hot Spring	?/??	547	91.2	2.80	0.0014	4.49	0	1.17	0.30	0.021	0.000	0.00033	99.97	-10.7	1.3	140
CL91-16	Grizzly Spring	03/09/91	19.4	98.3	0.0001	0.0000	1.11	0.0000	0.289	0.0001	0.0073	0.293	0.0000	100.02	-10.5	—	(48)
CL91-22	Sulphur Creek Spring	03/11/91	21.0	97.5	0.363	0.0000	0.791	0.0017	1.02	0.0004	0.021	0.0246	0.0000	99.70	-12.4	0.8	(126)
N	Sulphur Creek Spring	?/??	"cold"	97.6	0.17	0.0002	0.16	0.0005	1.56	—	—	0.30	0	99.76	-15.2(?)	—	103
CL91-24	Gas Spring	03/12/91	10.0	96.2	0.0001	0.0000	1.11	0.0000	2.81	0.0003	0.0000	0.0000	0.0000	100.07	-12.3	≤3.0	(49)
CL91-26	Howard Hot Spring	03/13/91	46.3	99.7	0.0000	0.0011	0.058	0.0000	0.204	0.0001	0.0049	0.0778	0.0000	99.99	-12.4	—	(60)
N	Howard Hot Spring	?/??	"hot"	99.0	0	0.0008	0.12	0.0001	0.61	—	—	0.91	0	100.60	-12.9	—	(83)
CL91-28	Borax Lake Gas Well	03/14/91	10.0	85.4	0.0138	0.0000	13.4	0.0000	1.14	0.0007	0.0000	0.0000	0.0060	99.94	-11.3	7.9	(89)
CL91-37	Allen Chahybeate Spring	06/03/92	17.0	87.5	0.0001	0.0000	0.010	0.0000	9.80	0.0020	0.118	2.65	0.0005	100.06	-12.8	—	(88)
CL92-39	Crabtree Gas Seep	06/03/92	28.0	94.1	0.0001	0.0014	1.27	0.0000	4.64	0.0005	0.0016	0.0355	0.0008	100.05	-11.3	—	(86)
N	Seigler Hot Sulphur Spring	?/??	"hot"	98.4	0	0.00041	1.10	0.0160	0.39	—	0.0066	0.11	0	99.97	-13.0	—	(69)
N	Moki Beach Gas Vent	?/??	"cold"	99.2	0	0.00003	0.63	0.0006	0.13	—	0.0033	0.0047	0	100.00	-11.8	—	(41)
N	Konocil Bay Gas Vent	?/??	"cold"	94.8	0	0	3.76	0.0150	1.48	—	0.025	0.041	0	100.08	-14.6(?)	—	(76)
N	Highland Springs Gas Vent	?/??	"cold"	99.8	0	0	0.20	0.0265	0.030	0.0068	0.0002	0.0002	0	100.02	-17.3(?)	—	(88)
Flow-through Gas Samples⁵																	
CL91-4	Hog Hollow Spring	03/07/91	30.0	84.7	<0.0005	<0.0002	1.23	0.0028	10.81	—	0.135	2.85	0.0004	99.68	-12.7	—	(50)
CL91-7	Kelseyville Methane Well	03/08/91	10.4	66.9	<0.0005	<0.0002	27.0	0.0718	5.73	—	0.0293	0.660	0.0016	100.42	-10.5	—	(16)
CL91-10	Spiers Spring	03/08/91	24.2	82.8	<0.0005	0.0002	0.0243	<0.0002	14.2	—	0.177	3.70	0.0008	100.85	-12.8	—	(79)
CL91-12	Jones Hot Spring	03/09/91	61.9	47.2	0.60	0.108	51.1	0.103	2.28	—	0.0118	0.144	0.0013	101.51	-9.0	1.7	157
CL91-19	Anderson Hot Spring	03/11/91	49.4	82.1	0.351	0.135	5.19	0.039	10.14	—	0.12	1.76	0.0006	99.85	-13.3 ⁶	—	218
OQ181B77	Wilbur Hot Spring Fresh Air	?/??	-55	95.6	2.92	<0.01	3.58	<0.05	0.28	—	<0.02	0.04	<0.02	99.41	-9.7	—	(136)
				0.032	<0.0005	<0.0005	<0.0002	<0.01	78.3	—	0.93	21.0	<0.005	100.26	—	—	—

209

¹ R/R_A means ³He/⁴He of sample divided by ³He/⁴He in air; analyses by B. M. Kennedy (LBL), except "P" sample number (Peters, 1993).

² Temperatures calculated using empirical gas geothermometer of D'Amore and Panichi (1980). Values in parentheses violate rules of application but are calculated assuming at least 0.001 mol-% H₂S and 0.001 mol-% H₂.

³ Analyses with "CL" sample prefix by P. E. Trujillo (LANL); Analyses with "N" sample number by Nehring (1981); analyses with "P" sample number by C. J. Janik (USGS); carbon-13 analyses by C. J. Janik except "N" sample numbers by Huebner (1981).

⁴ Average of three samples.

⁵ Analyses by W. C. Evans (USGS); carbon-13 analyses by L. D. White (USGS).

⁶ Analysis on separate sample is -13.8‰ (C. J. Janik).

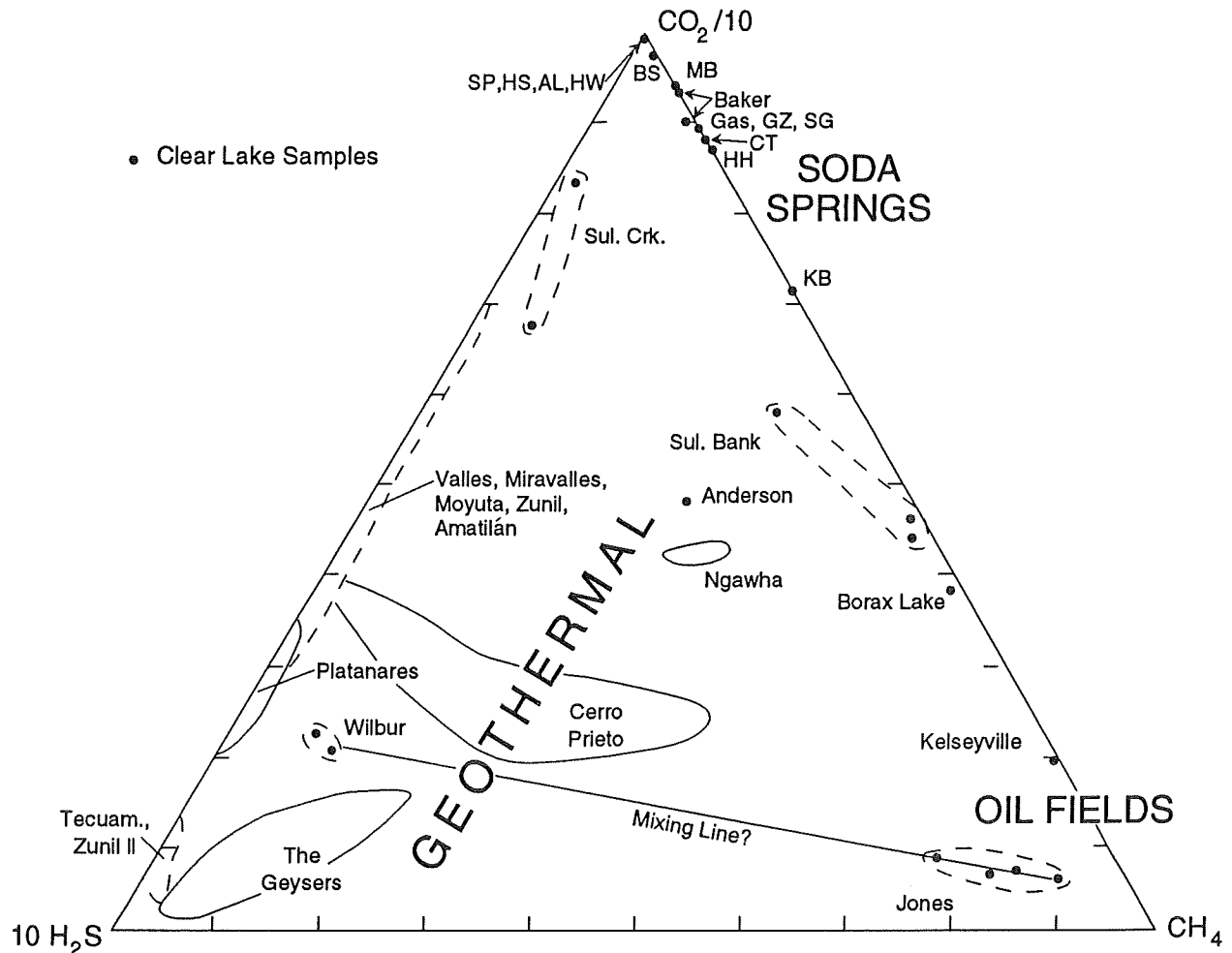


FIGURE 2. Triangular plot of $10\text{H}_2\text{S}$, CH_4 , $\text{CO}_2/10$ comparing gases in the Clear Lake region to gases from other geothermal systems (values in mol-%). Data sources: Valles caldera (Goff et al., 1985; Truesdell and Janik, 1986); Miravalles (Giggenbach and Corrales Soto, 1992); Moyuta (Goff et al., 1991b); Zunil and Zunil II (Adams et al., 1991; F. Goff, unpub. data); Amatitlán (F. Goff, unpubl. data); Platanares (Janik et al., 1991); Tecuamburro (Janik et al., 1992); The Geysers (Truesdell et al., 1987); Cerro Prieto (Nehring and D'Amore, 1984); Ngawha (Giggenbach and Lyon, 1977); this report. Abbreviations are explained in Fig. 1.

GAS COMPOSITIONS AND GEOTHERMAL COMPARISONS

As mentioned above, no natural features exist in the Clear Lake region that discharge at or near the boiling point; the hottest sampling site in Table 1 is Jones Hot Spring ($57\text{-}62^\circ\text{C}$). Although they contain the gas species typical of geothermal environments, most Clear Lake region gases are different from those derived from typical, high-temperature ($\geq 200^\circ\text{C}$) reservoirs because they contain relatively low H_2S , relatively high CH_4 , and, in several cases, > 99 mol-% CO_2 (Fig. 2). In addition, some Clear Lake region gases have N_2/Ar molar ratios between 84 and 38, the ratios in air and air-saturated water (Fig. 3). Such ratios indicate a meteoric source fluid or near-surface mixing with air and shallow groundwaters.

Thirteen of the 20 sites listed in Table 1 produce gases that have essentially no H_2S and only modest CH_4 contents; thus they have no apparent geothermal character (Fig. 2). Spring

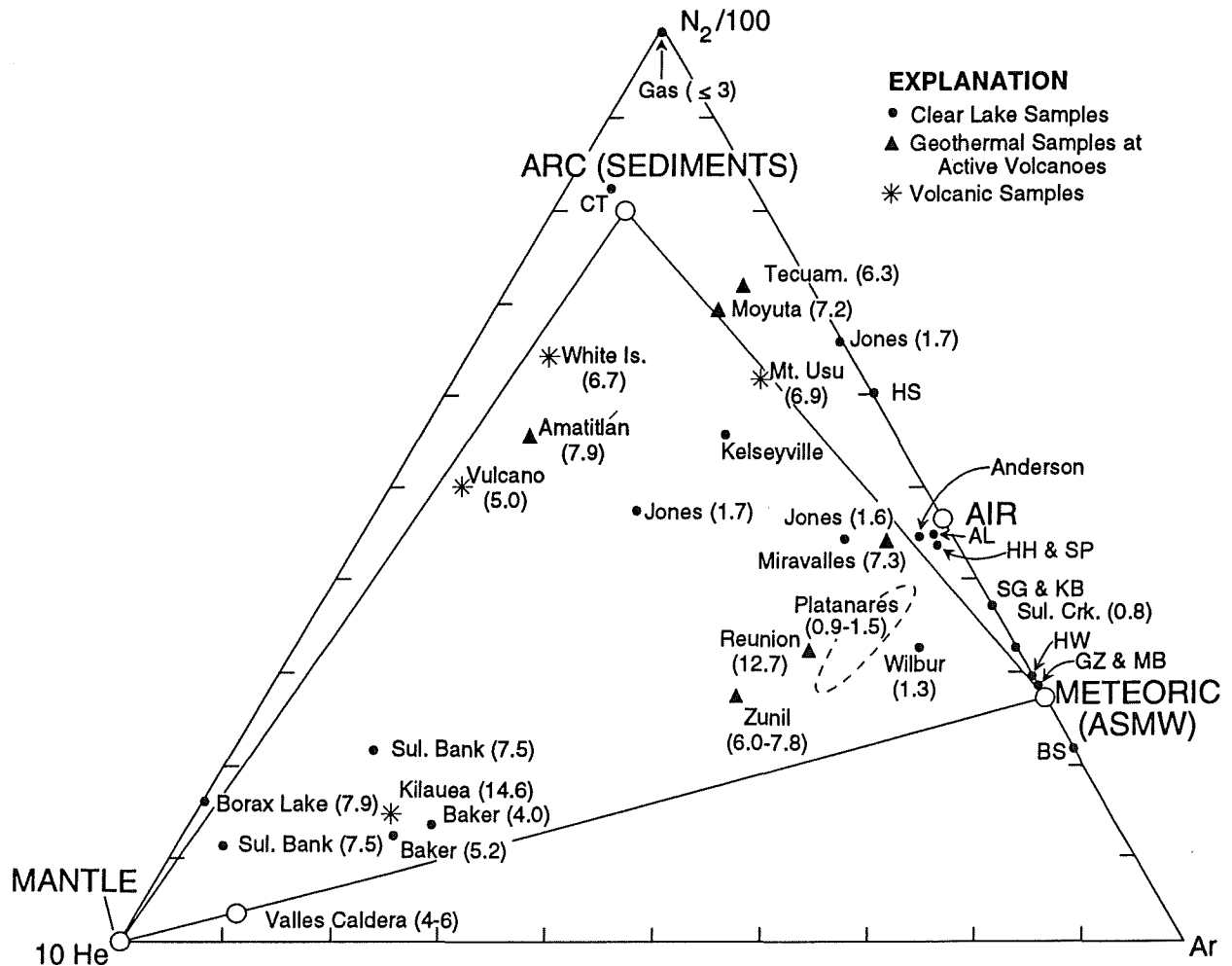


FIGURE 3. Triangular plot of 10He , Ar , $\text{N}_2/100$ comparing gases in the Clear Lake region to volcanic and geothermal gases (values in mol-%). R/R_A values are shown in parentheses. Data sources same as Fig. 2 except as follows: Vulcano, White Is., and Mt. Usu (Giggenbach and Matsuo, 1991); Reunion (Marty et al., 1993); Kilauea, Amatitlán, Zunil, and Moyuta (F. Goff, D. Hilton, and G. McMurtry, unpub. data); Platanarés (Kennedy et al., 1991); Valles caldera (Smith and Kennedy, 1985; Goff et al., 1992). Abbreviations are explained in Fig. 1.

waters at these sites have traditionally been called “soda springs” because of their early use as naturally carbonated beverages. Their high CO_2 and B contents have caused several investigators to call them metamorphic waters (e.g., Barnes et al., 1978) whereas the unusual stable isotope composition of some of these springs (e.g., Baker Soda and Grizzly) has resulted in the name connate or evolved connate waters (White et al., 1973; Donnelly-Nolan et al., 1993; Goff et al., 1993b; Peters, 1993). Note that gas compositions do not necessarily parallel water compositions and that these names (“metamorphic” or “connate”) are not useful terms for gas types.

Gases from Kelseyville and Jones Hot Spring contain so much CH_4 that they resemble typical oil field gases (i.e. Buzek, 1992) yet their co-existing waters are completely different in character from each other (Goff et al., 1977; Peters, 1993). Jones Hot Spring water resembles oil

field waters whereas Kelseyville water is much more dilute. Methane from the cluster of wells at Kelseyville was once used for heating and lighting (Waring, 1915) and the CH₄ probably originates in organic-rich sediments in the Clear Lake Basin.

Gases discharged at Sulphur Bank Mine and the nearby gas well at Borax Lake contain too little H₂S to be called typical geothermal gases. The three Sulphur Bank samples, however, may be unrepresentative due to gas flowing through water that fills the Herman Pit. Gases from both areas are similar in character and indicate a similar source.

Gas from Anderson Spring on the extreme southeast edge of The Geysers steam field (Fig. 1) is different from gases produced from Geysers production wells, primarily because it contains substantially less H₂S. Co-existing spring water is extremely low in Cl and trace elements and resembles steam-condensate fluids that exist on the tops and margins of vapor-dominated geothermal systems (Goff et al., 1977; 1993b; Donnelly-Nolan et al., 1993).

Gases from Wilbur Springs and Sulphur Creek Spring (near the Collayomi fault zone, Fig. 1) have compositions that resemble typical geothermal gases. Interestingly, Wilbur Springs gas lies at the H₂S-rich end of a projected mixing line with gas from Jones Hot Spring, which issues about 0.5 km west of Wilbur Springs (Fig. 1). The differences in results between various samples from Jones Hot Spring are too large to be analytical errors. We believe that this spring has two gas sources even though water composition of the spring is relatively constant. These unique gas sources supply gas at different rates during the cyclic, CO₂-induced eruptions of this spring. One gas source is clearly geothermal in character, whereas the dominant gas source resembles oil field gases.

Gases from other geothermal systems shown on Fig. 2 originate from high-temperature reservoirs ($\geq 200^{\circ}\text{C}$), with the possible exception of Platanares (maximum drilled temperature is 165°C , Goff et al., 1991a; Janik et al., 1991). Source rocks generally have a profound influence on gas geochemistry in geothermal systems. Gases from The Geysers, Cerro Prieto (Mexico), Ngawha (New Zealand), and Platanares (Honduras) originate in sedimentary source rocks that have some similarities to source rocks in the Clear Lake region. Sediments at Cerro Prieto are organic-rich, deltaic deposits filling the Salton Trough; gases from this field are notably rich in CH₄ and other organics (Nehring and D'Amore, 1984). Sediments at Platanares consist of organic-poor redbeds and conglomerates (Goff et al., 1991a); gases in this field contain considerable NH₃ but relatively little CH₄ (Janik et al., 1991). Sediments at Ngawha are composed of marine greywackes that resemble those in the Franciscan Complex (Skinner, 1981); gases and hot waters from this system have striking similarities to the geothermal fluids at Sulphur Bank Mine (Giggenbach and Lyon, 1977). Geothermal fluids at The Geysers issue from rocks of the Franciscan Complex and a young (≤ 1.3 Ma), shallow, composite intrusion (The Geysers felsite mentioned by Donnelly-Nolan et al., 1993). The relatively high H₂S content of Geysers steam may be a partial reflection of a magmatic source because the felsite contains abundant porphyry-copper mineralization (Hulen and Nielson, 1993). In contrast, the CH₄ contents may be derived from sedimentary sources (Truesdell et al., 1987). Gases from Valles caldera (New Mexico), Miravalles (Costa Rica), Moyuta, Zunil, Amatitlán, and Tecuamburro (all Guatemala) originate from volcanic and/or granitic host rocks at Quaternary volcanoes and have relatively low CH₄ and other organic components (Fig. 2).

MANTLE CONTRIBUTIONS

Preliminary results of a $^3\text{He}/^4\text{He}$ investigation of the region (Goff et al., 1993b) are listed in Table 1 along with three values reported by Peters (1993). To date the R/R_A values in the Clear Lake region range from 0.8 to 7.9. Values within the area from Sulphur Bank Mine to Borax Lake Gas Well are 7.5 to 7.9, respectively, indicating a definite mantle or young magmatic source (Kennedy et al., 1991). The coincidence of these values to the $\sim 200^\circ\text{C}$ hydrothermal system at Sulphur Bank Mine and close proximity to the youngest basaltic (≤ 44 ka) and silicic (~ 90 ka) eruptions in the Clear Lake volcanic field is noteworthy (Sims et al., 1981; Donnelly-Nolan et al., 1981).

R/R_A values of 4.0 to 5.2 have been obtained from Baker Soda Spring, also indicating a mantle signature. This spring issues from a northwest-trending fault zone (not shown in Fig. 1) in shale, serpentine, and silica-carbonate rock which is sub-parallel to other fault zones of the region (Brice, 1953; Hearn et al., 1981, 1988; Goff and Decker, 1983). The spring is located about midway between the McLaughlin gold mine which had hydrothermal activity as recent as 0.75 Ma (Lehrman, 1986) and the youngest Clear Lake eruptions in the Sulphur Bank-Borax Lake area.

R/R_A values of 1.3 to 1.7 occur in the Wilbur Springs district indicating considerably less mantle input. The youngest volcanic rock in the area is a basaltic dike dated at 1.66 Ma (McLaughlin et al., 1989). Present hydrothermal activity transports gold and mercury (Peters, 1991) but the geothermal system is $\leq 140^\circ\text{C}$ at about 1 km (G. Berry, written commun., 1989). Drilling to 2.9 km has not found higher temperatures, volcanic intrusions, or a commercial reservoir. Probably magmatic activity has long since waned (Smith and Shaw, 1978) and the present helium signature reflects mostly tectonic activity (Kennedy et al., 1991).

An R/R_A value of ≤ 3.0 was obtained from Gas Spring on the Bartlett Springs fault zone. No known exposures of the Clear Lake Volcanics occur this far north (Fig. 1); thus this relatively high value is suggestive of mantle leakage along a major fault zone. Similar associations between relatively high R/R_A values and tectonic features, instead of volcanic features, have been found in Honduras and Guatemala (Kennedy et al., 1991; Janik et al., 1992).

Sulphur Creek Spring along the Collayomi fault zone between The Geysers steam field and the Clear Lake region has an R/R_A value of only 0.8. Although values in The Geysers range from 6.6 to 9.5 (Torgersen and Jenkins, 1982) and this fault zone acts as a northeast boundary to the steam field (Goff et al., 1977), the spring has relatively little mantle helium. At this time, however, these results are scanty and considerably more helium ratios are needed to reveal tectonic, volcanic, and geothermal patterns.

Another way to evaluate mantle sources is to use the triangular plot of Fig. 3 which compares Clear Lake gases to those from active volcanoes and high-temperature geothermal systems. This plot, modified from Giggenbach and Goguel (1989) uses N_2 , Ar, and He as means for separating gases of predominantly mantle, arc (sedimentary), and meteoric affinities, particularly when combined with $^3\text{He}/^4\text{He}$ data. For convenience, R/R_A values are shown in parentheses next to the data points. The majority of Clear Lake region gases plot close to the points for air or air-saturated meteoric water (ASMW) indicating a possible influence from near-surface processes. Wilbur Springs gas also shows possible interactions with near-surface processes. Gases from Jones Hot Spring, Kelseyville, and Crabtree Gas Seep show the influence

of sedimentary organic sources. The R/R_A values of Jones and Wilbur Hot Springs are relatively low as stated above. On the other hand, gases from Sulphur Bank Mine, Borax Lake Gas Well and Baker Soda Spring have definite mantle characteristics due to excess total He and high $^3\text{He}/^4\text{He}$.

Of the four volcanic gases plotted on Fig. 3, three show high relative N_2 due to their arc settings and subsurface wedges of slab sediments (Vulcano, Italy; White Island, New Zealand; Mt. Usu, Japan) whereas the fourth (Kilauea) has excess He due to its hot spot setting. All have high R/R_A values. Six geothermal gases from reservoirs adjacent to or within recently active volcanoes also have high R/R_A values even though their relative proportions of N_2 , Ar, and He vary considerably. One of the examples (Miravalles) has an obvious association with air. Valles caldera geothermal gases have a significant mantle character and R/R_A values of 4 to 6 (Smith and Kennedy, 1985; Goff et al., 1992).

In contrast, the Platanares geothermal reservoir is not associated with any Quaternary volcanism; the system is strictly tectonic (Goff et al., 1991a). Platanares gases have an obvious association with near-surface processes due to mixing of reservoir waters with dilute groundwaters (Janik et al., 1991) and have R/R_A values of 0.9 to 1.5. Gases from the Wilbur Springs District resemble those from Platanares on this plot.

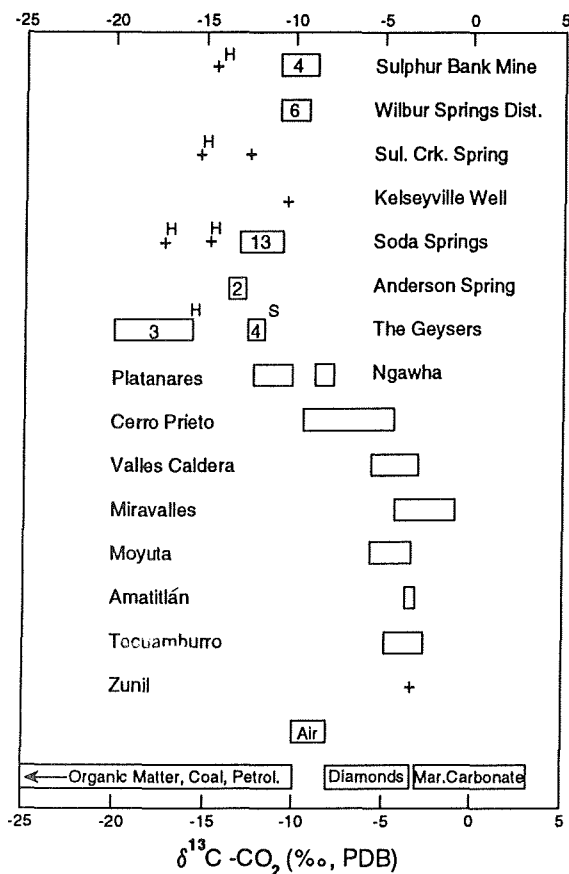


FIGURE 4. Diagram showing $\delta^{13}\text{C}-\text{CO}_2$ (‰, PDB) of Clear Lake region gases compared to gases from other geothermal systems and to $\delta^{13}\text{C}$ values of common carbon sources (Hoefs, 1973). A plus mark represents a single analysis whereas a box shows the range of analytical values for a site or area. Numbers inside boxes show the number of analyses. S means data from Shigeno et al. (1987); H means data from Huebner (1981). Cerro Prieto data from Janik et al. (1982). Other data comes from sources noted in Figs. 2 and 3.

CARBON SOURCES

Results of $\delta^{13}\text{C}-\text{CO}_2$ analyses for the Clear Lake region (Table 1) are compared to values from several high-temperature geothermal systems and to $\delta^{13}\text{C}$ values from common carbon sources (Fig. 4). All CO_2 samples from the Clear Lake region, including The Geysers, have $\delta^{13}\text{C}$ values with a distinct "organic" character ($\leq -9\text{‰}$) and are more depleted than mantle carbon values of -8 to -3‰ (represented by diamonds, Fig. 4). Recent samples collected and analyzed during our investigation are systematically more enriched in ^{13}C than analyses reported by Huebner (1981). In addition, Shigeno et al. (1987) report analyses for The Geysers that are also more enriched in ^{13}C than Huebner's results. Results of Shigeno et al. (1987) are similar to Craig (1963).

Interestingly, the two locations in the Clear Lake region known to host liquid-dominated geothermal reservoirs (Sulphur Bank Mine area and Wilbur Springs District) have $\delta^{13}\text{C}-\text{CO}_2$ values closest to mantle values. Quite possibly,

the carbon in these samples comes from a combination of mantle and organic sources. However, the $\delta^{13}\text{C}$ values of secondary carbonates from veins, fractures, and faults in regional basement rocks of the Clear Lake region have not been investigated to see if they represent viable carbon sources. Dissolution of Franciscan vein calcite and possibly aragonite has apparently created substantial matrix porosity throughout The Geysers steam field (Hulen et al., 1992) and may be a significant source of carbon in The Geysers and throughout the Clear Lake region. Lambert and Epstein (1992) report $\delta^{13}\text{C}$ values of -8 to -15‰ for 18 samples of hydrothermal calcite from steam zones in The Geysers, consistent with this hypothesis.

The $\delta^{13}\text{C}$ -CO₂ values of Clear Lake region gases are most similar to those in gases from geothermal systems hosted in sedimentary rocks (Platanares, Ngawha, Cerro Prieto). CO₂ produced from geothermal systems in volcanic rocks or from systems known to contain substantial amounts of marine carbonate (Valles caldera) have more enriched $\delta^{13}\text{C}$ -CO₂ values than Clear Lake region gases (Goff et al., 1985; 1992; Janik et al., 1992).

GAS GEOTHERMOMETRY

The apparent temperature of last equilibration of the gases can be calculated using the semi-empirical gas geothermometer of D'Amore and Panichi (1980). This geothermometer was derived from thermodynamic considerations of gas equilibria and from the relative proportions of CO₂, H₂S, H₂, and CH₄ in gases produced from 34 drilled, high-temperature geothermal systems. We have found that this geothermometer accurately estimates subsurface reservoir temperature in most high-temperature systems (Goff et al., 1985; Grigsby et al., 1989; Dennis et al., 1990; Adams et al., 1991; Janik et al., 1992). Because concentrations of H₂S and H₂ are <0.001 mol-% in many Clear Lake region gases most calculations violate rules of application for this geothermometer and calculated temperatures are maximum values (see Table 1). However, calculations show that Clear Lake region gases have equilibration temperatures $\leq 160^\circ\text{C}$, even for gases at Sulphur Bank Mine.

Calculated temperatures in the Wilbur Springs District range from 121 to 157°C (avg. 136°C) which brackets the maximum drilled temperature of about 140°C. Calculated temperatures for gas issuing at Sulphur Creek Spring are 103 to 126°C, although no commercial reservoir exists beneath that area. Temperatures in nearby exploration wells are roughly 200°C at 2000 m. A calculated temperature of 218°C is obtained for gas at Anderson Hot Spring on the southeast margin of The Geysers steam field (~240°C). All other Clear Lake region gases have calculated temperatures <100°C indicating substantial re-equilibration during their path to the surface or equilibration at relatively low temperatures. These results are similar to calculated reservoir temperatures based on water chemistry (Goff et al., 1993b).

CONCLUSIONS

Most Clear Lake region gases do not chemically resemble gases from typical, high-temperature geothermal reservoirs because of relatively low H₂S, relatively high CH₄, and exceptionally high CO₂ contents. Extremely CO₂-rich springs are common in the Clear Lake region and their carbon-13 contents suggest organic sources from marine sedimentary rocks or a mixture of mantle and organic sources. Some of these springs have elevated ³He/⁴He values

indicating the presence of mantle helium. The location of these springs along major northwest-trending fault zones is significant, and suggests that tectonics is as much a factor in their geochemistry as proximity to Clear Lake magma chambers (Barnes et al., 1978). In any event, the cool to moderate temperature soda springs are not connected to underlying high-temperature geothermal reservoirs (Goff et al., 1993b).

Two gas samples to date resemble oil field gases due to their exceptionally high CH₄. Carbon-13 contents of CO₂ in these gases indicate a mixture of carbon sources. Jones Hot Spring has a slightly elevated ³He/⁴He value and is derived from the 140°C reservoir in the Wilbur Springs District. Variations in gas chemistry suggest that Jones Hot Spring contains a minor geothermal gas component similar to Wilbur Springs gas. The association of past hydrothermal activity in the Wilbur Springs District with early Clear Lake volcanism (1.66 Ma) is certain (Donnelly-Nolan et al., 1993) but the association of present hydrothermal activity with present (hidden?) magma chambers is speculative.

Gases in the Borax Lake-Sulphur Bank Mine area are too depleted in H₂S to be called typical geothermal gases and their calculated equilibration temperatures are low (≤108°C). This may be a reflection of non-representative samples since maximum drilled temperatures are 218°C at 503 m. Carbon-13 contents of CO₂ also indicate a mixture of carbon sources. Total helium content and high ³He/⁴He values (7.5 to 7.9 R/R_A) indicate a significant mantle gas component. These gas sites are surrounded by the youngest basaltic to silicic eruptions in the Clear Lake volcanic field (~10 to 90 ka). The resemblance of the Sulphur Bank Mine system to the Ngawha geothermal system in New Zealand is remarkable. However, small reservoir size, aragonite scaling problems, and environmental obstacles will probably prevent development of the Sulphur Bank reservoir for many years.

First-Day Road Log: Geothermal Features Within the Main Clear Lake Volcanic Field

Summary — The route of the first day (Fig. 5) takes us on a loop through the main part of the Clear Lake volcanic field (northeast of the Collayomi fault zone) where we will look at thermal meteoric and steam condensate waters as defined by Donnelly-Nolan et al. (1993) and Goff et al. (1977; 1993b). Although features visited at the beginning of the day emerge from the Clear Lake Volcanics, most hot, warm, and mineralized springs issue around the edges of the volcanic field along fault zones related to the present tectonic regime (Hearn et al., 1976; 1981; 1988; Thompson et al., 1992). This region contained several famous spring resorts (Anderson, 1892; Waring, 1915; Berkstresser, 1968) that are now destroyed, closed, or converted into religious communities. Only Harbin Hot Springs (north of Middletown but south of today's loop) has commercial bathing facilities open to the public. Although the region has very high subsurface temperatures at relatively shallow depths (~200°C at 2000 m; Goff and Decker, 1983) and very high conductive heat flow (170 mW/m²; Walters and Combs, 1989), only the Agricultural Park south of Mount Konocti has seen recent geothermal development.

Mileage:

0.00 **Lower Lake Junction** between Highway 53 and Highway 29. **Head west on Highway 29** toward Lakeport. 1.35

- 1.35 Seigler Canyon Road on left. **Continue** straight ahead. **0.5**
- 1.85 Point Lakeview Road to Jago Bay on right. **Continue** straight ahead. **1.45**
- 3.3 Diener Drive on left. **Continue** straight ahead. **1.7**
- 5.0 Manning Flat on right (dry lake bed, deeply eroded by stream cut). **2.6**
- 7.6 Junction with Red Hill Road and Soda Bay Road (Highway 281). **Continue** straight ahead. **0.9**
- 8.5 **Turn left** off Highway 29 to the entrances to Sulphur Mound Mine (left gate) and the Geothermal Agricultural Heat Center (right gate). **NOTE: Access by special permission only; do not trespass. Proceed through gate on left road, up hill toward the mine. 0.35**

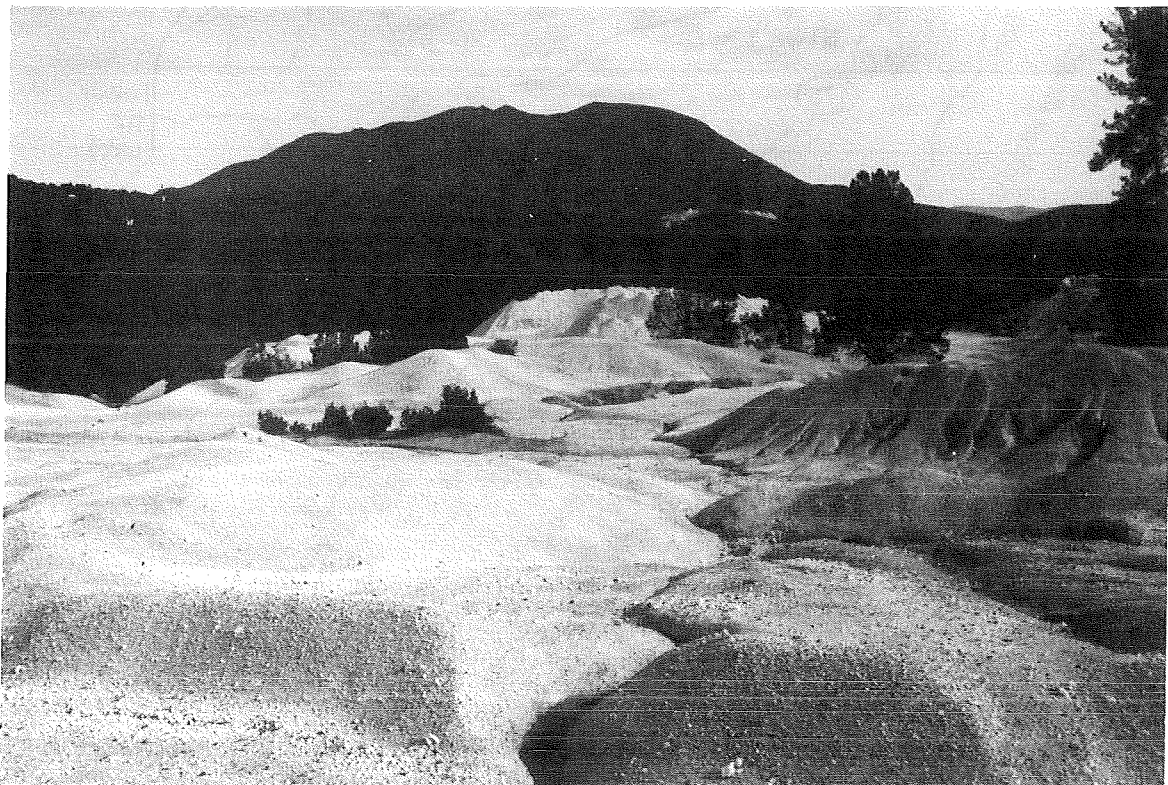


FIGURE 6. View looking north from quarry at Sulphur Mound Mine toward Mt. Konocti. This sector of the quarry was used as the well pad for the Neasham #1 exploration well. The brush covered ridge in foreground is the site for the Agricultural Park #3 production well. The white scar on the south flank of Mt. Konocti is the site of the Bell Mine. Two other exploration wells, Kettenhoffen #1 and Magma-Watson #1, were drilled in the vicinity of the Bell Mine.

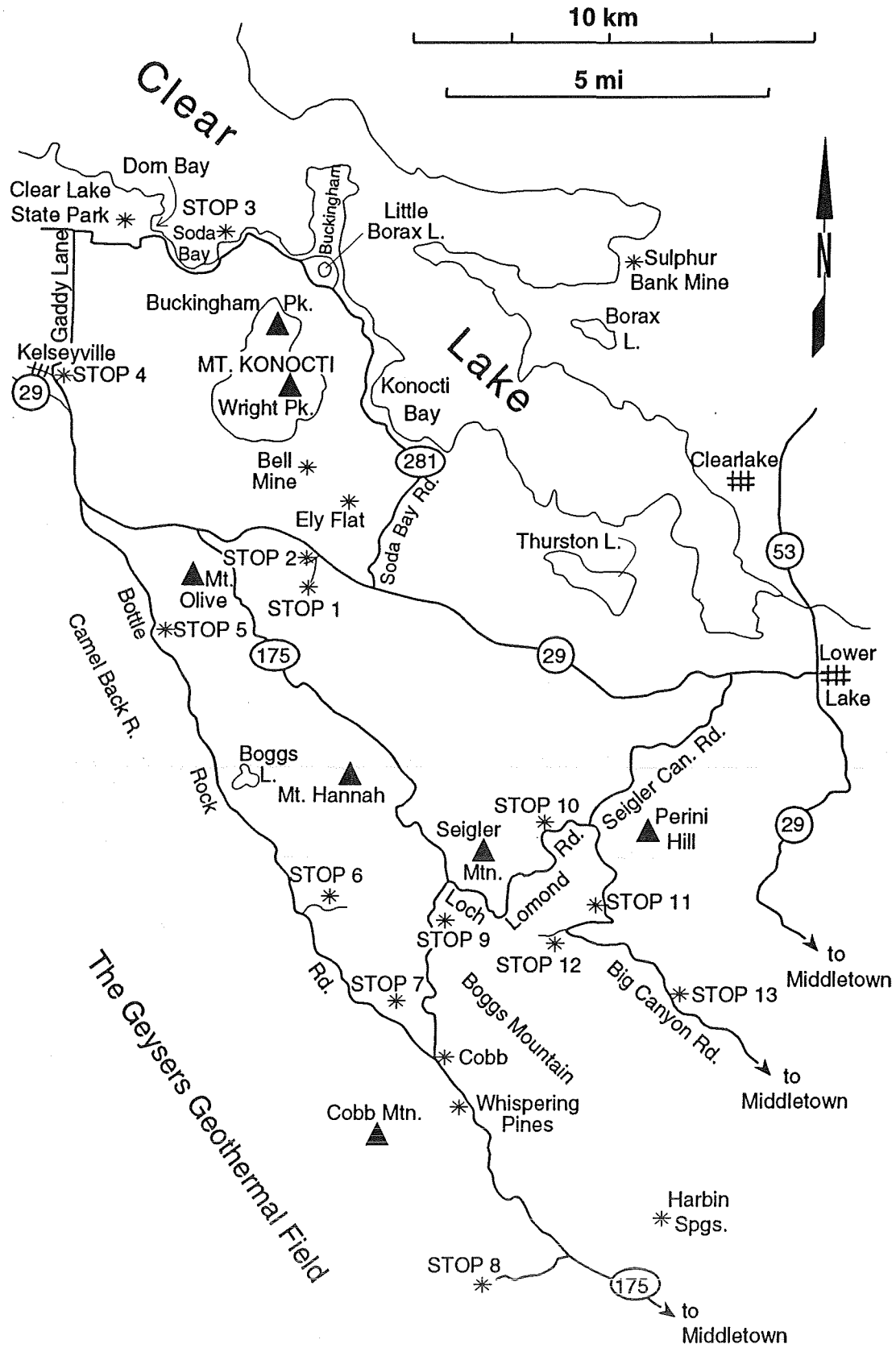


FIGURE 5. Route map, Day 1

8.85 Mine quarry. **Continue uphill** on road at right side of area presently being excavated.
0.1

8.95 **STOP 1. Sulphur Mound Mine.** Enter flat area and park vehicles. Walk uphill (~100 m south) toward the white, excavated scarp in bedded tuffs. Sulphur Mound Mine (Fig. 6) is developed within a complex sequence of dacitic and rhyolitic flows and pyroclastic deposits (<0.6 to >0.4 Ma) cut by the northeast-trending Sulphur Mound Fault, which is down to the northwest (Hearn et al., 1976). The silicic rocks are overlain by a basalt flow to the south and basalt agglomerate to the northwest.

The mine is located in a zone of opalized and kaolinized rocks with diffuse fumarolic activity and contains trace cinnabar as well as elemental sulfur. Cinnabar was mined near the turn of the century but agricultural sulfur is produced today. Note the strong smell of H₂S and patches of sulfur-rich ground. This is a locality containing acid-etched, flow-banded obsidian and sulfur-cemented obsidian breccia.

The Neasham #1 geothermal exploration well was drilled in the flat area by the vehicles to a depth of 3673 m. The well penetrated the base of the volcanic sequence at 728 m and entered serpentinite and rocks of the Franciscan Complex. A temperature of 275°C occurs at a fluid entry at 2615 m but flow could be sustained for only a couple of days. No data are available on fluid composition.

Agricultural Park #3 well is located on the nearest low ridge 0.5 km to the northwest providing 66°C fluid for the Agricultural Heat Center. The geothermal aquifer is intercepted at 120 m depth but a temperature reversal is encountered below the zone of hot water (Dellinger and Cooper, 1990). Apparently geothermal fluids ascend along the Sulphur Mound Fault and feed a hydrothermal outflow plume (Goff et al., 1988) that flows a few kilometers to the north. No hot springs occur in this area but hot fluids of similar geochemistry are present in several other nearby shallow wells (Thompson et al., 1981a; Goff et al., 1993b).

Elemental sulfur deposits form around the mouth of the AP #3 well crib but no free gas can be sampled at the well. There is no evidence that the fluid boils as it ascends from depth. Gases are apparently released as pressures decrease at shallow depths and rise along faults to produce the alteration. Dissolved gases react with rock in the saturated zone to produce HCO₃ (~400 mg/kg) and SO₄ (25 mg/kg). The water is of the thermal meteoric type and tastes strongly of H₂S (~17 mg/kg) and weakly of soda. The water contains only 0.09 T.U. tritium indicating a maximum mean residence time of 7500 yr (Goff et al., 1993a).

To the north on the shoulder of Mt. Konocti is the Bell Mine, another mercury prospect hosted in altered, bleached dacite. It is now mined for decorative rock. No active fumaroles or hot springs occur there. Mt. Konocti is a composite volcano consisting mostly of porphyritic dacite and accounting for over half of the volume of the Clear Lake

volcanic field (Donnally-Nolan et al., 1981). Dacite lavas at the summit of Wright Peak are 0.34 Ma in age. The rhyolitic and dacitic rocks of the Sulphur Mound Mine-Mt. Konocti area show clear textural and geochemical evidence of magma mixing between rhyolitic and basaltic andesite to andesitic magmas (Stimac et al., 1990; Stimac and Pearce, 1992).

Turn around and return downhill. 0.45

- 9.4 **Turn left** through gate to the Geothermal Agricultural Heat Center. Proceed to the greenhouse and park the vehicles. **0.1**
- 9.5 **STOP 2. Geothermal Agricultural Heat Center.** The greenhouse was built to utilize the low-temperature geothermal resource of the Sulphur Mound Mine area (Dellinger and Cooper, 1990). The geothermal project provides a heating distribution system for greenhouse operators, other agricultural businesses, and horticulture clubs, and provides vocational training in botany and horticulture, including methods using hydroponics. Sponsors are: 1) California Energy Commission, 2) County of Lake, and 3) Mendocino-Lake Community College District. Hot water is pumped into the greenhouses from AP #3 well, goes through a closed-loop heat exchanger, and then is re-injected into AP #1 well, which is located behind the greenhouse and intercepts the hot aquifer at about 70 m depth. The production well yields 400 l/min of water for the 650 m² (7000 ft²) greenhouse but could supply heat for an additional 2800 m² (30,000 ft²). A second production well (AP #2) could supply heat for up to 4600 m² (50,000 ft²). Unfortunately, the pipes that provide water from the well to the heat exchanger regularly need repairs. Primary demand when the system is working is during the months of October through mid-April.

Turn around and return through gate to Highway 29. 0.1.

- 9.6 **Turn right** on Highway 29, returning to Soda Bay Road. **1.0**
- 10.6 **Turn left** on Soda Bay Road, Highway 281 North. **0.3**
- 10.9 Passing through obsidian flow of the rhyolite of Thurston Creek (0.6 to 0.4 Ma). **0.1**
- 11.0 Good view of the Bell Mine and Ely Flat to the left. The first deep exploration well within the main Clear Lake volcanic field was drilled in 1971 in Ely Flat. The Kettenhoffen #1 well reached the base of the volcanic rocks at 744 m and had a maximum reported bottomhole temperature of 210 °C at 2610 m. The well was dry. About 0.5 km northwest of Bell Mine is the location of the Magma-Watson #1 wildcat well, which was drilled to 1754 m depth, with a bottomhole temperature >200 °C; it was also dry. **1.2**

- 12.2 View of Clear Lake from the community of Riviera. **0.3**
- 12.5 Point Lakeview Road on right. **Continue** straight ahead. **0.4**
- 12.9 View of Fraser Point and Konocti Bay. Many gaseous warm springs discharge from probable faults along the bottom of Konocti Bay (Sims and Rymer, 1976). Spring water was sampled in the drought years, 1974 to 1978; data were reported in Thompson et al. (1981a; 1981b). **0.2**
- 13.8 Cross fault scarp on Konocti Bay Fault Zone. **1.4**
- 15.2 Konocti Harbor Resort and Spa. Entrance by permission only. Warm springs issue along the lake shore. A warm water well (about 35 °C) is located in back of the boat house. The water is used for bathing and occasional space heating (Hinds and Dellinger, 1988). Chemical data are reported in Thompson et al. (1981a, 1981b; 1992). **Continue** on Soda Bay Road. **0.6**
- 15.8 Looking up at Buckingham Peak. **0.3**
- 16.1 View on right of Horseshoe Hot Spring, located on the nearest bank of the horseshoe-shaped cove flanked by two tall trees. This spring has been sampled only twice; data are reported in Thompson et al. (1981a; 1981b) but the springs in this area were noted by Waring (1915, p. 193). Exposed on the left side of the road are ash beds of a young (<50 ka?) basaltic andesite. **0.4**
- 16.5 **Turn right** on Crystal Drive. **0.2**
- 16.65 **Turn out on left** near golf course for view of Buckingham Peak, Buckingham Country Club, and Little Borax Lake, which fills a maar surrounded by basaltic pyroclastic deposits from a phreatomagmatic eruption (<50 ka?). There is no known spring or gas seep in the lake, but the water contains a high concentration of boron (Thompson et al., 1981a). Buckingham Peak is another composite dacite dome that formed about 0.35 Ma and it is capped by a basaltic andesite scoria dated at roughly 30 ka. **Continue** on Crystal Drive beyond the entrance to the county club. **0.05**
- 16.7 **Bear left** on Little Borax Lake Road. **0.7**
- 17.4 **Bear right** on Soda Bay Road. **0.3**
- 17.7 View of Horseshoe Bay and Buckingham Peninsula on right. The peninsula is composed mostly of north-trending, coalesced basaltic pyroclastic deposits ≤ 50 ka(?). **0.6**
- 18.3 View of Soda Bay. **1.1**

19.4 **STOP 3. Big Soda Spring.** Rent a boat from one of the docks in the community of Soda Bay and take the boat out about 1 km to the small islands near the northeast edge of the bay. Big Soda Spring (Fig. 7) upwells from a small bathing pool (usually submerged) at the base of iron-stained dacite boulders at the near-shore end of the northern-most island. At the turn of the century, this spring was called Geyser Spring or Omar-Ach-Hah-Bee (The Great Spring) and was an attraction for a boating and fishing resort that provided accommodations for about 150 people (Waring, 1915). Discharge rate of this spring is several hundred liters per minute and it is still a favorite swimming spot.

Four principal vents discharge gas and warm water (31°C) of the thermal meteoric type (Goff et al. 1977). The gas contains 99% CO₂ and the area smells musty (Table 1). There is no odor of H₂S. The water tastes strongly of soda (1200 mg/kg HCO₃) and iron. Tritium content of the spring water is very low (0.09 T.U.) indicating that the source is relatively old and deeply circulating (Goff et al., 1993a).



FIGURE 7. View looking north of Big Soda Spring, submerged beneath Clear Lake in May, 1993. The spring emits copious quantities of CO₂ from 3 to 4 principal vents at the edge of a small island of porphyritic dacite. The vents were visible in March, 1991 and June, 1992 (Goff et al., 1993a)

Bubble trains of gas are visible along the trend of the islands and parallel to the lake shore. The gases probably emerge along submerged faults and/or near submerged vents for relatively young (≤ 50 ka?) basaltic pyroclastic deposits that overlie the dacites on the north side of Mt. Konocti (Hearn et al., 1981). Over 30 ash beds beneath the muddy lake bottom have been penetrated in core and have ^{14}C ages of <44 to about 10 ka (Sims and White, 1981; Sims et al, 1981).

Return boat to dock, and **resume road trip. 0.2** for round trip from Soda Bay Road to boat dock and return.

- 19.6 **Continue west** on Soda Bay Road. **0.9**
- 20.5 View of Dorn Bay and Moki Beach to the right. Gas (primarily CO_2) and warm (27°C) bicarbonated water issue from Moki Beach Spring submerged near the lake shore (Thompson et al., 1981b; Nehring, 1981). **0.8**
- 21.3 Entrance to Clear Lake State Park and campground. **Continue** straight ahead. **1.0**
- 22.3 **Junction; turn left (south)** on Gaddy Lane toward Kelseyville. **2.1**
- 24.4 **Turn left** at junction with State Street, toward Kelseyville. **0.4**
- 24.8 **STOP 4. Kelseyville Methane Well.** Turn out on left and park vehicles near city park, just before intersection with Main Street in Kelseyville. Walk up low hill to southeast and stop at abandoned well head. Kelseyville methane well is one of several abandoned, shallow wells that were drilled around the turn of the century on this hill. The wells produced artesian, bicarbonated water of the thermal meteoric type (24°C), and the methane-rich gas was piped to buildings in the town for heating and lighting (Waring, 1915; Goff et al., 1977).

The abandoned well is surrounded by an area of altered, sulphurous ground with sparse to no vegetation. Gas discharges at the surface, especially in a few shallow pits. The air smells weakly of H_2S and more strongly of organics. A recent analysis shows the gas is 64% CO_2 and 27% CH_4 (Table 1). No water is produced from the well now, but an area of iron-staining north of the hill may indicate weak discharge of bicarbonated water.

The hill on which these wells were drilled is uplifted by a fault and consists of lacustrine, fluvial, and alluvial sediments of the Clear Lake basin that are probably <0.6 Ma in age (Hearn et al., 1981). The natural gas probably originates from burial and heating of organic-rich sediments in this old embayment of the lake (Fig. 1).

Turn left out of parking area **and continue** southeast. **0.1**

24.9 **Turn left** on Main Street at intersection. **0.45**

25.35 **Junction** with Highways 175 and 29. **Turn left** toward Lower Lake. **1.55**

26.9 Cole Creek Road on the right leads to Highland Springs Reservoir, site of the once-famous Highland Springs Resort and Diana Spring, which are now drowned by the reservoir (Waring, 1915; Nehring, 1981). **Continue** straight ahead. **0.7**

27.6 **Turn right** on Bottle Rock Road. **0.7**

28.3 View of Camel Back Ridge composed of dacite (0.59 Ma) on the right. At 10:00 is Mt. Olive (0.53 Ma), another dacite, with sulfurous gas seeps around its base (Hearn et al., 1976). **0.9**

29.2 Entering the area of obsidian flow-breccia of the rhyolite of Thurston Creek. The obsidian contains about 1% phenocrysts and 1% tiny (<2 cm) quenched andesitic inclusions (Stimac et al., 1990). **0.1**

29.3 **STOP 5. Carlsbad Spring.** Turn out on left into wide area opposite roadcut exposing obsidian flow-breccia. Park vehicles and descend road embankment to small gully. Cross gully and ascend to abandoned dirt road. Follow this road ~100 m east to junction with another dirt road. **Note: Access by special permission only; do not trespass.** Walk past gate and follow road downhill ~150 m. Carlsbad Spring issues from a 0.3 m diameter basin in a grassy area 6 m up from the right side of the dirt road. A small resort existed here at the turn of the century but it burned down in 1908 (Waring, 1915). Several other bicarbonated springs issue in this area near the banks of Cole Creek.

Carlsbad Spring flows 2 l/min of cool water (25°C) of the thermal meteoric type that tastes mildly of soda (550 mg/kg HCO₃) and iron (Goff et al., 1977). The outflow channel contains orange-stained algae. This spring was not flowing in March 1991 or June 1992 during the recent drought but flow had resumed by May 1993. No gas discharges from the spring or nearby area.

The spring issues near the contact of Thurston Creek Rhyolite and underlying sediments that are probably equivalent in age to many in the Clear Lake basin seen at Stop 4. The sediments contain abundant gravels with Franciscan chert fragments (Hearn et al., 1976).

Return to vehicles. **Continue** up Bottle Rock Road. **2.4**

31.7 Harrington Flat Road on the left. **Continue** on Bottle Rock Road. **0.6**

- 32.3 To right is entrance to Coldwater Creek geothermal field, The Geysers. **Continue on Bottle Rock Road. 0.4**
- 32.7 **Turn out on right** for view of serpentine ridge along the Collayomi fault zone where a deep well named Sullivan #1 was drilled to 1871 m depth, all in serpentine. The measured temperature in the dry hole was 190°C, but the temperature/depth profile near the bottom indicates a conductive gradient of 270°C/km. The Collayomi fault zone is the northeastern boundary to The Geysers vapor-dominated geothermal area (Goff et al., 1977). At 2:00 is Cobb Mountain, a composite rhyodacite dome (1.15 to 1.05 Ma). **1.5**
- 34.2 Sliver of Colloyami fault zone on left; serpentine and silica-carbonate rock are thrust over Quaternary gravels containing Franciscan lithologies and young volcanic clasts. **0.8**
- 35.0 **Turn left** on Sulphur Creek Road. **0.3**
- 35.3 **Turn left** on unmarked road where sign posts on tree indicate addresses 8300-8400. **0.3**
- 35.6 **STOP 6. Sulphur Creek Spring.** Park along creek at bottom of hill. **Note: Access by special permission only; do not trespass.** Walk down creek about 50-100 m to serpentinite where cool (~22°C) water and gas discharge into creek. Although the area smells strongly of H₂S, the gas contains 97.5% CO₂ and only 0.4% H₂S (Table 1). Undiluted spring water tastes mildly sweet and saline as well as sulfurated, and is of the thermal meteoric type. The sweet flavor comes from Mg (160 mg/kg) dissolved out of the serpentine. A sample of this spring collected in 1991 contained 4 T.U. tritium indicating it is composed mostly of young, near-surface groundwater (Goff et al., 1993a). These springs were briefly discussed by Waring (1915, p. 268). The serpentinite is fractured and incorporated into the Collayomi fault zone (Hearn et al., 1976). Shale belonging to the Knoxville Formation, part of the basal Great Valley sequence, occurs nearby.
- Turn around** and return to Sulphur Creek Road. **0.4**
- 36.0 **Turn right** (downhill) at Sulphur Creek Road. **0.3**
- 36.3 **Turn left** at Bottle Rock Road, and pass area called Glenbrook. **1.9**
- 38.2 Entrance (on right) to The Geysers over north side of Cobb Mountain. **Continue** straight ahead. **0.4**
- 38.6 **STOP 7. Gordon Warm Spring.** Turn out and park vehicles on left side of road at the south end of the meadow **Note: Access by special permission only; do not trespass.** Pass gate and walk along abandoned grassy road at the edge of the meadow. Cross Kelsey Creek as best you can. Walk ~200 m upstream along poorly defined path that

parallels the creek about 25 m away from the northeast bank. Gordon Warm Spring issues in a marshy area near the base of an old unpruned apple tree. Water from several small vents and seeps flows toward the creek through a blackberry thicket. Green, yellow-green, and orange algae form a mat over the main pool which measures 1m x 2m and about 0.2 m deep. A small bathhouse stood nearby at the turn of the century (Waring, 1915).

The spring water (35°C) is of the thermal meteoric type but is very dilute and has little taste. Very intermittent gas discharges are visible but may only be related to decomposing organic material in the algae pool.

The spring emerges near the base of linear ridges of serpentinite within the Collayomi fault zone (Hearn et al., 1976). The andesite of Boggs Mountain (1.50 Ma) overlies the serpentine uphill.

- Continue** on Bottle Rock Road. **0.3**
- 38.9 Community of Pine Grove. **0.7**
- 39.6 **Junction; turn right** on Highway 175 in the community of Cobb. **0.8**
- 40.4 Community of Whispering Pines. **2.0**
- 42.4 Landslide block (right) on south side of Cobb Mountain. **1.1**
- 43.5 Socrates Mine Road on right. **Continue** straight ahead. **0.3**
- 43.8 **Turn right** on Anderson Springs Road; **turn right** again past “not a through road” sign. Drive through dispersed vacation homes and past Anderson Springs Property Owners Association. **1.5**
- 45.3 **STOP 8. Anderson Springs.** Park at gate at end of road and walk uphill along dirt road. Pass by an old prospecting cave (to the left of road) that has calcite deposited on rock surfaces. Anderson Hot Spring is located at the base of a silicified cliff which is probably a fault scarp. Exposed rock includes bedded chert and metagreywacke of the Franciscan Complex. The spring issues from a small cave-like slot at about 2 ℓ/min into a shallow (<0.3 m deep) pool extending about 1 m from the mouth of the slot and which is partly contained on the right-hand side by a retaining wall. Black sulfides line the bottom of the slot and a scum of iron hydroxide floats on the surface of the pool.

At the turn of the century, nine mineralized springs of varying temperature issued from widely separated points in these ravines and were the main attraction for a resort that accommodated 150 people (Waring, 1915). All of the springs have surprisingly similar chemistry and are of the steam condensate type (Goff et al., 1977; 1993b). Anderson Hot

Spring discharges water that tastes of H₂S from gases that emerge from the pool of hot water near the base of the retaining wall. These gases contain 82% CO₂, 5% CH₄ and 0.4% H₂S among others (Table 1). The water contains 4.6 T.U. tritium indicating that it is primarily near-surface groundwater. Steam and acid gases from the vapor-dominated geothermal system of The Geysers condense into near-surface groundwaters to form these springs (White et al., 1971).

Anderson Springs is located southwest of the Collayomi fault zone near the southeast margin of The Geysers steam field (Fig. 1). The spring waters, spring deposits, and host rocks resemble those found in other parts of The Geysers (Waring, 1915, p. 91; Goff et al., 1977).

Turn around and return to Highway 175. **1.4**

46.7 **Turn left** on Highway 175 and return toward Cobb Mountain. **4.3**

51.0 **Junction** with Bottle Rock Road. **Continue** north on Highway 175. **0.7**

51.7 Andesite of Boggs Mountain along road. **0.8**

52.5 Hoberg's Resort, now owned by the Maharishi and named Capital of the Age of Enlightenment. Although the resort has no hot springs it was a popular retreat in the 1940's and 1950's. **0.6**

53.1 Bedded greywacke and shale (flysch) of the Great Valley sequence on right. **0.4**

53.5 **Turn right** on Adams Springs Road at junction with Harrington Flat Road (to left). **0.4**

53.9 **STOP 9. Adams Springs.** Park at intersection with Mineral Springs Lane. Walk down along old road bearing west (right) about 250 m to bottom of side ravine at head of Big Canyon. Adams Springs once boasted a large resort that accommodated about 400 people (Waring, 1915) but it fell into disuse in the 1940's.

The principal mineral spring (15°C) seeps from a concrete and metal drinking tank in the ruins of a rectangular, covered grotto. Iron oxides stain the outflow channel. The water tastes slightly sweet and strongly bicarbonated (3300 mg/kg HCO₃). Another spring seeps from the hillside northwest of the grotto and produces a bright iron oxide stain. No gases discharge from these springs. The springs were dry in March 1991 and June 1992 during drought conditions, but flow had resumed by May 1993.

The springs issue from flysch of the Great Valley sequence displaying very steep dip. However, very high content of Mg (≥ 400 mg/kg) indicates that the spring water flows through serpentine at depth.

Turn around and go back to Highway 175 via the return leg of the Adams Springs loop road. **0.3**

54.2 **Turn right** on Highway 175. **0.1**

54.3 White pyroclastic rocks of the rhyolite of Bonanza Springs (1.02 Ma) overlie steeply-dipping flysch deposits of the Great Valley sequence. **0.1**

54.4 Loch Lomond Church on right. **0.2**

54.6 **Turn right** on Loch Lomond Road, driving around Seigler Mountain, a dacite dome (0.61 Ma). Big Canyon is on the right. **3.0**

57.6 Junction with Seigler Springs Road North on left. **Continue** straight ahead. **0.3**

57.9 **STOP 10. Seigler Springs.** Turn out on right just below and opposite from prominent knob of silica-carbonate rock (altered serpentine) below the old resort buildings of Seigler Springs. **Note: Access by special permission only; do not trespass.** Seigler Springs is presently owned by the Free Communion Church and is no longer open to the public. Permission to enter is rarely given. The resort has been expanded and remodeled several times since the turn of the century and still retains much of its original charm (see Waring, 1915).

Over 10 thermal/mineral springs are spread out over the property and have a maximum temperature of about 52°C. One of the springs is known as the Hot Geyser (really a well 30 m deep) which spouted once a day until the 1906 earthquake caused this action to cease. The springs are of the thermal meteoric type and taste bicarbonated and slightly sweet. The springs are highlighted by Barnes et al. (1973b) in their study of silica-carbonate alteration of serpentine by hydrothermal fluids. The gases consist primarily of CO₂ (Nehring, 1981; Table 1). Low tritium content of the fluids (0.2 T.U.) indicates they are relatively old and deeply circulating (Goff et al., 1993a).

The springs issue from faulted serpentine and silica-carbonate rock in the Konocti Bay fault zone (Goff et al., 1977; Thompson et al., 1992). Greywacke of the Great Valley sequence is exposed to the northwest. These rocks are overlain by bedded pyroclastic deposits of the rhyolite of Bonanza Springs to the north. The opalized silica-carbonate rock exposed along the road is an excellent example of this type of alteration.

Continue on Loch Lomond Road. **0.2**

58.1 Gazebo housing a cool, carbonated spring on right. **0.4**

58.5 Hoberg's Airport on right. **0.1**

- 58.6 **Bear right** on Big Canyon Road at intersection with Seigler Canyon Road (to left). **0.1**
- 58.7 **Junction** with Perini Hill Road. **Continue** on Big Canyon Road. "Clear Lake diamonds", which are clear quartz crystals eroded from the andesite of Perini Hill (~0.9 Ma) can be found in Diamond Flat about 2.5 km up Perini Hill Road (Brice, 1953). The quartz is xenocrystic, and probably derived from metamorphic rocks that were assimilated by the andesite at midcrustal depths (Brice, 1953; Hearn et al., 1981; Stimac, this volume). **0.5**
- 59.2 Passing other leg of Perini Hill Road. **0.7**
- 59.9 Gated dirt/gravel road on right leads to the Bouscal #1A well, drilled to 2750 m through rocks of the Great Valley sequence, serpentinite, and the Franciscan Complex. The measured bottomhole temperature was 245 °C, but the well was essentially dry. **Continue** on Big Canyon Road. **0.2**
- 60.1 **STOP 11. Howard Hot Springs.** Turn out on right and park at chain across resort entrance. **Note: Access by special permission only; do not trespass.** Howard Hot Springs was first developed as a resort in about 1880 (Waring, 1915). Several improvements and renovations were made over the years but the resort was eventually closed to the general public in the early 1970's. The buildings are in an excellent state of preservation and provide an unparalleled glimpse of resort life from bygone days (Fig. 8).

There are roughly 40 different springs on the property but about 10 principle ones are used for bathing and drinking. Discharge temperatures are $\leq 46^{\circ}\text{C}$ and the largest spring discharges about 80,000 l/day. The springs are similar geochemically and are of the thermal meteoric type (Goff et al., 1977; 1993b; Thompson et al., 1992). Most of them produce deposits of iron oxides. The waters taste mildly saline, slightly sweet, and strongly bicarbonated from presence of Cl (460 mg/kg), Mg (300 mg/kg), and HCO_3 (1680 mg/kg). This water contains 0.0 T.U. tirtium indicating it is relatively old and deeply circulating. The gas contains over 99% CO_2 (Table 1).

The springs issue from faulted serpentine and shale of the Knoxville Formation near the southern end of the Konocti Bay fault zone where it interconnects with the faults in Big Canyon. White pyroclastic deposits of rhyolite of Bonanza Springs overlie the older rocks to the west.

Continue on Big Canyon Road. **0.2**

- 60.3 Descending into Big Canyon. The road cuts reveal rocks of the Great Valley sequence, serpentinite, silica-carbonate knobs, and chert. Across the canyon is Boggs Mountain. **1.2**
- 61.5 **Turn right** on Springs Road. **0.3**

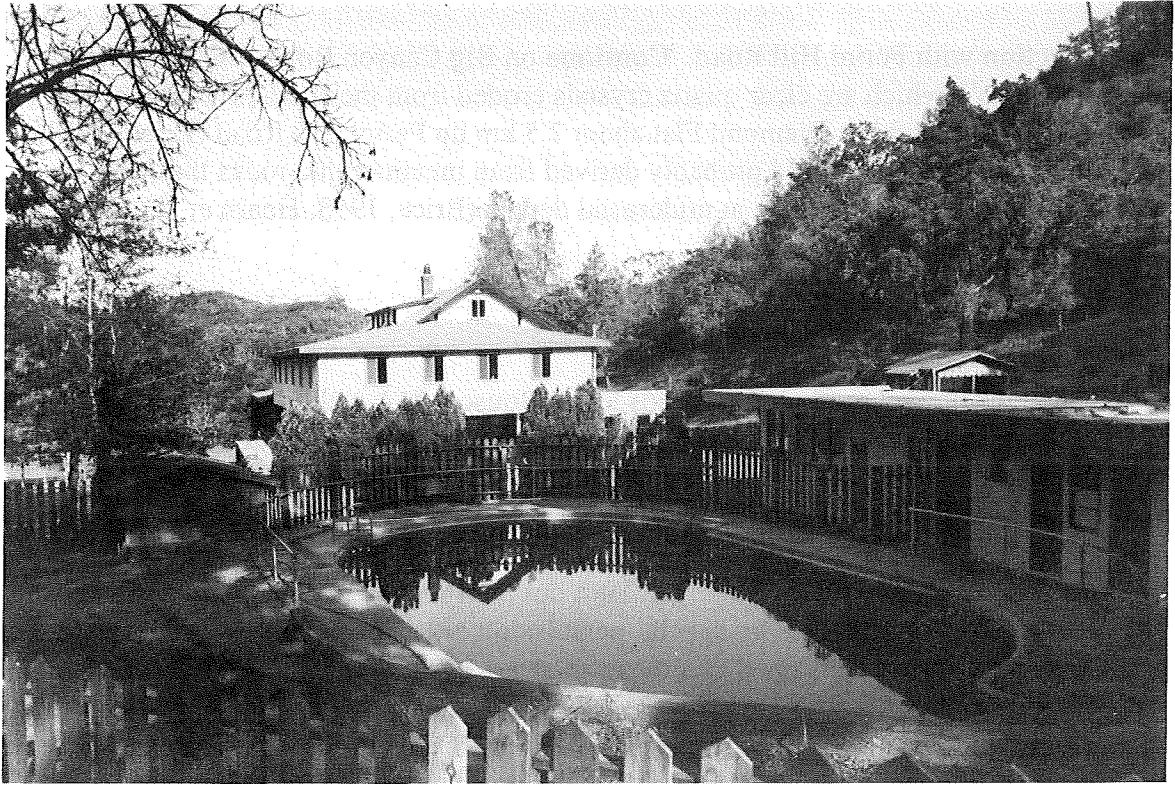


FIGURE 8. View looking east of the swimming pool and main resort building at Howard Hot Springs. Several warm to hot springs issue from the base of the low ridge of serpentinite and shale of the Knoxville Formation on the right side of the photo. Borax Beauty Bath and Iron-Sulphur Spring (46°C) issue from buildings to the right of the photo.

61.8 **STOP 12. Ettawa Spring (Pine Cone Spring).** Park in the lot by the house on the right. This is the local headquarters of Boggs Mountain Reserve, a nature reserve that encourages research and peaceful recreation. A ruined gazebo lies 50 m upslope south of the road and is reached by an unmarked trail opposite the house. The gazebo, which provided shelter for Pine Cone Spring, was destroyed sometime after 1976. It is now very difficult to sample or enjoy this spring. Ettawa Spring occurs a few meters west and downslope of Pine Cone Spring and issues from a black plastic pipe at 2 l/min. The property line between the reserve and the defunct resort of Ettawa Springs (further up the road) actually runs between the two springs. This is one of the few, easily accessible, bicarbonated springs of the region that is not mentioned by Waring (1915).

The springs are geochemically identical and are of the thermal meteoric type. Discharge temperatures range from 22 to 27°C depending on the season. The waters taste faintly saline, pleasantly sweet, strongly bicarbonated, and make great lemonade. Ettawa Spring

contains 1.1 T.U. tritium indicating a maximum mean residence time of 600 yr (Goff et al., 1993a). No gas is emitted by the springs.

The gazebo was constructed on a small apron of travertine deposited on landslide debris containing serpentine and greywacke of the Great Valley sequence. Occasional boulders of andesite of Boggs Mountain from upslope can also be found near the springs.

Probably the spring waters rise along one of the many faults that parallel the trend of Big Canyon.

Turn around and return to Big Canyon Road. **0.3**

62.1 **Turn right** (downstream) on Big Canyon Road. **1.3**

63.4 Bridge. **0.3**

63.7 Bridge. **0.5**

64.2 Bridge. **0.2**

64.4 **STOP 13. Spiers Springs.** Turn out and park on left side of road along the bank of Big Creek. Cross the creek and walk 50-60 m downstream. About three springs issue at the base of faulted serpentine. A knob of fault gouge filled with serpentine and greywacke is the prominent feature near the main spring which issues in a shallow gravel pan and has a constant, weak gas discharge. The outflow channel contains iron oxide deposits and a mat of green algae. The spring water tastes like iron and is somewhat sweet (310 mg/kg Mg) and bicarbonated (2100 mg/kg HCO_3). The waters are of the thermal meteoric type (Thompson et al., 1992; Goff et al., 1993b) and issue at 24°C and 15 l/min. The gas consists mostly of CO_2 and air components (Table 1). Water from this spring was bottled for sale around the turn of the century (Waring, 1915) but for many years it has been ignored and forgotten. When recrossing the creek, note the gas seeps that issue from the creek bottom; some bubbles are >3 cm in diameter.

Turn around and drive back up Big Canyon Road to return to Lower Lake Junction. **5.2**
[Option: Continue straight ahead on Big Canyon Road to Middletown, Calistoga, and return to the Bay Area.]

69.6 **Bear right** on Seigler Canyon Road. **0.8**

70.4 Rocks of the Great Valley sequence. **2.7**

73.1 Perini Hill Road on right. **Continue** straight ahead on Seigler Canyon Road. **0.5**

73.6 **Turn right** on Highway 29 toward Lower Lake. **1.4**

75.0 Lower Lake Junction. **End of Day 1.**

**Second Day Road Log:
Geothermal Phenomena and Mercury Deposits of the
Eastern Clear Lake Region**

Summary — On the second day (Fig. 9) we will visit several famous sites that produce connate waters (fossil seawater?). These relatively saline fluids have chemical similarities to oil field brines and seawater and have enriched $\delta^{18}\text{O}$ and δD values (White, 1957; White et al., 1973; Donnelly-Nolan et al., 1993; Goff et al., 1993b; Peters, 1993). Two areas, Sulphur Bank Mine and Wilbur Springs District, have high- to moderate-temperature connate fluids that are associated with contemporaneous ore deposits (White and Roberson, 1962; Moiseyev, 1968; Peters, 1991). The Sulphur Bank Mine deposit is surrounded by ≤ 90 ka basaltic to rhyolitic eruptions whereas the Wilbur Springs District contains small-volume basaltic dikes (1.66 Ma) representing early Clear Lake volcanism. Drilling encountered relatively small geothermal reservoirs at each site but, for various reasons, neither site has been developed commercially.

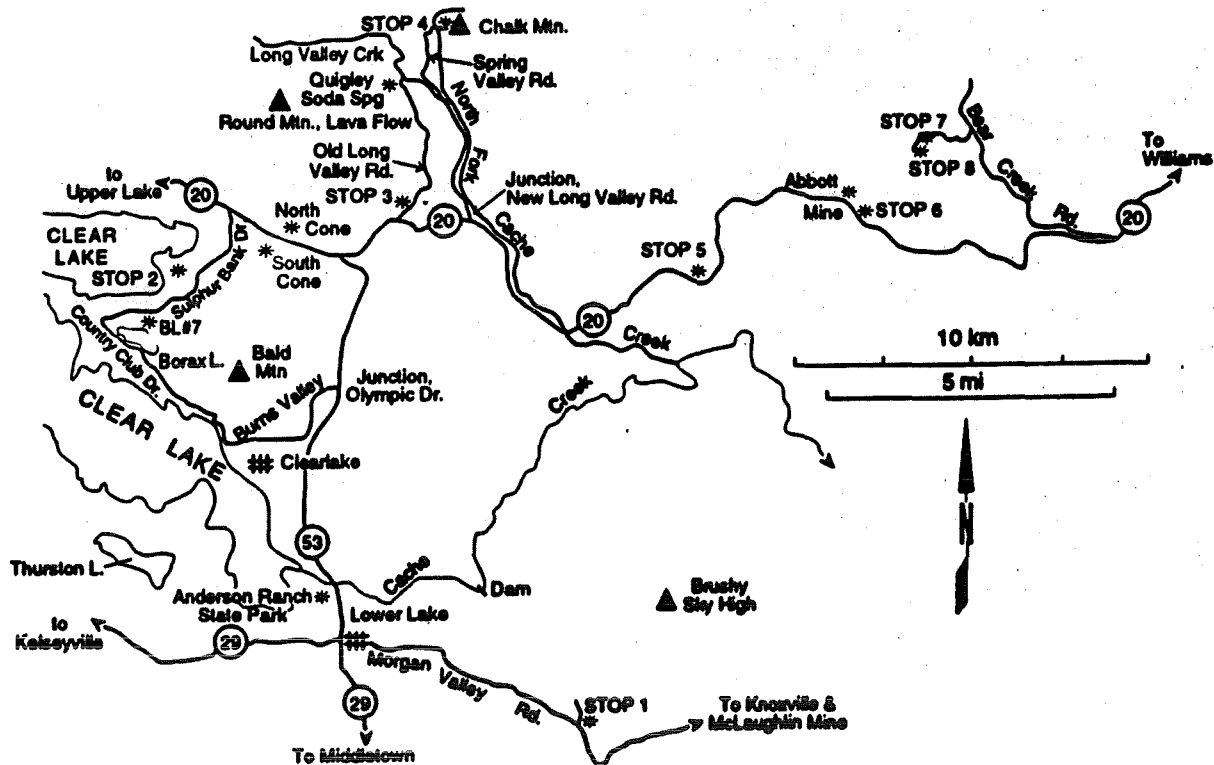


FIGURE 9. Route map, Day 2.

Mileage:

- 0.00 Lower Lake Junction, head east on Morgan Valley Road through the community of Lower Lake. Drive through rolling hills underlain by rocks of the Great Valley sequence. 4.7**
- 4.7 Turn left on Sky High Ridge Road. Baker Mercury Mine is seen on the hillside to the right, and is located on the Grizzly Peak fault zone; the mercury (cinnabar) is found in faulted serpentinite, silica-carbonate rock, and shale of the Knoxville Formation (Brice, 1953). The mine was never very productive. 0.1**
- 4.8 View of Baker Soda Spring. 0.1**
- 4.9 Faulted serpentinite in the roadbed. 0.1**
- 5.0 STOP 1. Baker Soda Spring. Park on either side of the road at the bottom of the gully. Walk toward the east about 400 m gradually contouring uphill. Baker Soda Spring forms a pool 6 m long by 2 m wide at the grassy summit of its iron-stained, travertine terrace (Fig. 10). The spring flows at about 3 l/min and discharge temperature ranges from 21 to 25°C depending on the season.**

Baker Soda Spring is a connate water (White et al., 1973; Donnelly-Nolan et al., 1993; Goff et al., 1993b; Peters, 1993) containing relatively high concentrations of Cl, HCO₃, Na, K, Mg, and trace elements As, B, Br, and Li. The water tastes salty (3000 mg/kg Cl) and bicarbonated (4650 mg/kg HCO₃). The water contains 0.04 T.U. tritium indicating that it is old and deeply circulating. Fehn et al. (1992) have estimated an age of roughly 84 ka for end-member connate waters of this type using ³⁶Cl. The gas that bubbles freely from the spring contains 99% CO₂ and has a distinct mantle/magmatic signature as described above (Table 1).

Baker Soda Spring issues from faulted serpentinite and shale of the Knoxville Formation in the northwest-trending Grizzly Peak(?) fault zone. Basalts of the Clear Lake volcanic field at the McLaughlin Mine southeast of Baker Soda Spring are dated at 2.2 Ma where relatively high-temperature hydrothermal activity persisted until 0.75 Ma (Lehrman, 1986). The spring lies 8 km southeast of the main Clear Lake volcanic field where rocks ≤0.4 Ma in age occur.

Turn around and return to Morgan Valley Road. 0.4

- 5.4 Turn right on Morgan Valley Road and retrace route to Lower Lake. 4.7**

[Option: Turn left on Morgan Valley Road to reach the Knoxville mercury district and the McLaughlin gold mine, a classic hot-spring gold deposit (Lehrman, 1986).]

- 10.1 Turn right on Highway 53 (north) at Lower Lake Junction. 0.7**

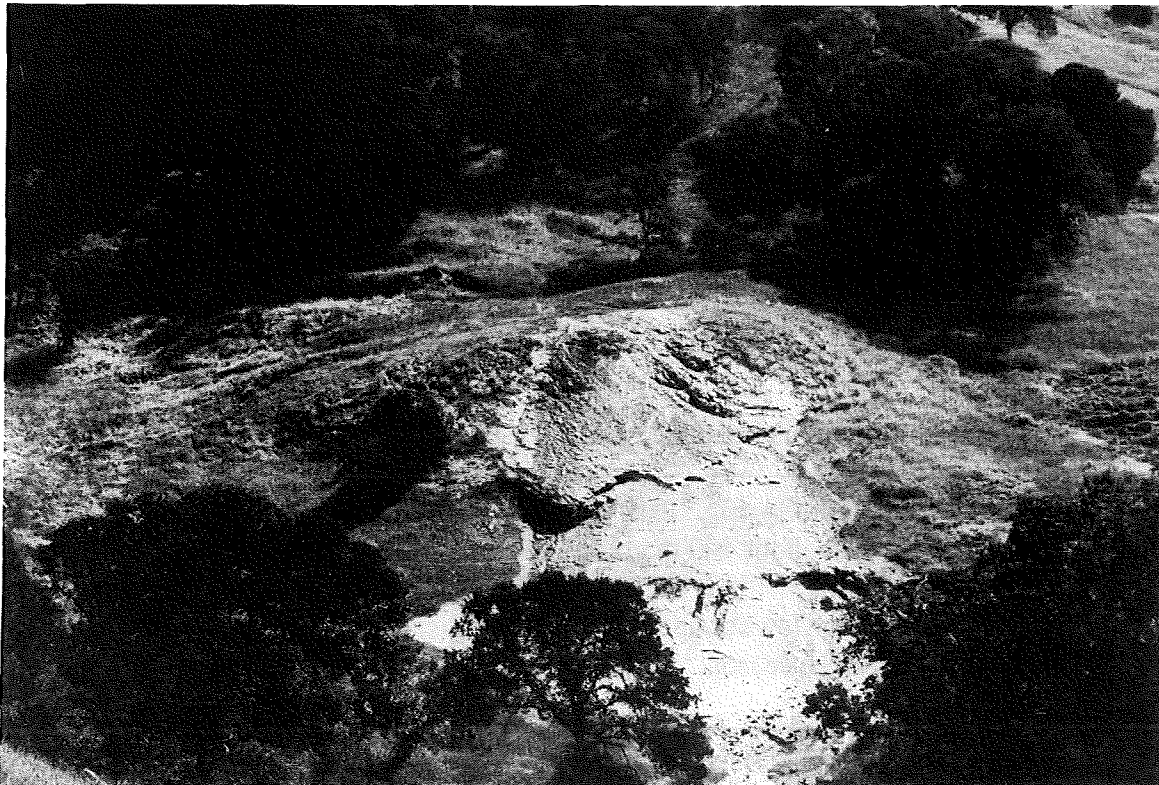


FIGURE 10. View looking north of the travertine terrace formed by Baker Soda Spring. The spring flows from a small pool at the summit of the terrace.

- 10.8 Anderson Park State Historic Ranch on left. **0.3**
- 11.1 Bridge over Cache Creek, the outlet of Clear Lake. **0.4**
- 11.5 Junction with old state highway. **Continue** straight ahead. **1.1**
- 12.6 White, poorly-bedded lacustrine rocks of the Cache Formation, a Pliocene to Pleistocene basin-fill deposit (Rymer, 1978). **0.4**
- 13.0 Junction with 40th Avenue, the main entrance to the community of Clearlake (to the left). **Continue** straight ahead on Highway 53. **1.0**
- 14.0 **Turn left** on Olympic Drive. Views of Burns Valley, Bald Mountain, and Mount Konocti. **0.7**
- 14.7 Junction with Burns Valley Road and old Highway 53. **Continue** straight ahead. **1.0**

- 15.7 **Turn right** on Lakeshore Drive. **0.3**
- 16.0 **Bear left** to stay on Lakeshore Drive. **0.4**
- 16.4 **Go straight ahead** on Park Street at junction with Lakeshore Drive. **0.45**
- 16.45 **Turn left** on Arrowhead Drive. Road is now on obsidian flow of the rhyolite of Borax Lake, the youngest (90 ka) rhyolite in the Clear Lake volcanic field. View of Highlands Arm of Clear Lake on left. **0.45**
- 16.9 **Continue straight ahead** to Country Club Drive at junction with several roads. Note chert, greenstone, and greywacke of the Franciscan Complex in outcrops on left beyond junction. **0.7**
- 17.6 View of closed-basin holding Borax Lake on the right. This was the first place in California to be mined for borax (in the 1850's). The lake forms at the end of the northwest-trending fault-controlled valley which was probably another arm of Clear Lake before closure by the obsidian flow of the rhyolite of Borax Lake. **0.5**
- 18.1 **Turn out on right** for view of Borax Lake #7 well pad on opposite side of the lake. This was an exploration well drilled to 3077 m in Franciscan rocks; bottomhole temperature was ≥ 250 °C, but the well was essentially dry. To the right (down valley) is a hill covered with live oak, exhibiting typical vegetation on obsidian flow of the rhyolite of Borax Lake. The unnamed ridge on the east side of the valley is largely composed of greenstone. Bald Mountain is at the southeast end of the ridge. Beyond the walnut orchard at the southeast end of the lake is an area of low-temperature gas seeps and altered ground. The gases display very definite mantle/magmatic affinities and resemble gases at Sulphur Bank Mine across the ridge to the north (Table 1).
- Continue straight ahead** along shore of Borax Lake. **1.0**
- 19.1 Ascending Sulphur Bank Ridge. Shattered greenstone and chert of the Franciscan Complex on left. **0.6**
- 19.7 **Bear right** on Sulphur Bank Drive at junction with Lakeshore Drive, and go east along crest of Sulphur Bank Ridge. **0.1**
- 19.8 View to the left of the Oaks Arm of Clear Lake. **0.1**
- 19.9 Greenstone knockers in the Franciscan Complex. **0.5**
- 20.4 Descending the ridge; view of Sulphur Bank Mine below. **1.1**
- 21.5 **STOP 2. Sulphur Bank Mine.** Turn hard left and park along entrance road to mine. **Note: Access by special permission only; do not trespass.** Access generally requires

signing a release form. Cross gate and follow old haul road to north side of Herman Pit. Sulphur Bank mine was one of the largest mercury mines in the United States (~130,000 flasks or ~4500 metric tons) before operations ceased in 1957 (Fig. 11). White and Roberson (1962) claimed it was “the most productive mineral deposit in the world that is clearly related to hot springs.” Much has been learned since then about the relation of hydrothermal fluids to ore deposits. The McLaughlin gold mine located southeast of Lower Lake is a “hot spring” gold deposit (Lehrman, 1986) but it was initially mined for mercury.

Sulphur Bank Mine has had an interesting history since its discovery in 1856 (Becker, 1888). It was first mined for sulfur (~2,000,000 tons) before it was realized that abundant cinnabar was deposited at the existing water table. Early mining of the cinnabar was done underground, mostly by Chinese laborers working 20-minute shifts. High subsurface temperatures and noxious levels of H_2S , NH_3 , CH_4 , and CO_2 took a heavy toll. Eventually open pit techniques were employed and the Herman Pit was excavated to a depth of roughly 50 m.

During early mining operations, water as hot as $80^{\circ}C$ was flowing into the deeper shafts (Waring, 1915) but, when operations ceased, the hottest water was produced from Geyser

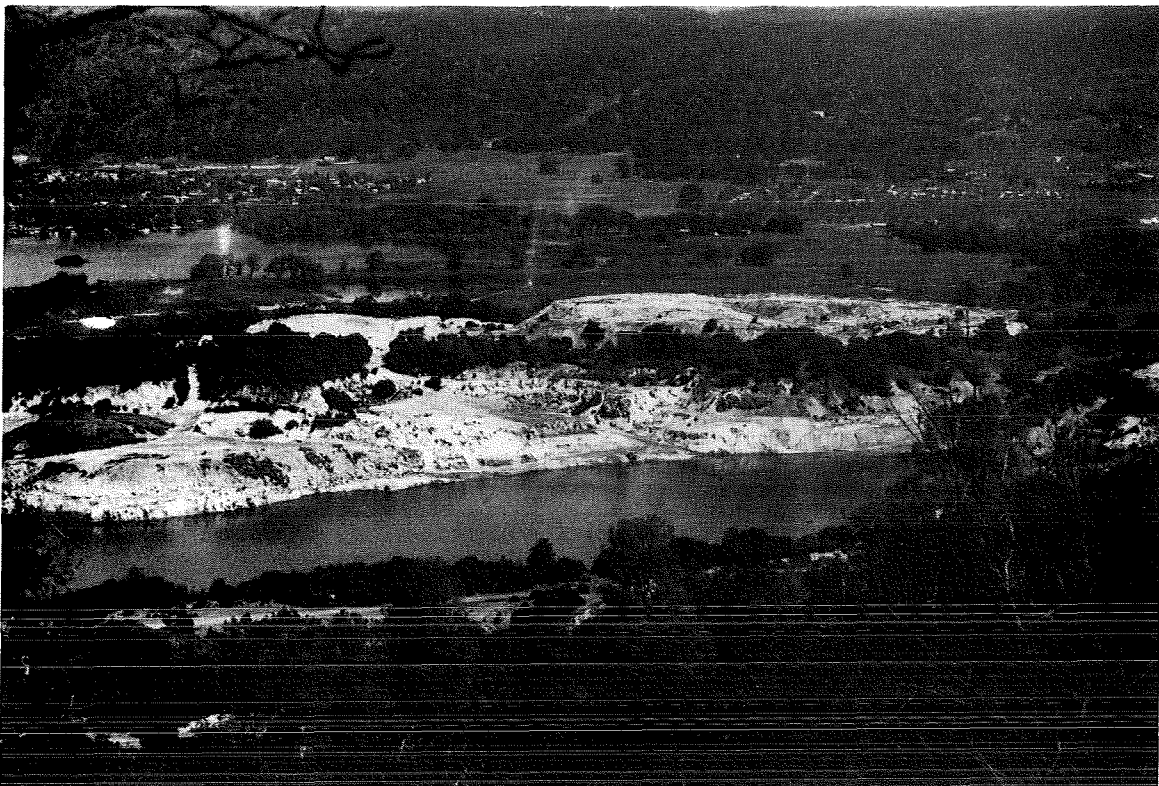


FIGURE 11. View looking northeast of Sulphur Bank mine and Herman Pit. Most of the rocks in the mine area are bleached white by near-surface argillic alteration. Gas vents occur throughout the small lake filling the pit, particularly on the north shore. Four geothermal exploration wells were drilled from flat areas excavated in the mine. The extreme eastern end of the Oaks Arm of Clear Lake is visible in left background of photo.

Spring (70°C) at the bottom of the pit. No hot springs presently issue at the surface but gas vents and standing pools of gas-rich water occur throughout the property. Clusters of gas vents can be seen at several points in the small lake filling the Herman Pit. Flow rate of the natural springs has been variously estimated at 150 to 1100 ℓ /min.

The spring waters have been called metamorphic waters by White (1957) and White et al. (1973) because of their extremely high B/Cl ratios (roughly 800 mg/kg of each component), relatively high salinity, high NH_4 contents (460 mg/kg) and abundant CH_4 . Isotopically, the waters are classified as connate waters (White et al., 1973; Goff et al., 1993b; Peters, 1993) because they closely resemble typical connate fluids located to the east. The fluids typically contain ~500 ppb of Hg (Chamberlin et al., 1990). A sample of Geyser Spring collected in 1957 contained 1.1 T.U. tritium implying that the water was a mixture of deep thermal water and near-surface groundwaters (Goff et al., 1993a).

Sulphur Bank gases have not been adequately studied. However, the gas emerging from the north edge of the Herman Pit contains 87% CO_2 , 10% CH_4 , 2.5% N_2 , 0.03% H_2S , and 0.002% NH_3 . Considerable NH_3 may be dissolved in the water filling the Herman Pit. The gas is distinctly mantle/magmatic in character and has relatively high ^3He ($R/R_A=7.5$; Table 1).

Four geothermal exploration wells have been drilled here and rusted wellheads and plumbing litter the mine. The best well was Bradley #1 which produced 218°C water from a fracture at 503 m. Drilling to depths of 1226 m did not find hotter, more productive horizons and all wells are considered subcommercial. Some wells suffered severe aragonite scaling problems, observable inside the fallen wellheads. The deep fluids resemble the hot spring fluids in their chemistry (White et al., 1973) and show many similarities to high-temperature fluids that enter other regional exploration wells in limited quantities (Beall, 1985).

The mine occurs in faulted, contorted greywacke and shale of the Franciscan Complex that is overlain by a thin sequence of unconsolidated conglomerate, silt, and cross-bedded sandstone. The andesite of Sulphur Bank Mine overlies the unconsolidated sediments and the source of the andesite is probably from South Cone located to the east (Hearn et al., 1981). Carbon-14 dating of wood fragments in sediments beneath the andesite yields an age of 44.5 ka (Sims and White, 1981).

Near-surface alteration and mercury transport mechanisms were most recently studied by Wells and Ghiorso (1988). The surface alteration is argillic to advanced argillic in character (silica, kaolin, alunite, other sulfates, pyrite/marcasite, sulfur, and cinnabar). Beneath the water table, silica, clays, pyrite, and cinnabar are deposited in fractures and breccia zones. Careful inspection of existing gas vents usually reveals disseminated cinnabar on altered rocks. This is also a locality for an ammonium feldspar, Buddingtonite. The mercury is probably transported from depth as sulfide complexes,

not as organomercury complexes. Oxidation of hot spring water at the water table is probably the most effective depositional mechanism. Because of relatively high volatility, some mercury is deposited above the water table.

Sulphur Bank Mine is now a Superfund Site and requires extensive environmental clean-up (Chamberlin et al, 1990). Approximately 100,000 kg of mercury exist within the upper sediments of the Oaks Arm of Clear Lake and the mine probably contributes another 100 kg/yr through sheet-wash erosion and slope failures. High concentrations of mercury occurring in deeper sediments of the lake have been correlated to periods of natural hydrothermal input (Sims and White, 1981).

Turn around and return to highway. **0.1**

21.6 **Turn left** to continue northeast on Sulphur Bank Drive. South Cone can be seen in the distance. **1.3**

22.9 **Junction; turn right** on Highway 20. **0.4**

23.3 View of North Cone on left. **1.6**

24.9 **Bear left** to stay on Highway 20 at junction with Highway 53. **1.3**

26.2 **Turn left** on Old Long Valley Road (sign has been removed). **0.2**

26.4 Outcrop of the Cache Formation (Pliocene to Pleistocene) on left. We have entered the southwest corner of a structural basin (Hearn et al., 1988). **0.2**

26.6 **STOP 3. Hog Hollow Spring.** Turn out on right side of road near stock tank and park. **Note: Access by special permission only; do not trespass.** Walk to left (west) following the gully uphill for about 200 m; go past little-used dirt road into brushy ravine. Hog Hollow Spring issues from the south side of the ravine into the gully. Additional seeps are located in the gully. This spring was first mentioned by Thompson et al. (1981a).

Hog Hollow Spring flows 8 l/min at 30°C and produces a brilliant orange deposit of iron oxides. The water is fairly dilute (~170 mg/kg Cl) but has elevated B (~15 mg/kg). It tastes of iron and soda (~800 mg/kg HCO₃). The spring water contains 0.3 T.U. tritium indicating a maximum mean residence time of 2500 yr (Goff et al., 1993a). It is classified as a thermal meteoric water. Weak gas emissions are produced constantly that contain 85% CO₂ and 1.2% CH₄ among others (Table 1).

A few meters further west is an outstanding exposure of the north-trending Cross Spring fault zone which juxtaposes shattered Franciscan greenstone (west) against sheared,

steeply-dipping sedimentary strata of the Cache Formation (McLaughlin et al., 1989). Other thermal/mineral springs flow from this fault zone further north.

Continue down Old Long Valley Road. **0.3**

26.9 **Turn around** in the driveway and retrace route to Highway 20. **0.65**

[Option: Continue straight ahead on Old Long Valley Road to cross the east end of the basaltic andesite of High Valley, the youngest lava flow in the Clear Lake volcanic field (estimated age is 10 ka). Quigley Soda Spring is located at the north end of the flow, west of the road in a marshy gully, near where the road descends to a dead end at Long Valley Creek.]

27.55 **Turn left** (east) on Highway 20. Drive by outcrops of Pliocene to Pleistocene basin-fill deposits of the Cache Formation. **1.45**

29.0 **Turn left** on New Long Valley Road. **0.1**

29.1 North Fork Cache Creek on right. **0.3**

29.4 Mouth of Benmore Canyon. The Benmore Well near the mouth of the canyon tapped highly mineralized 22°C connate water. Data are reported by Nehring et al. (1979), Thompson et al. (1981a) and Donnelly-Nolan et al. (1993). **1.9**

31.3 View of Chalk Mountain on right. **0.6**

31.9 Old Long Valley Road can be seen across creek on left. The old road now ends at the creek. Quigley Soda Spring is located at the upper end of the small marsh. **0.1**

32.0 **Turn right** on Spring Valley Road. **0.9**

32.9 **Turn right** on Wolf Creek Road. **0.25**

33.15 **Turn right** on Chalk Mountain Road. **0.05**

33.2 **Cross bridge** over North Fork Cache Creek. **0.1**

33.3 **STOP 4. Chalk Mountain.** Park in clearing at either side of the road. Chalk Mountain is an altered hypersthene dacite plug that intrudes rocks of the Franciscan Complex and the Cache Formation along the northwest-trending Bartlett Springs fault zone. The age of the intrusion is unknown but is estimated at about 0.9 Ma (Donnelly-Nolan et al., 1981). The summit area exhibits weak fumarolic activity and was mined for elemental sulfur. Travertine-depositing mineral springs occur all around the lower flanks of the intrusion

(Waring, 1915). To reach the most active spring area on the northern flank, contour up hill on the abandoned dirt road to the left of the parking area (in an easterly direction). After walking about 100 m, observe springs and seeps below and to the left issuing from cemented terrace gravels and colluvium above North Fork Cache Creek. Continue on contour up hill. Observe on the right a small, salty spring with an algae-laden outflow channel. Leave the abandoned road and continue contouring east for ~200 m, below outcrops of the dacite of Chalk Mountain. Cross over the jumbled talus below the dacite flow to reach the area of altered ground. [CAUTION: Beware of uneven footing and Rattlesnakes!] The first spring is easily visible. The main spring is located at slightly higher elevation, a few meters further to the north. This salty, sulfurous, soda spring issues intermittent gas and has filamentous bacteria growing in its outflow channel. It is classified as a mixed connate-meteoric water and contains 290 mg/kg B, 3400 mg/kg Cl, 4900 mg/kg HCO₃, and 590 mg/kg Mg (Goff et al., 1993b; Peters, 1993). The fluid also contains 1.1 T.U. tritium suggesting a mixture of deep and near-surface waters.

The area smells strongly of H₂S. About 15 m further uphill and to the right near manzanita trees and digger pines is a dry, cool, noisy gas vent; H₂S-rich gas is vigorously bubbling through water just below the ground surface. A now-dormant outflow channel provides evidence that water sometimes issues from this vent.

Before returning to the vehicle, look off toward the east for a view of the northwest-trending boundary fault to the Cache basin (part of Bartlett Springs fault zone) where bluish-colored rocks of the Cache Formation are faulted against brown-colored rocks of the Franciscan Complex. Slivers of serpentine and silica-carbonate rock occur along the fault (McLaughlin et al., 1989).

Turn around in parking area, cross bridge over North Fork Cache Creek, and turn left on Wolf Creek Road. 0.3

[Option: To reach the old sulfur mine, continue up hill on the dirt road beyond the parking area and bear left at the junction in ~0.2 mile.]

- 33.6 **Turn left on Spring Valley Road. 0.1**
- 33.7 **Turn out to right near intersection with Juniper Road for view of Alum Spring (Waring, 1915), the white-colored knob bearing N65E in the notch between Stony Top and Chalk Mountain. 0.8**
- 34.5 **Turn left on New Long Valley Road. 3.0**
- 37.5 **Turn left on Highway 20. The road enters a valley and then winds around heading east toward the same fault zone observed from Chalk Mountain springs. 5.5**

43.0 On the hill to the left side of road is a terrace of travertine deposited by Grizzly Spring. 0.1

43.1 **STOP 5. Grizzly Spring.** Turn out on right side of road and park. Walk back to the travertine apron and follow it up to the spring. Grizzly Spring is located on the Bartlett Springs fault zone (McLaughlin et al., 1989) and issues from sands and gravels of the Cache Formation just south of their contact with underlying shales of the Great Valley sequence. Slivers of serpentine occur in the faulted shales to the north and pieces of serpentine can be found in the Cache deposits.

Grizzly Spring issues from a rectangular concrete basin that was covered by a shed, but the shed burned down in a recent brush fire. The water was once piped to a small bathhouse and was bottled for drinking (Waring, 1915). The discharge channel is host to filamentous bacteria and the bottom of the pool contains blue-gray silt. The connate spring water flows at 6 l/min at temperatures between 19 and 22°C and contains substantial Mg (680 mg/kg), Cl (3750 mg/kg), and HCO₃ (4840 mg/kg); a true taste treat. The water contains 0.61 T.U. tritium indicating a maximum mean residence time of ~1100 yr. However, Grizzly Spring is a mixture of connate and meteoric waters and the connate end-member has a ³⁶Cl age of ~84 ka. This water has been studied by White et al. (1973), Thompson et al. (1981a), Fehn et al. (1992), Goff et al. (1993a; 1993b), and Peters (1993).

Gas discharge is moderate and continuous; the gas contains 98.3% CO₂ and 1.1% CH₄. Although the odor of H₂S is noticeable, it is present at levels of 0.0001%. The gas is meteoric in character (Table 1; Fig. 3).

Additional springs and seeps occur in this area leading to some confusion in previous reports as to the composition of the "real" Grizzly Spring.

Continue east on Highway 20. Two travertine-depositing mineral springs can be seen issuing from the hillside on the left side of the road, east of Grizzly Spring. 0.4

43.5 Cross a fault zone and enter an area of exposed shales of the Knoxville Formation. The Knoxville is the basal unit in the Great Valley sequence, which overlies the ophiolites that form the base of the Coast Range Thrust. 1.5

45.0 Serpentinite exposed in road cut on right. 1.0

46.0 "Watering Hole" on left. 0.8

46.8 Junction with Walker Ridge Road. **Continue** straight ahead on Highway 20. 0.4

47.2 The Abbott mercury mine is on the hill to the left. 0.6

- 47.8 **STOP 6. Turkey Run Mine.** Turn out on left side of highway and park at entrance to abandoned dirt road in narrow, north-trending gully. Walk up the old road following the water in the gully past the ruins of mine structures. Turkey Run Spring is located at the base of the ridge between two side gullies, flowing from a collapsed mine shaft at about 40 l/min. A small marsh occurs between the spring and one of the ruined buildings.

The spring water is of the connate type, containing 935 mg/kg Mg, 1110 mg/kg Cl, 2330 mg/kg HCO₃, and 2550 mg/kg SO₄. The sulfate content is one to two orders of magnitude higher than all other waters in the Clear Lake region. The water has a salty, bitter-sweet taste. The area smells weakly of organics and H₂S but no gas is visible at the source. Filamentous bacteria grow in the outflow channel.

Turkey Run Spring water is similar but slightly more concentrated than water discharged from the nearby Abbott Mine during operations in 1957 (White et al., 1973). The two waters are probably related by complex mixing between a deep connate component and shallow groundwaters that dissolve sulfates from alteration minerals in the mine workings, but further research in this area is warranted.

Turkey Run and Abbott Mines are part of the Wilbur Springs Mining District and produced most of the mercury (~1700 tons; Moiseyev, 1968). The district was featured by Moiseyev (1971) in his work on non-magmatic sources for mercury deposits. It was his opinion that the mercury was mobilized out of the sedimentary rocks. Both mines occur along the contact between serpentinite and Knoxville shales (McLaughlin et al., 1989). Sulphur Creek and most of the other mines of the district are located north of the ridge behind Turkey Run Mine.

Continue on Highway 20. 1.9

- 49.7 County line boundary between Colusa and Lake Counties. **2.6**
- 52.3 Paralleling Bear Creek. Observe the road to Wilbur Springs at the bottom of the canyon on the other side of the creek. **0.6**
- 52.9 Cross Bear Creek. **0.05**
- 52.95 **Turn left** on Bear Creek Road and head west up Bear Creek. **1.15**
- 54.1 Mineral springs form travertine-cemented terrace gravels above the creek on both sides of the road. **2.7**

- 56.8 **Turn left** on Wilbur Springs Road, cross the bridge over Bear Creek and proceed up the road following Sulphur Creek. **0.65**
- 57.45 Gate (unlocked, but kept latched) to Wilbur Springs. This is private property, and all visitors must stop to register at the lodge. Drive through fault zone exposing shale of the Knoxville Formation, greenstone, and serpentine. **0.45**
- 57.75 Old resort hotel on right; bathing pools on left. Wilbur Springs is a thriving hot spring resort open to the public. Stop and register your presence; then continue up road to parking area. **0.15**
- 57.9 Main springs at Wilbur Springs issue from concrete cribs by the creek on the left. **Continue** up road. **0.2**
- 58.1 **STOP 7. Wilbur Hot Springs.** Park in lot and walk back (downstream) to the springs. Wilbur Hot Springs were first developed as a resort in the 1870's but the present hotel and other buildings date after about 1908 (Waring, 1915). Roughly 30 different cold to hot mineralized springs issue on the property along Sulphur Creek upstream and downstream of the hotel. At one time they were used for bathing, drinking, and a variety of medicinal uses but the principal use now is bathing.

A cluster of concrete tanks isolate separate springs in the largest group. The main spring flows ~80 l/min, issues from a tank within a tank (the inner tank presently covered with plywood and polyurethane foam), and is piped downstream toward the bathhouses. The present temperature is 56°C but it was once as hot as 60°C. This spring has attracted considerable attention over the years for several reasons (White, 1957; White et al., 1973; Barnes et al., 1973b; Thompson et al., 1981a; Peters, 1991; 1993; Fehn et al., 1992; Goff et al., 1993a; 1993b): First, the spring water is very salty (~11,000 mg/kg Cl) and unusually rich in dissolved sulfide (~40 mg/kg S); filtered water has a distinctive dark yellow color; second, the spring and others like it occur in a zone of cinnabar and gold mineralization; third, the spring is closely associated with a zone of faulted serpentinite; fourth, the spring water isotopically approaches end-member connate water for the Clear Lake region. A crust of sulfur forms above the spring water in the inner tank and sulfur scum forms quickly on water in open tanks. Black precipitates in this spring contain 27 ppm Hg and 4.35 ppm Au (Peters, 1991). Main spring water contains 0.23 T.U. tritium suggesting a maximum mean residence time of roughly 3000 yr or mixing of connate water with a small fraction of near-surface groundwater. The ³⁶Cl data of Fehn et al. (1992) indicate an age of ~84 ka as mentioned before.

Gas from the main spring contains about 93% CO₂, 4% CH₄, and 3% H₂S (Table 1); much more H₂S than any spring in the region outside of The Geysers steam field. However, the gas compositions have a sedimentary signature and the R/R_A value is only 1.3 (Peters, 1993) indicating only minor mantle/magmatic contributions.

A second spring worth mentioning flows into the tank of pink water adjacent to the main spring. This is named Chromatic Spring (Waring, 1915) and yields a reddish water on filtering. Evaporation of the water forms crystals predominately of K_2SO_4 and $NaCl$. Various types of algae may contribute to the scums and colors of the many springs.

The group of principal springs issues from fractured, serpentinite breccia (or detrital serpentine?) along what is now called the Resort fault zone (McLaughlin et al., 1989). Massive serpentinite, greenstone, and shale of the Knoxville Formation occur nearby, generally as fault blocks and fault slices in this zone. A series of three, en echelon, olivine basalt dikes occur on Coyote Peak about 1.1 km northeast of Wilbur Springs. A K-Ar date on one dike sample is 1.66 Ma suggesting a close association between mineralization, hydrothermal activity, and early Clear Lake volcanism (Donnelly-Nolan et al., 1993). Lack of other volcanic rocks, particularly young (<0.5 Ma) silicic rocks, and relatively low R/R_A values indicate that very little, if any, magma presently resides beneath the area.

Continue up road. 0.2

- 58.3 **STOP 8. Jones Fountain of Life Spring.** Park at gate to Cherry Hill, Manzanita, and Elgin Mines. **Note: Access by special permission only; do not trespass.** Cross gate and walk up the road past the abandoned house on the right; then turn right and walk toward Sulphur Creek to the 4 m-high concrete and brick pillar (Fig. 12). The "spring" is really a well that was bored in a former gas vent. Water from the well rises under artesian pressure to the top of the tower where it was once piped to a small hotel and resort (Waring, 1915). Gas rises intermittently in the tower and causes the water to spurt, hence the name "Fountain of Life."

A spring has formed a 2-m-diameter basin at the foot of the pillar since the demise of the resort and water from the spring is piped to an open-air bathtub near the creek. This spring and the water in the pillar have a ~25-min cycle of activity in which the spring empties, fills, and gently erupts to a height of ~0.5 m. During every second or third eruption of the spring, water cascades out of the pillar.

Amazingly, this spring was almost forgotten after being described by Waring. Recent geothermal and gold exploration after the late 1970's have brought renewed interest (Thompson et al., 1981a; Peters, 1991; 1993; Donally-Nolan et al., 1993; Goff et al., 1993a; 1993b). For example, the black precipitate in the bottom of Jones Spring contains 163 ppm Hg and 3.70 ppm Au while the hot spring water of the Elgin Mine further up canyon contains roughly 1.5 ppb dissolved Au (Peters, 1991).

Jones Spring produces connate water similar to Wilbur Hot Spring water and many other hot springs in Sulphur Creek Valley (Thompson et al., 1981a; Peters, 1993). However, the gas produced by Jones Spring (48% CO_2 , 48% CH_4 , 1% H_2S) is considerably different than Wilbur Springs gas and it is not known if large differences occur among

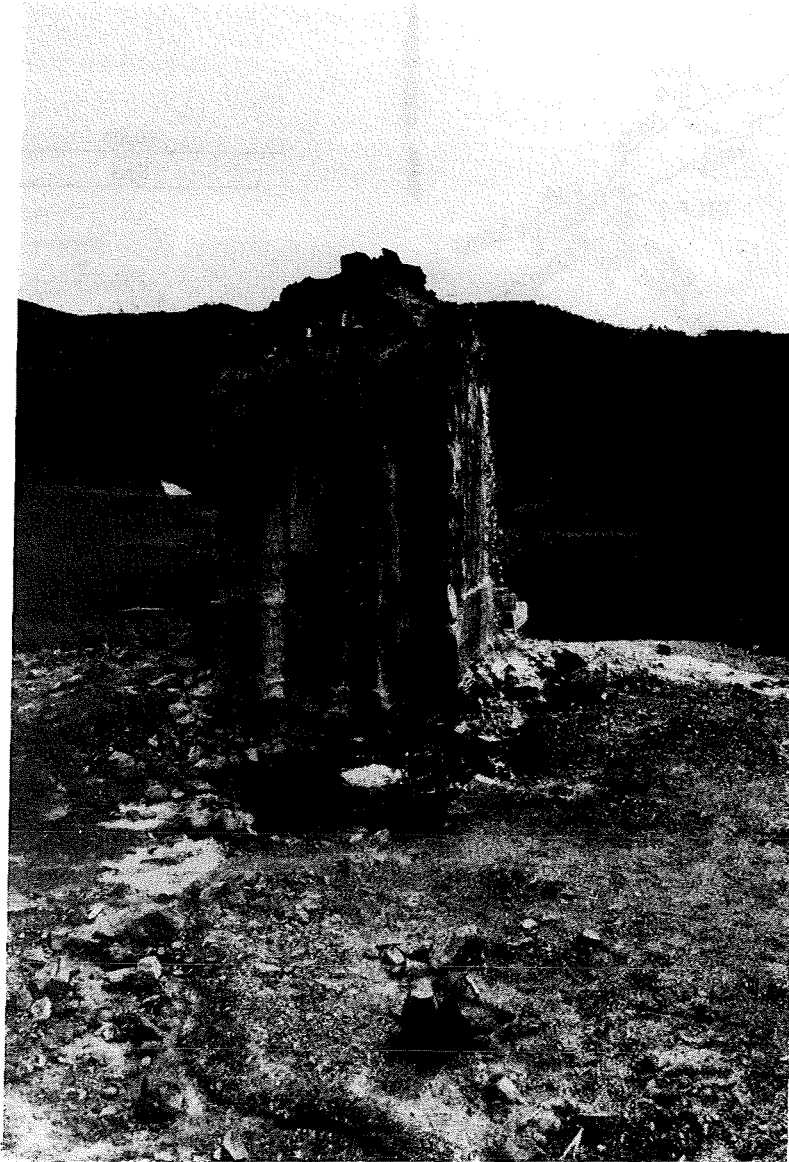


FIGURE 12. View looking west of the ruined concrete pillar that once contained Jones Fountain of Life Spring. The small pool in front of the pillar formed after the resort was abandoned. The photo shows hot water cascading out of the pillar and a low fountain of bubbles in the pool during an eruption. These eruptions are caused by excess pressure of CO₂-CH₄-rich gas, not by steam. Black sediment in the bottom of the pool contains high concentrations of gold (Peters, 1991).

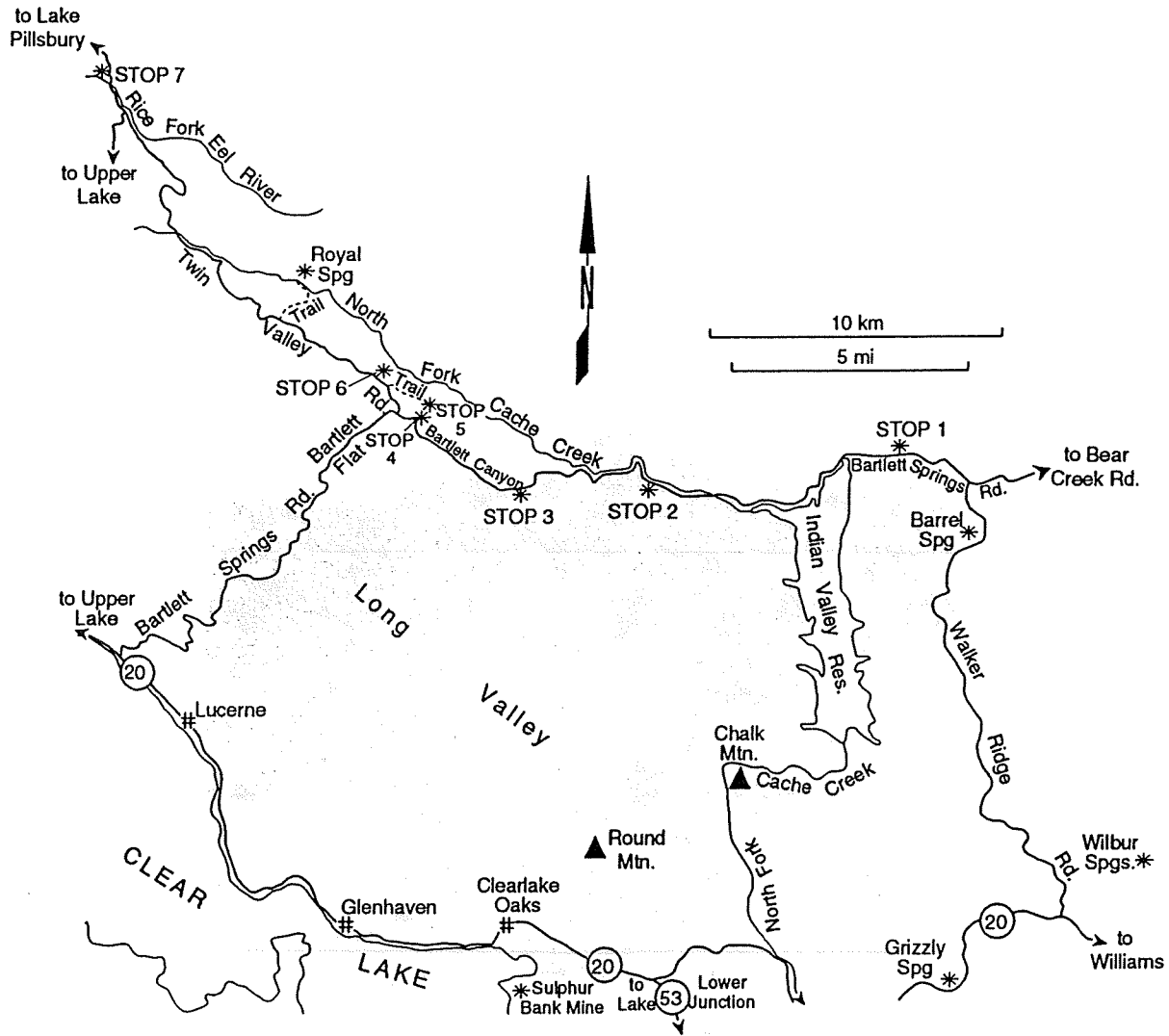


FIGURE 13. Route Map, Day 3.

the other springs. Differences in reported temperatures (56 to 62°C) and gas compositions (Table 1) suggest that Jones Spring has complicated subsurface plumbing with multiple feed points. The spring water contains as much as 0.49 T.U. tritium indicating some mixture with near-surface groundwater (Goff et al., 1993a).

Because of the abundance of hot spring waters, three geothermal exploration wells have been drilled in the flat areas and small gullies south of Jones Spring. Wilbur Hot Springs #1 hit a modest water entry (138°C) at 1020 m in serpentinite but a temperature reversal occurs beneath this zone. The deepest well is 2774 m and penetrates shale of the Knoxville formation and serpentinite. The maximum well temperatures ($\leq 140^\circ\text{C}$) agree with temperatures calculated from empirical gas geothermometers (135 to 157°C) whereas geothermometry on the waters yields confusing results (Goff et al., 1993b).

Jones Spring occurs in a complex structural zone where the NNW-trending Resort fault zone intersects the WNW-trending Indian Valley fault zone. Surface rocks in the area are shale of the Knoxville Formation and serpentinite (McLaughlin et al., 1989). The nearby mines contain quartz veins that cut silicified Knoxville rocks. These veins contain visible gold and carbonaceous material and have fluid-inclusion homogenization temperatures of 158 to 184°C (Thordsen, 1988), slightly hotter than the present hydrothermal system. Cinnabar, stibnite, and carbonaceous material are commonly associated with calcite veins at higher levels in the mine workings and have fluid-inclusion temperatures of 93 to 118°C. Cinnabar, stibnite, gold, carbonaceous material, and siliceous sinters and veins also characterize the McLaughlin deposit (Lehrman, 1986), which has fluid-inclusion temperatures of about 150°C (Peters, 1991). Carbonaceous products and cinnabar co-exist in many mercury prospects of the Coast Ranges (Bailey, 1959).

Turn around and return down the road past Wilbur Springs resort. **0.8**

59.1 **Exit** through the gate, remembering to latch it behind you. **0.6**

59.7 Cross the bridge over Bear Creek and retrace route back to Highway 20. **3.85**

63.55 **Turn right** (west) on Highway 20 to return to Clear Lake. **18.05**

[Option: Turn left (east) to go toward Williams and Sacramento]

81.6 **Junction; turn left** on Highway 53. **4.5**

86.1 Junction with 40th Avenue, the main entrance to Clearlake (to the right). **Continue** on Highway 53. **2.9**

89.0 Lower Lake Junction. **End of Day 2.**

Third Day Road Log:

Geothermal Features of Serpentine Belts Within and Near the Northern Bartlett Springs Fault Zone

Summary — The third day requires a long drive into the region northeast of Clear Lake (Fig. 13) to observe a diverse group of thermal/mineral waters and gases. The most famous sites are Complexion Spring which has been called a “serpentinizing” fluid (Barnes et al., 1972) and Bartlett Springs which was the main attraction of an old resort. Only two of the springs are distinctly thermal (Newman and Crabtree), yet most springs emerge from silica-carbonate rock within a narrow belt of serpentine along the Bartlett Springs fault zone (Waring, 1915; Donnelly-Nolan et al., 1993; Goff et al., 1993b). No rocks of the Clear Lake volcanic field are known in this region but it has been recently postulated

that unerupted or evolving magma chambers may lurk in the subsurface of this region (Benz et al., 1992; Lui and Furlong, 1992).

Mileage:

- 0.00 **Lower Lake Junction, head north on Highway 53. 2.9**
- 2.9 Junction with 40th Avenue at the town of Clear Lake. **Continue north on Highway 53. 4.5**
- 7.4 **Turn right (east) on Highway 20. 11.95**
- 19.35 **Turn left on Walker Ridge Road (graded dirt/gravel). There are many dirt roads that branch off, but keep on the ridge crest. 4.65**
- 24.0 Good views on left of Indian Valley Reservoir on North Fork Cache Creek; Clear Lake and Mount Konocti lie to the southwest; Round Mountain at S65W, the youngest cinder cone in the region, is vent for the basaltic andesite of High Valley; Chalk Mountain, the small low-lying white spot is in the draw at due west. **0.7**
- 24.7 **Turn right at intersection toward Bartlett Springs Road. 0.2**
- 24.9 View of Sutter Buttes (to the east) and Cortina Ridge that bounds the west side of the Central Valley. Sutter Buttes is a circular complex of andesite and rhyolite domes dated at 1.56 to 0.9 Ma (Hausback, 1991) **0.2**
- 25.1 Exposures of serpentinite. **2.7**
- 27.8 View turnout, looking down at Little Indian Valley, Round Mountain, Chalk Mountain, Clear Lake, and Mount Konocti. **1.1**
- 28.9 **Bear right at junction. 4.0**
- 32.9 On left is a small valley containing Barrel Spring, a cold, weakly mineralized spring issuing from serpentinite (Barnes et al., 1973b). **1.1**
- 34.0 **Junction with Bartlett Springs Road. Turn left toward Bartlett Springs. Robbers Roost is to right. 2.1**

36.1 Bridge. 0.2

36.3 Complexion Springs Canyon on right. 0.05

36.35 **STOP 1. Complexion Spring. Turn out on right** side of road and park. [CAUTION: this is Rattlesnake country!] Walk down to the stream and find a good point to cross. Walk up stream on the north bank about 100 m to Complexion Springs Canyon. Walk ~200 m along a poorly defined path on the west bank of the stream in Complexion Springs Canyon. Note well-preserved boulders of pyroxenite with antigorite (as pseudomorphs after pyroxenes) and chrysotile-lizardite. Cross the stream above the small (~1 m high) waterfall where serpentinite breccia is exposed in the stream bed. Note salt deposits on rocks along the stream. Contour up hill on the east bank ~ 15 m above the stream. Enter the first major gully to the east. Climb ~25 m up hill. The vegetation is very typical for serpentinite, with live oak, manzanita, digger pine, and cypress, but with very little grass. Complexion Spring issues as a seep from a small hole (0.3 m deep by 0.2 m high) in the side of a serpentinite hill on the south bank of the gully near the base of two cypress trees (Fig. 14). Brown/green algae grows around the mouth of the hole, and the spring water slowly flows into a shallow, milky-white pool with a film of salt on the surface. Brucite, $Mg(OH)_2$, deposition causes the milky appearance and evaporation of the highly saline water forms the salt scum. Two other seeps occur ≤ 10 meters away on either side of Complexion Spring and also have milky precipitates. At one time Complexion Spring water was used as a nasal douche and as a rinse for sores (Waring, 1915).

Complexion Spring discharges an alkaline brine ($pH \cong 11$ to 12; $Cl \leq 24,000$ mg/kg) that has a bitter salty taste with overtones of ammonia. Although NH_4 content is high (~110 mg/kg), it is half the concentration in water of the Wilbur Springs District. Mg contents are low due to precipitation of brucite. Contents of most trace elements are low to extremely low except for Br (56 mg/kg). The similarity of major constituent concentration to seawater was noted by Barnes et al. (1972). No gas discharges from the spring.

Several analyses of Complexion Spring water show that it varies widely in chemistry depending (probably) on the season. For example, the analysis reported in Waring (1915) shows only 15,400 mg/kg Cl whereas the analysis of Thompson et al. (1981a) shows a maximum of 24,100 mg/kg. Other constituents increase and decrease accordingly indicating that dilution with near-surface water changes the composition of the spring. As proof of this effect, the tritium content of a sample collected in March 1991 was 1.4 T.U., much too high for a deeply circulating, end-member, connate water (Goff et al., 1993a).

Barnes et al. (1972) called this water a "metamorphic" water because they believed that it and similar alkaline fluids were responsible for serpentinitization. However, Complexion Spring water is much different than the metamorphic waters in the Sulphur Bank Mine

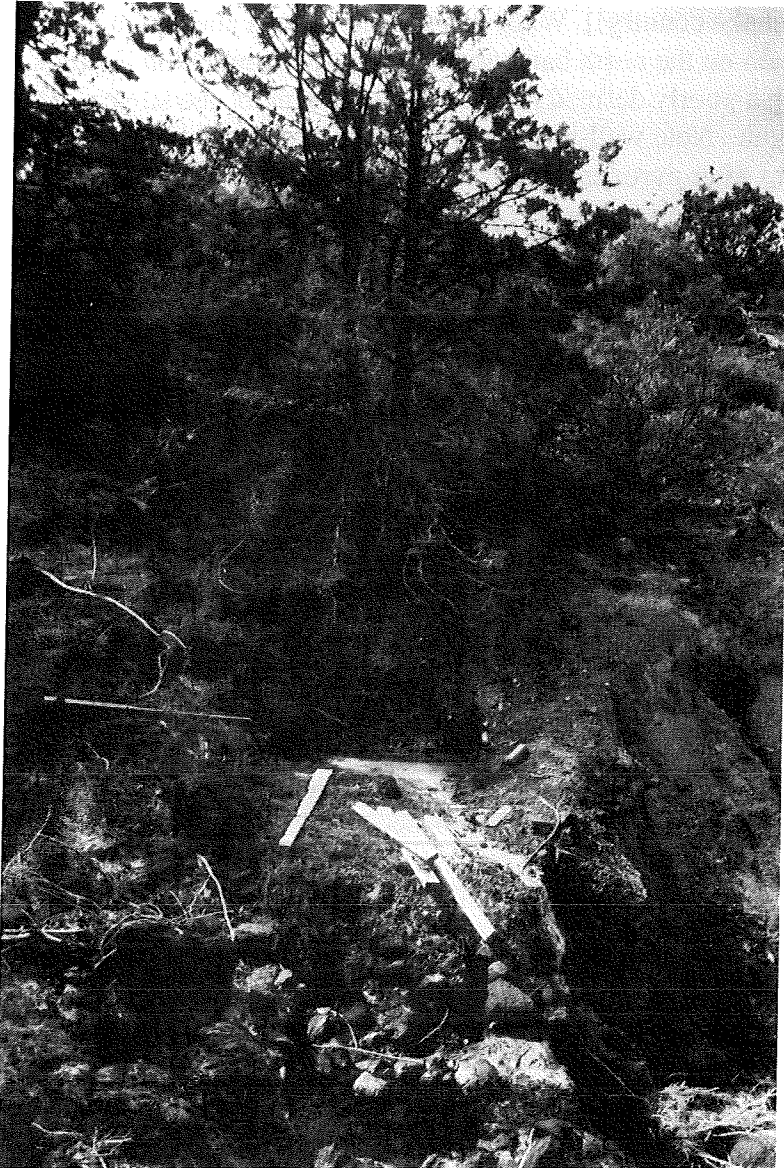


FIGURE 14. View looking south of Complexion Spring, the most concentrated spring in the Clear Lake region, which seeps from serpentinite and forms a milky precipitate of brucite ($Mg(OH)_2$). This spring water ranges in temperature from 9 to 18°C depending on the season. Total concentration of the connate fluid shows dilution effects, also depending on season. Although not thermal, Complexion Spring water has been cited as an example of a “serpentinizing” (or “metamorphic”) fluid (Barnes et al., 1972) and as the generic end-member of all connate fluids in the eastern Clear Lake region (Peters, 1993).

area described by White et al. (1973) and Beall (1985). At the other extreme, Peters (1993) has called this water a connate water that is the generic end-member of all connate waters in the Clear Lake region. Although Complexion Spring water is best classified as connate water, it has a unique stable isotope composition (except for the sample reported in Donnelly-Nolan et al., 1993) and has no isotopic resemblance to other connate waters in the region. Finally, Complexion Spring water is nothing like geothermal waters in chemical composition because of low temperature, low silica content, low trace element contents (except Br), and extremely high Na/K ratio (Goff et al., 1993b).

The rocks at Complexion Spring consist of relatively massive serpentinite that was originally a pyroxenite ultramafic rock. Relatively little slickenslided or gouged serpentine and no silica-carbonate rock are found at the site. Some rounded boulders of pyroxene gabbro are found in the main drainage of the canyon and have come from a source to the north. The serpentine is part of a large plate of the Coast Range ophiolite and is shown overlying deformed Franciscan argillites (McLaughlin et al., 1989); thus no Great Valley sequence rocks, which are usually identified as the source of regional connate waters, are found around or beneath the spring. Complexion Spring remains mysterious.

Continue down the road toward Bartlett Springs (west). **0.65**

- 37.0 Bridge. **0.1**
- 37.1 Entering upper Little Indian Valley. **2.5**
- 39.6 Leaving Little Indian Valley and following the North Fork Cache Creek. **1.2**
- 40.8 View of old abandoned bridge across North Fork Cache Creek to the left. **0.6**
- 41.4 Bridge across North Fork Cache Creek to the south bank. Continue up the valley. **1.6**
- 43.0 Ruined structures on left of Hough Springs, an abandoned resort that once served more than 100 people (Waring, 1915). **0.1**
- 43.1 Turn left on dirt road. **0.1**
- 43.2 **STOP 2. Hough Springs.** Park beyond the southern extent of a grove of black locust trees. Walk uphill along remnant of rock-lined path, bearing due south. Hough Spring forms a pool about 0.3 m wide and 0.2 m deep at the base of a hillside, near where old, travertine-cemented colluvium was dug out and a rock-line crib was constructed. Spring water was piped down to the resort. A second mineral spring reportedly occurs here but has not been found since the study of Waring (1915). In June 1992, Hough Spring was dry but flow had resumed by May 1993.

The bottom and sides of the pool are stained orange by iron oxide deposition and the surface of the water is covered by algae. The cool (14°C) spring water flows at 0.25 l/min and tastes of iron and soda. Hough Spring is primarily a dilute Ca-HCO₃ spring (430 mg/kg Ca). It has very low Cl (≤4 mg/kg) and trace element contents and has stable isotope values like local meteoric water. It is classified as a carbonated meteoric water by Donnelly-Nolan et al. (1993) although no free gas is discharged by the spring.

Rocks in the vicinity of the spring consist of metagreywacke and argillite of the Franciscan Complex but a klippe consisting of rocks of the Great Valley sequence surmounts the ridge south of the spring (McLaughlin et al., 1989).

Turn around and return to main road. **0.1**

43.3 **Turn left** and continue up North Fork Cache Creek. **2.4**

45.7 Entering Bartlett Canyon. **0.4**

46.1 Bridge over Bartlett Creek. **0.8**

46.9 Highly disturbed, vertically-dipping, bedded shale; resembles the Knoxville Formation. **0.55**

47.45 Allen Springs ruins on right. **0.1**

47.55 **STOP 3. Allen Springs. Turn out on right** side of road and park. Cross the road and descend the embankment. Several springs (17 to 20°C) issue from brecciated silica-carbonate rock in the Bartlett Springs fault zone. Most are on the northeast side of Bartlett Creek, but some discharge along the opposite bank and in the creek. During high water, all springs are flooded. Rocks around the orifices and in discharge channels are stained an intense orange color from iron oxide deposition. A weak, but constant flow of gas bubbles issue from most of the springs. The area smells a little of H₂S but the gas consists mostly of CO₂ and air components (Table 1). The water tastes rich in iron (13 mg/kg) and soda and has a faint salty sweet flavor (470 mg/kg Cl, 420 mg/kg Mg). The spring water contains 1.3 T.U. tritium indicating it has a component of near-surface groundwater. It is best classified as a "thermal" meteoric water.

The outcrop adjacent to the turnout displays an outstanding fault contact between silica-carbonate rock and sheared Knoxville shales. The trend of the fault is northwest. The shales are a thin wedge of the klippe composed of rocks of the Great Valley sequence that were mentioned at the previous stop. For the rest of the day we will criss-cross the Bartlett Springs fault zone which is easily recognized as a belt of serpentine and silica-carbonate rock.

Continue straight ahead. 2.95

- 50.5 **STOP 4. Bartlett Springs. Turn out on right** near the fence in front of the large gazebo. **Note: Access by special permission only; do not trespass.** The springs are owned by the Bartlett Mineral Springs Company. Bartlett Springs was once one of the largest resorts in Lake County having "a commodious hotel, stores, pleasure buildings, and a large bottling house" (Waring, 1915). The old buildings are mostly destroyed. A small motel was built north of the gazebo and still stands but it is not presently open for public use.

The main spring is located in a wood box between the gazebo and swimming pool. The overflow was once piped to a small wash basin at the fence by the road for public use but this convenience has been eliminated. The spring flows ~8 l/min at 18°C. It is primarily a Mg (290 mg/kg) - HCO₃ (1640 mg/kg) water with very low trace element contents and stable isotope values similar to local meteoric water. Although minor quantities of free gas issue from the spring, no gas analysis (and no tritium analysis) has been reported in the literature. Presumably, it is primarily CO₂. Like Hough Spring, this is a carbonated meteoric water (Donnelly-Nolan et al., 1993).

Bartlett Spring water was featured as an example of a fluid that causes silica-carbonate alteration of serpentine (Barnes et al., 1973b). The rocks immediately adjacent to the springs are metagreywacke and argillite of the Franciscan Complex, but faulted lenses and slivers of serpentine and silica-carbonate rock having a northwest trend are found in the slopes above the spring.

Continue along the main road, descending to Bartlett Creek. 0.3

- 50.8 **Turn right** on road to Twin Valley. 0.8

- 51.6 **STOP 5. Gas Spring. Turn out on right** at the entrance to a poorly maintained road, and park. The walk to Gas Spring is about 2 km long if this road is not negotiable by 4WD. Walk up along the road on a ridge crest which defines a major drainage divide between North Fork Cache Creek and Bartlett Canyon. The barren slope to the left of the road exhibits bleached rock and minor travertine deposits from springs that are no longer active. After about 0.3 km, the road ascends a hill into silica-carbonate rocks typical of the Bartlett Springs fault zone. About 1 km further, turn left and walk down the remnant of another road that now looks like a foot path. Continue down the hill about 0.3 km to the spring. Gas Spring is located in the Bartlett Springs fault zone and issues water and gas from an excavated ditch in deformed, clay-rich shale and greywacke. Silica-carbonate rocks are found as fault slices on both sides of the spring area.

Spring water flows into a marshy area and deposits iron oxide in the outflow channel. Gas bubbles up vigorously through the water creating a considerable noise and smelling of H₂S but the gas consists primarily of CO₂ (96%), N₂ (2.8%), and CH₄ (1.1%) (Table

1). The water tastes weakly of iron and slightly like lemon, with a tingle on the tongue from bicarbonate. Gas Spring water is extremely dilute and has a pH of ~5.7. The tritium value of 4.8 T.U. indicates that the water is entirely young, near-surface groundwater. Gas Spring represents an extreme (perhaps ideal) case of a carbonated meteoric water.

Continue northwest on road to Twin Valley. **0.2**

51.8 Soap Creek Canyon is on the right. 0.05

51.85 **STOP 6. Newman (also called Soap) Springs. Turn out on right at gate. Note: Access by special permission only; do not trespass.** Cross the gate and follow the road downhill about 250 m to an area of buildings. When the road forks, bear left to Soap Creek Canyon. At the edge of the canyon find a way into the canyon (no marked path). Head downstream by boulder-hopping, and enter a zone of iron-stained rocks where springs issue along both sides of the stream. The hottest is ~34 °C, issues no gas, and flows ~10 ℓ/min. Continue down stream through a prominent, 50-m-wide rib of serpentine. After cutting through the serpentine, the creek makes a short jog to the north and the Main Spring (29°C) issues from a fault contact between the serpentine and contorted black shale (Knoxville Formation). The spring is piped to a ledge of boulders along the creek and the water has formed an apron of iron-stained travertine. At one time the pipe crossed the creek to a small swimming pool that still exists. The Main Spring had a substantial flow of ~60 ℓ/min (Waring, 1915).

Newman Springs vary in salinity from about 1200 to 3300 mg/kg Cl; The Main Spring varies from 1200 to 1600 mg/kg Cl implying seasonal variations due to mixing with shallow groundwater (Thompson et al., 1981a; Peters, 1993; Goff et al., 1993b; unpub. data). The hottest, most concentrated spring has a tritium content of 0.3 T.U. indicating only a minor contribution from near-surface groundwater. In addition to relatively high Cl, the waters contain substantial HCO₃, Mg, Fe, B, and NH₄ making Newman Springs an interesting taste experience. Stable isotope values of the waters are midway between connate and thermal meteoric end-members (Donnelly-Nolan et al., 1993). Very little, if any, gas issues from the springs.

The rocks exposed along Soap Creek provide an interesting cross-section of the Bartlett Springs fault zone. West of the serpentine, the rocks consist of sheared, metagreywacke and argillite of the Franciscan Complex. The serpentine itself is faulted and gouged and contains local zones of silica-carbonate rock. The dip on the fault between serpentine and shale of the Knoxville Formation is ~75° to the west but the fault undulates to the north up the ridge above the creek.

Continue along road toward Twin Valley. **0.55**

- 52.4 Cross ford on Soap Creek. **0.2**
- 52.6 Cross Soap Creek again. **0.45**
- 53.05 Another ford. **1.85**
- 54.9 Road and gate on the right is entrance to Royal Spring. [**Optional side trip:** Royal Spring is located about 2 km up the trail on northeast side of North Fork Cache Creek. This spring (18°C) issues from a concrete basin at a rate of 8 l/min and has formed an iron-stained travertine apron. The spring emerges from a fault contact between greywacke-shale and serpentinite and silica-carbonate rock in the Bartlett Springs fault zone.] **1.2**
- 56.1 Cross Twin Valley Creek. **0.5**
- 56.6 Pass through a burned area near crest of hill. **1.3**
- 57.9 Ford stream. **0.1**
- 58.0 Another ford. **0.9**
- 58.9 Ford across North Fork Cache Creek. **0.05**
- 58.95 Junction with road to Crabtree Lodge on left. **Continue straight ahead** up the ridge on the main road. **0.65**
- 59.6 Fault zone with serpentine exposed. **0.5**
- 60.1 Small pond (similar to sag pond) on left at crest of ridge. **1.5**
- 61.6 Junction; **continue straight ahead** and descend into canyon of Rice Fork of Eel River. **0.9**
- 62.5 Junction with road to Upper Lake on left; **continue straight ahead** toward Bear Creek. **0.3**
- 62.8 Gouge zone in serpentinite on left. This road cut provides a great exposure of the Bartlett Springs fault zone. **0.5**
- 63.3 **STOP 7. Crabtree Gas Seep and Springs.** Cross Rice Fork Eel River and park on eroded greywacke just beyond the ford. Walk downstream on the right (north) bank about 0.4 km to Crabtree Gas Seep which issues from highly opalized silica-carbonate

rock along the edge of the river over a zone about 10 m long. The rocks are stained bright orange by iron oxides and resemble Allen Springs in appearance. However, here the rate and distribution of gas discharge is greater. The gas contains 94% CO₂, 4.6% N₂, 1.3% CH₄, and a trace of H₂S whose odor is obvious (Table 1). In high water the Gas Seep is submerged; the configuration of the pool changes almost yearly.

Follow the trail up on the ledge of silica-carbonate rock and descend to a very picturesque area of man-made pools constructed along the north bank which contain hot spring waters (Fig. 15). Crabtree Hot Springs vary from 39 to 42°C and the total flow is about 75 l/min. This is one of the most delightful swimming spots in Lake County. The hot waters are turbid with colloidal iron-hydroxide. The waters contain moderate Cl (1270 mg/kg), high B (330 mg/kg), and high HCO₃ (4000 mg/kg) and have a salty, soda, iron taste (Thompson et al., 1981a; Goff et al., 1993b). Tritium content is 0.9 T.U. indicating some mixture with relatively young groundwater. Crabtree Hot Spring water is also a mixture of connate and thermal meteoric water types based on stable isotope results (Donnelly-Nolan et al., 1993). The water was once "considered efficacious in the treatment of skin and blood diseases" (Waring, 1915).

The water also contains 0.9 mg/kg As and tiny veinlets of realgar occur sporadically in silica-carbonate rock across the river from the springs. Cinnabar also can be found here, but not in commercial quantities (Waring, 1915). No exposures of the Clear Lake Volcanics are known in this area (Donnelly-Nolan et al., 1993). Perhaps mineralization has just started here in response to the development of new magma chambers that may underlie this region (Benz et al., 1992; Liu and Furlong, 1992).

A near-vertical fault contact between silica-carbonate rock and metagreywacke of the Franciscan Complex can be observed on the southwest side of the creek. The silica-carbonate rib is about 30 m wide. Black contorted shale occurs northeast of the silica-carbonate rock which resembles shale of the Knoxville Formation. On the trail back to the vehicles, a zone of serpentine can be seen that occurs between the shale and the metagreywacke at the parking lot. These rocks all have northwest structural trends and lie within the Bartlett Springs fault zone.

Turn around and retrace route. **0.8**

64.1 Junction with road to Upper Lake to right (25 miles of very rough road); **continue straight ahead** heading toward Bartlett Springs. **11.7**

75.8 **Turn right** on Bartlett Springs Road to return to Clear Lake. **0.6**

[Option: turn left to go toward Williams and Sacramento.]

76.4 Bridge crossing Bartlett Creek at head of Bartlett Flat. **4.6**



FIGURE 15. View looking east (upstream) of Crabtree Hot Springs along the north bank of Rice Fork Eel River. The springs issue from fractures in a northwest-trending rib of silica-carbonate rock along the Bartlett Springs fault zone. The man-made pools make superb bathing spots but most pools must be rebuilt after high water levels of the river wash them away.

- 81.0 Magnificent view looking southeast into Long Valley. 2.8
- 83.8 Junction with road to Pinnacle Rocks. **Continue straight ahead**, descending into Clear Lake basin. 1.2
- 85.0 **Turn right** at junction with road to High Valley and continue descent toward Clear Lake to meet Highway 20. 4.95
- 89.95 **Turn left** on Highway 20. 1.35
- 91.3 Enter the community of Lucerne. 7.1
- 98.4 Enter the community of Glenhaven. 3.7
- 102.1 Clear Lake Oaks. 4.0
- 106.1 **Junction; turn right** on Highway 53. 4.5

110.6 Junction with 40th Avenue; **continue straight ahead. 2.9**

113.5 Lower Lake Junction. **End of Day 3.**

ACKNOWLEDGMENTS

The early work of Gerald Waring, Ivan Barnes, and Don White are fundamental to an understanding of the Clear Lake region and their efforts are gratefully appreciated. The first author benefitted from extensive collaborations with Carter Hearn, Julie Donnelly-Nolan, Bob McLaughlin, and Mike Thompson (all U.S. Geological Survey). Andrew Adams, James A. Stimac (both LANL) and Lynne Fahlquist (U.S. Geological Survey) contributed with some of the field work. The help and knowledge of Ester, Mario, and Adrienne Ciardella (Cobb and Buckingham) have become increasingly valuable. We thank the following people for their cooperation: V.A. "Kip" Neasham (Sulphur Mound Mine), Mark Dellinger (Geothermal Agricultural Park), Jim McLaughlin (Soda Bay Resort), Steve Ratislaw (C.M.E. Water Well Drilling), Elio R. Guisti (Giusti Enterprises), Carol Hills (Boggs Mountain Reserve), Donna and Larry Mayfield (Lower Lake), Frederick Bradley (Clearwater Mining Property), Richard and Ezzie Davis (Wilbur Hot Springs), and Norman Lehrman (Homestake Mining Company). Daniel Obermeyer (City of Clearlake) assisted with initial logistics. George Berry (Boulder, CO) provided valuable subsurface information and insights on early geothermal drilling. Some data in this paper were provided by a host of geothermal companies, many of which are now non-existent. The manuscript and figures were prepared by Carol White, Barbara Hahn, and James Archuleta (Los Alamos). The manuscript was reviewed by M. Nathenson, W. C. Evans (both U.S. Geological Survey), and James A. Stimac. This project was funded by the U.S. Department of Energy, Division of Geothermal Energy (Marshall Reed), by a grant to the City of Clearlake from the California Energy Commission, and by research funds from the Earth and Environmental Sciences Division of Los Alamos National Laboratory.

REFERENCES

- Adams, A., Dennis, B., Van Eeckhout, E., Goff, F., Lawton, R., Trujillo, P., Counce, D., Medina, V., and Archuleta, J., 1991, Results of investigations at the Zunil geothermal field, Guatemala: Well logging and brine geochemistry: Los Alamos Nat'l. Lab. Rept. LA-12098-MS, 47 p.
- Anderson, W., 1892, Mineral springs and health resorts of California: Bancroft Co., San Fran., 327 p.
- Bailey, E. H., 1959, Froth veins, formed by immiscible hydrothermal fluids, in mercury deposits, California: Geol. Soc. Amer. Bull., v. 70, p. 661-663.
- Barnes, I., Hirth, M., Rapp, J., Heropoulos, C., and Vaughn, W., 1973a, Chemical composition of naturally occurring fluids in relation to mercury deposits in part of north-central California: U.S. Geol. Surv. Bull. 1382-A, p. A1-A19.
- Barnes, I., Irwin, W. P., and White, D. E., 1978, Global distribution of carbon dioxide discharges and major zones of seismicity: U.S. Geol. Surv. Open-file Rept., Water Resour. Invest. 78-39, 12 p. w/map.
- Barnes, I., O'Neil, J., Rapp, J., and White, D. E., 1973b, Silica-carbonate alteration of serpentine: Wall rock alteration in mercury deposits of the California Coast Ranges: Econ. Geol., v. 68, p. 388-398.
- Barnes, I., Rapp, J., and O'Neil, J., 1972, Metamorphic assemblages and the direction of flow of metamorphic fluids in four instances of serpentinization: Contrib Mineral. and Petrol., v. 35, p. 263-276.
- Beall, J. J., 1985, Exploration of a high temperature, fault localized, nonmeteoric geothermal system at the Sulphur Bank Mine, California: Geotherm. Res. Counc. Trans., v. 9(1), p. 395-401.
- Becker, G. F., 1888, Geology of the quicksilver deposits of the Pacific slope: U.S. Geol. Surv. Mon. 13, 486 p.
- Benz, H. M., Zandt, G., Oppenheimer, D. H., 1992, Lithospheric structure of northern California from teleseismic images of the upper mantle: Jour. Geophys. Res., v. 97, p. 4791-4807.
- Berkstresser, C. F., Jr., 1968, Data for springs in the northern Coast Ranges and Klamath Mountains of California: U.S. Geol. Surv. Open-file Rept., 49 p.
- Brice, J. C., 1953, Geology of Lower Lake quadrangle, California: Calif. Div. Mines Geol. Bull. 166, 72 p.
- Buzek, F., 1992, Carbon isotope study of gas migration in underground gas storage reservoirs, Czechoslovakia: Applied Geochem., v. 7, p. 471-480.

- Chamberlin, C., Chaney, R., Fiinney, B., Hood, M., Lehman, P., McKee, M., and Willis, R., 1990, Abatement and control study: Sulphur Bank Mine and Clear Lake: Environ. Resour. Engineer. Dept., Humboldt State Univ., Arcata, Calif., 242 p.
- Craig, H., 1963, The isotopic geochemistry of water and carbon in geothermal areas, *in* (E. Tongiorgi, ed.) Nuclear Geology on Geothermal Areas: Consiglio Nazionale della Recherche, Pisa, p. 17-53.
- D'Amore, F., and Panichi, C., 1980, Evaluation of deep temperatures of hydrothermal systems by a new gas geothermometer: *Geochim. Cosmochim. Acta*, v. 44, p. 549-556.
- Dellinger, M. and Cooper, G., 1990, Greenhouse heating with low-temperature geothermal resources in Lake County, California: *Geotherm. Res. Counc. Trans.*, v. 14(1), p. 321-328.
- Dennis, B., Goff, F., Van Eeckhout, E., and Hanold, B., 1990, Results of investigations at the Ahuachapán geothermal field, El Salvador Part 1: Well logging and brine geochemistry: Los Alamos Nat'l. Lab. Rept., LA-11779-MS, 68 p.
- Donnelly-Nolan, J. M., Burns, M. G., Goff, F., Peters, E. K., and Thompson, J. M., 1993, The Geysers-Clear Lake area, California: Thermal waters, mineralization, volcanism, and geothermal potential: *Econ. Geol.*, v. 88, p. 301-316.
- Donnelly-Nolan, J. M., Hearn, B. C., Jr., Curtis, G. H., and Drake, R. E., 1981, Geochronology and evolution of the Clear Lake Volcanics: *U.S. Geol. Surv. Prof. Paper* 1141, p. 47-60.
- Evans, W. C., White, L. D., and Rapp, J. B., 1988, Geochemistry of some gases in hydrothermal fluids from the southern Juan de Fuca Ridge: *Jour. Geophys. Res.*, v. 93(B12), p. 15,305-15,313.
- Fahlquist, L. and Janik, C. J., 1992, Procedures for collecting and analyzing gas samples from geothermal systems: *U.S. Geol. Surv. Open-file Rept.*, 92-211, 19 p.
- Fehn, U., Peters, E. K., Tullai-Fitzpatrick, S., Kubik, P. W., Sharma, P., Tong, R., Gove, H., and Elmore, D., 1992, ^{129}I and ^{36}Cl concentrations in waters of the eastern Clear Lake area, California: Residence times and source ages of hydrothermal fluids: *Geochim. Cosmochim. Acta.*, v. 56, p. 2069-2079.
- Giggenbach, W. F. 1980, Geothermal gas equilibria: *Geochim. Cosmochim. Acta*, v. 44, p. 2021-2032.
- Giggenbach, W. F. and Corrales Soto, R., 1992, Isotopic and chemical composition of water and steam discharges from volcanic-magmatic-hydrothermal systems of the Guanacaste geothermal province, Costa Rica: *Applied Geochem.*, v. 7, p. 309-332.
- Giggenbach, W. F. and Goguel, R. L., 1989, Collection and analysis of geothermal and volcanic water and gas discharges: *Dept. Sci. Indus. Res. Rept. CD 2401*, Petone, N.Z., p. 69-81.
- Giggenbach, W. F. and Lyon, G. L., 1977, The chemical and isotopic composition of water and gas discharges from the Ngawha geothermal field, New Zealand: *Dept. Sci. Indus. Res.*, unnumbered report, Petone, N.Z., 37 p.
- Giggenbach, W. F. and Matsuo, S., 1991, Evaluation of results from second and third IAVECEI field workshops on volcanic gases, Mt. Usu, Japan and White Island, New Zealand: *Applied Geochem.*, v. 6, p. 125-141.
- Goff, F. and Decker, E. R., 1983, Candidate sites for future hot dry rock development in the United States: *Jour. Volcanol. Geotherm. Res.*, v. 15, p. 187-221.
- Goff, F., Adams, A. I., Trujillo, P. E., Counce, D., and Mansfield, J., 1993a, Geochemistry of thermal/mineral waters in the Clear Lake region, California and implications for hot dry rock geothermal development: *Los Alamos Nat'l. Lab. Rept. LA-12510-HDR*, 23 p.
- Goff, F., Donnelly, J. M., Thompson, J. M., and Hearn, B. C., Jr., 1977, Geothermal prospecting in The Geysers-Clear Lake area, northern California: *Geology*, v. 5, p. 509-515.
- Goff, F., Gardner, J. N., Hulen, J. B., Nielson, D. L., Charles, R., WoldeGabriel, G., Vuataz, F.-D., Musgrave, J. A., Shevenell, L., and Kennedy, B. M., 1992, The Valles caldera hydrothermal system, past and present, New Mexico, USA: *Sci. Drilling*, v. 3, p. 181-204.
- Goff, F., Gardner, J. N., Vidale, R., and Charles, R., 1985, Geochemistry and isotopes of fluids from Sulphur Springs, Valles caldera, New Mexico: *Jour. Volcanol. Geotherm. Res.*, v. 23, p. 273-297.
- Goff, F., Goff, S., Kelkar, S., Shevenell, L., Truesdell, A. H., Musgrave, J., Rufenacht, H., and Flores, W., 1991a, Exploration drilling and reservoir model of the Platanares geothermal system, Honduras, Central America: *Jour. Volcanol. Geotherm. Res.*, v. 45, p. 101-123.
- Goff, F., Janik, C. J., Fahlquist, L., Adams, A., Roldan, A., Revolorio, M., Trujillo, P. E., and Counce, D., 1991b, A re-evaluation of the Moyuta geothermal system, southern Guatemala: *Geotherm. Res. Counc. Trans.*, v. 15, p. 3-10.
- Goff, F., Kennedy, B. M., Adams, A. I., Trujillo, P. E., and Counce, D., 1993b, Hydrogeochemical evaluation of conventional and hot dry rock geothermal resource potential in the Clear Lake region, California: *Geotherm. Res. Counc. Trans.*, v. 17, 8 p.
- Goff, F., Shevenell, L., Gardner, J. N., Vuataz, F.-D., and Grigsby, C. O., 1988, The hydrothermal outflow plume of Valles caldera, New Mexico and a comparison with other outflow plumes: *Jour. Geophys. Res.*, v. 93(B6), p. 6041-6058.

- Grigsby, C. O., Goff, F., Trujillo, P. E., Counce, D. A., Dennis, B., Kolar, J., and Corrales, R., 1989, Results of investigation at the Miravalles geothermal field, Costa Rica part 2: Downhole fluid sampling: Los Alamos Nat'l. Lab. Rept., LA-11510-MS, 45 p.
- Hausback, B. P., 1991, Eruptive history of the Sutter Buttes volcano-review, update, and tectonic considerations: *Geol. Soc. Amer. Abst. w/Prog.*, v. 23, p. 34.
- Hearn, B. C., Jr., Donnelly, J. M., and Goff, F. E., 1976, Preliminary geologic map and cross-section of the Clear Lake volcanic field, Lake County, California: U. S. Geol. Surv. Open-file map 76-751, 1:24,000 scale.
- Hearn, B. C., Jr., Donnelly-Nolan, J. M., and Goff, F. E., 1981, The Clear Lake Volcanics: Tectonic setting and magma sources: U. S. Geol. Surv. Prof. Paper 1141, p. 24-45.
- Hearn, B. C., Jr., McLaughlin, R. J., and Donnelly-Nolan, J. M., 1988, Tectonic framework of the Clear Lake basin, California: *Geol. Soc. Amer. Spec. Paper* 214, p. 9-20.
- Hinds, A., and Dellinger, M., 1988, The Lake County geothermal resource and transmission element: *Geotherm. Res. Counc. Trans.*, v. 12, p. 89-93.
- Hoefs, J., 1973, Stable isotope geochemistry: Springer-Verlag, N.Y., 140 p.
- Huebner, M., 1981, Carbon-13 isotope values for carbon dioxide gas and dissolved carbon species in springs and wells in The Geysers-Clear Lake region: U.S. Geol. Surv. Prof. Paper 1141, p. 211-213.
- Hulen, J. B. and Nielson, D. L., 1993, Interim report on geology of The Geysers felsite, northwestern California: *Geotherm. Res. Counc. Trans.*, v. 17, 10 p.
- Hulen, J. B., Nielson, D. L., and Martin, W., 1992, Early calcite dissolution as a major control on porosity development in The Geysers steam field, California - additional evidence in core from UNOCAL well Negu-17: *Geotherm. Res. Counc. Trans.*, v. 16, p. 167-174.
- Janik, C. J., Goff, F., Fahlquist, L., Adams, A. I., Roldan-M., A., Chipera, S. J., Trujillo, P. E., and Counce, D., 1992, Hydrogeochemical exploration of geothermal prospects in the Tecuamburro Volcano region, Guatemala: *Geothermics*, v. 21, p. 447-481.
- Janik, C. J., Nehring, N. L., Huebner, M. A., and Truesdell, A. H., 1982, Carbon-13 variations in fluids from the Cerro Prieto geothermal system: *Proceed. Fourth Symp. Cerro Prieto Geotherm. Field, Guadalajara, Mexico*, Aug. 10-12, v. 2, 7 p.
- Janik, C. J., Truesdell, A. H., Goff, F., Shevenell, L., Stallard, M. L., Trujillo, P. E., and Counce, D., 1991, A geochemical model of the Platanares geothermal system, Honduras: *Jour. Volcanol. Geotherm. Res.*, v. 45, p. 125-146.
- Kennedy, B. M., Hiyagon, H., and Reynolds, J. H., 1991, Noble gases from Honduras geothermal sites: *Jour. Volcanol. Geotherm. Res.*, v. 45, p. 29-39.
- Lambert, S. J., and Epstein, S., 1992, Stable-isotope studies of rocks and secondary minerals in a vapor-dominated hydrothermal system at The Geysers, Sonoma County, California: *Jour. Volcanol. Geotherm. Res.*, v. 53, p. 199-226.
- Lehrman, N. J., 1986, The McLaughlin Mine, Napa and Yolo Counties, California: *Nevada Bur. Mines Geol. Rept.* 41, p. 85-89.
- Liu, M., and Furlong, K. P., 1992, Cenozoic volcanism in the California Coast Ranges: Numerical solutions: *Jour. Geophys. Res.*, v. 97, p. 4941-4951.
- Marty, B., Meynier, V., Nicolini, E., Griesshaber, E., Toutain, J. P., 1993, Geochemistry of gas emanations: A case study of the Réunion Hot Spot, Indian Ocean: *Applied Geochem.*, v. 8, p. 141-152.
- McLaughlin, R. J., Ohlin, H. N., Thormahlen, D. J., Jones, D. L., Miller, J. W., and Blome, C. D., 1989, Geologic map and structure sections of the Little Indian Valley-Wilbur Springs geothermal area, northern Coast Ranges, California: U. S. Geol. Surv. Map I-706, 1:24,000 scale.
- Moiseyev, A. N., 1968, The Wilbur Springs quicksilver district (California); example of a study of hydrothermal process combining field geology and theoretical geochemistry: *Econ. Geol.*, v. 63, p. 169-181.
- Moiseyev, A. N., 1971, A non-magmatic source for mercury ore deposits: *Econ. Geol.*, v. 66, p. 591-601.
- Nehring, N. L., 1981, Gases from springs and wells in The Geysers-Clear Lake area: U.S. Geol. Surv. Prof. Paper 1141, p. 204-209.
- Nehring, N. L., and D'Amore, F. D., 1984, Gas chemistry and thermometry of the Cerro Prieto, Mexico, geothermal field: *Geothermics*, v. 13, p. 75-89.
- Nehring, N. L., Mariner, R. H., White, L. D., Huebner, M. A., Roberts, E. D., Harmon, K., Bowen, P. A., and Tanner, L., 1979, Sulfate geothermometry of thermal waters in the western United States: U. S. Geol. Surv. Open-file Rept. 79-1135, 11 p.
- Peters E. K., 1993, D-¹⁸O enriched waters of the Coast Range Mountains, northern California: Connate and ore-forming fluids: *Geochim. Cosmochim. Acta*, v. 57, p. 1093-1104.
- Peters, E. K., 1991, Gold-bearing hot spring systems of the northern Coast Ranges, California: *Econ. Geol.*, v. 86, p. 1519-1528.

- Rymer, M. J., 1978, Stratigraphy of the Cache Formation (Pliocene and Pleistocene) in the Clear Lake basin, Lake County, California: U. S. Geol. Surv. Open-file Rept., 78-924, 102 p.
- Shigeno, H., Stallard, M. L., Truesdell, A. H., and Haizlip, J. R., 1987, $^{13}\text{C}/^{12}\text{C}$ and D/H ratios of CO_2 , CH_4 , and H_2 in The Geysers geothermal reservoir, California, and their implications: EOS, v. 68(14), p. 1537.
- Sims, J. D., Adams, D. P., and Rymer, M. J., 1981, Stratigraphy and palynology of Clear Lake, California: U. S. Geol. Surv. Prof. Paper 1141, p. 219-230.
- Sims, J. D., and Rymer, M. J., 1976, Map of gaseous springs and associated faults in Clear Lake, California: U. S. Geol. Surv. Misc. Field Invest. Map MF-721, 1:48,000 scale
- Sims, J. D., and White, D. E., 1981, Mercury in the sediments of Clear Lake: U. S. Geol. Surv. Prof. Paper 1141, p. 237-241.
- Skinner, D. N. B., 1981, Geological setting and sub-surface geology of Ngawha: Dept. Sci. Indus. Res. Geotherm. Rept. 7, Petone, N.Z., p. 14-35.
- Smith, R. L., and Shaw, H. R., 1978, Igneous-related geothermal systems: U. S. Geol. Surv. Circ. 790, p. 12-17.
- Smith, S. P., and Kennedy, B. M., 1985, Noble gas evidence for two fluids in the Baca (Valles caldera) geothermal reservoir: Geochim. Cosmochim. Acta, v. 49, p. 893-902.
- Stimac, J. A., this volume, The origin and significance of high-grade metamorphic xenoliths, Clear Lake Volcanics, California: Soc. Econ. Geol. Field Trip Guidebk. The Geysers-Clear Lake-McLaughlin area.
- Stimac, J. A., and Pearce, T. H., 1992, Textural evidence of mafic-felsic magma interaction in dacite lavas, Clear Lake, California: Amer. Mineral., v. 77, p. 795-809.
- Stimac, J. A., Pearce, T. H., Donnelly-Nolan, J. M., and Hearn, B. C., Jr., 1990, The origin and implications of undercooled andesitic inclusions in rhyolites, Clear Lake Volcanics, California: Jour. Geophys. Res., v. 95, p. 17,729-17,746.
- Thompson, J. M., Goff, F. E., and Donnelly-Nolan, J. M., 1981a, Chemical analyses of waters from springs and wells in the Clear Lake volcanic area: U. S. Geol. Surv. Prof. Paper 1141, p. 161-166.
- Thompson, J. M., Mariner, R. H., White, L. D., Presser, T. S., and Evans, W. C., 1992, Thermal waters along the Konocti Bay fault zone, Lake County, California: A re-evaluation: Jour. Volcanol. Geotherm. Res., v. 53, p. 167-183.
- Thompson, J. M., Sims, J. D., Yadav, S., and Rymer, M. J., 1981b, Chemical composition of water and gas from five near shore subaqueous springs in Clear Lake: U. S. Geol. Surv. Prof. Paper 1141, p. 215-218.
- Thorsen, J. J., 1988, Fluid-inclusion and geochemical study of epithermal gold mineralization in the Wilbur Springs District, Colusa and Lake Counties, California: Unpub. M. S. thesis, Ohio State Univ., 229 p.
- Torgersen, T., and Jenkins, W. J., 1982, Helium isotopes in geothermal systems: Iceland, The Geysers, Raft River, and Steamboat Springs: Geochim. Cosmochim. Acta, v. 46, p. 739-748.
- Truesdell, A. H., and Janik, C. J., 1986, Reservoir processes and fluid origins in the Baca geothermal system, Valles caldera, New Mexico: Jour. Geophys. Res., v. 91, p. 1817-1833.
- Truesdell, A. H., Haizlip, J. R., Box, W. T., and D'Amore, F. D., 1987, Fieldwide chemical and isotopic gradients in steam from The Geysers: Proceed. Twelfth Wksp. Geotherm. Res. Engin., Stanford Univ., Calif., p. 241-246.
- Trujillo, P. E., Counce, D., Grigsby, C. O., Goff, F., and Shevenell, L., 1987, Chemical analysis and sample techniques for geothermal fluids and gases at the Fenton Hill laboratory: Los Alamos Nat'l. Lab. Rept., LA-11006-MS, 84 p.
- Walters, M., and Combs, J., 1989, Heat flow regime in The Geysers-Clear Lake area of northern California, USA: Geotherm. Res. Counc. Trans., v. 13, p. 491-502.
- Waring, G. A., 1915, Springs of California: U. S. Geol. Surv. Water-Supply Paper 338, 410 p.
- Welhan, J. A., Poreda, R. J., Rison, W., and Craig, H., 1988, Helium isotopes in geothermal and volcanic gases of the western United States, I. Regional variability and magmatic origin: Jour. Volcanol. Geotherm. Res., v. 34, p. 185-189.
- Wells, J. T., and Ghiorsso, M. S., 1988, Rock alteration, mercury transport, and metal deposition at Sulphur Bank, California: Econ. Geol., v. 83, p. 606-618.
- White, D. E., 1957, Magmatic, connate, and metamorphic waters: Geol. Soc. Amer. Bull., v. 68, p. 1659-1682.
- White, D. E. and Roberson, C. F., 1962, Sulphur Bank, California, a major hot-spring quicksilver deposit: Geol. Soc. Amer., Buddington Vol., p. 397-428.
- White, D. E., Barnes, I., and O'Neil, J. R., 1973, Thermal and mineral waters of nonmeteoric origin, California Coast Ranges: Geol. Soc. Amer. Bull., v. 84, p. 547-560.
- White, D. E., Muffler, L. J. P., and Truesdell, A. H., 1971, Vapor-dominated hydrothermal systems compared with hot-water systems: Econ. Geol., v. 66, p. 75-97.

GOLD AND MERCURY DEPOSITS IN THE SULPHUR CREEK MINING DISTRICT, CALIFORNIA

Gordon C. Nelson¹, James J. Rytuba², Robert M. McLaughlin², and R. M. Tosdal²

¹Homestake Mining Company, McLaughlin Mine 26775 Morgan Valley Rd., Lower Lake, CA 95457

²U.S. Geological Survey, 345 Middlefield Road, Menlo Park CA 94025

INTRODUCTION

Within the central part of the Sulphur Creek Mining District six epithermal gold-mercury deposits have been mined, the West End, Central, Cherry Hill, Empire, Manzanita, and Wide Awake (Fig. 1). The mining district also includes the Abbott, Elgin and Rathburn mercury deposits and several hot springs that are depositing gold and cinnabar. The association of gold and mercury in the district was recognized early and gold was mined at the Cherry Hill and the Manzanita Mercury Mine from 1865 to 1891 with total production being about 3,000 oz of Au (Whitney, 1865, and Bradley, 1916). Whitney (1865) describes cobbles of cinnabar from the Sulphur Creek Mining District containing plumes of gold distributed through out the cinnabar. Fine placer gold is also present in drainages within the Sulphur Creek district, but has not been mined. Total mercury production from the district has been about 33,000 flasks, primarily from the Abbott mine. The Wide Awake mine was reported to have reserves of 24,000 flasks in 1899 and substantial unreported production may have come from this mine. In 1977, Homestake Mining Co. delineated a small gold deposit in the area of the Cherry Hill, West End, and Wide Awake Mines. The mineralization extends under the Sulphur Creek valley which separates these mines. Although numerous high-grade gold veins are present, typically greater than 0.3 oz of Au with multiple oz assays common, the veins are widely spaced and the deposit is presently uneconomic.

GEOLOGY

The gold-mercury deposits in the central part of the Sulphur Creek Mining district are hosted by the basal formation of the Great Valley sequence. The exceptions are the Wide Awake and Central Mines which are hosted in sedimentary serpentine. This Great Valley sequence consists of carbonaceous mudstone, sandstone, and conglomerate, and is equivalent to the Knoxville Formation in the McLaughlin Mine area. A detrital volcanic component is present in all of the sedimentary rocks, and fragments of wood and plant material are common in the sandstone. In areas adjacent to the gold-mercury deposits, the carbonaceous material has a high vitrinite reflectance resulting from the thermal effects of the geothermal system. Outside of geothermal areas, the sedimentary rocks of the Great Valley sequence typically have not been subjected to temperatures greater than 85° C (Phipps and Unruh, 1992). Sedimentary serpentinite consisting of coarse serpentine debris flows are interbedded in the basal strata of the Great Valley sequence and host the mercury ore body at the Wide Awake mine. The Abbott and Turkey Run

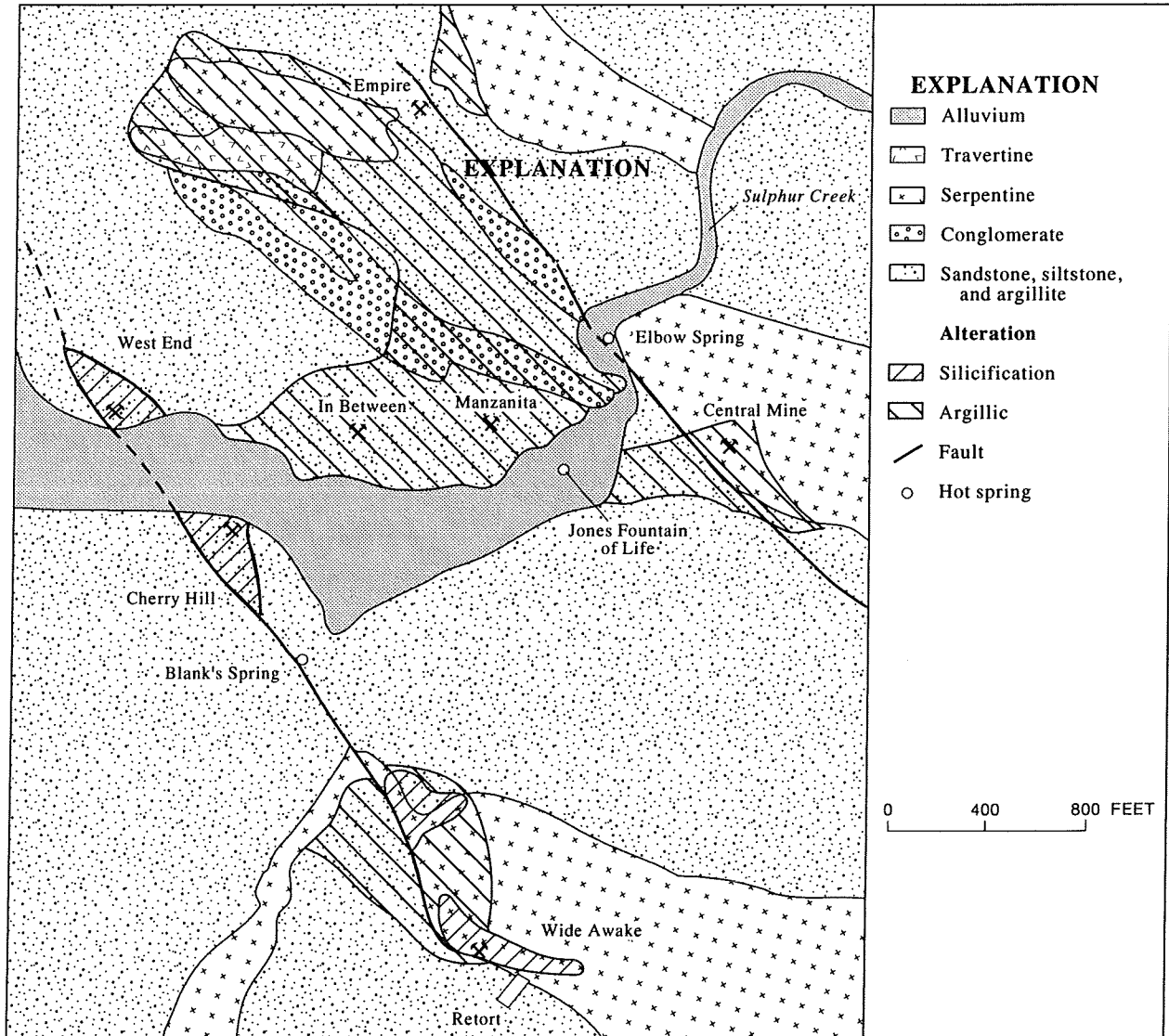


FIGURE 1. Geologic map of the central part of the Sulphur Creek Mining District. Gold and mercury depositing hot springs include the Elbow, Jones Fountain of Life, and Blank's.

Mercury Mines, about 1.5 km to the southwest, are hosted in equivalent sedimentary serpentinite within the lower Great Valley sequence strata of Tithonian to Valanginian age (McLaughlin and others, 1989).

The ore bodies are structurally bounded by northwest-trending, steeply-dipping faults that were active during and after mineralization (Fig. 1). A northwest-trending fault extending from the West End Mine to the Wide Awake Mine, bounds and cuts off gold veins on the west at the West End and Cherry Hill deposits. At the Wide Awake Mine, fault breccia in this fault was mineralized with stringers and veinlets of cinnabar and these extended into the footwall serpentinite along northeast trending fractures. Argillic alteration extends to the west of the fault zone toward Blank's hot spring (Fig. 1). During mining at the 300 foot level in the fault zone, flow from Blank's hot spring was disrupted indicating that this structure continued to provide structural control for the hydrothermal system. The east side of the West End and Cherry Hill deposits are cut off by a fault which splays off of the main northwest-trending fault (Fig. 1). The trace of one of these faults is well exposed at the West End mine (Fig. 2). A northwest-trending fault extending from the Empire to the Central mine (Fig. 1), limits mineralization to the east and provides the structural control for mineralization at these deposits. Recent left separations along this fault is evidenced by the offset of Sulphur Creek (Fig. 1).

The northwest striking faults in the district parallel the axis of the Wilbur Springs antiform and the Resort fault, a young, right lateral fault with a reverse component. In the district a conjugate set of discontinuous north, to northeast-trending faults locally provide ore controls especially where they intersect the northwest-trending structures such as at the Wide Awake Mine. The northwest-trending structures have a strike-slip and reverse component and the northeast-trending faults have a dip-slip component. The two set of faults are Neogene in age and have modified the morphology of the valley through which Sulphur Creek flows.

Veins in the district are typically sub-horizontal to gently dipping, with a maximum dip of about 30°. They outcrop especially well at the West End Mine (Figs. 2 and 3), at the open cut at the Cherry Hill Mine (Fig. 4), and at the In Between Mine (Fig. 5). No high angle veins are known at the Cherry Hill, West End, and the In Between deposits. All veins are cut by post-mineral, northwest-trending faults. The northwest-striking faults shallow with depth and cut off mineralization at the West End Mine.

Numerous veins are present in the gold deposit, but the veins are widely spaced and typically narrow, less than 1 cm in width and rarely as much as 40 cm. At the Cherry Hill deposit, spacing between the veins is about 2 m (Fig. 4). The largest vein occurs at the West End deposit and consists of an asymmetrically banded quartz vein with a central core of argillically altered hydrothermal sediment (Fig. 3). This vein displays botryoidal textures on the foot-wall and stalagmite forms hang from the hanging wall of the vein. These textures indicate that the present orientation of the vein reflects its original attitude and that no structural rotation of the veins has occurred.

The veins are hosted by adularized and silicified sandstone and siltstone except at the Wide Awake and Central Mines.. The most intense alteration present in at the West End Mine. In the near surface at the Manzanita Mine, advanced argillic alteration consisting of allophane, native sulfur, and opal is present. Veins typically consist of crustiform clear to milky quartz and amber to brown quartz containing abundant petroleum. Chalcedony



FIGURE 2. Overview of the West End gold deposit. Low angle veins are exposed from the top to the base of the hill with the largest vein present just below the cliff in the central part of the photograph. A northwest trending fault along the right side of the hill cuts off the vein system and juxtaposes adularized sandstone against unaltered sandstone of the Great Valley sequence.



FIGURE 3. View of the largest vein present at the West End mine shown in Figure 1. The vein is about 40 cm in width and consist of 2-4 cm of clear to petroliferous quartz deposited on each wall of the vein and a central zone of hydrothermal clay.

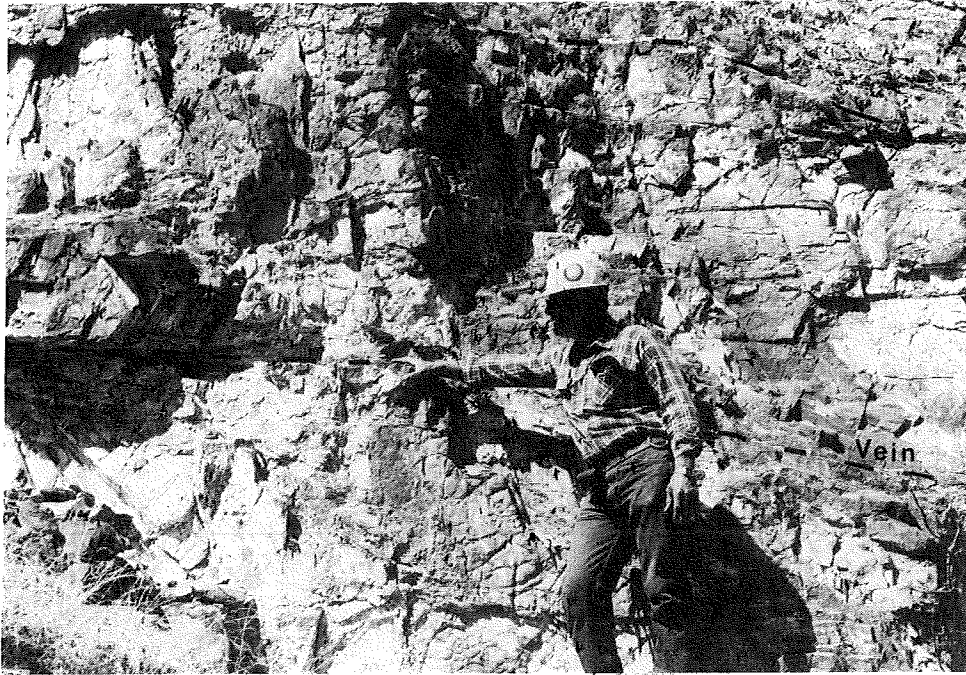


FIGURE 4. Beds of nearly vertical sandstone of the Great Valley sequence cut by low angle, gold-quartz veins at the Cherry Hill mine. Veins are generally less than 2 cm in width and consist of quartz and calcite filling fractures.

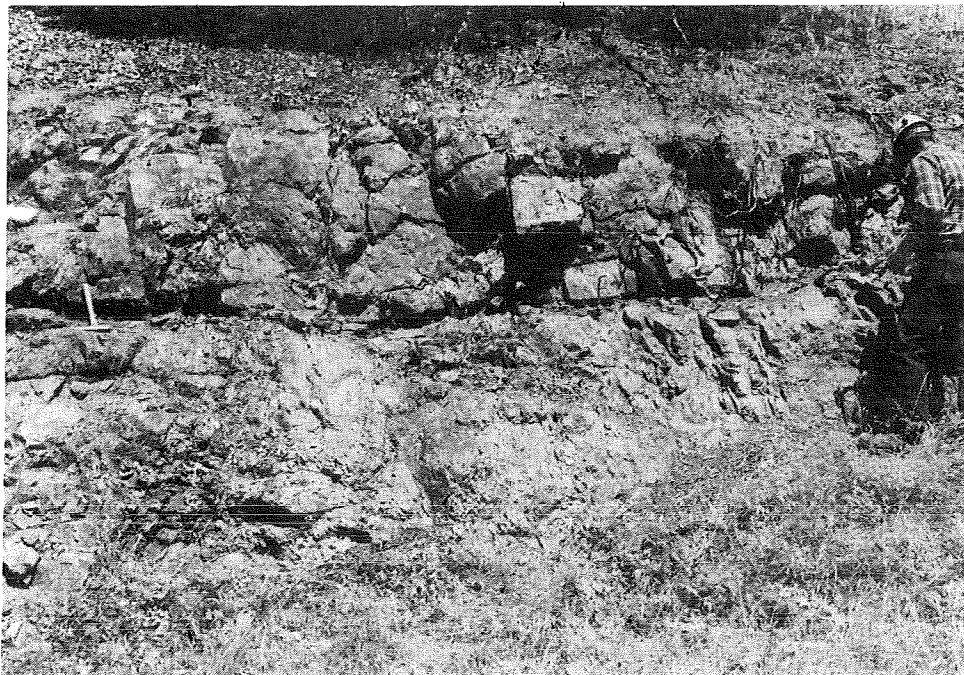


FIGURE 5. Nearly horizontal gold-quartz vein in the west part of the Manzanita mine (In Between mine). Vein is about 2-4 cm in width and contains abundant petroleum and visible gold.

and opal are only present at the Wide Awake Mine and the deeper levels of the Manzanita Mine. Froth vein textures and liquid petroleum filling vugs in quartz are commonly present. Some high-grade gold veins consist of coarse-grained gold in a matrix of petroleum with only traces of quartz gangue. Percy and Petersen (1990) recognized eleven stages in the vein paragenesis with vein stages characterized primarily by alternating from carbonate-dominant (magnesite, dolomite and calcite) and silica-dominant (quartz and chalcedony). However, most veins in the West End, Cheery Hill, In Between, and Manzanita Mines (Thordsen, 1988) have a simple paragenesis, an initial petroliferous quartz or quartz after calcite and clear comb quartz. Fluid inclusions indicate a steady decrease in temperature through the paragenetic sequence, from 190°C to 100°C, and the gold-mercury depositing hot springs reflect the waning stage of the hydrothermal system (Percy and Petersen, 1990). Gold is coarse grained and typically associated with pyrobitumen or petroliferous quartz. Electrum with a high mercury content, up to 5.2 wt. per cent is locally present (Percy and Petersen, 1990). In the west part of the Manzanita Mine (In Between Mine) (Fig. 1), quartz pseudomorphs after barite and calcite are present and marcasite is the main sulfide associated with the gold. The sulfide minerals at the Wide Awake deposit differ from the other deposits in that stibnite and silver sulfosalts are also present with cinnabar, gold and pyrite in petroliferous quartz-chalcedony veins that cut silica-carbonate altered serpentine. The deposit was mined primarily for mercury although coarse visible gold is present throughout the silica-carbonate altered serpentinite. The highest grade mercury ore occurred in a northwest trending fault gouge.

AGE OF MINERALIZATION

The earliest stage of mineralization in the Cherry Hill gold deposit has an age of 0.56 ± 0.14 Ma based on Ar^{40}/Ar^{39} dating of adularia (Percy and Petersen, 1990). The hydrothermal system has continued for the last 0.5 m. y. with gold and mercury presently being deposited in hot springs. The heat source for the hydrothermal system is uncertain. The only intrusive rocks exposed in the Sulphur Creek Mining District include three narrow, northwest-trending basalt dikes dated at 1.66 ± 0.08 Ma (McLaughlin and others, 1989). The basalt dikes intrude rocks of the lower Great Valley sequence in the eastern part of the district at Coyote Peak. These are too old and volumetrically insignificant to be the heat source for the mineralization. Donnelly-Nolan and others (1993) have postulated that a younger intrusive body is the heat source. A geothermal exploration well drilled at Wilbur Springs, about .25 km to the east, is reported to have encountered a mafic intrusion at depth, and but its age has not been determined.

Onset of mineralization in the Sulphur Creek Mining District coincides a major pulse of silicic volcanism in the central part of the Clear Lake volcanic field. It also coincides with a major pulse of plutonism in the composite felsite batholith present beneath The Geysers. This widespread increase in igneous activity suggests a regionally important change in heat flow beneath the Clear Lake volcanic field resulted in the development of the Sulphur Creek hydrothermal system.

DISCUSSION

The surface to shallow environment of mineralization in the Sulphur Creek Mining District is similar to that present at the McLaughlin Mine. However, in contrast to the McLaughlin Mine, the fluid flux and temperature of the hydrothermal system at the Sulphur Creek deposits has been lower and no large sinter terraces formed. The ore deposits in the Sulphur Creek Mining District are hosted by rocks at a structurally stratigraphic position higher in the lower Great Valley sequence than is the McLaughlin deposit. At depth in the area, the Great Valley sequence is underlain by the Stony Creek detachment fault and deformed ophiolitic and clastic rocks of the Grizzly Creek melange. A geothermal exploration well drilled near the Manzanita Mine encountered the base of the Great Valley sequence at about 0.67 km. In the drill hole about 0.3 km of the Coast Range ophiolite was present to a depth of about 1.0 km and below that about 0.3 km of Grizzly Creek melange to a depth of about 1.3 km. These rocks overlie about 1.0 km of serpentinized peridotite of the Coast Range ophiolite (McLaughlin and others, 1989). The Stony Creek fault underlies the Manzanita Mine area at a depth of about 1 km. This structure was important in channeling hydrothermal fluid to the surface at the McLaughlin mine and may also serve as a locus of hydrothermal flow and mineralization at depth in the Sulphur Creek Mining District. In the shallow levels of the Sulphur Creek Mining District, northwest-trending faults channeled hydrothermal fluids to the surface.

Repetition of the upper part of the Coast Range ophiolite below 2.3 km in the Sulphur Creek Mining District suggests contractional deformation and duplexing of the ophiolite beginning at this depth. Aeromagnetic data further indicate that magnetic basement rocks (probably ophiolitic) extend southwest from Wilbur Springs, to a depth of about 6 km beneath the Franciscan Complex near or at the Bartlett Springs fault. These relations imply that one or more tectonic wedges of Franciscan Complex are present beneath the Clear Lake region (McLaughlin and others, 1990; McLaughlin and Ohlin, 1984; Ramirez, 1993). Compression during wedge emplacement has been accommodated by uplift and shortening across oblique reverse faults at the surface, by blind thrusting at depth, and by growth of folds and warps in the hanging wall rocks, especially above blind thrusts. In this structural environment, detachment structures are important in the near surface. The low angle, open fractures that host the veins in the Sulphur Creek Mining District may have been generated above a near-surface low angle fault.

Alternatively, the shallow dipping auriferous veins may be related to reverse slip along the northwest-striking faults in a manner similar to the flat veins common in the shear zone hosted gold deposit. In this model, the vein represent extensional fractures that would be thickest adjacent to the faults, and thin laterally away (Sibson and others, 1988). Fluids would be channeled up the faults, and then flow laterally into the open fractures. This model predicts that shallow dipping veins should be distributed symmetrically about the reverse faults. This is not the case in the Sulfur Creek Mining District. It is likely that post-mineral reverse movement has displaced the hanging wall deposits from the footwall deposits. This scenario predicts that the other halves of the footwall deposits, like the Empire deposit, is eroded, and the other halves of hanging wall deposits, like the West End and Cherry Hill deposits, lie at depth.

REFERENCES

- Bradley, W. W., 1916, The counties of Colusa, Glenn, Lake, Marin, Napa, Solano, Sonoma, Yolo: California Mining Bureau Fourteenth Report State Mineralogist, p. 173-370.
- McLaughlin, R. J., and Ohlin, H. N., 1984, Tectonostratigraphic framework of the Geysers-Clear Lake region, California: Pacific Sec. Soc. Econ. Paleontologists Mineralogists, v. 43, p. 221-254.
- McLaughlin, R. J., Ohlin, H. N., Thormahlen, D. J., Jones, D. L., Miller, J. W., and Blome, C. D., 1989, Geologic map and structure sections of the Little Indian Valley-Wilbur Springs geothermal area, northern Coast Ranges, California: U. S. Geol. Survey Map I-1706, scale 1:24,000.
- Pearcy, E. C., and Petersen, Ulrich, 1990, Mineralogy, geochemistry and alteration of the Cherry Hill, California hot-spring gold deposit: *Journal of Geochemical Exploration*, v. 36, pp. 143-169.
- Phipps, S. P., and Unruh, J. R., 1992, Crustal-scale wedging beneath an imbricate roof-thrust system: geology of a transect across the western Sacramento Valley and northern Coast Ranges, California, in M. C. Erskine, J. Unruh, W. R. Lettis, and J. A. Bartow, eds., *Field Guide to the tectonics of the boundary between the California Coast Ranges and the Great Valley of California GB-70: American Association Petroleum Geologists Guidebook GB-70*, p. 117-140.
- Ramirez, V. R., 1993, Evolution of the Coast Range thrust as interpreted from seismic reflection data [abs.]: *Abstracts with Programs, Geol. Soc. America*, v. 25, p. 136.
- Sibson, R.H., Robert, Francois, and Poulsen K.H., 1988, High-angle reverse faults, fluid-pressure cycling, and mesothermal gold-quartz deposits: *Geology*, v. 16, p. 551-555.
- Thordsen, J. J., 1988, Fluid inclusion and geochemical study of epithermal gold mineralization in the Wilbur Springs district, Colusa and Lake counties, California: Master's Thesis, Ohio State University, 229 p.
- Whitney, J. D., 1865, *Geological Survey of California: Geology*, vol. I, Report of progress and synopsis of the field work from 1860 to 1864, 498 p.

DAY THREE

HOT SPRINGS AND DEPOSITS OF MERCURY AND GOLD IN THE CLEAR LAKE VOLCANIC FIELD: ROAD LOG

James J. Rytuba, Julie M. Donnelly-Nolan, and Robert J. McLaughlin

U.S. Geological Survey, 345 Middlefield Road, Menlo Park CA 94025

This tour begins and returns to Clearlake Highlands. The route for the trip is shown in Figure 1. Note that several stops on this trip are described in detail in the field guide that is part of the paper by Goff and Janik (this volume).

Mileage

0.0 Today's trip begins in the west (right side), back parking lot of the El Grande Hotel.

STOP 1.

STOP 1. OVERVIEW OF MOUNT KONOCTI AND THE CLEAR LAKE VOLCANIC FIELD

The Clear Lake volcanic field is the current locus of volcanism in the Coast Ranges with progressively older volcanic centers present to the south. Following the initial widespread phase of Clear Lake volcanism, activity focused primarily in the area between The Geysers and Clear Lake with some additional eruptions to the northeast. Within the main volcanic field, eruptive activity has moved northward through time in a general way (see Fig. 3 in Donnelly-Nolan and others, 1993). Vent trends tend to be either northwestward, parallel to the regional fault trends, or north to north-northeast, as in linear arrays of mafic vents that trend through Mt. Konocti and through this area from Roundtop Mountain near yesterday's final stop to just east of the Sulphur Bank Mine to High Valley, where an andesitic flow erupted from a cinder cone that is morphologically very young. Mafic tephra were also deposited around the shores of the Highlands arm of Clear Lake (the body of water between here and Mt. Konocti) and around the Oaks arm to the north. Bedding characteristics of these tephra indicate interaction with and likely eruption through water, and stratigraphic relations indicate that these are some of the youngest eruptions of the Clear Lake Volcanics. About 2 km to the northwest of us is the youngest rhyolite in the Clear Lake volcanic field, the 90,000 Ka rhyolite of Borax Lake. This rhyolite is part of a complex eruption sequence including dacite and basalt (Bowman and others, 1973). Basalt is one of the rarest rock types in the Clear Lake Volcanics.

Several hypotheses have been put forth to explain the Clear Lake Volcanics. Hearn and others (1981) suggested a hot spot origin. Johnson and O'Neil (1984) regarded the Clear Lake Volcanics as "triple-junction related," although the Mendocino Triple Junction lies 200 km to the northwest. Clear Lake volcanism has occurred entirely since subduction ceased at this latitude some 3 m. y. ago (Atwater and Molnar, 1973, McLaughlin, 1981). Donnelly-Nolan and others (1993) argued that the Clear Lake Volcanics result from extension within a pull-apart basin in the San Andreas transform-fault system. They suggested that extension over a slab window (Dickinson and

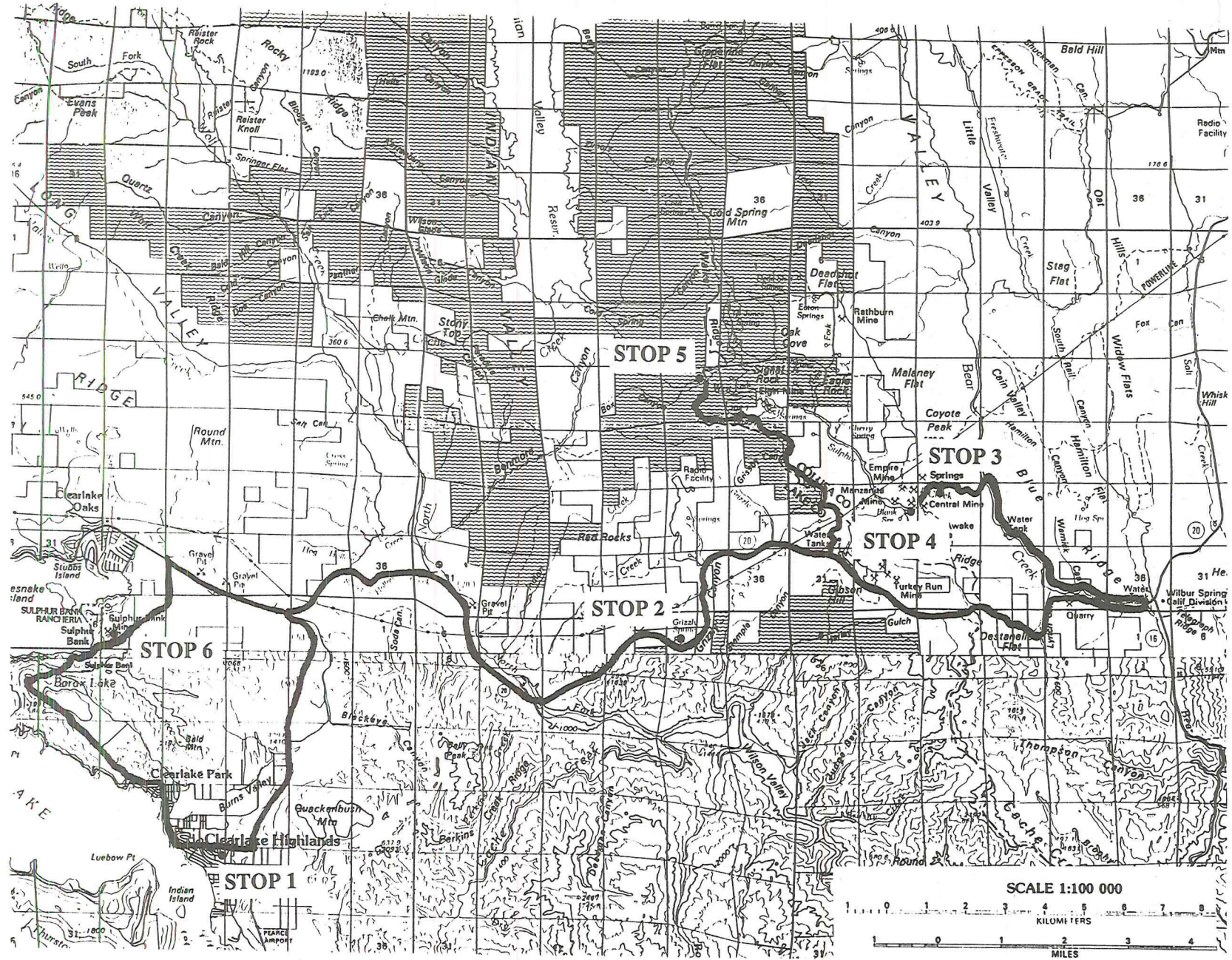


FIGURE 1. Route map for Day 3. Trip begins at El Grande Hotel parking lot and proceeds to Wilbur Springs. Trip returns to Clearlake Highlands.

Snyder, 1979) allowed mantle melts to intrude the relatively thin crust and generate derivative silicic melts, much of which have never reached the surface (for example the felsite in The Geysers). Hearn and others (1988) pointed out that Clear Lake basin and its associated igneous activity have the general characteristics of a pull-apart basin as defined by Crowell (1974).

Modeling of seismic data (Benz and others, 1992) is consistent with shallow asthenosphere in the area of the proposed slab window. A low-velocity anomaly was also observed north of Clear Lake, suggesting that magmatic intrusion is taking place there, which is consistent with the northward migration of volcanism in the Coast Ranges. Numerical simulations of Cenozoic volcanism in the Coast Ranges (Liu and Furlong, 1992) suggest that the spatial and temporal distribution of the volcanic rocks is directly related to the passage of the Mendocino triple junction. The more voluminous northern Coast Ranges volcanism correlates with a relatively high velocity between the Pacific and North American plates since 10 Ma, compared with smaller volumes of central California volcanism and rates of plate movement between 20 and 10 Ma. Modeling also shows that large amounts of basaltic magma may be produced by pressure-release partial melting in the area of the slab window, resulting in a high degree of thermally induced crustal anatexis.

Clear Lake is the largest natural freshwater lake entirely within California. There is a dam on its outlet stream, Cache Creek, but the dam only raises the level of the lake a few feet. Clear Lake fills a fault-bounded structural depression in which geometry has been largely controlled by tectonism and to a lesser extent by volcanism (Sims and others, 1988; Hearn and others, 1988). The lake has always been shallow although it formed about 600 ka (Hearn and others, 1988). It continues to exist because the lake basin is subsiding as fast as the lake is filling with sediment. Studies of sedimentary deposits in 10 cores taken from the bottom of Clear Lake (Sims, 1988) demonstrate changes in its shape, area, and depth (Sims and others, 1988) and numerous climatic changes through time (Adam, 1988).

Sedimentary deposits of the Pleistocene Kelseyville and Lower Lake Formations indicate that the lake formerly extended farther southwest and southeast. This hotel was built on top of interbedded lake sediments and tephra of the Lower Lake Formation. To the northeast is the older and much more extensive Cache Formation. It is composed primarily of fluvial sediments deposited within a fault-bounded basin from about 3.0 to 1.8 m. y. (Rymer, 1981; Rymer and others, 1988).

0.0	0.0	Exit parking lot of El Grande Hotel and turn right onto main road out of Clearlake (east.)
0.4	0.4	Turn left onto Highway 53.
1.5	1.9	Cache Formation sediments in road cuts on either side of road.
3.1	5.0	Turn right, east, onto Highway 20
2.8	7.8	The Cache Formation consists predominantly of Pliocene fluvial and alluvial gravel, siltstone, and sandstone, deposited in a rhombic structural basin between two northwest-trending strike slip faults, at least one of which (the Bartlett Springs fault zone) has a component of southwest-vergent

reverse slip. The Cache Formation is bounded on the NE by the northeast-trending, down to the southeast, Cross Springs fault. To the southwest, the Cache basin is bounded by a major splay of the Clover Valley fault zone (Hearn and others, 1988), and the northeast margin of the basin is the Bartlett Springs fault zone (McLaughlin and others, 1989). The age of the Cache Formation is greater than about 1.66 Ma based on the age of basalts in the upper part of the formation and about 2.9 Ma or less based on vertebrate fossils in the lower beds of the formation (Rymer and others, 1988, Hearn and others, 1988). The Cache Formation is up to 4 km thick and is compressed into broad north-northwest-trending warps between the Cross Springs and Bartlett Springs bounding fault zones. This suggests a component of northeast-southwest transpressional deformation since at least 1.66 Ma. Basaltic to dacitic volcanism is spatially associated with the northeast margin of the Cache basin, along the Bartlett Springs fault zone and with the Cross Spring fault on the northwest, suggesting that the basin-bounding faults also acted locally as conduits for venting of the volcanic rocks.

5.1 12.9 Grizzly Spring. Park on right side of road. **STOP 2.**

STOP 2. GRIZZLY SPRING AND TRAVERTINE TERRACE.

Grizzly Spring is at a dangerous bend in Highway 20; be sure to look carefully before crossing the road to climb up the travertine terrace, which has been partially undercut and broken by the highway. The spring has a low flow, measures about 20°C, and is moderately saline with 4,210 mg/l of chloride and 140 mg/l of boron. The source of water in the spring was interpreted by White and others (1973) to be metamorphic water derived from dehydration reactions during regional metamorphism (White, 1957). Donnelly-Nolan and others (1993) interpret this spring to be dominantly evolved connate water with a low B/Cl ratio similar to that of waters emerging in the Wilbur Springs area, although the chloride content is lower, suggesting mixing with meteoric water. Mixing is also indicated by the isotopic values, which are shifted (+0.55 $\delta^{18}\text{O}$, -32.5 δD), and lie along a line between meteoric water and evolved connate waters of the Wilbur Springs area. Grizzly Spring emerges along the Bartlett Springs fault zone at the east boundary of the Cache Formation and the water very likely interacts with underlying Great Valley sequence rocks, the likely source of the evolved-connate component of ancient sea water.

Numerous other low-flow, barely thermal springs with large travertine terraces emerge in the eastern part of the Clear Lake area. We will see another tomorrow just south of the McLaughlin Mine. These springs are more abundant in or near Great Valley sequence rocks than in the more metamorphosed Franciscan rocks to the west. They have high bicarbonate contents and commonly discharge CO_2 , which is thought to be a product of regional metamorphism (Barnes and others, 1973).

Numerous springs emerge along the Bartlett Springs fault zone with variable B/Cl ratios. Grizzly Spring is the most chloride-rich, but it has a relatively low boron content. Other springs appear to be mixtures of evolved connate and meteoric water with another high-boron water interpreted by Donnelly-Nolan and others (1993) as an evolved meteoric water. This water type is thought to be produced locally by concentration processes in rocks with

low permeability, and it is associated with Franciscan Complex rocks. Similar waters are found at Sulphur Bank Mine and are thought to occur in The Geysers.

For additional information about Grizzly Spring and other springs in the Geysers-Clear Lake area, see Goff and Janik (this volume). They reported the results of gas and tritium analyses. Grizzly Spring was originally described by Waring (1915), whose publication continues to be a valuable resource for information about springs of the area.

4.3 17.2 Walker Ridge Road. On the return from Wilbur Springs the trip will turn here.

0.3 17.5 Abbott Mercury Mine on left (north side of road) is a typical silica-carbonate mercury deposit developed in sedimentary serpentinite at the contact with Great Valley sediments. The mercury mineralization in this area, and in many of the mercury districts northeast of Clear Lake, is spatially associated with the contacts between clastic marine strata of the Great Valley sequence, and serpentinite. At the Abbott and Turkey Run Mines, the host rock is sedimentary serpentinite, consisting largely of coarse serpentinite debris flows, that locally grade upward into thin-bedded serpentinite sandstone turbidites. These rocks are interpreted to be derived from the exposure and erosion of subseafloor diapirs developed at (or) along a convergent margin (Carlson, 1981). The sedimentary serpentinite at the Abbott and Turkey Run Mines is within a section of lower Great Valley sequence strata of Tithonian to Valanginian age (McLaughlin and others, 1989) along the southwest flank of the southeastward-plunging Wilbur Springs antiform. This gross structural framework is overprinted by discontinuous steeply dipping northwest-trending strike-slip and reverse faults, and northeast-trending dip-slip faults, of probable Neogene age.

Froth veins with abundant petroleum are present at the mine. The hydrocarbons associated with the mercury deposits in this area were likely derived from associated strata of the Great Valley sequence, which has been the focus of oil exploration in the past. Hydrothermal fluids associated with hot springs and nearby oil and geothermal exploration wells, as will be discussed further at Stop 3, are characteristically high in chloride and probably have a significant connate component. This contrasts with waters from The Geysers and the Mayacmas mercury district, which mostly vent from the Franciscan Complex, have a comparatively low in chloride content, and are likely evolved meteoric water (Donnelly-Nolan and others, 1993).

0.2 17.9 Workings to the north of the road are from the Turkey Run mercury deposit, an extension of that at the Abbott Mine. The northwest-trending sedimentary serpentinite lens associated with mineralization at the Turkey Run and Abbott Mines merges eastward, along Highway 20, with a very thick section of sedimentary serpentinite, which laps over, and is offset (apparently right-laterally) along the crest of the Wilbur Springs antiform, by the northwest-trending Resort fault zone (McLaughlin and others, 1989).

Northwestward, along the antiform axis, the sedimentary serpentinite section and flanking *Buchia*-bearing mudstone and sandstone of the lower part of the Great Valley sequence overlie rocks of the Coast Range ophiolite and (or) an ophiolitic melange. The melange consists of boulder to house-size blocks of ophiolitic lithologies (ultramafic rocks, gabbro, diabase, basalt, chert, and mafic sedimentary breccias) tectonically mixed in a penetratively sheared matrix.

- 4.7 22.6 Turn left onto gravel road and proceed west to Wilbur Springs.
- 0.8 23.4 Contact of sedimentary serpentine and sediments of Great Valley sequence of Late Jurassic to Early Cretaceous age, based on *Buchia* index fossil.
- 0.2 23.6 Travertine terrace on right side of road from cool oxidized spring.
- 2.6 26.2 Turn left and cross bridge on road to Wilbur Springs.
- 0.6 26.8 Gate at Wilbur Springs-be sure to close gate.

Just north of the Wilbur Springs gate, three narrow northwest-trending inclusion-rich basalt dikes, dated at 1.66 ± 0.08 Ma (McLaughlin and others, 1989) cut the lower Great Valley rocks and underlie Coyote Peak. Sulphur Creek Canyon, along which the road into Wilbur Hot Springs Resort follows, cuts across the axial crest of the Wilbur Springs antiform here. As you cross the steeply dipping, folded Stony Creek detachment fault, you pass from lower Great Valley sequence strata to the east, into rocks of the Coast Range ophiolite exposed in the plunging core of the antiform. These rocks include basaltic flows, chert, and serpentinitized peridotite, all of which are hydrothermally altered, weathered, and iron stained. The ultramafic rocks also include ribs of silica-carbonate, exposed in the road cuts. At Wilbur Hot Springs Resort the road crosses back up section in the southwest limb of the Wilbur Springs antiform into intensely to weakly hydrothermally altered sedimentary serpentinite, and into sandstone and shale of the lower Great Valley sequence. The steeply dipping and very young Resort fault cuts through the southwest side of the antiform core here and overprints the older Stony Creek detachment fault.

- 0.2 27.0 Wilbur Springs vents and terraces on left side of road.
- 0.3 27.3 Parking lot for vehicles visiting Wilbur Springs. Walk back down road to Wilbur Springs.

STOP 3.

STOP 3. WILBUR SPRINGS TERRACE.

Hot springs vent along Sulphur Creek and are localized along the Resort fault zone. The spring deposits form a conspicuous terrace over basalt of the Coast Range ophiolite and sedimentary serpentinite in the core of the Wilbur Springs antiform. Hydrothermal flow and alteration are focused over the crest of this antiformal structure particularly around the plunging "apex" of exposures of the Coast Range ophiolite. Geyser activity at nearby Elbow and Jones Fountain of Life indicate that hydrothermal flow possibly may be enhanced in this area as the result of high pore pressures along the axis of the Wilbur Springs antiform.

Several springs form a coalescing travertine terrace along the north bank of Sulphur Creek, the hottest of which is known as Wilbur Main Spring. It emerges from a sulfur-lined box (Fig. 2) at about 50°C and flows on the terrace in channels containing filamentous bacteria (Fig. 3) and a wide variety of specialized insects (see Thompson and others, this volume). The water contains nearly 10,000 mg/l of chloride and 280 mg/l of boron, and the isotopes are strongly shifted to +4.95 $\delta^{18}\text{O}$ and -22.65 δD (Donnelly-Nolan and others, 1993). A black precipitate on the sulfur where the spring emerges contains 6.70 ppm of gold (J. M. Donnelly-Nolan, unpub. data, 1991), similar to values determined by Peters (1991), who studied the isotopically shifted springs of the eastern Clear Lake area emphasizing those associated with gold deposits. Peters (1993) interprets the chloride-rich springs as connate waters modified from Cretaceous sea water trapped in the rocks, a suggestion first put forward by White and others (1973) and supported by Donnelly-Nolan and others (1993). Several other chloride-rich springs including Elbow, Jones Fountain of Life, Blanks, and Elgin emerge within the greater than 10 mi² area of the Sulphur Creek drainage basin. The hottest (68°C) of these springs is at the Elgin mercury mine where greater than 100 l/minute of hot spring waters discharge in the vicinity of the mine, which is near the head of the drainage basin (White and others, 1973). See Goff and Janik (this volume) for additional information about Wilbur Springs.

The north easternmost exposures of the Clear Lake Volcanics are dikes of early Clear Lake Volcanics basaltic lava (K-Ar dated at 1.66 \pm 0.08 Ma) exposed less than 1 mi east and northeast of Wilbur Springs (McLaughlin and others, 1989). It is too old to be the heat source for the mercury and gold mineralization in the Sulphur Creek district, and later intrusive bodies probably have provided the heat (Donnelly-Nolan and others, 1993).

Perennial saline springs with isotopically shifted signatures are also reported farther southeast in the Rumsey Hills near the west edge of the Sacramento Valley (Unruh and others, 1992). They typically emerge near ridge crests and are thought to be surface expressions of anomalously high pore-fluid pressures resulting from active "tectonic wedging" and blind thrusting. The fluids are interpreted as formation waters being tectonically driven out of the rocks.

Retrace route back to parking lot.

- 0.2 27.5 Leave parking lot and turn left onto dirt road and stop at gate. Hike down to bend in creek to visit Elbow springs, Jones Fountain of Life and Cherry Hill gold deposit. **STOP 4.**
-

STOP 4. ELBOW AND JONES FOUNTAIN OF LIFE HOT SPRINGS AND THE CHERRY HILL GOLD DEPOSIT.

After crossing through the gate west of the Wilbur Springs parking lot, the road heads south. Where Sulphur Creek turns west away from the road, a small hot spring emerges at the base of the road embankment just south of the creek (Fig. 4) and is named the "Elbow Spring" by Peters (1991). It has a temperature of 62°C and a black precipitate (Fig. 5) from the hot spring pool yielded 12.1 ppm gold.

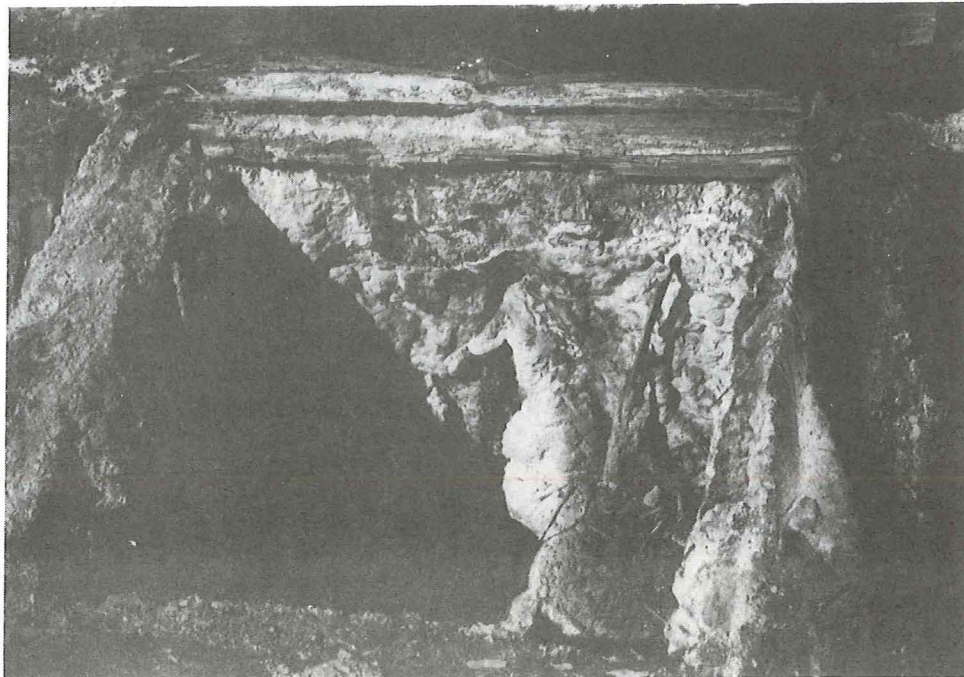


FIGURE 2. Hot spring vent area at Wilbur Springs enclosed in wooden structure coated with sulphur and dark gray precipitate.

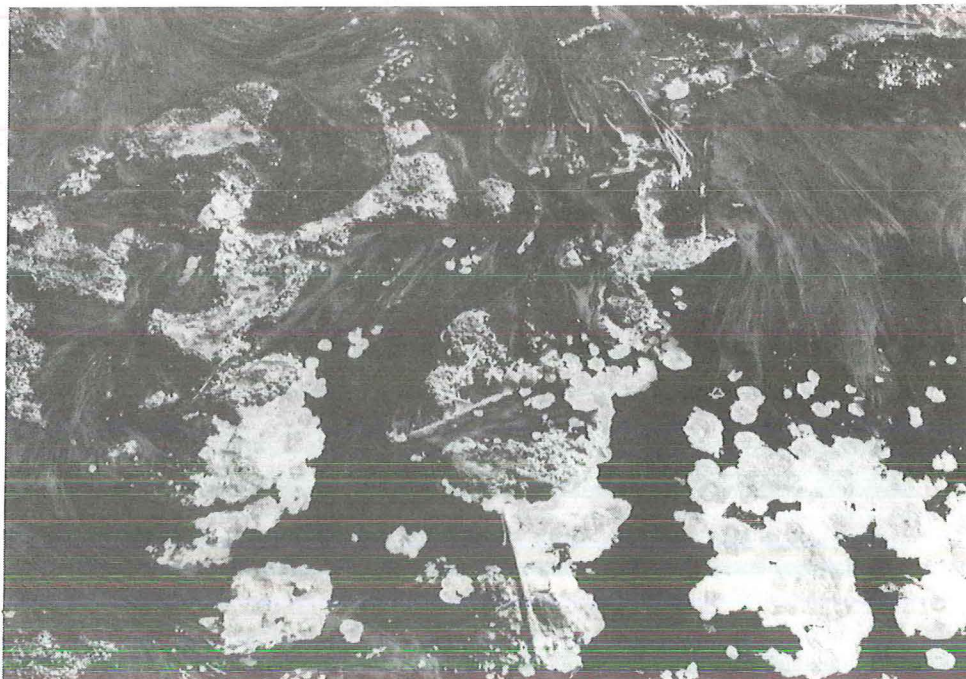


FIGURE 3. Filamentous bacteria and sulphur precipitate in hot spring terrace at Wilbur Springs.



FIGURE 4. Hot spring vent area at Elbow Springs with sulphur precipitate around the vent area. Although this spring has the highest gold content in sulfide mud precipitate, the spring is not forming a hot-spring terrace.

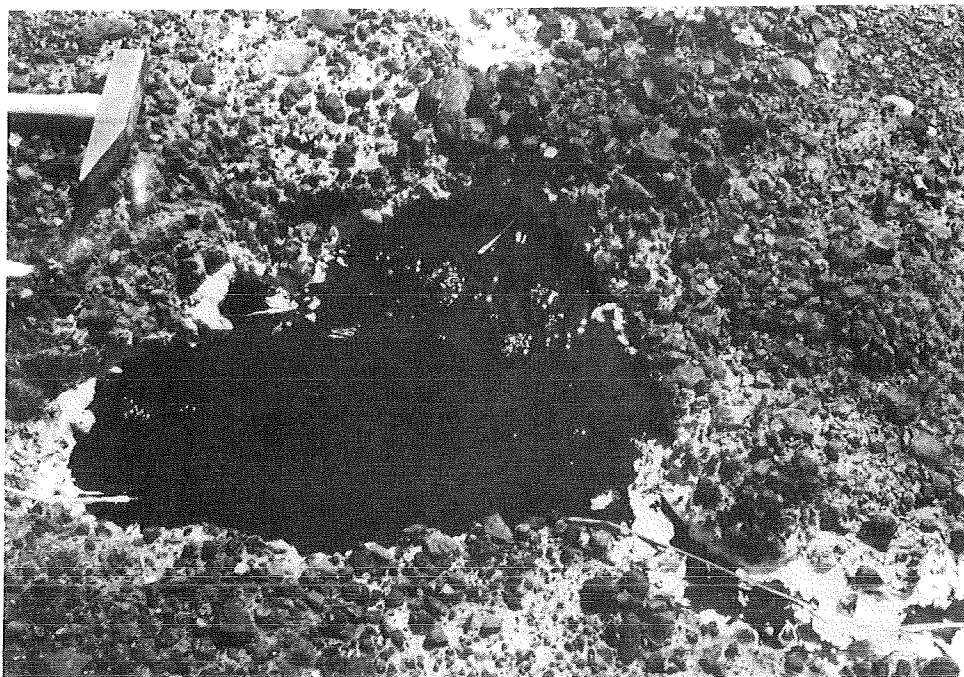


FIGURE 5. Vent of the Elbow hot springs surrounded by sulphur. Black sulfide mud in the bottom of the vent is several inches thick and contains 12.1 ppm gold and 179 ppm mercury (Peters, 1991).

Jones Fountain of Life spring is described elsewhere in this volume (Goff and Janik). It is similar in chemical and isotopic composition to the water of Wilbur Spring, but the gas is methane rich, markedly different from the CO₂-rich gas at Wilbur Main Spring.

Note that gold mineralization in The Geysers-Clear Lake area is located in the eastern part of the region, in or near Great Valley sequence rocks. As pointed out by Peters (1993), the gold was transported by saline fluids interpreted by her as connate waters which were derived from the Great Valley sequence.

Within the Sulphur Creek district several gold and mercury deposits have been developed including the West End, Central, Cherry Hill, Empire, and Wide Awake mines. The association of gold and mercury in the district was recognized early, and gold was mined at the Manzanita mercury mine from 1865 to 1891, with total production being about 3,000 oz of gold (Whitney, 1865, and Bradley, 1916). Fine placer gold is also present in drainages within the Sulphur Creek district. Total mercury production from the district has been only about 8,000 flasks. In 1977 Homestake Mining Co. delineated a small gold deposit in the area of the Cherry Hill, Empire and Central mines.

These gold and mercury deposits are primarily hosted by the basal unit of the Great Valley sequence, which consists of carbonaceous mudstone, sandstone, and conglomerate, all of which have a detrital volcanic component. This unit is equivalent to the Knoxville Formation at the McLaughlin Mine. Sedimentary serpentinite bodies are locally altered to silica-carbonate and locally host ore bodies. These deposits are along or near the crest of the Wilbur Springs antiform, where Coast Range ophiolite is exposed in the plunging apex of the antiform. The ore bodies are structurally controlled by northwest and northeast trending, steeply dipping faults; the northwest faults parallel the Resort fault and the axis of the Wilbur Springs antiform. A conjugate set of discontinuous north to northeast trending faults also provide important ore controls especially where they intersect the primary northwest trending structures. Fracture sets subparallel to bedding controlled alteration and mineralization. Veins in the Cherry Hill deposit are truncated by these structures and indicate that the faults were active during formation of the deposit.

The following summary of mineralization at Cherry Hill is taken from Percy and Petersen (1990). Several vein systems are present in the deposit but the veins are widely spaced and typically less than 1 cm wide but rarely as much as 10 cm. The veins are hosted by adularized and silicified mudstone at depth, which in the near surface advanced-argillic alteration consisting of allophane, native sulfur, and opal is present. Eleven stages in the vein paragenesis have been recognized, with vein stages characterized primarily by alternation from carbonate dominant (magnesite, dolomite, and calcite) to silica dominant (quartz and chalcedony). Fluid inclusions demonstrate a steady decrease in temperature from 190°C to 100°C, and the active gold-mercury-depositing hot springs reflect the waning stage of the hydrothermal system. Gold is present as electrum with a high mercury content, up to 5.2 wt. per cent and cinnabar typically formed late in the paragenetic sequence. Petroleum is abundant throughout the early and late stages of the paragenesis with some high grade gold veins consisting of dendritic gold in a matrix of petroleum. Adularia from the earliest stage of mineralization has an age of 0.56 ± 0.14 Ma based on Ar⁴⁰/Ar³⁹.

The level of exposure in the Sulphur Creek district may be similar to the mineralization depths at the McLaughlin deposit. However, the mercury and gold mineralization at the surface in the Sulphur Creek district occupies a structurally higher position, largely in relatively well-bedded, intact sandstone and argillite of the lower part of the Great Valley sequence, than the mineralization at the McLaughlin Mine. At depth, the Wilbur Springs area is underlain by the Stony Creek detachment fault, below which are deformed ophiolitic and clastic rocks of the Grizzly Creek melange. At the McLaughlin Mine, significant Au mineralization occurred in this deformed package of rocks equivalent to the Grizzly Creek melange. In both areas the melange is present below the Stony Creek detachment and above the Coast Range fault.

A deep geothermal-exploration well was drilled near the Manzanita Mine in 1980. The well (Bailey Minerals #1) encountered the base of the Great Valley sequence at about 0.67 km; below that about 0.3 km of the Coast Range ophiolite was present to a depth of about 1.0 km; about 0.9 km of Grizzly Creek melange was drilled to a depth of about 1.3 km; which in turn was underlain by about 1.0 km of serpentinized peridotite of the Coast Range ophiolite to about 2.3 km. Below the ultramafic rocks, about .57 km of basalt was drilled, to the bottom of the hole at about 2.9 km (McLaughlin and others, 1989) . Thus the Stony Creek detachment is projected to underlie the Manzanita Mine area at a depth of about 1.0 km, and rocks that are tectonically and stratigraphically equivalent to the mineralized Great Valley section at the McLaughlin Mine are about 0.3 km thick beneath the Stony Creek detachment in the Wilbur Springs area, extending to about 1.3 km. Repetition of the upper part of the Coast Range ophiolite section below 2.3 km suggests contractional deformation and duplexing of the ophiolite beginning at this depth. Aeromagnetic data further indicate that magnetic basement rocks (probably ophiolitic) extend southwestward from Wilbur Springs, to a depth of about 6 km beneath the Franciscan Complex near or at the Bartlett Springs fault. These relations independently support the interpretation of one or more eastwardly tapered tectonic wedges of Franciscan rocks beneath the Clear Lake region (McLaughlin and others, 1989; McLaughlin and Ohlin, 1984; Ramirez, 1993).

Retrace route back to vehicles.

-
- 1.4 28.9 Retrace route out from Wilbur Springs, cross bridge and turn right.
 - 3.6 32.5 Intersection with Highway 20, turn right.
 - 5.6 38.1 Turn right onto Walker Ridge Road, a BLM gravel road.
 - 1.1 39.2 Bear left and stay on good road.
 - 3.3 42.5 Park on side of road and walk up side road to top of hill at relay station for panoramic overlook of the Clear Lake volcanic field and west side of the Great Valley. **STOP 5.**

STOP 5. VIEW FROM WALKER RIDGE ROAD OF THE CLEAR LAKE VOLCANIC FIELD AND THE GREAT VALLEY.

From this vantage point along the crest of the eastern Coast Ranges, you can view the major volcanic edifices of the Clear Lake region, including Mount Konocti, and Mount Hannah within the main Clear Lake volcanic field and Cobb Mountain along the crest of the Mayacmas Mountains southwest of Clear Lake (Fig. 6). To the southeast of Cobb Mountain along the Mayacmas crest is Mt. St. Helena, which is at the northwest edge of the 2.9 Ma and older Sonoma volcanic field. The Clear Lake Volcanics occupy the intervening low-lying volcano-tectonic

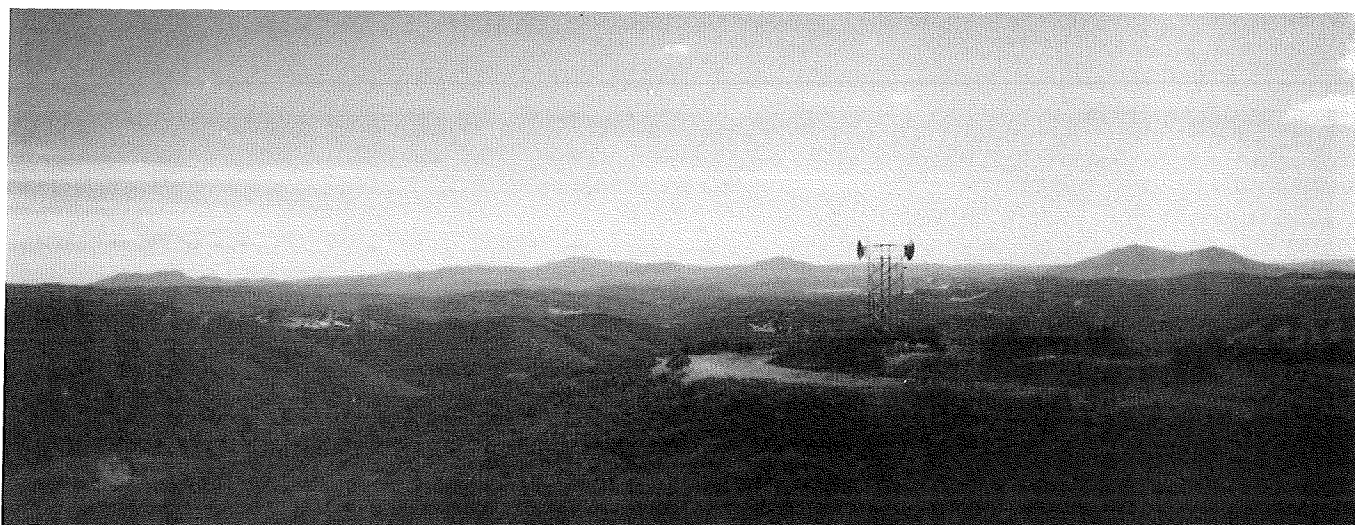


FIGURE 6. Overview of the Clear Lake volcanic field and northern part of the Sonoma volcanic field. Mount Konocti is to the far right, Mount Hannah is to the left and Cobb Mountain farther to the left. Mount St. Helena in the Sonoma volcanic field is on the extreme left. Rocks in the foreground are Great Valley sequence.

depressions between the crest of the Mayacmas Mountains and the Bartlett Springs fault zone. Some of the Neogene faults associated with, or superposed on, the Coast Range fault zone in this area (such as the Resort fault) may flatten at depth to root into the southwest-vergent roof thrust system of an underlying northeastwardly-propagating tectonic wedge. The existence of this wedge complex is based primarily on recent seismic reflection and refraction data (Wentworth and others, 1984; Ramirez, 1993; Unruh and Moores, 1992; Phipps and Unruh, 1992), and on stratigraphic relations discussed at previous stops near Wilbur Springs. The wedge complex, which extends under the entire length of the Coast Ranges, is composed predominantly of rocks of the Franciscan Complex, Coast Range ophiolite, and Great Valley sequence. Below depths of perhaps 6-8 km in the western Great Valley, the wedge complex appears to be thrust eastward (obducted) over rocks with the same velocity structure as the granitic and

metamorphic basement of the Klamath and Sierra Nevada Mountains to the north and east (Ramirez, 1993). The tip of the wedge complex is thought to lie east of Wilbur Springs, beneath the west side of the Great Valley.

Eastward propagation of this structure may be driven by the component of contractional deformation normal to the Pacific-North American plate transform boundary. This ongoing compression apparently is accommodated by uplift and shortening across oblique reverse faults at the surface, by blind thrusting at depth, and by growth of folds and warps in the hanging wall rocks, especially above blind thrusts. This model implies that much of the folding along the southwest side of Sacramento Valley is very young and underlain by southwest-vergent blind thrusts in the roof of the buried wedge complex. This model has also been used to explain the origin of unusually high fluid pore pressures in the Coast Ranges (Berry, 1973; Davisson, 1992). Visible northeast and east



FIGURE 7. On the skyline are the subparallel hogbacks that correspond to the Great Valley sequence. The Coast Range ophiolite occurs below the scarp toward this vantage point. In the distance on the left Sutter Buttes is barely visible.

of here are a series of northwest-trending, subparallel hogbacks that correspond to the upturned southwest side of the late Mesozoic and Tertiary Great Valley forearc basin (Fig. 7).

In the distance to the east is Sutter Buttes, a Pleistocene volcanic dome complex of andesite and rhyolite (Williams and Curtis, 1977) that erupted through the Sacramento Valley about 1.56 to 0.9 Ma (Hausback, 1991). It lies about 50 km northeast of Coyote Peak where the north easternmost lava of the Clear Lake Volcanics intruded the Great Valley sequence near Wilbur Springs. The age of Sutter Buttes volcanism corresponds with the age of widespread early Clear Lake volcanism, and Donnelly-Nolan and others (1993) speculated that the Sutter Buttes could be an extension of the Clear Lake volcanic field. They speculated further that intrusive bodies could exist in

the area between Wilbur Springs and Sutter Buttes, thus expanding possible sites of gold mineralization to the east. Lassen Peak, the southernmost active volcano of the Cascade Range may be visible on the far skyline along the northeast side of Sacramento Valley if the day is clear.

Retrace route back to highway 20.

- 2.05 44.55 Outcrop on west is small thrust in Great Valley sequence.
 - 2.35 46.9 Intersection with Highway 20, turn right.
 - 12.3 59.2 Proceed straight ahead at intersection with Highway 53.
 - 1.2 60.4 Basaltic cinder cone on left is South Cone and that on right is North Cone,, which is being mined for aggregate. South cone is the vent for the basaltic andesite flow that hosts mercury mineralization at Sulphur Bank.
 - 0.9 61.3 At intersection with Sulphur Bank Road, turn left at sign that says "Heritage Valley."
 - 1.4 62.7 Bear right onto middle gravel road.
 - 0.2 62.9 Park on left side of road opposite entrance into the Sulphur Bank mine. Proceed through gate down to gas vents on north side of Herman open pit. **STOP 6.**
-

STOP 6. SULPHUR BANK MINE.

The Sulphur Bank mercury deposit and Environmental Protection Agency (EPA) Superfund Site, is the fifth largest mercury deposit in the U.S. with a total production of 128,152 flasks of mercury, or about 4.0 per cent of total U.S. production. The deposit is still forming as evidenced by cinnabar+marcasite+sulphur+pyrite being deposited in vapor-dominated hot-spring vents on the margins of Herman lake (White, 1981). The deposit was discovered in 1856 and most of the production occurred in two periods, 1875 to 1895 and 1928 to 1942. Mining ceased in 1957. The mercury was deposited in an andesite flow of the Clear Lake Volcanics and in underlying rocks, including late Pleistocene sediments and the underlying Franciscan Complex. Shallow ore bodies were localized along faults that cut the andesite. Deposition was apparently controlled by the old ground-water table, below which the mercury was concentrated (White and Roberson, 1962; see also earlier studies by Anderson, 1936; Ross, 1940; Everhart, 1946; Becker, 1888; LeConte and Rising, 1882; and Whitney, 1865). Mineralization extends to a depth of about 100 m. Above the old ground-water table, native sulfur was abundant and two million tons of sulfur was mined before the pink "contamination" from cinnabar brought recognition of the mercury deposit. Most of the production from the mine took place before 1900. Early mining was done underground by Chinese miners on 20-minute shifts. Noxious fumes and temperatures up to about 175°F eventually led to open-pit mining.

The andesite of Sulphur Bank Mine overlies lacustrine and landslide deposits in which a carbonized log was found. Radiocarbon dating of the log gave an age of 44.5 ± 0.8 Ka (Sims and White, 1981), which is a maximum for the andesite and for the mercury deposition. No vent for the andesite has been found in the area of the mine, but the flow is traceable, in sporadic outcrops, for about half a mile to the northeast, to South Cone. It is one

of at least six mafic cinder cones that are aligned approximately north-south. Small areas of andesitic spatter within the andesite flow near the mine area occur where the flow crossed wet areas at the edge of Clear Lake.

The Franciscan Complex in the mine area is entirely metasediment of the Eastern belt. These rocks are part of the East Clear Lake terrane (McLaughlin and Ohlin, 1984) which, regionally, is probably correlative with the Yolla Bolly terrane of the Franciscan Eastern belt (Blake and others, 1988). The rocks of the East Clear Lake terrane, collectively, include alkaline basaltic volcanic flows, breccias, and aquagene tuffs tectonically interleaved with the metasediments; these metavolcanic rocks are in turn overlain by metamorphosed buff, red, or green tuffaceous ribbon chert, which exhibits up to three fold generations and is also complexly interleaved with the metavolcanic rocks and metasediments. Radiolarian assemblages from the chert indicate Late Jurassic (Tithonian?), and Early Cretaceous (Valanginian to Albian) ages. The metasediment, metachert, and metavolcanic rocks are texturally reconstituted, with a weak to moderately strong platy to crenulated foliation and with incipient metamorphic mineral assemblages that include lawsonite \pm sodic amphibole \pm minor jadeitic pyroxene.

Northwest-oriented strike-slip faults and northeast-oriented dip-slip faults of Quaternary age control the geomorphology and bound the east arms of Clear Lake as well as the structural basin of Borax Lake just over the ridge to the south. The Borax Lake basin is a classic fault-bounded pull-apart between two northwest-oriented faults with obvious dip-slip and probable dextral-slip components. The very youthful expression of this structural basin suggests it is bounded by active faults. In the vicinity of Sulphur Bank Mine, gas and fluid seeps and fumaroles vent along a prominent N. 20° to 40°E.-oriented normal fault zone aligned with the southeast shoreline of Clear Lake. Prominent hydrothermal alteration occurs along the trend of this fault. Beall (1985) delineated a prominent east-west zone of gas leakage in the mine area. Three sets of faults intersect in the mine, including northwest- and northeast-trending faults and the east-west gas leakage zone. According to Everhart (1946), mineralization was localized along a northeast-trending fault with high grade ore bodies forming where northwest-trending faults intersect the main structure.

The peak stage of mercury deposition likely occurred between 10.5 and 8.5 ka based on the highest content of mercury (up to 65 ppm) measured in cores of lake sediments in the Oaks arm of Clear Lake (Sims and White, 1981, Varekamp and Waibel, 1987). An estimated 2,400 metric tons of mercury have been naturally discharged into the sediments of Clear Lake from hot springs at Sulphur Bank (Varekamp and Waibel, 1987), equivalent to about half of the production from the deposit.

Cinnabar and metacinnabar are the main ore minerals and native mercury is present locally. In the andesite flow, alteration is fracture controlled and consists of an advanced argillic assemblage of kaolinite-alunite-opal-sulphur resulting from near surface oxidation of H_2S to form H_2SO_4 . Neutralization of the acid condensate fluid is exceptionally well displayed in these fractures. In the central part of the fracture, dissolution of all components except silica left a texture characterized by open vugs lined with opaline silica. Outward from the fracture-bounded core, alunite and kaolinite are present and the original rock texture is preserved. The outermost zone consists of propylitically altered andesite. Cinnabar typically is deposited in the central part of the fracture along with opaline silica. Wells and Ghiorso (1988) modeled the alteration as a coupled reaction-fluid transport system. Argillic-

carbonate alteration along with buddingtonite (ammonium feldspar) in the Franciscan rocks reflects the reducing to near- neutral pH conditions of the hydrothermal system below the paleo-ground-water table (White and Roberson, 1962). Transport and deposition of mercury has been ascribed to bisulfide complexes and subsequent destabilization of the complex by boiling and oxidation (Wells and Ghorso, 1988) and as dissolved elemental Hg at depth evolving to Hg vapor at the near surface (Varekamp and Buseck, 1984). Calculations by Reed and Spycher (1984) indicate that boiling probably caused cinnabar precipitation near 150°C and that the boiled fluids equilibrated with secondary minerals near 150°C even though temperatures up to 185°C have been measured at depth. That mercury vapor is presently being transported can be easily demonstrated by placing pH paper coated with lead acetate in the gas vents around Herman pit. It is quickly coated with native Hg and indicates that a substantial flux of mercury is being released into the atmosphere.

Four geothermal wells were drilled in the mine area, with the highest temperature (218°C) and largest fluid flow in the first of these, the Bradley Mining No. 1 well (drilled in 1964). The other three wells produced little or no fluid. Water as hot as 80°C emerged within the mine, but no thermal water can be sampled today because the springs vent into the bottom of the flooded Herman pit. Bubbles on the surface of the pond mark rising gases that consist dominantly of CO₂, which is also found in large quantities in the Audrey A-No. 1 geothermal well drilled about 0.5 mi southeast of Sulphur Bank Mine (Beall, 1985). Helium data indicate a magmatic contribution to the gases (Goff and Janik, this volume). Samples of geothermal well waters and of thermal springs that vented from the bottom of Herman pit before it was flooded are strongly enriched in B, NH₄, Cl, CH₄, and hydrocarbons and are isotopically heavy (White and Roberson, 1962). The highest boron value measured (880 ppm) exceeds that of chloride (830 ppm) (White and others, 1973). White and others (1973) interpreted the waters as metamorphic fluids, owing primarily to the high B and NH₄ of the waters and lower chloride than Wilbur Springs waters farther to the east. Peters (1993) and Goff and Janik (this volume) regarded the Sulphur Bank water as connate, derived from interstitial marine water of Mesozoic age. Donnelly-Nolan and others (1993) proposed that the waters are evolved meteoric waters resulting from closed- system boiling that shifted the isotopic signature of the original meteoric water and concentrated organic components derived from the Franciscan bedrock.

The EPA has developed a program to keep waters and sediment from the mine area out of Clear Lake. The dam which impounds water in Herman pit has been raised so that waters in the Herman Lake do not overtop the dam. Water in Herman pit has a pH of 3.0 and has high contents of B (270 ppm), NH₄ (180 ppm), and SO₄ (2,800) ppm. Tailings and waste dumps from the mine along Clear Lake have been stabilized to prevent erosion of this material into the lake.

-
- | | | |
|-----|------|---|
| 0.2 | 63.1 | Retrace route to paved road and turn right. |
| 1.5 | 64.6 | At ridge crest, Borax Lake is to the left and Clear Lake is to the right. |
| 1.7 | 66.3 | Borax Lake on left. |
| 1.6 | 67.9 | At multiple road junction at stop sign, proceed straight ahead. |

- 0.4 68.3 Turn right at stop sign.
- 0.1 68.4 Proceed straight ahead at stop sign.
- 2.2 70.6 At stop light proceed straight.
- 0.1 70.7 Turn right into El Grande parking lot.

REFERENCES

- Adam, D. P., 1988, Pollen zonation and proposed informal climatic units for Clear Lake, California, cores CL-73-4 and CL-73-7: Geological Society of America Special Paper 214, p. 63-80.
- Anderson, C.A., 1936, Volcanic history of the Clear Lake area, California: Geological Society of America Bulletin, v. 47, no. 3, p. 629-664.
- Atwater, Tanya, and Molnar, Peter, 1973, Relative motion of the Pacific and North American plates deduced from sea floor spreading in the Atlantic, Indian, and south Pacific Oceans, *in* Kovach, R. L., and Nur, Amos, eds., Proceedings of the conference on tectonic problems of the San Andreas fault system: Stanford University., Publications in the Geological Sciences, v. 13, p. 136-148.
- Barnes, Ivan, O'Neil, J. R., Rapp, J. B., and White, D. E., 1973, Silica-carbonate alteration of serpentine: Wall rock alteration in mercury deposits of the California Coast Ranges: Econ. Geol., v. 68, p. 388-398.
- Beall, J. J., 1985, Exploration of a high temperature, fault localized, non meteoric geothermal system at the Sulphur Bank mine, California: Geothermal Resources Council Trans., v. 9, p. 395-401.
- Becker, G. F., 1888, Geology of the quicksilver deposits of the Pacific slope: U.S. Geological Survey Monograph 13, 486 p.
- Benz, H. M., Zandt, G., and Oppenheimer, D. H., 1992, Lithospheric structure of northern California from teleseismic images of the upper mantle: Journal of Geophysical Research, v. 97, p. 4791-4807.
- Berry, F. A. F., 1973, High fluid potentials in the California Coast Ranges and their tectonic significance: American Association of Petroleum Geologists Bulletin, v. 57, p. 1219-1249.
- Blake, M. C., Jr., Jayko, A. S., McLaughlin, R. J., and Underwood, M. B., 1988, Metamorphic and tectonic evolution of the Franciscan Complex, northern California: *in* Ernst, W. G., ed., Metamorphism and Crustal Evolution of the Western United States, Ruby Vol., v. 11, Prentice-Hall, Englewood Cliffs, New Jersey, p. 1035-1060.
- Bowman, H. R., Asaro, Frank, and Perlman, I., 1973, On the uniformity of composition in obsidians and evidence for magmatic mixing: Journal of Geology, v. 81, no. 3, p. 312-327.
- Bradley, W. W., 1916, The counties of Colusa, Glenn, Lake, Marin, Napa, Solano, Sonoma, Yolo: California Mining Bureau Fourteenth Report State Mineralogist, p. 173-370.
- Carlson, Christine, 1981, Sedimentary serpentinites of the Wilbur Springs Area—A possible early Cretaceous structural and stratigraphic link between the Franciscan Complex and the Great Valley sequence: unpub. M.S. thesis, Stanford University, 105 p.
- Crowell, J. C., 1974, Origin of late Cenozoic basins in southern California, *in* W. R. Dickinson, ed., Tectonics and sedimentation: Society of Economic Paleontologists and Mineralogists Special Publication 22, p. 190-204.
- Dickinson, W. R., and Snyder, W. S., 1979, Geometry of subducted slabs related to San Andreas transform: Journal of Geology, v. 87, p. 609-627.
- Donnelly-Nolan, J. M., Burns, M. G., Goff, F. E., Peters, E. K., and Thompson, J. M., 1993, The Geysers-Clear Lake area, CA: thermal waters, mineralization, volcanism, and geothermal potential: Economic Geology, v. 88, pp. 301-316.
- Everhart, D. L., 1946, Quicksilver deposits at the Sulphur Bank mine, Lake County, California: California Journal of Mines and Geology, v.42, p. 125-153.
- Goff, F. E., and Janik, C. J., 1993, Gas geochemistry and guide for geothermal features in the Clear Lake region, California, *in* J. J. Rytuba ed., Active geothermal systems and gold-mercury deposits in the Sonoma-Clear Lake volcanic fields: California, Soc. Econ. Geol. Guidebook Series, (this volume)
- Hausback, B. P., 1991, Eruptive history of the Sutter Buttes volcano - review, update, and tectonic considerations: Geol. Soc. Am. Abs. with Prog., v. 23, no. 2, p. 34.
- Hearn, B. C., Jr., Donnelly-Nolan, J. M., and Goff, F. E., 1981, The Clear Lake Volcanics: Tectonic setting and magma sources: U.S. Geological Survey Professional Paper 1141, p. 25-45.
- Hearn, B. C., Jr., McLaughlin, R. J., and Donnelly-Nolan, J. M., 1988, Tectonic framework of the Clear Lake basin, California: Geol. Soc. America, Special Paper 214, p. 9-20.
- Johnson, C. M., and O'Neil, J. R., 1984, Triple junction magmatism: A geochemical study of Neogene volcanic rocks in western California: Earth and Planetary Science Letters, v. 71, p. 241-262.

- LeConte, Joseph, and Rising, W. B., 1882, The phenomena of metalliferous vein formation now in progress at Sulphur Bank, California: *American Journal of Science*, 3rd series, v. 24, p. 23-33.
- Liu, M., and Furlong, K. P., 1992, Cenozoic Volcanism in the California Coast Ranges: Numerical Solutions: *J. Geophys. Res.*, v. 97, p. 4941-4951.
- McLaughlin, R. J., 1981, Tectonic setting of pre-Tertiary rocks and its relation to geothermal resources in the Geysers-Clear Lake area: U. S. Geological Survey Prof. Paper 1141, p. 3-23.
- McLaughlin, R. J., and Ohlin, H. N., 1984, Tectonostratigraphic framework of the Geysers-Clear Lake region, California: *Pacific Sec. Soc. Econ. Paleontologists Mineralogists*, v. 43, p. 221-254.
- McLaughlin, R. J., Ohlin, H. N., Thormahlen, D. J., Jones, D. L., Miller, J. W., and Blome, C.D., 1989, Geologic map and structure sections of the Little Indian Valley-Wilbur Springs geothermal area, northern Coast Ranges, California: U.S. Geol. Survey Map I-1706, scale 1:24,000.
- Pearcy, E. C., and Petersen, Ulrich, 1990, Mineralogy, geochemistry and alteration of the Cherry Hill, California hot-spring gold deposit: *Journal of Geochemical Exploration*, v. 36, pp. 143-169.
- Peters, E. K., 1991, Gold bearing hot spring systems of the northern Coast Ranges, California: *Econ. Geol.*, v. 86, p. 1519-1528.
- Peters, E. K., 1993, $d^{18}O$ enriched waters of the Coast Range Mountains, northern California: Connate and ore-forming fluids: *Geochimica et Cosmochimica Acta*, v. 57, p. 1093-1104.
- Phipps, S. P., and Unruh, J. R., 1992, Crustal-scale wedging beneath an imbricate roof-thrust system: Geology of a transect across the western Sacramento Valley and northern Coast Ranges, California, *in* M. C. Erskine, J. Unruh, W. R. Lettis and J. A. Bartow, eds., *Field Guide to the tectonics of the boundary between the California Coast Ranges and the Great Valley of California: Pacific Section American Association of Petroleum Geologists GB-70*, pp. 117-140.
- Ramirez, V. R., 1993, Evolution of the Coast Range thrust as interpreted from seismic reflection data [abs.]: *Abstracts with Programs, Geol. Soc. America*, v. 25, p. 136.
- Reed, Mark, and Spycher, Nicolas, 1984, Calculation of pH and mineral equilibria in hydrothermal waters with application geothermometry and studies of boiling and dilution: *Geochimica et Cosmochimica Acta*, v. 48, p. 1479-1492.
- Ross, C. P., 1940, Quicksilver deposits of the Mayacmas and Sulphur Bank districts, California: U.S. Geological Survey Bulletin 922-L, p. 327-353.
- Rymer, M. J., 1981, Stratigraphic revision of the Cache Formation (Pliocene and Pleistocene) in Clear Lake basin, Lake County, California: U.S. Geological Survey Open-File Report 78-924, 102 p.
- Rymer, M. J., Roth, Barry, Bradbury, J. P., and Forester, R. M., 1988, Depositional environments of the Cache, Lower Lake, and Kelseyville Formations, Lake County, California: *Geological Society of America Special Paper 214*, p. 45-57.
- Sims, J. D., 1988, Late Quaternary climate, tectonism, and sedimentation in Clear Lake, northern California Coast Ranges: *Geological Society of America Special Paper 214*, p. 1-8.
- Sims, J. D., Rymer, M. J., and Perkins, J. A., 1988, Late Quaternary deposits beneath Clear Lake, California; physical stratigraphy, age, and paleogeographic implications: *Geological Society of America Special Paper 214*, p. 21-44.
- Sims, J. D., and White, D. E., 1981, Mercury in the sediments of Clear Lake: U.S. Geological Survey Professional Paper 1141, p. 237-241.
- Stimac, J. A., 1991, Evolution of the silicic magmatic system at Clear Lake, California from 0.6 to 0.3 Ma: Queen's University Ph. D. thesis, 399 p.
- Stimac, J. A., and Goff, F., and Hearn, B. C., Jr., 1992, Petrologic considerations for hot dry rock geothermal site selection in the Clear Lake region, California: *Geothermal Resource Council Trans.*, v. 16, p. 191-198.
- Stimac, J. A., and Pearce, T. H., 1992, Textural evidence of mafic-felsic magma interaction in dacitic lavas, Clear Lake, California: *Am. Mineral.*, v. 77, p. 795-809.
- Unruh, J. R., and Moores, E. M., 1992, Quaternary blind thrusting in the southwestern Sacramento Valley, California: *Tectonics*, v. 12, pp
- Unruh, J. R., Davisson, M. L., Criss, R. E., and Moores, E. M., 1992, Implications of perennial saline springs for abnormally high fluid pressures and active thrusting in western California: *Geology*, v. 20, p. 431-434.
- Varekamp, J. C., and Buseck, P. R., 1984, The speciation of Hg in hydrothermal systems, with applications for ore deposits: *Geochimica et Cosmochimica Acta*, v. 48, 177-185.
- Varekamp, J. C., and Waibel, A. F., 1987, Natural cause for mercury pollution at Clear Lake, California, and paleotectonic inferences: *Geology*, v. 15, p. 1018-1021.
- Waring, G. A., 1915, Springs of California: U. S. Geol. Survey, Water Supply Paper 338, 410 p.
- Wells, J. T., and Ghiorso, M. S., 1988, Rock alteration, mercury transport, and metal deposition at Sulphur Bank, California: *Econ. Geol.*, v. 83, p.606-618.

- Wentworth, C. M., Blake, M. C. Jr., Jones, D. L., Walter, A. W., and Zoback, M. D., 1984, Tectonic wedging associated with emplacement of the Franciscan assemblage, California Coast Ranges: *in* M. C. Blake Jr., ed., *Franciscan Geology of Northern California: Pacific Section SEPM Book 43*, p. 163-173.
- White, D. E., 1957, Magmatic, connate, and metamorphic waters: *Geol. Soc. America Bull.* v. 68, p. 1659-1682.
- White, D. E., 1981, Active geothermal systems and hydrothermal ore deposits: *Economic Geology*, 75th Anniversary Volume, p. 392-423.
- White, D. E., Barnes, Ivan, and O'Neil, J. R., 1973, Thermal and mineral waters of nonmeteoric origin, California Coast Ranges: *Geol. Soc. of America Bull.*, v. 84, p. 547-560.
- White, D. E., Muffler, L. J. P., and Truesdell, A. H., 1971, Vapor-dominated hydrothermal systems compared with hot-water systems: *Econ. Geol.*, v. 66, p. 75-97.
- White, D. E., and Roberson, C. E., 1962, Sulphur Bank, California, a major hot-spring quicksilver deposit: *Geol. Soc. America, Buddington Volume*, p. 397-428.
- Whitney, J. D., 1865, *Geological Survey of California: Geology*, v. I, Report of progress and synopsis of the field work from 1860 to 1864, 498 p.
- Williams, Howel, and Curtis, G. H., 1977, *The Sutter Buttes of California: University of California Publications in Geological Sciences*, v. 116, 56 p.

REGIONAL GEOPHYSICAL SETTING OF GOLD DEPOSITS IN THE CLEAR LAKE REGION, CALIFORNIA

Andrew Griscom, Robert C. Jachens, Phyllis F. Halvorson, and Richard J. Blakely

U.S. Geological Survey, Menlo Park, CA 94025

INTRODUCTION

The Geysers geothermal area and associated Clear Lake Volcanics have aroused much scientific interest and have been subjected to many sorts of geophysical investigations. Summaries of these studies have been published by Isherwood (1981) and Majer and others (1992). In this paper we provide a broad tectonic interpretation of the Clear Lake region and the relationship to the local gold mineralization, by interpreting magnetic and gravity data together with other available geologic and geophysical information. These results stem from work in progress and should be considered preliminary.

GEOLOGIC MAP

The simplified geologic map (Fig. 1) is taken from the digital map of Donnelly-Nolan and others (1993) plus additions from Jennings and Strand (1960), Wagner and Bortugno (1982), and McLaughlin and others (1989). The pre-Tertiary rocks of the Clear Lake area (Fig. 1) are described by McLaughlin (1981) and include: (1) the Upper Jurassic and Cretaceous sedimentary rocks of the Great Valley sequence and its basal oceanic crust, the Coast Range ophiolite, and (2) the essentially coeval Franciscan Complex, a Late Jurassic and Early Cretaceous subduction complex consisting predominantly of turbiditic graywacke, siltstone, shale, chert, and mafic igneous rocks. Additional rocks characteristically found in melange of the complex are serpentinite, limestone, amphibolite, and blocks of high pressure metamorphic rocks. The Franciscan Complex has been subdivided into several structural belts, or tectonostratigraphic terranes, that are metamorphosed to varying degrees, and at least seven such terranes are complexly faulted together in the Clear Lake area (McLaughlin and Ohlin, 1984).

The Great Valley sequence consists predominantly of mudstones and sandstones, forearc basin deposits that, near their base at Wilbur Springs, contain abundant serpentinite detritus and breccias (Carlson, 1981) extending in an irregular belt (based upon the magnetic map) at least as far south as the McLaughlin Mine (Fig. 1). This serpentinite may have been extruded on the sea floor from diapirs originating in the lower crust (Carlson, 1981; McLaughlin and Ohlin, 1984), though it is not clear how the serpentinite sands became entrained within the turbidites.

The Great Valley sequence, together with the Coast Range ophiolite, are thrust relatively westward over the Franciscan Complex and the ophiolite is attenuated by low-angle extensional faults (Jayko et al., 1982). In addition, some of the westernmost rocks of the Great Valley sequence and Coast Range ophiolite are penetratively sheared and deformed into a melange unit (McLaughlin and Ohlin, 1984; McLaughlin and others, 1989), possibly due to

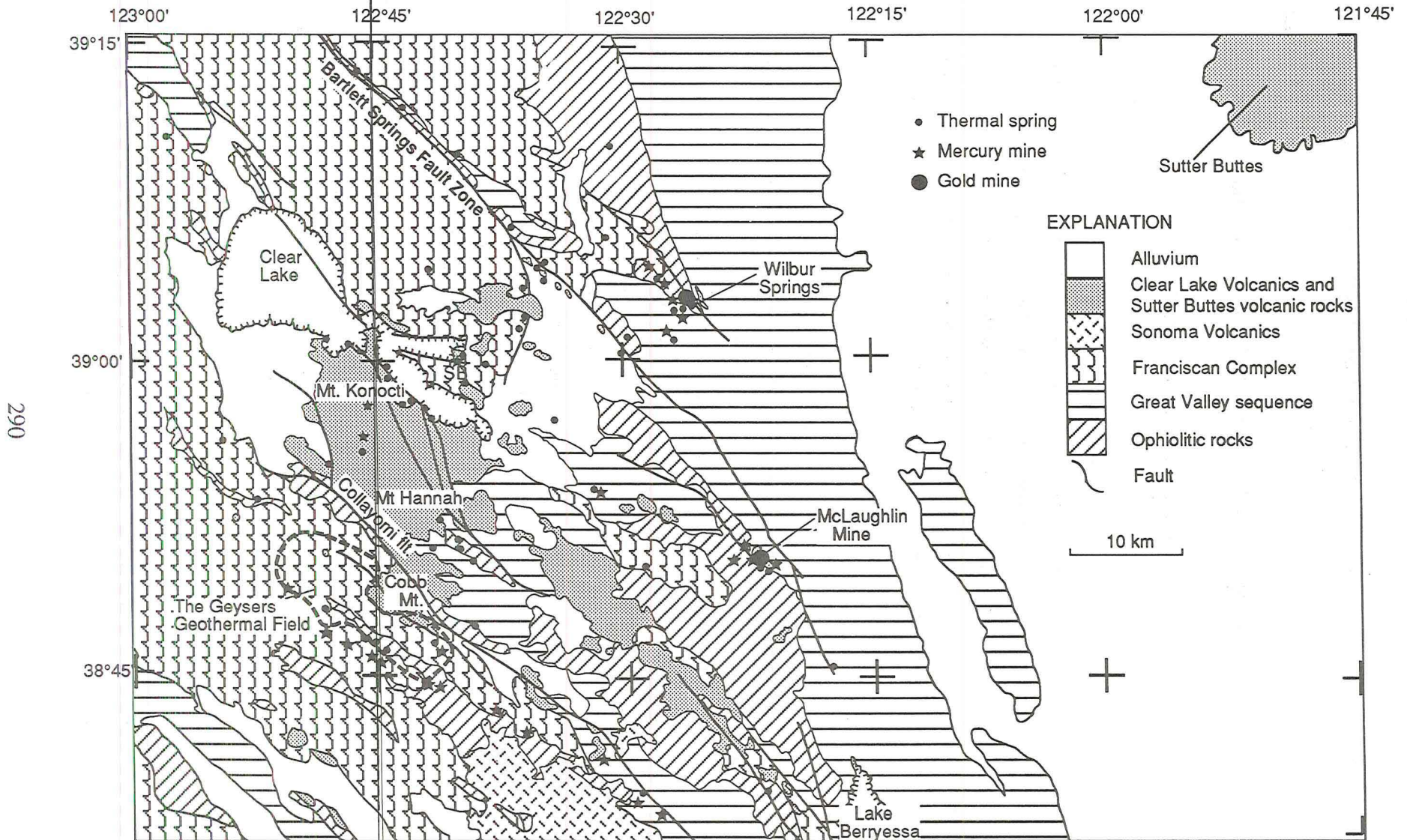


Figure 1. Geologic map of the Clear Lake-McLaughlin Mine area. Sources described in text.

tectonic wedging (described below). The geologic history of the contact between the coeval Franciscan Complex and Great Valley sequence is complex, but we emphasize here the process of tectonic wedging, which probably began in the Late Cretaceous, continued during the early Tertiary and Pleistocene (Unruh and others, 1991), and may still be going on today (Ramirez, 1993). This process is the development of major intrusive tectonic wedges (Wentworth and others, 1984) of the Franciscan Complex that have successively intruded eastward into the Great Valley sequence along or within its basement of the Coast Range ophiolite, resulting in uplift and eastward tilting of the basal rocks of the Great Valley sequence. The upper contact of a typical wedge displays the Franciscan Complex in thrust contact with the overlying Coast Range ophiolite that is in turn either in fault contact with or stratigraphically overlain by the Great Valley sequence. The key features distinguishing such wedges from other types of thrust faults are usually located in the subsurface and revealed only by seismic reflection or other geophysical techniques. These features include (1) an eastern tip to the wedge, beyond which no discontinuity is found, and (2) flat-lying Great Valley basement rocks (ophiolite) dipping gently to the west beneath the Franciscan Complex. Seismic reflection data also show that some internal wedging exists within the Great Valley sequence as well (Wentworth and others, 1984).

In Figure 2 we show a schematic cross-section across the Franciscan-Great Valley contact. A characteristic feature of this and other cross-sections is the chevron-shaped mass of the Coast Range ophiolite located at the Franciscan-Great Valley contact about 4 km below the surface. Tectonic wedges of the Franciscan Complex lie both above and below this feature, which we have termed the airfoil (Fig. 2) because of its generally curved or arched upper contact. The ophiolite airfoil is a tectonic feature of major regional importance, extending nearly continuously for 600 km along strike at the Great Valley-Franciscan contact (Griscom and Jachens, 1990). It may have been chiseled off the basement of the Great Valley by advancing lower wedges. Multiple wedging thus implies the possibility of multiple ophiolite airfoils stacked above each other, as shown in Figure 2. We discuss this feature more fully in the section on magnetic interpretation of the Great Valley magnetic anomaly.

Overlying the Mesozoic rocks west of the Great Valley are Pliocene and Quaternary alluvial and lacustrine deposits together with the coeval Clear Lake Volcanics. The volcanic rocks range in age from 2.1 to 0.01 Ma, but the more siliceous materials that dominate the volcanic section mostly range in age from 1.2-0.3 Ma (Hearn and others, 1981; Donnelly-Nolan and others, 1981, 1993). The associated silicic pluton (termed informally the "felsite") is observed only in drill holes in The Geysers geothermal area (Fig. 6) and has a possible age range of 0.9 Ma to 2.4 Ma (Thompson, 1992). More recent work indicates a minimum age of 1.3 to 1.4 Ma (Dalrymple, 1992) for the felsite. Deep wells in the Mt. Hannah area (Fig. 6) have not, to the writers' knowledge, penetrated any plutons but the Neasham well penetrated tourmalinized contact-metamorphic rocks at a depth of about 1.5 km below sea level (oral communication, J.M. Donnelly-Nolan, 1993). In addition, the Wilson No. 1 well penetrated rocks of epidote-actinolite metamorphic facies below 3.3 km (R.J. McLaughlin, oral communication, 1993) and, at the bottom (3.7 km), rocks with fluid inclusion temperatures of 370-395°C with no lower values found (written communication, R.O. Fournier, 1993). These data lead us to infer that a pluton is located less than 1 km below the bottoms of the two drill holes.

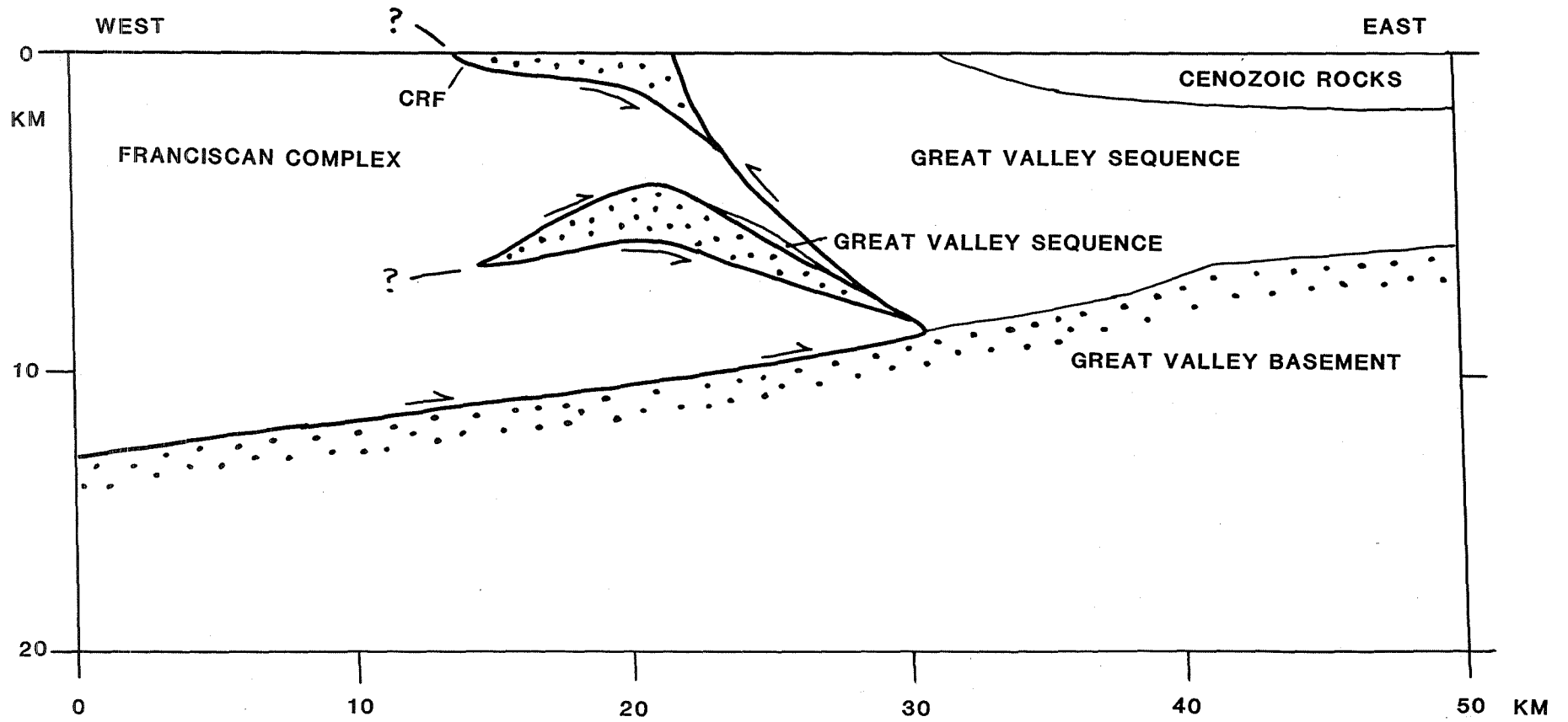


Figure 2. Generalized cross-section across the Franciscan-Great Valley contact as interpreted from geophysical data. Note two east-directed wedges of the Franciscan Complex between the ophiolite slices. Note also the Great Valley basement dipping west beneath the Franciscan Complex. All ophiolite elements are not necessarily present in all cross-sections of this contact. Stippled pattern is the Coast Range ophiolite. Heavy lines are wedge faults. CRF is Coast Range Fault.

Sutter Buttes (Fig. 1) are the remains of an eroded volcano in the center of the Great Valley. The volcanism began at approximately 1.56 Ma and continued at least until 0.9 Ma (Hausback, 1991), an age range similar to that of the older rocks of the Clear Lake Volcanics.

MAGNETIC MAP

The data for the magnetic map of the Clear Lake and McLaughlin Mine area (Fig. 3) are taken from the new aeromagnetic map of California compiled by Roberts and Jachens (1993). The data are derived from various surveys that were analytically continued to a common surface 300 m above mean terrain, adjusted to a common datum level, and merged to produce the final 1-km grid. The original aeromagnetic survey for the area west of long. 122°30'W. (U.S. Geological Survey, 1973) was flown at a constant barometric elevation of 1,370 m (4,500 ft) with east-west flight lines spaced about 1.6 km apart, and surveys east of long. 122°30' W. have the same or better specifications. These specifications indicate that the map of Figure 3 is a reasonable representation of the magnetic field of the study area.

The magnetic map has been converted to the pole, i.e. recalculated such that it depicts a magnetic map with the main magnetic field directed vertically downward. This procedure eliminates the paired, asymmetric magnetic highs and lows that are customarily observed over magnetic masses at these latitudes.

Magnetic susceptibilities of rocks in this area have been reported by Chapman (1975) and Isherwood (1975). Their results indicate that the only rocks with significant magnetizations are the Mesozoic serpentinite (ophiolite) and the Clear Lake Volcanics; serpentinites have average susceptibility values of $2-4 \times 10^{-3}$ (emu) and the volcanic rocks have average values of $1.5-3.2 \times 10^{-4}$ (emu). Mankinen and others (1981) reported results on 228 samples of the Clear Lake Volcanics; mean remanent magnetizations range from $2.79-13.2 \times 10^{-4}$ emu/cm³ (in some cases the directions of remanent magnetizations are opposite to the direction of magnetization induced by the earth's present field), while mean magnetic susceptibilities range from $1.0-2.3 \times 10^{-4}$ (emu), rather similar to those mentioned above. As is usual for young volcanic rocks, the remanent magnetization is significantly stronger than the induced magnetization (the magnitude of the magnetization induced in a rock by the earth's main field is roughly one-half the magnitude of the magnetic susceptibility). Magnetic anomalies produced by the Clear Lake Volcanics are in general subcircular high or lows, depending upon the direction of remanent magnetization, and tend to correlate with local volcanic edifices. There is no evident magnetic expression of any intrusions associated with the volcanic deposits, either because such rocks are only weakly magnetic or because they presently are heated (Chapman, 1975) above the Curie point of magnetite (580°C).

The Coast Range ophiolite and its associated serpentinite masses cause nearly all the major magnetic features located west of the Great Valley (west of long. 122°20'W.) on Figure 3. These anomalies form two general belts on Figures 3 and 6: (1) a western belt that trends northwest and extends along the southwest side of Clear Lake, and (2) a central belt trending more northerly along the major exposures of the Coast Range ophiolite.

As pointed out by Chapman (1975), the western anomaly belt extends without interruption along the northeast side of The Geysers geothermal area and across the associated gravity low and is generally associated with

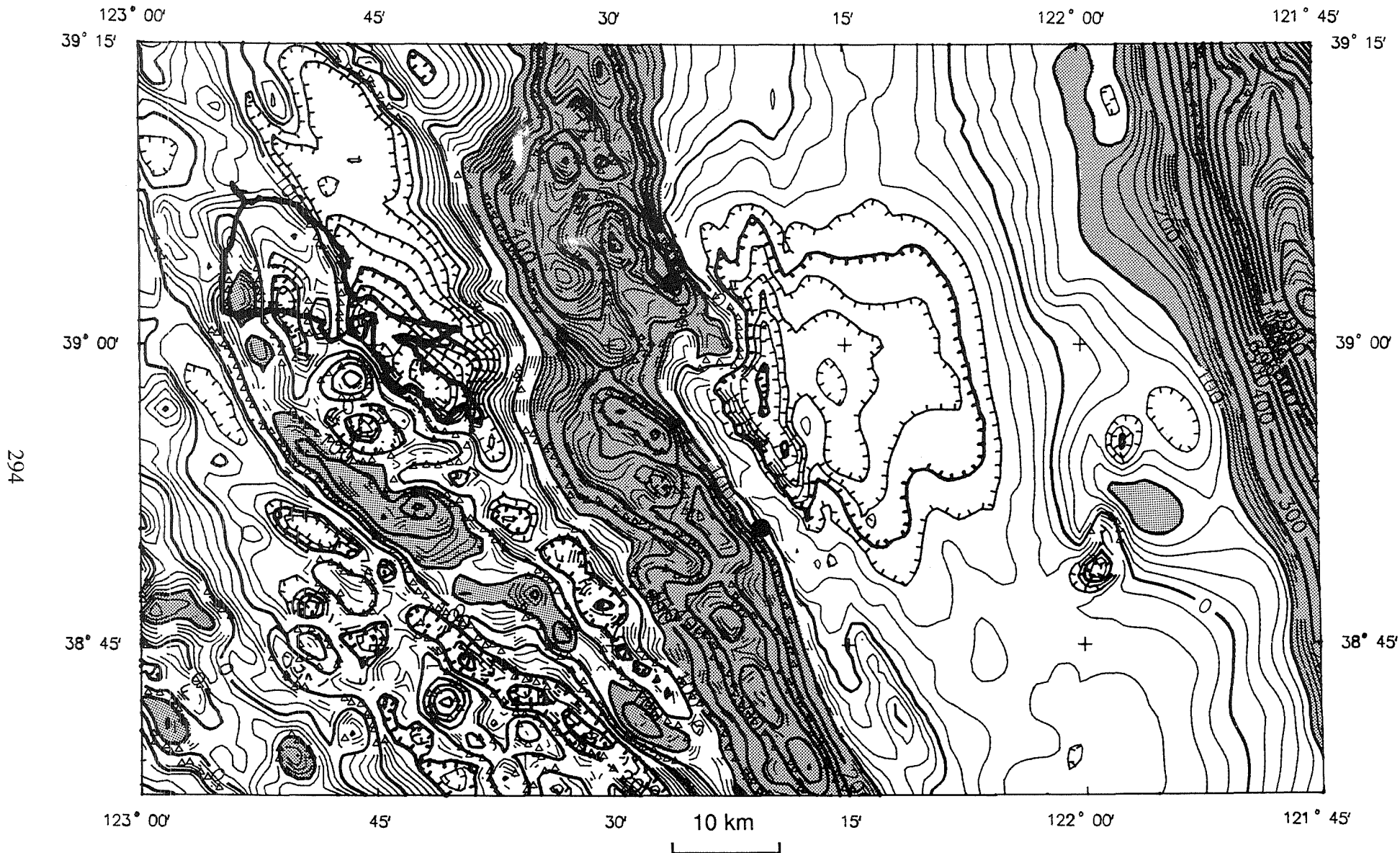


Figure 3. Magnetic map, converted to the pole, of the Clear Lake-McLaughlin Mine area. Gold deposits (dots) located as in Figure 1. Contour intervals 20 and 100 nT. Areas with magnetic values greater than 100 nT are shaded. Triangles indicate the calculated location of magnetic boundaries (at the steepest gradients).

a belt of rocks of the Great Valley sequence. Chapman (1975) interpreted the serpentinite to have the general form of a continuous flat slab underlying the rocks of the Great Valley sequence at relatively shallow depths. A similar slab configuration is modeled by Blakely and Stanley (in press), who also show that the main magnetic high in this belt is caused by the upturned southwest edge of the serpentinite slab. Calculations by Isherwood (1975) indicated maximum magnetic source depths of about 7.5 km for this area and he proposed this shallow result may be caused by a rise in the Curie isotherm.

We interpret the central belt magnetic anomalies to reflect an ophiolitic mass with the overall form of a relatively flat, antiformally folded slab with its east part dipping east and forming the base of the Great Valley sequence, and its west part dipping west within the Franciscan Complex. This feature is the airfoil described previously in the geologic section and its unusual structural relationships are considered to be the result of eastward-directed tectonic wedges of the Franciscan Complex (Griscom and Jachens, 1990). The airfoil here is evidently modified by northwest-trending faults and, perhaps, tight folds that have imbricated the slab somewhat to cause a series of right-lateral en echelon anomaly segments (Fig. 6).

The airfoil, at least along part of its length, consists of stacked fault slices of ophiolite. An example of such stacking can be seen near the north border of the study area (Figs. 1, 3, and 6) where the crest of the main ophiolite mass that comprises the central belt (delineated on Figure 6 by the magnetic anomaly axis symbol of feature 1) plunges north beneath the Franciscan Complex at about lat. 39°03'N. (the eastward protrusion of the Franciscan Complex that points toward Wilbur Springs on Figure 1), and then continues north beneath the exposed upper-level ophiolite sheet at lat. 39°08'N. Magnetic data show that this stacked pair of thrust slices extends to the north end of the Great Valley (Griscom, 1983), and our schematic cross-section (Fig. 2) shows the crest of the main ophiolite mass at a depth of about 4 km, separated from the ophiolite at the surface by a wedge of Franciscan rocks.

GRAVITY MAP

The data for the gravity map of the Clear Lake and McLaughlin Mine area (Fig. 4) are taken from the map of Roberts and others (1990). The data are presented as isostatic residual gravity values to emphasize those anomalies caused by density distributions in the middle and upper crust. Anomalies from deeper density distributions that buoyantly support the topography in a manner consistent with the concept of isostasy are suppressed by the process of calculating isostatic residual gravity values (Jachens and Griscom, 1985). Gravity stations are relatively sparse in the east half of Figure 4 where a few data gaps up to 10 km across exist. Station coverage is excellent in the southwest quadrant of the map.

Densities for rocks in this area are summarized by Blakely and Stanley (in press). We show here selected values from their Table 1.

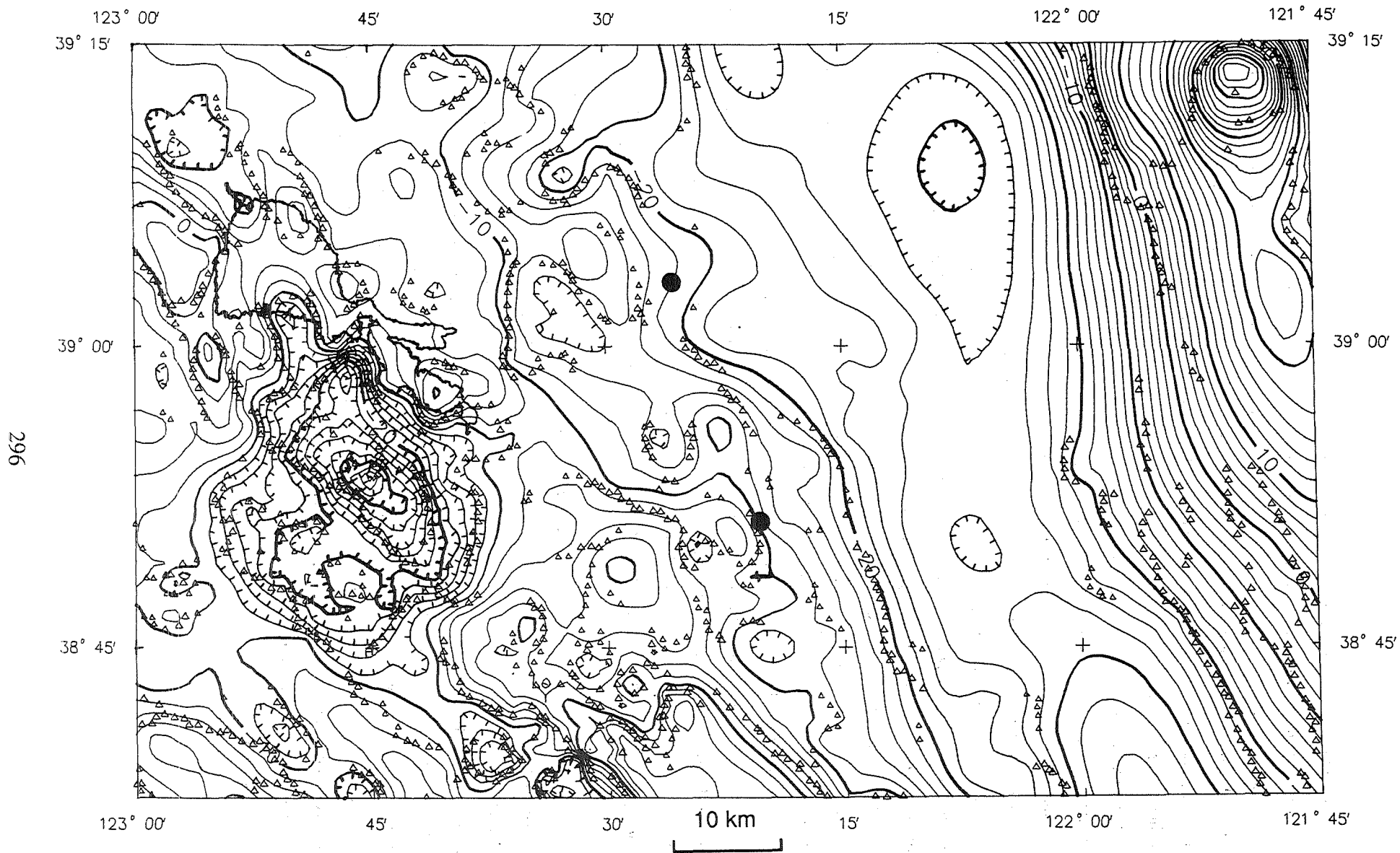


Figure 4. Isostatic residual gravity map of the Clear Lake-McLaughlin Mine area. Gold deposits (dots) located as in Figure 1. Contour intervals 2 and 10 mGal. Triangles indicate the calculated location of density boundaries (at the steepest gradients).

Table 1. Mean densities of rocks of the northern California Coast Ranges

Unit	Mean (g/cm ³)	No. of Samples
Clear Lake Volcanics	2.48	22
Felsite (batholith)	2.58	18
Great Valley sequence		
Upper Cretaceous	2.55	78
Lower Cretaceous	2.57	71
Upper Jurassic	2.59	40
Franciscan Complex		
sandstone	2.65	857
greenstone	2.88	29
Coast Range ophiolite		
serpentinite	2.42	56
mafic rocks	2.86	8

Within the Clear Lake volcanic field and associated gravity low the density of any Great Valley sequence rocks doubtless increases at depths below about 3 km because of high chlorite zone and epidote-actinolite zone metamorphism, as was sampled by the two deep wells (Fig. 6). We anticipate densities of about 2.65 g/cm³ in the metamorphic zones.

The features on the gravity map reflect lateral density variations associated with rocks beneath the surface (compare with Figure 1). Franciscan rocks lie generally west of the -10 mGal contour that crosses the center of the map whereas the somewhat lower density Great Valley sequence and ophiolite (serpentinite) are associated with lower gravity values to the east. Higher gravity values (above -4 mGal) at the south border of the map are probably caused by the more mafic parts of the ophiolite, whereas high values elsewhere over the Franciscan Complex are likely caused by Franciscan greenstone. The high gravity ridge at the east border of the map is caused by high density mafic basement rocks beneath the sedimentary rocks of the Great Valley and is discussed in a separate section.

Intrusive activity associated with Sutter Buttes volcano has locally elevated to the surface older, higher-density sedimentary rocks of the Great Valley, thus causing a circular gravity high (Fig. 6) with a local relief of about 20 mGal that is superimposed on the linear Great Valley gravity high. This local gravity high may also be caused in part by a near-surface pluton intruding the sedimentary rocks below the volcano. The pronounced gravity low in the southwest quadrant of the map is associated with The Geysers geothermal field and the Clear Lake Volcanics and is discussed in a subsequent section; it is predominantly caused by silicic intrusions.

THE GREAT VALLEY MAGNETIC AND GRAVITY ANOMALY

The Great Valley magnetic and gravity anomaly is the high-amplitude linear anomaly located at the east margins of Figures 3 and 4, respectively. This anomaly extends for over 600 km along the Great Valley and the source is interpreted to be a slab of Late Jurassic oceanic crust (Cady, 1975; Griscom and Jachens, 1990) now sutured to the rocks of the Sierra Nevada foothills beneath the central part of the Great Valley. Deep drill holes at Sutter Buttes have recovered basement samples of norite and quartz-hornblende diorite (Williams and Curtis, 1977) as well as cumulate gabbro (Harwood and Helley, 1987) below a Cretaceous unconformity. Using well data and seismic reflection data, our calculated magnetic and gravity models (Griscom and Jachens, 1990) show that the geophysical anomalies are caused by a slab of rock with the upper surface at the top of the Great Valley crystalline basement, or in other words, is probably the Coast Range ophiolite. We assume that the ophiolite at the longitude of Sutter Buttes was exposed to erosion during the Late Jurassic or Early Cretaceous, even though deposition was occurring farther to the west at the longitude of the exposed Coast Range ophiolite. Thus we can use the magnetic data to calculate the configuration of the Great Valley basement at the Franciscan-Great Valley contact. Seismic reflection data (Ramirez, 1993) show a smooth west-dipping interface at the basement surface that reaches maximum two-way travel times (depths) in excess of 5.5 seconds (roughly equivalent to 10 km depth) at the west end of a seismic line located about 10 km east of Wilbur Springs.

In order to calculate more accurately the shape of the basement surface from the magnetic map, we have calculated a pseudogravity or magnetic potential map (Fig. 5) from the magnetic map (Fig. 3) following Baranov (1957), with the result that the magnetic properties behave mathematically similar to rock densities. Our original magnetic data set actually extends over 2,000 km radially from Figure 5 in order to minimize the influence of possible problems associated with the edges of the data set. The magnetic potential emphasizes the magnetic effects of thick, wide bodies as compared with thin, narrow bodies. Examination of Figure 5 indicates only a few major magnetic (pseudogravity) features: the Great Valley magnetic anomaly at the east border, the anomaly produced by the mass of the Coast Range ophiolite trending NNW across the central part of the map, and, most importantly, a west-sloping gradient in the western third of the map. Our calculations indicate that this west-sloping pseudogravity gradient is probably caused by the west-sloping surface of the Great Valley magnetic basement which dips westward at low angles beneath the Franciscan Complex and The Geysers, extends westward for a distance of at least 20 km beyond Clear Lake, and lies at depths of about 15 km below sea level at Clear Lake. This approximate depth is confirmed independently by the seismic refraction data of Warren (1981) which located the top of a higher velocity

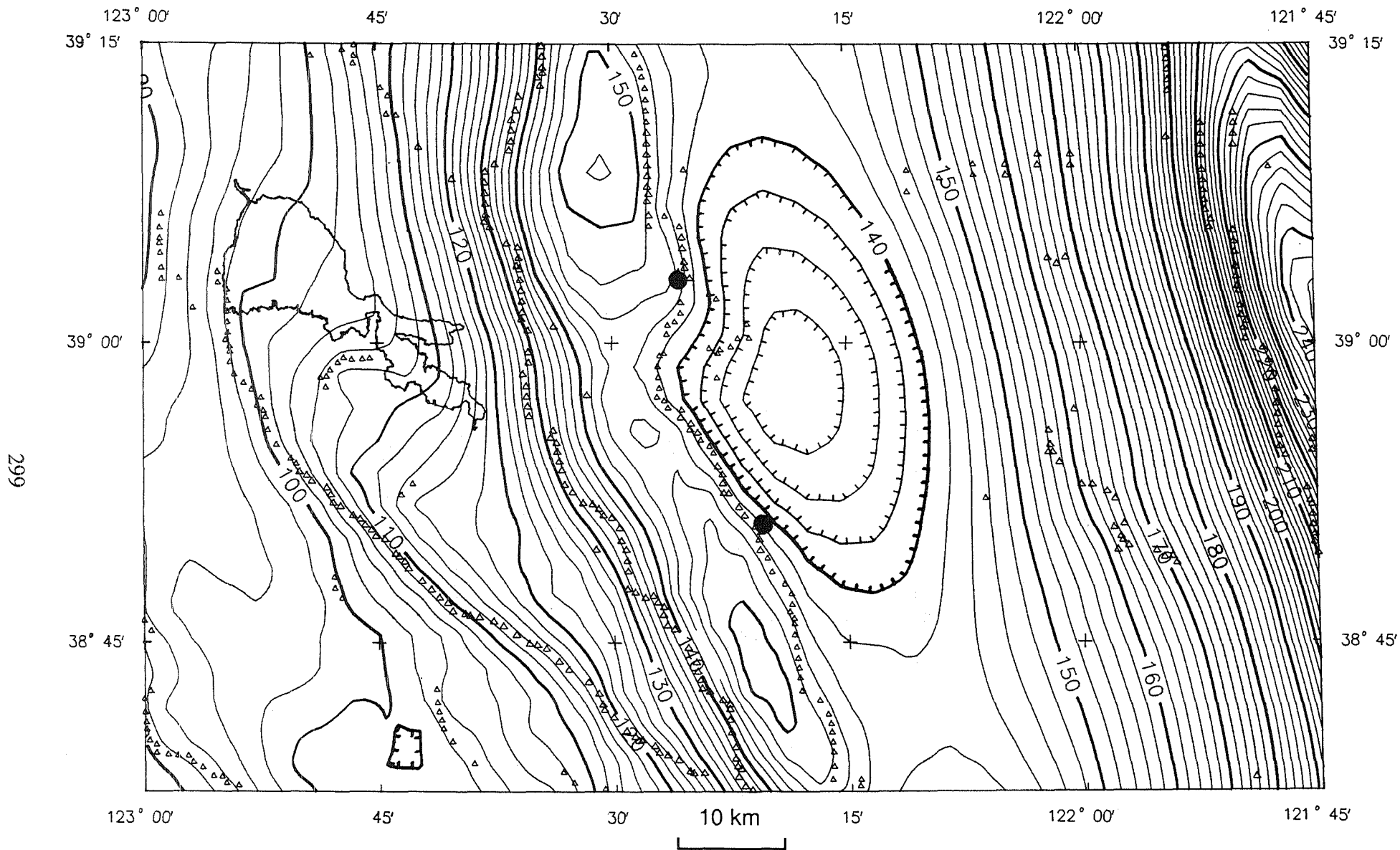


Figure 5. Pseudogravity (magnetic potential) map of the Clear Lake-McLaughlin Mine area. Gold deposits (dots) located as in Figure 1. Contour intervals 2 and 10 psmGals. Triangles indicate the calculated location of pseudodensity (magnetic) boundaries (at the steepest gradients). Magnetization of 1×10^{-3} emu/cm³ equals a pseudodensity of 0.1 g/cm³.

Explanation




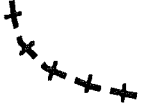
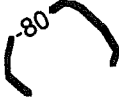

-  Boundary of aeromagnetic anomaly; teeth toward lower magnetization materials; R - reversely magnetized; N - normal magnetization.
-  Boundary of gravity anomaly; teeth toward lower density material.
-  Axis of linear magnetic high
-  Axis of linear gravity high
-  Contour from aeromagnetic map (-80 nT); encloses broad magnetic low
- 2 Numbers indicate magnetic features discussed in text
- K▲ Volcanoes; H - Mount Hannah, K- Mount Konocti
-  Contours on top of the felsite batholith; values in thousands of feet below sea level (from Thompson, 1992)
- M Gold deposit; M - McLaughlin Mine, W - Wilbur Springs
- ◆ Well; N - Neasham, W - Wilson No. 1

FIGURE 6. Explanation for Figure 6 map on adjacent page.

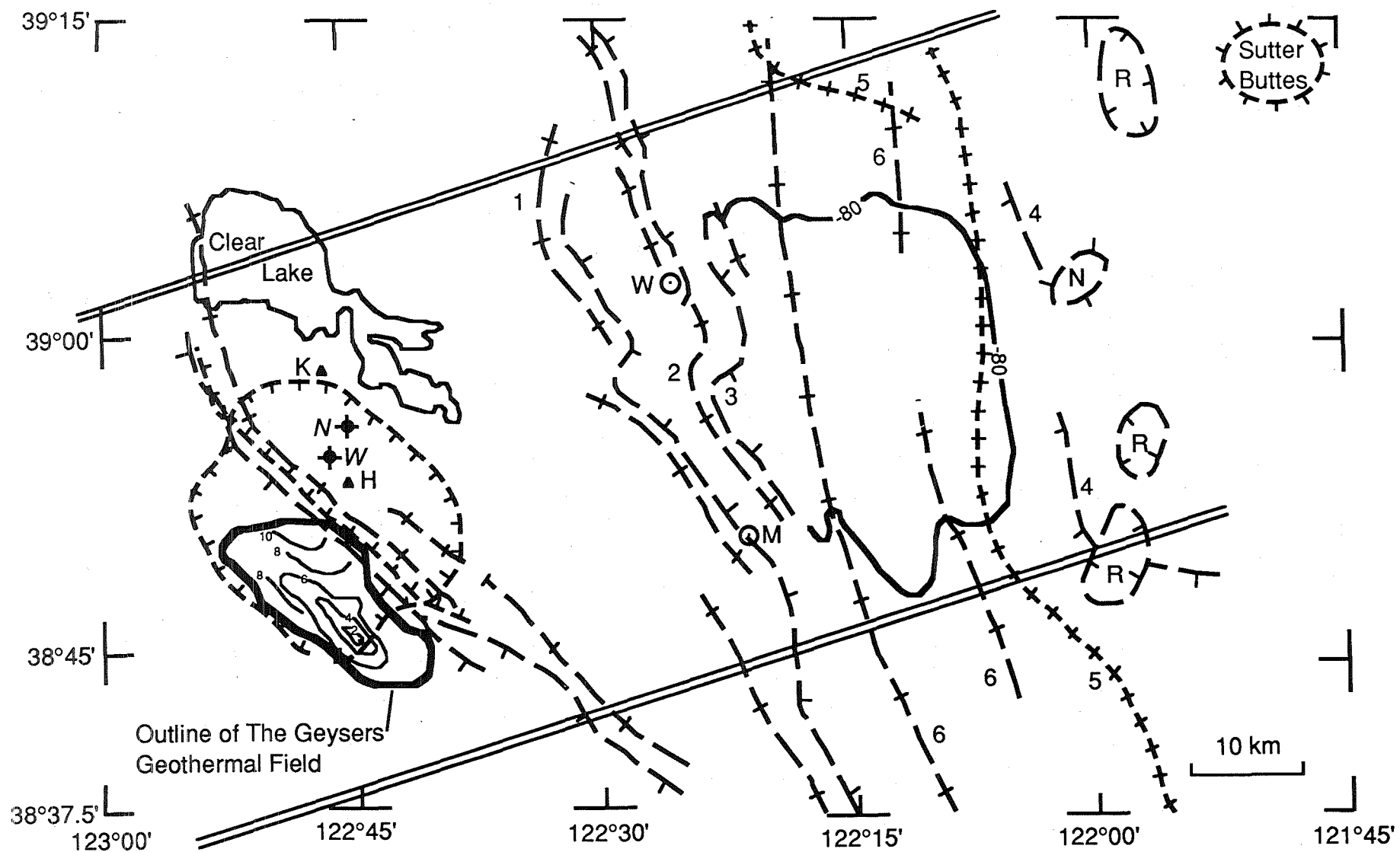


Figure 6. Interpretive geophysical map of the Clear Lake-McLaughlin Mine area, showing location of geophysical features discussed in the text. All the geophysical features possibly relating to gold mineralization are located within a belt defined by the two straight lines that trend N70°E. and are about 45 km apart.

layer (7.2 km/s) at a depth of about 15 km near Skaggs Springs, 20 km southwest of The Geysers. Our simple model (Fig. 7) calculated across the Franciscan-Great Valley contact at lat. 39°37'N., about 50 km north of Clear Lake, uses well data and seismic reflection data to constrain the basement surface beneath the Great Valley. This model implies eastward wedging of the Franciscan Complex over Great Valley basement for horizontal distances of at least 50 km. The interpretation has major consequences for understanding the tectonics of the California Coast Ranges.

MAGNETIC AND GRAVITY FEATURES IN THE GREAT VALLEY

A series of magnetic features caused by magnetic rocks generally at depths of less than 2 km in the Great Valley are described here in a separate section because some of the features have possible associations with the area of gold mineralization. The features listed below are shown in Figure 6 which should be compared with the magnetic map and the gravity map (Figs. 3 and 4).

1. Detrital serpentinite within the lower part of the Great Valley sequence causes magnetic anomalies south of Wilbur Springs and extending south to the McLaughlin Mine in a linear belt (feature 2 of Figure 6) parallel to the contact with the ophiolite which is located about 5 km to the west.
2. Magnetic anomalies over the detrital serpentinite on their east side are bounded by a relatively steep narrow curvilinear magnetic gradient (feature 3 of Figure 6) which implies either a fault or an abrupt stratigraphic termination above this unit. This steep gradient extends continuously between the latitudes of gold-bearing areas at Wilbur Springs and the McLaughlin Mine, but terminates abruptly opposite each mine, implying an association of some sort.
3. Low-amplitude linear magnetic highs (features labeled 6 on Figure 6) correlate with certain stratigraphic units of the Great Valley sequence. These anomalies extend many kilometers north and south of this study area and are probably not relevant to this discussion of local features related to mineralization.
4. Four small elliptical magnetic anomalies (Fig. 6) are observed in the eastern part of the map area; three are lows caused by rocks with reverse remanent magnetization (R) and one is a high, indicating normally magnetized rocks (N). The depths to the source rocks of these anomalies are less than 0.7 km below the surface based on the steepness of their bordering gradients. The two southern lows are probably caused by the Miocene Lovejoy Basalt, a reversely magnetized flow that extends from the northern Sierra Nevada west to the Great Valley and thence south in the subsurface to about lat. 38°20'N. This basalt was intersected by a well in the area of the southernmost magnetic low (Harwood and Helley, 1987). The small high may be only an apparent high on the northwest side of a local magnetic low because a well located 2 km southeast of the high penetrated Lovejoy Basalt (Harwood and Helley, 1987). Due to the wide distribution of this flow, these three magnetic features are probably not relevant to this discussion emphasizing local features related to mineralization.

The fourth or northernmost small anomaly, a magnetic low, is situated over the buried Colusa dome of Harwood and Helley (1987), a local feature displaying about 0.5 km of structural relief on the top of the Cretaceous section and containing intrusive volcanic rocks similar in composition and age to those in the Sutter Buttes. Williams and Curtis (1977) proposed that this dome formed solely by forceful magma injection contemporaneous

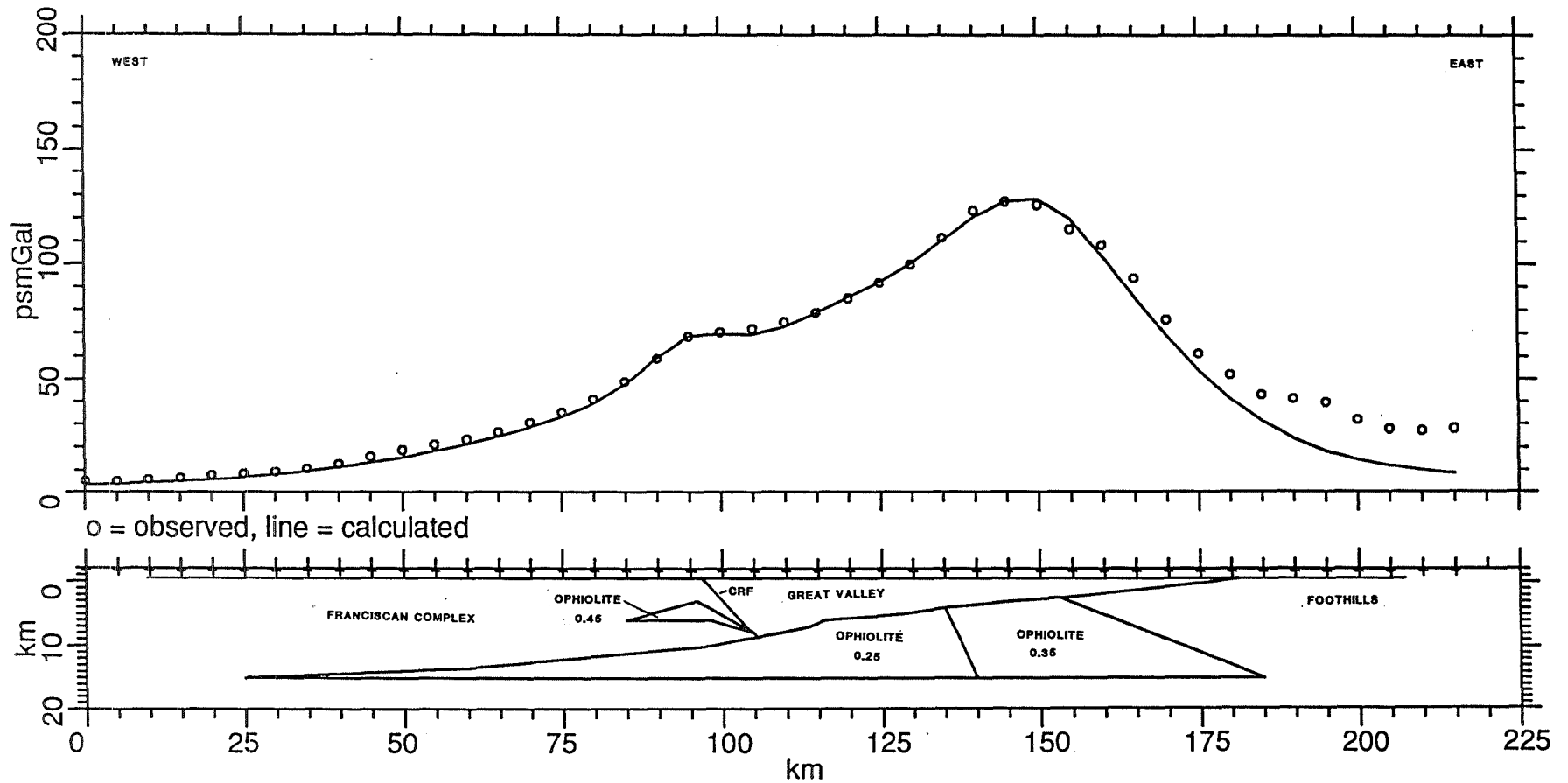


Figure 7. Calculated two-dimensional magnetic model from pseudogravity data (calculated from Roberts and Jachens, 1993) showing the configuration of the Great Valley basement and its extension west beneath the Franciscan Complex. Cross-section is located at lat. $39^{\circ} 37' N.$, about 50 km north of Clear Lake. CRF is Coast Range Fault. Numbers associated with the ophiolite indicate model pseudodensities (in g/cm^3).

with magmatism at Sutter Buttes but Harwood and Helley (1987) suggest earlier faulting may have localized the magmatism and caused some of the structure. These volcanic rocks appear to display reverse remanent magnetization, as evidenced by the associated magnetic low. A major fault on the west side of the dome causes the local steep gravity gradient striking north-south at long. $121^{\circ}58'W$. near the north edge of the gravity map (Fig. 4).

5. A magnetic boundary (feature 4 in Figure 6) is located near the small anomalies described in (4) above and is caused by a large area of magnetic rocks lying east of the boundary (feature 4) at depths of less than 2 km below the surface. These rocks are thus well up within the Great Valley sequence because the relatively smooth basement in this area lies at depths in excess of 4 km on the basis of well data and seismic reflection data (C.M. Wentworth, R.C. Jachens, and G.R. Fisher, unpublished basement contour map, 1991; Ramirez, 1993). The magnetic rocks may be sedimentary rocks or igneous rocks and their western boundary may be a wedge-fault lying within the Great Valley sequence.

6. Sutter Buttes volcano produces an insignificant effect on the magnetic map which indicates that any possible associated subsurface pluton (see gravity discussion) also might not be magnetic. This volcano is located on the crest of a linear magnetic high, the Great Valley magnetic anomaly.

7. A major magnetic feature that possibly relates to the area of gold and mercury mineralization is a large subcircular magnetic low within the area of the Great Valley. This magnetic low is depicted approximately on Figure 6 by a magnetic contour (-80 nT) that is taken from Figure 3. This low is a unique feature along the Great Valley where the more usual magnetic expression is similar to that at the north and south borders of Figure 3. Although the present study is only preliminary, we suggest that this low is caused by the local absence of magnetic material, specifically the absence of the east-dipping, magnetic part of the "airfoil" of the Coast Range ophiolite (Fig. 2) that customarily lies beneath the western part of the Great Valley.

Possible explanations for absence of magnetic ophiolite in this area include:

- a. This part of the ophiolite airfoil is missing because of local structural complications during the tectonic-wedging process which caused the tip of the eastward-moving Franciscan wedge to lie above the Great Valley basement rather than within the ophiolite basement. Thus the wedge here failed to chisel up a slab of ophiolite into the usual position of the airfoil. An additional implication of this hypothesis is that rocks of the basal part of the Great Valley sequence may here have been structurally isolated beneath the advancing wedge of the Franciscan Complex and thus their connate water, plus water derived from heated hydrous minerals, could become available later to form mineralizing fluids.
- b. The ophiolite slab is not missing but is simply too thin here to cause an anomaly.
- c. The ophiolite slab has been altered in such a way that it no longer contains significant amounts of magnetic minerals.

We favor hypothesis (a) and thus ascribe the magnetic low to a structural event that is probably of Late Cretaceous or early Tertiary age. Nevertheless, we find compelling the spatial association of this low with not only the gold mineralization (<2 Ma), but also the belt of magnetic detrital serpentinite (Cretaceous), and the youthful volcanic and geothermal area near Clear Lake.

8. The change in location of the axis of the gravity low (feature 5 of Figure 6) in the Great Valley may be related in some way to the magnetic boundary (feature 4) described in section 5 and to the magnetic low described in section 7. Elsewhere in the Great Valley, this gravity low is reasonably linear and is located approximately as shown on the north and south borders of the map (Fig. 4). Thus the position of the low between lat. 38°50'N. and lat. 39°12'N. is anomalously offset to the east. This offset gravity low is not caused by a local thickening of Tertiary sedimentary deposits because they here are less than 1 km thick (Harwood and Helley, 1987). Thus, the anomaly must have a deeper and unknown source. We tentatively interpret this eastern offset as in part the result of a subtle gravity high located on the west flank of the offset, the high being best displayed by the eastward bulge in the -26 and -24 mGal contours on the west side of the offset axial low. A possible cause for this gravity high is a local subsurface tectonic wedge of the Franciscan Complex that is either thicker or more dense than normal. A tabular pluton intruding the Great Valley sequence is another, less likely cause of the anomaly because there is little additional evidence supporting this hypothesis, but we cannot fully exclude the possibility of a non-magnetic siliceous pluton in this general area. The eastward offset of the axis of the gravity low cannot be entirely explained by the subtle high to the west, because most of the gravity contours that define the Great Valley gravity anomaly (high along the eastern edge of Figure 4) also reflect the eastward offset.

GRAVITY LOW SOUTH OF CLEAR LAKE

The gravity anomaly associated with the Clear Lake Volcanics and The Geysers geothermal area (Figs. 4 and 6) has crudely the outline of a square with two sides trending northwest parallel to the local structure and two sides trending northeast transverse to structures mapped at the surface. The outline of the main causative mass (Fig. 6) is determined from the location of the steepest marginal gradients. Analysis of both the relatively narrow gradients associated with the interior and sides of this anomaly as well as correlations with certain geologic features show that some of the density contrasts (sources) causing this anomaly are very shallow (Chapman, 1975; Blakely and Stanley, in press) and some, in fact, crop out at the surface. For example, the topography of Mount Hannah and Mount Konocti (Fig. 6) produces local gravity lows of approximately -5 and -15 mGal, respectively, that are 2-3 km wide; these volcanoes are composed of material with average density about 0.2-0.4 g/cm³ lower (as calculated from the topographic effects) than the assumed Bouguer anomaly reduction density of 2.67 g/cm³. The gravity gradient or step of about 6 mGal at the Collayomi Fault (Figs. 1 and 4) is caused by relatively lower density rocks (Great Valley sequence and, perhaps, serpentinite) lying on the northeast side of the fault (Blakely and Stanley, in press) compared to the Franciscan Complex on the southwest side. The small gravity ridge (amplitude of 2-4 mGal) trending northwest across the bottom of the gravity low lies on the southwest side of the Collayomi Fault, and may be caused in part by a thin slab of lawsonite-bearing rocks of the Franciscan Complex (Chapman *in* Majer and others, 1992) composed of a high-pressure metamorphic mineral assemblage (blueschist facies) probably having a bulk density in excess of 2.75 g/cm³. Highly altered rocks at the surface in the geothermal area are low in density and produce a local gravity low of about -2 mGal (the smaller -22 mGal contour on Figure 4).

Despite these somewhat minor causes of near-surface anomalies, the main gravity feature, a -20 mGal low that is at least 20 km wide, still requires explanation and, ever since its discovery in the 1960's (Chapman, 1966), has been interpreted as the gravity expression of a low-density partly molten granitic pluton (Chapman, 1975; Isherwood, 1976; Isherwood, 1981). The most recent model calculations (Blakely and Stanley, in press) show that the main anomaly is well-matched by a low-density mass having the configuration of a horizontal slab about 23 km wide with steep sides and a thickness of nearly 5 km, assuming a density contrast of -0.38 g/cm^3 . This slab in their model is located with its top at a depth of 15 km below sea level, in part because of interpretation of magnetotelluric soundings, but the authors do not rule out partial melting and smaller magma bodies in the upper crust. An earlier model calculation by Chapman (his Figure 8, 1975) depicts the source with a flat top at sea level, a maximum thickness of 8 km (density contrast of -0.20 g/cm^3), and tapering sides with inward-sloping bottom contacts.

Here we summarize evidence from magnetic studies and other data that in part supports the slab configuration of Blakely and Stanley (in press) and also supports, to some extent, the model of Chapman (1975) but that indicates significant low-density intrusions reaching within 4-5 km of the surface. Substantial evidence exists for relatively shallow depths to the tops of intrusions and includes: the very high temperatures and steep temperature gradients at depths of only a few kilometers, throughout the area of the gravity low; the presence of intrusive felsite beneath the geothermal area (contours on Figure 6); the observation of contact metamorphic hornfels near the bottom of two deep wells (over 3 km) in the Clear Lake Volcanics (well N and W in Figure 6); the absence of microseismicity below depths of about 6 km (Bufe and others, 1981); low resistivities in the Mt. Hannah area according to electrical geophysical studies (Stanley and others, 1973); and the shallow source-depths (tops no deeper than 2-4 km) for the relatively narrow gravity gradients that trend northeast along the sides of the gravity anomaly transverse to the regional structure. These gradients are important evidence because they do not correlate with any surface structure. The well data plus the uninterrupted continuity of the serpentinite-caused aeromagnetic anomalies across the gravity low (Figs. 3 and 6) indicate that the tops of the intrusions are generally somewhat deeper than about 3-4 km because the serpentinite belt has been neither intruded out nor heated above the Curie point of magnetite (about 580°C). The potentially contradictory evidence for intrusive source depths from the magnetic data (somewhat deeper than 3-4 km) and the steep gravity gradients (no deeper than 2-4 km) remains to be resolved.

On the basis of the substantial age range of the siliceous volcanic rocks (at least 1.3-0.3 Ma according to Donnelly-Nolan and others, 1981), and the age of the intrusive felsite of the geothermal area which is greater than 1.3 Ma (Dalrymple, 1992), multiple intrusions must have taken place. Repeated additions of magma would be necessary to maintain the high temperatures observed today and implied by older hot spring deposits and the volcanic rocks. If many of the older intrusions are already crystallized, then the density contrast between intrusive rock and country rock will be smaller than that associated with a granitic magma, and the calculated aggregate thickness of intrusions greater than that shown by Blakely and Stanley (in press), perhaps totaling as much as 8 or 9 km according to Chapman (1975), who assumed a density contrast of -0.20 g/cm^3 . Other uncertainties beset the gravity calculation, however, including the possibility of mafic igneous material located at depth (Stimac, this publication) and the possibility of an additional deep-seated low density (but long wavelength) contribution from

more mafic melts at the base of the crust (20-25 km). The presence of mafic igneous bodies high in the crust requires the low density granitic mass to be even thicker to balance the gravity effect of the associated high density mafic rocks, although little additional space remains for either material. The latter hypothesis permits the granitic body to be somewhat thinner.

The felsite intrusion beneath The Geysers area displays further shape complexities at its southeast end which extends across the border of the gravity low (Figs. 4 and 6) up to the top of the gravity gradient. Because the felsite has a density contrast of -0.1 g/cm^3 (Blakely and Stanley, in press), a slab 1 km thick will cause a gravity anomaly of about 4 mGal; because of the absence of such an anomaly on the gradient, we conclude that the southeastern 3 km of the felsite is less than 1 km thick, even though the rest of the felsite is underlain by at least 5 km of pluton. Such sill-like lateral protrusions are expected, may also be present elsewhere beyond the border of the gravity low as implied by the gravity model of Chapman (1975), and may similarly affect the location of potential geothermal reservoirs relative to the gravity low. Note that the measured density of the felsite (2.57 g/cm^3) is rather low for a granitic rock, but produces a density contrast of only about -0.1 g/cm^3 . The density contrasts used by Chapman (1975) and Blakely and Stanley (in press) require anomalous densities much lower than that of the felsite, implying the presence of significant proportions of low-density magma.

The Clear Lake region has been in an extensional environment for at least the past 2.1 m.y. (McLaughlin and Nilsen, 1982; Sims and others, 1981; Sims and others, 1988; Hearn and others, 1988) and has also been termed a volcano-tectonic depression. Evidence for extension includes a continuously existing series of lake basins plus associated sedimentary deposits and a nearly continuous record of extrusive volcanic activity. This environment has been favorable for the origin and movement of hot thermal waters together with associated deposits of mercury and gold. High heat flow (Walters and Combs, 1992) and hot springs extend well to the northeast of Clear Lake as also do P-wave teleseismic delays inferred to be caused by thermal effects between depths of 4 and 10 km (Iyer and others, 1981). The extension (and corresponding subsidence) at Clear Lake itself is closely balanced against sedimentation rates (Sims and others, 1981) such that this shallow lake has lasted for many times more than the estimated 10,000 years required to fill it with sediment. This observation about Clear Lake sedimentation may be analogous to a similar problem concerning the intrusive mass that produces the gravity low. This intrusion is calculated to be in excess of 5 km thick and yet there appears to be no evidence for significant vertical change in the topography above it over the past 1.3 m.y. Perhaps the crustal volume lost by continuing extension is to some extent correlated with the volume of successive injections of magma over this same time span.

The gravity low near Clear Lake is an unusual geologic feature relative to the late Cenozoic volcanism of the California Coast Ranges. Despite the large amounts of siliceous volcanism elsewhere in this province, there is no gravity evidence (Roberts and others, 1990) for such large siliceous intrusions associated with the other volcanic areas, although the Quien Sabe volcanic field (lat. $36^{\circ}55' \text{ N.}$, long. $121^{\circ}15' \text{ W.}$) displays a negative anomaly of -5 to -10 mGal. The pluton at Clear Lake is in this sense unique, and poses the question of why it is there.

RELATIONSHIPS OF GEOPHYSICAL FEATURES WITH GOLD MINERALIZATION

Elsewhere in this paper we have mentioned associations of various geophysical and geological features with the areas of gold mineralization. Here we summarize those associations and make some general observations.

1. The two gold deposits are located at the east margin of the exposed Coast Range ophiolite within about 1 km of a major magnetic gradient. Both deposits are also situated near the south extremity of ophiolite segments that, on the basis of magnetic anomalies form a right-lateral *en echelon* configuration (Fig. 6). Wilbur Springs is above a folded ophiolite slice that is one structural level above the slice at the McLaughlin Mine.
2. The two deposits are located near the north and south ends of a belt of magnetic detrital serpentinite located in the Late Jurassic and Early Cretaceous parts of the Great Valley sequence (Carlson, 1981; McLaughlin and others, 1989) at distances of 0-5 km from the ophiolite. The east side of the detrital serpentinite causes a steep narrow curvilinear magnetic gradient (Fig. 6), the two ends of which are directly opposite the two deposits, implying a possible structural association. The steep gradient is caused either by a fault or a relatively abrupt stratigraphic termination above the magnetic detrital unit which otherwise has a rather irregular configuration (McLaughlin and others 1989).
3. The gold-bearing areas are associated, to the west, with The Geysers-Clear Lake area, an area of high heat flow, thermal springs and hot spring deposits, plutonism and volcanism, and an extensional environment, all at least moderately continuous since about 2.1 Ma (Donnelly-Nolan and others, 1993).
4. The Geysers-Clear Lake area and the two gold deposits are associated, on the east, with an unusual broad magnetic low in the Great Valley (Figs. 3 and 6). This magnetic low is 30-40 km across in its northwest dimension, very similar to the dimensions of the thermal anomaly in The Geysers-Clear Lake area (Walters and Combs, 1992, Figure 3). The magnetic low is also rather precisely bounded on the west by the detrital serpentinite anomaly and its associated steep eastern magnetic gradient (Figs. 3 and 6). We interpret the magnetic low to be caused by a local structural complication (Cretaceous or early Tertiary in age), namely the absence of an east-dipping tabular mass of magnetic ophiolite that elsewhere is uniformly found beneath the west side of the Great Valley sequence. Nevertheless, we cannot fully exclude other less likely explanations such as the ophiolite slab being too thin here to cause an anomaly, or the ophiolite being altered and its magnetic minerals destroyed. It is not clear why this magnetic low should be associated so precisely with an older belt of detrital serpentinite.
5. On the east side of the magnetic low (see section 4) the axial gravity low (feature 5 of Figure 6) of the Great Valley is uniquely offset as much as 13 km to the east by a small-amplitude broad gravity high generally similar in dimensions and location with the magnetic low. This high may be caused by an unusually thick or dense tectonic wedge of the Franciscan Complex beneath this part of the Great Valley sequence, but other explanations, including that of a concealed pluton within the Great Valley sequence, are possible.
6. We define here a belt of seemingly associated geophysical and geologic features (Fig. 6) by using The Geysers geothermal field, the gravity boundary around the silicic intrusions, the location of the gold mineralization, the belt of detrital serpentinite, the broad magnetic low in the Great Valley, the associated offset axial gravity low in the Great Valley, the volcano at Sutter Buttes together with the associated intrusive volcanic rocks in the buried

Colusa dome (10 km west of the volcano), and a basement-offsetting fault, striking N60°E., and located at 9 km northwest of Sutter Buttes (Harwood and Helley, 1982).

This belt trends about N70°E. for a distance of at least 105 km and has a width of about 45 km. The belt is approximately normal to the strike of the San Andreas Fault system. The features west of the Great Valley and east at Sutter Buttes are younger than about 2.1 Ma, whereas the features in the Great Valley probably are Mesozoic in age. We suggest that this belt may represent the location of a linear Mesozoic structural feature. This feature was reactivated at around 3 Ma when the Mendocino Triple Junction passed by, subduction ended at the latitude of Clear Lake, and the cold base of the crust of the North American plate came in contact with hot asthenosphere at a depth of about 20-25 km (Warren, 1981; McLaughlin, 1981; Jachens and Griscom, 1983). These events initiated volcanism, plutonism, and movement of thermal waters in the Clear Lake area. The gold deposits themselves are thus located at the intersection of two structural trends: (1) the contact, trending about N20°W., between the Coast Range ophiolite and the Great Valley sequence, a complex structural feature predominantly of Mesozoic age, and, (2) this newly proposed belt, trending about N70°E., that may represent a reactivated Mesozoic structure.

Perhaps the area of missing ophiolite and this Mesozoic structural feature offered more favorable opportunities for minor intrusions of relatively fluid basaltic andesite to work their way to the east side of the exposed Coast Range ophiolite and here provide suitable local environments for later gold mineralization.

REFERENCES

- Baranov, V., 1957, A new method for interpretation of aeromagnetic maps: pseudogravimetric anomalies: *Geoph.*, v. 22 p. 359-383.
- Blakely, R.J., and Stanley, W.D., in press, The Geysers magma chamber, California: constraints from gravity data, density measurements, and well information: Geothermal Resources Council, Spec. Rept. ___.
- Bufe, C.G., Marks, S.M., Lester, F.W., Ludwin, R.S., and Stickney, M.C., 1981, Seismicity of The Geysers-Clear Lake region: U.S. Geol. Survey Prof. Paper 1141, p. 129-137.
- Cady, J.W., 1975, Magnetic and gravity anomalies in the Great Valley and western Sierra Nevada metamorphic belt, California: *Geol. Soc. America Spec. Paper* 168, 56 p.
- Carlson, Christine, 1981, Sedimentary serpentinites of the Wilbur Springs Area—A possible early Cretaceous structural and stratigraphic link between the Franciscan Complex and the Great Valley sequence: unpub. M.S. thesis, Stanford University, 105 p.
- Chapman, R.H., 1966, Gravity map of Geysers area: *Calif. Div. Mines Geology Mineral Inf. Serv.*, v. 19, p. 148-149.
- _____, 1975, Geophysical study of the Clear Lake region, California: *Calif. Div. Mines Geology Spec. Rept.* 116, 23 p.
- Dalrymple, G.B., 1992, Preliminary report on $^{40}\text{Ar}/^{39}\text{Ar}$ incremental heating experiments on feldspar samples from the felsite unit, Geysers geothermal field, California: U.S. Geol. Survey Open-File Rept. 92-407, 15 p.
- Donnelly-Nolan, J.M., Hearn, B.C., Jr., Curtis, G.H., and Drake, R.E., 1981, Geochronology and evolution of the Clear Lake Volcanics: U.S. Geol. Survey Prof. Paper 1141, p. 47-60.
- Donnelly-Nolan, J.M., Burns, M.G., Goff, F.E., Peters, E.K., and Thompson, J.M., 1993, The Geysers-Clear Lake area, California: thermal waters, mineralization, volcanism, and geothermal potential: *Econ. Geol.*, v. 88, p. 301-316.
- Griscom, Andrew, 1983, The contact between the Great Valley sequence and the Franciscan assemblage, California, from magnetic data [abs.]: *EOS, Trans., American Geoph. Union*, v. 64, p. 867-868.
- Griscom, Andrew, and Jachens, R.C., 1989, Tectonic history of the north portion of the San Andreas fault system, California, inferred from gravity and magnetic anomalies: *Jour. Geoph. Res.*, v. 93, p. 3089-3099.
- _____, 1990, Tectonic implications of gravity and magnetic models along east-west seismic profiles across the Great Valley near Coalinga, Chap. 5 of Rymer, M.J., and Ellsworth, W.L., eds., *The Coalinga, California, earthquake of May 2, 1983*: U.S. Geol. Survey Prof. Paper 1487, p. 69-78.

- Harwood, D.S., and Helley, E.J., 1987, Late Cenozoic tectonism of the Sacramento Valley, California: U.S. Geol. Survey Prof. Paper 1359, 46 p.
- Hausback, B.P., 1991, Eruptive history of the Sutter Buttes volcano—review, update, and tectonic considerations [abs.]: Geol. Soc. America Abstracts with Programs, v. 23, no. 2, p. 34.
- Hearn, B.C., Jr., Donnelly-Nolan, J.M., and Goff, F.E., 1981, The Clear Lake Volcanics: Tectonic setting and magma sources: U.S. Geol. Survey Prof. Paper 1141, p. 25-45.
- Hearn, B.C., Jr., McLaughlin, R.J., and Donnelly-Nolan, J.M., 1988, Tectonic framework of the Clear Lake basin, California: Geol. Soc. America Spec. Paper 214, p. 9-20.
- Isherwood, W.F., 1975, Gravity and magnetic studies of the Geysers-Clear Lake geothermal region, California, U.S.A.: U.S. Geol. Survey Open-File Rept. 75-368, 37 p.
- Isherwood, W.F., 1976, Gravity and magnetic studies of The Geysers-Clear Lake geothermal region, California, U.S.A.: United Nations symposium on the development and use of geothermal resources, 2nd, San Francisco, California, 20-29 May 1975, Proc., v. 2, p. 1065-1073.
- Isherwood, W.F., 1981, Geophysical overview of The Geysers: U.S. Geol. Survey Prof. Paper 1141, p. 83-95.
- Iyer, H.M., Oppenheimer, D.H., Hitchcock, T., Roloff, J.N., and Coakley, J.M., 1981, Large teleseismic P-wave delays in The Geysers-Clear Lake geothermal area: U.S. Geol. Survey Prof. Paper 1141, p. 97-116.
- Jachens, R.C., and Griscom, Andrew, 1983, Three-dimensional geometry of the Gorda plate beneath northern California: Jour. Geoph. Research, v. 88, p. 9375-9392.
- Jachens, R.C., and Griscom, Andrew, 1985, An isostatic residual gravity map of California—a residual map for interpretation of anomalies from intracrustal sources, *in* Hinze, W.J., ed., The utility of regional gravity and magnetic anomaly maps: Tulsa, Okla, Soc. Expl. Geophysicists, p. 347-360.
- Jayko, A.S., Blake, M.C., Jr., and Harms, T., 1987, Attenuation of the Coast Range ophiolite by extensional faulting, and nature of the Coast Range "thrust", California: Tectonics, v. 6, p. 475-488.
- Jennings, C.W., and Strand, R.G., 1960, Geologic map of California, Ukiah sheet: Calif. Div. Mines Geology, 2 sheets, scale 1:250,000.
- Majer, E.L., and McEvilly, T.V., 1977, Seismological investigations at the Geysers geothermal field: Berkeley, Univ. California, Lawrence Berkeley Laboratory Rept. LBL-7023, 71 p.
- Majer, E.L., Chapman, R.H., Stanley, W.D., and Rodriguez, B.D., 1992, Geophysics at The Geysers, *in* Stone, Claudia, ed., Monograph on The Geysers Field: Geothermal Resources Council, Spec. Rept. No. 17, p. 97-110.
- Mankinen, E.A., Donnelly-Nolan, J.M., Grommé, C.S., and Hearn, B.C., Jr., 1981, Paleomagnetism of the Clear Lake Volcanics and new limits on the age of the Jaramillo normal-polarity event: U.S. Geol. Survey Prof. Paper 1141, p. 67-82.
- McLaughlin, R.J., 1981, Tectonic setting of pre-Tertiary rocks and its relation to geothermal resources in the Geysers-Clear Lake area: U.S. Geol. Survey Prof. Paper 1141, p. 3-23.
- McLaughlin, R.J., and Nilsen, T.H., 1982, Neogene non-marine sedimentation and tectonics in small pull-apart basins of the San Andreas fault system, Sonoma County, California: Sedimentology, v. 29, p. 865-876.
- McLaughlin, R.J., and Ohlin, H.N., 1984, Tectonostratigraphic framework of the Geysers-Clear Lake region, California: Pacific Sec. Soc. Econ. Paleontologists Mineralogists, v. 43, p. 221-254.
- McLaughlin, R.J., Ohlin, H.N., Thormahlen, D.J., Jones, D.L., Miller, J.W., and Blome, C.D., 1989, Geologic map and structure sections of the Little Indian Valley-Wilbur Springs geothermal area, northern Coast Ranges, California: U.S. Geol. Survey Map I-1706, scale 1:24,000.
- Pulka, F.S., 1991, Recent intrusives at Ford flat and relationships to faulting and the geothermal heat source, Geysers geothermal field, California [abs.]: Geol. Soc. America Abstracts with Programs, v. 23, p. 90.
- Ramirez, V.R., 1993, Evolution of the Coast Range thrust as interpreted from seismic reflection data [abs.]: Abstracts with Programs, Geol. Soc. America, v. 25, p. 136.
- Roberts, C.W., Jachens, R.C., and Oliver, H.W., 1990, Isostatic residual gravity map of California and offshore southern California: Calif. Div. Mines Geology, Geologic Data Map No. 7, scale 1:750,000.
- Roberts, C.W., and Jachens, R.C., 1993, Draped aeromagnetic map of California—a new tool for regional structural and tectonic analysis [abs.]: EOS, Trans. American Geoph. Union, v. 74, p. 379.
- Sims, J.D., Adam, D.P., and Rymer, M.J., 1981, Stratigraphy and palynology of Clear Lake, California: U.S. Geol. Survey Prof. Paper 1141, p. 219-230.
- Sims, J.D., Rymer, M.J., and Perkins, J.A., 1988, Late Quaternary deposits beneath Clear Lake, California: Physical stratigraphy, age, and paleogeographic implications, Geol. Soc. America Spec. Paper 214, p. 21-41.
- Stanley, W.D., Jackson, D.B., and Hearn, B.C., Jr., 1973, Preliminary results of geoelectrical investigations near Clear lake, California: U.S. Geol. Survey Open-File Rept., 20 p.

- Thompson, R.C., 1992, Structural stratigraphy and intrusive rocks at The Geysers geothermal field, *in* Stone, Claudia, ed., Monograph on The Geysers geothermal field: Davis, California, Geothermal Resources Council Spec. Rept. 17, p. 59-63.
- U.S. Geological Survey, 1973, Aeromagnetic map of the Clear Lake area, Lake, Sonoma, Napa, and Mendocino Counties, California: U.S. Geol. Survey Open-File Rept. 73-299, scale 1:62,500.
- Unruh, J.R., Ramirez, V.R., Phipps, S.P., and Moores, E.M., 1991, Tectonic wedging beneath fore-arc basins: ancient and modern examples from California and the Lesser Antilles: *GSA Today*, v. 1, p. 185, 188-189.
- Wagner, D.L., and Bortugno, E.J., 1982, Geologic map of the Santa Rosa Quadrangle: Calif. Div. Mines Geology Map 2A, 5 sheets, scale 1:250,000.
- Walters, M., and Combs, J., 1992, Heat flow in The Geysers-Clear Lake geothermal area of northern California, U.S.A., *in* Stone, Claudia, ed., Monograph on The Geysers geothermal field: Davis, California, Geothermal Resources Council Spec. Rept. 17, p. 43-53.
- Wentworth, C.M., Blake, M.C., Jr., Jones, D.L., Walter, A.W., and Zoback, M.D., 1984, Tectonic wedging associated with emplacement of the Franciscan assemblage, California Coast Ranges, *in* Blake, M.C., Jr., ed., Franciscan geology of northern California: Pacific Section, Soc. Econ. Paleontologists Mineralogists, v. 43, p. 163-173.
- Williams, H., and Curtis, G.H., 1977, The Sutter Buttes of California: A study of Plio-Pleistocene volcanism: Univ. California Pub. in Geol. Sciences, v. 116, 56 p.

**OVERVIEW OF THE McLAUGHLIN PRECIOUS METAL DEPOSIT,
NAPA AND YOLO COUNTIES, NORTHERN CALIFORNIA**

Richard M. Tosdal¹, Dean A. Enderlin², Gordon C. Nelson², and Norman J. Lehrman³

1. U.S. Geological Survey, 345 Middlefield Road, Menlo Park, CA 94025

2. Homestake Mining Company, 26775 Morgan Valley Road, Lower Lake, CA 95457

3. Homestake Mining Company, 1375 Greg Street, Suite 105, Sparks, NV 89431

ABSTRACT

A late Pliocene and Pleistocene hot-spring deposit consisting of sinter terraces underlain by veins is the site of the McLaughlin Mine in northern California. The deposit is localized along the contact between hanging wall mudstone of the Upper Jurassic Knoxville Formation (basal formation of the Upper Jurassic and Cretaceous Great Valley sequence) and serpentinized ultramafic and mafic rocks of the Middle Jurassic Coast Range ophiolite in the footwall. The Stony Creek fault separates the two units, and dips moderately northeasterly. Pliocene basaltic andesite and volcanoclastic rocks unconformably overlie the sedimentary and ophiolitic rocks in the mine area. These rocks intruded as sills to shallow depths or erupted after phreatomagmatic explosions from small volcanic centers. Magmatism was also localized along the Stony Creek fault. The volcanic rocks are part of the older phase of the Clear Lake Volcanics, which formed in a Pliocene to Holocene volcanic field that lay mostly to the west and northwest.

The deposit consists of two epithermal orebodies, the north and south orebodies, which are connected by a narrow zone of mineralization. The oldest hydrothermal event recognized in the deposit was adularization of the hanging wall mudstone and silicification of the footwall serpentinite. Alteration formed a roughly tabular body that is discontinuous along the Stony Creek fault. Basaltic andesite sills, plugs, and flows are propylitized and locally argillized. Precious metals are present in opal, chalcedony, and quartz veins that cut brittle rocks, including altered rocks, basaltic andesites, and tabular lithons present in the footwall serpentinite. The south orebody is dominated by a sheeted vein complex, which contained as much as 25% of the total gold content of the deposit before mining. The sheeted vein complex formed along the southeast margin of a tabular greenstone (metabasalt) block in footwall serpentinite. The north orebody and the south orebody outside of the sheeted vein complex consist of mutually crosscutting veins, millimeters to 0.6-meter wide. Three sets of moderately to steeply dipping veins are recognized based on different orientations. The vein sets strike northeasterly (010°-045°), east-southeasterly (090°-130°), and southeasterly to southerly (130°-180°). The sheeted vein complex and the veins outside of the complex formed in one hydrothermal system, and do not represent superposed hydrothermal events. Post-mineral faults of limited displacement disrupt parts of the deposit.

Formation of the deposit apparently resulted from the interplay of magmatism of the Clear Lake volcanic field and transpressional tectonics of the San Andreas transform fault system.

INTRODUCTION

The McLaughlin Mine is the largest producer of gold in the state of California (1992) (Burnett, 1993). Located in the Knoxville Mining District in Napa and Yolo Counties of northern California (Figs. 1 and 2), the mine is developed at the site of a hot spring mercury deposit hosted in and below a sinter terrace at the surface (Lehrman, 1986, 1990). Warm water springs are still active in the district, including several within the present open pit in the McLaughlin Mine (Berkstresser, 1968; Sherlock et al., 1993). The Knoxville Mining District is the southern of two gold-mercury mining districts in the Clear Lake area (Fig. 2). The northern district, known as the Sulphur Creek Mining District, contains gold- and mercury-bearing hot spring deposits and active hot springs depositing these elements (Pearcy and Petersen, 1990; Peters, 1991). Gold deposits in both districts are closely associated with a major lithotectonic contact between ophiolitic rocks representing ancient sea floor and sedimentary rocks of a forearc basin. Mercury deposits in each district are developed in silica-carbonate altered serpentinite (Peters, 1991; Sherlock et al., 1993), and contain only minor amounts of gold.

The McLaughlin deposit is spatially associated with isolated exposures of basaltic andesite, part of the Pliocene to Holocene Clear Lake Volcanics, that unconformably overlie and intrude polydeformed Jurassic and Cretaceous oceanic sedimentary and igneous rocks (Figs. 2 and 3). The deposit lies to the east of the main outcrops of the Clear Lake Volcanics. The Clear Lake Volcanics represent the youngest and northernmost of a series of volcanic centers, that become progressively older to the south along the California Coast Ranges (McLaughlin, 1981, Hearn et al., 1981, Fox et al., 1985). The volcanic centers are interpreted to have formed in response to the northward passage of the Mendocino triple junction along the coast of California. A major tectonic change from convergence associated with subduction to strike-slip and transpression associated with the modern San Andreas transform margin accompanied the passage of the triple junction. The Clear Lake Volcanics, and the McLaughlin deposit, formed after this important tectonic transition. This contribution reviews the setting of the McLaughlin deposit, focusing on the structural setting and sequence of events that formed the deposit. Mineralogic and geochemical aspects of the deposit are briefly summarized from Lehrman (1986, 1990), Peters (1991), Rytuba (1992), Donnelly-Nolan et al., (1993), Sherlock (1993a,b), Sherlock et al., (1993), and unpublished work of the staff of Homestake Mining Company.

The McLaughlin Mine was discovered in 1978 at the site of the Manhattan Mercury Mine, and produced its first gold in 1985. Initial ore reserves were approximately 2.9 million troy ounces of gold (19,300,000 tons at an average grade of 0.152 troy ounces per ton (oz/ton)). Continued exploration has increased reserves (1992) to about 3.5 million troy ounces of gold (26.8 million tons at average grade of 0.131 troy oz/ton). The deposit is presently (1993) mined in two contiguous open pits. Mining is scheduled to extend to depths of 200 to 230 m below the surface. Precious metal mineralization extends to deeper levels, but it is not presently economic.

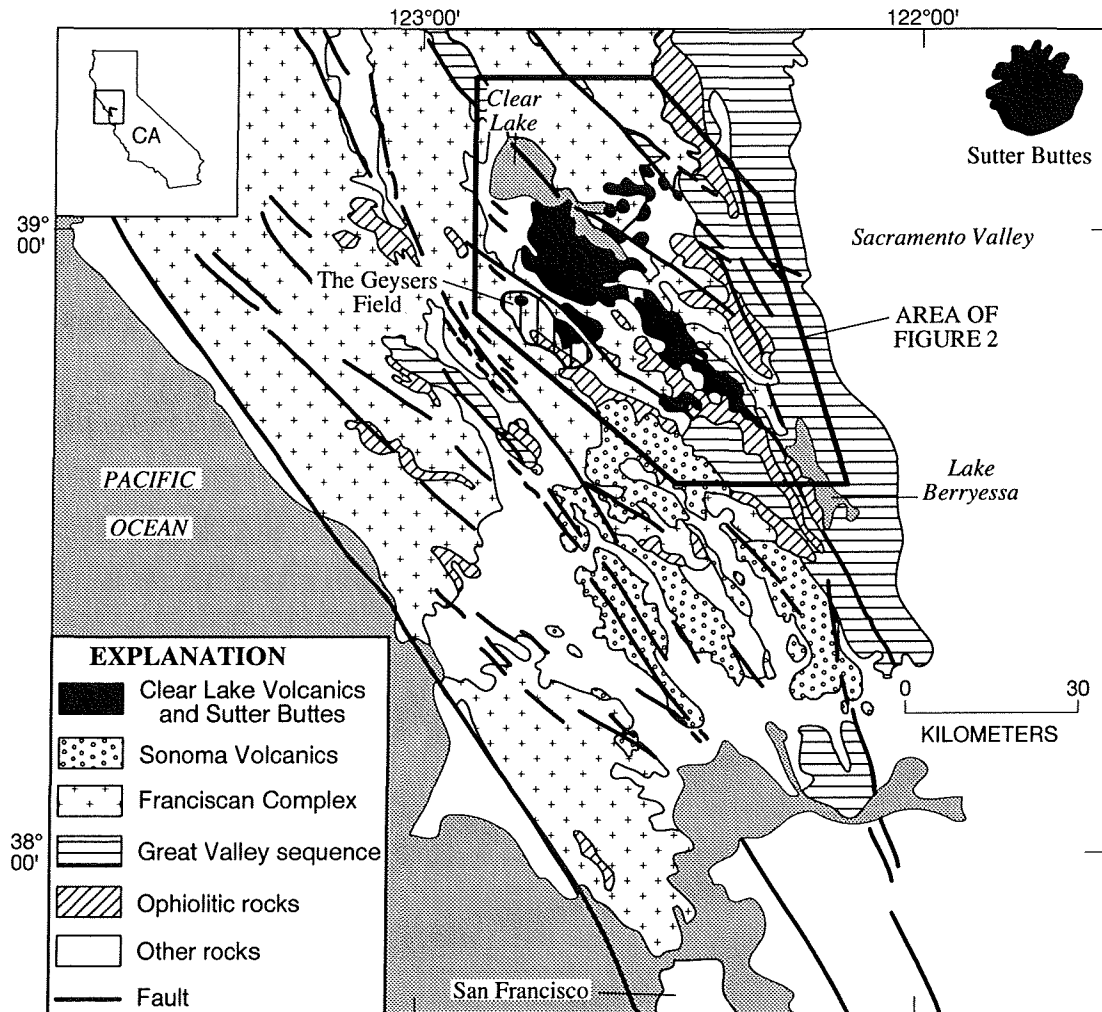


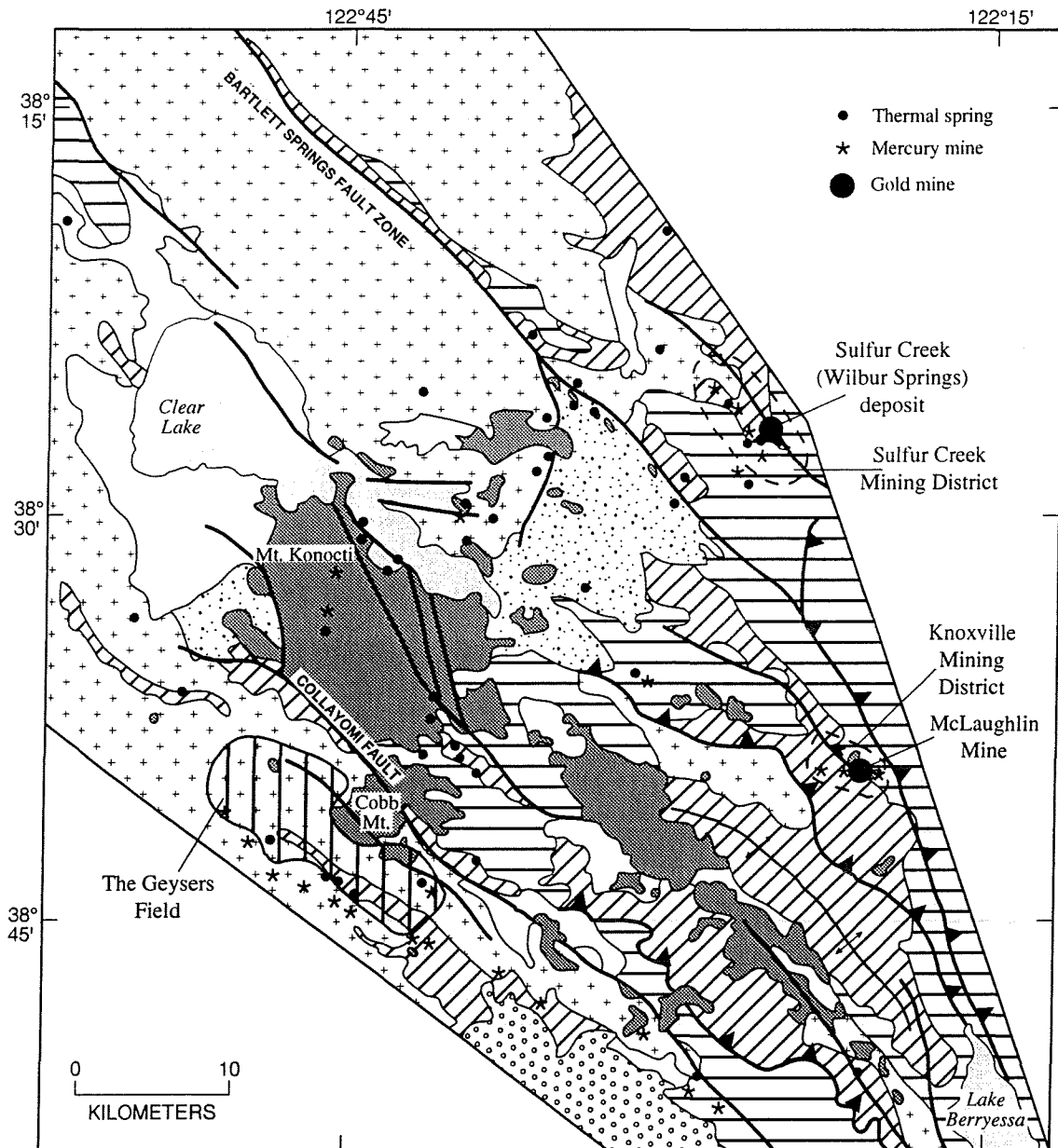
FIGURE 1. Geologic and location map of the Coast Ranges of northern California. Box encloses map shown in figure 2. From Donnelly-Nolan et al. (1993).

GEOLOGIC FRAMEWORK

Basement rock units and structure

Mesozoic and Cenozoic plate margin tectonics shaped the geologic framework of the Coast Ranges of northern California where the McLaughlin deposit is located. During this time, oceanic crust of the Kula or Farallon plate was subducted obliquely eastward beneath the leading margin of the North American continent. Mesozoic and Cenozoic trench and forearc deposits formed in the area that is now the Coast Ranges, with progressively younger deposits lying to the west. The magmatic arcs lay to the east and north. In the Mesozoic, the arc was located in the area of the Sierra Nevada and the Klamath Mountains.

The Mesozoic trench and forearc deposits in the Coast Ranges are divided into three lithotectonic units (Figs. 1 and 2). Trench deposits include sedimentary rocks derived from the continent to the east and rocks representative of



EXPLANATION

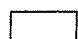
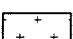


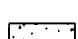
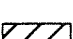
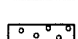



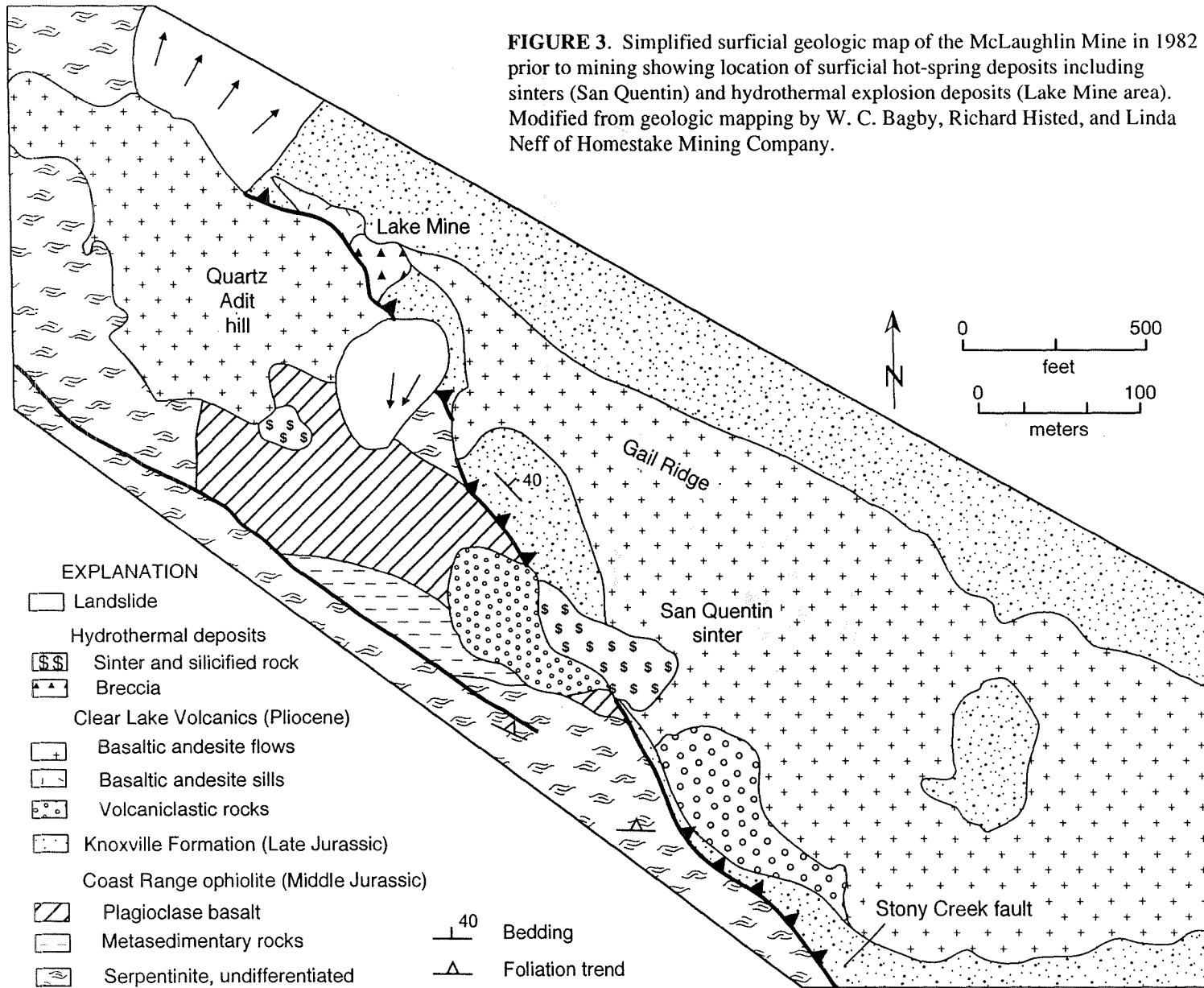
- | | |
|--|--|
|  Alluvium (Quaternary) |  Franciscan Complex (Cenozoic and Mesozoic) |
|  Clear Lake Volcanics (Quaternary and Pliocene) |  Great Valley sequence (Cretaceous and Late Jurassic) |
|  Cache Formation and related rocks (Pliocene and Pleistocene) |  Coast Range ophiolite (Middle Jurassic) |
|  Sonoma Volcanics (Pliocene and Miocene) |  Contact |
| |  Fault |
| |  Thrust fault |

FIGURE 2. Geologic map of the Clear Lake area, northern Coast Ranges of California. Only Late Cenozoic strike-slip, normal, and thrust faults are shown. Early Cenozoic and older faults are treated as lithologic contacts. Modified from Rymer (1981), Phipps and Unruh (1992), and Donnelly-Nolan et al. (1993).



oceanic crust that were scraped off the subducting oceanic plate and accreted to the leading edge of the overriding plate. These rocks constitute the Mesozoic and Cenozoic Franciscan Complex, the structurally lowest lithotectonic unit in the Coast Ranges. The forearc region is represented by two units that are separated from the accretionary complex by a polygenic fault system, the Coast Range fault. Along most of the Coast Range fault, the Middle Jurassic Coast Range ophiolite lies in the hanging wall. It is generally interpreted to have formed in a suprasubduction zone spreading center in the forearc region (McLaughlin et al., 1988; Saleeby, 1992). Sedimentary rocks buried the ophiolite in a marine forearc basin. The sedimentary rocks are now included in the Upper Jurassic and Cretaceous Great Valley sequence. Detritus was derived principally from the distal magmatic arc with a minor component being derived from the subjacent ophiolite and accretionary complex (Ingersoll and Dickinson, 1981; Phipps and Unruh, 1992).

The Great Valley sequence, Coast Range ophiolite, and Franciscan Complex are structurally interleaved to the west, north, and south of the McLaughlin deposit (Figs. 1 and 2), as they are in most of the California Coast Ranges. Shuffling of the lithotectonic packages in the Coast Ranges occurred during several episodes of thrusting, strike-slip, and extension both in the Mesozoic and Cenozoic (McLaughlin et al., 1988; Phipps and Unruh, 1992). The McLaughlin deposit lies near the transition between the terrane of fault-bounded lithotectonic packages on the west and the eastward dipping Great Valley sequence in the Sacramento Valley on the east (Figs. 1 and 2).

The Coast Range ophiolite and basal formation of the Great Valley sequence are important host rocks to the McLaughlin deposit. The Franciscan Complex is not exposed in the mine area, but it probably lies at depth beneath the deposit because of Cenozoic strike-slip and contractile deformation (McLaughlin and Ohlin, 1984; Phipps and Unruh, 1992).

In the area of the McLaughlin deposit, the highly tectonized Coast Range ophiolite has been subdivided into two fault-bounded packages, both of which strike west-northwest and dip moderately to the north-northeast (Figs. 4 and 5). Brittle faults marked by breccia and gouge separate the two packages. Internal stratigraphy, faults, and fabrics within the two packages are subparallel to the strikes of the major rock units. The structurally lowest package consists of serpentinite melange derived from mafic and ultramafic rocks of the ophiolite; this part of the ophiolite does not host mineralization. The upper package consists of polymictic melange and serpentinite. Tabular blocks or lithons floating in a serpentinite matrix form the polymictic melange. Greenstone (massive and pillowed basalt) and metasedimentary rocks are the most common rock types composing lithons. Mudstone and less common sandstone are protoliths for metasedimentary lithons. Lithons range in size from meters to kilometers long, and commonly are as much as tens of meters thick. The serpentinite matrix is highly sheared and broken into a foliated groundmass consisting of fragments of varying sizes. In addition, a large body of serpentinitized peridotite structurally overlies polymictic melange in the north orebody (Fig. 5). Tectonic interleaving of the various rocks within the ophiolite preceded formation of the McLaughlin deposit.

The Coast Range ophiolite in the mine area is overlain structurally by the Upper Jurassic Knoxville Formation, the basal formation of the Upper Jurassic and Cretaceous Great Valley sequence. The Knoxville Formation consists of mudstone, siltstone, fine-grained graywacke, and minor conglomerate. Bedding dips moderately northeastward.

The contact between the Knoxville Formation and the subjacent Coast Range ophiolite is the Stony Creek fault. Mudstone and serpentinite were structurally interleaved along the fault prior to mineralization. The fault dips moderately (30-45°) northeast in the deposit, but is vertical ($90^{\circ}\pm 20$) along strike to the northwest and to the southeast. Regionally, however, the Stony Creek fault is a shallowly dipping structure that is interpreted to have formed along the depositional contact between the hanging wall Knoxville Formation and the footwall Coast Range ophiolite (McLaughlin and Ohlin, 1984).

In the deposit, the Knoxville Formation, Coast Range ophiolite, and Stony Creek fault have been folded and faulted before and after mineralization. Pre-mineral folds in the Knoxville Formation have ramp-flat style geometry and are cut by bedding-parallel thrust faults. Bedding in the Knoxville Formation is broadly subparallel to the Stony Creek fault. Pre-mineral faults are also common in the footwall ophiolite where they bound lithologic packages. Footwall faults generally strike north-northwest at an angle to the more northwesterly to northerly striking faults in the hanging wall Knoxville Formation. Post-mineral deformation is summarized in a following section.

The Stony Creek fault in the deposit separates two domains of contrasting structural orientations. It is curvilinear through the deposit with minor to moderate changes in strike (Figs. 4 and 5). Right-separation, west-northwest trending and left-separation, northeast trending faults cut the Stony Creek fault (Figs. 5 and 6). Many of the small post-Stony Creek faults are post-mineral although some may have syn- or premineral displacements. Within the deposit, slip along the Stony Creek fault during mineralization was minimal to absent. Rather, the fault acted as a planar boundary separating two packages of rocks containing distinct structural fabrics.

Clear Lake Volcanics

The Clear Lake Volcanics are the youngest unit in the area of the McLaughlin deposit (Figs. 2, 3, and 4). The volcanics were erupted over the past 2.2 million years; the youngest rocks erupted 10,000 years ago (Donnelly-Nolan et al., 1981; Lehrman, 1986). Evolution of the volcanic field overlapped development of two basins that formed between late Cenozoic strike-slip faults. The older basin began forming prior to eruption of the Clear Lake Volcanics with its depocenter located east of Clear Lake in the area now occupied by the Pliocene and Pleistocene Cache Formation (Fig. 2) (Rymer, 1981; Hearn et al., 1988). The younger basin is occupied by Clear Lake (Fig. 2), and is the locus of younger volcanism and sedimentation.

Basaltic to rhyolitic rocks compose the Clear Lake Volcanics, with dacitic rocks being volumetrically dominant (Donnelly-Nolan et al., 1981; Hearn et al., 1981; Stimac and Pearce, 1992). Within the field, basaltic andesite erupted over a large region during the early evolution of the field (2.2 to 1.3 Ma) (Donnelly-Nolan et al., 1981, 1993). Mafic volcanism began synchronous with deposition in the late stages of the Cache Formation basin and continued after deposition ceased. Felsic rocks erupted during the younger stage (0.6 to 0.3 Ma) contemporaneous with onset of deposition in the Clear Lake basin (Hearn et al., 1988). The most recent volcanic rocks have basaltic compositions (Donnelly-Nolan et al., 1981).

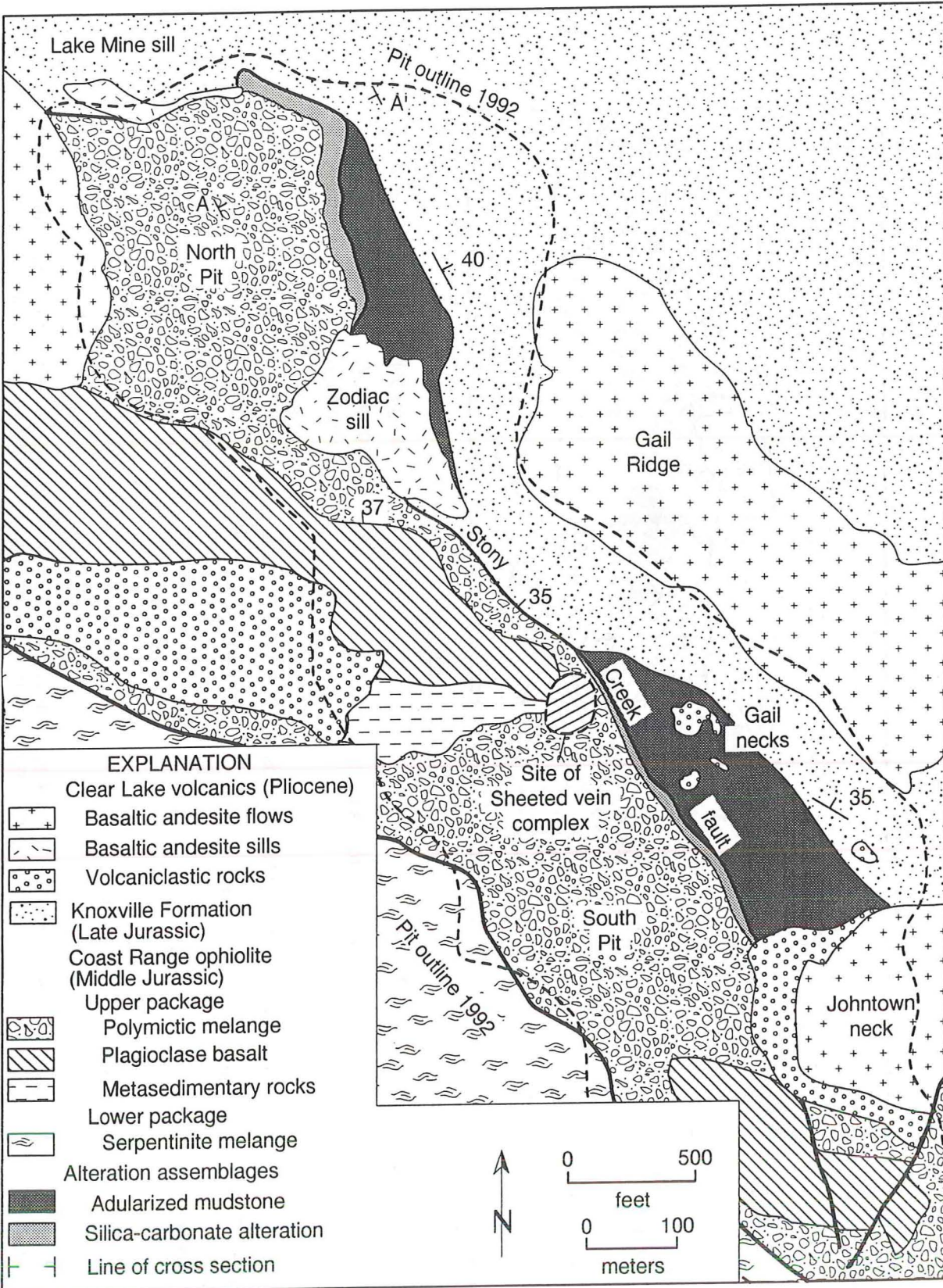
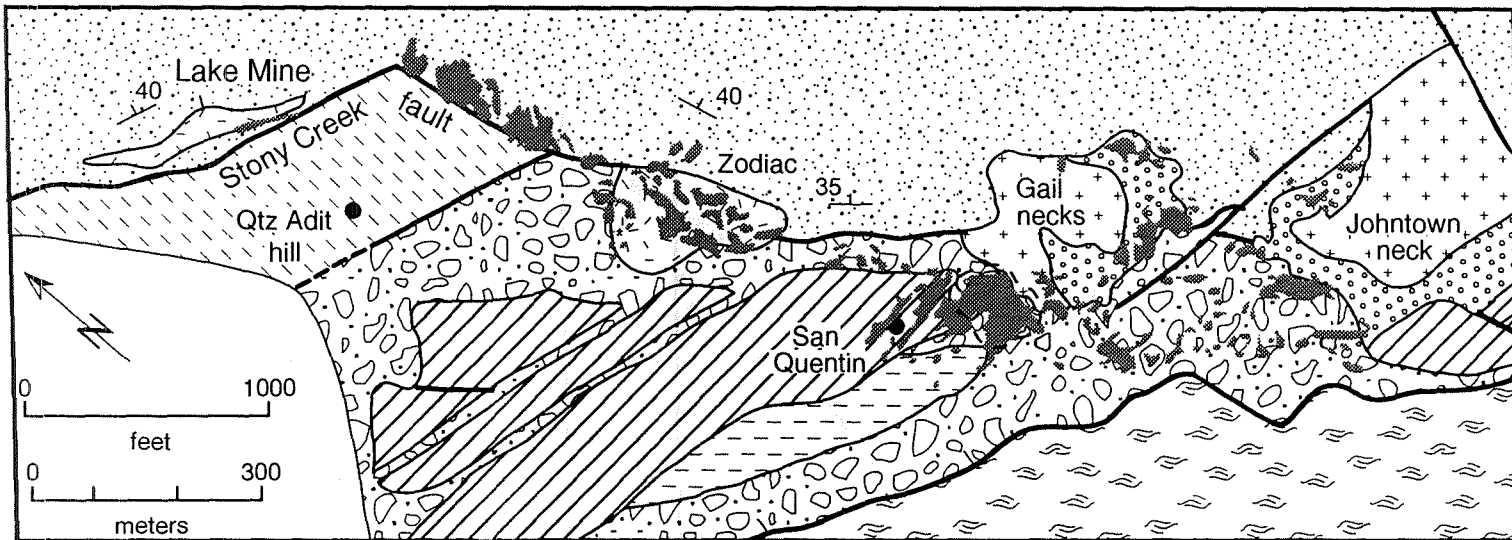


FIGURE 4. Simplified geologic maps of the McLaughlin Mine in 1992 showing the outline of the north and south open pits. Only the larger lithons in the Coast Range ophiolite are shown. Silica-carbonate alteration in the south pit is highly disrupted by post-mineral faulting and is not shown. Modified from geologic mapping by N.J. Lehrman, D.A. Enderlin, and G.C. Nelson of Homestake Mining Company.



EXPLANATION


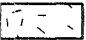
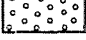


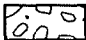
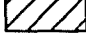

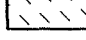

<p>Clear Lake volcanics (Pliocene)</p> <p> Basaltic andesite flows and intrusive rocks</p> <p> Basaltic andesite sills</p> <p> Volcaniclastic rocks and fragmental deposits</p> <p> Knoxville Formation (Late Jurassic)</p> <p>> 0.1 oz/ton Au symbol" data-bbox="141 702 181 726"/> > 0.1 oz/ton Au</p> <p> Outline of sheeted vein complex</p>	<p>Coast Range ophiolite (Middle Jurassic)</p> <p>Upper package</p> <p> Polymictic melange</p> <p> Plagioclase basalt</p> <p> Metasedimentary rocks</p> <p> Serpentinized peridotite</p> <p>Lower package</p> <p> Serpentine melange</p>
--	--

FIGURE 5. Geologic map of the McLaughlin deposit showing distribution of gold at the 0.1 troy ounces per ton cut-off grade on the 1780 bench level. Grade distributions are based upon assay values determined during mining. Basaltic andesite lava along Gail Ridge on the northeast margin of the deposit are not shown on the map. Pit outlines are not shown.

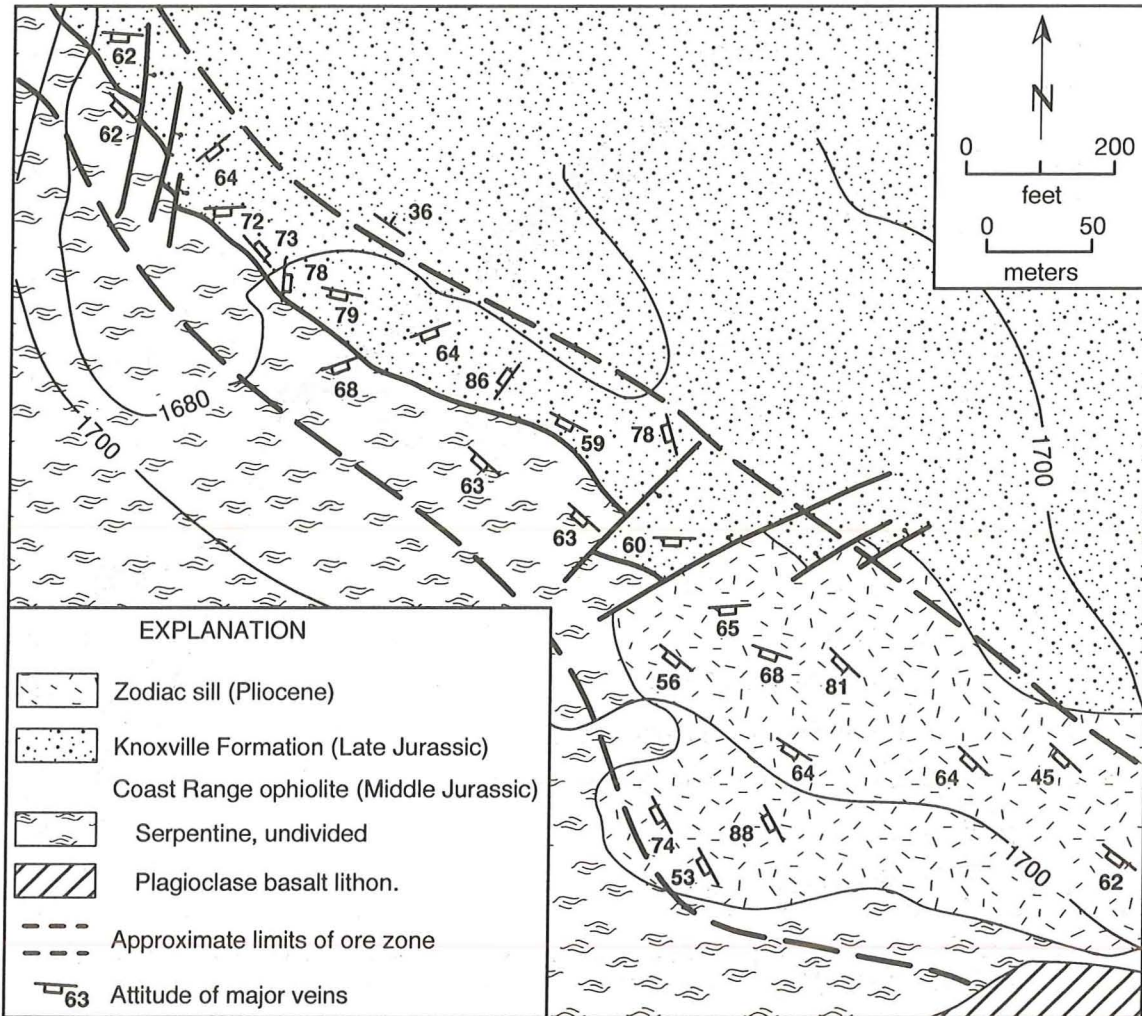


FIGURE 6. Simplified geologic map of the 1720 bench in the north pit showing the representative orientations of auriferous veins and their relation to the altered zone along the Stony Creek fault. Broad outline of altered rock composing the ore zone is simplified. Post-mineral faults cut and offset veins and ore zone. From pit geologic maps prepared by G.C. Nelson.

The Clear Lake Volcanics in the area of the McLaughlin Mine are characterized by basaltic andesite. Associated rocks include volcanoclastic deposits from phreatomagmatic eruptions, reworked fluvial deposits, and tuffs. Basaltic andesite forms sills, volcanic necks, and flows (Figs. 3, 4 and 5). The intrusions are localized along inflections in the Stony Creek fault. The northern sill, known as the Lake Mine sill, is a narrow lenticular body that plunges to the north down the dip of the Stony Creek fault. The Zodiac sill near the center of the deposit formed a triangular body near the surface and it narrowed and elongated down plunge eastward along the Stony Creek fault. A third intrusion has only been encountered in drill holes to the immediate east of the Lake Mine sill (Fig. 7). Remnants of explosion craters and intense brecciation overlay or characterized the Zodiac and Lake Mine sills, respectively, at shallow depths. One of these sills is probably also the source of basaltic andesite flows on Gail

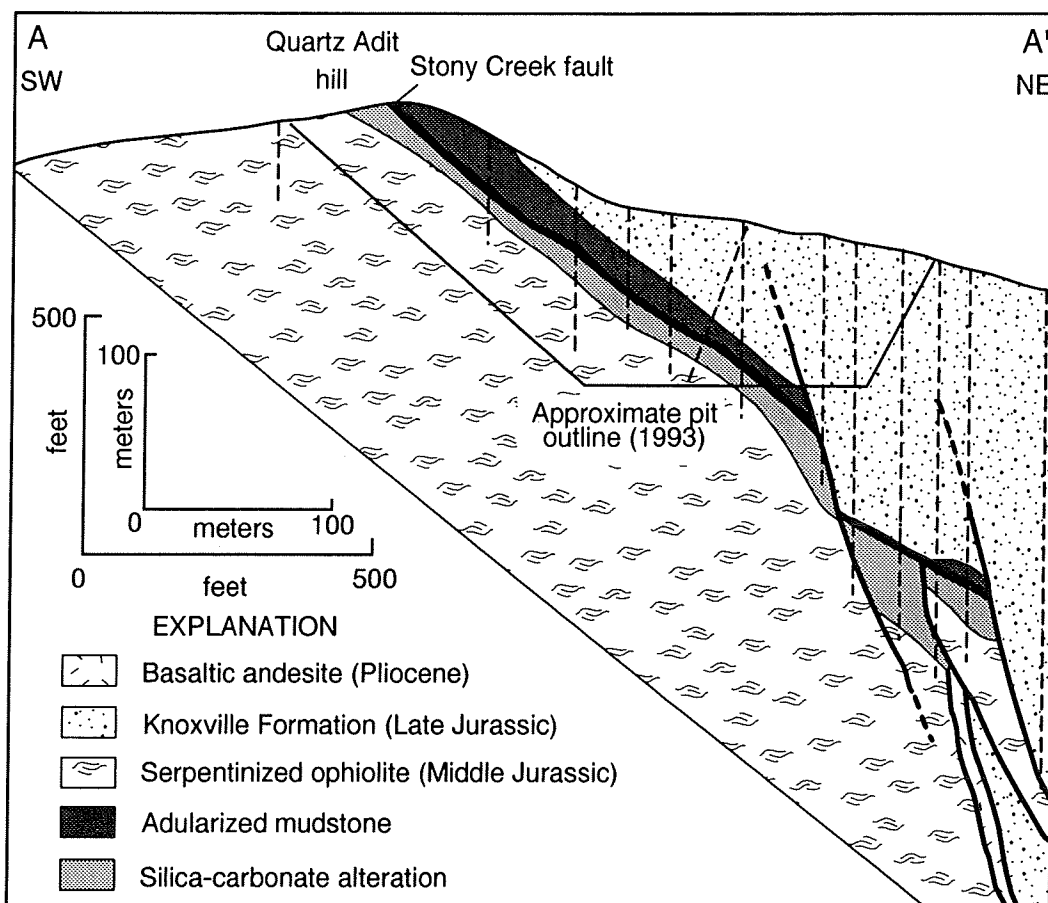


FIGURE 7. Cross section of northeastward dipping Sony Creek fault and subparallel altered rocks in the northern end of the north orebody. See figure 4 for location.

Ridge and Quartz Adit hill (Fig. 3). Flows filled a west-northwest trending valley that lay parallel to the structural grain in the footwall ophiolite. The paleovalley is now a topographic high because of post-volcanism erosion. One sample of basaltic andesite from Gail Ridge yielded a whole rock K-Ar date of 2.2 ± 0.2 Ma (Lehrman, 1986), which together with their composition indicate that the volcanic and intrusive rocks in the McLaughlin deposit correlate with the older parts of the Clear Lake Volcanics.

A subcircular basaltic andesite intrusion, known as the Johntown neck, forms an intrusive-extrusive complex at the southeast end of the deposit (Fig. 4). The intrusion plunges to the northeast. The Johntown neck filled a crater formed by a phreatomagmatic eruption. Intrusions filled the crater, and buried the volcanoclastic deposits that had blanketed the crater following the explosive event(s). The volcanoclastic rocks, composed of angular to subrounded fragments of basaltic andesite, ophiolite, mudstone, and serpentinite in a fine grained matrix, forms a funnel shaped deposit that underlies basaltic andesite. Fragmental volcanoclastic rocks also fill pipes, known as Gail necks (Fig. 4), that vented at the surface. Unlike the other explosive craters, no magma is present in the Gail necks, although

basaltic andesite derived from elsewhere did fill the crater. The Gail necks plunge shallowly (25°-30°) north-northeast, and the fragmental rocks of the necks are encountered in drill holes adjacent to the Zodiac sill. Fragmental volcanoclastic rocks also underlie or are interbedded with basaltic andesite flows on Gail Ridge and Quartz Adit hill. Clearly, vigorous and repeated phreatomagmatic activity was an integral part of volcanism in the late Pliocene.

Important sedimentary rocks crop out on the west side of the deposit (Fig. 3). Here, fine-grained sedimentary rocks, which were deposited in a lacustrine environment, overlie unconformably the Coast Range ophiolite. Detritus in the lacustrine rocks is exclusively ophiolitic, and fossils include reeds and wood fragments similar to modern redwoods. The lacustrine rocks grade into pumice-lapilli tuff, which represents the initial products of volcanic activity in the area. Fluvial deposits of sandstone and conglomerate overlie tuff and lacustrine rocks. Locally derived clasts of basaltic andesite, mudstone, and ophiolitic rocks are present, with fragments of hydrothermal vein, explosion breccia, and sinter becoming common near the stratigraphic top of the sequence. Sinter deposits overlay the fluvial rocks before mining. In addition, beds of fluvial and lacustrine sedimentary rocks are locally replaced by opal. These observations together with the evidence for vigorous phreatomagmatic activity are critical. Evidently, lakes and water-saturated ground characterized the area prior to eruption of basaltic andesite. Moreover, the rocks also attest to the presence of surface water during the life of the hydrothermal system that formed the McLaughlin deposit.

Late Cenozoic structure

Polyphase deformation on strike-slip, thrust, and normal faults characterizes the structural evolution of the Coast Ranges (Fig. 2). Most faults dip moderately to steeply northeasterly and easterly. Deformation began in the Mesozoic and continued episodically through the Cenozoic (McLaughlin et al., 1988; Phipps and Unruh, 1992). Many structures are still active (e.g. Hearn et al., 1988; Wong et al., 1988). Deformation since the Miocene resulted from two contrasting tectonic regimes that formed in response to transpressive strains in the San Andreas transform fault system (Fox, 1983; Hearn et al., 1988; McLaughlin et al., 1988; Phipps and Unruh, 1992). The relationship between the two regimes is unclear.

One regime consists of faults that are part of the present San Andreas transform fault system. Northwest-striking, right-lateral strike-slip faults and north-striking normal faults are characteristic. These structures record approximately north-south oriented shortening and east-west oriented extensional strains (Fox, 1983; Hearn et al., 1988). The inferred present-day stress field in the Geyser geothermal field, in the Clear Lake area, and along parts of the contact between the Coast Ranges and the Sacramento Valley (Figs. 1 and 2) is consistent with these strains (Bufe et al., 1981; Wong et al., 1988).

The second regime is formed by a fold and thrust belt that strikes subparallel to the San Andreas fault system (Phipps and Unruh, 1992). The fold and thrust belt formed during approximately northeast-southwest directed shortening normal to the strike-slip faults and to the plate margin. Wedging of slabs of the Franciscan Complex and the Coast Range ophiolite into the Great Valley Complex along folds and thrust faults is characteristic of this regime

(Phipps and Unruh, 1992). In many locations, thrust faults coincide with traces of strike-slip faults at the surface, whereas in other locations, thrust faults are cut or are reactivated by right-lateral strike-slip faults (Phipps and Unruh, 1992).

The McLaughlin deposit is located in the eastern part of the area widely cut by late Cenozoic dextral strike-slip faults and in the area cut by the late Cenozoic fold and thrust belt. It lies in that part of the Coast Ranges where northwest-striking strike-slip or thrust faults merge with more north-northwesterly striking folds and thrust faults (Fig. 2). Thus, it seems likely that the two tectonic regimes deformed the area of the deposit. How these two regimes interacted, if they did, during formation of the McLaughlin deposit is not completely understood. It is also uncertain which tectonic regime was dominant during formation of the deposit. Most workers have assumed that strains related to the strike-slip fault system were dominant during formation of the McLaughlin deposit (Lehrman, 1986, Enderlin et al., 1993), but this has yet to be demonstrated.

McLAUGHLIN DEPOSIT

General characteristics

The McLaughlin Mine lies in the center of the Knoxville Mining District (Fig. 2). Mercury mines, the Knoxville and Reid Mines, lie southeast and northwest of the McLaughlin Mine along the Stony Creek fault (Averitt, 1945). Smaller mercury prospects occupy the remainder of the district. Gold is relatively rare in the district outside of the McLaughlin deposit. For example, deep exploration in the Knoxville and Reid deposits demonstrates that although mercury mineralization extends to depths of 200 m, little gold is found. In these deposits, gold concentrations are usually less than 100 parts per billion (ppb). The highest gold concentrations averaged 1400 ppb over a 2 m interval at about a 160-m depth in the Knoxville Mine.

The McLaughlin Mine (1993) consists of two orebodies, referred to as the north and south orebodies, present along a 2 km strike-length of the Stony Creek fault (Fig. 4). A narrow area of limited mineralization separates the two orebodies. The south orebody contained a high-gold-grade vein complex that was the focus of initial mining. It also includes spatially distinct concentrations of auriferous veins, as does the north orebody (Fig. 5). There is no disseminated mineralization in the deposit. The orebodies plunge moderately to the east and northeast, subparallel to the Stony Creek fault. Deep drilling suggests that the two orebodies may converge with depth toward the projection of the Zodiac sill beneath the lower limits of economic mineralization.

One and perhaps two hot-spring sinter deposits were present prior to mining. One sinter is present only as blocks within a landslide on the north flank of the north orebody (Fig. 3). A source for the landslide blocks was not exposed, but the landslide was derived from the area of the Lake Mine sill and Quartz Adit hill at the northwestern end of the McLaughlin deposit. The second sinter, known as the San Quentin sinter (Fig. 3), was the location of one of the primary mining sites in the Manhattan mercury deposit, which produced 17,000 flasks of mercury (Lehrman, 1986). Lehrman (1986) has previously described the characteristics of the sinter, which reached about 35 m thick and 130 m long. Of particular interest was the abundance of hydrocarbons in some parts of the opaline silica sinter.

Low gold concentrations characterized the sinter with the notable exception of exceedingly rich gold veins cutting its base. Gold concentrations ranged from 3 to 2000 ppb, with the typical laminated sinter containing less than 300 ppb. The higher gold concentrations were present in explosion breccias interbedded in the sinter terrace. The sinter formed along the southwest margin of basaltic andesite flows that had filled a paleovalley lying parallel to what is now Gail Ridge (Fig. 3). Sinter laminations dipped shallowly ($\sim 10^\circ$) southward, and current indicators demonstrate southward flow away from the basaltic andesite. The San Quentin sinter lay in the approximate center of the hydrothermal system and formerly covered the northwest part of the south orebody where it overlay the richest concentration of gold in the deposit.

Gold is present free or as electrum, with varying Au/Ag ratios, either as dendrites or in association with amber to brown hydrocarbon-containing opal or chalcedony (Lehrman, 1986). Within petroliferous opal, gold occurs in 20-50 micron diameter oval shapes that represent former large fluid inclusions, as 2 to 4 micron size crystals that coalesce to form dendrites of gold along primary vein banding, and in syneresis cracks that cut crustiform banding (Rytuba, 1992). Hydrocarbons range from microscopic particles included within opal to macroscopic concentrations of oil, tar, bitumen, and curtisite ($C_{12}H_{18}$). All hydrocarbons are present over the vertical extent of the deposit, although tar, oil, and bitumen are more concentrated in shallow and peripheral areas where veins are present. Gold is not generally associated with tar, bitumen, and oil. However, high gold grades are commonly present in amber-colored petroliferous opal. Visible gold and electrum are common in deeper parts of the deposit.

Silver-bearing minerals are dominantly pyrrargarite (Ag_3SbS), myargarite ($AgSbS_2$), electrum, and less commonly polybasite ($(Ag,Cu)_{16}Sb_2S_{11}$). Other argentiferous sulfosalts are rare.

Cinnabar is present locally throughout the deposit, and was mined in the shallower levels of the deposit (Lehrman, 1986). Two stages of cinnabar deposition are recognized. The early stage consists of massive dark red cinnabar and black metacinnabar. Bright red, late stage cinnabar coats fractures. Quicksilver is rare. Base metal sulfides (chalcopyrite, galena, and sphalerite) are also rare, but become slightly more common with depth.

Multiple generations of non-auriferous pyrite and marcasite are present as gangue minerals (Lehrman, 1986). Both are widely distributed, but their presence does not positively correlate with gold content. Pyrite is present as a diagenetic mineral along bedding in mudstones and as a hydrothermal mineral in veins. Hydrothermal pyrite is locally rich in arsenic. Where a diagenetic pyrite-rich bed is cut by a vein, dendritic gold or electrum commonly nucleated on the pyrite. Stibnite is common throughout the orebodies and is particularly abundant in late stage veins. Many other sulfide and sulfosalts minerals are also present in the deposit, but most of these minerals are rare and only identified petrographically. Included are trace minerals of chromium oxides, indium-tin-gallium alloys, argyrodite (Ag_8GeS_6), arsenopyrite, orpiment, realgar, gersdorffite ($NiAsS$), and scheelite.

Barite and carbonate minerals, including calcite, dolomite, siderite and magnesite, are present in the gangue. Calcite is most common peripheral to the ore zone, whereas dolomite, siderite, and magnesite are associated with the ore zone. Magnesite is more common at depth.

The elemental association of the deposit is typical of hot-spring-type deposits (Table 1) (Lehrman, 1986, 1990). Concentrations of base metals, Mn, Se, Te, F, and Mo are not anomalous in the deposit (Lehrman, 1986). In fact,

the McLaughlin deposit has lower base metal concentrations than does the surrounding mafic rocks of the Coast Range ophiolite, and is thus a negative anomaly within the region. Ag/Au shows considerable variation both with depth and with location in the deposit (Fig. 8). In the south orebody, Ag/Au ranges between 10/1 at the surface in the base of the sinter to in excess of 20/1 at depths of about 200 meters (Lehrman, 1986) (Fig. 5). A similar range of Ag/Au characterizes most of the north orebody. In the vicinity of the Lake Mine sill in the northern part of the north orebody, Ag/Au increases from about 20/1 in the shallow part of the orebody to greater than 40/1 with depth. The changing ratio with depth reflects an increase in silver concentration with an almost constant gold concentration.

Fluid inclusion data and oxygen and deuterium isotopic analysis suggest that the ore forming fluids were boiling, low salinity meteoric fluids dominated by NaCl with low CO₂ concentrations (Sherlock, 1993a, b). Fluid evolution and metal deposition was controlled by boiling along a hydrostatic pressure gradient (Sherlock, 1993a, b). Other chemical data and stable isotopic studies of the McLaughlin deposit and other hot springs in the region suggest that at least three fluids are potentially responsible for the deposits (Peters, 1991; Rytuba, 1992; Donnelly-Nolan et al., 1993; Sherlock, 1993a, b). These include hydrocarbon transporting fluids, fluids from a contemporaneous cooling pluton at depth, and near surface meteoric waters. The relative role of each fluid in the formation of the auriferous deposits is not completely understood.

TABLE 1. Anomalous elements found in the McLaughlin deposit, northern California. Concentration ranges are in parts per million (ppm).

Element	Concentration range (ppm)
Au	1 to 10's
Ag	10's to 100's
Sb	100's to 1000's
As	0 to 100's
Hg	up to 30,000
Tl	10's

Age of mineralization

Basaltic andesite hosts mineralization and the 2.2 ± 0.2 Ma age on a flow on Gail Ridge (Fig. 3) places a maximum age on the mineralization. A minimum age is provided by a 750 ka K-Ar age on a whole rock sample of vein material. The vein contained alunite interlayered with cinnabar, and cut basalt and underlying volcanoclastic rocks in the base of the sinter. The alunite has been interpreted to be hypogene (Lehrman, 1986). Several other whole rock K-Ar ages from veins are intermediate between the 750-ka age and the age of the basaltic andesite (N.J. Lehrman, 1986, and unpublished data). The deposit is loosely dated as late Pliocene and Pleistocene.

Anatomy of the deposit

Precious metal mineralization is part of a sequence of events that formed the McLaughlin deposit. The deposit evolved in three stages. Locally pervasive alteration of host rocks and intrusion or eruption of basaltic andesite were

the earliest events. Once competent rocks were present in a near surface environment, cross-cutting fractures were filled by precious metal-bearing veins. Post-mineral faulting formed the last stage. Each stage is described below.

Alteration and magmatism

Adularization of the hanging wall mudstone of the Knoxville Formation and silicification of the footwall serpentinite of the Coast Range ophiolite were an important first stage in the formation of the deposit (Figs. 4). Mudstone lithons in the footwall ophiolite were also adularized. Silicification of the serpentinite consist of low-temperature silica-carbonate alteration typical of that found throughout the Coast Ranges (Sherlock et al., 1993), and opalite silica alteration formed during hot spring activity. Adularization and silicification formed a tabular body about the moderately dipping Stony Creek fault. The body of altered rocks is well preserved in the north orebody where it is thickest near the surface and narrows with depth (Fig. 7). It is still present at the deepest levels of exploration drilling. In the south orebody, the altered rocks are thickest adjacent to the Johntown neck, and thin abruptly northwest of the Gail necks toward the Zodiac sill (Fig. 4). Incompetent mudstone in the hanging wall and serpentinite in the footwall surround the competent altered rocks. The strong rheological contrast between altered and unaltered rocks was important for subsequent vein formation (Enderlin et al., 1993).

Intrusion and eruption of basaltic andesite were also part of the first stage. An unequivocal relationship between basaltic andesite intrusion and alteration is not yet demonstrated. There are, however, four observations important to understanding their potential relations. One, basaltic andesite is not silicified or adularized where in contact with the altered rocks. Rather, basaltic andesite is propylitized in these locations, just as it is outside of the deposit. Basaltic andesite is locally argillized adjacent to crosscutting veins. Two, adularized mudstone clasts are present in volcanoclastic explosion deposits and the matrix of these deposits is also altered. Three, adularized and silicified rocks are spatially associated with basaltic andesite intrusions (Fig. 4). Furthermore, the thickness of the altered zone decreases away from these intrusions, particularly to the northwest of the Johntown and Gail necks. Four, Sherlock et al. (1993) argued that silica-carbonate alteration did not form from hot-spring fluids; this alteration apparently preceded and postdated hot spring activity. Although these observations lead to an ambiguous conclusion, it seems probable that there is a genetic relationship between alteration and basaltic andesite. Most alteration evidently preceded intrusion. Some alteration probably was contemporaneous with and postdated intrusion. We propose that heat preceding rising magma interacted with ground water and drove convective circulation at a shallow level. Potassium-rich sedimentary rocks were converted to fine-grained adularia and serpentinitized ophiolite were silicified along fluid pathways. Vigorous phreatomagmatic activity followed as hot intrusions interacted with ground water.

Vein formation

Vein mineralization postdated alteration and intrusion. Hydrothermal breccias are also mineralized, and are common in the shallower levels but become sparse with depth. Veins are less than 1 mm thick to as much as 60 cm thick, and are composed of either a single vein or subparallel and crosscutting veins. Veins are present in two types

of occurrences. One occurrence is a sheeted vein complex that lay near the center of the deposit and represents the roots to the San Quentin sinter (Figs. 4 and 5). The sheeted vein complex contained about 25% of the total gold content of the deposit in only about 6% of the total rock volume before mining (Figs. 4 and 5). The remainder of the precious metal-bearing veins outside of the sheeted vein complex lie in discrete zones (Fig. 5). Veins cut (1) silicified and adularized rocks along the Stony Creek fault, as in the north orebody; (2) lithons and fault wedges of competent rocks within the polymictic melange, as in most of the south orebody; or (3) basaltic andesite necks, sills, and volcanoclastic rocks in both orebodies. Veins are rare in unaltered serpentinite or mudstone.

Veins in the sheeted vein complex strike northeast and dip steeply southeast (Fig. 9). In addition to the sheeted vein complex, three other sets of veins are recognized based on different orientations (Fig. 9). Veins of each set are mutually cross cutting, are subparallel to curvilinear, and anastomose along their strikes and down their dips. Intersection angles between individual veins within each set are typically between 20° and 30°. Veins of one set strike northeasterly (010°-045°) and dip steeply ($90^{\circ}\pm 15^{\circ}$) northwest or southeast. This set, known as group B veins, commonly contains the highest gold grades in the north orebody. A second set, known as group C veins, strike east-southeasterly (090°-130°) and dip moderately (40°-70°) southward. Where present in footwall lithons, they dip perpendicular to the external contacts between lithons and their serpentinite matrix (Fig. 10). In a few lithons, group C veins form small-scale swarms morphologically similar to the sheeted vein complex. Veins of the third set, known as group D veins, strike southwesterly (130°-180°) subparallel to the Stony Creek fault. Group D veins dip moderately southwesterly (40°-70°) normal to the dip of bedding in the Knoxville Formation and to the dip of altered rocks along the Stony Creek fault (Fig. 10). Some veins in groups C and D are thicker adjacent to bedding, lithologic contacts, and faults; these veins become thinner away from the planar structures. Groups B and C veins have limited strike continuity in the altered rocks along the Stony Creek fault. In contrast, group B veins extend for several tens of meters parallel to the strike of the altered rocks.

Along the 2 km length of the deposit outside of the sheeted vein complex, there are domains where specific sets of veins dominate. In the Lake Mine sill in the north orebody, group D veins are more common than the other two vein sets (Fig. 4). At depth in the northern part of the north orebody, group B veins are more common than are group C veins. Group C veins dominate the shallower levels of that orebody. Group D veins are ubiquitous at all levels in the north orebody. In contrast, group C veins are prevalent in the south orebody, outside of the sheeted vein complex, where much of the orebody is formed by veins in lithons within the footwall serpentinite or by veins in the Johntown and Gail necks (Fig. 5). Veins are not well developed in the tabular body of altered rock along the Stony Creek fault in the south orebody. Also in the north orebody, a general sequence of vein formation can be discerned. Group B are generally the oldest veins, whereas groups C and D veins are younger. The latest veins are most commonly group D veins, which are also the only veins that cut the sheeted vein complex. Because veins are mutually crosscutting, we infer that they formed during one hydrothermal system, and not during superposed events.

Veins consist of opal, chalcedony, and crystalline quartz. Where present in the thicker veins, growth bands on vein walls are crustiform, consisting of multiple and alternating layers of variously pigmented silica polymorphs. Quartz filled vugs or comb-textured quartz commonly occupy the center of a vein. Compositional growth bands

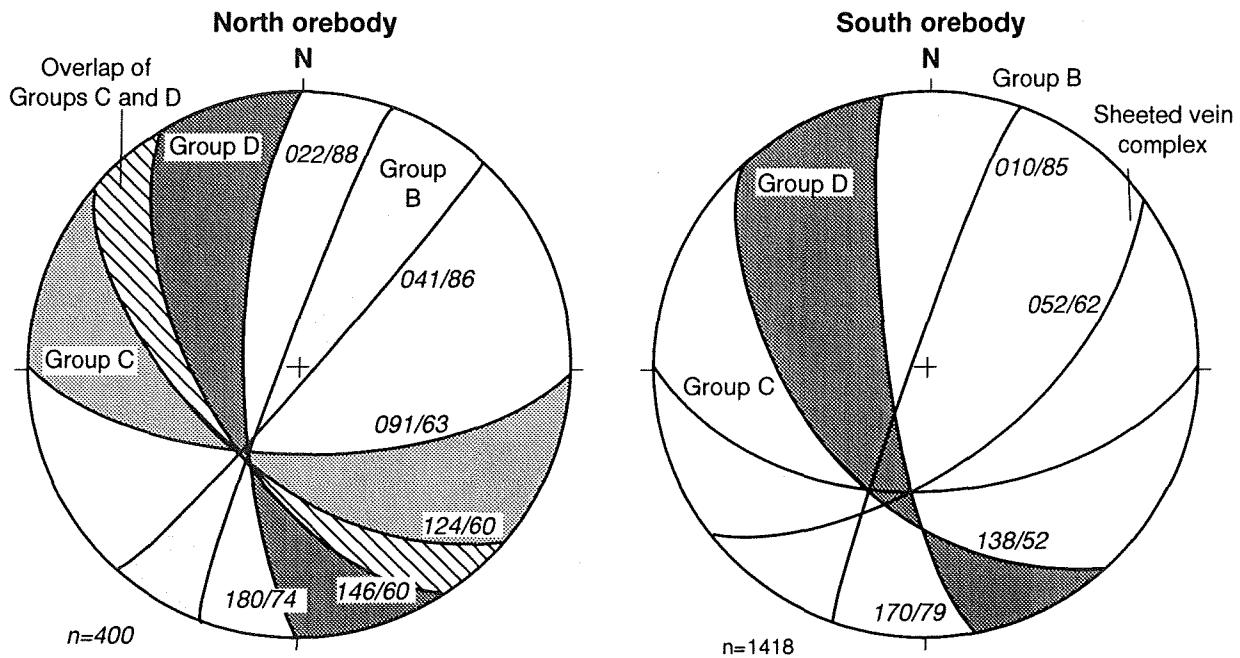


FIGURE 9. Lower hemisphere stereonets showing orientations of vein sets in the north and south orebodies. Vein orientations are depicted in two ways. For most of the data, a range of vein orientations for each group is shown, with the attitude of the limiting planes for each group noted. For some of the data from the south orebody, only an average plane can be shown as these data are derived from a single site. Data from the north orebody was collected on 1660-, 1680-, 1700-, and 1720-ft benches by R.M. Tosdal and G.C. Nelson in 1992, and contoured using 1%/1% area using Stereonet program written by Rick Allmendinger. Data from the south orebody was collected from 1985 to 1990 by N.J. Lehrman, D.A. Enderlin, G.C. Nelson, and other geologists of Homestake Mining Company.

in a vein are usually symmetric; that is, crustified banding on each vein wall is the compositional mirror image of the other. Other veins have asymmetric growth bands. In these veins, the hanging wall side is formed by rhythmically layered crustified silica whereas the footwall is formed by contorted bands of silica. The contorted banding is best explained by gravitational slumping of silica gel down the moderately dipping veins. Because of the preservation of the delicate crustified banding, each vein, regardless of its thickness, probably records a single episode of vein filling, with the growth bands reflecting changing fluid compositions. Where subparallel or crosscutting veins are present, repeated episodes of fracturing and fluid flux must have occurred during the dynamic evolution of the hydrothermal system.

The sheeted vein complex is up to 30 m thick, consisting of subparallel veins. The complex is spatially restricted to the southeast dipping contact between the end of a large lithon, composed of plagioclase-phyric basalt, and polymictic melange in the footwall of the Stony Creek fault. Few veins extend outside the cone-shaped complex. The complex narrows abruptly at depth into a few isolated veins. It grades laterally into barren rock over distances of less than 1 m to the east and south. The Stony Creek fault is the edge of the complex on the northeast. To the northwest, the complex overlapped the edge of the basalt lithon where it merged with east-southeast striking

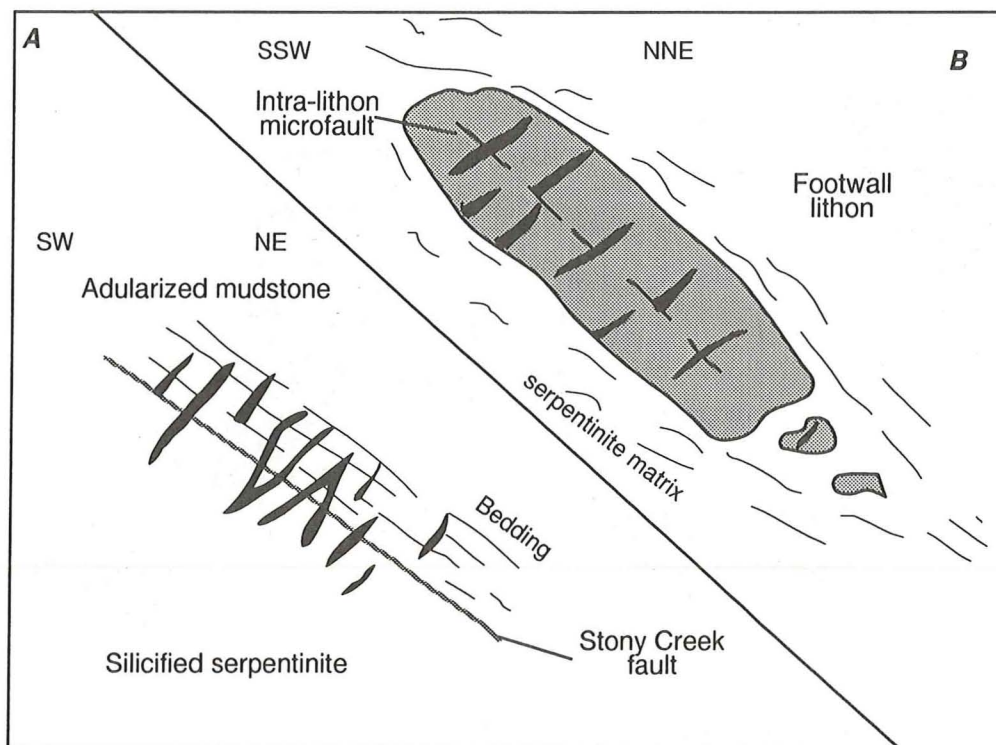


FIGURE 10. Cross sectional sketches showing the geometric relations between veins and planar structures. (A) Relation of group D veins to the Stony Creek fault, bedding in mudstones of the hanging wall Knoxville Formation, and the zone of altered rocks that parallels the Stony Creek fault. (B) Relation of group C veins to the lithons in the footwall ophiolite and to lithon-parallel microfaults. Not drawn to scale.

group C veins in the basalt lithon. The close spatial association of the sheeted veins and the southeast edge of basalt lithon suggests that the complex formed in a pressure shadow at the edge of the lithon.

Veins in the sheeted vein complex were apparently fed from group C veins emanating from the basalt lithon. Group C veins in the basalt lithon consist of crustified chalcedony and quartz with symmetrical growth bands. Nearer the sheeted vein complex, the same veins consist of angular remnants of crustified vein material attached to the hanging wall and broken angular fragments of crustified quartz and chalcedony floating unsupported in a matrix of gelatinous chalcedony. These veins pass into spheroidal opal veins. The compositional and textural variations along single veins not only support the concept of fluid flow from the lithon into the sheeted vein complex, but also indicate that fluid flux was locally rapid. It seems likely that throttling and seismic pumping were important mechanisms in the formation of the sheeted vein complex.

Group D veins always exhibit extension normal to vein walls, as do most groups C and D veins. There are, however, deviations from simple extension during vein formation. In the north orebody, limited evidence suggests some component of oblique opening on both groups B and C veins. Offset veins and microjogs suggest that sinistral shear accompanied opening of some group B veins and dextral shear accompanied opening of some group C veins. Similar evidence also indicates small components of normal slip on veins. In the south orebody, sinistral shear was

noted on some group C veins, particularly those in the southeastern part of the plagioclase basalt lithon (Fig. 5). The shear component on the veins is usually small, with offsets ranging from a few mm to 4 or 5 cm. Even where there is a shear component, there is also a component of dilation, commonly of equal magnitude, normal to the vein walls. In these cases, comb quartz crystal-growth textures are normal to vein walls, as they generally are in all veins including the sheeted vein complex.

Dilational during vein formation implies that extensional strains dominated. However, a significant number of veins also are extensional shear veins. In the north orebody, the sense of shear, where it could be determined, was consistent for each vein set. These observations imply that the incremental strain field probably did not shift significantly during formation of the veins. We suggest that the veins formed in an area characterized by low differential stress. In addition, the hydrothermal fluids under hydrostatic pressures (Sherlock, 1993b) probably also lowered the local effective stresses during mineralization. These conditions permit fractures to form in a wide variety of orientations with respect to the ambient stress field (Hill and Thatcher, 1992). Regardless of the details of the paleostress field, vein textures and kinematics are interpreted to indicate that the orientation of group D veins best approximates the direction of finite shortening strain (north-northwest to south-southeast shortening, $\sim 340^{\circ} \pm 20^{\circ}$) with finite extensional strain being oriented normal to it (east-northeast to west-southwest; $070^{\circ} \pm 20^{\circ}$). The inferred strain field in the deposit deviates from a strain field consistent either with (1) northwest-striking, right-lateral strike-slip faulting or (2) northeast-southwest directed thrusting, both of which have deformed the Coast Ranges since the Miocene (see above). A satisfying explanation for the differences is not known, but two possibilities are suggested. One, the strain field deduced for the McLaughlin deposit does not reflect the regional strain field, but was reoriented locally in response to structural heterogeneities. Two, post-mineral deformation could have rotated the area of the McLaughlin deposit. Evidence supporting either explanation is lacking.

Post-mineral deformation

Post-mineral deformation affects the orebody to varying extents, but is more intense in the south orebody than in the north orebody. Moderately to steeply dipping faults with north-northwest and northeast strikes are present. North-northwest striking faults are most common in the ophiolite where they dip moderately northeast parallel to the lithons. Post-mineral faults are marked by gouge and, locally, cataclasite. Where faults cut the ore zone, veins and altered rocks are brecciated and offset. Kinematics of these faults are poorly understood and probably complex. Normal or lateral separations less than 10 meters have been observed, as have low-angle faults with a thrust geometry. Northeast-striking faults cut the flows on Gail Ridge. These faults have normal separations with the blocks on the northwest side being downdropped. Post-mineral deformation has also reactivated the Stony Creek fault in the northern part of the north orebody where left-slip has occurred along the fault as it bends towards a west-northwest strike.

SUMMARY

The McLaughlin deposit is a hot-spring ore deposit that is spatially associated with late Pliocene and younger volcanism of the Clear Lake Volcanics in the northern California Coast Ranges. The deposit lies along the Stony Creek fault, a major lithotectonic contact that formed in the Mesozoic or early Cenozoic. Magmatism in the deposit area preceded mineralization, and was also localized along the fault. Multiple precious metal-bearing veins were deposited from ascending, boiling fluids. Gold, silver, and mercury were deposited in veins beneath two surficial sinters, only one of which was preserved before mining began. The largest concentration of gold lies beneath one sinter in a sheeted vein complex. Veins are not restricted to the areas beneath sinters, but are present over a 2-km long area.

The deposit formed after a major tectonic transition in the northern Coast Ranges at a time when tectonism changed from that associated with subduction-driven convergence to that associated with transpressional tectonics characteristic of the present San Andreas transform plate margin. The deposit lies at the eastern edge of the strike-slip system and within the zone of thrusting. How the regional tectonics influenced the structural evolution of the deposit is still ambiguous, and requires continued work within and outside of the deposit. Nevertheless, the McLaughlin deposit does represent a major precious metal deposit, and its presence, along with the auriferous Sulphur Creek deposit in the Sulphur Creek Mining District to the north (Fig. 2), raises the question of whether there are other deposits of their type located elsewhere in the Coast Ranges of California.

ACKNOWLEDGEMENTS

We thank Homestake Mining Company for access to the deposit and for the permission to include unpublished data in this contribution. Diana Mangan drafted the figures.

REFERENCES CITED

- Averitt, Paul, 1945 Quicksilver deposits of the Knoxville district, Napa, Yolo, and Lake Counties, California: *California Jour. Mines and Geol.*, v. 41, no. 2, p. 65-89.
- Berkstresser, C.F., Jr., 1968, Data for springs in the northern Coast Ranges and Klamath Mountains of California: U.S. Geol. Survey Open-File Rept., 49 p.
- Bufe, C.G., Marks, S.M., Lester, F.W., Ludwin, R.S., and Stickney, M.C., 1981, Seismicity of the Geysers-Clear Lake region: U.S. Geol. Survey Prof. Paper 1141, p. 129-137.
- Burnett, J.L., 1993, The mineral industry of California-1992: *California Geol.*, v. 46, no. 3, p. 219-224.
- Donnelly-Nolan, J.M., Hearn, B.C., Jr., Curtis, G.H., and Drake, R.E., 1981, Geochronology and evolution of the Clear Lake Volcanics: U.S. Geol. Survey Prof. Paper 1141, p. 47-60.
- Donnelly-Nolan, J.M., Burns, M.G., Goff, F.E., Peters, E.K., and Thompson, J.M., 1993, The Geysers-Clear Lake area, California: Thermal water, mineralization, volcanism, and geothermal potential: *Econ. Geol.*, v. 88, p. 301-316.
- Enderlin, D.A., Lehrman, N.J., Nelson, G.C., and Tosdal, R.M., 1993, Structural evolution of Au-Ag veins, McLaughlin Mine, northern California [abs.]: *Geol. Soc. America Abstracts with Programs*, v. 25, no. 5, p. 34-35.
- Fox, K.F., Jr., 1983, Tectonic setting of late Miocene, Pliocene, and Pleistocene rocks in part of the Coast Ranges north of San Francisco, California: U.S. Geol. Survey Prof. Paper 1239, 33 p.
- Fox, K.F., Jr., Fleck, R.J., Curtis, G.H., and Meyer, C.E., 1985, Implications of the northwestwardly younger age of the volcanic rocks of west-central California: *Geol. Soc. America Bull.*, v. 96, p. 647-654.
- Hearn, B.C., Jr., Donnelly-Nolan, J.M., and Goff, F.E., 1981, The Clear Lake volcanics: Tectonic setting and magma sources: U.S. Geol. Survey Prof. Paper 1141, p. 25-45.

- Hearn, B.C., Jr., McLaughlin, R.J., and Donnelly-Nolan, J.M., 1988, Tectonic framework of the Clear Lake basin, California, *in* Sims, J.D., ed., Late Quaternary climate, tectonism, and sedimentation in Clear Lake, northern California Coast Ranges: Geol. Soc. America Spec. Paper 214, p. 9-20.
- Hill, D.P., and Thatcher, Wayne, 1992, An energy constraint for frictional slip on misoriented faults: *Bull. Seismol. Soc. America*, v. 82, p. 883-897.
- Ingersoll, R.V., and Dickinson, W.R., 1981, Great Valley Group (Sequence), Sacramento Valley, California, *in* Frizzel, Virgil, ed., Upper Mesozoic Franciscan Rocks and Great Valley Sequence, central Coast Ranges, California: Pacific Section, Soc. Economic Paleontologists Mineralogists, p. 1-33.
- Lehrman, N.J., 1986, The McLaughlin Mine, Napa and Yolo Counties, California, *in* Tingley, J.V., and Bonham, Jr., H.F., eds., Precious-metal mineralization in hot spring systems, Nevada-California: Nevada Bur. Mines and Geol. Rept. 41, p. 85-89.
- Lehrman, N.J., 1990, The McLaughlin Mine, California: An update [abs.]: Program with abstracts Geol. Assoc. Canada, v. 15, p. A75.
- McLaughlin, R.J., 1981, Tectonic setting of the pre-Tertiary rocks and its relation to geothermal resources in the Geysers-Clear Lake area: U.S. Geol. Survey Prof. Paper 1141, p. 3-23.
- McLaughlin, R.J., and Ohlin, H.N., 1984, Tectonostratigraphic framework of the Geysers-Clear Lake region, California, *in* Blake, M.C., Jr., ed., Franciscan Geology of Northern California: Pacific Section, Soc. Economic Paleontologists Mineralogists, v. 43, p. 221-254.
- McLaughlin, R.J., Blake, M.C., Jr., Griscom, A., Blome, C.D., and Murchey, B., 1988, Tectonics of formation, translation, and dispersal of the Coast Range ophiolite of California: *Tectonics*, v. 7, p. 1033-1056.
- Nilsen, T.H., and Clarke, S.J., Jr., 1989, Late Cenozoic basins of northern California: *Tectonics*, v. 8, p. 1137-1158.
- Pearcy, E.C., and Petersen, U., 1990, Mineralogy, geochemistry, and alteration of the Cherry Hill, California, hot-spring deposit: *Jour. Geochem. Explor.*, v. 36, p. 143-169.
- Peters, E.K., 1991, Gold-bearing hot spring systems of the northern Coast Ranges, California: *Econ. Geol.*, v. 86, p. 1519-1528.
- Phipps, S.P., and Unruh, J.R., 1992, Crustal-scale wedging beneath an imbricate roof-thrust system: Geology of a transect across the western Sacramento Valley and northern Coast Ranges, California, *in* Erskine, M.C., Unruh, J.R., Lettis, W.R., and Bartow, J.A., eds. Field Guide to the tectonics of the boundary between the California Coast Ranges and the Great Valley of California: Pacific Section, Am. Assoc. Petroleum Geologists, p. 117-140.
- Rymer, M.J., 1981, Stratigraphic revision of the Cache Formation (Pliocene and Pleistocene), Lake County, California: U.S. Geol. Survey Bull. 1502-C, 35 p.
- Rytuba, J.J., 1992, Hot-Spring precious metal deposits in the Sonoma and Clear Lake volcanic field, CA, USA, *in* Frazee, Portia, eds, Proc. MineExpo Symposium, 15 p.
- Saleeby, J.G., 1992, Prototectonic and paleogeographic settings of U.S. Cordilleran ophiolites, *in* Burchfiel, B.C., Lipman, P.W., and Zoback, M.L., eds., The Cordilleran Orogen: Conterminous U.S.: Boulder, Geol. Soc. America, The Geology of North America, v. G-3, p. 653-682.
- Sherlock, R.L., 1993a, The geology and geochemistry of the McLaughlin sheeted vein complex, northern Coast Ranges, California: Waterloo, Ontario, University of Waterloo, Ph.D. thesis, 309 p.
- Sherlock, R.L., 1993b, The genesis of the McLaughlin Mine sheeted vein complex, Fluid inclusion and stable isotope evidence, *in* Rytuba, J.J., ed., Active geothermal systems and gold/mercury deposits in the Sonoma/Clear Lake volcanic fields, California: Soc. Econ. Geol. Guidebook Series, [this volume].
- Sherlock, R.L., Logan, M.A., and Jowett, E.C., 1993, Silica carbonate alteration of serpentinite, implications for the association of precious metal and mercury mineralization in the Coast Ranges, *in* Rytuba, J.J., ed., Active geothermal systems and gold/mercury deposits in the Sonoma/Clear Lake volcanic fields, California: Soc. Econ. Geol. Guidebook Series, [this volume].
- Stimac, J.A., 1992, and Pearce, T.H., 1992, Textural evidence of mafic-felsic magma interaction in dacite lavas, Clear Lake, California: *Am. Mineral.*, v. 77, p. 795-809.
- Wong, I.G., Ely, R.W., and Kollmann, A.C., 1988, Contemporary seismicity and tectonics of the northern and central Coast Ranges-Sierran Block boundary zone, California: *Jour. Geophys. Res.*, v. 93, no. B7, p. 7813-7833.

THE GENESIS OF THE McLAUGHLIN MINE SHEETED VEIN COMPLEX, FLUID INCLUSION AND STABLE ISOTOPE EVIDENCE

Ross L. Sherlock

Mineral Deposit Research Unit, Department of Geological Sciences, University of British Columbia, Vancouver, B.C. V6T 1Z4

ABSTRACT

The McLaughlin Mine is a hot-spring type gold-mercury deposit located in the Coast Ranges of northern California. The "sheeted vein complex" is the center of the hot-spring system that formed the McLaughlin deposit. The sheeted vein complex merges from a subaerial siliceous sinter into a bilaterally symmetric, subparallel, multistage vein swarm. The precious metals are well zoned with gold largely restricted to the upper 200 m of the deposit. Silver can dominate anywhere in the system but is always more abundant than gold below 200 m. Below 350 m, silver is rare, gold has not been observed and mineralization is dominated by base metal sulfides. Fluid inclusion analysis suggest that the ore forming fluids were low salinity NaCl dominated, low CO₂ fluids. The deepest samples (> 800 m below the paleosurface) have an average temperature of 235°C. The ascending hydrothermal fluid intersected the hydrostatic boiling curve at ~400 m below the surface and paralleled the hydrostatic boiling curve to the surface. Boiling of an ascending hydrothermal fluid accounts for the metal zoning observed in the sheeted vein complex. During boiling CO₂ is partitioned into the vapor phase faster than H₂S, resulting in the deeper portions of the ore body being enriched in silver with respect to gold and the shallow portions of the ore body enriched in gold with respect to silver. On the basis of the physical and chemical conditions of the ore forming fluids, gold grade, as well as silica and temperature gradients the hydrothermal fluid is undersaturated with respect to gold prior to the onset of boiling. There is a strong trend for increasingly light $\delta^{18}\text{O}_{\text{Qtz}}$ with depth. The most isotopically enriched samples are from the subaerial sinter and the lightest sample are from the deepest samples. This trend is a temperature effect and is the result of increasing fractionation with decreasing temperature. The oxygen isotopic composition of the hydrothermal fluid remained fairly constant at ~9.3‰. The oxygen and deuterium composition of the hydrothermal fluids are consistent with a meteoric water origin. The hydrothermal fluids have a pronounced oxygen shift due to water/rock interaction but do not have a deuterium shift. The water/rock ratios are low but similar to other geothermal systems in the Coast Ranges and other epithermal deposits emplaced within sedimentary sequences.

INTRODUCTION

The McLaughlin Mine is a hot-spring type gold-mercury deposit located in the northern Coast Ranges of California. The McLaughlin deposit is unique among epithermal systems in that an *in situ* subaerial sinter is preserved. The sinter represents the ground surface at the time of hydrothermal activity and allows the depth at which the veins formed to be directly measured. Located below and continuous with the sinter is a large precious metal mineralized vein swarm and associated smaller veins (Fig. 1). The subaerial sinter and the veins are collectively referred to as the "sheeted vein complex". Below the sheeted vein complex are small quartz veins with base metal mineralization. Although direct continuity of these base metal bearing veins with the sheeted vein complex has not been established, they likely represent the root zone of the hydrothermal system. The sheeted vein complex represents a complete epithermal system from the paleosurface to the base metal root zone (e.g. Buchanan, 1981).

Geothermal systems are often considered modern analogs of epithermal ore deposits. However, comparisons are often unconvincing because of the general absence of a preserved sinter in epithermal deposits and the lack of economically significant precious metal mineralization in active geothermal systems. The sheeted vein complex represents a fully preserved fossil geothermal system with economic concentrations of precious metals that bridges the gap between modern geothermal systems and epithermal ore deposits.

The sheeted vein complex is the center of hydrothermal activity that formed the McLaughlin hot-spring gold deposit and is the focus of this study. The sheeted vein complex is a pipe-like body ~50 m in diameter composed of centimeter- to meter-wide subparallel veins showing bilateral symmetry. The sheeted vein complex formed in a large dilatant zone at the contact between a tholeiitic basalt lithon and serpentinite melange. The subparallel, symmetric vein configuration suggests that the dilation zone was repeatedly opened maintaining high permeability and focusing fluid flow. Although the veins are dominantly subparallel, cross-cutting relationships are common and extremely complex making the many paragenetic stages impossible to identify with certainty.

METHODOLOGY

This manuscript summarizes some the author's research on the sheeted vein complex. The metal zoning is based on gold and silver assays from exploration drill core as well as conventional petrography of over 100 polished sections throughout the depth profile.

Fluid inclusion analysis were conducted on a Fluid Inc. USGS gas flow heating freezing stage. Calibrations were made with organic and inorganic standards with known melting points as well as with synthetic fluid inclusions. The accuracy of the thermocouple is considered to be better than $\pm 0.2^{\circ}\text{C}$ over the temperature range of the study. Over one hundred doubly polished fluid inclusion sections were prepared from eighty samples over the full depth range available.

Oxygen was extracted from silicates using bromine pentafluoride and converted to CO_2 over a heated graphite rod (Taylor and Epstein, 1962; Clayton and Mayeda, 1963) and analyzed at the University of Western Ontario on a gas source mass spectrometer. Fluid inclusion extracts were produced by crushing clean quartz samples, that had large and abundant fluid inclusions, in a vacuum using a modified technique of Rye (1966). The fluid

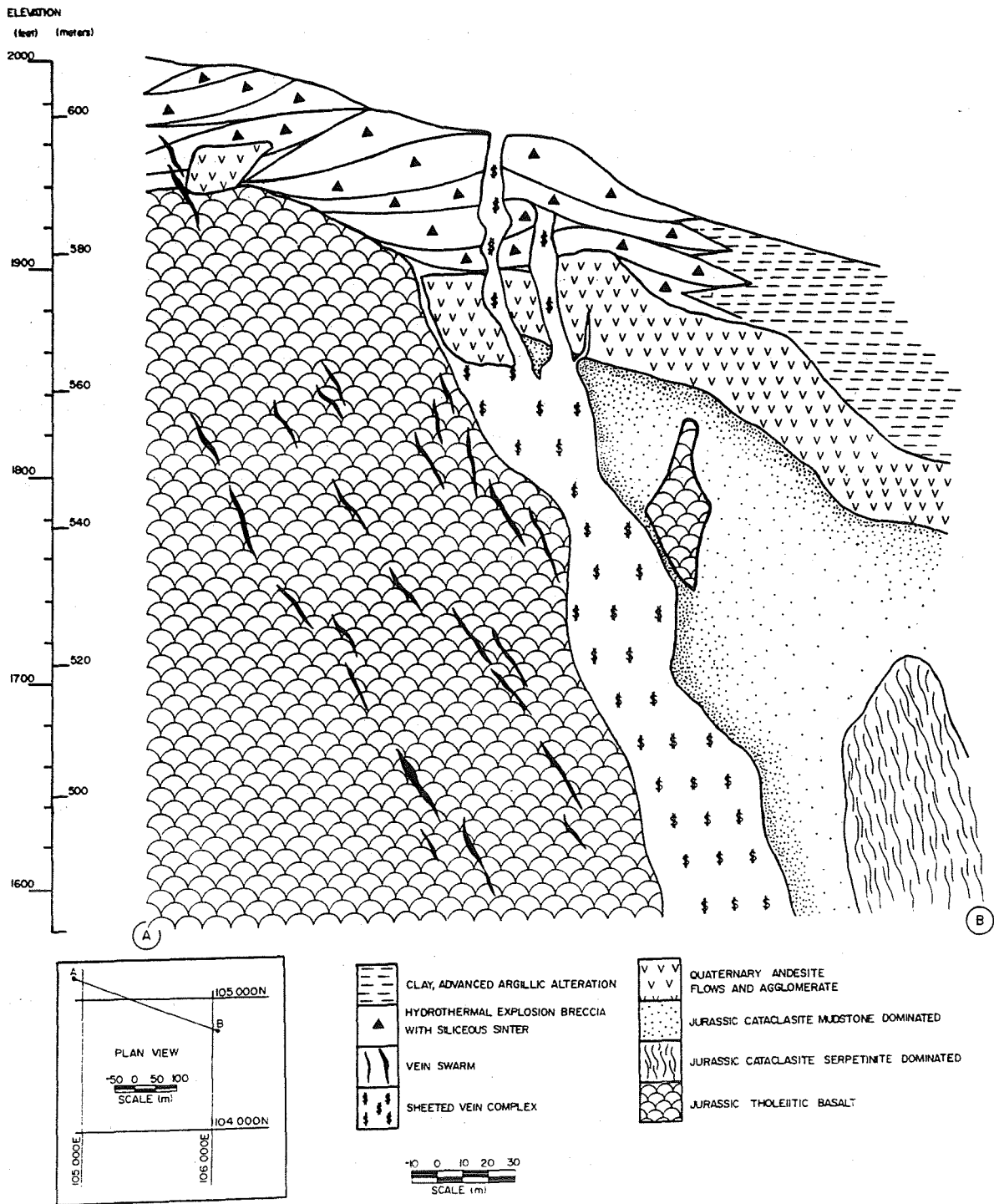


FIGURE 1. Simplified cross section through the sheeted vein complex. The section is approximately parallel to the Stony Creek Fault and shows only footwall lithologies. Compiled from geological bench maps from Homestake Mining Company, and mapping by the author.

extracts were frozen onto metallic zinc and reduced to H₂ gas using the method of Coleman et al. (1982) and analyzed using a gas source mass spectrometer at the University of Waterloo. Deuterium composition of montmorillonite was determined commercially at Krueger Enterprises Inc.

PREVIOUS WORK

Two previous works on fluid inclusion and stable isotope relations have been conducted on the McLaughlin deposit. The data from both of these studies is consistent with the results presented here. T. James Reynolds (Homestake internal report, 1982) examined twelve samples, for fluid inclusion analysis, from the sheeted vein area at depths between 33 and 112 m below the sinter. Fluid inclusion homogenization temperatures varied between 120 and 160°C, with some as high as 190°C. The homogenization temperatures for each sample straddled the depth to boiling point curve for pure water. Salinities calculated from the final melting temperatures and the equations of Potter et al., (1978) were generally less than 4 wt. % NaCl eq. but did range up to 14.5 wt. % NaCl eq. for one sample. The samples were crushed under oil and no evidence of CO₂ was observed.

Peters (1991) analyzed twelve samples for both fluid inclusions and $\delta^{18}\text{O}_{\text{Qtz}}$ from the sheeted vein complex at a depth of 49 m below the sinter. The average homogenization temperature was ~150°C which is similar to the boiling temperature of pure water (160°C) for that elevation. Fluid salinities averaged ~1.5 and ranged up to ~4 wt. % NaCl eq. Samples were crushed under oil and no evidence for CO₂ was found. The samples had an average $\delta^{18}\text{O}_{\text{Qtz}}$ value of 23.8‰. Using the average homogenization temperature of 150°C, the average $\delta^{18}\text{O}_{\text{Qtz}}$, and the fractionation factor of Clayton et al., (1972) the isotopic composition of the fluid in equilibrium with the quartz is 8.4‰.

METAL ZONING

A compilation of 1646 gold and silver assays, from exploration drill core in the sheeted vein complex shows the metal zoning as a function of depth below the sinter (Fig. 2). In the upper 200 m of the sheeted vein either gold or silver is the dominate precious metal. However, below 200 m gold is seldom greater than 20% of the total precious metal content and below 350 m gold has not been observed.

There is a very generalized mineralogical zoning in the sheeted vein. The sinter is typically barren of gold (< 10 ppb), only when it has been hydrothermally brecciated or cross-cut by hydrothermal veins does it contain up to several ppm gold. In the upper 50 m of the sheeted vein gold is relatively common, generally very fine grained and associated with minor silver sulfosalts. Below the upper 50 m the silver sulfosalt content increases and gold is generally coarser in size and present as discrete grains within the sulfosalt rich zones. Below 200 m, mineralization is dominated by silver sulfosalts and subordinate gold. Below 350 m, gold has not been observed, silver sulfosalts are present but uncommon, and mineralization is dominated by base metal sulfides.

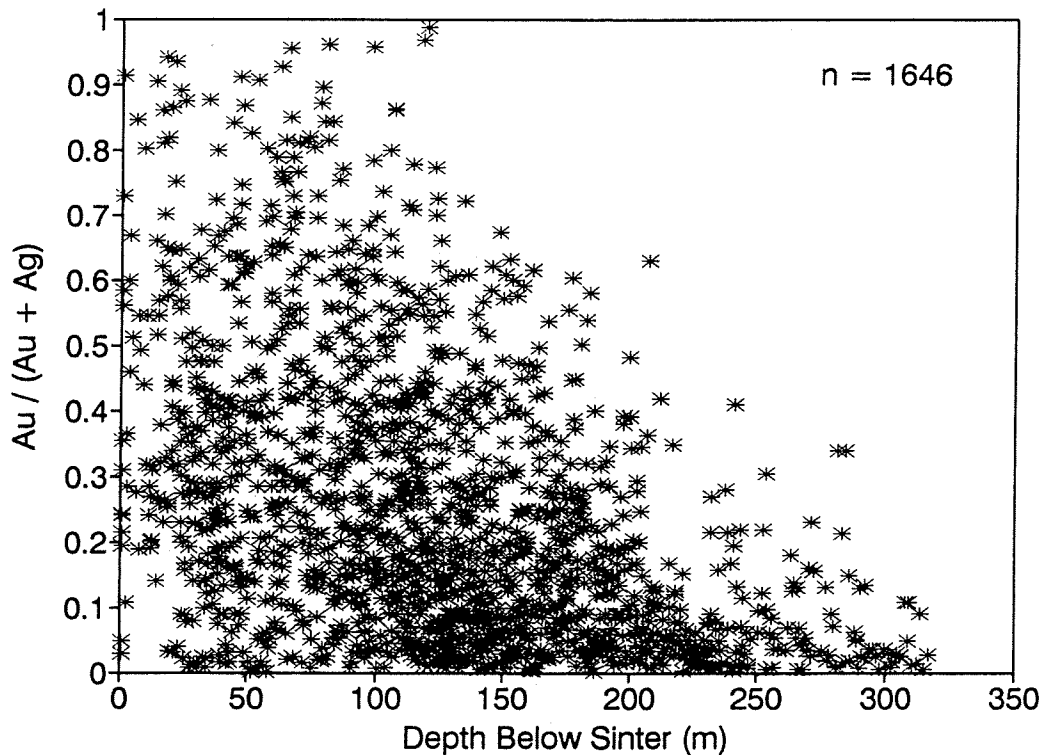


FIGURE 2. Compilation of Au and Ag assays from exploration drill core, plotted against depth below the sinter.

FLUID INCLUSION DATA

Petrography

The fluid inclusion study was conducted on vein quartz from the sheeted vein complex. Due to the complex cross-cutting vein relationships it was not possible to identify and analyze a single paragenetic phase. To avoid comparing different vein stages only samples with gold, silver, or in the deep samples base metal mineralization were analyzed. Although the samples are not of the same paragenetic phase they are all representative of ore stage fluids.

Only samples of crystalline quartz were used for fluid inclusion analysis. Chalcedony and opal may form by direct precipitation from solution or by transformation of an amorphous phase (Fournier, 1985). In the case of direct precipitation, primary fluid inclusions would represent the conditions at the time of precipitation. If the chalcedony or opal formed as a result of transformation of an amorphous phase then primary fluid inclusions would have little meaning. Due to the indeterminate origin of the chalcedony and opal these materials were not used in this study.

Fluid inclusions are rare, however, when present they are commonly large (> 10 μm) and always contain two phases, liquid and vapor. Liquid-dominated inclusions are the most common and typically have 10 to 20% visually estimated vapor phase and always homogenize to a liquid. Vapor-dominated inclusions typically have greater than 90% visually estimated vapor phase and when heated homogenize to a vapor. For vapor-dominated inclusions

total homogenization could never be convincingly determined so for these fluid inclusions homogenization temperatures must be regarded as minimum values (Stern, 1992).

Fluid inclusions analyzed were either primary or pseudosecondary (Roedder, 1984). Primary fluid inclusions occur along growth bands or as isolated inclusions or clusters of inclusions. Pseudosecondary inclusions occur along fractures that originate and terminate within a single quartz grain. Secondary inclusions were not analyzed due to their indeterminate origin.

In general approximately 5 inclusions were analyzed from each sample. If the data for the five inclusions is consistent then no more were analyzed. This ensures that the data are not biased by samples with abundant inclusions.

Freezing Data

Temperatures of first melt were obtained on 87 fluid inclusions from 33 samples over the full depth range available. The data ranges from -44.6 to -21.0°C with a median of -36.0°C (Fig. 3). This temperature is consistent with the melting of salt hydrates in the H₂O-NaCl system (Davies et al., 1990).

Temperatures of final melt were obtained on 107 fluid inclusions from 33 samples over the entire depth range available. The data ranges from -4.6 to -0.2°C with a median of -1.4°C (Fig. 4). Salinities, calculated from the final melting temperatures and the relationship of Oakes et al. (1990; XCaCl₂ = 0.0), range from 7.3 to 0.3 weight percent NaCl equivalent (wt. % NaCl eq.) with a median of 2.4 wt. % NaCl eq. or 0.4 molal.

Crushing Data

Fluid inclusion plates were crushed under oil to determine the presence of non-condensable gases. The crushing tests, as described by Roedder (1984) were successfully performed on twelve fluid inclusion chips over the entire depth range available. In each test the vapor bubble of individual inclusions was observed to rapidly collapse and disappear. This suggests that the vapor phase is a near vacuum and that the concentration of non-condensable gases, including CO₂, is less than 0.1 to 0.2 mole percent (Bodnar et al., 1985).

Heating Data

Depth to Boiling Point Calculations

The presence of a subaerial sinter makes the sheeted vein complex unique since the depth at which the veins formed can be directly measured. The depth constraint allows the depth to boiling point curves to be calculated for various hydrothermal solutions. Five different solutions were considered that bracket the inferred composition of the ore forming fluids. Under hydrostatic conditions, pure water and a 5 wt. % NaCl fluid are used. Also under hydrostatic conditions pure water with 0.5 mole % CO₂, and a fluid with 5 wt. % NaCl and 0.5 mole % CO₂ are used. These fluids represent the maximum amount of dissolved gases present in the ore forming fluids indicated by crushing data. The actual amount of dissolved gas present is likely less than what these curves represent. A fifth

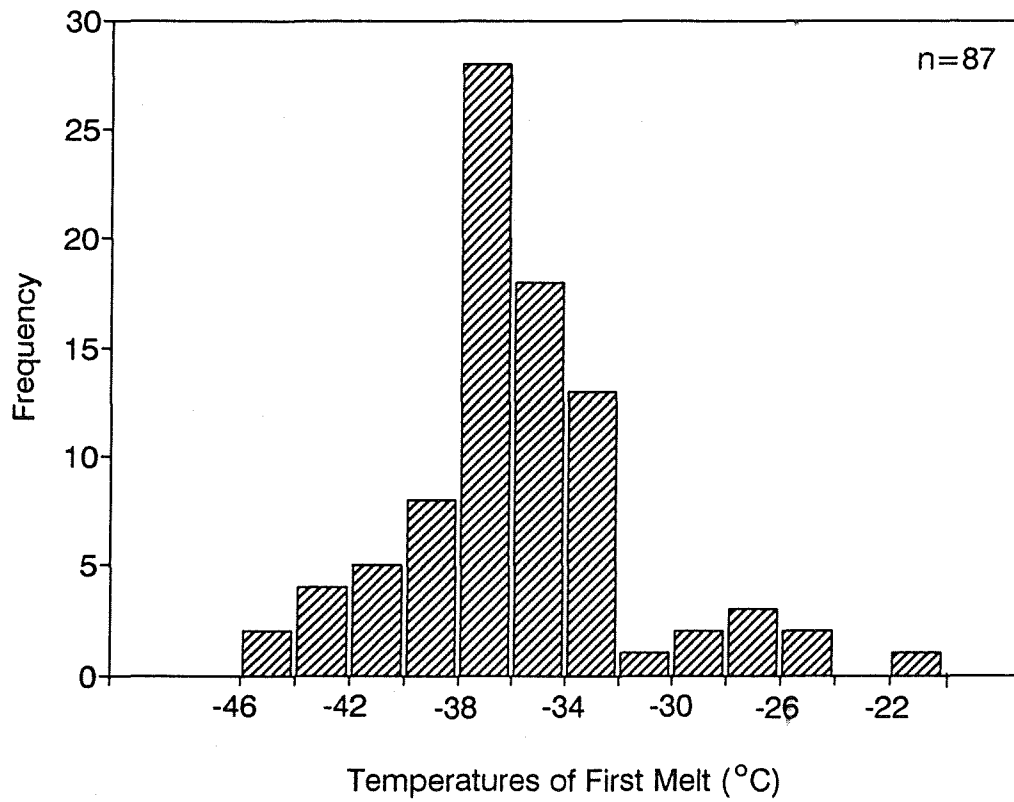


FIGURE 3. Histogram of fluid inclusion temperatures of first melt.

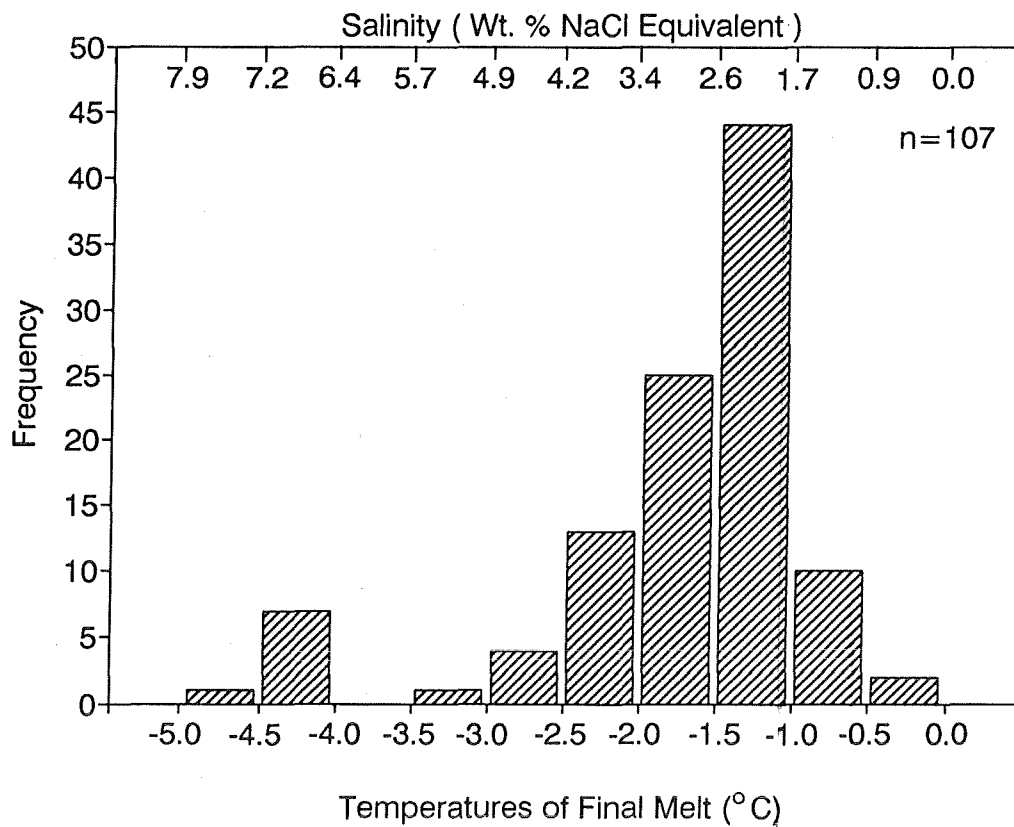


FIGURE 4. Histogram of fluid inclusion final melting temperature. Also shown is the corresponding salinities calculated using the relationship of Oakes et al., (1990).

solution of pure water under lithostatic conditions was also used. These fluid compositions bracket the range in compositions seen in fluid inclusions.

The depth to boiling point curves for the fluids with no dissolved gases were taken from Haas (1971). The depth to boiling point curves for fluids with dissolved CO₂ were calculated using the technique of Henley (1984a). The fluid is assumed to boil adiabatically with the vapor phase removed after each boiling increment. The partitioning of CO₂ into the vapor phase during boiling and the concentration of CO₂ left in the fluid phase is calculated after each boiling increment. The depth to boiling point curves were calculated from 250 to 100°C in 10° increments. A starting temperature of 250°C was used as an approximation of the deepest reservoir fluids at McLaughlin based on fluid inclusion data. During boiling volatiles are rapidly partitioned into the vapor phase therefore the shape of these curves is dependent on the initial few increments of boiling. For this reason these curves can not be extrapolated to higher temperatures or greater depths.

Homogenization Data

Homogenization temperatures were obtained for 287 fluid inclusions from 53 samples over the entire depth profile available (Fig. 5). The homogenization temperatures are plotted on the same diagram as the depth to boiling point curves. The circles represent the mean homogenization temperature and the horizontal line represents the standard deviation. Open circles represent samples that homogenized to a vapor phase and the closed circles represents samples that homogenized to a liquid phase. For clarity samples from the same elevation are represented as a single point

For samples below 400 m the homogenization temperatures remain fairly constant and are always lower than the depth to boiling point curve. For the deepest samples, below 800 m, the fluid inclusion homogenization temperature varies from 184 to 263°C averaging 235°C. At ~400 m the fluid temperatures intersect the hydrostatic boiling curve. Above 400 m the homogenization temperature varies from ~230°C at 400 m to ~150°C at 50 m (Fig. 5). Discharge temperatures are likely around 80 to 100°C, consistent with the discharge temperatures of large hot-spring systems (Henley, 1984b).

Pressure Gradients

A histogram of homogenization temperatures (Fig. 6) for all the samples at the 1580 bench (128 m below the sinter) are plotted along with the hydrostatic and lithostatic boiling temperatures for pure water. The bulk of the data falls between the hydrostatic and lithostatic boiling temperatures. There is a small population of inclusions with homogenization temperatures below the hydrostatic boiling temperature but none with temperatures in excess of the lithostatic boiling temperature. The mean homogenization temperature is 201°C, but the boiling temperature of pure water at this depth under hydrostatic conditions is 189°C suggesting that the hydrothermal fluid pressure is generally in excess of the hydrostatic pressure. White et al. (1975) measured the down hole pressure gradients at Yellowstone and suggested that convective or buoyancy pressures combined with permeability restrictions may lead to pressures in excess of the hydrostatic load. Grant et al. (1982) suggested that for fluid flow to occur in a geothermal well

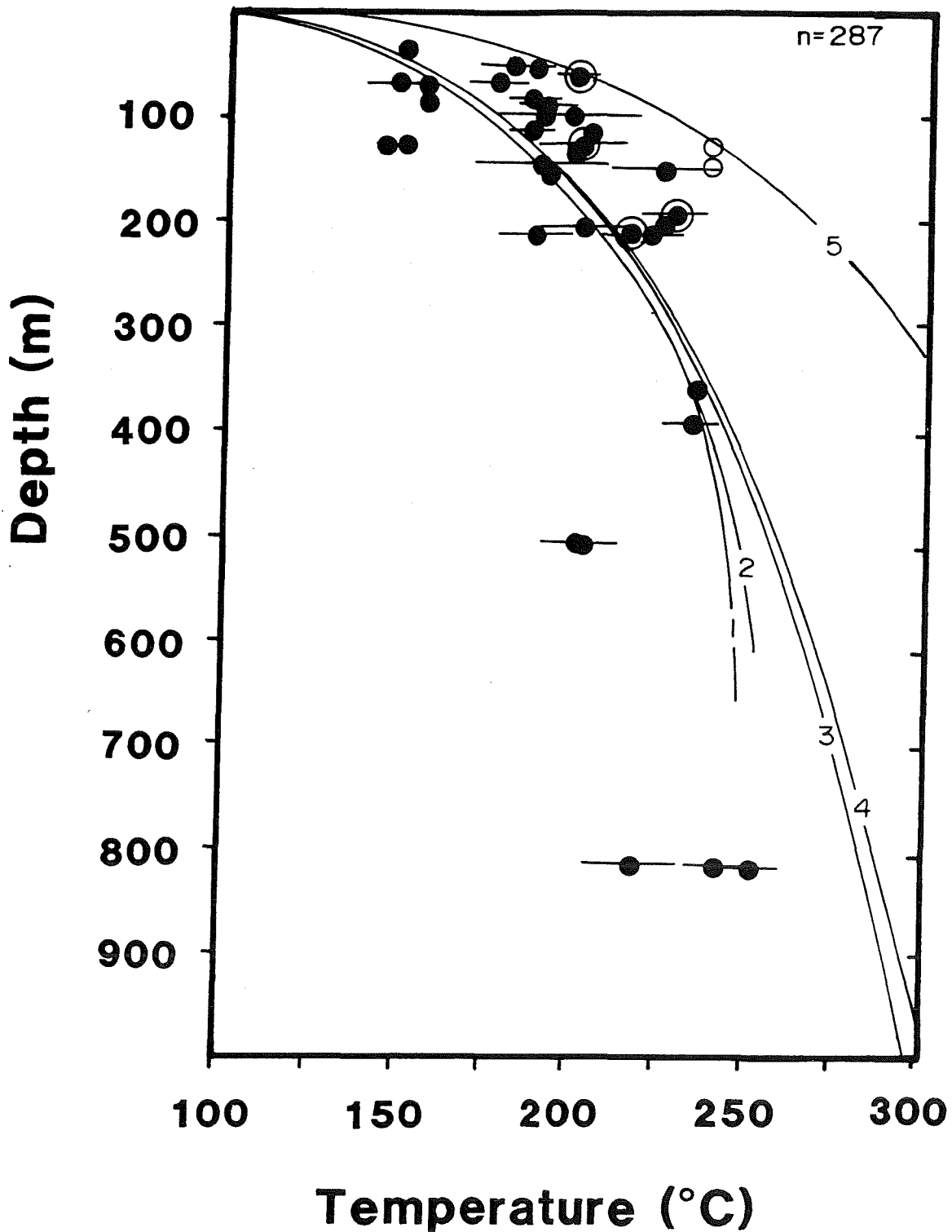


FIGURE 5. Compilation of fluid inclusion homogenization temperatures plotted against depth below the sinter. Circles are average homogenization temperatures for samples from that elevation, and the horizontal line is the standard deviation in the data. The closed circles represent fluid inclusions that homogenized to a liquid phase and the open circles represent fluid inclusion that homogenized to a vapor phase. For clarity some of the circles have been made larger. Also shown are the depth to boiling point curves (Haas, 1971; Henley, 1984a) for various fluid compositions under hydrostatic conditions unless specified differently. Curve 1 is 0.5 mole % CO_2 and pure water; curve 2 is 0.5 mole % CO_2 and 5 wt. % NaCl eq.; curve 3 is pure water; curve 4 is 5 wt. % NaCl; and curve 5 is pure water under lithostatic pressures.

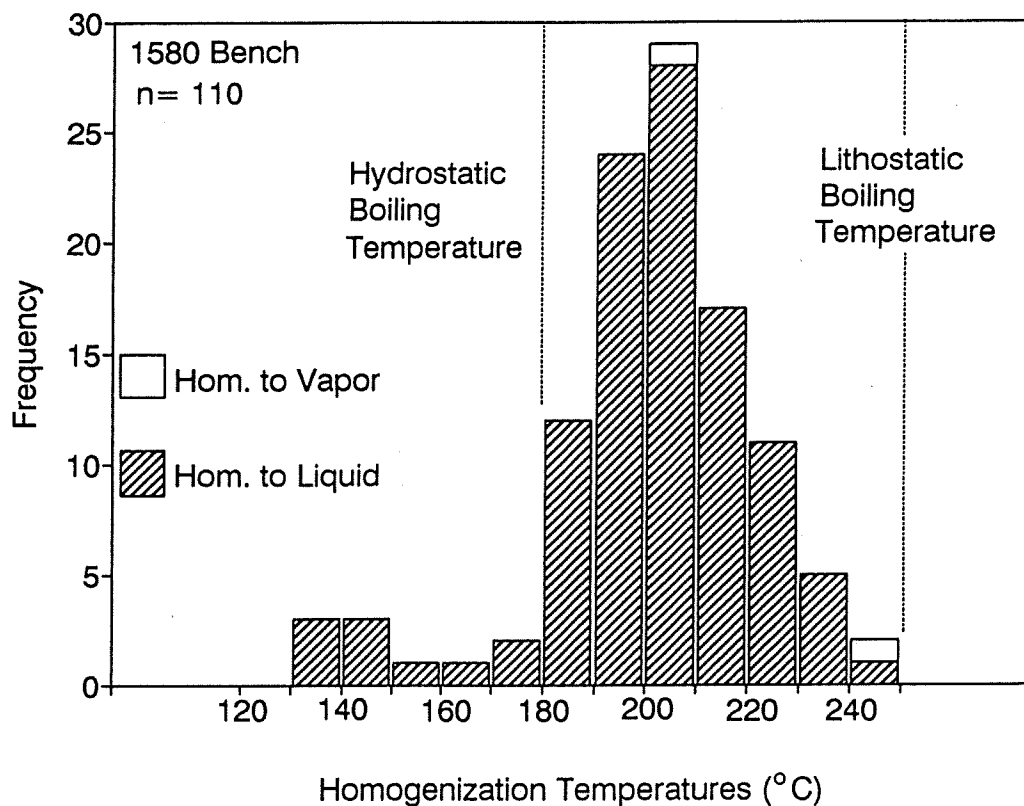


FIGURE 6. Histogram of fluid inclusion homogenization temperatures for samples from the 1580 bench (128 m below the sinter). Also shown are the hydrostatic and lithostatic boiling temperatures for pure water.

pressure gradients up to 10% in excess of the hydrostatic pressure must be present. In the case of the sheeted vein complex at the 128 m elevation the mean temperature is ~6% in excess of the hydrostatic boiling temperature.

Fluid pressures in excess of the lithostatic boiling curve have not been observed, suggesting that fluid pressure approached but did not exceed the lithostatic load. The lack of supralithostatic pressures is consistent with observations from modern geothermal systems. Active geothermal systems show a rapid propagation of pressure fluctuations from the geothermal systems to the surrounding cold water hydrologic systems (Hedenquist and Henley, 1985). This suggests that field wide silica sealing and therefore supralithostatic pressures did not occur.

Precipitation Mechanism and Metal Zoning

The coincident onset of precious metal mineralization and fluid boiling strongly suggests that boiling, and the associated physical and chemical changes, is the mechanism that precipitated the precious metals. On the basis of fluid inclusion data, alteration assemblages and sulfide mineral stability's, Sherlock (1993) outlined the conditions of the ore forming fluids. Fluid inclusion data suggests that the ore forming fluids were low salinity (0.4 m) NaCl

dominated fluids at ~200°C, but ranged from 263 to ~100°C. Alteration assemblages and fluid salinities indicate that the fluid pH was ~6.2, which is slightly alkaline at 200°C. The presence of abundant hydrocarbons suggest that the oxygen fugacity is low ($\log f_{O_2} = -43$) likely buffered by the C-CH₄-CO₂ assemblage. Arsenic mineral stability relationships suggest that the sulfur activity is also low ($\Sigma S = 0.001 m$).

Under these conditions of low f_{O_2} , f_{S_2} and temperature, gold is likely transported predominately as a sulfide complex (Seward, 1973, 1984; Romberger, 1988, 1989). Under these conditions the solubility of gold is ~52 ppb. Silver and base metals are likely transported predominantly as chloride complexes (Henley, 1984c).

During boiling the dominant control on the precipitation of precious metals is the partitioning of volatiles (CO₂ and H₂S) into the vapor phase and the resulting change in fluid chemistry (Drummond and Ohmoto, 1985; Cole and Drummond, 1986). The partitioning of volatiles during boiling is very rapid, occurring within the first few percent phase separation (Drummond and Ohmoto, 1985). The first volatile, typically present in significant quantities, to partition into a vapor phase is CO₂. Loss of CO₂ from the liquid phase causes a rapid pH increase. The effect of a pH increase on metal solubility's is to decrease the stability of chloride complexed metals and increase the stability of bisulfide complexed metals (Drummond and Ohmoto, 1985; Cole and Drummond, 1986). The pH increase will cause chloride complexed metals to precipitate as sulfides and sulfosalts.

During the same boiling event H₂S will be partitioned into a vapor phase slower than CO₂, because of the higher solubility of H₂S in a aqueous phase (Giggenbach, 1980). The loss of H₂S to a vapor phase decreases the activity of aqueous sulfur and decreases the solubility of bisulfide complexed metals. If the system is open so that H₂S is removed after phase separation then the decrease in the solubility of gold caused by the reduction in the activity of sulfur is much greater than the increased solubility caused by the pH increase so that gold will be precipitated (Seward, 1988; Clark and Williams-Jones, 1990).

As an ascending hydrothermal fluid intersects the depth to boiling point curve the initial pH increase, resulting from the loss of CO₂, causes silver and other chloride complexed metals to be precipitated. The same boiling event causes H₂S to be separated into a vapor phase slower than CO₂ resulting in the precipitation of gold and other bisulfide complexed metals at higher elevations than the chloride complexed metals. The difference in partitioning of volatiles into a vapor phase during boiling as the hydrothermal fluid is ascending results in the metal zoning that is observed at the McLaughlin deposit. The deeper portions of the ore zone are enriched in silver with respect to gold and the upper portions are enriched in gold with respect to silver.

Concentration of Gold in the Hydrothermal Solution

The solubility of gold in the hydrothermal fluid was calculated in the previous section to be 52 ppb. This is the maximum amount of gold that the hydrothermal fluid can transport as a sulfur ligand. It is not necessarily the concentration of gold in the fluid. The fluid could be undersaturated with respect to gold.

An estimate of the gold content of the hydrothermal fluid can be made by considering the gold grade of the sheeted vein complex and the thermal gradients observed in the fluid inclusion data. The average gold grade of the

sheeted vein complex is ~9 ppm (Lehrman, 1990). The sheeted vein complex is a large vein swarm with minor wall rock inclusions, therefore the average grade of the sheeted vein is representative of the average grade of the hydrothermal silica. The hydrothermal fluids likely precipitated 100% of its gold content before being discharged. This is shown by the contrasting gold content of the sheeted vein complex and the siliceous sinter. Therefore it is a reasonable assumption that, 9 ppm is a representative value for the gold content of hydrothermal silica precipitated from fluids that formed the sheeted vein complex.

Fluid inclusion studies indicate that the hydrothermal fluids cooled from ~235°C depth to a discharge temperature of ~100°C. If we assume that the hydrothermal fluid maintains saturation with respect to chalcedonic silica, consistent with active geothermal systems (Fournier, 1985), then the silica solubility varied from 600 mg/kg at 235°C to 90 mg/kg at 100°C (Fournier, 1985). Over this temperature and silica solubility gradient each liter of fluid would precipitate ~0.5 grams of silica. Therefore approximately 2.0E6 liters of water (2.0E3 tonnes of water) are needed to precipitate one tonne of hydrothermal silica. To form an ore body with an average grade of 9 ppm gold, then each tonne of hydrothermal silica would contain 9 grams of gold, which would precipitate from 2.0E6 liters of water. Therefore one tonne of hydrothermal water would contain approximately 5.0E-3 grams of gold. This suggests that the concentration of gold in the hydrothermal fluid is approximately 5 ppb. This calculated gold content of the fluid is undersaturated with respect to gold solubility calculations made above.

This calculation, although a gross generalization, is relatively insensitive to errors inherent in estimating the gold content of the sheeted vein system. For example, if the average gold content of the sheeted vein was 20 ppm, then using similar arguments the gold content of the fluid would be 10 ppb, still well undersaturated with respect to gold. Alternatively, if the fluid was initially saturated with respect to gold (52 ppb) then the gold content of the sheeted vein complex would be approximately 100 ppm, which is certainly not the case.

The calculated saturation of gold in the hydrothermal fluid is 52 ppb, yet the calculated gold content of the hydrothermal fluid is 5 ppb. This suggests that the hydrothermal fluid was undersaturated with respect to gold. The calculated gold content of 5 ppb is very similar to the Ohaaki-Broadlands (11.1 ppb) and Rotokawa (7.2 ppb) active geothermal systems (Seward, 1988). The observation that the McLaughlin geothermal fluids were initially undersaturated with respect to gold is consistent with observations from active geothermal systems (Brown, 1986).

STABLE ISOTOPES

Oxygen

There is a strong trend for increasingly enriched $\delta^{18}\text{O}_{\text{Qtz}}$ values towards the surface. The deepest sample at 821 m below the sinter has the lowest value at 18.2‰ and the sinter samples have the highest values averaging 31.5‰. There is a smooth curve from the deepest lightest samples to the surficial heaviest samples (Fig. 7). Using the fluid inclusion homogenization temperatures and the appropriate fractionation factors (Kita et al., 1985; Clayton et al., 1972) the isotopic composition of the fluid in equilibrium with the silica can be calculated. The isotopic composition of the fluid is much more uniform averaging 9.3‰. This suggests that the trend of increasingly more

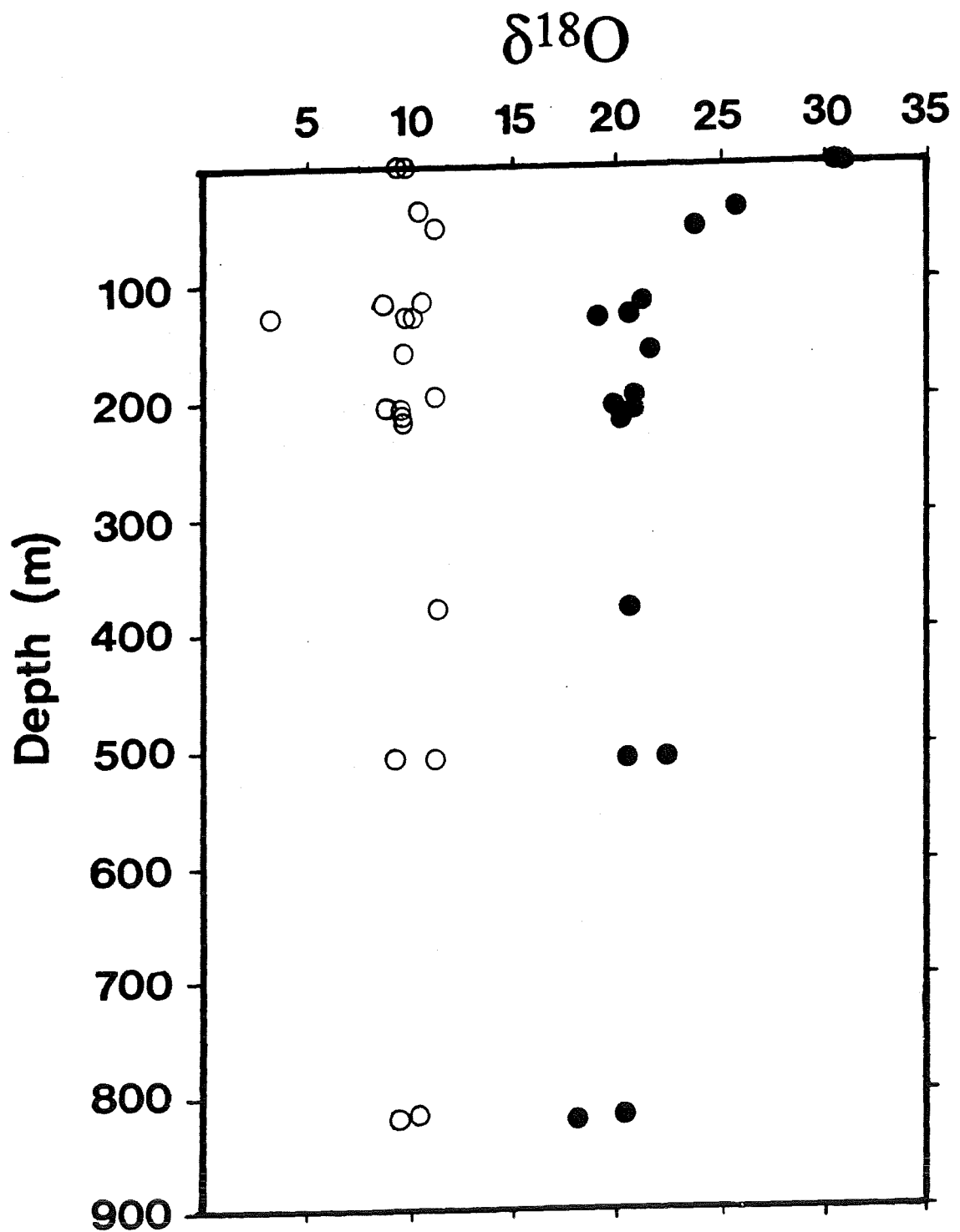


FIGURE 7. Variations in $\delta^{18}\text{O}$ with depth below the sinter. Closed circles are the measured data and the open circles are the composition of the water in equilibrium with the quartz.

enriched samples towards the surface is a temperature effect and that the actual fluid composition remained fairly uniform throughout the depth profile.

Calculations of the oxygen isotopic shift resulting from boiling (Truesdell, 1984) suggest that the shift was small between 1.3‰ and 0.9‰ for single stage and continuous vapor loss respectively. Mass balance calculations suggest that dilution of the hydrothermal fluid with local meteoric groundwater was also small likely less than 10% (Sherlock, 1993).

Deuterium

Twelve samples of quartz were crushed under vacuum and analyzed for deuterium. Samples were selected based on their abundance of large primary and pseudosecondary fluid inclusions and the general lack of secondary fluid inclusions. Although it is impossible to quantify the contribution of secondary fluid inclusions to the δD values the samples were selected to minimize their effect. In addition, four samples of hydrothermal montmorillonite were analyzed for both oxygen and deuterium. The data from both methods are consistent and indicate that the deuterium composition of the ore forming fluids varied between -48‰ and -68‰ with two samples ranging down to -82‰ (Fig. 8). There is no systematic variation observed in the deuterium data with depth. The data derived by both techniques are independent of each other and are corroborating suggesting that the deuterium composition, as indicated by the fluid inclusion extracts and the hydrous alteration assemblages, reflect the composition of the hydrothermal fluid. The deuterium data of the hydrothermal fluids, is very similar to the composition of present day meteoric waters, which have a composition of -60‰ (Peters, 1993)

FLUID SOURCE

The isotopic composition of the hydrothermal fluids are consistent with a meteoric source. The hydrothermal fluids show a strong oxygen shift resulting from water/rock interaction but do not show a deuterium shift (Fig. 8). This classic isotopic signature is characteristic of a meteoric water dominated hydrothermal system. The overwhelming majority of geothermal waters have a meteoric origin based on the δD and $\delta^{18}O$ composition of the hydrothermal fluids that plot in close proximity to or by lateral shift away from the meteoric water line (Truesdell and Hulston, 1980). Epithermal ore deposits are often compared to geothermal systems and numerous studies have demonstrated that the $\delta^{18}O$ of the hydrothermal fluids may vary considerably, as a result of water/rock exchange, but the δD of the fluid is consistent with local meteoric water (Taylor, 1971, 1973, 1974, 1979; O'Neil et al., 1973; O'Neil and Silberman, 1974; compilation of Field and Fifarek, 1985)

A meteoric water source for the ore forming fluid is consistent with the geology of the deposit. Large amounts of fluid are required to form a deposit the size of McLaughlin, the most abundant and obvious source for this fluid is surficial water or groundwater. Lacustrine deposits are locally common around the McLaughlin deposit.

Interlayered with the sediments are lapilli tuff and vein fragments, as well as opalized wood (Lehrman personal communication, 1992). This relationship strongly suggests that a standing body of water occupied the area around

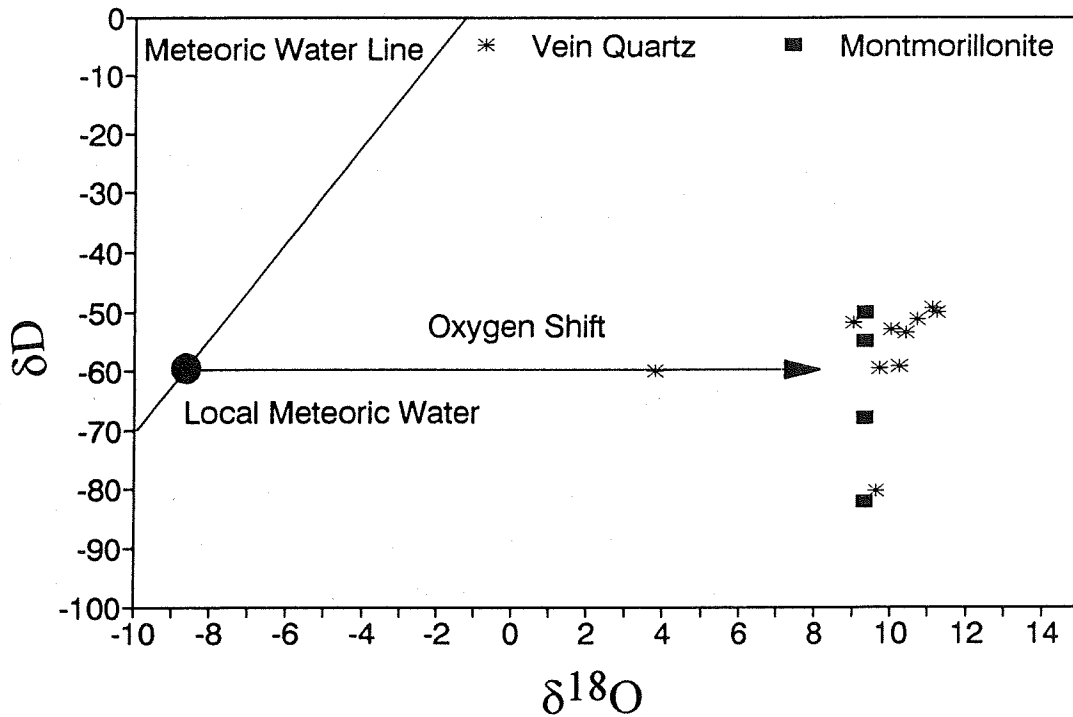


FIGURE 8. $\delta^{18}\text{O}$ vs δD showing data derived for the McLaughlin hydrothermal fluids, the meteoric water line and the composition of local meteoric water.

the McLaughlin deposit during hydrothermal activity. This is consistent with epithermal districts in Nevada. Berger and Henley (1988) have noted the spatial and temporal association of epithermal mineralization and periods of high water availability, often seen as standing bodies of water or variations in vegetation.

The water/rock ratio needed to evolve the hydrothermal fluid from a meteoric water is low ~ 0.1 but similar to other geothermal systems in the Coast Ranges and other epithermal deposits emplaced within sedimentary rocks. The Geysers Geothermal System is a meteoric water, vapor dominated, geothermal system, ~ 20 km west of McLaughlin (White et al., 1971). An early fluid dominated phase and associated hydrothermal veins show variable water/rock ratios between 0.1 and 2 (Sternfeld, 1981; Gunderson, 1989; Sherlock, 1993). The pronounced oxygen shift seen at McLaughlin is generally larger than what is observed in volcanic hosted epithermal deposits but is similar to the shift observed in sedimentary hosted epithermal deposits such as Humbolt and Tenmile (O'Neil and Silberman, 1974), Cortez (Rye et al., 1974) and Carlin (compiled in Field and Fifarek, 1985). The large oxygen shift and the lower water/rock ratios in sediment hosted epithermal deposits is attributed to the hydrothermal systems being emplaced within less permeable (lower water/rock ratios) and isotopically heavier sedimentary rocks, compared to volcanic rocks (Taylor, 1979). The hydrothermal fluids that formed the McLaughlin deposit have exchanged and equilibrated with sedimentary rocks, as indicated by the presence abundant hydrocarbons in hydrothermal silica, which produced the pronounced isotopic shift.

Relationship of the McLaughlin Deposit to Active Hydrothermal Systems in the Coast Ranges

Although it is beyond the scale of this document to delve into this relationship in detail, the scope of this publication demands that the relationship between the McLaughlin deposit and other hydrothermal systems in the Coast Ranges be commented on. Previous studies (Peters, 1991, 1993) have suggested that the McLaughlin deposit is related to active hot- and mineral-springs, most notably in the Sulphur Creek District (Wilbur Springs) but also throughout the Coast Ranges. The geological relationships strongly support this, however the isotopic relationships of the two systems are different.

Previous workers have suggested that the active springs are a combination of either, connate fluids derived from the Great Valley Sequence, metamorphic fluids derived from the Franciscan Complex, or evolved meteoric waters that have been diluted with local meteoric waters (Barnes et al., 1973; White et al., 1973; Peters, 1991, 1993; Donnelly-Nolan et al. 1993). On the basis of similar oxygen isotopes and a suggested connate origin for the active springs Peters (1991) suggests that the hydrothermal fluids responsible for the formation of the McLaughlin deposit were connate in origin. However, Peters (1991) did not obtain deuterium data for the McLaughlin hydrothermal fluids. In addition, all previous works have suggested that many of the active springs have a distinctly different origin than the Geysers Geothermal System despite their similar geological setting.

Sherlock (1993) suggests, based on geological relationships, spatial distribution, chemical and isotopic relationships as well as cation geothermometers that the hydrothermal systems in the Coast Ranges are all related and originated as meteoric fluids. The chemistry and isotopic composition of the active springs are the result of a thermally activated process modified by vapor loss. Sherlock (1993) suggests that there are two end-member meteoric water hydrothermal systems in the Coast Ranges, fluid and vapor dominated. The McLaughlin deposit is a fluid dominated hydrothermal system and the Geysers Geothermal System is a vapor dominated system. The active springs are in between these two end-members, they are meteoric water systems that have undergone high degrees of vapor loss.

CONCLUSIONS

The sheeted vein complex is the center of the hot-spring system that formed the McLaughlin deposit. The sheeted vein merges from a subaerial sinter into a bilaterally symmetric, subparallel vein swarm, suggesting syntectonic vein formation.

Precious metals show a well defined zonation with gold largely restricted to the upper 200 m of the deposit. Silver can be dominant anywhere in the system but is always more abundant than gold below 200 m. Below 350 m, silver is rare, gold has not been observed, and mineralization is dominated by base metal sulfides.

Fluid inclusion analysis suggests that the ore forming fluids were low salinity NaCl dominated, low CO₂ fluids. The deepest samples (> 800 m below the paleosurface) have an average temperature of 235°C. The ascending

hydrothermal fluid intersected the hydrostatic boiling curve at ~400 m below the surface. The fluids boiled and followed the hydrostatic boiling curve to the surface, precipitating metals due to the physical and chemical changes associated with boiling. Pressure gradients were ~6% in excess of the hydrostatic pressure and did not exceed the lithostatic pressure. There were very steep thermal and pressure gradients in the near surface environment that resulted in very effective precipitation mechanisms.

Boiling of an ascending hydrothermal fluid accounts for the metal zoning observed in the sheeted vein complex. An ascending hydrothermal fluid will rapidly partition CO₂ into the vapor phase during the first few percent boiling. The loss of CO₂ will cause a rapid increase in pH that destabilizes chloride complexed metals and results in the precipitation of silver and base metals. As the hydrothermal fluid continues to ascend and boil, H₂S will be partitioned into the vapor phase which destabilizes sulfide complexed metals and results in the precipitation of gold. During boiling CO₂ is partitioned into the vapor phase faster than H₂S, resulting in the deeper portions of the ore body being enriched in silver with respect to gold and the shallow portions of the ore body enriched in gold with respect to silver.

On the basis of the physical and chemical conditions of the ore forming fluids the gold solubility is calculated to be ~52 ppb. However, on the basis of gold grade, as well as silica and temperature gradients the gold content of the hydrothermal fluid is calculated to be ~5 ppb. This suggests that the hydrothermal fluids were undersaturated with respect to gold prior to the onset of boiling.

There is a strong trend for increasingly light $\delta^{18}\text{O}_{\text{Qtz}}$ with depth. The most enriched samples are from the subaerial sinter and the lightest sample are from the deepest samples. This trend is a temperature effect and is the result of increasing fractionation with decreasing temperature. The oxygen isotopic composition of the hydrothermal fluid remained fairly constant at ~9.3‰.

The oxygen and deuterium composition of the hydrothermal fluids are consistent with a meteoric water origin. The hydrothermal fluids have a pronounced oxygen shift due to water/rock interaction but do not have a deuterium shift. The water/rock ratios are low but similar to other geothermal systems in the Coast Ranges and other epithermal deposits emplaced within sedimentary sequences.

ACKNOWLEDGMENTS

This paper represents a summary of part of the author's research on the sheeted vein complex. I would like to acknowledge the enthusiastic support of Norman Lehrman, Gordon Nelson and the rest of the geological staff at McLaughlin. This work would not have been possible without the support of Homestake Mining Company as employment through the 1990, 1991 and 1992 field seasons as well as through a research grant to the author. I would also like to acknowledge the financial support of an Ontario Post Graduate Scholarship. I would like to thank Dr. J. Rytuba and the organizers of this field trip for the invitation to present my research in this forum.

REFERENCES

- Barnes, I., Hinkle, M.E., Rapp, J.B., Heropoulos, C., and Vaughn, W.W., 1973, Chemical composition of naturally occurring fluids in relation to mercury deposits in part of north central California: U.S. Geol. Survey Bull. 1382-A, 19 pp.
- Berger, B.R. and Henley, R.W., 1988, Advances in the understanding of epithermal gold-silver deposits, with special reference to the western United States: in The Geology of Gold Deposits: The Perspective in 1988, edited by R.R. Keays, W.R.H. Ramsay and D.I. Groves, Econ. Geol. Monograph 6, p. 405-423
- Bodnar, R.J., Reynolds, T.J., and Kuehn, C.A., 1985, Fluid-inclusion systematics in Epithermal Systems: in Geology and Geochemistry of Epithermal Systems, edited by B.R. Berger and P.M. Bethke, Reviews in Econ. Geol., v. 2, p. 73-98
- Brown, K.L., 1986, Gold deposition from geothermal discharges in New Zealand: Econ. Geol., v. 81, p. 979-983
- Buchanan, L.J., 1981, Precious metal deposits associated with volcanic environments in the southwest: in Relations of Tectonics to Ore Deposits in the South Cordillera, edited by W.R. Dickinson and W.D. Payne. Arizona Geol. Soc. Digest, v. XIV, p. 237-261
- Clark, J.R., and Williams-Jones, A.E., 1990, Analogs of epithermal gold-silver deposition in geothermal well scales: Nature, v. 346, p. 644-645
- Clayton, R.N., and Mayeda, T.K., 1963, The use of BrF₅ in extraction of oxygen from oxides and silicates for isotopic analysis: Geochim. et Cosmochim. Acta, v. 27, p. 43-52.
- Clayton, R.N., O'Neil, J.R., and Mayeda, T.K., 1972, Oxygen isotope exchange between quartz and water: Jour. Geoph. Res., v. 77, p. 3057-3067
- Cole, D.R., and Drummond, S.E., 1986, The effect of transport and boiling on Ag/Au ratios in hydrothermal solutions: a preliminary assessment and possible implications for the formation of epithermal precious-metal ore deposits. Jour. Geochem. Explor., v. 25, p.45-79
- Coleman, M.I., Shepherd, T.J., Durham, J.J., Rouse, J.E., Moore, G.R., 1982, Reduction of water with zinc for hydrogen isotope analysis: Anal. Chem., v. 54, p. 993-995
- Davis, D.W., Lowenstein, T.K., and Spencer, R.J., 1990, The melting behavior of fluid inclusions in laboratory-grown halite crystals in the systems NaCl-H₂O, NaCl-KCl-H₂O, NaCl-MgCl₂-H₂O and NaCl-CaCl₂-H₂O: Geochim. et Cosmochim. Acta, v. 54, p. 591-601.
- Donnelly-Nolan, J.M., Burns, M.G., Goff, F.E., Peters, E.K., and Thompson, J.M., 1993, The Geysers-Clear lake Area, California: thermal waters, mineralization, volcanism, and geothermal potential: Econ. Geol., v. 88, p. 301-316
- Drummond S.E. and Ohmoto, H., 1985, Chemical evolution and mineral deposition in boiling hydrothermal systems: Econ. Geol., v. 80, p. 126-147
- Field C.W., and Fifarek, R.H., 1985, Light stable isotope systematics in the epithermal environment: in Geology and Geochemistry of Epithermal Systems, edited by B.R. Berger and P.M. Bethke, Reviews in Econ. Geol., v. 2, p. 99-128
- Fournier, R.O., 1985, The behavior of silica in hydrothermal solutions in epithermal systems: in Geology and Geochemistry of Epithermal Systems, edited by B.R. Berger and P.M. Bethke, Reviews in Econ. Geol., v. 2, p. 45-62
- Giggenbach, W.F., 1980, Geothermal gas equilibria: Geochim. et Cosmochim. Acta, v. 44, p. 2021-2032
- Grant, M.A. Donaldson, I.G., and Bixley, P.F., 1982, Geothermal reservoir engineering: Academic Press, New York 369 p.
- Gunderson, R.P., 1989, Distribution of oxygen isotopes and non-condensable gas in steam at the Geysers: Geotherm. Resour. Council Trans., v. 13, p. 449-454.
- Haas, J.L., 1971, The effect of salinity on the maximum thermal gradient of a hydrothermal system at hydrostatic pressure: Econ. Geol., v. 66, p. 940-946
- Henley, R.W., 1984a, Gaseous components in geothermal systems. in Fluid Mineral Equilibria in Hydrothermal Systems: edited by R.W. Henley, A.H. Truesdell, and P.B. Barton Jr., Reviews in Econ. Geol., v. 1, p. 45-56
- Henley, R.W., 1984b, Chemical structure of geothermal systems: in Fluid Mineral Equilibria in Hydrothermal Systems, edited by R.W. Henley, A.H. Truesdell, and P.B. Barton Jr., Reviews in Econ. Geol., v. 1, p. 9-30
- Henley, R.W., 1984c, Metals in hydrothermal fluids: in Fluid Mineral Equilibria in Hydrothermal Systems, edited by R.W. Henley, A.H. Truesdell, and P.B. Barton Jr., Reviews in Econ. Geol., v. 1, p. 115-129

- Hedenquist, J.W., and Henley, R.W., 1985, Hydrothermal eruptions in the Waiotapu geothermal system, New Zealand: their origin associated breccias, and relation to precious metal mineralization: *Econ. Geol.*, v. 80, p. 1640-1668
- Kita, I., Taguchi, S., and Matsubaya, O., 1985, Oxygen isotope fractionation between amorphous silica and water at 34 - 93°C: *Nature*, v. 314, p. 63-64.
- Lehrman, N.J., 1990, The McLaughlin Mine, California: an update. GAC-MAC Joint Annual Meeting, Program with Abstracts, Vancouver, v. 15, p. A75
- Oakes, C.S., Bondar, R.J., and Simonson, J.M., 1990, The system NaCl-CaCl₂-H₂O: I. The ice liquidus at 1 atm total pressure: *Geochim. et Cosmochim. Acta*, v. 54, p. 603-610
- O'Neil, J.R., Silberman, M.L., Fabbi, B.P., and Chesterman, C.W., 1973, Stable isotope and chemical relations during mineralization in the Bodie mining district, Mono county, California: *Econ. Geol.*, v. 68, p. 765-784
- O'Neil, J.R., and Silberman, M.L., 1974, Stable isotope relations in epithermal Au-Ag deposits: *Econ. Geol.*, v. 68, p. 902-909.
- Peters, E.K., 1991, Gold-bearing hot spring systems of the northern Coast Ranges, California: *Econ. Geol.*, v. 86, p. 1519-1528
- Peters, E.K., 1993, D-18O enriched waters of the Coast Range Mountains, northern California: connate and ore-forming fluids: *Geochim. et Cosmochim. Acta*, v. 57, p. 1093-1104
- Potter, II, R.W., Clynne, M.A., and Brown, D.L., 1978, Freezing point depression of aqueous sodium chloride solutions: *Econ. Geol.*, v. 73, p. 284-285
- Roedder, E., 1984, Fluid inclusions: *Min. Soc. America, Reviews in Min.* v. 12, 644 pp.
- Romberger, S.B., 1988, Geochemistry of gold in hydrothermal deposits: *U.S. Geol. Survey Bull.* 1857-A, p. A9-A25
- Romberger, S.B., 1989, Mechanisms of gold transport and deposition in low temperature hydrothermal systems: Short Course, University of Western Ontario
- Rye, R.O., 1966, The carbon, hydrogen and oxygen isotopic composition of the hydrothermal fluids responsible for the lead-zinc deposits at Providencia, Zacatecas, Mexico: *Econ. Geol.*, v. 61, p. 1399-1427
- Rye, R.O., Doe, B.R., and Wells, J.D., 1974, Stable isotope and lead isotope study of the Cortez, Nevada, gold deposit and surrounding area: *Jour. of Research, U.S. Geol. Survey*, v. 2, p. 13-23.
- Seward, T.M., 1973, Thiocomplexes of gold and transport of gold in hydrothermal solutions: *Geochim. et Cosmochim. Acta*. v. 37, p. 379-399
- Seward, T.M., 1984, The transport and deposition of gold in hydrothermal systems: in *Gold'82, The Geology and Geochemistry and Genesis of Gold Deposits*, edited by R.P. Foster, A.A. Balkema, p. 165-182
- Seward, T.M., 1988, The hydrothermal chemistry of gold and its implications for ore formation: boiling and conductive cooling as examples: in *The Geology of Gold Deposits: The Perspective in 1988*, edited by R.R. Keays, W.R.H. Ramsay and D.I. Groves, *Econ. Geol. Monograph* 6, p. 398-404
- Sherlock, R.L., 1993, The geology and geochemistry of the McLaughlin Mine sheeted vein complex, northern Coast Ranges, California. Unpub. Ph.D. Thesis, University of Waterloo, 309 pp.
- Serner, S.M., 1992, Homogenization of fluid inclusions to the vapor phase: the apparent homogenization problem: *Econ. Geol.* v. 87, p. 1616-1623
- Sternfeld, J.N., 1981, The hydrothermal and stable isotope geochemistry of two wells in the Geysers Geothermal Field, Sonoma County, California: Unpub. M.Sc. Thesis, University of California, Riverside, 202 pp
- Taylor, H.P. Jr., 1971, Oxygen isotope evidence for large-scale interaction between meteoric ground waters and tertiary granodiorite intrusions, Western Cascade Range, Oregon: *Jour. of Geoph. Res.*, v. 76, p. 7855-7874
- Taylor, H.P. Jr., 1973, O¹⁸/O¹⁶ evidence for meteoric-hydrothermal alteration and ore deposition in the Tonopah, Comstock lode and Goldfield mining districts, Nevada: *Econ. Geol.*, v. 68, p. 747-764
- Taylor, H.P. Jr., 1974, The application of oxygen and hydrogen isotope studies to problems of hydrothermal alteration and ore deposition: *Econ. Geol.*, v. 69, p. 843-883.
- Taylor, H.P. Jr., 1979, Oxygen and hydrogen isotope relationships in hydrothermal ore deposits: in *Geochemistry of hydrothermal ore deposits*, second edition, edited by H.L. Barnes, Wiley, p. 236-277.
- Taylor, H.P. Jr., and Epstein, S., 1962, Relationship between ¹⁸O and ¹⁶O in coexisting minerals of igneous and metamorphic rocks: Part 1 - Principles and experimental results: *Geol. Soc. America Bull.*, v. 73, p. 461-480
- Truesdell, A.H., 1984, Stable isotopes in hydrothermal systems: in *Fluid Mineral Equilibria in Hydrothermal Systems* edited by R.W. Henley, A.H. Truesdell, and P.B. Barton Jr., *Reviews in Econ. Geol.*, v. 1, p. 129-142

- Truesdell, A.H., and Hulston, J.R., 1980, Isotopic evidence on environments of geothermal systems, Chapter Five: in Handbook of Environmental Isotope Geochemistry, v. 1, The Terrestrial Environment. edited by P. Fritz and J.C. Font, Elsevier, Amsterdam, p. 170-226
- White, D.E., Muffler, J.P., and Truesdell, A.H., 1971, Vapor-dominated hydrothermal systems compared with hot-water systems: Econ. Geol., v. 66, p.75-97
- White, D., Barnes, I., and O'Neil, J.R., 1973, Thermal and mineral waters of nonmeteoric origin, California Coast Ranges: Geol. Soc. America Bull., v. 84, p. 547-560
- White, D.E., Fournier, R.O., Muffler, L.J., and Truesdell, A.H., 1975, Physical results of research drilling in the thermal areas of Yellowstone Park, Wyoming: U.S. Geol. Survey Pro. Paper 892, 70 pp.

DAY FOUR

McLAUGHLIN GOLD AND KNOXVILLE MERCURY DEPOSITS : ROAD LOG

James J. Rytuba¹, Dean A. Enderlin², Julie M. Donnelly-Nolan¹, and Robert McLaughlin¹

¹U.S. Geological Survey, 345 Middlefield Road, Menlo Park CA 94025

²Homestake Mining Company, McLaughlin Mine 26775 Morgan Valley Rd., Lower Lake, CA 95457

This tour begins in Clearlake Highlands and proceeds to the Homestake Mining Company's McLaughlin Mine and the Knoxville mercury deposit. The route for the trip is shown in Figure 1.

Mileage

0.0	0.0	Exit parking lot of El Grande Hotel and turn right onto main road out of Clearlake (east).
0.35	0.35	Turn right onto Highway 53.
2.95	3.3	Turn left (east) at main intersection in downtown Lower Lake and proceed east on Morgan Valley Road.
1.8	5.1	Exposures along road and in creek under bridge east of town are Paleocene Martinez and Eocene Tejon Formation consisting of marine sandstone and siltstone.
0.3	5.4	Paleocene sandstone of the Martinez Formation and massive white sandstone of the Tejon Formation are exposed along the road. An angular unconformity exists between these marine clastic rocks and underlying Great Valley sequence.
1.7	7.1	Southwest of the Baker Mine a structural window in the lower beds of the Great Valley sequence exposes rocks of the eastern belt of the Franciscan Complex, in which serpentine delineates thrusts that outline a semi-circular window through rocks of the Great Valley sequence.
1.0	8.1	The Baker mercury mine is on the left (east) side of road. On the hillside in the foreground, connate water emerges at Baker Soda Spring to form a large travertine terrace; see Goff and Janik (Day 2, stop 1, this volume) for further information. The spring and mine are along a northwest-trending fault zone. Mercury production from the Baker mine was small, less than 500 flasks, and came from several zones of silica-carbonate alteration in serpentinite. Alteration around the Baker mine is extensive and rocks of the Great Valley sequence are bleached and argillically altered.

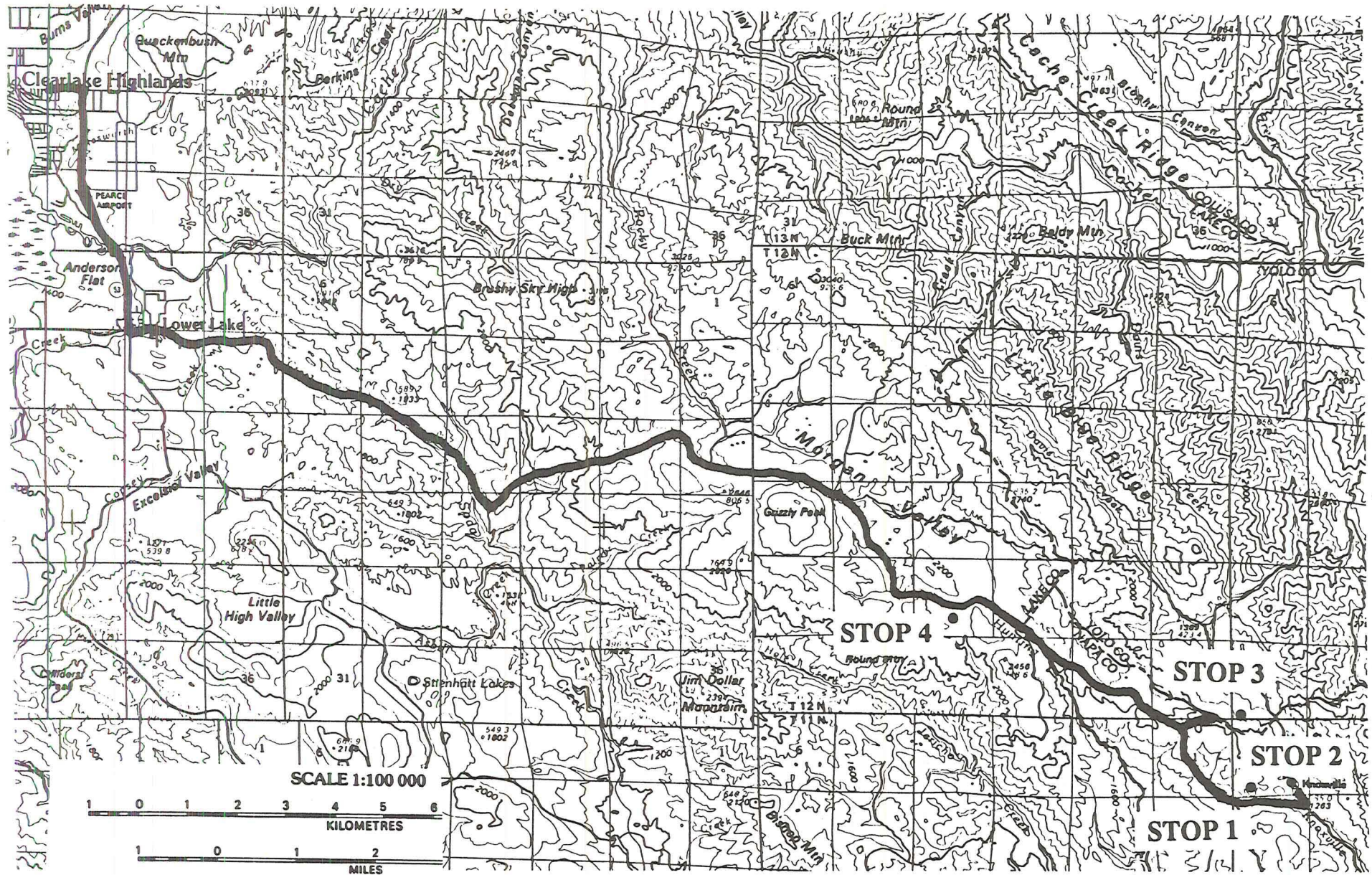


FIGURE 1. Route map for Day 4: from Clearlake Highlands to the Knoxville mercury deposit and the McLaughlin gold deposit.

- Silica-carbonate alteration in serpentinite is typically reddish-brown due to oxidation of marcasite and pyrite.
- 2.5 10.6 Good exposures of Great Valley sequence consisting of tan sandstone and siltstone in road cuts on left side of road.
- 0.1 10.7 Grizzly Peak at the right of the road (west) consists of aphyric dacite of the Clear Lake Volcanics, age unknown. The dacite contains 67.2 wt. per cent SiO₂ but has an MgO content of 5.20 per cent, as high as most basaltic andesites in the volcanic field. Large blocks of dacite occupy flank of the hill and it is likely that the topography here is a reflection of a small dome.
- 0.6 11.3 For the next 0.2 mi, good exposures of Great Valley sequence consisting primarily of tan sandstone can be seen to the right of the road.
- 3.2 14.5 Tailings pond from the Homestake's McLaughlin Mine in the distance, right side of road. Ore is transported to the mill, which is about 8 km north of the open pit.
- 1.8 16.3 Turn right at sign for Homestake Mine and proceed to guard house. Buildings of the mill are visible on the skyline.
- 0.25 16.55 Park adjacent of Homestake Mining guard house and check in with the guard to obtain permission to visit the mine. A signature is required of each individual on trip. Retrace route back to main road.
- 0.25 16.8 Turn right onto Morgan Valley Road.
- 4.3 21.1 Pass under tunnel created under haulage road used to transport rock to waste dumps on the right side of the road.
- 0.2 21.3 Entrance to McLaughlin mine on left. Proceed on road toward Knoxville Mercury Mine.
- 1.4 22.7 Large travertine terrace occupies slope to left of road, continues under road, and is exposed in the creek walls to the right of the road. **STOP 1 . (Optional)**

STOP 1 . CARBONATE SPRINGS AND TRAVERTINE TERRACE

The springs depositing this travertine terrace (Fig. 2) vent from fractures southeast of the Stony Creek fault, the major structural feature in the McLaughlin Mine which is just over the hill. The travertine is dominantly calcite and magnesian calcite (up to 10 per cent magnesium) but some layers contain barite (Fig. 3a) and sulfosalts of Pb-Bi-Fe and Pb-Bi sulfide (Fig. 3b) as well as Ni-Fe-Mn oxide, and Fe-Cr oxide. These springs reflect continued hydrothermal activity along the McLaughlin-Knoxville trend with deposition of base metals and barite. This mineral assemblage is present in the McLaughlin gold deposit where it typically is present as late cross-cutting fracture coatings and veins that cut earlier quartz-chalcedony-gold mineralization.

Continue down road.

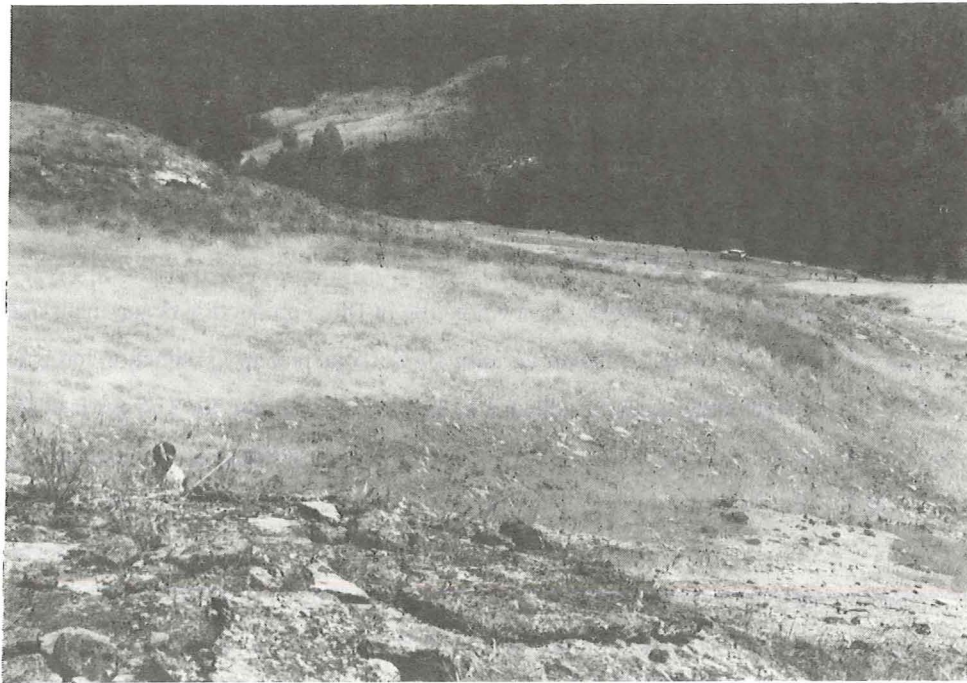


FIGURE 2. Travertine terrace along trace of Stony Creek fault just south of the McLaughlin Mine. View is from the top of the terrace toward road to Knoxville. The terrace extends from the foreground to the creek bed below the road. Several vents are present but the fluid flow is very low. Beds of barite and Pb-Bi-Fe sulfosalts are interbedded with the travertine.

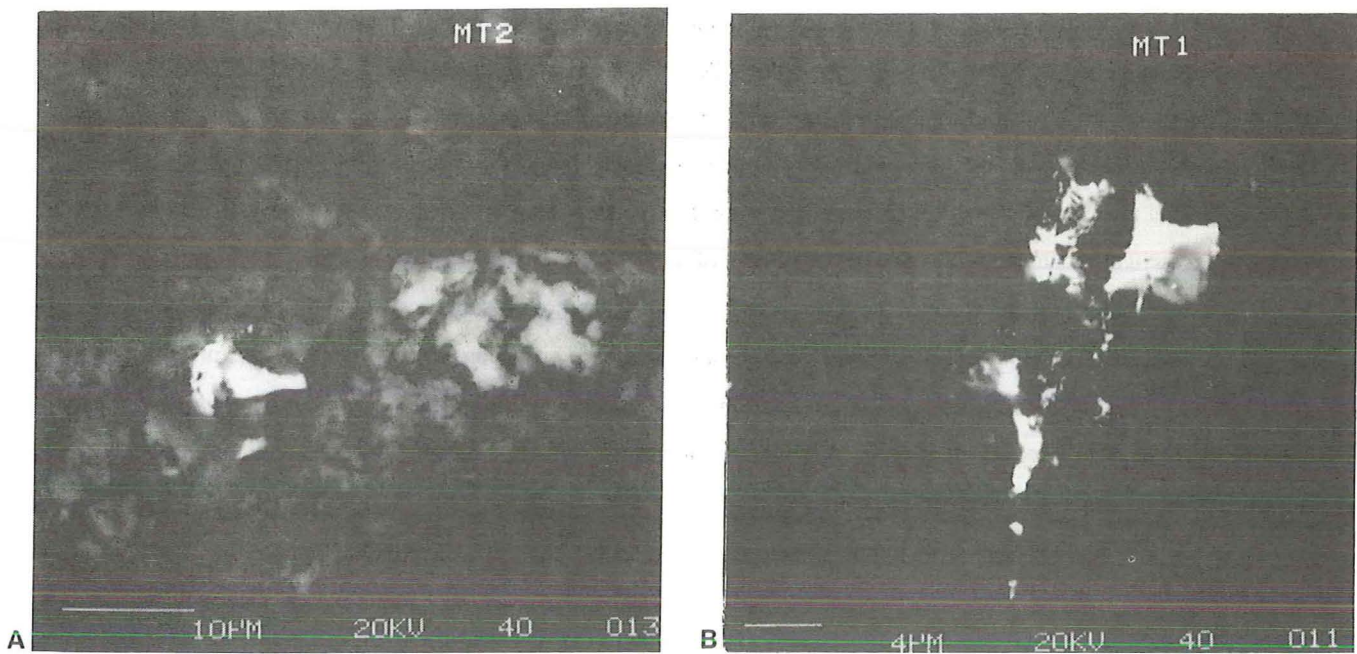


FIGURE 3. A. Barite, light gray grains in center of SEM photograph, intergrown with magnesian calcite from travertine terrace shown in Figure 1. White grains to left of barite are Mn-Fe-Ni oxide. **B.** Grains of Pb-Bi-Fe sulfide, white areas in backscatter SEM image within matrix of calcite, dark low reflectivity areas, from travertine shown in Figure 2.

- 0.5 23.2 Turn left onto road to Knoxville mercury deposit.
- 0.2 23.4 Turn left onto road to working of Knoxville mercury deposit.
- 0.3 23.7 Park and hike up to working of the Knoxville mercury deposit. **STOP 2.**

STOP 2. KNOXVILLE MERCURY DEPOSIT.

Mercury mineralization was first discovered at Knoxville in 1862; production began that same year and was continuous until about 1910 but only sporadic thereafter until 1948. Total mercury production has been 120,850 flasks, making Knoxville the sixth largest mercury deposit in the U.S., accounting for 3.75 per cent of total U.S. production. The deposit is localized along the Stony Creek fault, the same feature that provides important structural control in the McLaughlin gold deposit 2.5 km to the northwest. Other mercury deposits in the Knoxville district include, in decreasing order of importance, the Manhattan (now the McLaughlin gold mine), Reed, Harrison, and Red Elephant and total production in the district has been about 156,000 flasks. Although gold and cinnabar are found in surface soils at the Knoxville deposit (Vredenburg, 1982), several drill holes to depths of 200 m by Homestake Mining Co. indicate mercury mineralization persists with depth but gold contents are generally less than 100 ppb except for one intercept at 160 m of 1.4 ppm (Tosdal and others, this volume).

The ore bodies at Knoxville are in silica-carbonate altered serpentinite adjacent to the Stony Creek fault, which dips 45° to the east, an anomalously low angle compared to the typical near-vertical dip of the fault elsewhere (Averitt, 1945). The curvilinear fault trends generally northwest and separates serpentinite melange from Great Valley sequence mudstone and shale called the Knoxville Formation. Mineralization has a strike length of 0.3 km and is bounded on the north and south by east-trending cross faults, the southern fault being locally mineralized. These faults are analogous to the footwall faults and veins in the McLaughlin deposit. In the upper part of the mine several parallel zones of silica-carbonate veins are present in the fault zone but these coalesce into one narrow vein at depth. Silica-carbonate alteration persists to a depth of at least 800 feet. In contrast to Knoxville Formation rocks at McLaughlin, mudstone and shale of the Knoxville Formation here are not silicified or adularized. Cinnabar, the dominant ore mineral, was deposited late in the paragenetic sequence as discontinuous veins and fracture fillings and as irregular masses in silica-carbonate altered serpentinite and fault gouge. Minor native mercury and metacinnabar as well as pyrite and marcasite are present. Liquid and solid petroleum are abundant and petroleum-carbonate veins characterizes the last stage of mineralization.

Retrace route back to main road.

-
- 0.3 24.0 Turn right onto road out from Knoxville mercury deposit.
 - 0.2 24.2 Turn right onto road.
 - 2.0 26.2 Turn right into main entrance of McLaughlin Mine.

0.2 26.4 Proceed into mine area visitor parking lot and follow Homestake staff directions. In the open pit area driving is on the left side of the road. **STOP 3.**

STOP 3. McLAUGHLIN GOLD DEPOSIT.

The McLaughlin gold deposit lies along the Stony Creek fault, a major structural feature that separates Great Valley sequence from serpentinite melange containing fragments of Coast Range ophiolite and Franciscan Complex rocks (Fig. 4). The fault dips moderately (45°) northeast and strikes northwest. The Great Valley sequence in the mine area consists of shales and mudstones of the Knoxville Formation, which are adularized adjacent to the fault zone. Where it is mineralized in the north ore body, the serpentinite melange is altered to silica-carbonate rock (light colored area, Fig. 4). A basaltic andesite flow capping the ridge northeast of the pit represents the earliest phase of Clear Lake volcanism and has an age of 2.2 Ma (Lehrman, 1986). Equivalent flows extend southeastward toward the Knoxville mercury deposit and northward along the trace of the Stony Creek fault. Four distinct intrusive bodies have been emplaced along the Stony Creek fault with the largest being the Johntown neck, an andesitic vent complex consisting of a tuff ring-agglomerate apron surrounding a central plug (Lehrman, 1986). The central plug of the Johntown neck is mineralized and the Gailmercury deposit is localized in a maar agglomerate occurring just to the northwest of the Johntown neck. Other intrusions include sills and dikes that are important hosts for mineralization in the north ore body (Fig. 5). The only high-silica rhyolite in the mine area consists of a pumice-lapilli air-fall tuff that is present west of the open pit.



FIGURE 4. McLaughlin Mine looking northwest into the north ore body. In the north ore body, the Stony Creek fault separates adularized mudstones and shales of the Knoxville formation from serpentinite melange, which is altered to silica-carbonate rock along the fault zone, light colored area left of fault. The Zodiac sill occupies the fault zone in the central part of the photo. Basaltic andesite flows cap ridges to the right (Gail Ridge) and left of pit.



FIGURE 5. Overview of the northeast wall of the south ore body at the McLaughlin gold deposit. On the skyline, Gail Ridge is capped by a basaltic andesite flow about 20m thick (see Figure 6). The flow caps the hill to the extreme right (east) and was deposited on adularized mudstones and shales of the Knoxville Formation. The Johntown neck, a basaltic-andesite plug with an agglomerate apron, occurs in the right foreground. Agglomerate beds in the Gail maar deposits to the left (west) of the Johntown neck hosted mercury mineralization (see Figure 6). The San Quentin sinter occupied the area in the central part of the open pit, see Figure 6 for comparison to view prior to development of McLaughlin gold deposit.

The Manhattan mercury deposit (Fig. 6) occupied the area of what is now the south ore body. The main part of the south ore body occurred just below the San Quentin sinter and consisted of a sheeted vein 60 m by 60 m in area occurring over a vertical interval of 130 m and contained 721,000 oz of gold, about 25 per cent of the gold within the deposit (Lehrman, 1986). Numerous closely spaced veins with no intervening country rock comprise the sheeted vein. Vein banding, defined by several silica phases, includes white to clear opal, amber to brown opal, and clear to milky quartz and chalcedony. The rest of the south ore body consisted of veins hosted by the Johntown neck and serpentinite melange. The north ore body contains three distinct types of veins (Tosdal and others, this volume). In adularized mudstone the ore body consists of numerous closely spaced high-grade chalcedony-quartz-adularia veins. Gold often occurs in spectacular coarse-grained dendrites in these veins. The other two types of veins occur in silica-carbonate altered andesite sills and serpentinite melange. They consist of (1) banded quartz, chalcedony, petroliferous chalcedony, and carbonate with the brown petroliferous chalcedony having the highest gold values, and (2) quartz-chalcedony froth veins in which sufficient concentrations of petroleum are present to fill large voids and vugs that also contain abundant acicular stibnite crystals.

Retrace route back to main road.

0.2	26.6	Turn right onto paved road and retrace route back toward Lower Lake
3.5	30.1	Turn left onto dirt road and proceed straight ahead to parking area.
0.2	30.3	Park in area adjacent to Homestake boulder museum. STOP 4.

STOP 4. BOULDER MUSEUM FROM THE McLAUGHLIN GOLD DEPOSIT.

Large samples of sinter and veins from the surface and shallow subsurface of the McLaughlin gold deposit are displayed in this "boulder museum." Hot-spring sinter, locally known as the San Quentin sinter, was present over the main sheeted vein complex of the south ore body. The sinter was about 35 m thick, 130 m in maximum width, and hosted the mercury mineralization of the Manhattan Mine (Fig. 6). The sinter displayed many features typically found in hot-spring systems and these textures are easily seen in this boulder museum. Terraces in the sinter were formed when organic debris formed curvilinear dams and restricted fluid flow (Fig. 7). Filamentous bacteria, seen as sinuous ridges on the sinter surface, form in channels where fluid flow is not restricted (Fig. 8). In contrast, conophyton bacteria form stromatolites of vertical columns in quiescent pools on the sinter terrace and typically form an open, irregular texture quite different from planar laminated sinter formed in channels and high flow regimes on the sinter terrace. Silica deposited at the surface consisted of amorphous silica with a high water content. Dehydration of the silica resulted in polygonal dehydration (syneresis) cracks now preserved in the chalcedonic sinter (Fig. 9).

Hydrothermal explosion breccias are interbedded with the sinter (Fig. 10). Numerous beds of explosion breccia were present in the sinter terrace indicating multiple overpressuring events in the McLaughlin hydrothermal

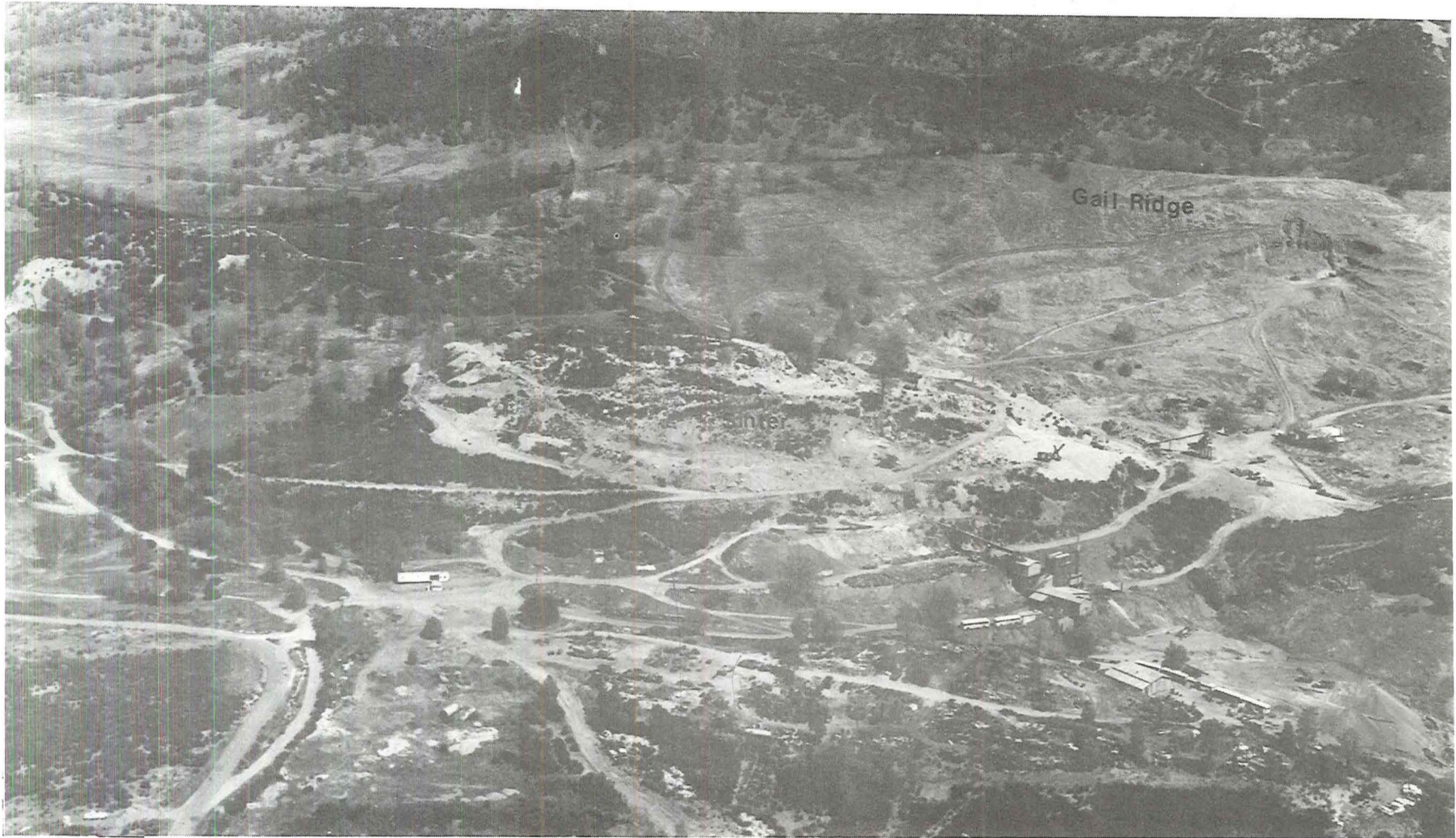


FIGURE 6. View of the Manhattan Mercury Mine prior to development of the McLoughlin gold deposit. The San Quentin sinter occupies the oval hill in the foreground and was 35 m thick and 130 m in length. The sheeted vein complex of the McLoughlin deposit was just below the sinter. Note the steam shovel on the right side of the sinter. Gail Ridge is just behind sinter hill and consists of a nearly flat lying basaltic andesite flow. Open cuts on the right side of the ridge are the workings of the Gail mercury deposit.



FIGURE 7. Surface of sinter terrace displaying ridges where organic debris formed curvilinear dams and restricted fluid flow. Flow was toward the right side of photo.



FIGURE 8. Filamentous bacteria form sinuous ridges on the sinter surface where unrestricted fluid flow occurred in channels. Fluid flow was toward the right side of photograph.

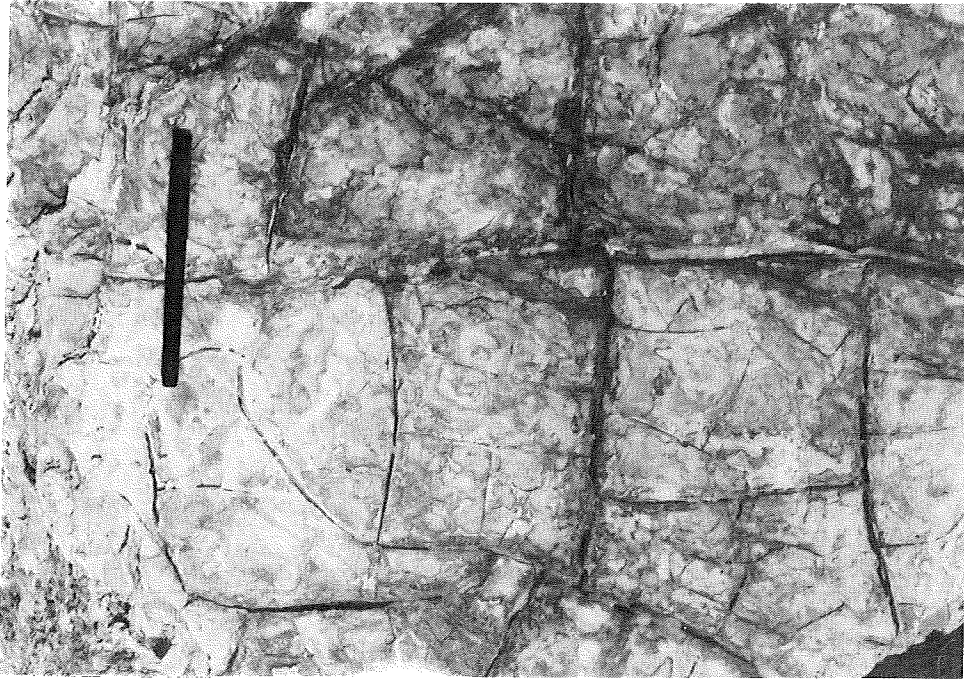


FIGURE 9. Dehydration of amorphous silica in the sinter resulted in polygonal dehydration (syneresis) cracks.



FIGURE 10. Hydrothermal explosion breccias are interbedded with banded sinter and consist of country rock and sinter fragments in an open-texture breccia cemented by silica.

system. The base of the sinter terrace was cut by high-grade gold veins displaying banded texture. Just below the sinter surface, numerous crosscutting banded veins comprised the upper part of the sheeted vein complex.

Retrace route back to main road.

- 0.2 30.5 Turn left onto paved road and retrace route back toward Lower Lake.
0.9 31.4 Homestake guard station. Stop and sign out.
13.0 44.4 Intersection of Highway 53, end of trip.

REFERENCES

- Averitt, Paul, 1945, Quicksilver deposits of the Knoxville district, Napa, Yolo, and Lake Counties, California: California Journal of Mines and Geology, v. 41, no. 2, p. 65-89.
- Goff, F. E., and Janik, C. J., 1993, Gas geochemistry and guide for geothermal features in the Clear Lake region, California, in J. J. Rytuba ed., Active geothermal systems and gold-mercury deposits in the Sonoma-Clear Lake volcanic fields: California, Soc. Econ. Geol. Guidebook Series, (this volume)
- Lehrman, N. J., 1986, The McLaughlin mine, Napa and Yolo counties, California: Nevada Bureau of Mines and Geology, Report 41, p. 85-89.
- Tosdal, R. M., Enderlin, D. A., Nelson, G. C., and Lehrman, N. J. 1993, Overview of the McLaughlin precious metal deposit, Napa and Yolo Counties, northern California, in J. J. Rytuba ed., Active geothermal systems and gold-mercury deposits in the Sonoma-Clear Lake volcanic fields: California, Soc. Econ. Geol. Guidebook Series, (this volume)
- Vredenburg, L. M. , 1982, Tertiary gold bearing mercury deposits of the Coast Ranges of California: California Geology, v. 35, no. 2, p. 23-27.

